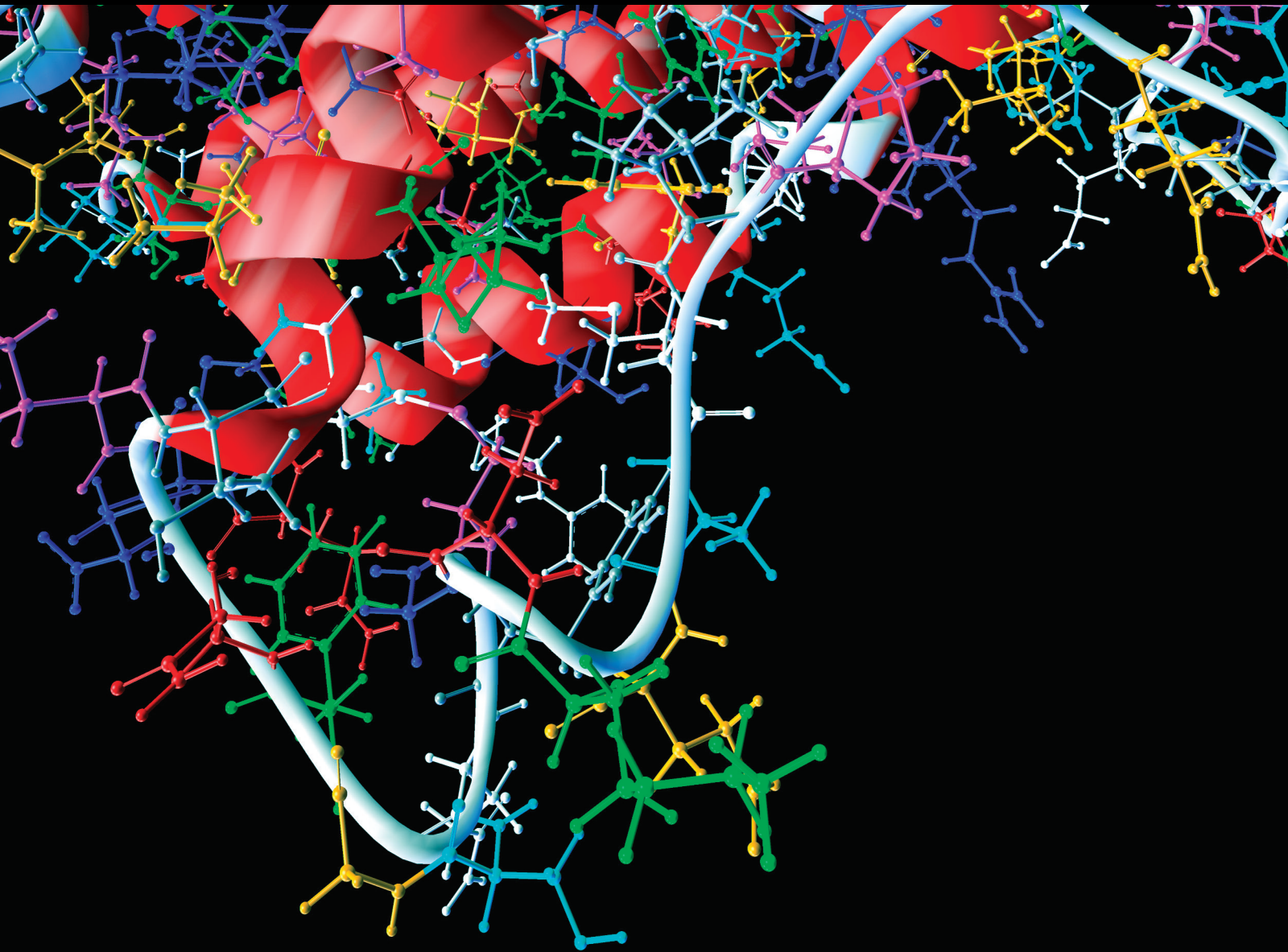# Social Network-Based Medical Informatics with a Deep Learning Perspective 2022

Lead Guest Editor: Muhammad Zubair Asghar
Guest Editors: Ibrahim Hameed and Shakeel Ahmad

Social Network-Based Medical Informatics with a Deep Learning Perspective 2022

Social Network-Based Medical Informatics with a Deep Learning Perspective 2022

Lead Guest Editor: Muhammad Zubair Asghar
Guest Editors: Ibrahim Hameed and Shakeel Ahmad

Hyuntae Park, Japan
Jovana Paunovic, Serbia
Manuel F. G. Penedo, Spain
Riccardo Pernice, Italy
Kemal Polat, Turkey
Alberto Policriti, Italy
Giuseppe Pontrelli, Italy
Jesús Poza, Spain
Maciej Przybyłek, Poland
Bhanwar Lal Puniya, USA
Mihai V. Putz, Romania
Suresh Rasappan, Oman
Jose Joaquin Rieta, Spain
Fathalla Rihan, United Arab Emirates
Sidheswar Routray, India
Sudipta Roy, India
Jan Rychtar, USA
Mario Sansone, Italy
Murat Sari, Turkey
Shahzad Sarwar, Saudi Arabia
Kamal Shah, Saudi Arabia
Bhisham Sharma, India
Simon A. Sherman, USA
Mingsong Shi, China
Mohammed Shuaib, Malaysia
Prabhishek Singh, India
Neelakandan Subramani, India
Junwei Sun, China
Yung-Shin Sun, Taiwan
Min Tang, China
Hongxun Tao, China
Alireza Tavakkoli, USA
João M. Tavares, Portugal
Jlenia Toppi, Italy
Anna Tsantili-Kakoulidou, Greece
Markos G. Tsipouras, North Macedonia
Po-Hsiang Tsui, Taiwan
Sathishkumar V E, Republic of Korea
Durai Raj Vincent P M, India
Gajendra Kumar Vishwakarma, India
Liangjiang Wang, USA
Ruisheng Wang, USA
Zhouchao Wei, China
Gabriel Wittum, Germany
Xiang Wu, China

KI Yanover, Israel
Xiaojun Yao, China
Kaan Yetilmezsoy, Turkey
Hiro Yoshida, USA
Yuhai Zhao, China

Contents

Retracted: Analysis of Rotator Cuff Muscle Injury on the Drawing Side of the Recurve Bow: A Finite Element Method
Computational and Mathematical Methods in Medicine
Retraction (1 page), Article ID 9765751, Volume 2023 (2023)

Retracted: MiR-579 Inhibits Lung Adenocarcinoma Cell Proliferation and Metastasis via Binding to CRABP2
Computational and Mathematical Methods in Medicine
Retraction (1 page), Article ID 9892542, Volume 2023 (2023)

Retracted: Advances in the Application of Liquid Chromatography in the Detection of Pollutants
Computational and Mathematical Methods in Medicine
Retraction (1 page), Article ID 9891424, Volume 2023 (2023)

Retracted: 23G Minimally Invasive Vitrectomy Combined with Glaucoma Drainage Valve Implantation and Phacoemulsification Cataract Extraction for Neovascular Glaucoma Secondary to Proliferative Diabetic Retinopathy with Vitreous Hemorrhage
Computational and Mathematical Methods in Medicine
Retraction (1 page), Article ID 9868749, Volume 2023 (2023)

Retracted: The Efficacy and Safety of Bisoprolol in the Treatment of Myocardial Infarction with Cardiac Insufficiency
Computational and Mathematical Methods in Medicine
Retraction (1 page), Article ID 9863585, Volume 2023 (2023)

Retracted: Magnetic Resonance Image Compilation Was Used in Conjunction with Prostate PI-RADS v2.1 Score Has Diagnostic Relevance for Benign and Malignant Prostate Lesions
Computational and Mathematical Methods in Medicine
Retraction (1 page), Article ID 9862310, Volume 2023 (2023)

Retracted: Myopia in Chinese Adolescents: Its Influencing Factors and Correlation with Physical Activities
Computational and Mathematical Methods in Medicine
Retraction (1 page), Article ID 9861925, Volume 2023 (2023)

Retracted: Effect of Stereotactic Body Radiation Therapy Combined with Thermoplastic Fixation on Set-Up Errors in Breast Cancer Patients Undergoing Radiotherapy
Computational and Mathematical Methods in Medicine
Retraction (1 page), Article ID 9857125, Volume 2023 (2023)

Retracted: Clinical Evaluation of the Medium-Term Efficacy of Laparoscopic Sleeve Gastrectomy against Obstructive Sleep Apnea-Hypopnea Syndrome in Obese Patients
Computational and Mathematical Methods in Medicine
Retraction (1 page), Article ID 9848635, Volume 2023 (2023)

Contents

Contents

[Retracted] Effects of Bevacizumab Combined with Chemotherapy on CT, CyFRA21-1, and ProGRP and Prognosis of Lung Cancer Patients under Nursing Intervention

Chao Xi (iD), Hong Jiang (iD), Yinling Xue (iD), Yongmei Lv (iD), and Chao Wang (iD)

Retraction

Retracted: Effects of Quantitative Nursing Combined with Psychological Intervention in Operating Room on Stress Response, Psychological State, and Prognosis of Patients Undergoing Laparoscopic Endometrial Cancer Surgery

Computational and Mathematical Methods in Medicine

This article has been retracted by Hindawi following an investigation undertaken by the publisher [1]. This investigation has uncovered evidence of one or more of the following indicators of systematic manipulation of the publication process:

(1) Discrepancies in scope

(2) Discrepancies in the description of the research reported

(3) Discrepancies between the availability of data and the research described

(4) Inappropriate citations

(5) Incoherent, meaningless and/or irrelevant content included in the article

(6) Peer-review manipulation

The presence of these indicators undermines our confidence in the integrity of the article's content and we cannot, therefore, vouch for its reliability. Please note that this notice is intended solely to alert readers that the content of this article is unreliable. We have not investigated whether authors were aware of or involved in the systematic manipulation of the publication process.

Wiley and Hindawi regrets that the usual quality checks did not identify these issues before publication and have since put additional measures in place to safeguard research integrity.

We wish to credit our own Research Integrity and Research Publishing teams and anonymous and named external researchers and research integrity experts for contributing to this investigation.

The corresponding author, as the representative of all authors, has been given the opportunity to register their agreement or disagreement to this retraction. We have kept a record of any response received.

References

[1] X. Chen, H. Li, S. Wang et al., "Effects of Quantitative Nursing Combined with Psychological Intervention in Operating Room on Stress Response, Psychological State, and Prognosis of Patients Undergoing Laparoscopic Endometrial Cancer Surgery," *Computational and Mathematical Methods in Medicine*, vol. 2022, Article ID 6735100, 8 pages, 2022.

Retraction

Retracted: Early Assessment of Cardiac Function by Echocardiography in Patients with Gestational Diabetes Mellitus

Computational and Mathematical Methods in Medicine

This article has been retracted by Hindawi following an investigation undertaken by the publisher [1]. This investigation has uncovered evidence of one or more of the following indicators of systematic manipulation of the publication process:

(1) Discrepancies in scope

(2) Discrepancies in the description of the research reported

(3) Discrepancies between the availability of data and the research described

(4) Inappropriate citations

(5) Incoherent, meaningless and/or irrelevant content included in the article

(6) Peer-review manipulation

The presence of these indicators undermines our confidence in the integrity of the article's content and we cannot, therefore, vouch for its reliability. Please note that this notice is intended solely to alert readers that the content of this article is unreliable. We have not investigated whether authors were aware of or involved in the systematic manipulation of the publication process.

Wiley and Hindawi regrets that the usual quality checks did not identify these issues before publication and have since put additional measures in place to safeguard research integrity.

We wish to credit our own Research Integrity and Research Publishing teams and anonymous and named external researchers and research integrity experts for contributing to this investigation.

The corresponding author, as the representative of all authors, has been given the opportunity to register their agreement or disagreement to this retraction. We have kept a record of any response received.

References

[1] P. Wang, Y. Peng, L. Liu et al., "Early Assessment of Cardiac Function by Echocardiography in Patients with Gestational Diabetes Mellitus," *Computational and Mathematical Methods in Medicine*, vol. 2022, Article ID 6565109, 7 pages, 2022.

Retraction

Retracted: Analysis of Intervention Effect and Satisfaction of Holistic Nursing after Oral Tumor Resection

Computational and Mathematical Methods in Medicine

This article has been retracted by Hindawi following an investigation undertaken by the publisher [1]. This investigation has uncovered evidence of one or more of the following indicators of systematic manipulation of the publication process:

(1) Discrepancies in scope

(2) Discrepancies in the description of the research reported

(3) Discrepancies between the availability of data and the research described

(4) Inappropriate citations

(5) Incoherent, meaningless and/or irrelevant content included in the article

(6) Peer-review manipulation

The presence of these indicators undermines our confidence in the integrity of the article's content and we cannot, therefore, vouch for its reliability. Please note that this notice is intended solely to alert readers that the content of this article is unreliable. We have not investigated whether authors were aware of or involved in the systematic manipulation of the publication process.

Wiley and Hindawi regrets that the usual quality checks did not identify these issues before publication and have since put additional measures in place to safeguard research integrity.

We wish to credit our own Research Integrity and Research Publishing teams and anonymous and named external researchers and research integrity experts for contributing to this investigation.

The corresponding author, as the representative of all authors, has been given the opportunity to register their agreement or disagreement to this retraction. We have kept a record of any response received.

References

[1] L. Qu, Y. Yin, N. Zhao, Y. Lv, and H. Xu, "Analysis of Intervention Effect and Satisfaction of Holistic Nursing after Oral Tumor Resection," *Computational and Mathematical Methods in Medicine*, vol. 2022, Article ID 3788605, 7 pages, 2022.

Retraction

Retracted: Effects of Chinese Herbal Formula on Immune Function and Nutritional Status of Breast Cancer Patients

Computational and Mathematical Methods in Medicine

This article has been retracted by Hindawi following an investigation undertaken by the publisher [1]. This investigation has uncovered evidence of one or more of the following indicators of systematic manipulation of the publication process:

(1) Discrepancies in scope

(2) Discrepancies in the description of the research reported

(3) Discrepancies between the availability of data and the research described

(4) Inappropriate citations

(5) Incoherent, meaningless and/or irrelevant content included in the article

(6) Peer-review manipulation

The presence of these indicators undermines our confidence in the integrity of the article's content and we cannot, therefore, vouch for its reliability. Please note that this notice is intended solely to alert readers that the content of this article is unreliable. We have not investigated whether authors were aware of or involved in the systematic manipulation of the publication process.

Wiley and Hindawi regrets that the usual quality checks did not identify these issues before publication and have since put additional measures in place to safeguard research integrity.

We wish to credit our own Research Integrity and Research Publishing teams and anonymous and named external researchers and research integrity experts for contributing to this investigation.

The corresponding author, as the representative of all authors, has been given the opportunity to register their agreement or disagreement to this retraction. We have kept a record of any response received.

References

[1] M. Liu, "Effects of Chinese Herbal Formula on Immune Function and Nutritional Status of Breast Cancer Patients," *Computational and Mathematical Methods in Medicine*, vol. 2022, Article ID 5900024, 6 pages, 2022.

Retraction

Retracted: Clinical and Biological Significances of a Ferroptosis-Related Gene Signature in Lung Cancer Based on Deep Learning

Computational and Mathematical Methods in Medicine

This article has been retracted by Hindawi following an investigation undertaken by the publisher [1]. This investigation has uncovered evidence of one or more of the following indicators of systematic manipulation of the publication process:

(1) Discrepancies in scope

(2) Discrepancies in the description of the research reported

(3) Discrepancies between the availability of data and the research described

(4) Inappropriate citations

(5) Incoherent, meaningless and/or irrelevant content included in the article

(6) Peer-review manipulation

The presence of these indicators undermines our confidence in the integrity of the article's content and we cannot, therefore, vouch for its reliability. Please note that this notice is intended solely to alert readers that the content of this article is unreliable. We have not investigated whether authors were aware of or involved in the systematic manipulation of the publication process.

Wiley and Hindawi regrets that the usual quality checks did not identify these issues before publication and have since put additional measures in place to safeguard research integrity.

We wish to credit our own Research Integrity and Research Publishing teams and anonymous and named external researchers and research integrity experts for contributing to this investigation.

The corresponding author, as the representative of all authors, has been given the opportunity to register their agreement or disagreement to this retraction. We have kept a record of any response received.

References

[1] X. Yang, X. Hu, and N. Guo, "Clinical and Biological Significances of a Ferroptosis-Related Gene Signature in Lung Cancer Based on Deep Learning," *Computational and Mathematical Methods in Medicine*, vol. 2022, Article ID 6495301, 15 pages, 2022.

Retraction

Retracted: KIF11 Is a Promising Therapeutic Target for Thyroid Cancer Treatment

Computational and Mathematical Methods in Medicine

This article has been retracted by Hindawi following an investigation undertaken by the publisher [1]. This investigation has uncovered evidence of one or more of the following indicators of systematic manipulation of the publication process:

(1) Discrepancies in scope

(2) Discrepancies in the description of the research reported

(3) Discrepancies between the availability of data and the research described

(4) Inappropriate citations

(5) Incoherent, meaningless and/or irrelevant content included in the article

(6) Peer-review manipulation

The presence of these indicators undermines our confidence in the integrity of the article's content and we cannot, therefore, vouch for its reliability. Please note that this notice is intended solely to alert readers that the content of this article is unreliable. We have not investigated whether authors were aware of or involved in the systematic manipulation of the publication process.

In addition, our investigation has also shown that one or more of the following human-subject reporting requirements has not been met in this article: ethical approval by an Institutional Review Board (IRB) committee or equivalent, patient/participant consent to participate, and/or agreement to publish patient/participant details (where relevant).

Wiley and Hindawi regrets that the usual quality checks did not identify these issues before publication and have since put additional measures in place to safeguard research integrity.

We wish to credit our own Research Integrity and Research Publishing teams and anonymous and named external researchers and research integrity experts for contributing to this investigation.

The corresponding author, as the representative of all authors, has been given the opportunity to register their agreement or disagreement to this retraction. We have kept a record of any response received.

References

[1] Y. Han, J. Chen, D. Wei, and B. Wang, "KIF11 Is a Promising Therapeutic Target for Thyroid Cancer Treatment," *Computational and Mathematical Methods in Medicine*, vol. 2022, Article ID 6426800, 8 pages, 2022.

Hindawi

Retraction

Retracted: Effects of Bevacizumab Combined with Chemotherapy on CT, CyFRA21-1, and ProGRP and Prognosis of Lung Cancer Patients under Nursing Intervention

Computational and Mathematical Methods in Medicine

This article has been retracted by Hindawi following an investigation undertaken by the publisher [1]. This investigation has uncovered evidence of one or more of the following indicators of systematic manipulation of the publication process:

(1) Discrepancies in scope

(2) Discrepancies in the description of the research reported

(3) Discrepancies between the availability of data and the research described

(4) Inappropriate citations

(5) Incoherent, meaningless and/or irrelevant content included in the article

(6) Peer-review manipulation

The presence of these indicators undermines our confidence in the integrity of the article's content and we cannot, therefore, vouch for its reliability. Please note that this notice is intended solely to alert readers that the content of this article is unreliable. We have not investigated whether authors were aware of or involved in the systematic manipulation of the publication process.

Wiley and Hindawi regrets that the usual quality checks did not identify these issues before publication and have since put additional measures in place to safeguard research integrity.

We wish to credit our own Research Integrity and Research Publishing teams and anonymous and named external researchers and research integrity experts for contributing to this investigation.

The corresponding author, as the representative of all authors, has been given the opportunity to register their agreement or disagreement to this retraction. We have kept a record of any response received.

References

[1] C. Xi, H. Jiang, Y. Xue, Y. Lv, and C. Wang, "Effects of Bevacizumab Combined with Chemotherapy on CT, CyFRA21-1, and ProGRP and Prognosis of Lung Cancer Patients under Nursing Intervention," *Computational and Mathematical Methods in Medicine*, vol. 2022, Article ID 9422902, 8 pages, 2022.

Retraction

Retracted: A Meta-Analysis of CT as a Tool for Diagnosing and Treating Shoulder Joint Bankart Injuries

Computational and Mathematical Methods in Medicine

This article has been retracted by Hindawi following an investigation undertaken by the publisher [1]. This investigation has uncovered evidence of one or more of the following indicators of systematic manipulation of the publication process:

(1) Discrepancies in scope

(2) Discrepancies in the description of the research reported

(3) Discrepancies between the availability of data and the research described

(4) Inappropriate citations

(5) Incoherent, meaningless and/or irrelevant content included in the article

(6) Peer-review manipulation

The presence of these indicators undermines our confidence in the integrity of the article's content and we cannot, therefore, vouch for its reliability. Please note that this notice is intended solely to alert readers that the content of this article is unreliable. We have not investigated whether authors were aware of or involved in the systematic manipulation of the publication process.

In addition, our investigation has also shown that one or more of the following human-subject reporting requirements has not been met in this article: ethical approval by an Institutional Review Board (IRB) committee or equivalent, patient/participant consent to participate, and/or agreement to publish patient/participant details (where relevant).

Wiley and Hindawi regrets that the usual quality checks did not identify these issues before publication and have since put additional measures in place to safeguard research integrity.

We wish to credit our own Research Integrity and Research Publishing teams and anonymous and named external researchers and research integrity experts for contributing to this investigation.

The corresponding author, as the representative of all authors, has been given the opportunity to register their agreement or disagreement to this retraction. We have kept a record of any response received.

References

[1] Y. Yang, L. Zou, and Z. Li, "A Meta-Analysis of CT as a Tool for Diagnosing and Treating Shoulder Joint Bankart Injuries," *Computational and Mathematical Methods in Medicine*, vol. 2022, Article ID 9137706, 8 pages, 2022.

Retraction

Retracted: A Study on the Preventive Effect of Esketamine on Postpartum Depression (PPD) after Cesarean Section

Computational and Mathematical Methods in Medicine

This article has been retracted by Hindawi following an investigation undertaken by the publisher [1]. This investigation has uncovered evidence of one or more of the following indicators of systematic manipulation of the publication process:

(1) Discrepancies in scope

(2) Discrepancies in the description of the research reported

(3) Discrepancies between the availability of data and the research described

(4) Inappropriate citations

(5) Incoherent, meaningless and/or irrelevant content included in the article

(6) Peer-review manipulation

The presence of these indicators undermines our confidence in the integrity of the article's content and we cannot, therefore, vouch for its reliability. Please note that this notice is intended solely to alert readers that the content of this article is unreliable. We have not investigated whether authors were aware of or involved in the systematic manipulation of the publication process.

Wiley and Hindawi regrets that the usual quality checks did not identify these issues before publication and have since put additional measures in place to safeguard research integrity.

We wish to credit our own Research Integrity and Research Publishing teams and anonymous and named external researchers and research integrity experts for contributing to this investigation.

The corresponding author, as the representative of all authors, has been given the opportunity to register their agreement or disagreement to this retraction. We have kept a record of any response received.

References

[1] Q. Wang, M. Xiao, H. Sun, and P. Zhang, "A Study on the Preventive Effect of Esketamine on Postpartum Depression (PPD) after Cesarean Section," *Computational and Mathematical Methods in Medicine*, vol. 2022, Article ID 1524198, 5 pages, 2022.

Retraction

Retracted: Analysis of Rotator Cuff Muscle Injury on the Drawing Side of the Recurve Bow: A Finite Element Method

Computational and Mathematical Methods in Medicine

This article has been retracted by Hindawi following an investigation undertaken by the publisher [1]. This investigation has uncovered evidence of one or more of the following indicators of systematic manipulation of the publication process:

(1) Discrepancies in scope

(2) Discrepancies in the description of the research reported

(3) Discrepancies between the availability of data and the research described

(4) Inappropriate citations

(5) Incoherent, meaningless and/or irrelevant content included in the article

(6) Peer-review manipulation

The presence of these indicators undermines our confidence in the integrity of the article's content and we cannot, therefore, vouch for its reliability. Please note that this notice is intended solely to alert readers that the content of this article is unreliable. We have not investigated whether authors were aware of or involved in the systematic manipulation of the publication process.

Wiley and Hindawi regrets that the usual quality checks did not identify these issues before publication and have since put additional measures in place to safeguard research integrity.

We wish to credit our own Research Integrity and Research Publishing teams and anonymous and named external researchers and research integrity experts for contributing to this investigation.

The corresponding author, as the representative of all authors, has been given the opportunity to register their agreement or disagreement to this retraction. We have kept a record of any response received.

References

[1] C. Guo, X. Liu, Y. Yang, D. Zhang, D. Yang, and J. Yin, "Analysis of Rotator Cuff Muscle Injury on the Drawing Side of the Recurve Bow: A Finite Element Method," *Computational and Mathematical Methods in Medicine*, vol. 2022, Article ID 8572311, 10 pages, 2022.

Hindawi

Retraction

Retracted: MiR-579 Inhibits Lung Adenocarcinoma Cell Proliferation and Metastasis via Binding to CRABP2

Computational and Mathematical Methods in Medicine

This article has been retracted by Hindawi following an investigation undertaken by the publisher [1]. This investigation has uncovered evidence of one or more of the following indicators of systematic manipulation of the publication process:

(1) Discrepancies in scope

(2) Discrepancies in the description of the research reported

(3) Discrepancies between the availability of data and the research described

(4) Inappropriate citations

(5) Incoherent, meaningless and/or irrelevant content included in the article

(6) Peer-review manipulation

The presence of these indicators undermines our confidence in the integrity of the article's content and we cannot, therefore, vouch for its reliability. Please note that this notice is intended solely to alert readers that the content of this article is unreliable. We have not investigated whether authors were aware of or involved in the systematic manipulation of the publication process.

Wiley and Hindawi regrets that the usual quality checks did not identify these issues before publication and have since put additional measures in place to safeguard research integrity.

We wish to credit our own Research Integrity and Research Publishing teams and anonymous and named external researchers and research integrity experts for contributing to this investigation.

The corresponding author, as the representative of all authors, has been given the opportunity to register their agreement or disagreement to this retraction. We have kept a record of any response received.

References

[1] Q. Yi, Y. Miao, Y. Kong et al., "MiR-579 Inhibits Lung Adenocarcinoma Cell Proliferation and Metastasis via Binding to CRABP2," *Computational and Mathematical Methods in Medicine*, vol. 2022, Article ID 9111681, 9 pages, 2022.

Retraction

Retracted: Advances in the Application of Liquid Chromatography in the Detection of Pollutants

Computational and Mathematical Methods in Medicine

This article has been retracted by Hindawi following an investigation undertaken by the publisher [1]. This investigation has uncovered evidence of one or more of the following indicators of systematic manipulation of the publication process:

(1) Discrepancies in scope

(2) Discrepancies in the description of the research reported

(3) Discrepancies between the availability of data and the research described

(4) Inappropriate citations

(5) Incoherent, meaningless and/or irrelevant content included in the article

(6) Peer-review manipulation

The presence of these indicators undermines our confidence in the integrity of the article's content and we cannot, therefore, vouch for its reliability. Please note that this notice is intended solely to alert readers that the content of this article is unreliable. We have not investigated whether authors were aware of or involved in the systematic manipulation of the publication process.

Wiley and Hindawi regrets that the usual quality checks did not identify these issues before publication and have since put additional measures in place to safeguard research integrity.

We wish to credit our own Research Integrity and Research Publishing teams and anonymous and named external researchers and research integrity experts for contributing to this investigation.

The corresponding author, as the representative of all authors, has been given the opportunity to register their agreement or disagreement to this retraction. We have kept a record of any response received.

References

[1] X. Hu, "Advances in the Application of Liquid Chromatography in the Detection of Pollutants," *Computational and Mathematical Methods in Medicine*, vol. 2022, Article ID 2152615, 11 pages, 2022.

Retraction

Retracted: 23G Minimally Invasive Vitrectomy Combined with Glaucoma Drainage Valve Implantation and Phacoemulsification Cataract Extraction for Neovascular Glaucoma Secondary to Proliferative Diabetic Retinopathy with Vitreous Hemorrhage

Computational and Mathematical Methods in Medicine

This article has been retracted by Hindawi following an investigation undertaken by the publisher [1]. This investigation has uncovered evidence of one or more of the following indicators of systematic manipulation of the publication process:

(1) Discrepancies in scope

(2) Discrepancies in the description of the research reported

(3) Discrepancies between the availability of data and the research described

(4) Inappropriate citations

(5) Incoherent, meaningless and/or irrelevant content included in the article

(6) Peer-review manipulation

The presence of these indicators undermines our confidence in the integrity of the article's content and we cannot, therefore, vouch for its reliability. Please note that this notice is intended solely to alert readers that the content of this article is unreliable. We have not investigated whether authors were aware of or involved in the systematic manipulation of the publication process.

Wiley and Hindawi regrets that the usual quality checks did not identify these issues before publication and have since put additional measures in place to safeguard research integrity.

We wish to credit our own Research Integrity and Research Publishing teams and anonymous and named external researchers and research integrity experts for contributing to this investigation.

The corresponding author, as the representative of all authors, has been given the opportunity to register their agreement or disagreement to this retraction. We have kept a record of any response received.

References

[1] X. Shi, N. Dong, Y. Liang, L. Zheng, and X. Wang, "23G Minimally Invasive Vitrectomy Combined with Glaucoma Drainage Valve Implantation and Phacoemulsification Cataract Extraction for Neovascular Glaucoma Secondary to Proliferative Diabetic Retinopathy with Vitreous Hemorrhage," *Computational and Mathematical Methods in Medicine*, vol. 2022, Article ID 7393661, 8 pages, 2022.

Retraction

Retracted: The Efficacy and Safety of Bisoprolol in the Treatment of Myocardial Infarction with Cardiac Insufficiency

Computational and Mathematical Methods in Medicine

This article has been retracted by Hindawi following an investigation undertaken by the publisher [1]. This investigation has uncovered evidence of one or more of the following indicators of systematic manipulation of the publication process:

(1) Discrepancies in scope

(2) Discrepancies in the description of the research reported

(3) Discrepancies between the availability of data and the research described

(4) Inappropriate citations

(5) Incoherent, meaningless and/or irrelevant content included in the article

(6) Peer-review manipulation

The presence of these indicators undermines our confidence in the integrity of the article's content and we cannot, therefore, vouch for its reliability. Please note that this notice is intended solely to alert readers that the content of this article is unreliable. We have not investigated whether authors were aware of or involved in the systematic manipulation of the publication process.

Wiley and Hindawi regrets that the usual quality checks did not identify these issues before publication and have since put additional measures in place to safeguard research integrity.

We wish to credit our own Research Integrity and Research Publishing teams and anonymous and named external researchers and research integrity experts for contributing to this investigation.

The corresponding author, as the representative of all authors, has been given the opportunity to register their agreement or disagreement to this retraction. We have kept a record of any response received.

References

[1] Y. Wang, "The Efficacy and Safety of Bisoprolol in the Treatment of Myocardial Infarction with Cardiac Insufficiency," *Computational and Mathematical Methods in Medicine*, vol. 2022, Article ID 3098726, 5 pages, 2022.

Retraction

Retracted: Magnetic Resonance Image Compilation Was Used in Conjunction with Prostate PI-RADS v2.1 Score Has Diagnostic Relevance for Benign and Malignant Prostate Lesions

Computational and Mathematical Methods in Medicine

This article has been retracted by Hindawi following an investigation undertaken by the publisher [1]. This investigation has uncovered evidence of one or more of the following indicators of systematic manipulation of the publication process:

(1) Discrepancies in scope

(2) Discrepancies in the description of the research reported

(3) Discrepancies between the availability of data and the research described

(4) Inappropriate citations

(5) Incoherent, meaningless and/or irrelevant content included in the article

(6) Peer-review manipulation

The presence of these indicators undermines our confidence in the integrity of the article's content and we cannot, therefore, vouch for its reliability. Please note that this notice is intended solely to alert readers that the content of this article is unreliable. We have not investigated whether authors were aware of or involved in the systematic manipulation of the publication process.

Wiley and Hindawi regrets that the usual quality checks did not identify these issues before publication and have since put additional measures in place to safeguard research integrity.

We wish to credit our own Research Integrity and Research Publishing teams and anonymous and named external researchers and research integrity experts for contributing to this investigation.

The corresponding author, as the representative of all authors, has been given the opportunity to register their agreement or disagreement to this retraction. We have kept a record of any response received.

References

[1] W. Xu, H. Cao, F. Du, L. He, F. Jiang, and C. Hu, "Magnetic Resonance Image Compilation Was Used in Conjunction with Prostate PI-RADS v2.1 Score Has Diagnostic Relevance for Benign and Malignant Prostate Lesions," *Computational and Mathematical Methods in Medicine*, vol. 2022, Article ID 3613540, 10 pages, 2022.

Retraction

Retracted: Myopia in Chinese Adolescents: Its Influencing Factors and Correlation with Physical Activities

Computational and Mathematical Methods in Medicine

This article has been retracted by Hindawi following an investigation undertaken by the publisher [1]. This investigation has uncovered evidence of one or more of the following indicators of systematic manipulation of the publication process:

(1) Discrepancies in scope

(2) Discrepancies in the description of the research reported

(3) Discrepancies between the availability of data and the research described

(4) Inappropriate citations

(5) Incoherent, meaningless and/or irrelevant content included in the article

(6) Peer-review manipulation

The presence of these indicators undermines our confidence in the integrity of the article's content and we cannot, therefore, vouch for its reliability. Please note that this notice is intended solely to alert readers that the content of this article is unreliable. We have not investigated whether authors were aware of or involved in the systematic manipulation of the publication process.

Wiley and Hindawi regrets that the usual quality checks did not identify these issues before publication and have since put additional measures in place to safeguard research integrity.

We wish to credit our own Research Integrity and Research Publishing teams and anonymous and named external researchers and research integrity experts for contributing to this investigation.

The corresponding author, as the representative of all authors, has been given the opportunity to register their agreement or disagreement to this retraction. We have kept a record of any response received.

References

[1] Y. Yin, C. Qiu, and Y. Qi, "Myopia in Chinese Adolescents: Its Influencing Factors and Correlation with Physical Activities," *Computational and Mathematical Methods in Medicine*, vol. 2022, Article ID 4700325, 10 pages, 2022.

Retraction

Retracted: Effect of Stereotactic Body Radiation Therapy Combined with Thermoplastic Fixation on Set-Up Errors in Breast Cancer Patients Undergoing Radiotherapy

Computational and Mathematical Methods in Medicine

This article has been retracted by Hindawi following an investigation undertaken by the publisher [1]. This investigation has uncovered evidence of one or more of the following indicators of systematic manipulation of the publication process:

(1) Discrepancies in scope

(2) Discrepancies in the description of the research reported

(3) Discrepancies between the availability of data and the research described

(4) Inappropriate citations

(5) Incoherent, meaningless and/or irrelevant content included in the article

(6) Peer-review manipulation

The presence of these indicators undermines our confidence in the integrity of the article's content and we cannot, therefore, vouch for its reliability. Please note that this notice is intended solely to alert readers that the content of this article is unreliable. We have not investigated whether authors were aware of or involved in the systematic manipulation of the publication process.

Wiley and Hindawi regrets that the usual quality checks did not identify these issues before publication and have since put additional measures in place to safeguard research integrity.

We wish to credit our own Research Integrity and Research Publishing teams and anonymous and named external researchers and research integrity experts for contributing to this investigation.

The corresponding author, as the representative of all authors, has been given the opportunity to register their agreement or disagreement to this retraction. We have kept a record of any response received.

References

[1] L. Zhu, J. Liu, Y. Li et al., "Effect of Stereotactic Body Radiation Therapy Combined with Thermoplastic Fixation on Set-Up Errors in Breast Cancer Patients Undergoing Radiotherapy," *Computational and Mathematical Methods in Medicine*, vol. 2022, Article ID 8370842, 7 pages, 2022.

Retraction

Retracted: Clinical Evaluation of the Medium-Term Efficacy of Laparoscopic Sleeve Gastrectomy against Obstructive Sleep Apnea-Hypopnea Syndrome in Obese Patients

Computational and Mathematical Methods in Medicine

This article has been retracted by Hindawi following an investigation undertaken by the publisher [1]. This investigation has uncovered evidence of one or more of the following indicators of systematic manipulation of the publication process:

(1) Discrepancies in scope

(2) Discrepancies in the description of the research reported

(3) Discrepancies between the availability of data and the research described

(4) Inappropriate citations

(5) Incoherent, meaningless and/or irrelevant content included in the article

(6) Peer-review manipulation

The presence of these indicators undermines our confidence in the integrity of the article's content and we cannot, therefore, vouch for its reliability. Please note that this notice is intended solely to alert readers that the content of this article is unreliable. We have not investigated whether authors were aware of or involved in the systematic manipulation of the publication process.

Wiley and Hindawi regrets that the usual quality checks did not identify these issues before publication and have since put additional measures in place to safeguard research integrity.

We wish to credit our own Research Integrity and Research Publishing teams and anonymous and named external researchers and research integrity experts for contributing to this investigation.

The corresponding author, as the representative of all authors, has been given the opportunity to register their agreement or disagreement to this retraction. We have kept a record of any response received.

References

[1] J. Wu, H. Ge, S. Lei et al., "Clinical Evaluation of the Medium-Term Efficacy of Laparoscopic Sleeve Gastrectomy against Obstructive Sleep Apnea-Hypopnea Syndrome in Obese Patients," *Computational and Mathematical Methods in Medicine*, vol. 2022, Article ID 7682706, 9 pages, 2022.

Retraction

Retracted: The Expression of miR-205 in Prostate Carcinoma and the Relationship with Prognosis in Patients

Computational and Mathematical Methods in Medicine

This article has been retracted by Hindawi following an investigation undertaken by the publisher [1]. This investigation has uncovered evidence of one or more of the following indicators of systematic manipulation of the publication process:

(1) Discrepancies in scope

(2) Discrepancies in the description of the research reported

(3) Discrepancies between the availability of data and the research described

(4) Inappropriate citations

(5) Incoherent, meaningless and/or irrelevant content included in the article

(6) Peer-review manipulation

The presence of these indicators undermines our confidence in the integrity of the article's content and we cannot, therefore, vouch for its reliability. Please note that this notice is intended solely to alert readers that the content of this article is unreliable. We have not investigated whether authors were aware of or involved in the systematic manipulation of the publication process.

Wiley and Hindawi regrets that the usual quality checks did not identify these issues before publication and have since put additional measures in place to safeguard research integrity.

We wish to credit our own Research Integrity and Research Publishing teams and anonymous and named external researchers and research integrity experts for contributing to this investigation.

The corresponding author, as the representative of all authors, has been given the opportunity to register their agreement or disagreement to this retraction. We have kept a record of any response received.

References

[1] Z. Guo, X. Lu, F. Yang et al., "The Expression of miR-205 in Prostate Carcinoma and the Relationship with Prognosis in Patients," *Computational and Mathematical Methods in Medicine*, vol. 2022, Article ID 1784791, 9 pages, 2022.

Review Article

Psychological Impact and Influence of Animation on Viewer's Visual Attention and Cognition: A Systematic Literature Review, Open Challenges, and Future Research Directions

C. K. Praveen [ID][1] and Kathiravan Srinivasan [ID][2]

[1]*VIT School of Design, Vellore Institute of Technology, Vellore 632 014, India*
[2]*School of Computer Science and Engineering, Vellore Institute of Technology, Vellore 632 014, India*

Correspondence should be addressed to Kathiravan Srinivasan; kathiravan.srinivasan@vit.ac.in

Animation is an excellent method to associate with the audience in a fun and innovative manner. In recent span, animation has been employed in various fields to enhance knowledge, marketing, advertisement, and age groups from infants to adults. The present communication expounds the systematic review on the impact created by animation on the viewer's visual attention. For this review, a database such as Google Scholar, ScienceDirect, Taylor & Francis, and IEEE Xplore were pursued for publications on the impact of animation on viewer's visual attention from January 2015 to December 2021. The search results showcased 175 titles with 114 full articles, out of which 35 were related to viewers' visual attention towards animation. These reviewed studies comprised of physical outcome ($n = 9$), psychological outcome ($n = 15$), and cognitive outcome ($n = 11$) from which the attention-related factors, physical effects, and cognitive effects of animation were assessed. The animation has influenced the viewer's visual attention through the integration of the different stimuli and the highly organized presentation. Furthermore, the animation has also aided the viewer in attaining greater conceptual understanding, thereby facilitating their cognitive response. As a result, the animation was found to be helpful in enhancing learning skills, food marketing, and teaching strategy. Furthermore, the drawbacks and future recommendations of the studies were elaborated. In addition, challenges and open issues faced during the studies were discussed. Finally, the priority areas in animation identified for promising future directions to visualize large pool data, provide smart communication, and design 3D modeling structures were highlighted.

1. Introduction

Animation is a comprehensive introduction to animated films, from cartoons to computer animation. In layman's terms, it can be described as a state of being full of life. It brings the life of unanimated objects to moving objects, thereby attracting the modern world with its features [1]. In other words, it is a form of pictorial presentation that has become the most prominent feature of technology-based learning environments. In the modern world, it has become an essential tool for presenting multimedia materials for learners to understand them better [2].

Animation techniques have been developed over a while, either in 2D drawings or 3D objects like clay, stop motion, or motion graphics. It has become a reliable and significant platform for various fields that have impacted viewers' visual attention through its magic. The animation need not be a full-length movie to attract the viewers' visual attention; rather, it can be a clip of a few seconds comprised of just a few frames. The animation videos can be processed as represented in Figure 1.

An idea of integrating traditional animation with the digital 2D animation technique was proposed by Purwaningsih [3]. It provides an alternative pipeline for hand-drawn 2D animation shorts, thereby optimizing the production time.
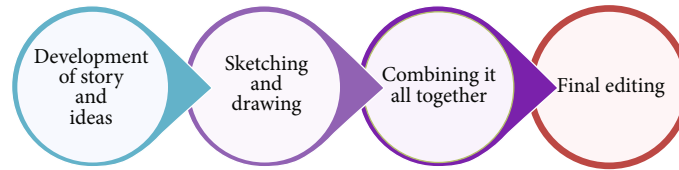
Figure 1: Process of animation.

The impact of animation on viewer's visual attention and attention span was reviewed and reported either with respect to animated characters or character motion. The research on considering both as influencing factors for viewer's visual attention is insignificant. The present survey focuses on how animated characters and their motions create an impact on the viewer's visual attention. Also, it emphasizes the physiological and cognitive impact created by the animation on the viewers.

1.1. Need and Objectives of the Study. Animation is capable of attracting a large audience in every field. As a result, most people are exposed to this interesting field of knowledge. The major objectives of this systematic review are summarized as follows:

(i) To exemplify the impact and influence of animation and animated characters on viewers visual attention and cognition

(ii) To elucidate the various approaches and techniques used in attention based animation studies

(iii) To elicit the standards, regulations, guidelines, and best practices that could assist the animation professionals in understanding the viewers' cognitive behavior

(iv) To exemplify the current trends and open issues of the impact of animation on viewers' attention and cognition

(v) To elucidate the future research directions in animation-based attention studies

1.2. Related Work. Etemad et al. [4] have analyzed the motivating factors for processing motion features and their relative degrees of significance in a general paradigm called the perceptual validity (PV) model. The PV consists of four components: association, contextual dependency, internal consistency, and external consistency with underlying elements (bodily action, bodily expressions, facial action, and facial expression). A case study was conducted with this paradigm based on the contextual dependency and finally discussed with Disney's principles of animation. Zong et al. [5] have discussed the importance of character expression shaping in animated films. The features of facial expression design, such as exaggeration, accuracy, and virtuality, were briefed. Likewise, the expression techniques such as association, personification, exaggeration, and deformation were discussed. Finally, a case analysis of animation expression shaping with respect to every character depicted in the Kung Fu Panda film was carried out in-depth.

Kim et al. [6] studied character-audience similarity's impact on evaluating public service announcements (PSAs). The characters of smokers and persuaders are differentiated to explore their different roles in message effectiveness. Shao [7] has discussed the performance of visual humor in animation from the point of view of image, color, action, and rhythm. The image of an animated character is suggested as a bearer of visual humor. It suggested that the humor can be enhanced/created either in the form of body proportion (genius rat in Ratatouille) or structural reorganization (Pigsy's head in Journey to the West). The animated character's color is considered to render emotional visual humor (Panda Po in Kung Fu Panda). The action of the animated character is proposed to be surreal humor (Tom cat and Jerry mouse in Tom and Jerry). Finally, the rhythm of animated films was proposed to affect the audience's visual and psychological feelings.

Shah et al. [8] studied the application of animation in pharmaceutical advertisements and its impact on consumer perception of the risks and benefits of the drug. Two sets of studies have been carried out for the analysis. Rotoscoping was used to test the effects of animation in this study. Study 1 was carried out to assess whether any shift in perception exists and whether it agrees with a memory effect. In study 2, the findings from study 1 were extended by including consumer implications in order to demonstrate the downstream consequences of the use of animation in pharmaceutical advertisements. Smith and Neff [9] have investigated the influence of animated gestures in controlling personality perception. A sequence of four diverse gestures with twelve motion adjustments was selected as stimuli for the study. The correlation in personality perception was determined. In addition, the potential and possible limits of motion editing approaches were discussed. Two constellations of motion adjustments were selected for the study.

Vijayakrishnan et al. [10] analyzed the importance of animated cartoon characters in product marketing through advertisement. The preference of children over products having cartoon characters was scrutinized. The strategies used in the global market for selling the products using animated characters were also discussed. Geal [11] has explored how animation can manipulate a reflexive intertextual framework related to religious prohibitions on artistic mimesis that might replicate and threaten God's creative act. The limitations of the existing survey are listed briefly in Table 1.

This paper is divided into seven sections and its general layout is depicted in Figure 2. The first section introduces the animation, its impact on the viewer's psychology, and attention span. It also briefs the objective of this study, the limitations of the existing research, and the present study's

TABLE 1: Comparison of existing surveys with the current review (✓: yes; x: no).

S.No	Reference	Title of research	Objective and details	Shortcomings of existing survey	Impact of animation on the viewer's visual attention and cognition	Open challenges	Future directions
1	The present study	Psychological impact and influence of animation on viewer's visual attention and cognition: a systematic literature review, open challenges, and future research directions	The impact of animation on viewers' attention and attention span was reviewed and reported either with respect to animated characters or character motion.	—	✓	✓	✓
2	Yang [12]	Research on the influence of the nature and behavior of animated characters on the audience	The influence of nature and animated characters' behavior on different audiences was analyzed. The personality classification of the animated design was discussed based on modes such as absolute justice, negative energy, and yes man mode. The study suggested that shaping character image with good temperament and behavior in animated films is necessary for guiding the children to establish a correct world outlook, outlook on life, and values.	A systematic survey protocol was not followed.	x	x	x
3	Van Rooij [13]	Carefully constructed yet curiously real: how major American animation studios generate empathy through a shared style of character design	The computer-animated characters portrayed by major American animation studios Pixar, Disney, and DreamWorks were analyzed for an overwhelming emotional response in the audience. In addition, a case study on the animation movies by these studios was carried out. The study proposed that audiences can feel equal levels of empathy for computer-animated characters and real human actors. It also suggested that the animated characters created by these studios using digital sets, virtual	A systematic survey protocol was not followed.	Talks about the impact on viewer's attention alone	x	x

TABLE 1: Continued.

S.No	Reference	Title of research	Objective and details	Shortcomings of existing survey	Impact of animation on the viewer's visual attention and cognition	Open challenges	Future directions
			cameras, and perceptual cues seem to be accepted by the audience as real and authentic, and it evoked empathy.				
4	Sen & Rong [14]	The influence of Japanese anime on the values of adolescent	The influence of Japanese anime on Chinese youth was elaborated. The positive and negative effects on forming correct values for adolescents were determined.	A systematic survey protocol was not followed.	x	x	x
5	Ghazali & Ghani [15]	The important of great storytelling in Malaysia animation industries	The importance of great storytelling to grab the audience's attention was exposed. Furthermore, the importance of animation story structure, such as appeal, believability, story, collaboration, and research, was elaborated.	A systematic survey protocol was not followed.	x	x	x
6	Liu & Elms [16]	Animating student engagement: the impacts of cartoon instructional videos on learning experience	The use of a series of animated videos for teaching advanced accounting at an Australian university was explored. The benefits of various demographic groups of students from these animation videos were also explored.	The design, development, and production of animated videos require more resources, and this survey did not provide a direct cost analysis.	✓	✓	✓
7	Jintapitak [16]	Use of animation characters to motivate students in a higher education class	The influence of animation on the educational field, especially for the higher education class, was explored.	A systematic survey protocol was not followed.	Talks about the impact on viewer's attention alone	x	x
8	Flynn [17]	Discovering audience motivations behind movie theater attendance	The factors that currently attract the audience to movie theaters were compared with the factors which attracted in the past. The top box office films within the past six years were selected for the study. The films were categorized into preexisting fandom,	Only a tiny portion of the top box office of all time was chosen for the study.	x	x	x

Table 1: Continued.

S.No	Reference	Title of research	Objective and details	Shortcomings of existing survey	Impact of animation on the viewer's visual attention and cognition	Open challenges	Future directions
			remake/sequel, superhero movies, and cinematic first.				
9	Zhou [18]	The narrative construction of Chinese animation from the perspective of adolescent audience	The direction of sustainable development of Chinese animation with adolescents as an object was analyzed. The characteristics of adolescence under the historical background were analyzed with respect to the phenomenon of idol worship, the dependence on networks, and the lack of knowledge of traditional culture.	A systematic survey protocol was not followed.	Talks about the impact on viewer's attention alone	x	x
10	Agarwal & Adhikari [19]	Survey of trends in 3D animation	The techniques which are in trend that are used to convert a 3D design into a 3D object on screen were analyzed. Furthermore, the techniques used to enhance state-in-art, such as texture space (continuity mapping), object space (cages), and screen space (I-Render), were elaborated.	A systematic survey protocol was not followed.	x	x	x
11	Goel & Upadhyay [20]	Effectiveness of the use of animation in advertising: a literature review	The basic concepts related to animation and its use in advertising were elaborated. Then, the animation process was discussed, including developing ideas and stories, sketching and drawing, combining it, and final editing. Also, animation styles like Walt Disney, Warner Brothers, and Japanese styles were briefed. Finally, various factors influencing the effective use of animation like attention, memory, recall and recognition, click-through rate, and attitude were discussed.	A systematic survey protocol was not followed.	Talks about the impact on viewer's attention alone	x	x

TABLE 1: Continued.

S.No	Reference	Title of research	Objective and details	Shortcomings of existing survey	Impact of animation on the viewer's visual attention and cognition	Open challenges	Future directions
12	Zaky [21]	Once Upon a Time, We Were All Little Kids Too!!! Influence of Cartoon on Children's Behavior; Is it Just a World of Fantasy or a Nightmare???	The influence of cartoons on toddlers and children's behavior was investigated. The cartoon's beneficial effects (independent learning and proper communication) and possible harmful effects (behavior, social, and emotional development) were discussed.	A systematic survey protocol was not followed.	x	x	x
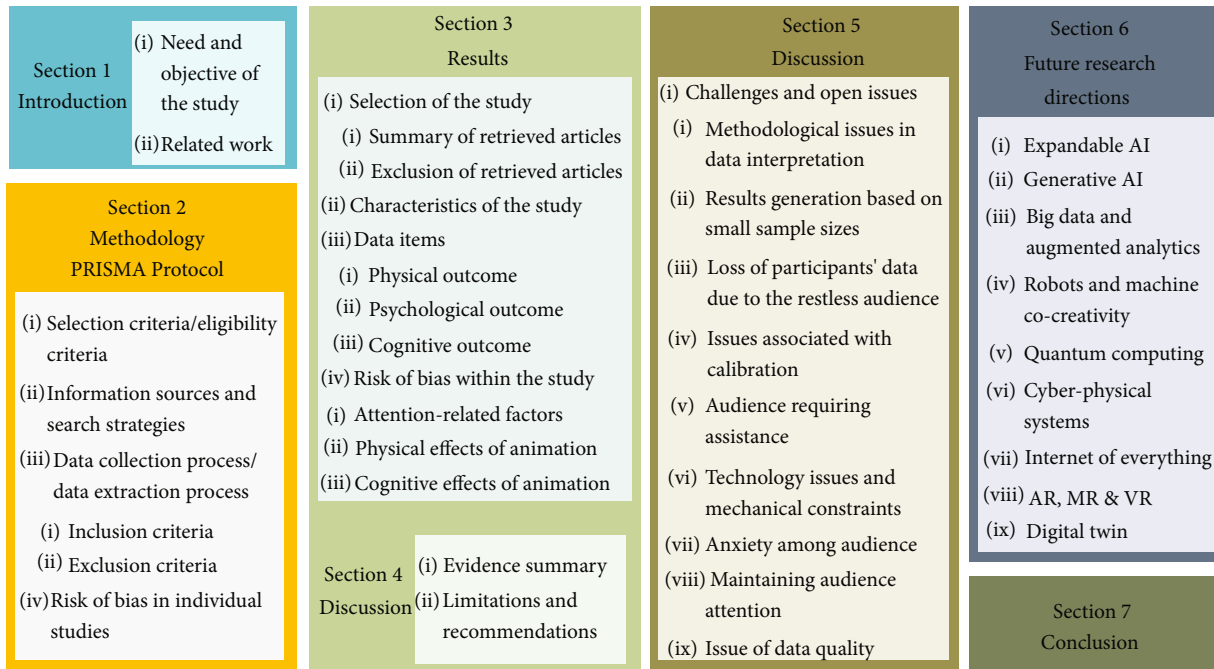
FIGURE 2: Structure of this review.

contribution. The second section explains the application of the PRISMA protocol to evaluate the reviewing of other types of research. The evaluation is based on the survey's selection criteria, its information sources and search strategies, data collection process, and risk of bias in individual studies. The third section elaborates on the selection of the present study, its characteristics, selected data items, and the risk of bias within the studies. It also assesses animation's attention-related factors and physical and cognitive effects. The fourth section briefly presents the summary along with the limitations and recommendations. The fifth section elaborates on the challenges and open issues the researchers face during the study. The sixth section highlights the future research directions in the field of animation. Finally, the last section summarizes all the facts and concludes the reviewed results.

2. Methodology

2.1. PRISMA Protocol. The present study is reviewed based on the PRISMA (Preferred Reporting Items for Systematic Reviews and Meta-Analyses) Protocol [22, 23]. It is a set of

recommendations designed for reporting systematic reviews. These guidelines aid authors in improving the reporting of systematic reviews and meta-analyses and ensuring the accuracy and transparency of the studies reported [24]. The present study's reporting quality can be optimized by completing the review report based on the PRISMA–P statement and checklist. Moreover, it also improves the efficiency of the peer review process and enables the readers to get a clear view of the author's work.

The steps followed in the PRISMA protocol are represented in Figure 3. It is provided briefly as follows: (a) Identification, the records are identified through database searching and additional sources. (b) Removal of duplicates, the records that appear more than once should be removed to avoid reviewing the duplicate records. The entire list of records is exported to a citation manager to remove the duplicate records. The remaining records are entered in the second top box. (c) Screening, the number of screened articles are entered in the following box. Furthermore, this value will be the same as that of the number entered in the duplicate removed box. Further, the articles are screened based on their titles and abstracts. The number of articles excluded in this screening process is recorded in the relevant box. (d) Eligibility, the number of excluded articles after the screening process is subtracted from the total number of records screened. Full-text articles are assessed for eligibility. All these full-text articles are eligible for the final reviewing process. The number of excluded articles at this point is recorded in the appropriate box. (e) Inclusion, the number of excluded articles is subtracted from the total number of articles reviewed for eligibility. Furthermore, this number is entered in the qualitative analysis box. The number of studies list is entered in the quantitative synthesis box to perform the meta-analysis.

2.1.1. Selection Criteria/Eligibility Criteria. The criteria selected were defined before undergoing screening of any articles. The selection criteria are listed in Table 2.

The criteria selection helps to limit the broad topic to direct relevance for the research questions. The language is selected as English as it is the primary publication language for scientific articles. The year of publication is limited to providing a review based on recently published research works. Finally, peer-reviewed articles are considered to provide good quality of work and confirmed results. Also, published thesis work is considered, providing more detail about the research work introduced in peer-reviewed articles by the same or similar authors. Animation-based attention-creating articles were selected for the reviewing process.

2.1.2. Information Sources and Search Strategies. The search databases selected for article retrieval should have good coverage of the body of the relevant work. For this purpose, the two major exiting multidisciplinary databases, Web of Science and Scopus, were selected. Also, scientific databases like Google Scholar and ResearchGate are included as they cover good reporting of animation-related attention-creating articles. In recent times, these research articles can also be retrieved from general databases. However, Google Scholar

gains superiority due to its positive correlation with the citation counts from various sources. Many of the works relevant to animation-based attention-creating articles can be retrieved from this database. The publishers such as IEEE, ScienceDirect, Springer, and SAGE also provide direct access to their publications, and their databases were also assessed for their yield of additional relevant results. All the relevant papers can be expected to be available online as the year of publication selection is from 2015 and above. So the analogue search was not conducted separately. Therefore, the electronic database searches were executed from January 2015 to the year 2021 until the preparation of the review. The reference list of all the relevant articles was analyzed for their significance with the research objectives and screened accordingly. The same selection criteria were applied here.

The search strategies need to be fine-tuned to get a better search of articles. Meanwhile, it should expose all relevant research works under a manageable level with no increase in the overall workload of the reviewing process. For the given research objective, the attention-creating articles published in the field of animation were chosen. The research terms for the search were used in either form of individual keywords or a combination of keywords. And specifically, the research terms used were 'animation' OR 'impact of animation' 'Animation' AND 'psychology' OR 'animation' AND 'audience' OR 'animation' AND 'cognitive psychology' OR 'animation' AND 'audience visual attention'.

2.1.3. Data Collection Process/Data Extraction Process. The title of the articles retrieved from the databases is evaluated for their significant relevance to the research objectives. Furthermore, their respective abstracts are read thoroughly. Based on this, the most relevant articles were segregated and organized in a Microsoft Excel sheet.

(1) Inclusion Criteria. Inclusion criteria for this study include the year of publication, country of origin, methodological base, experimental context, sample characteristics, study duration of existing articles, outcome measures, and exposure to animation duration.

(2) Exclusion Criteria. The criteria excluded for this study comprise lack of access to the full article, unsuitable research articles, letters to the editor, and retraction articles review articles.

The study's key findings mainly focused on how effective the animation in the existing articles. And no attempts are made to contact the authors for missing details in their respective articles.

2.1.4. Risk of Bias in Individual Studies. All the articles were independently evaluated based on the inclusion and exclusion criteria to assess the risk of bias in individual studies. The information extracted from each study is evaluated using the quality assessment tool. For the effective quality assessment, the checklist is made based on the following criteria: yes, no, not applicable (NA), and not reported (NR).
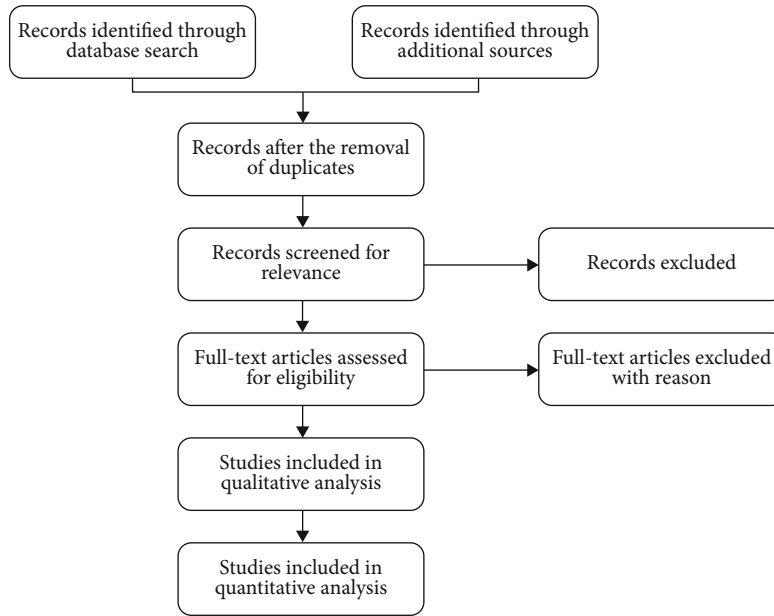
FIGURE 3: Flow diagram of PRISMA protocol.

TABLE 2: Selection criteria.

S.No	Criteria	Selected criteria
1	Topic	Impact of animation on viewer's attention
2	Language	English
3	Year of Publication	2015 or later
4	Journals and conferences	Any
5	Scientific	Academic articles such as a published thesis or peer-reviewed articles

The checklist of quality assessment tools includes the following criteria mentioned in Table 3.

3. Results

3.1. Selection of the Study

3.1.1. Summary of Retrieved Articles. The summary of the search databases visited and the number of articles obtained from the respective sources is presented in Table 4. Further, this table shows the percentage of articles retrieved from each academic database and reveals that the highest number of articles were retrieved from Google Scholar ($n = 199$). It comprises research articles, conference papers, and students' dissertations. Other databases like Springer, Science Direct, and Taylor and Francis account for 6.76%, 6.41%, and 6.05% of the total number of articles. The rest of the articles were retrieved from IEEE Xplore (4.27%), ResearchGate (3.20%), and Wiley Online Library (2.49%).

3.1.2. Exclusion of Retrieved Articles. The number of articles retrieved from the search database was reduced with the following eliminated procedure based on PRISMA protocol.

(i) Elimination of the articles based on language ($n = 6$), irrelevant titles ($n = 75$), and reduction of duplica-

tion ($n = 25$) from various search databases, leading to reduction from 281 to 175

(ii) Elimination of articles after the examination of abstracts, leading to the reduction of articles from 175 to 114

(iii) Elimination of articles based on thoroughly reading the full article led to a reduction from 114 to 35. The articles were eliminated for the following reasons:

(a) Report on animation impact, 37

(b) Not focused on animation, 18

(c) Report on animation application, 14

(d) Case study, review, and others, 5

(e) Not enough information, 5

The procedure flow for selecting articles for the study is depicted in Figure 4, which shows the elimination procedure.

3.2. Characteristics of the Study. Based on the selection process, 35 articles were shortlisted for the systematic review. Each article was reviewed, and the information gathered from it was tabulated. The following information was

TABLE 3: Design quality analysis.

S.No	Criteria	S.No	Criteria
1.	Randomization	2.	Missing data
3.	Control	4.	Power analysis
5.	Isolation	6.	Validity measures
7.	Pre- and post-test	8.	Baseline method comparison
9.	Retention	10.	Follow up

extracted from the articles: description of the study, sample and design applied in the study, type and duration of animation used in the study, and outcome and findings of the study and case-control applied within the study. The study's characteristics, as itemized above, are summarized in Table 5.

3.3. Data Items. The study participants' ages ranged from 30 months to 30 years, and most of the studies included both sex samples, with the exception of three studies with female samples alone and gender not mentioned in eight studies. In addition, most of the studies included 3D animation ($n = 10$) followed by 2D animation ($n = 6$) and flash ($n = 4$), and the remaining studies included motion graphics, VR, and AR. Further, the outcomes reviewed from all these studies, namely, physical outcome ($n = 9$), psychological outcome ($n = 15$), and cognitive outcome ($n = 11$), are presented in Table 5.

3.3.1. Physical Outcome. The importance and necessity of physical exercise was easily delivered to the primary grade students. The results showed a significant difference in self-efficacy, learning, benefits, importance, personal best, and fun between the control and experimental groups ($p \leq 0.05$) [31]. The hand manipulative tasks was made better with the help of animation. The results showed that the animation groups ranked their difficulty levels (cognitive load) significantly lower than the static groups. Moreover, viewing hand or not made no difference for the animation group [36].

The effects of visual cueing depend on the subject matter and the learner's learning strategies [40]. The pretest scores revealed insignificant scores between the test and control groups. However, there is a significant difference between the test and control group in the sequential memory test [55]. The microintervention study revealed the positive impact of animation on creating awareness on body image among the adolescents. It helped them to understand the importance of telling a bully to stop. The study results showed a significant difference in body satisfaction between the groups. However, it is insignificant to media literacy and self-efficacy [29]. There is a significant difference in the learning outcomes between each PK (prior knowledge) group for reading comprehension. The animation annotation was easily noticed by the low PK group, whereas the text zone was noticed by the high PK group [38]. The results obtained from SPQ and BMI revealed the following results: Pororo - So-Yang type boy, Petty - So-Yang type girl, Loopy - So-Eum type girl, Pobby & Harry -most obvious contrast

[50]. There is a significant difference between lip-syncing and gaze to target for perceived speech intelligibility [43].

3.3.2. Psychological Outcome. Food marketing industries have efficiently utilizing animation as a tool to attract the children, and they were assessing their attention towards healthy/unhealthy food items. Children are attracted to the food and beverages product with or without animated characters. Children were significantly chosen the less healthy product with or without character. Children significantly preferred more or less healthier products irrespective of character [51]. Children's pupil diameter increased on watching the candy condition. However, no significant difference was observed in the children's visual attention or emotional arousal towards candy or food conditions. There is a significant difference in children's emotional arousal to unhealthy products due to the parent's restriction of candy at home [32].

The children recalled the story and more content words significantly from animated conditions than a static conditions. Children's visual attention was significant with animated conditions compared to static conditions [57]. The children were able to recognize the facial identity through dynamic facial animation. However, they failed to learn the facial expression. There is no significant difference observed between the pre- and post-familiarization tests [47].

The animation has delivered a better opportunity to have self-awareness and knowledge on the health issues without any hesitation. The implementation of computer-animated agent provides assistance to deliver personally relevant information on breast cancer. It helps to reduce anxiety, support psychological needs, and boost confidence. The results showed a significant difference in the proportion of participants with unanswered questions for the post-intervention period [30]. The health awareness regarding the conditions of glaucoma was perceived by the patients through animation video. There is a significant difference in the patients' knowledge scores between pre- and post-intervention ($p \leq 0.001$). Rural residence, low income, and unemployment were identified as influencing factors for acquiring glaucoma knowledge [45].

There is a positive correlation between the learning experience between the VR simulation and traditional practice [52]. There is no significant difference between the real and hybrid CG characters ($p = 1.00$). A less significant difference existed between real and CG characters ($p < .001$) as well as between CG and hybrid characters ($p < .001$). The CGI could feature the actor those who are alive or dead and are capable of enhancing the parasocial interaction and relatability [25]. The animated character influenced the viewer's attention. There is a significant difference in eeriness between the Pixar character and the Toon character ($p < 0.05$). There is a significant difference in eeriness between the photorealistic human character and the Toon character ($p < 0.05$) [48].

The prior knowledge about the techniques behind the making of stop motion films may influence the impact of viewer's attention towards the technical aspects rather than focusing on the story. However, the viewer's attention can

TABLE 4: Article sources and number of articles.

S.No	Search databases	URL	No. of articles	Percentage (%)
1	Google Scholar	https://www.scholar.google.com/	199	70.82
2	Springer	https://www.springer.com/	19	6.76
3	Science Direct	https://sciencedirect.com/	18	6.41
4	Taylor & Francis	https://taylorandfrancis.com/	17	6.05
5	IEEE Xplore	https://www.ieeexplore.ieee.org/	12	4.27
6	ResearchGate	https://www.researchgate.net/	9	3.20
7	Wiley Online Library	https://onlinelibrary.wiley.com/	7	2.49
		Total	*281*	*100.00*
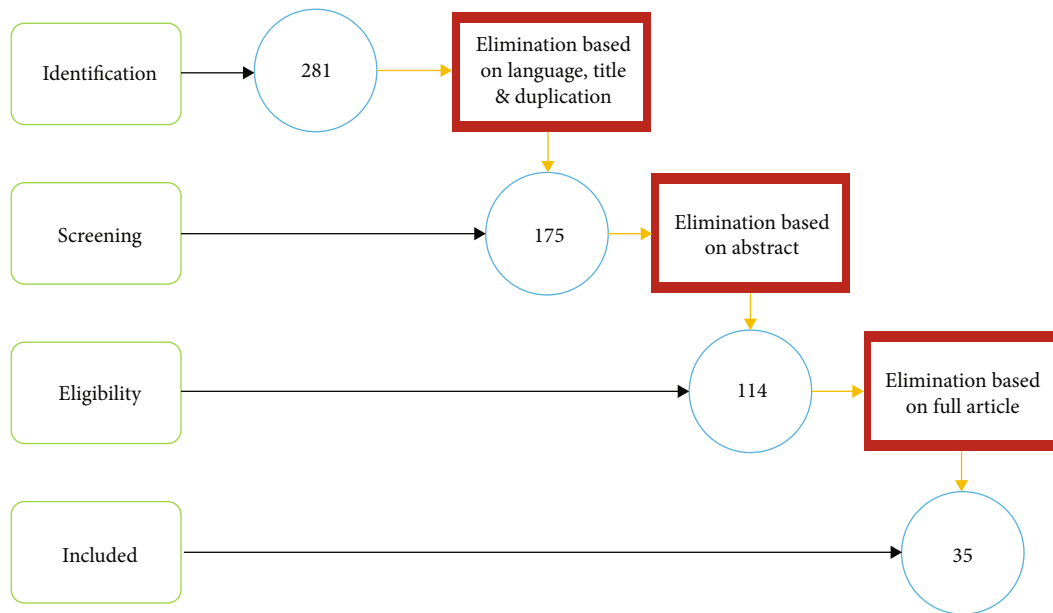
FIGURE 4: Elimination process of articles based on PRISMA protocol.

be engrossed in the film, and it may develop a deeper connection with the story [26]. The level of exaggeration in animated cat is insignificant to the audience's perception of the appeal of the realistic feline character. Moreover, the significance of believability is higher for high exaggeration clips than for low exaggeration clips [37]. The frequency of exposure to animated television cartoons is higher among females, and it is greatly influenced based on their level of education. The perception of such cartoons varies with the level of education [56]. The viewer's pleasantness feeling toward animated character design aesthetics is insignificant to their gender and age group [44].

The animated virtual ads attracted the participants than the static ads. The virtual ads presented in the nonbattle scene attracted the participants than those ads in the battle scene. The interaction effect between ad animation and in-game context on fixation count is insignificant [41]. The animation intensity and animation color on the sponsorship signage showed negative effect on the viewer's attention. The arousal of the viewer's confusion due to increased levels of animation intensity was explored. And the results showed an insignificant effect of animation intensity on viewer con-

fusion [46]. Also, there is no significant difference in color [59].

3.3.3. Cognitive Outcome. The studies reported that animation played an essential role in the cognitive development of children ($n = 6$). The children who read the AR storybook were more confident in retelling and recalling the story when compared to those who read its printed version [27]. The mother's video prompted larger pupil dilations and a more smiling and cheerful eye blinking rate among the infants. The highest value cartoons prompted long looking time, reduced blinking, but no increased smiling or pupil dilation [34, 40]. Animated films positively affect a child's involvement in symbolic mediation and the level of arbitrary behavior [54]. Also, it was observed that the executive functions of the preschoolers were disrupted after watching the animated fantastical events [28]. A significant effect of animated features in ebooks (motion and sound) was observed on children's vocabulary acquisition, story retelling, and visual attention [35]. There is no significant difference in birth weight, age, parental educational level, or preintervention performance levels between the groups. The trained

TABLE 5: Summary of animation studies.

Reference	Study description	Sample and design	Types of animation	Outcomes	Duration of animation	Findings	Case control
[25]	The audience's interaction with digital characters and the emotional impact of such films were examined. Undergraduate students of film, media, communication, and psychology courses from the Southwestern United States have participated in the study.	$n = 144$ (65 male and 79 female) Mean age: 20.6 years Design not reported	Computer-generated imagery (CGI)	Psychological outcome	60-100 min	CGI is very effective in creating a scene with characters featuring an actor either alive or passed away. In addition, it enhanced their parasocial interaction and relatability with such characters.	Real condition ($n = 49$): real human characters played by real actors CGI condition ($n = 44$): all-CG characters Hybrid condition ($n = 51$): a hybrid of characters with real humans and CG
[26]	A qualitative analysis was performed to learn the visual impacts of stop motion animated films towards the audience.	$n = 9$ (gender not mentioned) Age: 21-23 years Qualitative analysis	Stop motion	Psychological outcome	NR	The participant unknowingly noticed the techniques behind the making of stop motion film. Some of them even observed the sense of space in them.	NA
[27]	The comprehension reading of children was investigated by making them read an augmented reality (AR) storybook and was compared with those reading its printed version. The participants were selected from five children's libraries in Tehran.	$n = 34$ (20 girls and 14 boys) Age: 7-9 years Quasi-experimental methodology	2D animation AR	Cognitive outcome	NR	The AR storybooks with more interactive 3D images with added value can be used as a tool to support children's literacy learning.	Experimental group ($n = 18$; 11 girls and 7 boys): read AR storybooks Control group ($n = 16$; 9 girls and 7 boys): read the printed version of the same book
[28]	The influence of watching an animated show with fantastical events on the Chinese preschooler's executive function (EF) was investigated. The preschoolers from urban public schools in central China participated in the study.	Experiment 1 $n = 90$ (41 girls and 49 boys) Mean age: 60.37 months Latin square design Experiment 2 $n = 20$ (9 girls and 11 boys) Mean age: 63.94 months Eye-tracking technology Experiment 3 $n = 20$ (9 girls and 11 boys) Mean age: 63.94	3D animation	Cognitive outcome	Experiments 1 and 2 19 min 25 s (low fantasy) 18 min 37 s (high fantasy) Experiment 3 6 min 50 s (low fantasy and high fantasy)	The animated videos with high fantastical events have a negative impact on the preschooler's executive function.	Experiment 1 (30 participants each): high fantasy, low fantasy, no viewing Experiment 2 (10 participants each): high fantasy and low fantasy No control group Experiment 3 (10 participants each): high fantasy and low fantasy No control group

TABLE 5: Continued.

Reference	Study description	Sample and design	Types of animation	Outcomes	Duration of animation	Findings	Case control
		months Strengths and difficulties questionnaire					
[29]	The study investigated the effectiveness of employing animated films as a measure of microintervention in a possible way to improve children's body image. Participants were selected from eastern, central, and western regions of six major US cities through a commercial research agency.	$n = 1,329$ (41% girls and 59% boys) Age: 7-14 years Randomized controlled trial	3D	Physical outcome	60 s	Microintervention effects played an essential role in creating awareness in adolescents who concern more about their body image.	Appearance teasing and bulling animation showing positive appearance self-talk ($n = 442$), media and celebrities animation showing unrealistic social media images ($n = 441$), and active control showing no body image ($n = 446$)
[30]	An interactive computer-animated agent (prototype) was developed to provide information on breast density to the women. The effectiveness of the prototype was assessed for its approval. Mammography-eligible English-speaking women were selected for the study.	$n = 44$ (all female) Age: 40-74 Cross-sectional study	Computer animation	Psychological outcome	3 min	The computer-animated agent delivers satisfied informational needs of women regarding breast density. It can be more beneficial if it is designed to deliver the psychological needs of the women undergoing the diagnosis.	NA
[31]	The changes in the student attitudes toward physical activity were evaluated by implementing Brain Breaks®videos for four months. The participants are primary grade students (3rd, 4th, and 5th) from 16 schools like Croatia, Lithuania, Macedonia, Poland, Romania, Serbia,	$n = 3,036$ (1,496 males and 1,540 females) Quasi-experimental design	NR	Physical outcome	3-5 min 2 times per day 5 days each week	The student's attitude towards physical health and self-efficacy in doing exercises improved.	Experimental group (1914 participants) participated in group activity exercises and Brain Breaks®videos, and the control group (1122 participants) standard teaching materials

TABLE 5: Continued.

Reference	Study description	Sample and design	Types of animation	Outcomes	Duration of animation	Findings	Case control
	South Africa, and Turkey.						
[32]	The effect of children's reactions towards unhealthy versus healthy products was investigated. The children's visual attention, such as dwell time and pupil dilation, was measured. The children from primary school in Austria participated in the study.	$n = 68$ (34 boys and 34 girls) Age: 6-11 years Fruit condition $n = 34$ Candy condition $n = 34$ Eye-tracking technology	2D animation cartoon style	Psychological outcome	6 min	The attractive and cartoonistic media presentation did not automatically influence the children's visual attention or emotional arousal toward unhealthy foods. However, it may prompt them when there is a restriction on taking healthy foods imposed by the parents at home.	NA
[33]	The adoption of 3D animation as a teaching tool for illustrating surgical skills in medical education was investigated. The 3D animation was hosted on Moodle platform. Third- and fifth-year medical students from the University of Botswana have participated in the study.	$n = 90$ (gender not mentioned) Age: not mentioned Randomized comparative study	Motion graphics in the form of 3D animation	Cognitive outcome	8 mins	The students preferred the adoption of 3D animation and the traditional teaching method.	Group A (traditional teaching group) is the control group, and group B (3D animation teaching group) is the experimental group
[34]	The reward learning mechanism in an infant's visual behavior was investigated. Participants are the infants recruited from the community via ads and birth records.	$n = 51$ (23 females and 28 males) Mean age: 7 months Eye-tracking technology	Animation using Adobe flash	Cognitive outcome	8 s $*$ six videos 2 times per session	Reward learning of the infant is significantly observed in the infant's mother. It played an essential role in enhancing the early cognitive development of infants.	NA
[35]	The influence of animated storybooks (motion and sound) on preschoolers' visual attention and Mandarin language learning was investigated.	$n = 102$ (49 boys and 53 girls) Age: 4-5 years Eye-tracking technology	ebook motion animation	Cognitive outcome	245 sec	The animated ebooks featuring sound and motion facilitate the children's attention, enhancing story comprehension and word learning.	Animation ebook reading group, static ebook with sound, static ebook with no motion and no sound and no reading exposure control group

TABLE 5: Continued.

Reference	Study description	Sample and design	Types of animation	Outcomes	Duration of animation	Findings	Case control
	Children from 21 kindergartens of PAP community foundation, Singapore, were selected for the study.						
[36]	The observation of hand action in visualizing the animation and static graphics was investigated. Also, the respective influence on learning the hand manipulative tasks was explored. The psychology students from Erasmus University Rotterdam have participated in the study.	$n = 100$ (20 males and 80 females) Mean age: 20.26 years	Animations were recorded in video clips	Physical outcome	NR	In learning hand manipulative tasks (i.e., knot tying), the animation delivers better knowledge than static graphics. The motor task performance was not hindered by hand appearance.	Animation with hands ($n = 24$), animation without hands ($n = 25$), statics with hands ($n = 25$), and statics without hands ($n = 26$)
[37]	The possible application of traditional animation principles to photorealistic animated animal characters was analyzed. The influence of varying degrees of exaggeration on perceived believability was investigated.	$n = 82$ (gender not mentioned) Age: 18 years Randomized block design	3D	Psychological outcome	18 sec	The animated characters should be presented realistically to achieve a higher level of the audience's perception of believability and appeal	No exaggeration, low exaggeration, high exaggeration
[38]	The influence of learning Japanese using an interactive manga-based ebook on the university students' visual attention and learning performance was investigated. The university students from the applied foreign languages department at the university in Taiwan have	$n = 60$ (gender not mentioned) Age: NR Eye-tracking technology	2D graphics (annotation animation)	Physical outcome	NR	Overall, students spent more time reading text and annotation than graphic information.	High prior knowledge (PK) group ($n = 30$) and low prior knowledge group ($n = 30$)

TABLE 5: Continued.

Reference	Study description	Sample and design	Types of animation	Outcomes	Duration of animation	Findings	Case control
	participated in the study.						
[39]	The effectiveness of using animation and static pictures to support the learning of genetics was assessed and compared. Seventh-grade students from a public junior high school participated in the study.	$n = 181$ (gender not mentioned) Age: NR	2D animation	Cognitive outcome	40 min	The animation approach is an easy and effective way to help students learn invisible infinitesimal phenomena as it lowers the perceived extraneous cognitive load.	Static pictures group ($n = 89$) and animation group ($n = 92$)
[40]	The influence of attention cueing on the learner's prior knowledge of cognitive load was investigated. Participants were students from a technology university in southeastern China.	$n = 55$ (7 male and 48 female) Mean age: 19.85 years Quasi-experimental design	Adobe flash-based animation	Physical outcome	255 sec	The interactive features of the animation help to explore knowledge	Animation only group ($n = 27$) Animation plus cueing group ($n = 28$)
[41]	The influence of characteristics of eSports virtual ads on viewers' attention was examined. It also determined how the dynamic nature of gameplay can influence those, as mentioned earlier.	$n = 114$ (40 female and 74 male) Mean age: 22.83 Eye-tracking technology	Ad animation	Psychological outcome	5 min	The advertising practitioners should take care of virtual ad designs for eSports and their placing timing.	Static condition ($n = 58$) and animated conditions ($n = 56$).
[42]	Infants' responsiveness to social attention was observed by providing training on essential attentional functions. The participants were recruited from a population-based database from the Tampere area in Finland.	$n = 70$ (37 females and 33 males) Age: 9 months Eye-tracking technology	NR	Cognitive outcome	NR	Basic training on visual attention plays an essential role in the early development of socio-cognitive skills in infants. It helps to increase the infant's responsiveness to social-communicative cues.	Training group ($n = 35$; 19 females, 16 males): four gaze-interactive games in terms of attention switching, visual search, sustained attention, and interference control and control group ($n = 35$; 18 females, 17 males), watching noncontingent, child-appropriate animations, and television clips
[43]	The virtual audiovisual		3D animation	Physical outcome	NR	The realistic animation	NA

TABLE 5: Continued.

Reference	Study description	Sample and design	Types of animation	Outcomes	Duration of animation	Findings	Case control
	environment with animated characters was employed to study hearing aid benefits. The influence of visual cues on the head and eye movements during listening talks in such an environment was investigated. Participants were young normal hearing students from the Oldenburg University.	n = 14 (7 males and 7 females) Age: 19-35 years				condition was more comfortable investigating the effects of hearing aid signal processing on motion behavior. Also, it helps to identify the limitations of the technology developed.	
[44]	The experiences of pleasantness in viewer's emotions which stimulates the perception of pleasure portrayed in Malaysian animated cartoon characters were investigated.	n = 143 (78 male and 65 female) Age: 17-27 years Questionnaire's survey	3D animation	Psychological outcome	NR	During the early stage of animation production, the relationship between a character's theme and the character's appearance plays a significant role	NA
[45]	An attempt was made to increase the knowledge of glaucoma patients through animation. The factors influencing the knowledge level of such patients were determined. The patients who were diagnosed with glaucoma for six months at the King Khaled Eye Specialist Hospital were included in the study.	n = 196 (108 males and 88 females) Mean age: 55.7 ± 15.5 years Self-identification	Motion graphics	Psychological outcome	3 min	The animated video was influential in spreading the knowledge of glaucoma among its patients. The video should contain more information regarding the importance of long-term follow-ups with an ophthalmologist.	NA
[46]	The influence of sponsorship signage's animation intensity on the sports viewer's attention was investigated. The arousal of the viewer's confusion due to increased levels of animation	n = 52 (40.4% female and 59.6% male) Mean age: 24.98 years Eye-tracking technology	Flash	Psychological outcome	3 min 19 sec	The visual animation has drawn sports viewers' attention to sponsorship signage even in an attractive sports environment. The animation intensity played a significant role in	NA

TABLE 5: Continued.

Reference	Study description	Sample and design	Types of animation	Outcomes	Duration of animation	Findings	Case control
	intensity was explored. Participants were undergraduate and graduate sports students from the German Sport University Cologne.					attracting the sports viewer's attention.	
[47]	The infants' recognizing ability to facial expression changes were investigated. The participants were infants recruited through newspaper ads.	$n = 25$ (15 boys and 10 girls) Mean age: 226 days Principles of the Helsinki Declaration	NR	Physical outcome	1,800 ms	The infants' ability to recognize expression was disturbed by dynamic change of facial identity using dynamic morphing animation.	Pre- and post-familiarization tests were conducted under two conditions: expression test condition and ID test condition
[48]	The audience's response to the uncanny valley, while observing different types of 3D animated characters were assessed. Also, the audience's response towards the animation films rendered in different styles was evaluated.	$n = 50$ (gender not mentioned) Age: 18-23 years Volunteer sampling	3D Computer-generated and motion capture	Psychological outcome	3 min	The participants could not feel the warmth of the real human character.	NA
[49]	The significant effect on learning idioms through English animated movies was investigated. Iranian intermediate EFL learners were selected randomly from the English language institutes in Sari for the study.	$n = 40$ (all female) Age: 14-18 years Oxford Placement Test	Animated movies	Cognitive outcome	NR	Animated movies can motivate the learners to understand the idioms in a much better way.	Experimental group ($n = 20$) provided idioms using English animated movies, and the control group ($n = 20$) exposed to those during the instruction session
[50]	The usefulness of Sasang typology in providing a theoretical backbone to the animation industry was investigated. The biopsychological features of seven animated	$n = 41$ (17 males and 24 females) Mean age: 30.64 ± 9.08 (male) and 28.62 ± 4.08 (female) Body mass index (BMI) Sasang Personality	3D animation cartoon	Physical outcome	15 min	The SPQ and BMI help analyze the biopsychosocial features as well as patients. It remained a valuable tool to educate health-care professionals and the general public	NA

TABLE 5: Continued.

Reference	Study description	Sample and design	Types of animation	Outcomes	Duration of animation	Findings	Case control
	characters in Pororo the Little Penguin were analyzed. The analysis was validated with the standardized measures of Sasang typology. The graduate school students from Pusan National University were selected for the analysis.	Questionnaire (SPQ)				regarding Korean medicine.	
[51]	The impact of licensed cartoon characters on children's attention to healthy food/ beverages packages and their preferences was investigated. Participants were children aged 6-9 years selected via online and in-person techniques in 2012 and 2013.	$n = 149$ (gender not mentioned) Age: 6-9 years Eye-tracking technology	2D	Psychological outcome	60 trials	Healthy food and beverage packages with featured cartoon characters may enhance the children's attention and product choice.	NA
[52]	The pharmacology interleaved learning virtual reality (PILL-VR) simulation was developed to learn medication administration procedures. Its effectiveness was evaluated by employing it in nursing education.	$n = 129$ (97 female and 32 male) Mean age: 23 ± 3 years Quasi-experimental design	3D virtual reality	Psychological outcome	45 min	The VR simulations provide an affordable and flexible environment to practice medical administration. The learning practice may be made more accessible by improving students' sense of control.	Experimental group ($n = 82$; 67 female and 21 male) learned via PILL-VR environment for 3 h Comparison group ($n = 47$; 36 female and 11 male) learned via normative lecture with PowerPoint presentation for 3-4 h
[53]	The 12th grade female students from Ad Dakhiliyah Governorate in the Sultanate of Oman participated in the study. The corresponding students' spatial ability and scientific reasoning skills were observed.	$n = 60$ (all female) Mean age: NR Quasi-experimental design	2D and 3D	Cognitive outcome	8 weeks	Visualizing the chemistry concepts in 2D and 3D enhanced the spatial ability and reasoning skills of the participants	Experimental group ($n = 32$) and control group ($n = 28$).

Table 5: Continued.

Reference	Study description	Sample and design	Types of animation	Outcomes	Duration of animation	Findings	Case control
[54]	The influence of animated film culture on the child's involvement in extended meditation in animated films is derived. Participants were preschoolers from Moscow kindergarten.	$n = 50$ (gender not mentioned) Age: 6-7 years	Animated films	Cognitive outcome	NR	Animated films enhance the child's capacity for symbolic mediation and their level of arbitrary behavior.	NA
[55]	The five-year-old children's visual perception development using 3D animated movies and interactive applications was investigated. The children from two kindergartens in Turkey participated in the study.	$n = 38$ (22 girls and 16 boys) Age: 5 years Test of visual perceptual skills-3	3D	Physical outcome	10 min Every 15 days for 16 weeks	The 3D animated movies, as well as interactive applications such as worksheets and touchscreen, can enrich the visual perceptual development of infants	Test group 1 ($n = 12$; 7 girls and 5 boys) trained with 3D animated movies and interactive application with computer Test group II ($n = 12$; 7 girls and 5 boys) trained with 3D animated movies and worksheets of the interactive application Control group ($n = 14$; 8 girls and 6 boys) trained with preschool program
[56]	The audience's perception of animated cartoons telecasted on television for political communication was investigated. The frequency of exposure to such cartoons among males and females and the audience with primary, secondary, and tertiary levels of education was determined.	$n = 357$ (182 male and 175 female) Multistage sampling	TV animated cartoons	Psychological outcome	NA	Females are more exposed to animated TV cartoons. Furthermore, the perception depends on the level of education. The cartoons should be in such a way to motivate voting behavior.	NA
[57]	The influence of animated storybooks (motion) on children's visual attention and story comprehension was	$n = 39$ (22 boys and 17 girls) Mean age: 61.26 months Eye-tracking technology	2D	Psychological outcome	120 s	The motion in animated illustrations caused the children to focus longer and steadily, which enhanced their	Storybook with animated illustrations, a storybook with static illustrations, and a control condition (only

TABLE 5: Continued.

Reference	Study description	Sample and design	Types of animation	Outcomes	Duration of animation	Findings	Case control
	investigated. Participants were children from three public schools in the Netherlands.					capability of retelling the stories.	post-testing and no reading).
[58]	The influence of pedagogical agents with cueing on the students' learning ability was investigated. Seventh-grade students from a large junior high school in Taipei, Taiwan, have participated in the study.	$n = 133$ (67 boys and 66 girls) Age: 12 years	3D animation	Cognitive outcome	40 min	Implementing a pedagogical agent with cueing may help reduce the complexity of animation. It may support the learners to have a clear-cut view of the complex concepts of the biology domain.	Experimental group ($n = 64$): animation with a pedagogical agent and control group ($n = 69$), animation without a pedagogical agent
[59]	The impact of color and animation types on the sports viewer's attention to sponsorship signage was investigated. The arousal of confusion among sports viewers due to the animated sponsor signage was analyzed. Participants were assigned to four highlighted video clips (soccer, handball, biathlon, and formula one) according to their treatment conditions.	$n = 176$ (56.3% male and 43.7% female) Mean age: 24.4 ± 5 years Eye-tracking technology	Flash	Psychological outcome	15-20 min	Attention measures are more important than exposure quantities while designing sports sponsorship signage boards	Animation treatment (blinking, running, twisting, and spotlight) and color treatment (four chromatic primary hues such as red, green, blue, and yellow).

group showed tremendous results immediately after the training and at 6 weeks follow-up [42].

Some of the studies reported the role of animation in the teaching field ($n = 5$). The adoption of 3D animation as a teaching tool for illustrating surgical skills in medical education was investigated. The test scores showed higher significance for the 3D animation group when compared to the traditional teaching group ($p < 0.0001$) [33]. The animation lecture with instructional design helps in guiding learner's attention, thereby making them focus on the important instructions in the instructions. The animated group required less cognitive load, and they outperformed on the open-ended questions. It was further confirmed with insignificant differences between the two groups in the Genetic Foundation Test [39]. Idioms learning can be made

easier by watching an English animated movies. There is a significant effect on learning idioms through English animated movies ($p < 0.05$) [49]. The spatial features of the animations and the simulations facilitated the development of spatial ability of the 12th grade students. The experimental group's spatial ability and reasoning skills have higher significance than the control group ($p < 0.05$) [53]. The cueing by pedagogical agents positively affected learning performance and instructional efficiency. The cognitive load measures between the two groups were insignificant [58].

3.4. Risk of Bias within the Study. The risk of bias assessment within the studies is summarized in Table 6. The criteria for the assessment were based on the study design and data analysis. Nearly all the study participants were randomly selected

($n = 28$) with control group ($n = 15$) assigned. Some of the studies were conducted in isolation ($n = 31$), and the pretest and post-test ($n = 16$) method was employed to assess the significance of the hypothesis developed. The participants' visual perception of the animation was determined by their capability to recall or retell ($n = 27$). The data obtained in most of the studies were analyzed using power analysis ($n = 12$), validity measures ($n = 10$), and baseline comparisons ($n = 7$) and were employed in some studies. Follow-up on the influence of the animation was further assessed in a few studies ($n = 3$), and missing data were reported in a few studies ($n = 5$).

3.5. Attention-Related Factors.

Some of the studies reported in this review are solely concentrated on the visual attention of the participant's towards animation ($n = 12$). The attention-related factors among these studies are animation's interactive features ($n = 3$), intensity ($n = 1$), design ($n = 1$), motion ($n = 3$), sound ($n = 1$), annotation ($n = 1$), and character ($n = 3$). The factors that are insignificant with the viewer's visual attention was animation's color.

In twelve out of thirty-five papers, eye-tracking technology was employed to assess the participants' visual attention to the animation. The pupil movement and fixation time was observed to assess the viewer's attention towards the animation.

3.6. Physical Effects of Animation.

Animation has created awareness among adolescents about their body images and provided knowledge about the necessity of physical activity. It also helped women get a detailed report on mammographic procedures without hesitation. Moreover, it also delivered a knowledge on the health issues related to glaucoma.

3.7. Cognitive Effects of Animation.

As mentioned earlier, the animation has created some cognitive effects towards infants to adults. The animated ebook has helped the children understand the story's structure and content. Furthermore, animation made it easy to learn the surgical procedures like intercostal drain insertion and suprapubic catheter insertion. Also, the concepts of genetics, such as cell division, mitosis, and meiosis, were presented in animation, and the participant's performance was found to be improved. Moreover, the student's spatial ability and reasoning skills were improved by watching the animation lectures.

4. Discussion

4.1. Evidence Summary.

From the overall studies, it was evident that the animation was employed in various applications to attract and assess the viewer's attention. Among thirty-five studies, five briefed about the animated characters and one study about the animation motion.

The rest of the studies described the perception of audience towards implementing animation in the following phenomenon: learning skill improvement ($n = 15$), teaching strategy ($n = 2$), health awareness ($n = 5$), advertisement ($n = 3$), food marketing ($n = 2$), validating hearing aid ($n = 1$), and political awareness ($n = 1$).

4.2. Limitations and Recommendations.

Although the studies reported in this survey showed a significant difference and the hypothesis generated was accepted, some limitations still exist. The common limitations identified in the studies are short period of time for implementation [53], smaller sample size [27, 37], nongeneralizability [25, 27, 32, 39, 53], nonrandomization trials [52], and no control group and post only group [45]. Few other studies have reported the possibility of cross-contamination among the control and experimental group [33], increased dropout of participants before completing the post-test questionnaire [52], and underestimation of participant's knowledge of expressing words which might directly affect the animation [57].

Arshad et al. [44] have examined the "Pleasure" as a sole emotional response to describe the pleasure level of human emotion towards the Malaysian animation cartoon characters. In contrast, the PAD (pleasure, arousal, and dominance) model utilized in the study has two other dimensions: arousal and dominance.

The audience could not feel the warmth of the real human character in the animated short film as the animation span is too short [48]. In another study, there is a possible way for the audience to have different perceptions regarding the meaning of the word "believability." Moreover, the cat's exaggerated motion alone studied might express the intrinsic characteristics of its particular character design [37]. While studying the viewer/character relationships, the PSI (parasocial interaction) scores remained low, which may be due to the cause that it features nonhuman characters in all-CGI conditions. At the same time, the other conditions featured only humans [25].

Some of the typical future recommendations mentioned in the studies are an extension of the study period [53], increasing the study sample size [37] and implementing a randomized sample approach from various situations to overcome the limitation of result generalization [37, 52, 53].

The audience's perception of various anthropomorphic animal characters performing various actions in different situations should be examined [37]. In addition to the animation, the story's narration is more concentrated when designing a storybook app [57]. Moreover, TV animated cartoons can be designed to attract people with tertiary education for political promotions and political mobilization [56].

5. Challenges and Open Issues

The challenges and open issues faced by the researchers during the study are elaborated in this section, and it is shown in Figure 5.

5.1. Methodological Issues in Data Interpretation.

The methodological issues in data interpretation may occur due to animation completion time, fixation duration, and other confounding variables. Fixation duration may be employed to determine the participant's eye or head movements. Mostly eye-tracking devices and gaze movement trackers are utilized for this purpose. Any fault with these devices will affect the data quality, data loss, and data interpretation bias.

TABLE 6: Risk of bias within the studies.

Article	Randomization	Control	Isolation	Pre- and post-test	Retention	Missing data	Power analysis	Validity measure	Baseline method comparison	Follow up	Score	Reference
Sheldon et al.	Yes	No	Yes	No	No	No	No	Yes	No	No	3	[25]
Arora	Yes	No	No	No	Yes	No	No	No	No	No	2	[26]
Danaei et al.	Yes	Yes	Yes	No	Yes	No	No	No	No	No	4	[27]
Li et al.	Yes	Yes	Yes	No	Yes	No	No	No	Yes	No	5	[28]
Matheson et al.	Yes	Yes	Yes	Yes	Yes	Yes	Yes	Yes	Yes	Yes	10	[29]
Gunn et al.	No	No	Yes	Yes	Yes	Yes	No	No	Yes	No	5	[30]
Mok et al.	Yes	Yes	Yes	Yes	No	No	Yes	Yes	No	No	6	[31]
Binder et al.	Yes	No	Yes	No	Yes	No	Yes	Yes	Yes	No	6	[32]
Bedada et al.	Yes	Yes	Yes	Yes	Yes	No	No	No	No	No	5	[33]
Tummeltshammer et al.	Yes	No	Yes	Yes	Yes	Yes	No	No	Yes	No	6	[34]
Sun et al.	Yes	Yes	Yes	Yes	Yes	No	No	No	No	No	5	[35]
de Koning et al.	Yes	No	Yes	No	Yes	No	Yes	No	No	No	4	[36]
Hammer	Yes	Yes	No	No	Yes	No	No	No	No	No	3	[37]
Wang et al.	No	No	Yes	Yes	Yes	No	No	No	No	No	3	[38]
Yang et al.	Yes	No	Yes	No	No	No	No	No	No	No	2	[39]
Yang	Yes	Yes	Yes	No	No	No	No	No	No	No	3	[40]
Seo et al.	Yes	No	Yes	No	Yes	No	Yes	No	No	No	4	[41]
Forssman & Wass	Yes	Yes	Yes	Yes	Yes	No	Yes	No	No	Yes	7	[42]
Hendriikse et al.	Yes	No	Yes	No	Yes	Yes	No	Yes	No	No	5	[43]
Arshad et al.	No	No	No	No	Yes	No	Yes	No	No	No	2	[44]
Al Owaifeer et al.	No	No	No	Yes	Yes	No	No	Yes	Yes	Yes	5	[45]
Otto & Rumpf	Yes	No	Yes	No	Yes	Yes	Yes	No	No	No	5	[46]
Ichikawa et al.	Yes	No	Yes	Yes	Yes	No	Yes	No	No	No	5	[47]
Bouwer & Human	Yes	No	Yes	No	Yes	No	No	No	No	No	3	[48]
Sanaeifar	Yes	Yes	Yes	Yes	No	No	Yes	Yes	No	No	5	[49]
Yoon et al.	No	No	No	No	No	No	No	Yes	No	No	1	[50]
Ogle et al.	No	No	No	No	Yes	No	Yes	No	No	No	2	[51]
Dubovi et a.l	Yes	Yes	Yes	Yes	Yes	No	No	Yes	Yes	No	7	[52]
Al-Balushi et al.	Yes	Yes	Yes	Yes	No	No	No	No	No	No	4	[53]
Martynenko	Yes	No	Yes	No	No	No	No	No	No	No	2	[54]
Yucelyigit & Aral	Yes	Yes	Yes	Yes	Yes	No	No	Yes	No	No	6	[55]
Okoro & Onakpa	Yes	No	No	Yes	Yes	No	No	Yes	No	No	4	[56]
Takacs & Bus	No	Yes	Yes	No	Yes	No	Yes	No	No	No	4	[57]
Yung & Paas	Yes	Yes	Yes	Yes	Yes	No	No	No	No	No	5	[58]

Table 6: Continued.

Article	Randomization	Control	Isolation	Pre- and post-test	Retention	Missing data	Power analysis	Validity measure	Baseline method comparison	Follow up	Score	Reference
Breuer & Rumpf	Yes	No	Yes	No	Yes	No	No	No	No	No	3	[59]
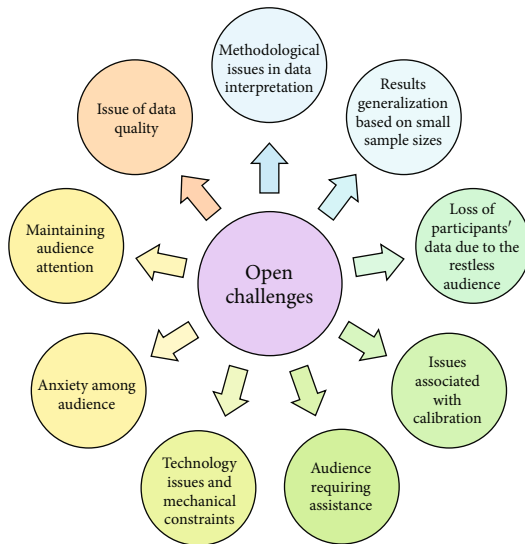
FIGURE 5: Challenges and open issues.

Li et al. [28] have suggested that fixation data points showed the preschooler's more significant mobilization and limited processing capacity. Tummeltshammer et al. [34] have determined the unfiltered eye movement data using SMI's BeGaze analysis software to overcome the error caused by the tracking device or participants in attention.

5.2. Results Generalization Based on Small Sample Sizes. The generalization of results based on small sample sizes may not be appropriate for all the cases. Most of the studies mentioned it as a limitation due to various concerns such as participants' demographical features and socio-economical features. Al-Balushi et al. [53] have reported improving logical thinking and spatial thinking skills of 12th grade students of Oman. He has also stated that further investigations are required due to the small sample size. Danaei et al. [27] have reported that the children who read the AR storybook were more confident in retelling and recalling the story.

The specific format or instructions employed in the research can also affect the generalization among the same or different populations. For instance, a specific pedagogical agent format that shows attraction towards the younger population might not show the same effects on adolescents and adults [58]. Similarly, the instructions designed to visualize in animation may not be appropriate for visualizing the same in real phenomena [39]. Binder et al. [32] suggested conducting more eye-tracking experiments with integrated food cues to attract children's attention toward healthy foods.

5.3. Loss of Participants' Data due to the Restless Audience. The audience becomes restless when the study duration is too long. This may be overcome by regular contact with them or follow-up studies. In some cases, participants find it difficult to spare their free time voluntarily. For instance, many students find it difficult to complete the questionnaire in their free time due to the stressful semester [52]. Some-

times, it is difficult to compel the participants to make things if they are children or infants. Among 39 children, one refused to retell the comprehensive stories learned through animated storybooks, so the corresponding data was removed from the study [57]. Two children in an experimental group refused to participate during the middle of the study [55].

In some cases, the data will be collected indirectly through random websites or by issuing pamphlets to random people. For example, Okoro and Onakpa [56] have collected data from selected towns in North Central Nigeria by issuing 385 copies of the questionnaire. Among these, 2% of the questionnaire were not received due to the restless audience.

5.4. Issues Associated with Calibration. The calibration of devices employed for measuring participants' visual attention plays a vital role in acquiring good quality data and aids in providing a better focus on the participants. Unfortunately, due to poor calibration (> 1) of the eye-tracking device, deviated results were obtained from five children, which may negatively impact the overall results [32].

5.5. Audience Requiring Assistance. The most important challenge faced in the study is to find the audience who requires assistance to participate in the study. Furthermore, this might help in acquiring better and more appropriate results. For example, Danaei et al. [27] have identified and helped the children who had struggled to start retelling the story learned through AR story book. And they were encouraged to continue the story.

5.6. Technology Issues and Mechanical Constraints. The technological issues may be caused due to unavoidable faults in the devices employed in the study. Due to this issue, the data points measured will be low, resulting in removing those data points. For example, in a study by Hendrikse et al. [43], the electrodes reached saturation due to the loose connection in the EOG (electrooculogram) electrodes for some participants. This, in turn, affected the data quality, and the corresponding data point was removed until it was adjusted to drift compensation. Similarly, two children were excluded from the study due to the problem that occurred in the stimulus presentation of fruit and candy [32].

5.7. Anxiety among Audience. Anxiety among the audience is another challenge faced during experimenting with new ideas. For example, al-Balushi et al. [53] have attempted to teach the critical concepts of 12th grade chemistry through animation. However, the students facing stressful periods due to the important exam in 12th grade made them anxious about the adoption of new teaching technology, which negatively affected the results. Nevertheless, the study still showed healthier results with improved spatial ability and reasoning skills of those students.

5.8. Maintaining Audience Attention. Another challenge in making animation successful is maintaining the viewer's attention. Attention can be influenced by various factors like animation span, animation intensity, animated character,

the motion of the animated character, and sound. Likewise, it may be affected by intervening factors such as restlessness of the audience in the real-time study settings and eye irritation. This situation can be overcome by conducting studies in a silent room where the audience can focus on the visual animation without getting distracted by external factors [49]. In some cases, the audience may get distracted by the instructions provided in the animation video [39].

5.9. Issue of Data Quality. One of the significant issues faced while carrying out studies is the quality of data obtained. And it may be influenced by the missing data due to an error in the instruments employed. It can either affect the result or may be corrected. For instance, due to the eye-tracking device's problem, children's eye movements were not clearly captured, which resulted in extremely low fixation time [57]. Similarly, 31.4% of EOG data were missing due to some error in the device. However, the missing data points are adjusted by entering them as not-a-number in the analysis [43]. Figure 5 illustrates the open challenges associated with this research.

6. Future Research Directions

The priority areas identified for future research directions are elaborated to strengthen the body of evidence. These include the advanced applications of animations that may make life easier and are listed in Figure 6 and are elaborated below.

The foremost application could include artificial intelligence (AI) that may generate 3D motion from video without any capture equipment [60]. The AI and advanced hardware can bring breathing life into animation by blurring the lines between the virtual and real characters. The application of AI into animation has reduced the post-production time, limited the need for character design, and aids in improved lip-syncing [61]. The explainable AI is an artificial intelligence operation that runs on deep neural networks. The practical applicability and promotion of the AI tool are enhanced by developing computational help [62]. The major challenges in AI are to succeed explainability in its program, which can be facilitated with animation techniques [63]. The explainable AI can be adopted in autonomous car decision-making and energy efficiency in smart homes [64] and medical imaging [65, 66]. Meanwhile, generative AI is a machine learning algorithm that can generate new content through text, images, and audio content. In addition, it can generate human-like language output [67].

Analyzing a large amount of fragmented data can be simplified by converging the big data and augmented analytics. Moreover, it helps to provide simplified statements to the customers in an understandable manner [68]. The visualization of a large pool of data can be made easier with the help of animation. Moreover, the data visualization can be integrated with augmented and virtual reality [69]. The big data and augmented analytics play a major role in video gaming. For instance, Pokemon Go is a location-based Japanese video game franchise. This game transforms the gamer's physical location into an augmented world where
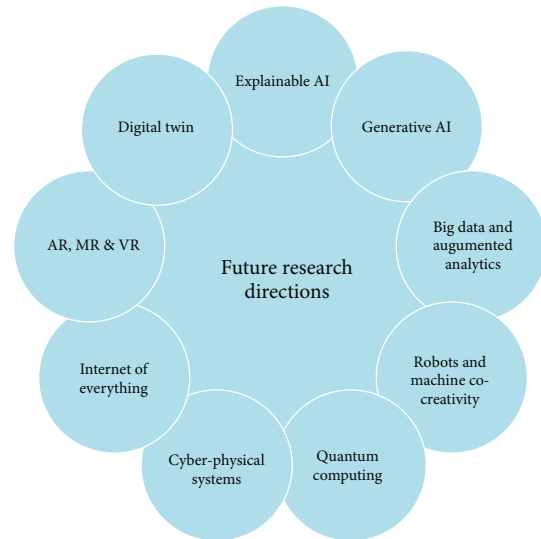
FIGURE 6: Future research directions.

the characters are superimposed on the reality seen through their mobiles. The Global Positioning System (GPS), a major staple of big data, makes this possible by allowing data collection and storing it upon the crowd-sourced data [70].

Quantum computing deals with pulling together the theoretical ideas of computer science and fundamental physics. It has been the focus of many large companies such as Google, IBM, and Microsoft. The algorithm created from quantum computing concepts can be employed to design a 3D modeling [71]. It is based on the qubits that give rise to new logic gates, which enable constructing a new algorithm. However, it is still in its emerging phase, and for future development, it is necessary to overcome the obstacles like decoherence and scalability issues [72].

The collaboration of robots and machines to perform a day-to-day task will be the perception of the modern era. However, its ethical issues are yet to be analyzed and eradicated [73]. Internet of Everything (IoE) provides interconnection of physical items to frame an information network that provides smart communication services to the users. The IoE finds applications in the fields like health care, smart grids, smart cities, smart homes, manufacturing, and transport [74].

Digital twin technology provides a virtual representation of a physical product consisting of information from the product's origin to its life cycle management. The general applicability of the digital twin lies in physical entities like agricultural supply chains, automotive wiring harnesses, smart cars, and farms, and virtual entities like health monitoring and scheduling [75]. The animation concepts play a vital role in mirroring the design concepts and visualizing them during the conceptual designing stage of the digital twin [76]. For instance, while designing the speed of the machines, synchronization can be achieved by controlling the rate of animation frames [77].

Another major industrial revolution is the cyber-physical system (CPS), composed of highly integrated computation, communication, control, and physical elements.

The CPS research is emerging in education [78], agriculture [79], and manufacturing. For instance, in the manufacturing sector, the CPS may bridge the gap between design and manufacturing [80]. It extends the manufacturing process with a communication interface that mimics the worker assistance system. Furthermore, the animation is used to assist the operation flow of instruments in the worker assistance system [81]. However, the CPS development is still in the embryonic stage as it faces challenges such as security, privacy, efficiency, and interoperability [82].

The interaction and fusion between the physical space and virtual space are facilitated with the advancements in the 3R technology (virtual reality (VR), augmented reality (AR), and mixed reality (MR)). The VR is a simulated environment designed in real time using computer graphics and pictures of the scene in 3D. It will immerse the viewer into the virtual environment, closing them completely away from the outside world. Meanwhile, AR is an interactive environment that is designed by increasing this fusion between the physical and virtual space. The viewers can interact with the animated data and instructional information superimposed over the real-world view through devices such as mobile phones or tablets. At the same time, the MR simulation environment is designed from the fusion of real-world and virtual space comprising the co-existence interaction of physical objects and digital objects. Two or more viewers can be networked together in a virtual environment where they can interact with computer-generated objects on the real world [83, 84]. In recent span, the AR, VR and MR applications have been widely used in health-care monitoring [84, 85], clinical applications in oral and maxillofacial surgery [86, 87], improvising nursing skills [52], and enhanced teaching strategy [27].

7. Conclusions

This paper highlighted a systematic review of 35 publications about animation's importance and its impact on viewer's visual attention and cognition. These publications were collected from 2015 to 2021 and are grouped into 3 categories. The risk of bias in the study design carried out in these publications was briefed. The attention-related factors such as animation motion, animated character, color, and intensity were assessed in the field of food marketing, teaching, entertainment, and advertisement. The animation motion and animated character are significant, whereas color and intensity are insignificant. The cognitive effects developed in the viewers are executive function, comprehension, spatial ability, and symbolic mediation. Meanwhile, the physical effects included confidence in their own body image and the importance of physical exercise. The limitations and recommendations associated with these 35 publications were elaborated. Also, the open challenges and issues under each category were summarized. The identified future research directions ideas may further strengthen the necessity for improving the visual quality of the animation.

The major limitation of this study is that the recently published articles were not included (i.e., publications in 2022). Several important animation research fields, such as gaming, medical, and entertainment, were not covered in this paper. Future research should include the recently published articles to enhance the quality and validate the findings in this study. In addition, the future study focuses on assessing the influence of animation motion and animated characters on the viewer's visual attention.

Data Availability

The original contributions generated for this study are included in the article; further inquiries can be directed to the corresponding author.

Conflicts of Interest

The authors declare that there are no conflicts of interest regarding the publication of this paper.

References

[1] P. Wells, *Understanding animation*, Routledge, 2013.

[2] G. A. Bhutto, Z. Bhatti, S. U. Rehman, and S. Joyo, "Multimedia based learning paradigm for school going children using 3D animation," *University of Sindh Journal of Information and Communication Technology*, vol. 2, no. 4, pp. 202–207, 2018.

[3] D. A. Purwaningsih, "Optimizing 2D animation production time in creating traditional watercolor looks by integrating traditional and digital media," *International Journal of Asia Digital Art and Design Association*, vol. 21, no. 1, pp. 57–63, 2017.

[4] S. A. Etemad, A. Arya, A. Parush, and S. DiPaola, "Perceptual validity in animation of human motion," *Computer Animation and Virtual Worlds*, vol. 27, no. 1, pp. 58–71, 2016.

[5] M. Zong, Z. Qi, and Z. Zong, "Research on character expression shaping in animation movies," in *4th International Conference on Culture, Education and Economic Development of Modern Society (ICCESE 2020)*, pp. 151–155, Atlantis Press, 2020.

[6] M. Kim, R. Shi, and J. N. Cappella, "Effect of character–audience similarity on the perceived effectiveness of antismoking PSAs via engagement," *Health Communication*, vol. 31, no. 10, pp. 1193–1204, 2016.

[7] Z. Shao, "Discussion on the performance of visual humor in animation," in *2nd International Conference on Contemporary Education, Social Sciences and Humanities (ICCESSH 2017)*, pp. 419–422, Atlantis Press, 2017.

[8] E. D. Shah, L. R. Larson, and L. L. Denton III, "Animation and consumer perceptions of DTC pharmaceutical advertisement," *Journal of Consumer Affairs*, vol. 53, no. 4, pp. 1456–1477, 2019.

[9] H. J. Smith and M. Neff, "Understanding the impact of animated gesture performance on personality perceptions," *ACM Transactions on Graphics (TOG)*, vol. 36, no. 4, pp. 1–12, 2017.

[10] V. Vijayakrishnan, D. Harikrishnan, D. Babu, and A. V. V. Kochi, "Marketing strategy in advertisements using animated characters," *International Journal of Pure and Applied Mathematics*, vol. 119, no. 12, pp. 2841–2852, 2018.

[11] R. Geal, "Animated images and animated objects in the Toy Story franchise: reflexively and intertextually transgressive mimesis," *Animation*, vol. 13, no. 1, pp. 69–84, 2018.

[12] T. Yang, "Research on the influence of the nature and behavior of animated characters on the audience," in *4th International Conference on Contemporary Education, Social Sciences and Humanities (ICCESSH 2019)*, pp. 862–864, Atlantis Press, 2019.

[13] M. van Rooij, "Carefully constructed yet curiously real: how major American animation studios generate empathy through a shared style of character design," *Animation*, vol. 14, no. 3, pp. 191–206, 2019.

[14] L. Sen and Z. Rong, "The influence of Japanese anime on the values of adolescent," in *2019 4th International Conference on Humanities Science and Society Development (ICHSSD 2019)*, pp. 272–274, Atlantis Press, 2019.

[15] M. N. B. M. Ghazali and D. A. Ghani, "The important of great storytelling in Malaysia animation industries," *International Journal of Innovative Technology and Exploring Engineering*, vol. 8, no. 11S2, pp. 230–235, 2019.

[16] C. Liu and P. Elms, "Animating student engagement: the impacts of cartoon instructional videos on learning experience," *Research in Learning Technology*, vol. 27, 2019.

[17] E. Flynn, "Discovering audience motivations behind movie theater attendance," *Elon Journal of Undergraduate Research in Communications*, vol. 9, no. 2, pp. 94–103, 2018.

[18] H. Zhou, "The narrative construction of Chinese animation from the perspective of adolescent audience," in *Proceedings of 4th International Conference on Education, Language, Art and Intercultural Communication (ICELAIC 2017)*, pp. 519–523, Moscow, Russia, 2017.

[19] P. Agarwal and N. Adhikari, "Survey of trends in 3D animation," *International Journal of Scientific & Engineering Research*, vol. 8, no. 5, pp. 97–101, 2017.

[20] D. Goel and R. Upadhyay, "Effectiveness of use of animation in advertising: a literature review," *International Journal of Scientific Research in Network Security and Communication (IJSRNSC)*, vol. 5, no. 3, pp. 146–159, 2017.

[21] E. A. Zaky, "Once Upon A Time, We were All Little Kids too!!! Influence of Cartoon on Children's Behavior; Is It Just A World of Fantasy or A Nightmare???," *International Journal of Science and Research*, vol. 5, no. 5, pp. 1296–1298, 2016.

[22] M. J. Page, J. E. McKenzie, P. M. Bossuyt et al., "The PRISMA 2020 statement: an updated guideline for reporting systematic reviews," *Systematic Reviews*, vol. 10, no. 1, p. 89, 2021.

[23] I. Penuelas-Calvo, L. K. Jiang-Lin, B. Girela-Serrano et al., "Video games for the assessment and treatment of attention-deficit/hyperactivity disorder: a systematic review," *European Child & Adolescent Psychiatry*, vol. 31, pp. 5–20, 2020.

[24] R. Sarkis-Onofre, F. Catalá-López, E. Aromataris, and C. Lockwood, "How to properly use the PRISMA statement," *Systematic Reviews*, vol. 10, no. 1, pp. 1–3, 2021.

[25] Z. Sheldon, M. Romanowski, and D. M. Shafer, "Parasocial interactions and digital characters: the changing landscape of cinema and viewer/character relationships," *Atlantic Journal of Communication*, vol. 29, no. 1, pp. 15–25, 2021.

[26] P. Arora, "A qualitative study of the visual impact of stop-motion animation films on its audience," *International Journal of Modern Agriculture*, vol. 10, no. 2, pp. 936–945, 2021.

[27] D. Danaei, H. R. Jamali, Y. Mansourian, and H. Rastegarpour, "Comparing reading comprehension between children reading augmented reality and print storybooks," *Computers & Education*, vol. 153, article 103900, 2020.

[28] H. Li, Y. Hsueh, H. Yu, and K. M. Kitzmann, "Viewing fantastical events in animated television shows: immediate effects on Chinese preschoolers' executive function," *Frontiers in Psychology*, vol. 11, p. 3423, 2020.

[29] E. L. Matheson, H. Lewis-Smith, and P. C. Diedrichs, "The effectiveness of brief animated films as a scalable micro-intervention to improve children's body image: a randomised controlled trial," *Body Image*, vol. 35, pp. 142–153, 2020.

[30] C. Gunn, A. Maschke, T. Bickmore et al., "Acceptability of an interactive computer-animated agent to promote patient-provider communication about breast density: a mixed method pilot study," *Journal of General Internal Medicine*, vol. 35, no. 4, pp. 1069–1077, 2020.

[31] M. M. C. Mok, M. K. Chin, A. Korcz et al., "Brain breaks® physical activity solutions in the classroom and on attitudes toward physical activity: a randomized controlled trial among primary students from eight countries," *International Journal of Environmental Research and Public Health*, vol. 17, no. 5, p. 1666, 2020.

[32] A. Binder, B. Naderer, and J. Matthes, "A "forbidden fruit effect": an eye-tracking study on children's visual attention to food marketing," *International Journal of Environmental Research and Public Health*, vol. 17, no. 6, p. 1859, 2020.

[33] A. G. Bedada, G. Ayane, and M. J. Motsumi, "The role of Moodle-based surgical skills illustrations using 3D animation in undergraduate training," *African Journal of Health Professions Education*, vol. 11, no. 4, pp. 149–152, 2019.

[34] K. Tummeltshammer, E. C. Feldman, and D. Amso, "Using pupil dilation, eye-blink rate, and the value of mother to investigate reward learning mechanisms in infancy," *Developmental Cognitive Neuroscience*, vol. 36, article 100608, 2019.

[35] H. Sun, J. Loh, and A. Charles Roberts, "Motion and sound in animated storybooks for preschoolers' visual attention and mandarin language learning: an eye-tracking study with bilingual children," *AERA Open*, vol. 5, no. 2, p. 19, 2019.

[36] B. B. de Koning, N. Marcus, B. Brucker, and P. Ayres, "Does observing hand actions in animations and static graphics differentially affect learning of hand-manipulative tasks?," *Computers & Education*, vol. 141, article 103636, 2019.

[37] M. Hammer, *Audience perception of exaggerated motion on realistic animated creatures, [Ph.D. thesis]*, Purdue University, 2020.

[38] C. C. Wang, J. C. Hung, S. N. Chen, and H. P. Chang, "Tracking students' visual attention on manga-based interactive e-book while reading: an eye-movement approach," *Multimedia Tools and Applications*, vol. 78, no. 4, pp. 4813–4834, 2019.

[39] C. Yang, C. H. Jen, C. Y. Chang, and T. K. Yeh, "Comparison of animation and static-picture based instruction: effects on performance and cognitive load for learning genetics," *Journal of Educational Technology & Society*, vol. 21, no. 4, pp. 1–11, 2018.

[40] H. Y. Yang, "The effects of visual cueing on pictorial and verbal tests through mobile-phone-based animation," *Journal of Computers in Education*, vol. 5, no. 4, pp. 393–414, 2018.

[41] Y. N. Seo, M. Kim, D. Lee, and Y. Jung, "Attention to eSports advertisement: effects of ad animation and in-game dynamics on viewers' visual attention," *Behaviour & Information Technology*, vol. 37, no. 12, pp. 1194–1202, 2018.

[42] L. Forssman and S. V. Wass, "Training basic visual attention leads to changes in responsiveness to social-communicative

cues in 9-month-olds," *Child Development*, vol. 89, no. 3, pp. e199–e213, 2018.

[43] M. M. Hendrikse, G. Llorach, G. Grimm, and V. Hohmann, "Influence of visual cues on head and eye movements during listening tasks in multi-talker audiovisual environments with animated characters," *Speech Communication*, vol. 101, pp. 70–84, 2018.

[44] M. R. Arshad, K. H. Yoon, and A. A. Manaf, "Character pleasantness in Malaysian animated cartoon characters," *SHS Web of Conferences*, vol. 53, 2018.

[45] A. M. Al Owaifeer, S. M. Alrefaie, Z. M. Alsawah, A. A. Al Taisan, A. Mousa, and S. I. Ahmad, "The effect of a short animated educational video on knowledge among glaucoma patients," *Clinical Ophthalmology (Auckland, NZ)*, vol. 12, p. 805, 2018.

[46] F. Otto and C. Rumpf, "Animation intensity of sponsorship signage," *Sport, Business and Management: An International Journal*, vol. 8, no. 2, pp. 177–194, 2018.

[47] H. Ichikawa, S. Kanazawa, and M. K. Yamaguchi, "Infants recognize identity in a dynamic facial animation that simultaneously changes its identity and expression," *Visual Cognition*, vol. 26, no. 3, pp. 156–165, 2018.

[48] W. Bouwer and F. Human, "The impact of the uncanny valley effect on the perception of animated three-dimensional humanlike characters," *The Computer Games Journal*, vol. 6, no. 3, pp. 185–203, 2017.

[49] S. H. Sanaeifar, "The effect of watching English language animation movies on learning idioms: a case of Iranian EFL learners," *European Journal of English Language Teaching*, vol. 2, no. 3, pp. 20–38, 2017.

[50] Y. J. Yoon, B. K. Hwang, S. J. Lee, J. O. Lee, and H. Chae, "Analysis of seven animation characters in Pororo the Little Penguin with Sasang typology," *Integrative medicine Research*, vol. 6, no. 2, pp. 156–164, 2017.

[51] A. D. Ogle, D. J. Graham, R. G. Lucas-Thompson, and C. A. Roberto, "Influence of cartoon media characters on children's attention to and preference for food and beverage products," *Journal of the Academy of Nutrition and Dietetics*, vol. 117, no. 2, pp. 265–270.e2, 2017.

[52] I. Dubovi, S. T. Levy, and E. Dagan, "Now I know how! The learning process of medication administration among nursing students with non-immersive desktop virtual reality simulation," *Computers & Education*, vol. 113, pp. 16–27, 2017.

[53] S. M. Al-Balushi, A. S. Al-Musawi, A. K. Ambusaidi, and F. H. Al-Hajri, "The effectiveness of interacting with scientific animations in chemistry using mobile devices on grade 12 students' spatial ability and scientific reasoning skills," *Journal of Science Education and Technology*, vol. 26, no. 1, pp. 70–81, 2017.

[54] M. N. Martynenko, "Comprehension of the animated films culture as a factor of development of capacity for symbolic mediation by a senior preschool-age child," *Procedia-Social and Behavioral Sciences*, vol. 233, pp. 211–215, 2016.

[55] S. Yücelyiğit and N. Aral, "The effects of three dimensional (3D) animated movies and interactive applications on development of visual perception of preschoolers," *Education & Science/Egitim ve Bilim*, vol. 41, no. 188, pp. 255–271, 2016.

[56] N. Okoro and M. S. Onakpa, "Audience perception of television animated cartoons as tool for political communication: a study of selected towns in north central Nigeria," *AFRREV IJAH: An International Journal of Arts and Humanities*, vol. 5, no. 4, pp. 232–249, 2016.

[57] Z. K. Takacs and A. G. Bus, "Benefits of motion in animated storybooks for children's visual attention and story comprehension. an eye-tracking study," *Frontiers in Psychology*, vol. 7, p. 1591, 2016.

[58] H. I. Yung and F. Paas, "Effects of cueing by a pedagogical agent in an instructional animation: a cognitive load approach," *Journal of Educational Technology & Society*, vol. 18, no. 3, pp. 153–160, 2015.

[59] C. Breuer and C. Rumpf, "The impact of color and animation on sports viewers' attention to televised sponsorship signage," *Journal of Sport Management*, vol. 29, no. 2, pp. 170–183, 2015.

[60] A. Mathis, S. Schneider, J. Lauer, and M. W. Mathis, "A primer on motion capture with deep learning: principles, pitfalls, and perspectives," *Neuron*, vol. 108, no. 1, pp. 44–65, 2020.

[61] https://analyticsindiamag.com/how-ai-is-breathing-life-into-animation/.

[62] W. J. Clancey and R. R. Hoffman, "Methods and standards for research on explainable artificial intelligence: lessons from intelligent tutoring systems," *Applied AI Letters*, vol. 2, no. 4, p. e53, 2021.

[63] C. Rubio-Manzano, A. Segura-Navarrete, C. Martinez-Araneda, and C. Vidal-Castro, "Explainable hopfield neural networks using an automatic video-generation system," *Applied Sciences*, vol. 11, no. 13, p. 5771, 2021.

[64] N. Petrović and M. Tošić, "Explainable artificial intelligence and reasoning in smart cities," *YuInfo*, vol. 2020, pp. 1–6, 2020.

[65] Z. Papanastasopoulos, R. K. Samala, H. P. Chan et al., "Explainable AI for medical imaging: deep-learning CNN ensemble for classification of estrogen receptor status from breast MRI," *Medical Imaging 2020: Computer-Aided Diagnosis*, vol. 11314, article 113140Z, 2020.

[66] T. Folke, S. C. H. Yang, S. Anderson, and P. Shafto, "Explainable AI for medical imaging: explaining pneumothorax diagnoses with Bayesian teaching," *Artificial Intelligence and Machine Learning for Multi-Domain Operations Applications III*, vol. 11746, pp. 644–664, 2021.

[67] J. Sun, Q. V. Liao, M. Muller et al., "Investigating explainability of generative AI for code through scenario-based design," in *27th International Conference on Intelligent User Interfaces*, pp. 212–228, Helsinki, Finland, 2022.

[68] C. Tominski, G. Andrienko, N. Andrienko et al., "Toward flexible visual analytics augmented through smooth display transitions," *Visual Informatics*, vol. 5, no. 3, pp. 28–38, 2021.

[69] E. Olshannikova, A. Ometov, Y. Koucheryavy, and T. Olsson, "Visualizing big data with augmented and virtual reality: challenges and research agenda," *Journal of Big Data*, vol. 2, no. 1, pp. 1–27, 2015.

[70] B. Joseph, "The secret sauce in Pokémon Go: big data," 2016, https://dmlcentral.net/secret-sauce-Pokémon-go.

[71] F. Olart, E. Tassin, L. Capdeville, L. Pinguet, T. Gautier, and A. Lioret, "Quantum nodes: quantum computing applied to 3D modeling," in *ACM SIGGRAPH 2021 Posters*, pp. 1-2, Virtual Event, USA, 2021.

[72] V. Moret-Bonillo, "Can artificial intelligence benefit from quantum computing?," *Progress in Artificial Intelligence*, vol. 3, no. 2, pp. 89–105, 2015.

[73] A. Kantosalo, M. Falk, and A. Jordanous, "Embodiment in 18th century depictions of human-machine co-creativity," *Frontiers in Robotics and AI*, vol. 8, 2021.

[74] F. A. Alaba, M. Othman, I. A. T. Hashem, and F. Alotaibi, "Internet of things security: a survey," *Journal of Network and Computer Applications*, vol. 88, pp. 10–28, 2017.

[75] D. Jones, C. Snider, A. Nassehi, J. Yon, and B. Hicks, "Characterising the digital twin: a systematic literature review," *CIRP Journal of Manufacturing Science and Technology*, vol. 29, pp. 36–52, 2020.

[76] J. Guo, N. Zhao, L. Sun, and S. Zhang, "Modular based flexible digital twin for factory design," *Journal of Ambient Intelligence and Humanized Computing*, vol. 10, no. 3, pp. 1189–1200, 2019.

[77] G. C. Deac, C. N. Georgescu, C. L. Popa, and C. E. Cotet, "Virtual reality digital twin for a smart factory," *International Journal of Modeling and Optimization*, vol. 10, no. 6, pp. 190–195, 2020.

[78] A. K. Azad and R. Hashemian, "Cyber-physical systems in STEM disciplines," in *2016 SAI Computing Conference (SAI)*, pp. 868–874, London, UK, 2016.

[79] S. I. Caramihai and I. Dumitrache, "Agricultural enterprise as a complex system: a cyber physical systems approach," in *2015 20th International Conference on Control Systems and Computer Science*, pp. 659–664, Bucharest, Romania, 2015.

[80] E. Frontoni, J. Loncarski, R. Pierdicca, M. Bernardini, and M. Sasso, "Cyber physical systems for industry 4.0: towards real time virtual reality in smart manufacturing," in *International Conference on Augmented Reality, Virtual Reality and Computer Graphics*, L. Paolis and P. Bourdot, Eds., vol. 10851, pp. 422–434, Springer, Cham, 2018.

[81] B. Röhm, J. Olbort, and R. Anderl, "AR based assistance for the tool change of cyber-physical systems," *Procedia CIRP*, vol. 104, pp. 536–541, 2021.

[82] H. Chen, "Applications of cyber-physical system: a literature review," *Journal of Industrial Integration and Management*, vol. 2, no. 3, article 1750012, 2017.

[83] S. Ke, F. Xiang, Z. Zhang, and Y. Zuo, "A enhanced interaction framework based on VR, AR and MR in digital twin," *Procedia Cirp*, vol. 83, pp. 753–758, 2019.

[84] M. Sugimoto, "Extended reality (XR: VR/AR/MR), 3D printing, holography, AI, radiomics, and online VR Tele-medicine for precision surgery," in *Surgery and Operating Room Innovation*, pp. 65–70, Springer, Singapore, 2021.

[85] M. C. Hsieh and J. J. Lee, "Preliminary study of VR and AR applications in medical and healthcare education," *Journal of Nursing and Health Studies*, vol. 3, no. 1, p. 1, 2018.

[86] X. Chen and J. Hu, "A review of haptic simulator for oral and maxillofacial surgery based on virtual reality," *Expert Review of Medical Devices*, vol. 15, no. 6, pp. 435–444, 2018.

[87] D. Holzinger, P. Juergens, K. Shahim et al., "Accuracy of soft tissue prediction in surgery-first treatment concept in orthognathic surgery: a prospective study," *Journal of Cranio-Maxillofacial Surgery*, vol. 46, no. 9, pp. 1455–1460, 2018.

Retraction

Retracted: Effects of Quantitative Nursing Combined with Psychological Intervention in Operating Room on Stress Response, Psychological State, and Prognosis of Patients Undergoing Laparoscopic Endometrial Cancer Surgery

Computational and Mathematical Methods in Medicine

This article has been retracted by Hindawi following an investigation undertaken by the publisher [1]. This investigation has uncovered evidence of one or more of the following indicators of systematic manipulation of the publication process:

(1) Discrepancies in scope

(2) Discrepancies in the description of the research reported

(3) Discrepancies between the availability of data and the research described

(4) Inappropriate citations

(5) Incoherent, meaningless and/or irrelevant content included in the article

(6) Peer-review manipulation

The presence of these indicators undermines our confidence in the integrity of the article's content and we cannot, therefore, vouch for its reliability. Please note that this notice is intended solely to alert readers that the content of this article is unreliable. We have not investigated whether authors were aware of or involved in the systematic manipulation of the publication process.

Wiley and Hindawi regrets that the usual quality checks did not identify these issues before publication and have since put additional measures in place to safeguard research integrity.

We wish to credit our own Research Integrity and Research Publishing teams and anonymous and named external researchers and research integrity experts for contributing to this investigation.

The corresponding author, as the representative of all authors, has been given the opportunity to register their agreement or disagreement to this retraction. We have kept a record of any response received.

References

[1] X. Chen, H. Li, S. Wang et al., "Effects of Quantitative Nursing Combined with Psychological Intervention in Operating Room on Stress Response, Psychological State, and Prognosis of Patients Undergoing Laparoscopic Endometrial Cancer Surgery," *Computational and Mathematical Methods in Medicine*, vol. 2022, Article ID 6735100, 8 pages, 2022.

Research Article

Effects of Quantitative Nursing Combined with Psychological Intervention in Operating Room on Stress Response, Psychological State, and Prognosis of Patients Undergoing Laparoscopic Endometrial Cancer Surgery

Xiaojing Chen,[1] Huiyan Li [ID],[2] Shouyan Wang,[1] Yu Wang,[1] Li Zhang,[1] Dandan Yao,[3] Li Li,[1] and Ge Gao[1]

[1]*Department of Clean Operation, Harbin Medical University Cancer Hospital, Harbin 150081, China*
[2]*Department of Nursing, Harbin Medical University Cancer Hospital, Harbin 150081, China*
[3]*Department of Anesthesiology, Harbin Medical University Cancer Hospital, Harbin 150081, China*

Correspondence should be addressed to Huiyan Li; 2411@ecupl.edu.cn

Objective. To investigate the effects of quantitative nursing and psychological interventions on stress response, mental health, and prognosis in endometrial cancer patients having laparoscopic surgery. *Methods.* The random number table approach was used to identify and split 98 patients with endometrial cancer undergoing laparoscopic surgery at our hospital's Obstetrics and Gynecology Hospital ($n = 49$) into observation and control groups ($n = 49$) from May 2020 to February 2022. Both groups received standard care in the operating room, while those in the observation group received quantitative and psychological interventions in the operating room. Both groups were compared for perioperative markers, stress indicators, coping strategies, and pain levels. *Results.* In terms of age, TNM stage, or pathology, there was no statistically significant difference between the two groups ($P > 0.05$). Both the observation and control groups experienced statistically significant ($P < 0.05$) reductions in the perioperative markers of operation time, intraoperative blood loss, and overall hospital stay. Both groups' SAS and SDS scores were lower than they had been prior to surgery, but the observation group had lower scores than the control group, and these differences were statistically significant ($P < 0.05$). Postsurgery, the observation group's cortisol and adrenaline levels were lower than those of the control group, and both groups' levels were higher than before surgery, with statistical significance ($P < 0.05$) in both groups. Neither coping style nor pain level differed significantly between the two groups before surgery ($P > 0.05$). Postoperatively, while yield item scores were lower and faces scores were higher than the control group, the observation group's avoidance item score was lower than the control group. All with statistical significance. There were substantial differences in NRS SCORE between observers and controls. *Conclusion.* After laparoscopic surgery to remove endometrial cancer, patients may benefit from the combination of quantitative nursing and psychological intervention in the operating room to alleviate postoperative anxiety and sadness and reduce stress reaction.

1. Introduction

During the perimenopausal and postmenopausal periods, women are more likely to develop endometrial cancer. It is mainly treated by surgery in clinic [1]. Laparoscopic surgery has the advantages of high safety and less complications during the perioperative period. However, it still causes certain damage to the body. At the same time, due to the impact on the body shape of patients, patients are prone to strong psychological and physical stress reactions, which is not conducive to the work of anesthesiologists and surgeons, leading to poor rehabilitation. Therefore, it is necessary to give patients better medical care and services [2]. The success of the operation, the patient's recovery, and the patient's

Table 1: Comparison of the general material between the two groups.

Group	Control group	Observation group	Total value	P value
Age (years, $\bar{x} \pm s$)	52.54 ± 10.72	52.12 ± 10.68	1.252	0.062
TNM grade (cases, n)				
Grade II	27	28	0.874	0.312
Grade III	22	21		
Pathological type (cases, n)				
Endometrioid adenocarcinoma	23	24		
Adenosquamous carcinoma	17	19	0.754	0.385
Clear cell carcinoma	9	6		

Table 2: Comparison of perioperative indicators of patients between the two groups ($\bar{x} \pm s$).

	Control	Observation
Operative time (min)	188 ± 11.74	145 ± 9.52
Intraoperative blood loss (ml)	321 ± 23.01	245 ± 18.45
Total length of hospital stay (d)	10.33 ± 2.97	7.35 ± 1.13
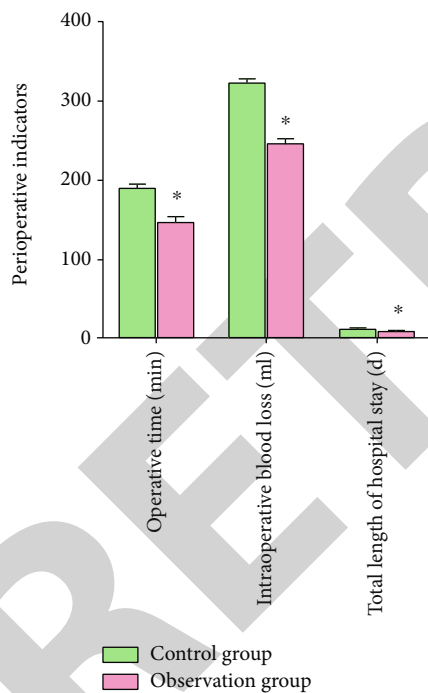
Figure 1: Perioperative indicators of patients between the two groups. Compared with control group, $^{*}P < 0.05$, the differences were statistically significant.

quality of life after surgery can all be influenced by the quality of the nursing care provided, and the patient's postoperative rehabilitation but conventional nursing cannot meet the above needs and affect the surgical effect to a certain extent, delaying the rehabilitation process [3]. Quantitative nursing in operation room means that through strictly controlling various details and good communication with patients during the whole perioperative period, risks caused by insufficient preparation are avoided, which can effectively remedy the disadvantages of conventional nursing in operation room and quantify the nursing scheme in operation room, thus ensuring the smooth operation and safety of patients [4]. Although relevant studies in China and overseas have demonstrated that psychological counseling can successfully improve patients' physical and mental status, the influence on whether stress response is improved is still unclear [5]. In 98 patients who underwent laparoscopic surgery for endometrial cancer and were admitted to the Department of Obstetrics and Gynecology Hospital at our hospital from May 2020 to February 2022, the stress response and psychological state of our patients were compared and observed following various nursing interventions. The following are the outcomes of the study.

2. Material and Methods

2.1. General Material. Using the random number table, 98 patients who underwent laparoscopic surgery for endometrial cancer at our hospital between May 2020 and February 2022 were chosen as research participants and split into two groups: an observation group ($n = 49$) and a control group ($n = 49$). In the observation group, quantitative nursing in the operating room was paired with psychological intervention, and the control group received standard intervention, however. The participant in this experiment gave informed consent, which was authorized by a hospital's Ethics Committee.

2.2. Criteria of Inclusion and Exclusion. Inclusion criteria [6] are (1) endometrial cancer is diagnosed according to clinical manifestations and auxiliary examinations such as imaging, (2) tolerant to surgery, (3) the I–II scale set by the American Association of Anesthesiologists, (4) no surgery or hemorrhagic disease within six months, and (5) informed consent forms are signed by patients and their families.

Exclusion criteria [7] are (1) tumor metastasis has occurred, (2) together with other cancerous tumors, (3) combination of cardiovascular and cerebrovascular illness, (4) liver and kidney dysfunction, and (5) confusion or cognitive impairment.

2.3. Nursing Methods. Treatment was kept to a minimum for those in the control group. The preoperative diet guidance, explain the complications; Active cooperation with doctors

TABLE 3: Comparison of patients' coping styles between the two groups ($\bar{x} \pm s$).

	Control	Observation
SAS		
Before	61.45 ± 9.88	61.47 ± 9.13
After	42.31 ± 7.56	32.78 ± 5.20
SDS		
Before	51.51 ± 8.20	51.53 ± 7.98
After	45.26 ± 7.31	28.66 ± 2.19
Cortisol, ng/L		
Before	101.23 ± 10.11	101.16 ± 11.63
After	140.89 ± 20.17	120.36 ± 15.08
Drenaline, ng/L		
Before	90.15 ± 8.75	90.12 ± 8.34
After	150.05 ± 21.53	128.88 ± 16.89
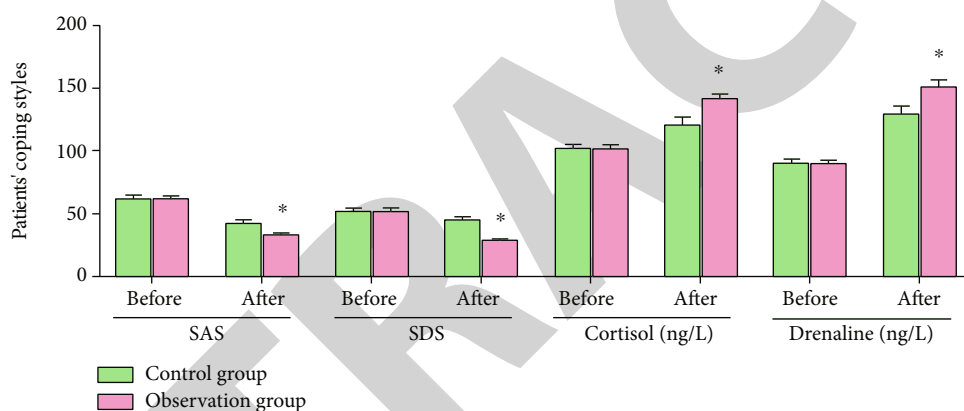
FIGURE 2: Patients' coping styles between the two groups. Compared with control group, $^*P < 0.05$, the differences were statistically significant.

TABLE 4: Comparison of patients' coping styles between the two groups ($\bar{x} \pm s$).

	Control	Observation
Duck		
Before	25.21 ± 3.78	24.96 ± 3.83
After	19.53 ± 3.06	7.53 ± 1.10
Yield		
Before	24.1 ± 3.75	23.64 ± 3.96
After	18.53 ± 3.51	7.83 ± 1.09
Face		
Before	7.03 ± 1.07	6.98 ± 1.01
After	9.36 ± 1.09	15.73 ± 2.74

and nurses during the operation and strict monitoring of patients' vital signs; Postoperative guidance on the correct medication and discharge guidance, etc. Quantitative nursing in operation room is combined with psychological intervention for patients in observation group. Specific measures are as follows:

(1) *Presurgery Quantification*. The age, disease status, and combined disease status of patients were obtained. (1) In terms of age, one point before the age of 50, two points from 50 to 60, and three points above the age of 60 are counted. (2) There were 10 items on the SAS and SDS scales, which both used the four-grade scoring approach, and disease quantification was assessed using the SAS and SDS scales. The total scores were 100 points. A lower score indicated a milder anxiety or depression. Mild anxiety or depression 50–60 points were scored as one point, moderate anxiety or depression 61–70 points were scored as two points and >70 points were scored as three points. (3) Quantification of combined diseases: 1 point without complications, 2 points with one disease, and 3 points with more than two diseases. (4) The total scores of low-risk nursing patients undergoing surgery were <4 points, with medium-risk of 4–6 points and high-risk of >6 points. The grades were N1, N2, and N3 according to the nurse's title, seniority, and nursing skills. Patients with low risk of surgery, equipped with N1
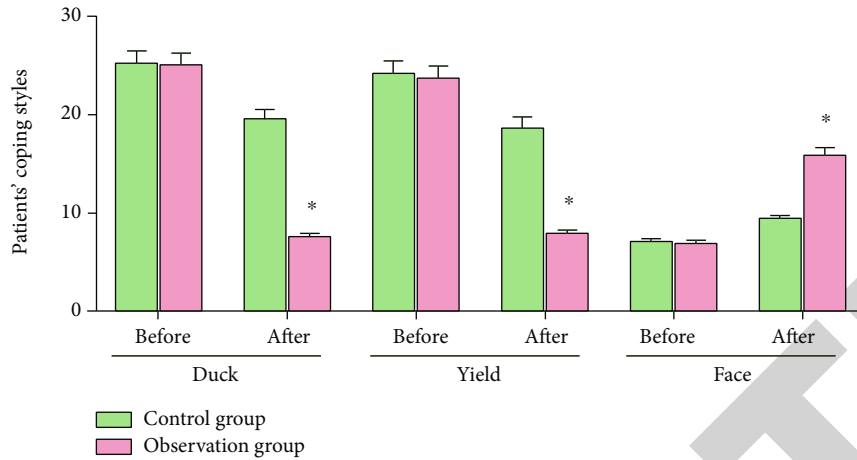
FIGURE 3: Patients' coping styles between the two groups. Compared with control group, $^*P < 0.05$, the differences were statistically significant.

TABLE 5: Comparison of pain levels between the two groups ($\bar{x} \pm s$).

Group		Control	Observation
NRS	Before	6.29 ± 1.12	6.36 ± 1.04
	After	4.52 ± 1.01	2.18 ± 0.43
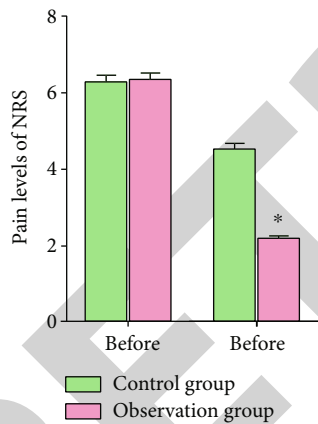
FIGURE 4: Pain levels between the two groups. Compared with control group, $^*P < 0.05$, the differences were statistically significant.

level nurses, nurse-patient ratio of 1 : 2. Patients at risk during the operation were equipped with N2-level nurses, and the ratio of nurses to patients was 1 : 1. High-risk patients undergoing surgery were equipped with N3-level nurses, and the nurse-patient ratio was 2 : 1. During the implementation, the nurses were evaluated and adjusted according to the timely feedback information

(2) *Preoperative Cognitive Intervention.* Knowledge seminars and health handbooks were used to explain the disease-related knowledge and treatment plan to the patients. The medical staff explained the possible dis-

comfort during the operation and the possible complications after operation to the patient with the help of videos and pictures and issued the certificate, with emphasis on the effect of the operation on his physiological function. Spouse is an important participant in patient education. While educating and educating patients, medical staff explained the care methods and related knowledge of female reproductive system to the spouse, in order to reduce the psychological burden of the patient's spouse and encourage them to care for the patient

(3) *Intraoperative Care.* Cooperate with the surgeon in skin preparation, posture placement, device link, and pipeline examination, and cooperate with the anesthesiologist in the anesthesia, ventilator, and other device examinations. Patients' vital signs were closely observed during the operation, and the parameters of various instruments were adjusted timely according to needs. After the operation, cooperate with the doctor for instrument inspection, assist the doctor for disinfection and incision suture, etc. Meanwhile, the mental state and vital signs of the patients after anesthesia and sobriety were observed

(4) *Postoperative Care.* Cooperate with the doctor to check the placement of drainage tube and drainage, and record the pain of the patients as well as the use of analgesic pump after operation. The postoperative precautions were informed, and the patients were advised to choose their favorite exercise mode and take reasonable exercise every day to enhance physical strength. The exercise time was controlled at 20 min, and it was conducted twice a day

(5) *Psychological Intervention.* Nursing staff chose an appropriate time every day to communicate with the patients and their families to understand the root causes of negative emotions in patients. It was shown that hypnosis, image dialogue therapy, cognitive

therapy, and other methods were effective in helping patients destress and unwind in order to alleviate symptoms of stress, such as anxiety and depression. As well as being educated on how their emotional state affects the treatment of sickness, so that they could understand that the good or bad mood directly affected the prognosis and subsequent treatment. In addition, patients are taught some psychological adjustment methods to guide relaxation training and to enter a relaxed state consciously by feeling the difference between muscle tension and relaxation. Medical staff organized patients with similar symptoms to participate in the communication meeting so as to encourage and help each other and give full play to the peer effect. During this period, medical staff also need to do a good job in the ideological work of their families, to guide them to play their due role of supervision and accompanying them, to affect the patients with their own optimistic state, and to enable the patients to deal with the treatment in a positive attitude

2.4. Serum Test. All patients collected 5 mL of venous blood in the morning on an empty stomach and allowed to stand at room temperature for half an hour. When serum appeared in their layers, they were placed in a centrifuge, and the upper layer of serum was sucked after centrifuging at a speed of 3000 r/min for 10 minutes. The test samples were stored in a refrigerator at −80°C. Cortisol was determined by radioimmunoassay, and epinephrine was determined by immunofluorescence assay.

2.5. Observational Index

(1) In terms of perioperative indicators, the two groups were compared in terms of operation time, intraoperative bleeding volume, and hospital stay

(2) The stress levels of the two groups were evaluated before and 24 hours after the operation. Psychological and physical indicators are also included. Cortisol and epinephrine levels were measured using the SAS and SDS scores to examine psychological and physiological signs

(3) A comparison of the two groups' coping styles before and 24 hours after surgery was made. Medical coping model questionnaire (MCMQ) was used. The questionnaire consisted of three dimensions of avoidance (7 items), submission (6 items), and facing (7 items), with a total of 20 items. Each item adopted a 4-level scoring system, which represented that it had never been like this, sometimes like this, often like this, and always like this. The higher score indicated that patients were more inclined to the coping style of this item

(4) Prior to and 24 hours after surgery, both groups were tested for pain levels. Each patient's level of pain was evaluated using the numerical rating scale (NRS),

with 0 denoting no pain at all and 10 denoting the most painful and extreme agony

2.6. Statistical Analysis. SPSS22.0 statistical software was used to conduct the analysis. They employed the t-test to compare the groups based on the mean standard deviation of the measurement data ($\bar{x} \pm s$). The percentage (percent) and number (N) of enumeration data were compared using the χ^2 test. The difference was deemed statistically significant at <0.05.

3. Results

3.1. General Material. As indicated in Table 1, there was no significant difference between the two groups in terms of age, TNM stage, and pathological type ($P > 0.05$).

3.2. Perioperative Indicators of Patients. There was a statistically significant difference ($P < 0.05$) in perioperative markers such operation duration, intraoperative bleeding volume, and total hospital stay between the observation group and the control group, as shown in Table 2 and Figure 1.

3.3. Stress Indicators of Patients. Following surgery, patients' SAS and SDS ratings were lower in both groups than they were before to surgery, as indicated in Table 3, the observation group's scores were lower than the control group, which had a statistically significant difference ($P < 0.05$). In terms of physiological indicators, the postoperative observation group's cortisol and epinephrine levels were lower than those in the control group, and the postoperative two groups' levels were higher than those prior to surgery in the two postoperative groups. $P < 0.05$ was the threshold for statistical significance in this study, as shown in Table 3 and Figure 2.

3.4. Two Groups of Patients' Coping Styles. Before surgery, there were no significant differences in the two groups' coping methods ($P > 0.05$). The avoidance and yielding item scores of the observation group were lower than those of the control group, however, the facing item scores of the observation group were higher than those of the control group. Table 4 and Figure 3 show that the differences were statistically significant. Cores are between the observation and control groups.

3.5. Pain Severity in Two Groups. Both groups saw no significant differences in discomfort prior to surgery ($P > 0.05$). Table 5 and Figure 4 show that after the operation, there was a statistically significant ($P < 0.05$) difference in NRS scores between the observation and control groups.

4. Discussion

At present, for patients with early endometrial cancer clinically, surgical resection is generally adopted to avoid the lesions from further development. There are numerous advantages to laparoscopic surgery, including reduced trauma. However, since the operation involved reproductive

organs, and the patients' immune function was lower than that of the healthy ones, there was a certain operation risk. At this time, bad emotions and body damage would easily induce stress response in the body [8]. Excessive stress response will destroy the endocrine and nervous system balance of patients, affecting the surgical effect and subsequent rehabilitation. Obviously, simple routine care can no longer solve such problems.

Studies have shown that developing targeted care programs based on patients' disease characteristics can reduce patients' anxiety and depression during the operation and urge patients to actively cooperate with medical work during the operation [9]. Quantitative nursing in operation rooms is a brand-new clinical nursing mode, in which the nursing plan is reasonably formulated based on the patient state, standardized, and quantified evaluation and classification, as a means to improve the overall prognosis of the patient by increasing their participation with surgery and decreasing their perioperative trauma psychologically and physiologically [10]. For patients undergoing laparoscopic surgery to remove uterine fibroids, clinical trials have indicated that a nursing intervention in the operating room improves both the surgical outcomes and the patients' emotional well-being. Other studies have demonstrated that psychological assistance in patients having laparoscopic resection can improve their psychological condition and stabilize their vital signs [11, 12].

According to the findings of this study, the observation group's perioperative indicators, such as operating time, the amount of blood lost during surgery, and the length of time the patient spent in the hospital, were both less than in the control group. It has been found that endometrial cancer patients who got quantitative nursing during surgery in addition to psychological assistance recovered more quickly. It was analyzed that in the present study, nurses with different qualifications and nursing skills were assigned to patients of different grades through quantitative classification of age, disease status, and combined diseases of endometrial cancer patients; and targeted intervention [13] was conducted to enable patients to receive treatment with an understanding of endometrial cancer and the process of laparotomy, ensure that patients with different psychological states and conditions can receive professional care, eliminate fear of diseases and surgery, and enhance confidence in coping with the discomfort caused by surgical trauma, so that they can actively receive treatment, improve the treatment effect, and promote the stable improvement of the condition [14].

According to reports, when the mental state of the human body is in extreme conditions, such as anxiety, depression, or excessive tension, the sympathetic nerve will be overexcited, causing the release of excessive catecholamine, promoting the increase of cortisol and epinephrine levels, and resulting in the excessive increase or decrease of heart rate and blood pressure [15, 16]. It has been noted that psychological intervention may be able to lower the body's stress reaction by inhibiting the natural defense system's increase in adrenocortical hormone. Both groups' SAS and SDS scores were lower after surgery than they were before, but the observation group's scores were lower than those

of the control group, and the differences were statistically significant. All three groups had higher levels of cortisol and epinephrine after surgery than before, indicating that they had been exposed to more stress than their presurgical counterparts. Statistically significant differences were found. Patients undergoing laparoscopic surgery for endometrial cancer could benefit from quantitative nursing in the operating room, as well as psychosocial counseling, according to the study. The analysis showed that some extreme emotions such as fear and anxiety were avoided through popularization of disease-related knowledge, correction of patients' wrong cognition, and establishment of correct concept of treatment during nursing [17]. In addition, psychological counseling is conducted for the patients to achieve the optimal psychological state as much as possible so as to regulate the hypothalamic and adrenal sympathetic nervous system of the patients and reduce the massive secretion of cortisol and adrenocortical hormone in the body caused by negative emotions, thereby avoiding stress response to a great extent [18].

Research has shown that when patients develop fear of death due to lack of understanding of cancer, they are prone to develop cancer-related fatigue and adopt such methods as "avoiding" and "yielding" to cope with the disease. The above two coping methods not only aggravate the negative emotions of patients but also lead to physiological discomforts such as pain, aggravate the development of the disease, and lead to the decline of patients' life quality [19]. A lower avoidance and yield item score in the observation group after surgery, as well as a significantly higher face item score, was seen in comparison to the control group. Endometrial cancer patients who received quantitative nursing in the operating room as well as psychological assistance improved their coping methods following laparoscopic surgery, according to these findings. The analysis suggests that the quantitative nursing in operation room combined with psychological intervention can promote the patients to affirm their life values and stimulate their positive potentials [20] by improving their treatment concepts and giving them the confidence to fight against diseases and face treatment actively with the help of spouse's encouragement and family support, thus alleviating the loneliness caused by illness and enabling patients to correctly treat the physiological reactions caused by diseases with an optimistic attitude, thus avoiding the states of avoidance and submission, and thus becoming stronger [21].

The experimental group's postoperative NRS scores were much lower than those of the controls, despite the fact that preoperative pain levels did not differ significantly between the two groups, and this difference was statistically significant. Preoperative pain levels did not change substantially between the two groups; however, postoperative NRS scores were markedly lower in the experimental group compared to controls, indicating a meaningful effect of surgery. It was analyzed that quantitative nursing in operation room combined with psychological intervention helped patients to be willing to face the disease directly, and the state of patients at this time was extremely beneficial to the implementation of various medical operations, equivalent to improving their

treatment compliance, and beneficial to transferring patients' attention to pain and reducing their pain perception [22]. In addition, after the patients have a certain understanding of disease management, some wrong behavior patterns can be avoided as far as possible to greatly reduce the generation of additional pain, wherein the prognosis is much enhanced [23, 24].

The combination of quantitative nursing and social psychological intervention in operating room is a new nursing model that appears with the rapid development of psychology. It affects the psychological state of patients through various nursing and psychological means, so as to achieve the purpose of creating a good psychological environment for treatment and rehabilitation for patients. The research results show that the team nursing after the SAS and SDS scores was lower than the control group, indicating that the operating room quantitative nursing combined with social psychological intervention can effectively relieve patients with endometrial cancer perioperative anxiety and depression, and the quantitative results show the operating room nursing combined with social psychological intervention to improve the patients quality of life also have certain help, this is for In psychological care is also a kind of comprehensive care, its targeted psychological counseling to patients at the same time, also other factors that is likely to affect the psychological status of patients with nursing intervention, so as to reduce the patients fear of the unknown, to guide the patient is distracting to avoid overly concerned about their disease patients, and families with help to urge patients to feel from the family Care. This study also has obvious clinical application value. However, the sample size of this study is small, and the survival rate of patients has not been determined, so the results have certain limitations, and it is necessary to further accumulate the sample size to conduct in-depth research.

Data Availability

The data used to support the findings of this study are available from the corresponding author upon request.

Conflicts of Interest

The authors declare that they have no conflicts of interest.

Acknowledgments

References

[1] D. W. Doo, K. G. Essel, M. H. Vetter et al., "The effect of adjuvant therapy for high intermediate-risk endometrial cancer on patients with recurrent disease," *Gynecologic Oncology*, vol. 153, no. 3, pp. 6-7, 2019.

[2] T. S. Lee, J. Y. Jung, J. W. Kim et al., "Feasibility of ovarian preservation in patients with early stage endometrial carcinoma," *Gynecologic Oncology*, vol. 104, no. 1, pp. 52–57, 2007.

[3] W. Guo, J. Cai, M. Li, H. Wang, and Y. Shen, "Survival benefits of pelvic lymphadenectomy versus pelvic and para-aortic lymphadenectomy in patients with endometrial cancer," *Medicine*, vol. 97, no. 1, pp. 9520–9520, 2018.

[4] M. Bazzi, I. Bergbom, and M. Hellstrom, "Team composition and staff roles in a hybrid operating room: a prospective study using video observations," *Nursing*, vol. 6, no. 3, pp. 1245–1253, 2019.

[5] C. Wang, J. Chen, Y. Wang et al., "Effects of family participatory dignity therapy on the psychological well-being and family function of patients with haematologic malignancies and their family caregivers: a randomised controlled trial," *International Journal of Nursing Studies*, vol. 118, p. 103922, 2021.

[6] K. J. Eoh, E. J. Nam, S. W. Kim et al., "Nationwide comparison of surgical and oncologic outcomes in endometrial cancer patients undergoing robotic, laparoscopic, and open surgery: a population-based cohort study," *Cancer Research and Treatment*, vol. 53, no. 2, pp. 549–557, 2021.

[7] P. Cybulska, M. B. Schiavone, B. Sawyer et al., "Trocar site hernia development in patients undergoing robotically assisted or standard laparoscopic staging surgery for endometrial cancer," *Gynecologic Oncology*, vol. 147, no. 2, pp. 371–374, 2017.

[8] N. Lucic, D. Draganovic, S. Sibincic, V. EcimZlojutro, and S. Milicevic, "Myometrium invasion, tumour size and lymphovascular invasion as a prognostic factor in dissemination of pelvic lymphatics at endometrial carcinoma," *Medical Archives*, vol. 71, no. 5, pp. 325–329, 2017.

[9] K. Hongmei, "The role of fine nursing in improving the safety management of operating room," *Journal of Medicine*, vol. 41, no. 3, pp. 207-208, 2019.

[10] T. F. Wei, "Study on the application effect of detail nursing in operating room to ensure the safety of operating room nursing," *Journal of Clinic Medicine Literature*, vol. 6, no. 44, pp. 123-124, 2019.

[11] J. Safdieh, Y. C. Lee, A. Wong et al., "A comparison of outcomes between open hysterectomy and robotic-assisted hysterectomy for endometrial cancer using the national cancer database," *International Journal of Gynecological Cancer*, vol. 27, no. 7, pp. 1508–1516, 2017.

[12] D. C. Ding, T. Y. Chu, and H. W. Liu, "Reciprocal crosstalk between endometrial carcinoma and mesenchymal stem cells via transforming growth factor-β/transforming growth factor receptor and C-X-C motif chemokine ligand 12/C-X-C chemokine receptor type 4 aggravates malignant phenotypes," *Oncotarget*, vol. 8, no. 70, pp. 115202–115214, 2017.

[13] Q. H. Guo, H. M. Chochinov, S. McClement, G. Thompson, and T. Hack, "Deve-lopment and evaluation of the dignity talk question framework for palliative patients and their families: a mixed-methods study," *Palliative Medicine*, vol. 32, no. 1, pp. 195–205, 2018.

[14] G. Kaur, G. Kumari, and S. Sharma, "Functional matrix hypothesis: a review of literature," *Surface Plasmon Resonance*, vol. 1, no. 2, pp. 33–42, 2021.

[15] A. von Heymann-Horan, P. Bidstrup, M. B. Guldin et al., "Effect of home-based specialised palliative care and dyadic psychological intervention on caregiver anxiety and depression: a randomised controlled trial," *British Journal of Cancer*, vol. 119, no. 11, pp. 1307–1315, 2018.

[16] L. A. Johnson, A. M. Schreier, M. Swanson, J. P. Moye, and S. H. Ridner, "Stigma and quality of life in patients with advanced lung cancer," *Oncology Nursing Forum*, vol. 46, no. 3, pp. 318–328, 2019.

Research Article

IOT-Based Medical Informatics Farming System with Predictive Data Analytics Using Supervised Machine Learning Algorithms

Ashay Rokade [ID],[1] Manwinder Singh [ID],[1] Sandeep Kumar Arora [ID],[1] and Eric Nizeyimana [ID][2]

[1]*School of Electronics and Electrical Engineering, Lovely Professional University, Punjab, India*
[2]*College of Science and Technology, University of Rwanda, Rwanda*

Correspondence should be addressed to Manwinder Singh; manwinder.25231@lpu.co.in,
Sandeep Kumar Arora; sandeep.16930@lpu.co.in, and Eric Nizeyimana; nizerik@yahoo.fr

In the farming industry, the Internet of Things (IoT) is crucial for boosting utility. Innovative agriculture practices and medical informatics have the potential to increase crop yield while using the same amount of input. Individuals can benefit from the Internet of Things in various ways. The intelligent farms require the creation of an IoT-based infrastructure based on sensors, actuators, embedded systems, and a network connection. The agriculture sector will gain new advantages from machine learning and IoT data analytics in terms of improving crop output quantity and quality to fulfill rising food demand. This paper described an intelligent medical informatics farming system with predictive data analytics on sensing parameters, utilizing a supervised machine learning approach in an intelligent agricultural system. The four essential components of the proposed approach are the cloud layer, fog layer, edge layer, and sensor layer. The primary goal is to enhance production and provide organic farming by adjusting farming conditions as per plant needs that are considered in experimentation. The use of machine learning on acquired sensor data from a prototype embedded model is investigated for regulating the actuators in the system. Then, an analytics and decision-making system was built at the fog layer, employing two supervised machine learning approaches including classification and regression algorithms using a support vector machine (SVM) and artificial neural network (ANN) for effective computation over the cloud layer. The experimental results are evaluated and analyzed in MATLAB software, and it is found that the classification accuracy using SVM is much better as compared to ANN and other state of art methods.

1. Introduction

Data gathering and using data to inform practical farming decisions is undergoing a significant agricultural revolution. Intelligent culture is the request of modern news and ideas of technology (ICT) in farming, to degree machine intelligence algorithms, and the rationalization of raw material use, as a capital-located system and state-of-the-art electronics in drink farming in tenable and environmentally intimate habits. Innovative technologies are helping the plurality of people everywhere the experience in a type of ways. The Internet of Things (IoT) and dossier data, such as grown dossier data and data learning, are immediately playing a more and more critical duty in people's everyday lives, admitting them to change their environment more surely [1–3]. In general, IoTs and data reasoning are secondhand in the agromodern and environmental subdivisions for two together diagnostics and control of brilliant culture arrangements, to provide essential facts to the final laborer and services about the footing and properties of agroproduction and structures [4–6]. Figure 1 shows the overview of IoT-based smart agriculture factors.

Machine learning is being used to regulate actuators' intelligence. The algorithm uses data acquired about the plants' climatological and soil conditions to advise the farmer on what should be done efficiently. IoT is also

utilized to collect sensor data from the field so that the data and ML algorithm recommendations may be made available on a UI platform, making it easier to keep track of the field in real time. In intelligent farming, supervised machine intelligence algorithms are used to create predictions on dossier acquired by sensors and to deliver agriculture solutions. The utilization of IoT devices gives an automatic data prediction solution. The obtained results will assist the farmer in making an informed decision [6, 7]. The proposed technology will boost system efficiency and forecast superior intelligence control options. The plant's growth will be affected by changing climatic circumstances in agriculture, resulting in a lower yield after the cultivation. As a result, environmental sensing parameters such as greenhouse gases, temperature, soil moisture, and light must all be maintained and monitored. This issue could be solved by implementing an Internet of Things (IoT) innovation in intelligent agriculture, which entails the precise application of certain greenhouse factors for optimal plant development, such as temperature management, water flow control, and light radiation, among other things [8, 9]. The main contributions of the paper are as follows.

(i) Develop efficient analytics and decision-making model which can be used for precise and intelligent farming using supervised machine learning

(ii) Design of a four-layer framework for IoT-based intelligent farming system that can support the deployment of the low-cost farming system with intelligent solutions

(iii) Presented a case study on adoption of IoT and data analytics on two greenhouse plants, Gerbera and Broccoli

(iv) Evaluate the proposed analytics and decision-making model based on supervised machine learning performances through different experiment

The rest of the paper is organized as follows: In Section 2, the related work regarding intelligent model using various data analytic algorithms is discussed. The details of proposed intelligent farming framework are presented in Section 3. Section 4 describes an experimental evaluation with results. Section 5 finally presented conclusions towards proposed scheme.

2. Literature Review

Several researchers have developed an intelligent agriculture system with predictive intelligence for various applications. The summaries of those papers are listed below.

Suma [5] gives a survey of predicting analysis, Internet of Things (IoT) designs accompanying cloud presidency, and security wholes for multibreeding in the farming area, all while taking into account farmers' previous experiences. It also emphasizes the difficulties and issues that might be expected when incorporating contemporary technologies into traditional farming practices. For adequate decision
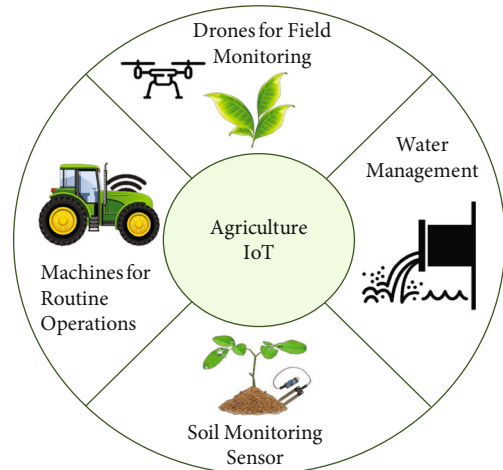
Figure 1: Overview of an agriculture IoT [1].

support in IoT-based intelligent farming systems, Rezk et al. [6] propose an IoT-located intelligent production system linked with an effective prediction means called WPART established machine intelligence techniques to think crop productivity and dryness. Araby et al. [7] used a sensor network to collect field data from a variety of crops (potatoes, tomatoes, and so on). They before shipped the dossier to a machine-education invention to produce a warning meaning before effecting both the dossier and the warning communication by way of a graphical user interface (GUI). Several machine learning techniques have been built by Tageldin et al. [8] to predict plant infestation with CLW. The current research established a framework for machine learning to forecast CLW infestation in greenhouse plants. Aliar et al. [9] present a complete analysis of the various intelligent farming methods and architectures. It also examines various designs in depth and suggests acceptable solutions to today's intelligent farming issues. Sethy et al. [10] projected an arrangement that uses deep knowledge and IoT to monitor paddy fields by chance. The VGG16 preprepared network is being surveyed for paddy leaf ailment discovery and nitrogen rank belief. Kaushik et al. [11] propose an intelligent agriculture method that monitors the agricultural field and can help farmers increase productivity significantly. Siddiquee et al. [12] projected an IoT-based creative agriculture listening system accompanying different algorithms for discovery, quantification, adulthood testing, and diseased produce detection.

Nourelhouda et al. [13] developed and deployed a ground-breaking wireless mobile robot that uses the Internet of Things (IoT) to conduct a range of outdoor chores. More precise and efficient data, as well as a reduction in the workforce, are among the benefits of this endeavor. Sekaran et al. [14] grew a structural foundation that integrates the Internet of things (IoT) accompanying crop results, utilizing cloud estimating to monitor crops using different measures and orders. The procedure supplies a certain-time dossier study from sensors established in crops and produces a result for the grower, which is necessary for crop progress listening and saves the grower's time and strength. The concept of
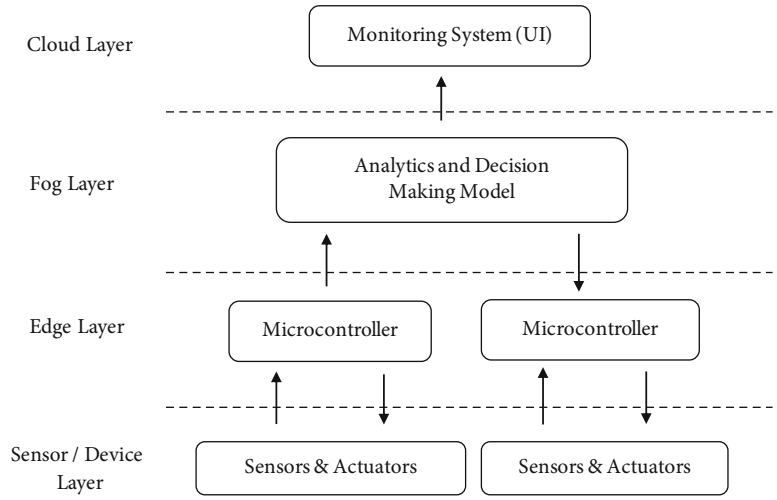
Figure 2: Intelligent farming framework for greenhouse management.
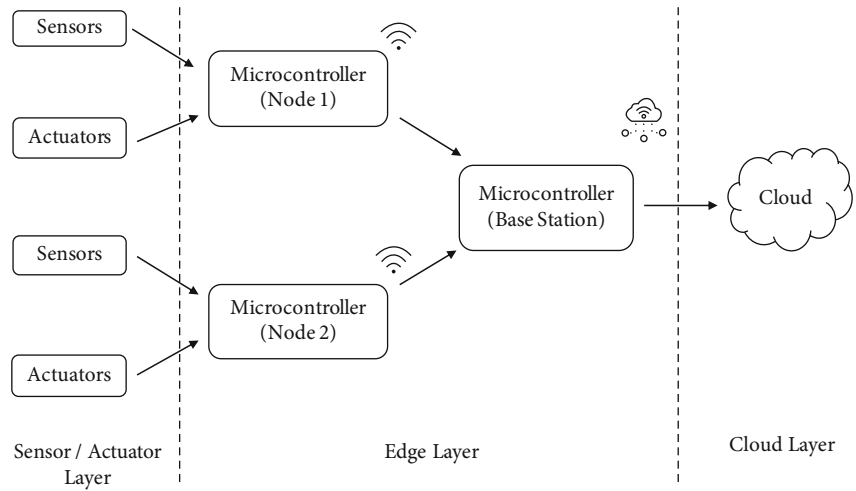
Figure 3: Proposed framework for acquisition of data in the greenhouse environment.
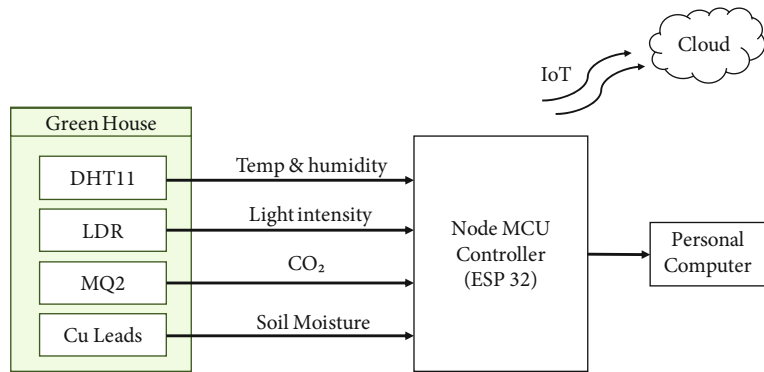
Figure 4: Proposed experimental model.
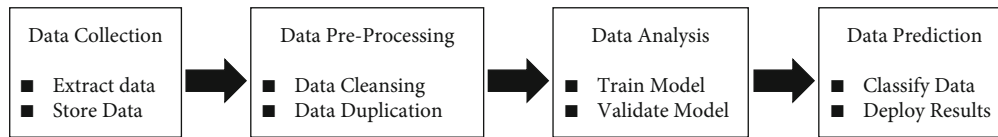
Figure 5: Analytics and decision-making model.
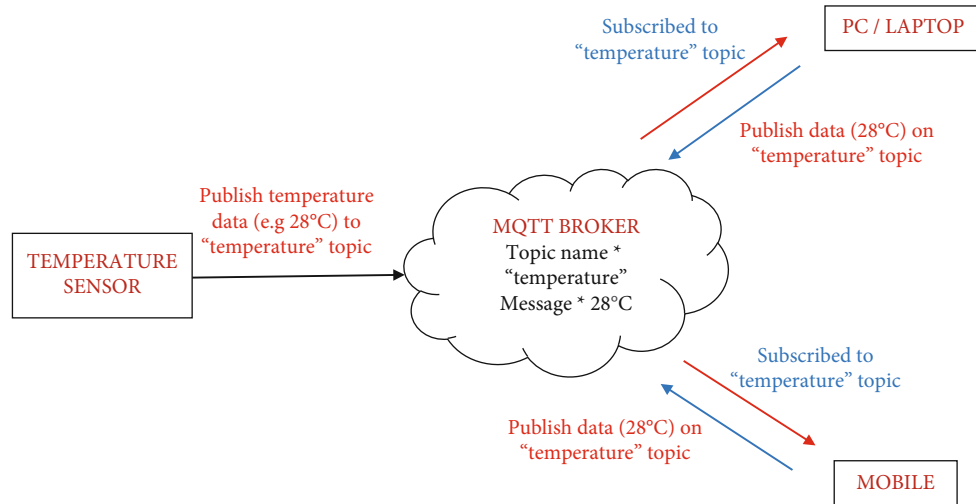
Figure 6: Workflow of MQTT for sensor data.

Input:
"Features Set"
Input (CO_2 gas level (ppm), soil moisture (percent), light intensity (lux), humidity (percent), temperature (Celsius))
Output (on/off pump, on/off ventilation fan, low/medium/high amount of light)
Output:
Predicted output with label values.
Procedure:
Step 1: Collect and prepare the feature data and label data from raw dataset values from datasets.
Step 2: apply feature engineering to each feature data, find the missing and unknown values, replace the mean values, calculate the normalized value of all feature set, and scale all feature data into a specific range.
Step 3: select the machine learning model for classification, SVM, and MLP
Step 4: choose the range of possible values for hyperparameters of ML algorithms.
Step 5: optimize the values of the hyperparameters using the Grid Search CV Optimization algorithm.
Step 6: evaluate and find the best score and estimator for the selected classifier.
Step 7: validate the model using the K-fold validation learning method.
Step 8: set best-selected hyperparameters tuned for the ML training process.
Step 9: initialize the feature data and label data for the training dataset.
Step 10: train the model for respective ML algorithms.
Step 11: validate the model performance using the K-fold crossvalidation method.
Step 12: if validation is successful, then save/deploy the trained model, and if not, repeat from steps 2 or 8.
Step 13: initialize the feature data for the testing dataset.
Step 14: load the trained model of ML algorithms.
Step 15: predict the results for its label values (classification).
Step 16: evaluate system performance using a confusion matrix.

Algorithm 1: Proposed algorithms.
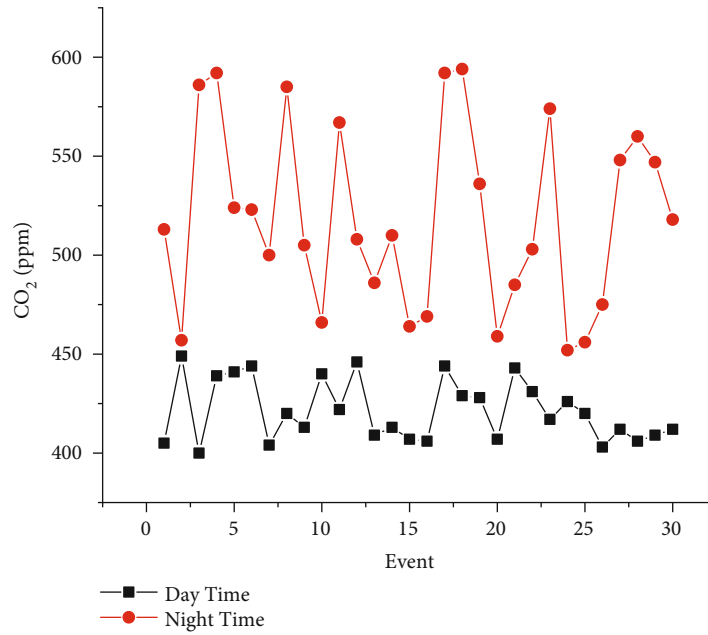
Figure 7: Day and night time CO_2 representation.
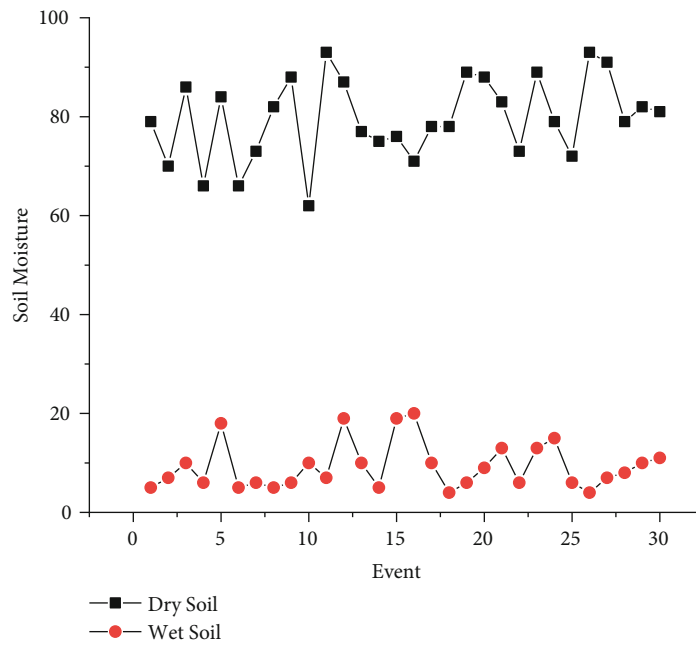
Figure 8: Dry and wet soil moisture representation.

security and privacy in cloud computing can be implemented to design prototype for cloud layer devices [15–17]. and the demonstration of space time coding for MDL mitigation and capacity enhancement of FTS gives right direction for transmission criteria [18–20].

Kaur et al. [21] specify a scheme for capably monitoring and ruling abundant crop progress and result in limits. The system also engages machine intelligence and the Internet of Things (IoT) to predict crop yield. Liu [22] integrates the needs of knowledgeable agriculture complete happening to create an inventive farming floor based on Internet of Things electronics and machine intelligence, in addition to designing experiments to verify the policy's acting. Sharma et al. [23] grew a strategy that may be used to boost livestock productivity by predicting reproductive patterns, detecting consuming problems, and envisioning cow behavior using machine intelligence models and dossier from collar sensors, among other things. Lela Madhav and Sandeep [24] investigated a variety of machine learning algorithms, each with its own set of advantages and disadvantages ranging from the
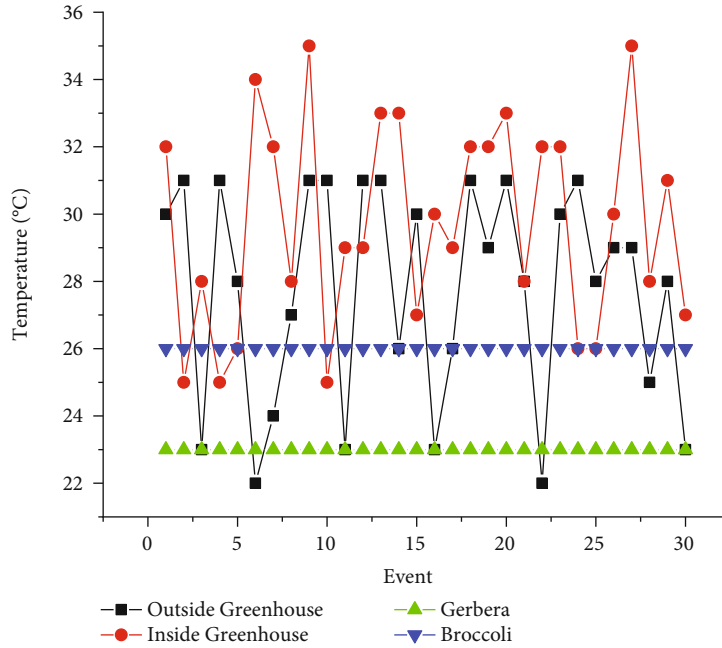
FIGURE 9: Outside and inside greenhouse temperature representation.
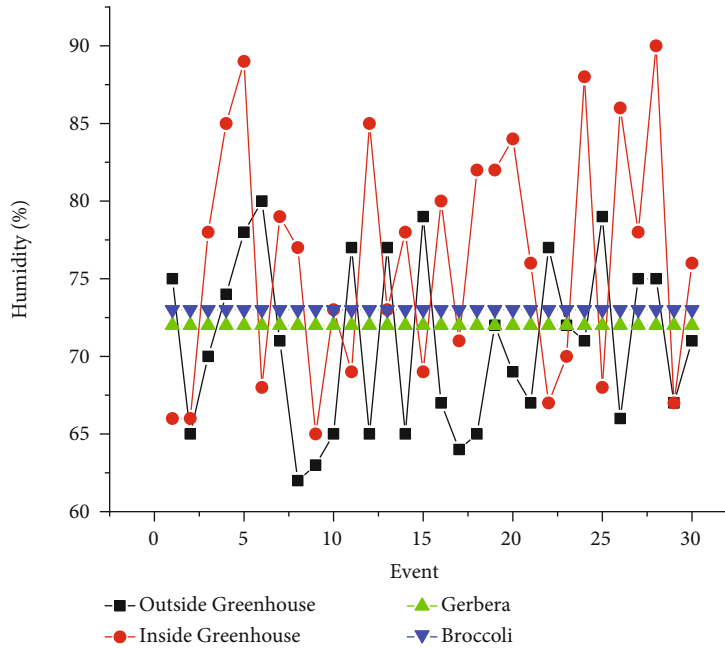
FIGURE 10: Outside and inside greenhouse humidity representation.

process to the final product. To get the most out of the model utilized, the user must first comprehend each model before implementing it to their application. Mekonnen et al. [25] provide a thorough examination of several machine learning algorithms in sensor data analytics in the agricultural environment. Perales Gómez et al. [26] detail a novel design for continuous land crop value listening established IoT and machine learning/deep learning technologies. Perales Gómez et al. [27] characterize an intelligent culture

arrangement for crop production, namely, buxom on low-cost IoT sensors and common data storage and dossier science of logical analysis services connected to the Internet of Things Yang and Xu et al. [28] help and guide researchers in completely comprehending the strengths and potential drawbacks of deep learning in the horticultural sector. Cafuta et al. [29] present a whole replacement sensor dossier information with machine intelligence for plant well-being belief. Estimating plant strength admits for more
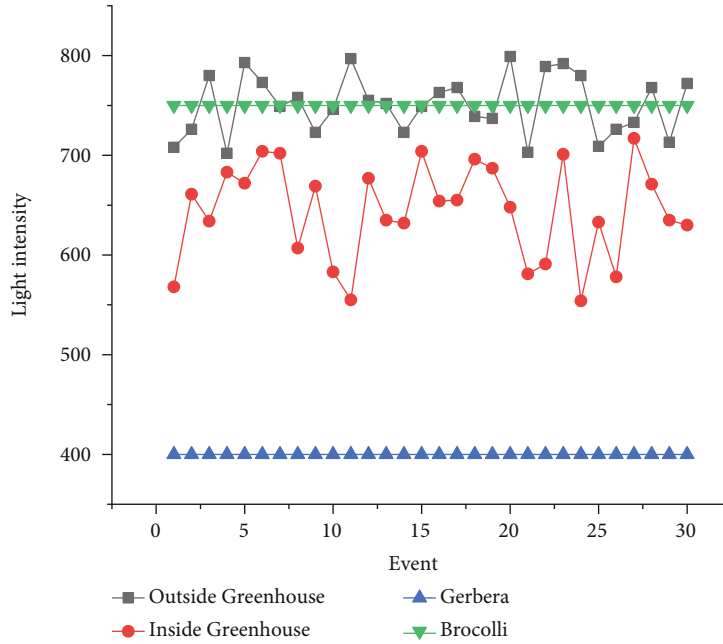
FIGURE 11: Outside and inside greenhouse light intensity representation.

TABLE 1: Hyperparameter tuning for classifier modeling.

Prediction algorithm	Model parameters	Range searched	Range selected
SVM classifier and regressor	Kernel	rbf, poly, sigmoid	Poly
	max_iter	10, 30, 50	10
MLP classifier and regressor	hidden_layer_size	10, 50, 100	100
	max_iter	100, 200, 300	200

comprehensive ebb periods and raises the nutritional content of the things produced. The fundamental goal of this case study, according to Bakthavatchalam et al. [30], is to evolve a model that forecasts extreme yield crops and precision farming. The projected method posing incorporates contemporary science, the Internet of Things, and farming's detracting measurements. Khalaf et al. [31] have given the efficiencies in cognitive radio enable 5G network which guarantees the use of 5G network to enhance system performance. Walia et al. [32] have emphasized on localization of dynamic wireless sensor networks. Singh et al. [33] give a brief idea about the energy-efficient cognitive body area network. Hassan et al. [34] proposed a survey for data sharing techniques for 5G. A. Rokade and Singh [35] give a brief analysis of intelligent farming techniques which helps us to propose a sustainable intelligent farming model. A. Kadu and Singh [36] emphasize on distinguish data analysis for telemedicine systems which describes the uses of IoT and machine learning. Hassan et al. [37–39] focus on the cognitive radio networks for improvement of capacity rate in 5G. Roy at el. [40] proposed a filter model for system enhancement. Moreover, the clustering technique can also be followed for the collection and aggregation of data, and data can be filtered through machine learning algorithms

[41–46]. As part of the industry's technological progress, Teferaa et al. [47] emphasize emerging different automation approaches such as IoT, wireless communications, machine learning, artificial intelligence, and deep learning. Ha et al. [48] described a set of modern sensing applications that use machine learning-enabled intelligent sensor systems. In an intelligent greenhouse, Jin et al. [49] offer a bidirectional self-concentrating encoder-translator framework (BEDA) to build a seasoned prophet for numerous material limits with important nonlinearity and turbulence. Akhter et al. stated that [50] secondhand dossier data and machine intelligence in an IoT system to present an indicator model for Apple ailment in the sphere gardens of Kashmir basin. Quy et al. [51] judge the architecture (IoT designs, communication sciences, ample data conversion, and transform), applications, and research schedule of IoT-enabled brainy agriculture environments. The IoT ecosystem is described by Elijah et al. [52], who show how the integration of IoT and DA is enabling intelligent agriculture.

3. Methodology

3.1. Proposed Framework. The proposed intelligent farming system model for greenhouses is depicted in figure 2. The
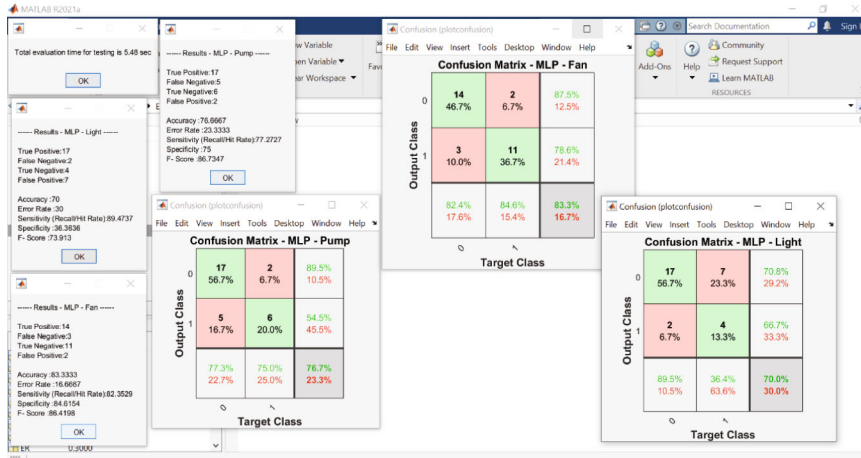
Figure 12: Classification approach result and confusion matrix MLP.
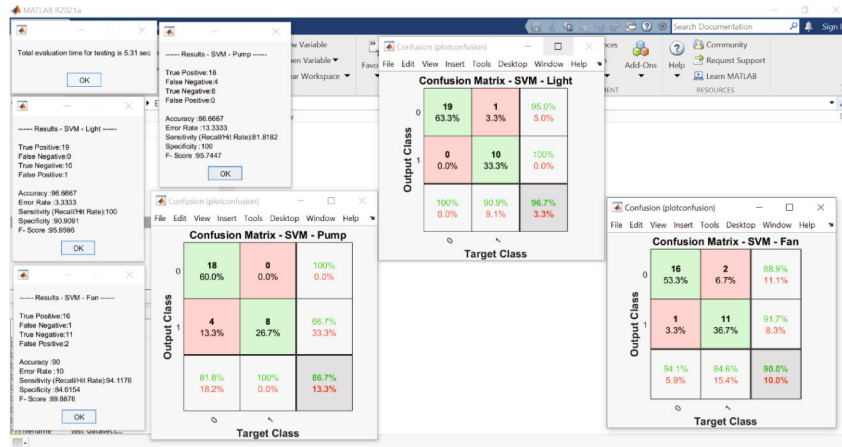
Figure 13: Classification approach result and confusion matrix SVM.

Table 2: Performance evaluation of classification model.

Attributes	Accuracy (%)		Sensitivity (%)		Specificity (%)		F-score (%)	
	SVM	MLP	SVM	MLP	SVM	MLP	SVM	MLP
Pump	86.66	76.66	81.81	77.27	100	75	95.74	86.73
Light	96.66	70	100	89.47	90.90	36.36	95.95	73.91
Fan	90	83.33	94.11	82.35	84.61	84.61	89.88	86.41

four basic architectural layers are the cloud layer, fog layer, edge layer, and sensor/device layer. The sensor layer includes the various sensors and actuators related to the field environment. The edge layer mainly consists of controller unit to which various sensors and actuators are interfaced for data acquisition and sending to fog layer for further process. The main objective of the fog layer is developing the analytics and decision-making model based on data acquired from the edge layer and provide the control signals to the edge layer for controlling of actuators. And finally, data represen-

tation of sensors and actuators is displayed on the cloud layer in the form of user interface (UI) dashboard. The suggested system is notable for its ability to assist farmers by providing greenhouse management using an IoT-based precision farming framework. The purpose is to supply agriculturists with remotely controlled greenhouse agricultural elements such as soil moisture, CO_2, light, and temperature from afar, and depending on the soil moisture values, a controlling move for the greenhouse doors/windows to roll off/ on may be made. Agriculturists are unable to visit the fields as a result of this physically.

3.1.1. Sensor Layer. In this experiment, Gerbera and Broccoli are the crops that considered in the greenhouse, which is primarily a climate-sensitive environment. The sensors used to monitor factors in the greenhouse environment include a gas sensor, a dht11 sensor for temperature and humidity, a light sensor, a gas sensor, and a moisture sensor. Actuators will be chosen and deployed to control equipment such as fans and pumps by relaying parameters. Controlled RH, temperature, light, protection from rain, storms, and
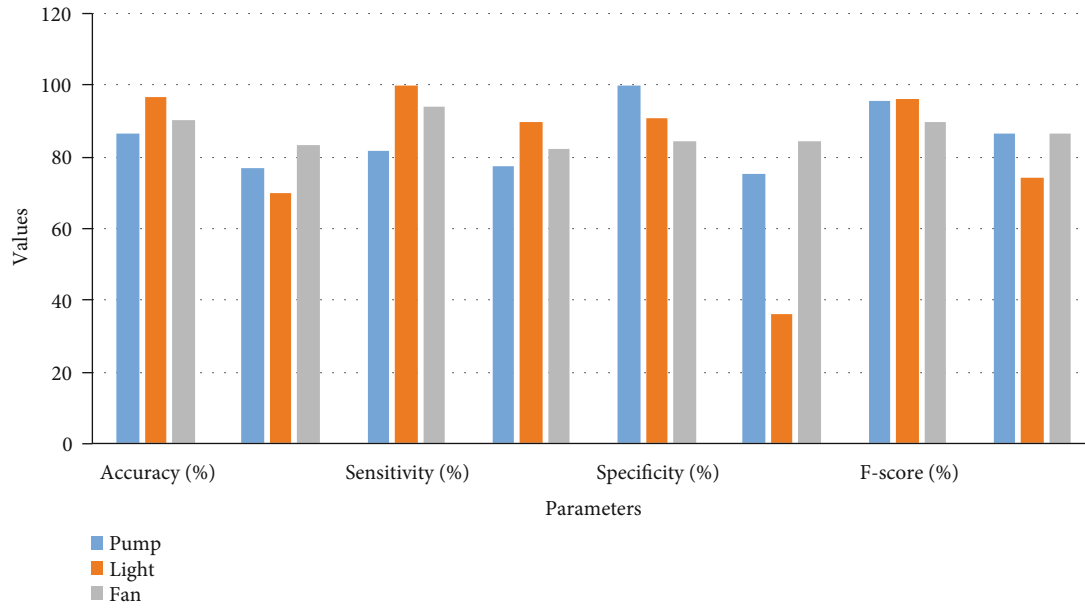
FIGURE 14: Performance of classification model.
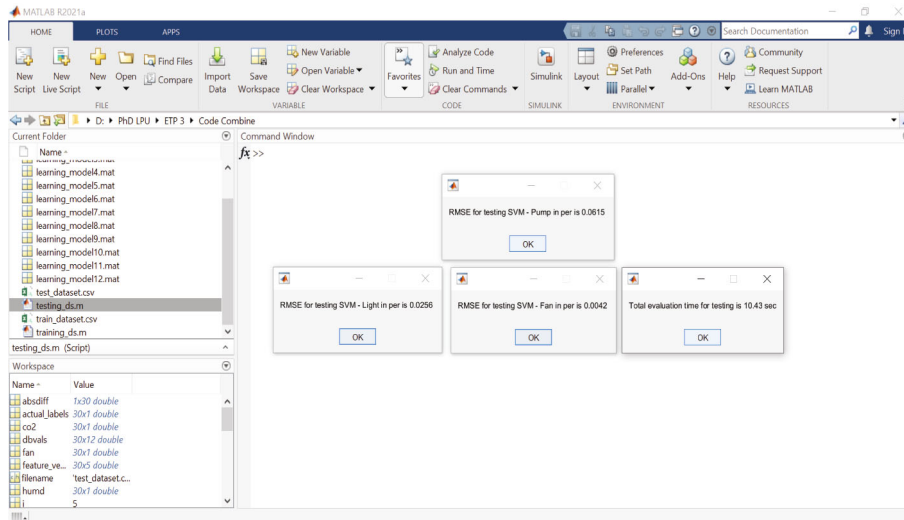
FIGURE 15: Regression approach result for RMSE SVM.

scorching sun, as well as pest and disease control, are all advantages of using a greenhouse management system for such a crop.

3.1.2. Edge Layer. Sensors, known as nodes or edges, are put in the field at various locations and connected to a low-power microcontroller designed for IoT. We used a Node MCU ESP 32 in our experiment, which can gather and analyze data from sensors before transferring it to the edge layer's base station. Sensors must be calibrated and checked against an expected value to collect data in analog or digital form according to requirements. Data is collected for various climate variables, both healthy and

unhealthy, to better comprehend all possible environmental situations and to assure crop survival through accurate crop management.

To test an intelligent greenhouse management system, a prototype experimental model was created using an embedded system device based on three primary layers that includes several sensors and a microprocessor at first layer, microcontrollers for a node at second layer, and cloud at third layer for data representation, as shown in Figure 3.

The proposed model tracks several greenhouse characteristics for two crops, Gerbera and Broccoli, in different climates. A microcontroller Node MCU ESP 32 is connected to all of the needed sensors for obtaining the greenhouse
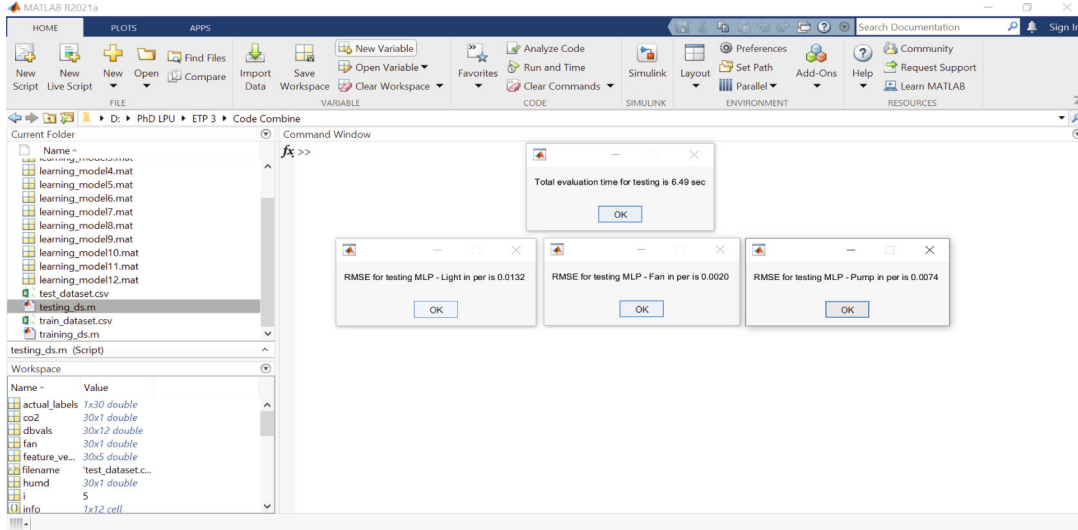
FIGURE 16: Regression approach result for RMSE MLP.

TABLE 3: Performance evaluation of regression model.

Attributes	RMSE	
	SVM	MLP
Pump	0.0615	0.0074
Fan	0.0042	0.0020
Light	0.0256	0.0132

parameters. A personal computer collects data serially with timestamp values for data logging of various parameters. Temperature and humidity, which is taken from the DHT11 sensor, light intensity, which is taken from LDR sensor, CO_2, which is taken from MQ2 sensor, and soil moisture, which is taken from Cu leads, are all continually monitored for ten days on the Adafruit IO cloud platform utilizing the MQTT protocol under day and night conditions within specific time intervals. Operational work flow of the proposed system is defined in Figure 4 in which four sensors are deployed at farm site with Node MCU ESP32 controller interfaced. The real-time data from sensors are monitored serially on personal computer through controller, and same data is sent on cloud.

3.1.3. Fog Layer. The basic responsibility of the analytics and decision-making model is to control the actions at the edge layer and communicate the accompanying report to the cloud layer for the use of farmers. The in-charge order will create a machine intelligence treasure accompanying many processing states. The proposed methodology developed at the fog layer for data analytics system using machine learning algorithms typically classification modeling is as shown in Figure 5 and discussed in detail below.

At first, data from sensors is generated at the edge layer and then is acquired. Preprocessing of stored data is used to clean and correct the data. Data classification is based on its

intended use by initializing the classifier, later after training of machine learning algorithms and validation of classifier so as to store trained classifier. Data was gathered by IoT devices, particularly sensors, which can collect data in real time or in small batches (temperature, humidity, camera vision, light intensity, etc.) (e.g., when to pump water). Decision-making based on predictions and data visualization through reports or dashboards were as follows: support vector machine (SVM) and multilayer perceptron neural network (MLP-ANN) are the two machine learning techniques that were primarily chosen for implementation. The advantages of selecting this algorithm are effective in high dimensional spaces and capability to learn nonlinear models.

Support vector machines (SVM) are a supervised classification and regression method. SVM's main idea is shifting nonlinear data to a new space for which the data may be separated linearly by employing a hyperplane that accurately separates the data by following two important conditions: because distinct classes of vectors will have various aspects, the distances between the hyperplane and the vectors must be used. The assumption function f has the following definition:

$$f(x_i) = \begin{Bmatrix} +1 \text{ if } w.x \ + \ b \geq 0 \\ -1 \text{ if } \ \ w.x + b < 0 \end{Bmatrix}. \tag{1}$$

Class +1 will be filling a place points above or on the hyperplane; when in fact, class -1 will be filling a place points beneath the hyperplane.

An artificial neural network (ANN) with one or more hidden layers is known as a Multilayer perceptron neural network. A perceptron is an interconnected system amounting to just an individual affecting the animate nerve organs model. It simulates high nonlinear functions, which are the foundation for deep learning neural networks. The degree of inaccuracy in an output node j in the nth data point (training example) can be represented by

$$e_j(n) = d_j(n) - y_j(n), \tag{2}$$
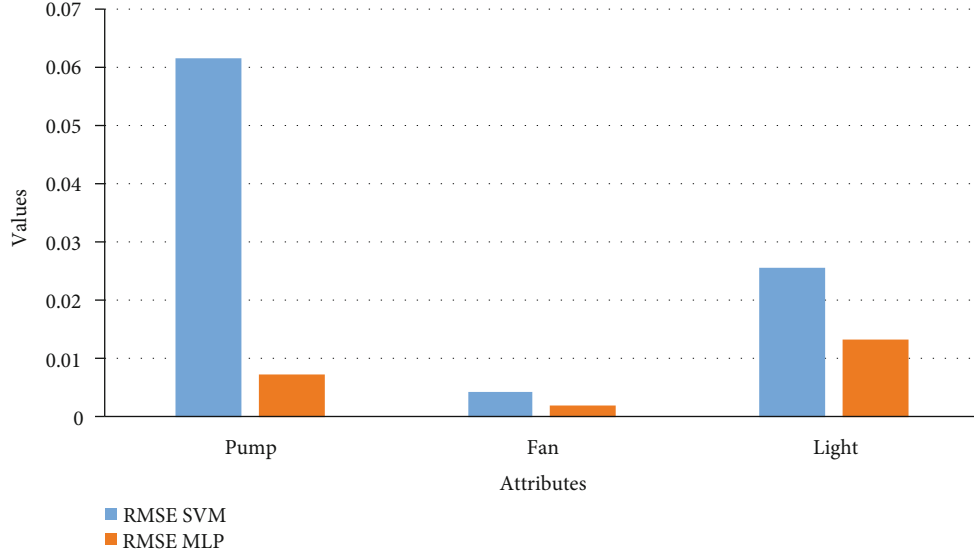
Figure 17: Performance of the regression model.

Table 4: Comparative analysis.

Ref	Accuracy (%)	Sensitivity (%)	Specificity (%)	F-score (%)	Latency (sec)	RMSE
[2]	—	93.59	94.63	96.30	—	—
[4]	—	—	—	—	—	0.2431
[6]	87.35	87.33	95.76	87.17	224.6	—
[7]	90	—	—	—	—	—
[13]	—	—	—	—	—	0.02726
Proposed work	91.10	91.97	91.83	92.1	6.49	0.0615

where "d" is the goal value, and "y" is the perceptron's output value. The node weights can then be modified depending on adjustments that reduce the overall output error, as determined by

$$\epsilon(n) = \frac{1}{2} \sum_j e_j^2(n).$$ (3)

The trouble of selecting a set of ideal hyperparameters for a model knowledge invention is famous as hyperparameter bringing into harmony or optimization. An energetic limit is a profit for a limit that is to say used to influence the education process. The gridiron search method is utilized, which is an ultimate fundamental form of hyperparameter bringing into harmony. We merely produce a model each reasonable combination of all of the energetic-limit principles provided, judge each model, and pick the construction that gives the best results utilizing this arrangement. Below is a writing of the method for energetic limit regulating the model.

Step 1. Define a machine learning model.

Step 2. For the selected approach, define the range of possible values for all hyperparameters.

Step 3. Define a sampling mechanism for hyperparameter values.

Step 4. Create a criterion for judging the model.

Step 5. Develop a crossvalidation technique for determining the system's efficiency.

3.1.4. Cloud Layer. Data from each node in the edge layer, which is subsequently processed and controlled at the base station, will be visualized at the cloud layer using an Adafruit IO cloud platform; farmers can track crop cultivation progress using a graphical interface- (UI-) based application. Adafruit IO is a platform for visualizing, responding to, and interacting with sensor data. With the support of MQTT, the dossier is likewise observed private and secure. MQTT (Message Queue Telemetry Transport) is a TCP/IP-located inconsequential issue-contribute contract. MQTT employs a message broker to route messages between senders who send them and receivers who are interested in

receiving them. Messages can be published and subscribed to using the same client. Each message is associated with a specific subject, for example, as shown in Figure 6, how temperature sensor data from a greenhouse system is sent.

4. Experimental Result and Discussion

The proposed experimental plan is implemented on a prototype that has been tested practically on two crops, Gerbera and Broccoli, for various conditions. The acquired dataset has feature attribute of CO_2 gas level (ppm), soil moisture (percent), light intensity (lux), humidity (percent), and temperature (Celsius) with output attribute pump (on/off), ventilation fan (on/off), and amount of light (low/medium/high). The values of dataset are taken under various conditions for several days and one hour per day. The mean of each day reading for every sensor's attribute is as shown in Figures 7–11. The two primary phases of experimentation are the creation of basic model embedded systems for plant growth and feeding, the construction of a sensor net for intelligent greenhouse monitoring, and the automation of actuators using supervised machine learning algorithms. The analytics and decision-making model classification was done on a laptop with a 2.30 GHz Intel ™ Core ™ CPU, 8 GB RAM, and Windows 10 (64 bit) operating system, with no other processes running in the background. MATLAB IDE is used to program the intelligent model, statistics, and machine learning toolbox from MATLAB that was utilized as tools. A confusion matrix as performance metrics is used to evaluate the system performance. Also, the accuracy, sensitivity, specificity, and F-score for the classification model and RMSE for the regression model are calculated from confusion matrix parameters: true positive (TP), false positive (FP), true negative (TN), and false negative (FN).

$$
\begin{aligned}
\text{Accuracy} &= \frac{(\text{TP} + \text{TN})}{\text{TP} + \text{TN} + \text{FP} + \text{FN}}, \\
\text{Sensitivity} &= \frac{\text{TP}}{\text{TP} + \text{FN}}, \\
\text{Specificity} &= \frac{\text{TN}}{\text{TN} + \text{FP}}, \\
F - \text{score} &= 2 * \frac{\text{TP}}{2\text{TP} + \text{FP} + \text{FN}}, \\
\text{RMSE} &= \text{sqrt}\left(\frac{\text{sum}\left((\text{predicted}_{\text{label}} - \text{actual}_{\text{label}})^2\right)}{\text{total}} \text{predictions}\right).
\end{aligned}
\tag{4}
$$

The proposed approach employs an embedded system to analyze greenhouse execution parameters like as CO_2, soil moisture, temperature, and plant light, yielding accurate results. All the readings are observed under several conditions and monitored on the personal computer over serial communication. All these sensor data are monitored over the Internet on the Adafruit IO cloud dashboard by publishing data from nodes to the broker of Adafruit.

Then, the user can subscribe to this data to access it in real time.

The greenhouse doors/windows can also be rolled on/off depending on the soil moisture conditions. The plant photosynthesis process requires a high level of CO_2 concentration and water in the evenings rather than during the day; with these two sources of energy, the photosynthesis method keeps the plant cool and encourages rapid growth. Because the greenhouse absorbs CO_2 from day to night, it maintains a CO_2 level maximum at night after completing a CO_2 concentration level experiment in a greenhouse, as illustrated in Figure 6. As a result, as seen in Figure 6, the CO_2 level decreases during the day. Figure 7 depicts that moisture level of soil in wet and dry condition and accordingly motor turns on/off with amount of water. The environmental temperature and humidity are shown in Figures 8 and 9 inside and outside greenhouse; accordingly, and actuator fan or humidifier is controlled. The light intensity inside and outside greenhouse as shown in Figure 10 indicates that sufficient light is required for photosynthesis purpose; so, accordingly, artificial light is provided in accordance with it.

In the decision-making model, the confusion matrix for regression and classification model has been evaluated to get the desired result and calculate the different parameters such as accuracy, sensitivity, and latency after applying the proposed algorithms to the standard dataset. The two supervised machine learning models, SVM and MLP-ANN, were used to train and test the model using MATLAB software with statistics and machine learning toolbox. The both algorithms required best hyperparameters to train the model which are obtained by using the grid search CV algorithm which is mentioned in Table 1.

The simulation results for classification modeling are shown in Figures 12 and 13 mentioned below for the SVM and MLP algorithm, respectively. In these results, classification report results and confusion matrix for three output attributes pump, fan, and light are displayed. The performance of the classification model using confusion matrix is shown in Table 2. From this table, it is found that for all three output attributes, the SVM algorithm performed better as compared to MLP in all performance metrics; also, its graphical representation is as shown in Figure 14.

The simulation results for regression modeling are shown in Figures 15 and 16 mentioned below for the SVM and MLP algorithm, respectively. In these results, regression report results for three output attributes pump, fan, and light are displayed. The performance of the regression model using RMSE metric is shown in Table 3. From this table, it is found that for all three output attributes, the SVM regressor algorithm is performed better as compared to MLP regressor; also, its graphical representation is as shown in figure 17.

Finally, Table 4 shows the comparative analysis with the existing state of art methods. From the results, it is found that the proposed classification and regression model which is used for intelligent and precise smart farming for greenhouse model gives better results considering the classification model parameters using accuracy, sensitivity, specificity, and the regression model using RMSE.

5. Conclusion

This paper presented a machine learning-based smart farming system that makes use of IoT principles and capabilities. The suggested strategy can be applied in a smart agricultural setting where the decision-making model is supported by IoT-based systems. The data required for the analytics model is collected by using IoT-based embedded system device for two greenhouse plants with sensing parameters as input and related actuators as output. The two different analytics model is developed for intelligent and precise farming using classification and regression model. For both types of modeling, SVM and MLP are used. Finally, classification- and regression-based supervised machine learning algorithms are used to evaluate how well the smart farming system performs in intelligent and precise farming. The results demonstrated that SVM is perform better as compared to MLP and other existing state of art classification model. The suggested approach is also successful in creating smart agricultural systems with intelligent prediction-based decision support. On the basis of the experimental results, the proposed strategy also proved to be the most effective at providing actuators with predictions and control. Further, this proposed model can be used in real world scenario by making it robust and whether proof. Also, the analytics model will be varied as per the crop or plant consideration for certain scenario. The performance of the model can be improved by employing deep learning models with large dataset samples.

Data Availability

The data will be availableupon request.

Conflicts of Interest

All authors declare that they have no conflicts of interest.

References

[1] J. Pei, Z. Yu, J. Li, M. A. Jan, and K. Lakshmanna, "TKAGFL: a federated communication framework under data heterogeneity," *IEEE Transactions on Network Science and Engineering.*, 2022.

[2] N. Gundluru, D. S. Rajput, K. Lakshmanna et al., "Enhancement of detection of diabetic retinopathy using Harris hawks optimization with deep learning model," *Computational Intelligence and Neuroscience*, vol. 2022, 13 pages, 2022.

[3] K. Lakshmanna, N. Subramani, Y. Alotaibi, S. Alghamdi, O. I. Khalafand, and A. K. Nanda, "Improved metaheuristic-driven energy-aware cluster-based routing scheme for IoT-assisted wireless sensor networks," *Sustainability*, vol. 14, no. 13, p. 7712, 2022.

[4] K. Lakshmanna, R. Kavitha, B. T. Geetha, A. K. Nanda, A. Radhakrishnan, and R. Kohar, "Deep learning-based privacy-preserving data transmission scheme for clustered IIoT environment," *Computational Intelligence and Neuroscience*, vol. 2022, Article ID 8927830, 11 pages, 2022.

[5] V. Suma, "Internet of Things (IoT) based intelligent agriculture in India: an overview," *Journal of ISMAC*, vol. 3, no. 1, pp. 1–15, 2021.

[6] N. G. Rezk, E. E. D. Hemdan, A. F. Attia, A. el-Sayed, and M. A. el-Rashidy, "An efficient IoT based smart farming system using machine learning algorithms," *Multimedia Tools and Applications*, vol. 80, no. 1, pp. 773–797, 2021.

[7] A. Araby, M. M. Abd Elhameed, N. M. Magdy, N. Abdelaal, Y. T. Abd Allah, and M. S. Darweesh, "Intelligent IoT monitoring system for agriculture with predictive analysis," in *2019 8th International Conference on Modern Circuits and Systems Technologies (MOCAST)*, pp. 1–4, 2019.

[8] A. Tageldin, D. Adly, H. Mostafa, and H. S. Mohammed, "Applying machine learning technology in the prediction of crop infestation with cotton leafworm in greenhouse," *bioRxiv*, 2020.

[9] A. A. S. Aliar, J. Yesudhasan, M. Alagarsamy, K. Anbalagan, J. Sakkarai, and K. Suriyan, "A comprehensive analysis on IoT-based intelligent farming solutions using machine learning algorithms," *Bulletin of Electrical Engineering and Informatics*, vol. 11, no. 3, pp. 1550–1557, 2022.

[10] P. Sethy, S. Behera, C. Pandey, and S. Narayanand, "Intelligent paddy field monitoring system using deep learning and IoT," *Concurrent Engineering Research and Applications*, 2020.

[11] N. Kaushik, S. Narad, A. Mohature, and P. Sakpal, "Predictive analysis of iot based digital agriculture system using machine learning," *International Journal of Engineering Science and Computing*, vol. 9, 2019.

[12] K. N.-E.-A. Siddiquee, M. Islam, N. Singh et al., "Development of algorithms for an iot-based smart agriculture monitoring system," *Wireless Communications and Mobile Computing*, vol. 2022, Article ID 7372053, 16 pages, 2022.

[13] F. Nourelhouda, A. Haqiq, and M. W. Ahmad, "Smart farming system based on intelligent Internet of Things and predictive analytics," *Journal of Food Quality*, vol. 2022, Article ID 7484088, 2022.

[14] K. Sekaran, M. N. Meqdad, P. Kumar, S. Rajan, and S. Kadry, "Smart agriculture management system using Internet of Things," *TELKOMNIKA (Telecommunication Computing Electronics and Control)*, vol. 18, no. 3, pp. 1275–1285, 2020.

[15] Y. Simpa Abdulsalam and M. Hedabou, "Security and privacy in cloud computing:technical review," *Future Internet*, vol. 14, no. 1, 2022.

[16] G. S. Gaba, M. Hedabou, P. Kumar, A. Braeken, M. Liyanage, and M. Alazab, "Zero knowledge proofs based authenticated key agreement protocol for sustainable healthcare," *Sustainable Cities and Society Journal*, vol. 80, p. 103766, 2022.

[17] M. Hedabou, "Cloud key management based on verifable secret sharing," in *15th International Conference on Network and System Security. Lecture Notes in Computer Science*, pp. 289–303, 2021.

[18] E. M. Amhoud, G. R. B. Othman, L. Bigot et al., "experimental demonstration of space-time coding for MDL mitigation in few-mode fiber transmission systems," in *2017 European Conference on Optical Communication (ECOC)*, pp. 1–3, 2017.

[19] E. M. Amhoud, G. Rekaya-Ben Othman, and Y. Jaouën, "Capacity enhancement of few-mode fiber transmission systems impaired by mode-dependent loss," *Applied Sciences*, vol. 8, no. 3, p. 326, 2018.

[20] O. Alkhazragi, X. Sun, V. Zuba et al., "Spectrally resolved characterization of thermally induced underwater turbulence using

a broadband white-light interrogator," *IEEE Photonics Journal*, vol. 11, no. 5, pp. 1–9.

[21] R. Kaur, K. Havish, T. K. Dutt, and G. M. Reddy, "Agrocompanion: a intelligent farming approach based on iot and machine learning," *International Journal of Innovative Technology and Exploring Engineering (IJITEE)*, vol. 9, no. 12, pp. 254–262, 2020.

[22] Y. Liu, "Intelligent analysis platform of sustainable agricultural development based on the Internet of Things and machine learning," *Acta Agriculturae Scandinavica, Section B—Soil & Plant Science*, vol. 71, no. 8, pp. 718–731, 2021.

[23] A. Sharma, P. G. Jain, and V. Chowdary, "Machine learning applications for precision agriculture: a comprehensive review," *Access*, vol. 9, pp. 4843–4873, 2021.

[24] K. Lela Madhav and N. Sandeep, "Machine learning approach for agriculture iot using svm&ann," *INTERNATIONAL JOURNAL OF ENGINEERING RESEARCH & TECHNOLOGY (IJERT)*, vol. 7, no. 11, 2019.

[25] Y. Mekonnen, S. Namuduri, L. Burton, A. Sarwat, and S. Bhansali, "Review—machine learning techniques in wireless sensor network based precision agriculture," *Journal of the Electrochemical Society*, vol. 167, no. 3, p. 037522, 2020.

[26] Á. L. Perales Gómez, P. E. López-de-Teruel, A. Ruiz, G. García-Mateos, G. Bernabé García, and F. J. García Clemente, "FARMIT: continuous assessment of crop quality using machine learning and deep learning techniques for IoT-based smart farming," *Cluster Computing*, vol. 25, no. 3, pp. 2163–2178, 2022.

[27] L. Colombo-Mendoza, M. Paredes-Valverde, M. del Pilar Salas-Zárate, and R. Valencia-García, "Internet of Things-driven data mining for smart crop production prediction in the peasant farming domain," *Applied Sciences*, vol. 12, no. 4, p. 1940, 2022.

[28] B. Yang and Y. Xu, "Applications of deep-learning approaches in horticultural research: a review," *Horticulture Research*, vol. 8, no. 1, p. 123, 2021.

[29] D. Cafuta, I. Dodig, I. Cesar, and T. Kramberger, "Developing a modern greenhouse scientific research facility-a case study," *Sensors*, vol. 21, no. 8, p. 2575, 2021.

[30] K. Bakthavatchalam, B. Karthik, V. Thiruvengadam et al., "IoT framework for measurement and precision agriculture: predicting the crop using machine learning algorithms," *Technologies*, vol. 10, no. 1, p. 13, 2022.

[31] O. I. Khalaf, K. A. Ogudo, and M. Singh, "A fuzzy-based optimization technique for the energy and spectrum efficiencies trade-off in cognitive radio-enabled 5G network," *Symmetry*, vol. 13, no. 1, p. 47, 2021.

[32] G. S. Walia, P. Singh, M. Singh et al., "Three dimensional optimum node localization in dynamic wireless sensor networks," *CMC-Computers, Materials & Continua*, vol. 70, no. 1, pp. 305–321, 2022.

[33] M. Singh, M. Kumar, and J. Malhotra, "Energy efficient cognitive body area network (CBAN) using lookup table and energy harvesting," *Journal of Intelligent & Fuzzy Systems*, vol. 35, no. 2, pp. 1253–1265, 2018.

[34] M. Hassan, M. Singh, K. Hamid, R. Saeed, M. Abdelhaq, and R. Alsaqour, "Modeling of NOMA-MIMO-Based Power Domain for 5G Network under Selective Rayleigh Fading Channels," *Energies*, vol. 15, no. 15, p. 5668, 2022.

[35] A. Rokade and M. Singh, "Analysis of precise green house management system using machine learning based Internet of Things (IoT) for intelligent farming," in *2021 2nd International Conference on Intelligent Electronics and Communication (ICOSEC)*, pp. 21–28, 2021.

[36] A. Kadu and M. Singh, "Comparative analysis of e-health care telemedicine system based on Internet of Medical Things and artificial intelligence," in *2021 2nd International Conference on Intelligent Electronics and Communication (ICOSEC)*, pp. 1768–1775, 2021.

[37] M. Hassan, M. Singh, and K. Hamid, "Impact of power and bandwidth on the capacity rate and number of users in Sc-Noma," *Harbin Gongye Daxue Xuebao/Journal of Harbin Institute of Technology*, vol. 53, no. 9, pp. 118–124, 2021.

[38] M. Hassan, M. Singh, and K. Hamid, "Survey on NOMA and spectrum sharing techniques in 5G," in *2021 IEEE International Conference on Intelligent Information Systems and Technologies (SIST)*, pp. 1–4, 2021.

[39] M. Hassan, M. Singh, and K. Hamid, "Overview of cognitive radio networks," *Journal of Physics: Conference Series*, vol. 1831, 2021.

[40] S. K. Roy, M. Singh, K. K. Sharma, C. Bhargava, and B. P. Singh, "Mathematical modelling of simple passive RC filters using floating admittance technique," in *2020 IEEE International Conference for Innovation in Technology (INOCON)*, pp. 1–6, 2020.

[41] M. Alazab, K. Lakshmanna, T. Reddy, Q. V. Pham, and P. K. Maddikunta, "Multi-objective cluster head selection using fitness averaged rider optimization algorithm for IoT networks in smart cities," *Sustainable Energy Technologies and Assessments.*, vol. 43, no. 43, article 100973, 2021.

[42] G. T. Reddy, M. P. Reddy, K. Lakshmanna et al., "Analysis of dimensionality reduction techniques on big data," *IEEE Access*, vol. 8, no. 8, pp. 54776–54788, 2020.

[43] K. Lakshmanna, R. Kaluri, N. Gundluru et al., "A review on deep learning techniques for IoT data," *Electronics*, vol. 11, no. 10, p. 1604, 2022.

[44] K. Lakshmanna, F. Shaik, V. K. Gunjan, N. Singh, G. Kumar, and R. M. Shafi, "Perimeter degree technique for the reduction of routing congestion during placement in physical design of VLSI circuits," *Complexity*, vol. 2022, Article ID 8658770, 11 pages, 2022.

[45] N. Singh, V. K. Gunjan, G. Chaudhary, R. Kaluri, N. Victor, and K. Lakshmanna, "IoT enabled HELMET to safeguard the health of mine workers," *Computer Communications*, vol. 193, pp. 1–9, 2022.

[46] D. S. Rajput, S. M. Basha, Q. Xin et al., "Providing diagnosis on diabetes using cloud computing environment to the people living in rural areas of India," *Journal of Ambient Intelligence and Humanized Computing*, vol. 13, no. 5, pp. 2829–2840, 2022.

[47] H. A. Teferaa, H. Dongjunb, and K. Njagic, "Implementation of iot and machine learning for intelligent farming monitoring system," *International Journal of Sciences: Basic and Applied Research (IJSBAR)*, vol. 52, no. 1, pp. 67–77, 2020.

[48] N. Ha, K. Xu, G. Ren, A. Mitchell, and J. Ou, "Machine learning-enabled smart sensor systems," *Advanced Intelligent Systems.*, vol. 2, no. 9, p. 2000063, 2020.

[49] X.-b. Jin, W.-Z. Zheng, J.-L. Kong et al., "Deep-learning temporal predictor via bidirectional self-attentive encoder-decoder framework for IoT-based environmental sensing in intelligent greenhouse," *Agriculture*, vol. 11, no. 8, p. 802, 2021.

[50] R. Akhter and S. Sofi, "Precision agriculture using IoT data analytics and machine learning," *Journal of King Saud University-Computer and Information Sciences*, 2021.

[51] V. K. Quy, N. V. Hau, D. V. Anh et al., "IoT-enabled smart agriculture: architecture, applications, and challenges," *Applied Sciences*, vol. 12, no. 7, p. 3396, 2022.

[52] O. Elijah, T. A. Rahman, I. Orikumhi, C. Y. Leow, and M. N. Hindia, "An overview of Internet of Things (IoT) and data analytics in agriculture: benefits and challenges," *IEEE Internet of Things Journal*, vol. 5, no. 5, pp. 3758–3773, 2018.

Retraction

Retracted: The Expression of miR-205 in Prostate Carcinoma and the Relationship with Prognosis in Patients

Computational and Mathematical Methods in Medicine

This article has been retracted by Hindawi following an investigation undertaken by the publisher [1]. This investigation has uncovered evidence of one or more of the following indicators of systematic manipulation of the publication process:

(1) Discrepancies in scope

(2) Discrepancies in the description of the research reported

(3) Discrepancies between the availability of data and the research described

(4) Inappropriate citations

(5) Incoherent, meaningless and/or irrelevant content included in the article

(6) Peer-review manipulation

The presence of these indicators undermines our confidence in the integrity of the article's content and we cannot, therefore, vouch for its reliability. Please note that this notice is intended solely to alert readers that the content of this article is unreliable. We have not investigated whether authors were aware of or involved in the systematic manipulation of the publication process.

Wiley and Hindawi regrets that the usual quality checks did not identify these issues before publication and have since put additional measures in place to safeguard research integrity.

We wish to credit our own Research Integrity and Research Publishing teams and anonymous and named external researchers and research integrity experts for contributing to this investigation.

The corresponding author, as the representative of all authors, has been given the opportunity to register their agreement or disagreement to this retraction. We have kept a record of any response received.

References

[1] Z. Guo, X. Lu, F. Yang et al., "The Expression of miR-205 in Prostate Carcinoma and the Relationship with Prognosis in Patients," *Computational and Mathematical Methods in Medicine*, vol. 2022, Article ID 1784791, 9 pages, 2022.

Hindawi

Research Article

The Expression of miR-205 in Prostate Carcinoma and the Relationship with Prognosis in Patients

Zhuifeng Guo [ID],[1] **Xuwei Lu** [ID],[1] **Fan Yang** [ID],[1] **Liang Qin** [ID],[1] **Ning Yang** [ID],[1] **Peiran Cai** [ID],[2] **Conghui Han** [ID],[3] **Jiawen Wu** [ID],[1] and **Hang Wang** [ID][4]

[1]*Department of Urology, Minhang Hospital, Fudan University, Shanghai, China*
[2]*Center for Traditional Chinese Medicine and Gut Microbiota, Minhang Hospital, Fudan University, Shanghai, China*
[3]*Department of Urology, Xuzhou Central Hospital, Xuzhou, Jiangsu, China*
[4]*Department of Urology, Zhongshan Hospital, Fudan University, Shanghai, China*

Correspondence should be addressed to Hang Wang; zsurology@126.com

Purpose. We aimed to investigate the changes of serum and cell exosome miR-205 levels in patients with prostate carcinoma and its clinical significance. *Materials and Methods*. Firstly, pronouncement of miR-205 in normal and prostate carcinoma tissues was analyzed by using UALCAN database. The relationship between miR-205 in tumor tissues and the pathological and clinical characteristics of patients with prostate carcinoma were analyzed. Consequently, 60 people with prostate carcinoma were collected to the Minhang Hospital from August 2016 to August 2021. Serum of patients in the two groups was collected, and RNA in serum exosomes was extracted, and qRT-PCR was used to analyze the expression of miR-205 mediated by serum exosomes. Meanwhile, the relationship among the clinical as well as pathological aspects and bodement of patients with prostate carcinoma and the pronouncement level of miR-205 mediated by exosome was compared. Next, assays like wound healing and CKK-8 were used to investigate the effects of miR-205 in exosomes extracted from prostate carcinoma on the augmentation and metastasis of prostate carcinoma. *Results*. The results showed that the pronouncement level of miR-205 in tissues with prostate carcinoma was significantly lower than that in normal prostate tissues. In addition, the pronouncement level of miR-205 in fluid exosome of people with prostate carcinoma and exosomes derived from the lines of prostate carcinoma was considerably less than that in serum exosomes of healthy patients and that of normal cell lines of prostate. The pronouncement level of miR-205 in fluid exosomes of people with prostate carcinoma was negatively associated with cancer phase, uncontrolled cell division in lymph nodes, distant metastasis, and PSA level at initial diagnosis. Analysis (multivariate and univariate) showed that miR-205 pronouncement was a sovereign threat cause for prognosis of prostate cancer patients. Additionally, the pronouncement and metastasis of prostate carcinoma can be restricted by the overexpression of miR-205. *Conclusion*. The pronouncement of miR-205 in liquid derived exosomes is correlated with the prediction of people with prostate carcinoma and may be a new marker for identification and cure of prostate carcinoma.

1. Introduction

Prostate cancer is the second largest virulence in males around the world, and in the genital and urinary system among males, it is the most common spreading lump [1].

Many prostate cancer patients do not respond to therapy through androgen stripping, and as a result, they are affected by a disease in which metastatic castration is permanent.

Early diagnosis and treatment can reduce the mortality and cost of patients. Screening for prostate cancer is usually done through two methods: first is the clinical manifestation, and the second one is test of serum prostate-specific antigen.

PSA screening often misdiagnoses certain ailments like hyperplasia in part prostate and prostatitis as carcinoma of prostate and leads to unnecessary invasive biopsy and overtreatment [2, 3]. PSA levels are also commonly used to

monitor the recurrence of the disease, but the standard interval of PSA after radical surgery has been controversial. Therefore, there is a dire need of a new method to improve the quality of diagnosis of prostate cancer and the monitoring quality of progression of cancer.

Exosomes are actually some membraned vesicles like substances having about 30-150 nm diameter. They are released outside the cell after the mixing of cell membranes with the intracellular polyvesicles. They are mostly present in saliva, breast milk, amniotic fluid, blood, and urine. He et al. demonstrated that circulating exosomes in patients with SLE could be associated with disease activity and might therefore serve as biomarkers of disease activity [4]. Zhang et al. found that circulating exosomes suppressed the induction of regulatory T cells via let-7i-mediated blockade of the IGF1R/TGFBR1 pathway in multiple sclerosis [5].

Through recent experiments, it is proved that exosomes can be a medium for intracellular communication, and the content from donor cells such as DNA, mRNA, and miRNA can be transmitted towards the receiving cells in the future to regulate or interfere with specific physiological and pathological processes [6, 7]. Among RNAs contained in exosomes, miRNA content is the most abundant, and the types of miRNA in exosomes are selectively enriched, and their content directly reflects the expression level of miRNA in donor cells [8]. miRNAs are those RNAs which are noncoding. They are composed of 18-25 subunits called as nucleotides that results in the control of gene pronouncement after transcription [9, 10]. Each miRNA can regulate hundreds of transcripts through base complementary pairing, and the same transcript can bind more than one miRNA. Therefore, miRNA has a wide regulatory spectrum [11, 12]. In this study, the pronouncement levels of serum and cell exosome miR-205 in prostate cancer patients were analyzed to explore miR-205 amount in the early diagnosis and bodement test of prostate carcinoma, aiming to provide reference for the diagnosis and treatment of clinical diseases.

2. Methods and Materials

2.1. Clinical Specimens. A total of 60 prostate cancer patients admitted to the Minhang Hospital from August 2016 to August 2021 were objects in the research, and 60 healthy people were selected as the control group. Our study was approved by the Institutional Review Board of the Minhang Hospital, and written informed consent was obtained from each participant.

Inclusion criteria are as follows: (1) a participant had not injected with any form of anticarcinoma therapy before surgery. (2) All patients were confirmed by histopathological diagnosis of prostate cancer. (3) All patients or their family members understand the purpose and requirements of this study, agree to participate in this study, and sign consent in a printed form, and this study has been approved by the ethics committee of the Minhang Hospital. Elimination measures are as follows: (1) missing visitors or patients with incomplete clinical data; (2) patients with other tumors; and (3) complicated with severe cardiac, hepatic and renal insufficiency, and acute or chronic active pulmonary infection.

The demographic characteristics and clinicopathological data of prostate cancer patients were recorded and summarized in Table 1.

2.2. Peripheral Blood Sample Collection. 5mL of peripheral blood samples from tumor patients was extracted by anticoagulant tube, and the sample was extracted and kept at -80°C for subsequent experiments. Extract exosomes according to the instructions of the Exosome Extraction Kit (System Biosciences, USA) and do as follows: 500 μL of serum sample was absorbed with a pipetting gun, and 126 μL of extraction reagent was added and mixed by shaking. The serum was placed and incubated at 4°C for 30 min. The supernatant was removed by centrifugation, and 200 μL of PBS was added for resuspension to obtain exosome suspension.

2.3. Extraction and Identification of Serum Exosomes. Cleared media were centrifuged at 100,000g for 70 min at 4°C following a method described previously [1]. The subsequent pellet was resuspended in PBS and washed three times by centrifugation at 100,000g for 70 min at 4°C. The clean pellet was then resuspended in 100 μL of PBS or in NuPAGE™ LDS sample buffer. After polymerization at 60°C overnight, the precipitate was sliced, and the ultrathin sections were observed under a transmission electron microscope.

2.4. Extraction of RNA from Serum Exosomes. Follow the instructions for RNA extraction from serum exosomes (Qiagen, Valencia, CA, USA) kit. NanoDrop 2000 was used to detect RNA concentration, and a260/230 and A260/280 values and concentrations were recorded. If a260/230 value >2.1 (RNA degradation) and A260/280 <1.8, organic matter contaminated the extracted products.

2.5. The Extent of Pronouncement of miR-205 Mediated by Serum Exosome Was Detected by qRT-PCR. In accordance with the kit of TaqMan microRNA reverse transcription, there was a backward transcription of RNA into cDNA. The reaction conditions were as follows: reaction time was 15 min at 37°C, reaction 5 s at 85°C, and 4°C for 60 min. TaqMan microRNA Assay Kits (Applied Biosystems) are utilized to evaluate the pronouncement level of miR-205 in sample, which is mediated by exosome. PCR primers are miR-205: forward 5′-CTTGTCCTTCATTCCACCGGA-3′ and reverse 5′-TGCCGCCTGAACTTCACTCC-3′ and GAPDH: forward 5′-GAACGGGAAGCTCACTGG-3′ and reverse 5′-GCCTGCTTCACCACCTTCT-3′.

2.6. Cell Line Culture. Cell lines of patient with prostate tumor (DU145, 22RV1, and PC3) and RWPE-1 (normal prostatic epithelial cells) were acquired from Shanghai Yaji Biotechnology Co., Ltd. (Shanghai, China). RPMI-1640 medium or DMEM was used to incubate all the cells, and 10% FBS was the temperature for process of seeding at 37°C; they were cultured with 5% CO_2.

2.7. Cell Transfection. PC3 cells at logarithmic growth stage were obtained, and trypsin was used for their digestion for 2-3 min. DMEM medium was used to make the suspension

Table 1: The relationship between the expression of exosome miR-205 secreted by serum of prostate cancer patients and clinicopathological features of prostate cancer patients ($n = 60$).

Characteristics	miR-205 expression		Chi-squared test	P value
	Low no. cases	High no. cases		
All patients	($n = 25$)	($n = 35$)		
Age(years)			0.156	0.693
≤60	13	20		
>60	12	15		
Tumor stage			9.16	0.002
≤T2	8	25		
>T2	17	10		
Lymph node metastasis			5.173	0.023
Negative	9	23		
Positive	16	12		
Distant metastasis			7.837	0.005
M0	8	24		
M1	17	11		
PSA at initial diagnosis (ng/mL)			11.051	0.001
≤20	7	25		
>20	18	10		

of cells and inoculated in 6-well culture plates for 6 h. Follow-up experiments were conducted when the cell density reached 50-80%. According to the Lipofectamine 2000 liposome kit specification, microRNA blank sequence (miR-205 NC) and miR-205 mimics (Shanghai Jima Biotechnology Co., LTD.) were transferred into prostate cancer PC3 cells, respectively. After routine overnight culture in the incubator, a mixture containing miR-205 mimics and transfection reagent was configured with a transfection concentration of 50 nmol/L. After reaction at room temperature for 30 min, the mixed reagents were added into 6-well culture plates, respectively, according to the grouping. After 4 h culture in the incubator at 37°C, the reagents were replaced with complete medium. Human prostate cancer cell line PC3 was collected from each group 24 h after transfection, and the extent of pronouncement of miR-205 was evaluated by qRT-PCR to detect the cell transfection efficiency. The RNA sequences were as follows: miR-205 NC: UUUGUACUACACAAAAGUACUG and miR-205 mimics: UCCUUCAUUCCACCGGAGUCUG.

2.8. Isolation of Cell Line Exosomes. Exosomes were extracted and purified from supernatant of cell culture collected super centrifugation from cell lines of prostate carcinoma and epithelial cell lines of normal prostate. The product was centrifuged at 300g for 10 min, at 2000g for 10 min, and at 10000g for 30 min. After each centrifugation, the supernatant was collected for the next centrifugation operation. The product was finally put in the centrifuge at 100000g for 70 min, and the product was wasted to collect sediment. After centrifugation at 100000g for 70 min, the

precipitate was taken to obtain exosomes. Resuspended exosomes with 100 μL PBS buffer should be stored in 4°C refrigerator when immediately used and stored in -80°C urtra-low temperature refrigerator when long-term storage. The ELISA kit is used for overall exosome capture and quantification (Biovision, ExoQuant™, Catalog # K1201).

2.9. Detection of Cell Proliferation Ability (CCK-8 Assay). 24 h after transfection, prostate cancer cells PC3 were digested with trypsin for 2-3 min and then inoculated into 96-well plates. 100 μL was added to each well, with about 3 $\times 10^3$ cells. After incubating at 37°C for 0 h, 24 h, 48 h, 72 h, and 96 h, add CCK-8 solution 20 μL/well to 6-well cells at each time and incubate at 37°C for 6 h, wavelength of enzyme plate was set at 450 nm of the microplate reader, absorbance of 96-well plate was measured, and growth curve was drawn. Repeat the experiment 3 times.

2.10. Detection of Cell Migration Ability (Wound Healing Assay). First, use marker pen behind 6-hole plate, compare with ruler, equally make lines on the x-axis, with a continuous difference of 0.5-1 cm, across the hole, and the difference of each hole at least 5 lines. About 1×10^5 cells were added into each well, and the specific number varied with different cell types. The inoculation principle was that the cell fusion rate reached 100% overnight. The next day with 200 μL spear head than ruler, try to hang as far as the back of the horizontal line scratches; if the spear head is vertical, do not tilt. PBS was used for three times to clean the cells, the cells were removed, and medium without serum was added. After incubation at 37°C and 5%CO$_2$ for 24 h, samples were taken and photos were taken. Finally, the migration distance of the two groups was compared.

2.11. Analysis Based on Statistics. The data was evaluated by utilizing SPSS 25.0, and for evaluation and mapping, we used GraphPad Prism 7.0 software. All measurement data in the form of mean ± standard deviation (SD), according to two groups and multiple groups of measuring data comparison using Student's t-test and analysis of variance (one-way). The relationship between the pronouncement of exosome miR-205 secreted by serum of people with prostate carcinoma and pathological and clinical manifestations of prostate carcinoma was examined through Pearson's chi-squared test, and the relationship amid the expression of miR-205 and the embodiment of prostate cancer patients was evaluated by the Kaplan-Meier survival analysis and Cox proportional hazard model. For a significant difference, $P < 0.05$ was selected.

3. Results

3.1. The Expression of miR-205 Was Significant Lower in the Prostate Tumor Tissues. Firstly, we used UALCAN database to analyze the pronouncement of miR-205 in prostate tumor tissues and normal tissues and revealed that the extent of pronouncement of miR-205 in c was significantly lesser than in normal prostate tissues (Figure 1(a)). Furthermore, the UALCAN database was used to evaluate the relationship between the pronouncement of miR-205 in prostate
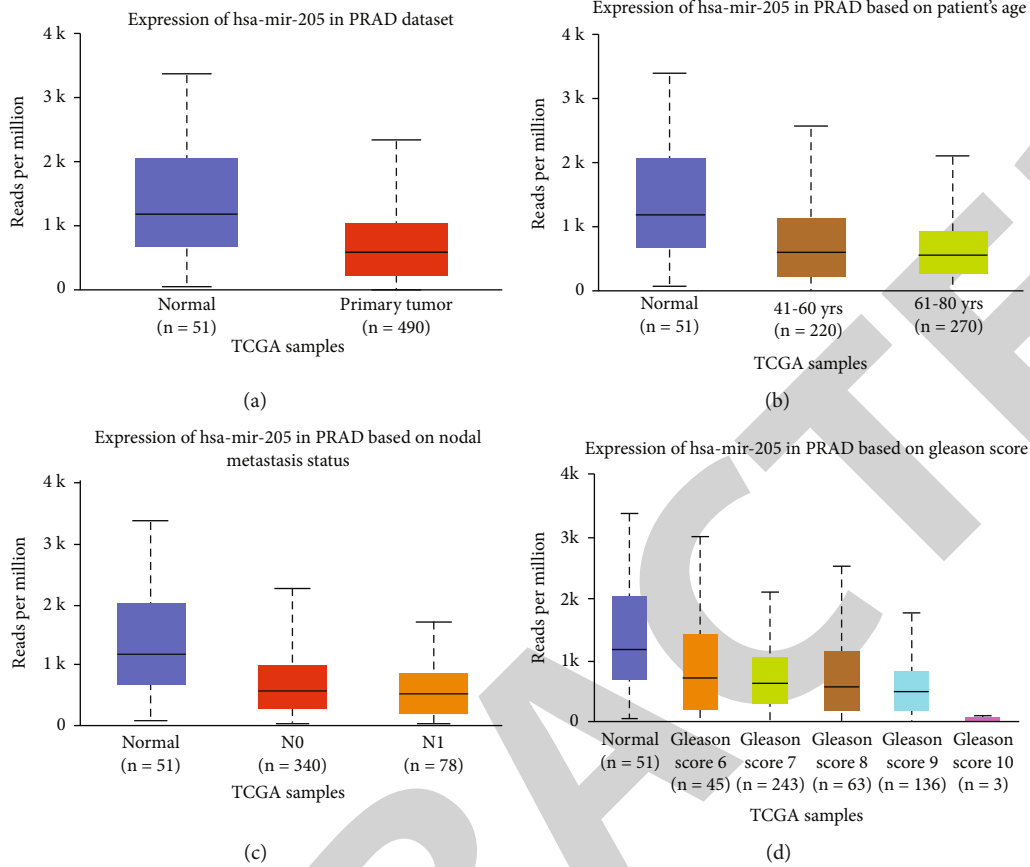
Figure 1: The miR-205 expression in the database. (a) The miR-205 expression in prostate tumor tissues and normal tissues. (b) The relationship between the expression of miR-205 expression and age in prostate cancer tissues. (c) The relationship between miR-205 expression and lymph node metastasis in prostate cancer tissues. (d) The relationship between miR-205 expression and Gleason score in prostate cancer tissues.

carcinoma tissues and the clinicopathological features of prostate cancer patients, and it was revealed that the relationship between miR-205 expression level in prostate cancer tissues and age, lymph node metastasis, and Gleason score was not statistically significant (Figures 1(b)–1(d)).

3.2. The Expression Level of Serum Exosome-Mediated miR-205 Is Negatively Correlated with Pathological as well as Clinical Features. The 120 serum samples (including 60 prostate cancer patient serum and 60 healthy subject serum) were selected to analyze the pronouncement of miR-205 in serum exosomes of people with prostate carcinoma by qRT-PCR. The findings suggested that the miR-205 pronouncement in serum exosomes of people with prostate tumor was lesser than that in serum exosomes of healthy patients (Figure 2(a)). To reveal the relationship between miR-205 expression and pathological and clinical manifestations of prostate carcinoma, the mentioned sections were divided into high (above the mean, $n = 35$) and low (below the mean, $n = 25$) miR-205 pronouncement classes (Figure 2(b)). The association between miR-205 pronouncement level and pathological and clinical manifestations of people with prostate tumor was analyzed using chi-squared test, and the findings revealed that the miR-205 pronouncement in serum exosomes of prostate

tumor patients was significantly negatively linked with carcinoma stage, uncontrolled cell division in lymph node, distant metastasis, and PSA level at initial diagnosis in prostate cancer patients (Figures 2(c) and 2(d)), while the relationship with age of patients was not statistically significant (Table 1).

3.3. The Expression of miR-205 Pronouncement in Serum Exosomes Predicts Good Prognosis of Prostate Carcinoma. We firstly utilized the Kaplan-Meier survival analysis to investigate the correlation among miR-205 pronouncement in exosomes present in the serum of people with prostate cancer and prognosis of patients with prostate cancer. The findings revealed that the inclusive survival rate of people with more miR-205 pronouncement in serum exosomes was higher than that of people with less miR-205 pronouncement (Figure 3), which suggested that miR-205 in serum exosomes played a significant part in the prognosis of patients with prostate tumor. Next, we conducted COX proportional risk model analysis, and the findings of univariate analysis showed that carcinoma stage, PSA level at initial diagnosis, and miR-205 pronouncement were significantly correlated with the inclusive survival rate of people with prostate carcinoma. Furthermore, the results of multivariate investigation indicated that miR-205 utterance in serum
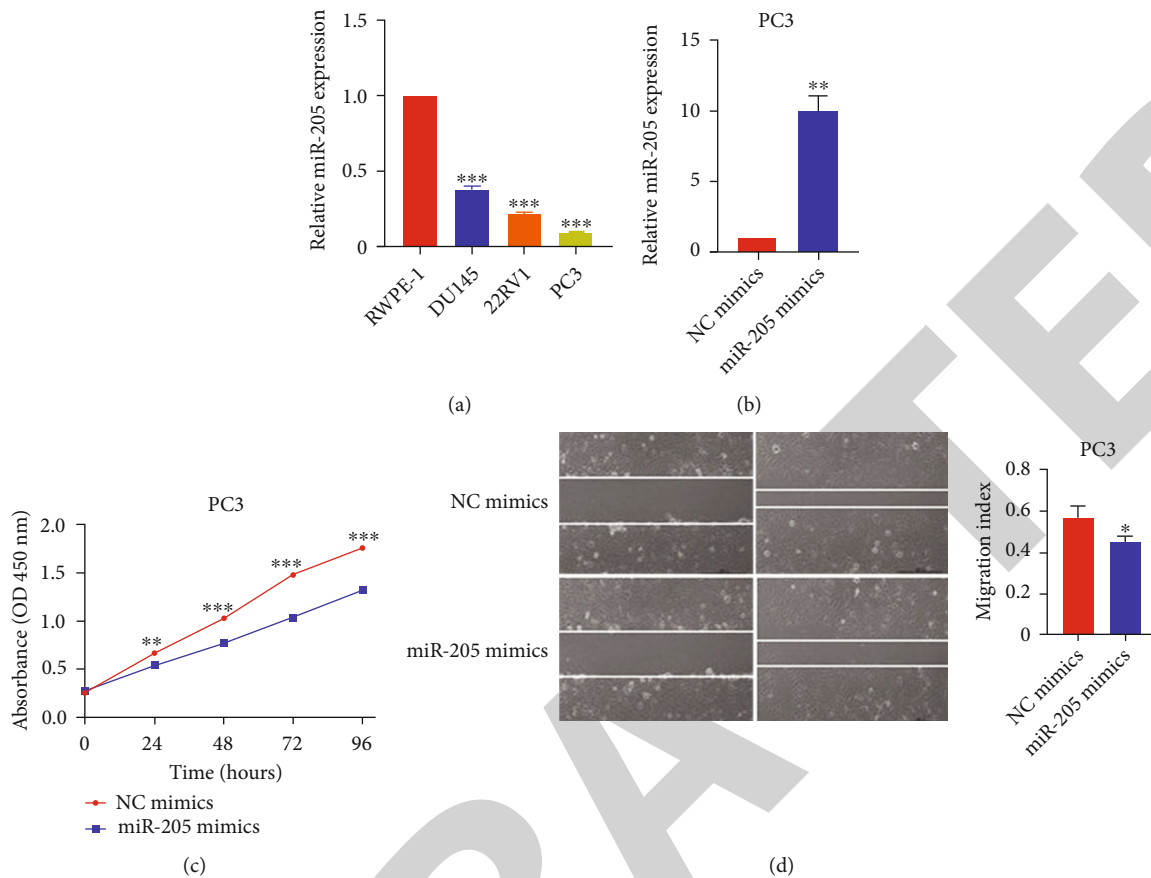
Figure 2: The miR-205 expression in exosomes extracted from prostate carcinoma cell lines and the biological function. (a) The miR-205 expression in exosomes extracted from prostate carcinoma cell lines and normal prostatic cell line of epithelium. (b) The miR-205 expression in exosomes extracted from miR-NC group and miR-205 mimics. (c) The miR-205 promotes the proliferation of prostate cancer cells. (d) The miR-205 promotes the migration of prostate cancer cells. $^{*}P < 0.05$, $^{**}P < 0.01$, and $^{***}P < 0.001$ (Student's t-test). Abbreviations: HR: hazard ratio; CI: confidence interval.

exosomes was an impartial risk aspect for prognosis in people with prostate tumor (Table 2).

3.4. *The miR-205 Extent of Pronouncement in Exosomes Extracted from Prostate Carcinoma Cell Lines.* Cell lines of prostate tumor (DU145, 22RV1, and PC3) and normal prostatic cell line of epithelium RWPE-1 were selected to analyze the miR-205 expression in exosomes derived from cell lies of prostate carcinoma by qRT-PCR. The findings suggested that the miR-205 pronouncement in exosomes of prostate cancer cell lines was significantly lower than that in exosomes of normal cell line of epithelium (Figure 4(a)).

3.5. *The miR-205 Promotes the Spread and Migration of Prostate Carcinoma Cells.* In order to further study the role of miR-205 in prostate carcinoma cells, in this study, the miR-NC and miR-205 mimics were transfected into PC3 cell line, and the RT-PCR was applied to identify cell transfection efficiency of miR-205. The findings revealed that contrasted with miR-NC group, after transfection with miR-205 mimics, the pronouncement level of miR-205 in PC3 was higher with statistically significant difference (Figure 4(b)). Subsequently, proliferation and migration experiments were conducted, and the

results of proliferation detection revealed that overexpression of miR-205 could significantly activate the spread of prostate carcinoma linked with the miR-NC class (Figure 4(c)). In addition, the migration detection findings revealed that overexpression of miR-205 promoted the migration of prostate cancer cells contrasted with the miR-NC group (Figure 4(d)).

4. Discussion

Prostate cancer is one of the extremely widespread cancerous growths in the genitourinary system in elderly men. Its death rate and morbidity rate rank the 2nd and 5th in the global malignant tumor incidence and mortality spectrum, the 1st and 3rd in men in Europe and America, and the 6th and 7th in men in China, respectively [1, 13]. In recent years, with the aging of China's population and other reasons, the incidence and death of prostate cancer have increased significantly, and the disease burden is increasing [14, 15]. Prostate-specific antigen is commonly used biomarker for the screening of prostate carcinoma, but it cannot distinguish the benign and malignant prostate diseases well [16–18]. The Gleason histopathological score is used to assess the prognosis of patients, who often experience additional pain due to invasive procedures [19,
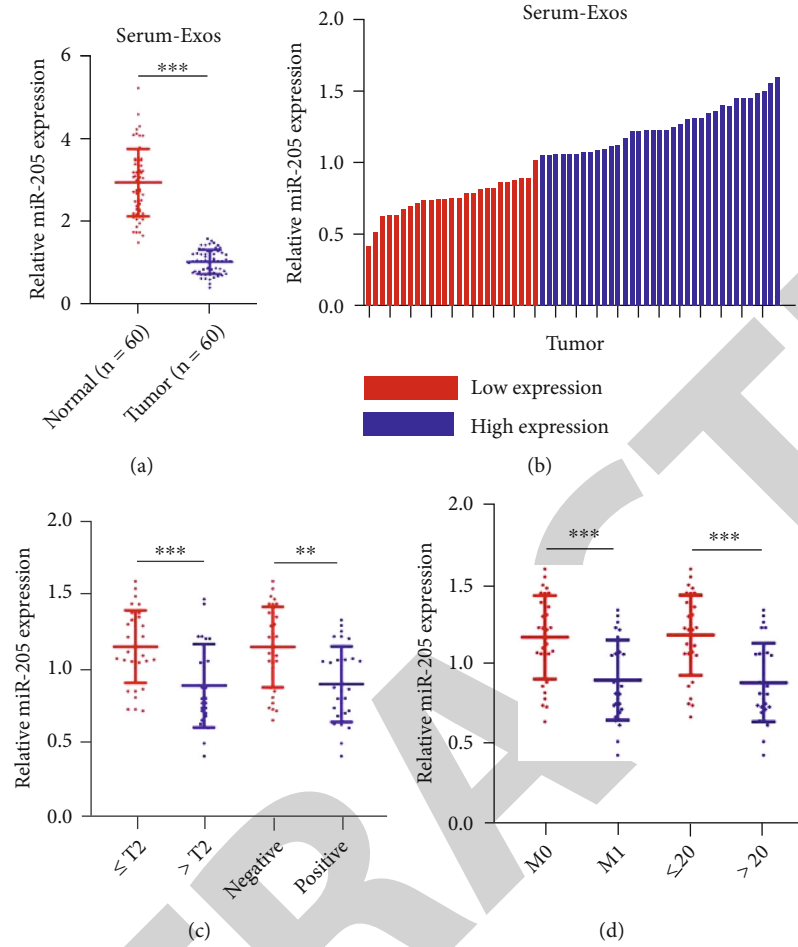
Figure 3: The relationship between the expression level of serum exosome-mediated miR-205 and pathological, clinical features in prostate cancer patients. (a) The miR-205 expression in serum exosomes of people with prostate tumor and healthy patients. (b) The miR-205 expression was divided into high (above the mean, $n = 35$) and low (below the mean, $n = 25$) miR-205 expression classes. (c) The relationship between the expression level of serum exosome-mediated miR-205 and carcinoma stage, lymph node metastasis in prostate carcinoma. (d) The relationship between the expression level of serum exosome-mediated miR-205 and distant metastasis, PSA level in prostate carcinoma at initial diagnosis. $*P < 0.05$, $**P < 0.01$, and $***P < 0.001$ (Student's t-test).

Table 2: Univariate and multivariate analysis of overall survival in patients with prostate cancer ($n = 60$).

Variable for overall survival	Univariate analysis			Multivariate analysis		
	HR	95% CI	P	HR	95% CI	P
Age(years)			0.897			
≤60 vs. >60	1.043	0.547-1.989				
Lymph node metastasis			0.071			
Negative vs. positive	1.819	0.950-3.485				
Distant metastasis			0.218			
M0 vs. M1	1.501	0.786-2.863				
Tumor stage			0.011			0.105
≤T2 vs. >T2	2.364	1.220-4.580		0.565	0.283-1.128	
PSA at initial diagnosis (ng/mL)			0.008			0.294
≤20 vs. >20	2.45	1.263-4.754		0.671	0.318-1.414	
miR-205 expression			$P < 0.001$			0.021
Low vs. high	3.251	1.675-6.313		0.417	0.198-0.878	
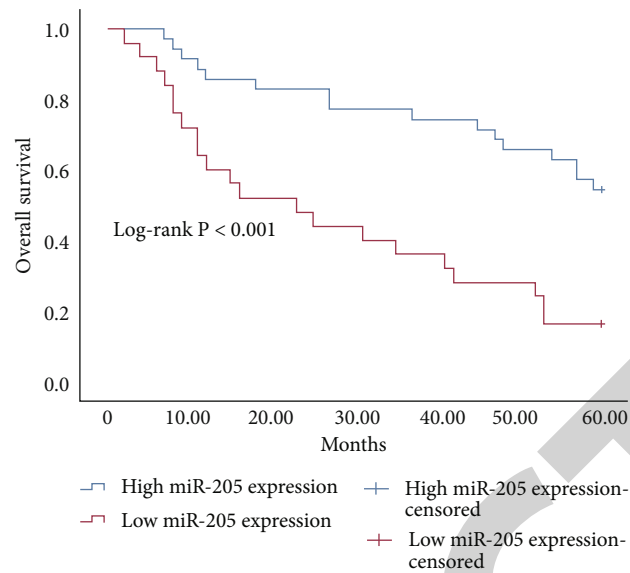
FIGURE 4: The relationship between miR-205 expression in serum exosomes of people with prostate cancer and prognosis of patients.

20]. Therefore, highly specific and noninvasive biomarkers are required to lead the analysis and cure of prostate cancer on urgent basis.

Exosomes are vesicles present outside the cell. They have a diameter of 30-150 nm and lipid bilayer membrane, which are mostly found in numerous body liquids [21, 22]. The main substances of exosomes include proteins, nucleic acids, and lipids. Exosomes secreted by different tissues have different compositions [23]. The lipid bilayer structure of exosomes can protect its contents from degradation by protease and RNA enzyme, and it has high biological stability. Protein is the main component of exosome content, which can directly change the invasion and relocation capability of tumor carcinoma and stimulate tumor progression and uncontrolled cell division [24]. Nucleic acids in exosomes, including mRNA, miRNA, and DNA, can be transferred and change the receptor cell signaling pathway through the fusion of exosomes and target cell membranes [25, 26].

Recent studies have found that miRNAs carried by exosomes derived from cancer cells are engaged in the genesis, angiogenesis, invasion, and uncontrolled cell division of nasopharyngeal carcinoma, breast carcinoma, and other tumor tissues [27, 28]. Prostate cancer cells create a microenvironment conducive to tumor growth by releasing exosomes containing specific components. The miR-424 in exosomes secreted by prostate cancer could induce tumor transformation of normal prostate epithelial cells and further promote the progression of the disease through intercellular transmission, and miR-183 in exosomes secreted by prostate cancer could indorse the propagation, invasion, and uncontrolled cell divisions of cancer cells by downregulating TPM1 pronouncement [29, 30].

Human miR-205 is in the LOC642587 gene of chromosomal lq32.2, which has significant tissue specificity and can be particularly shown in human thymus, breast, prostate, and other tissues, and can control the appearance of multiple target genes. It is involved in the proliferation, apoptosis, differentiation, angiogenesis, drug resistance, infiltration, and uncontrolled cell division of tumor cells. Moreover, miR-205 is expressed differently in different cancer tissues, with high expression in bladder cancer, ovarian cancer, and lung cancer, but low expression in breast cancer, and no difference in colon cancer tissue, indicating that miR-205 cannot only indorse the incidence and growth of lump as a carcinogen miRNAs. It can also be involved in the occurrence and development of tumors as tumor suppressor miRNAs [31, 32]. To study the link between miR-205 pronouncement level and prognosis in prostate cancer, we first examined the UALCAN database and discovered that the pronouncement level of miR-205 in prostate carcinoma tissues was lesser than that in normal prostate tissues. Next, we selected 120 serum samples to analyze the miR-205 pronouncement in serum exosomes of people with prostate carcinoma, and the results suggested that the miR-205 pronouncement in serum exosomes of people with prostate carcinoma was significantly lesser than that in serum exosomes of healthy people. Furthermore, the miR-205 utterance in serum exosomes of people with prostate carcinoma was significantly negatively connected with tumor stage, uncontrolled cell division in lymph node, distant metastasis, and PSA level at initial diagnosis in prostate cancer patients and could be used as a sovereign risk aspect for prognosis in people with prostate carcinoma. In addition, we also found that the miR-205 expression in exosomes of prostate carcinoma cell lines was significantly less than that in exosomes of normal human prostatic cell line of epithelium, and miR-205 could encourage the proliferation and migration of prostate tumor cells. Our results suggested that miR-205 could be implicated in the incidence and progress of prostate tumor as tumor suppressor miRNAs.

5. Conclusion

The pronouncement of miR-205 mediated by serum exosomes and cell exosomes in prostate cancer patients can be used as an indicator of tumor progression and poor prognosis

and also indicates that exosome-mediated miRNA may be utilized as biological markers for early analysis and prediction of malicious carcinomas.

Data Availability

The data could be obtained from contacting the corresponding author.

Conflicts of Interest

The authors declare that they have no conflicts of interest.

Authors' Contributions

Zhuifeng Guo and Xuwei Lu contributed equally to this work.

Acknowledgments

References

[1] H. Sung, J. Ferlay, R. L. Siegel et al., "Global cancer statistics 2020: GLOBOCAN estimates of incidence and mortality worldwide for 36 cancers in 185 countries," *CA: a Cancer Journal for Clinicians*, vol. 71, no. 3, pp. 209–249, 2021.

[2] P. Liu, H. M. Lai, and Z. Guo, "Prostate cancer early diagnosis: circulating microRNA pairs potentially beyond single microRNAs upon 1231 serum samples," *Briefings in Bioinformatics*, vol. 22, no. 3, article bbaa111, 2021.

[3] Y. Miyai, N. Esaki, M. Takahashi, and A. Enomoto, "Cancer-associated fibroblasts that restrain cancer progression: hypotheses and perspectives," *Cancer Science*, vol. 111, no. 4, pp. 1047–1057, 2020.

[4] C. J. He, S. Zheng, Y. Luo, and B. Wang, "Exosome theranostics: biology and translational medicine," *Theranostics*, vol. 8, no. 1, pp. 237–255, 2018.

[5] H. T. Zhang, L. Wang, C. Y. Li et al., "Exosome-induced regulation in inflammatory bowel disease," *Frontiers in Immunology*, vol. 10, p. 1464, 2019.

[6] I. Wortzel, S. Dror, C. M. Kenific, and D. Lyden, "Exosome-mediated metastasis: communication from a distance," *Developmental Cell*, vol. 49, no. 3, pp. 347–360, 2019.

[7] S. Gurung, D. Perocheau, L. Touramanidou, and J. Baruteau, "The exosome journey: from biogenesis to uptake and intracellular signalling," *Cell Communication and Signaling: CCS*, vol. 19, no. 1, p. 47, 2021.

[8] W. Yu, J. Hurley, D. Roberts et al., "Exosome-based liquid biopsies in cancer: opportunities and challenges," *Annals of Oncology*, vol. 32, no. 4, pp. 466–477, 2021.

[9] M. L. Zhang, X. Bai, X. M. Zeng, J. Liu, F. Liu, and Z. Zhang, "circRNA-miRNA-mRNA in breast cancer," *Clinica Chimica Acta*, vol. 523, pp. 120–130, 2021.

[10] K. Yoshida, A. Yokoi, Y. Yamamoto, and H. Kajiyama, "ChrXq27.3 miRNA cluster functions in cancer development," *Journal of Experimental & Clinical Cancer Research*, vol. 40, no. 1, p. 112, 2021.

[11] S. R. Prabhu, A. P. Ware, and A. V. Saadi, "Erythrocyte miRNA regulators and malarial pathophysiology," *Infection, Genetics and Evolution*, vol. 93, article 105000, 2021.

[12] S. Khan, H. Ayub, T. Khan, and F. Wahid, "MicroRNA biogenesis, gene silencing mechanisms and role in breast, ovarian and prostate cancer," *Biochimie*, vol. 167, pp. 12–24, 2019.

[13] T. Tsujino, K. Komura, T. Inamoto, and H. Azuma, "CRISPR screen contributes to novel target discovery in prostate cancer," *International Journal of Molecular Sciences*, vol. 22, no. 23, p. 12777, 2021.

[14] R. J. Rebello, C. Oing, K. E. Knudsen et al., "Prostate cancer (primer)," *Nature Reviews: Disease Primers*, vol. 7, no. 1, p. 9, 2021.

[15] E. Schaeffer, S. Srinivas, E. S. Antonarakis et al., "NCCN guidelines insights: prostate cancer, version 1.2021," *Journal of the National Comprehensive Cancer Network*, vol. 19, no. 2, pp. 134–143, 2021.

[16] S. Dowlatshahi and M. J. Abdekhodaie, "Electrochemical prostate-specific antigen biosensors based on electroconductive nanomaterials and polymers," *Clinica Chimica Acta*, vol. 516, pp. 111–135, 2021.

[17] C. Özyurt, I. Uludağ, B. İnce, and M. K. Sezgintürk, "Biosensing strategies for diagnosis of prostate specific antigen," *Journal of Pharmaceutical and Biomedical Analysis*, vol. 209, article 114535, 2022.

[18] G. Ploussard, N. Fossati, T. Wiegel et al., "Management of persistently elevated prostate-specific antigen after radical prostatectomy: a systematic review of the literature," *European urology oncology*, vol. 4, no. 2, pp. 150–169, 2021.

[19] M. Apfelbeck, S. Tritschler, D.-A. Clevert et al., "Postoperative change in Gleason score of prostate cancer in fusion targeted biopsy: a matched pair analysis," *Scandinavian Journal of Urology*, vol. 55, no. 1, pp. 27–32, 2021.

[20] W. Y. Zhang, G. W. Wang, F. L. Lan et al., "Exploration on Gleason score variation trend of patients with prostate carcinoma from 1996 to 2019: a retrospective single center study," *Gland Surgery*, vol. 10, no. 2, pp. 607–617, 2021.

[21] A. M. Gleason, E. G. Woo, C. McKinney, and E. Sidransky, "The role of exosomes in lysosomal storage disorders," *Biomolecules*, vol. 11, no. 4, p. 576, 2021.

[22] M. D. Hade, C. N. Suire, and Z. C. Suo, "Mesenchymal stem cell-derived exosomes: applications in regenerative medicine," *Cell*, vol. 10, no. 8, p. 1959, 2021.

[23] L. Y. Zhang, Y. C. Ju, S. Chen, and L. Ren, "Recent progress on exosomes in RNA virus infection," *Viruses*, vol. 13, no. 2, p. 256, 2021.

[24] S. Benjamin-Davalos, M. Koroleva, C. L. Allen, M. S. Ernstoff, and S. L. Shu, "Co-isolation of cytokines and exosomes: implications for immunomodulation studies," *Frontiers in Immunology*, vol. 12, article 638111, 2021.

[25] A. Dutta, "Exosomes-based cell-free cancer therapy: a novel strategy for targeted therapy," *Immunological Medicine*, vol. 44, no. 2, pp. 116–123, 2021.

[26] K. Z. Yi, Y. Rong, L. X. Huang et al., "Aptamer-exosomes for tumor theranostics," *ACS sensors*, vol. 6, no. 4, pp. 1418–1429, 2021.

[27] M. L. Liu, K. R. Zhu, X. M. Qian, and W. Li, "Identification of miRNA/mRNA-negative regulation pairs in nasopharyngeal carcinoma," *Medical Science Monitor*, vol. 22, pp. 2215–2234, 2016.

Retraction

Retracted: Magnetic Resonance Image Compilation Was Used in Conjunction with Prostate PI-RADS v2.1 Score Has Diagnostic Relevance for Benign and Malignant Prostate Lesions

Computational and Mathematical Methods in Medicine

This article has been retracted by Hindawi following an investigation undertaken by the publisher [1]. This investigation has uncovered evidence of one or more of the following indicators of systematic manipulation of the publication process:

(1) Discrepancies in scope

(2) Discrepancies in the description of the research reported

(3) Discrepancies between the availability of data and the research described

(4) Inappropriate citations

(5) Incoherent, meaningless and/or irrelevant content included in the article

(6) Peer-review manipulation

The presence of these indicators undermines our confidence in the integrity of the article's content and we cannot, therefore, vouch for its reliability. Please note that this notice is intended solely to alert readers that the content of this article is unreliable. We have not investigated whether authors were aware of or involved in the systematic manipulation of the publication process.

Wiley and Hindawi regrets that the usual quality checks did not identify these issues before publication and have since put additional measures in place to safeguard research integrity.

We wish to credit our own Research Integrity and Research Publishing teams and anonymous and named external researchers and research integrity experts for contributing to this investigation.

The corresponding author, as the representative of all authors, has been given the opportunity to register their agreement or disagreement to this retraction. We have kept a record of any response received.

References

[1] W. Xu, H. Cao, F. Du, L. He, F. Jiang, and C. Hu, "Magnetic Resonance Image Compilation Was Used in Conjunction with Prostate PI-RADS v2.1 Score Has Diagnostic Relevance for Benign and Malignant Prostate Lesions," *Computational and Mathematical Methods in Medicine*, vol. 2022, Article ID 3613540, 10 pages, 2022.

Research Article

Magnetic Resonance Image Compilation Was Used in Conjunction with Prostate PI-RADS v2.1 Score Has Diagnostic Relevance for Benign and Malignant Prostate Lesions

Wenjuan Xu [iD],[1,2] **HaiYan Cao** [iD],[3] **Fang Du** [iD],[2] **Ling He** [iD],[2] **FangLian Jiang** [iD],[2] **and ChunHong Hu** [iD][1]

[1]*Department of Radiology, The First Affiliated Hospital of Soochow University, Suzhou, Jiangsu Province 215006, China*
[2]*Department of Radiology, Medical Image Center, The Affiliated Hospital of Yangzhou University, Yangzhou, Jiangsu Province 225001, China*
[3]*Department of Ultrasound, Yancheng First Hospital, Affiliated Hospital of Nanjing University Medical School(the First People, S Hospital of Yancheng), Yancheng, Jiangsu Province224001, China*

Correspondence should be addressed to ChunHong Hu; sdhuchunhong@sina.com

Objective. To assess the diagnostic usefulness of magic in conjunction with PI-RADS v2.1 for prostate cancer malignant foci. *Methods.* A total of 202 lesions (97 transitional zone lesions and 105 peripheral zone lesions) from 198 people were investigated retrospectively using traditional MRI and magic images. Each lesion has a unique pathological consequence. Lesions T1, T2, and PD values were employed as magic observation markers. The locations of the lesions were aggregated, and the paired *t*-test and receiver operating characteristic curve (ROC) were employed to find the indices with statistical significance in separating benign from malignant prostatic nodules (+1 point) and (−1 point) respectively. Draw a ROC curve and compare it to the PI-RADS v2.1 score using the magic positive and negative indices as well as the PI-RADS v2.1 score. By comparing the ROC curves scored separately, the diagnostic efficiency of the two scoring approaches for benign and malignant prostate lesions was investigated. *Results.* T2 value has the highest diagnostic efficiency among the magic observation indices. T2 value of 77 ms for transitional zone lesions and T2 value of 89 ms for peripheral zone lesions are positive indices, whereas T2 value >77 ms and T2 value >89 ms are negative indexes. PI-RADS v2.1 combines one score and magic. In the transitional zone, the sensitivity, specificity, positive predictive value, and negative predictive value of the two scoring methods were 57.52, 87.70, 76.70, and 74.6 percent and 82.50, 73.68, 95.5, and 74.7 percent, respectively, and the AUC values were 0.735 and 0.846, respectively (*P* = 0.004); in the peripheral zone, the AUC values were 86.15 percent, 68.42 percent, 82.4. *Conclusions.* Magic T2 value is a favorable sign for diagnosing benign and malignant prostate cancers when used in conjunction with PI-RADS v2.1. The end product exceeds PI-RADS v2.1 on its own, which is more useful in identifying benign and malignant prostate lesions, decreasing unnecessary puncture and alleviating patient pain.

1. Introduction

Prostate cancer (PCA) is the world's second most frequent male cancer and the fourth major cause of cancer mortality in males [1, 2]. Early detection and appropriate staging seem to be particularly critical for PCA therapy and prognosis [3]. Digital rectal examination, traditional transrectal ultrasound (TRUS)-guided biopsy, PSA testing, and magnetic resonance imaging are now used to diagnose prostate disease (MRI). MRI, with its excellent soft tissue contrast capacity and non-invasive nature, has been extensively employed in the identification, localization, and staging of benign and malignant prostate tumors [2]. The first and second editions of the prostate imaging reporting and data system (PIRADS) were

introduced, respectively, at the 2012 annual European Urogenital Radiology meeting, the 2014 American College of Radiology, and the European Society of Urogenital Radiology joint AdMeTech foundation, to standardize MRI image acquisition, image interpretation, and report writing, as well as to improve diagnostic accuracy and reduce unnecessary punctures for benign and malignant prostate. In 2019, this data system was upgraded to PI-RADS v2.0 Version 1 of the PI-RADS data system application streamlines reporting and scanning definitions, as well as surgeon and patient interpretation of findings. Previous clinical investigations have also shown that the PI-RADS score system correlates better with clinical diagnoses [4].

These quantitative approaches, such as apparent diffusion coefficient (ADC), diffusion kurtosis imaging (DKI), diffusion tensor imaging (DTI), and intravoxel incoherent motion (IVIM), have been increasingly employed for MRI detection of prostate disorders in recent years [5, 6]. Magic (magnetic resonance image preparation), also known as synthetic MRI, has recently developed a new MRI quantitative sequence, one-stop relaxation quantitative MRI, by optimizing the multi delay versus multi echo technique with saturation pulses alternating with signal acquisition and additionally incorporating estimation and correction for radiofrequency field inhomogeneities. The relaxation periods and proton density were quantified using a multisaturation recovery multiecho paired fast spin echo readout. Its benefit is its capacity to give absolute quantitative maps of T1, T2, and PD maps in a single scan, giving objective quantitative data for illness diagnosis. The purpose of this research was to look into the cutoff values of magic technology in distinguishing benign from malignant prostate disorders, as well as the combination of magic-related quantitative factors with prostate PI-RADS v2.1 score value for the correction of benign and malignant prostate lesions.

2. Materials and Methods

2.1. Study Subjects. Patients with routine pathology findings who had prostate puncture or surgery in our institution between October 2020 and December 2021 had their MR imaging data evaluated retrospectively. Inclusion criteria are as follows: (1) no medication or surgical therapy prior to prostate MRI examination; (2) no needle biopsy performed prior to the prostate MRI test; and (3) all patients receiving the magic examination. Exclusion criteria are as follows: (1) no pathological findings after magnetic resonance examination and a time interval of more than 3 months between biopsy and MRI examination; (2) lesions in the context of diffuse type lesions of the prostate; (3) prostate lesions ≤5 mm; (4) insufficient data on MRI imaging; and (5) magnetic resonance images of poor quality with significant image artifacts. This study included 198 patients, 202 lesions, 97 of which were transitional band lesions and 105 of which were peripheral band lesions, with the most common complaints being PSA elevation or/and urinary frequency, dysuria, urinary retention, hematuria, and other symptoms; radical prostatectomy was performed in 129 patients (58 lesions in the peripheral band and 71 lesions

in the transitional band). The medical ethics review board of Yangzhou University's Affiliated Hospital authorized this research, and all patients provided written informed permission. The age range was 29-87 years old, with a mean age of (68.48 ±0.69)

2.2. MRI Scanning Techniques. The scanner utilized was a GE- architect 3.0 T MRI scanner with 16 channel coils (anterior array, AA) and a 40 channel coil (posterior array). Before the examination, the patient's urine was correctly preserved, and the scan body position comprised axial, coronal, and sagittal, with the axial direction perpendicular to the long axis of the prostate. T1WI and T2WI scans with rapid spin echo sequences, small field high-resolution T2WI and DWI scans, DCE scans (DCE scans were not frequently conducted), and magic scans were among the sequences used. Axial parameters for T1WI sequences were entered: repetition time (TR) =620 ms, echo time (echo time, TE) =15 ms, slice thickness/interslice spacing 3.0 mm/0 mm, scan field 200×200 mm, matrix (matrix) 320×320, number of excitations (nex) 2 times, and image duration 2 min 35 s. On T1WI sequences, the following parameters were used: TR =620 ms, TE= 15 ms, slice thickness/interslice distance 3.0 mm/0 mm, scan field 340×340 mm, matrix 320×320, nex 2 times, and picture duration 2 minutes 28 seconds. On T2WI sequences, the axial parameters were TR =3500 ms, TE =100 ms, slice thickness/interslice distance 3.0 mm/0 mm, scan field 200 ×200 mm, matrix 320×320, nex 2.5 times, and picture duration 2 minutes 28 seconds. On T2WI sequences, the coronary parameters were TR =3700 ms, TE =106 ms, slice thickness/interslice distance 3.0 mm/0 mm, scan field 340 ×340 mm, matrix 320×320, nex 2.5 times, and image duration 2 minutes 14 seconds. On T2WI sequences, the sagittal parameters were TR = 4100 ms, TE = 140 ms, slice thickness /interslice distance = 3.0 mm / 0 mm, scan field = 280×280 mm, matrix 320×320, nex 2 times,and picture acquisition duration 2 minutes 6 seconds. On DWI sequences, the axialparameters were TR=3600 ms,TE=86 ms, slice thickness / interslice distance 3.0mm / 1.0 mm, scan field 280×140 mm, matrix 120× 60, nex 2 times, picture duration 2 minutes 6 seconds.On MAGIC sequencws, the axial parameters were TR= 4300ms, TE= 20 / 108ms, slice thickness/ slice spacing 3.0mm/0.5mm, scan field of view 300×300 mm, matrix 320×256, nex 1 time,picture time 4 minutes 23 seconds.On DCE sequencesTR= 5 ms, TE = 2 ms, slice thickness / interslice distance 6.0 mm / 0 mm, scan field = 288 ×245 mm, matrix 224×192, no nex, picture collection time 5min 6 s, total scan duration 30 periods.The time resolution is 10 seconds. tr = 4100 MS, TE = 140 ms, slice thickness/interslice distance = 3.0 mm/0 mm, scan field = 280 280 mm, Gadopentetate dimeglumine (GD DTPA) was given intravenously by the elbow using a two barrel high-pressure syringe at an injection rate of 2–3 ml/s and a bolus of 0.1 mmol/kg in 20 ml tubes.

2.3. Pathological Examination and Zonation. Rectal ultrasonography was used to identify the perineal route after MRI in 198 patients, and the puncture was performed by an

experienced chief physician who preoperatively analyzed the patient's MRI data and coordinated with the imaging physician to determine the targeted puncture. Ultrasonography-magnetic resonance fusion navigation biopsy (TRUS-MRI FB) and ultrasound-guided systematic biopsy (TRUS-SB) "10 needles" combined prostate puncture method TRUS and guided the piercing of the MRI-targeted targets. TRUS-MRI fusion navigation puncture (TRUS-MRI FB) and ultrasound-guided system puncture (TRUS-SB) prostate puncture method TRUS guided the piercing of the MRI-targeted targets. Each chosen target received 2-4 needles; conventional puncture used 10 needles, one for each of the prostate's peripheral bands, notably the anterior, lateral, central, paramedian, and transitional bands (Figure 1). In this research, histopathological samples of radical prostatectomy were chosen as the ultimate pathological reference for individuals who had simultaneous radical prostatectomy and biopsy.

2.4. Image Processing and PI-RADS v2.1 Scoring Criteria. The scanned images were sent to a diagnostic workstation, and the enrolled cases were co-analyzed in a double blinded manner by two physicians with more than 5 and 10 years of experience in MRI diagnosis and analyzed according to find PI-RADS v2.1 standard scoring, with consensus achieved when scoring was discordant [7, 8]. The peripheral zone of the prostate (PZ) is dominated by DWI (ADC) scores, such as: DWI (ADC) of 3 points, T2WI is arbitrary, DCE is negative, and the total score remains unchanged, remaining 3 points; DCE was positive with a total score of $3 + 1$, which was 4 points. T2WI scores dominated the transitional zone (TZ), for example: T2WI of 2 points, if DWI (ADC) ≤ 3 points, total score unaltered, if DWI (ADC) ≥ 4 points, and total score 3 points; T2WI of 3 points, DWI (ADC) ≤ 4 points, total score unaltered, if DWI (ADC) of 5 points, total score 4 points, and negative or positive DCE in the mobility band score had no effect on the overall score. Finally, use the PI-RADS v2.1 score to determine the probability of PCA: 1 point = very unlikely to exist; 2 points = unlikely to be present; 3 points = dubious existence; 4 points = probable presence; and 5 points = highly likely to be present. In our research, the biggest diameter of the lesion was at the PZ according to the PZ score, and the largest diameter was at the TZ according to the TZ score of the migrating band, when the lesion was substantial and included either the PZ or the TZ. Two radiologists (with over 5 and 10 years of experience in MRI diagnostic work-up, respectively) manually drew the area of interest (ROI) based on T2WI and DWI images based on the pathological findings. For each enrolled case, GE aw4 was used to create a ready view in the system. First, the prostate tissue was mirror segmented, and two levels displaying the most typical clarity of prostate cancer were chosen to avoid necrosis, cystic change, hemorrhage areas, and so on, and the dedicated magic postprocessing software on the GE- architect device was used to acquire T1 value, T2 value, and PD value of the focal area of the prostate (Figure 2).

2.5. Statistical Methods. Results were analyzed using SPSS21.0 statistical software, and measurement data were represented as mean standard deviation ($x \pm s$). The intergroup comparison of counting data was done using paired t-test to establish the differential indicators of the magic approach in discriminating benign and malignant prostate cancers, and $P < 0.05$ was judged statistically significant. If there was more than one statistically significant indication, the differential indicators were scored again (1 point for the positive indicator and -1 point for the negative indicator). Using the MedCalc 19.2 statistical program, the differential index of the final inclusion score was derived by calculating the receiver operating characteristic curve (ROC) and comparing the area under the curve with pathological results as status factors (AUC). PI-RADS v2.1 was plotted separately with pathological findings as the status variable scoring, the Z-test was used to compare the difference between the AUCs, and the MAGIC combined PI-RADS v2.1 ROC curve of the score was used to determine its optimal diagnostic cut-off value, sensitivity, specificity, positive predictive value (PPV), and negative predictive value (NPV) in the diagnosis of benign and malignant lesions of the prostate.

3. Results

3.1. Pathological Findings. In the peripheral band region, all 202 lesions from 197 individuals displayed unambiguous conventional pathology findings, including 40 (38.1%) benign and 65 (61.9%) malignant lesions. The benign nodules had a maximum diameter of 5-24 mm and a mean diameter of 11.8-64.77%; the malignant nodules had a maximum diameter of 5-27 mm and a mean diameter of (13.1-95.19%). In the group of peripheral benign and malignant lesions, the transitional zone was home to 57 (58.78%) benign lesions and 40 (41.2%) malignant lesions. The benign nodules had a maximum diameter of 7-38 mm and a mean diameter of 13.93 ± 6.17 mm; the malignant nodules had a maximum diameter of 3-30 mm and a mean diameter of 15.82 ± 6.87 mm.

3.2. PI-RADS v2.1 Ratio of Benign to Malignant Lesion Composition in Different Scores. The prostatic lesions included in this investigation had PI-RADS values of 2, 3, 4, and 5. The percentage of malignant foci with shifted bands in PI-RADS 2-5 scores was 0.25%, 76%, 75.22%, and 83.33%; the percentage of peripheral band malignant foci in PI-RADS 2-5 scores was 0%.31.03%, 74.51%, and 94.74% (see Table 1).

3.2.1. Differences in Quantitative Parameters of Benign and Malignant Lesions of the Prostate. Table 2 shows the T1, T2, and PD values in benign and malignant prostate tumors. T1, T2, and PD values were lower in transitional and peripheral PCA lesions than in noncancerous regions. T1 and T2 values of PCA lesions in the transitional zone were lower than those of benign hyperplasia ($P = 0.03, 0.001$), and PD values of PCA lesions were not significantly different from those of benign hyperplasia ($P = 0.209$); T2 value was significantly different ($P < 0.001$) between peripheral band PCA and non cancerous tissue, while T1 and PD values were not significantly different ($P = 018, 0.25$).

(a)

(b)

(c)

(d)

(e)

(f)

(g)

(h)
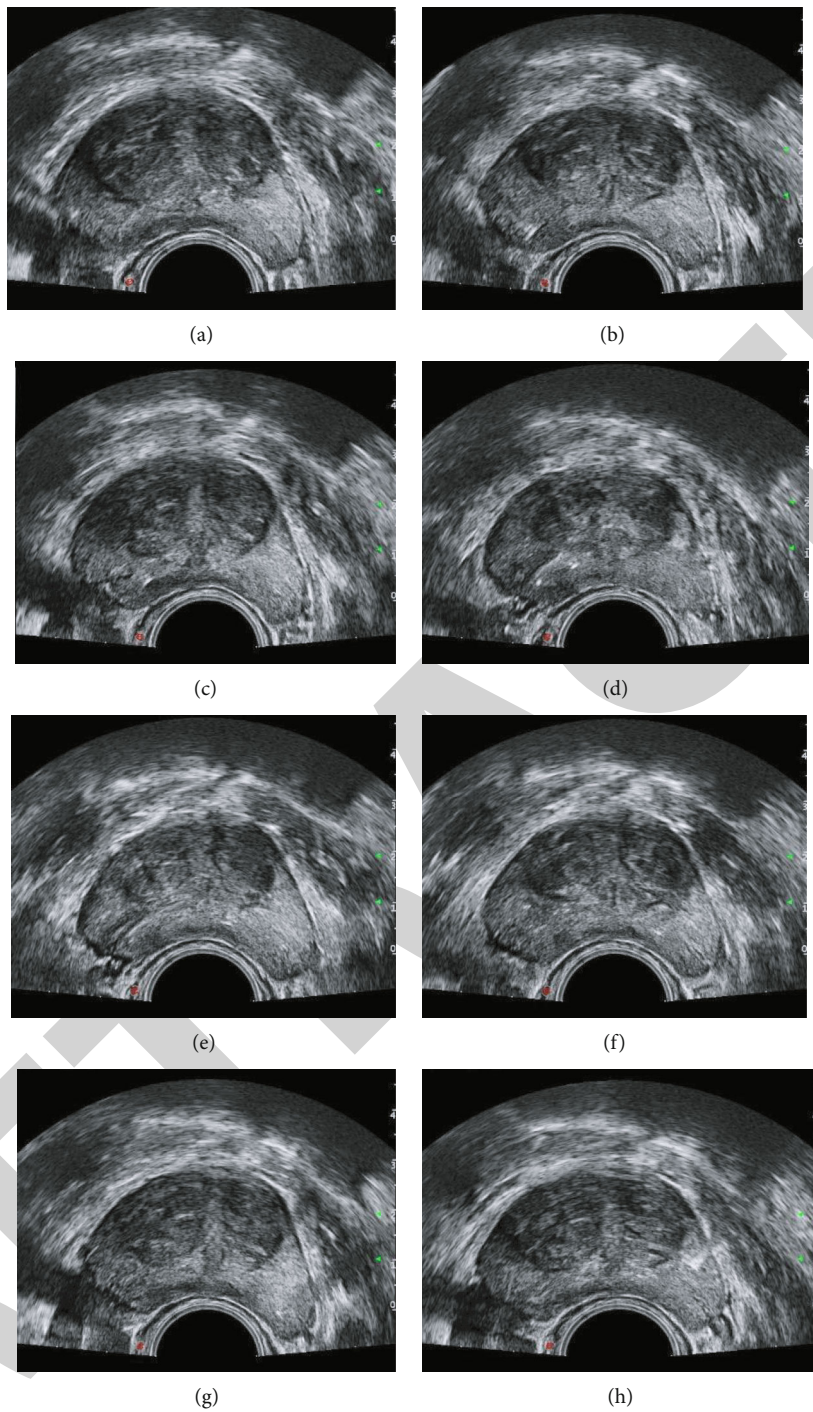
Figure 1: Continued.
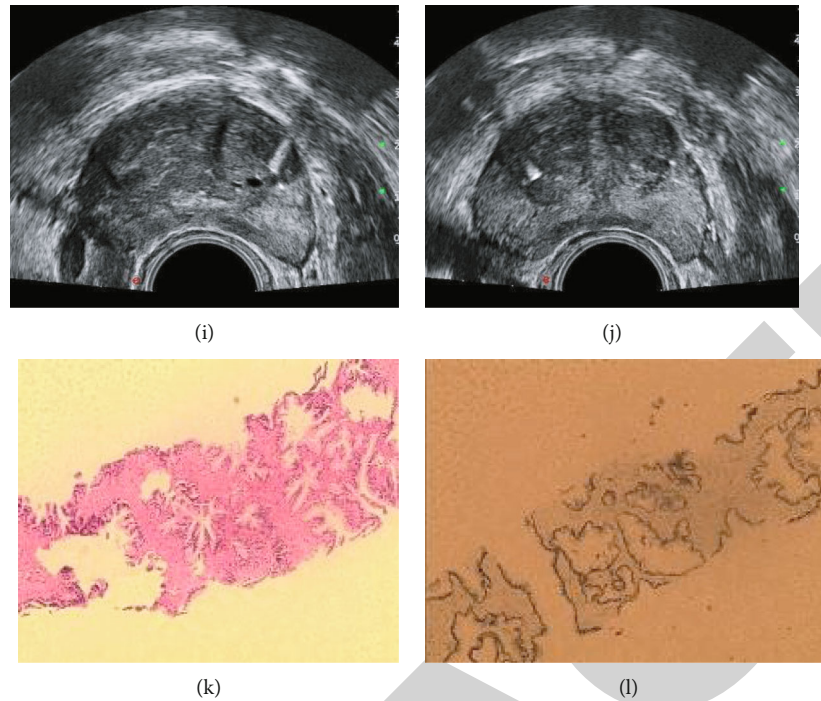
FIGURE 1: Prostate sb 10 gauge. The puncture points of (a)–(j) were the following: anteroposterior, lateral, medial, and paramedian of the right peripheral band and the paramedian, medial, lateral, and anteroposterior of the left peripheral band and the transitional band on the right side; (k)–(l) is the pathology result of puncture; immunohistochemistry results are prostate hyperplasia.

3.2.2. Diagnostic Efficacy of Different Quantitative Parameters in Differentiating Benign and Malignant Foci of Prostate. Figure 3 depicts the findings of ROC analysis of the quantitative parameters T1, T2, and PD values of the migrating and peripheral bands in distinguishing benign from malignant tumors. The AUC of T2 value was significantly higher than that of T1 and Pd ($P = 0.0063$ and 0.0023, respectively) for discriminating PCA from benign hyperplasia in the region of the migrating band, and the AUC of T1 value was slightly higher than that of PD value without statistical significance ($P = 0.3683$). For PCA and noncancerous tissue discriminating peripheral band regions, the AUC of T2 value was still significantly higher than that of T1 and Pd (the AUC values of T2 value in the migrating band and peripheral band sections in this research were 0.819 and 0.813, respectively).

3.3. PI-RADS v2.1 Scoring and T2 Values Combined PI-RADS v2.1 Diagnostic Efficacy for Benign and Malignant Lesions of the Prostate. T2 values in this research demonstrated good diagnostic effectiveness in the identification of benign and malignant prostate disorders, with cutoffs of 77 ms for T2 values in the transitional zone and 89 ms for T2 values in the peripheral zone. The sensitivity, specificity, PPV, and NPV of the two scoring methods, PI-RADS V2.1 scoring and T2 value, combined with PI-RADS V2.1 scoring in the diagnosis of benign and malignant diseases of the prostate transitional zone were 57.52, 87.70, 76.70, and 74.6 percent and 82.50, 73.68, 95.5, and 74.7 percent, respectively, and the AUC values were 0.735 and 0.846, respectively (see Table 3). The sensitivity, specificity, PPV, and

NP are shown in Table 4. The combination of PI-RADS v2.1 scores and quantitative parametric T2 value demonstrated a higher diagnostic value for benign and malignant prostate lesions, regardless of whether they were migration band or peripheral band lesions (migration band $z = 2.878$, $P = 0.0040$; peripheral band $z = 2.103$, $P = 0.0355$), as shown in Figure 4.

4. Discussion

PI-RADS, a standardized reporting system for magnetic resonance diagnostic of prostate imaging, was released in 2012 by the European Society of Urological Radiology (ESUR). The American College of Radiology, the European Society of Genitourinary Radiology, and the AdMeTech Foundation scoring standards released PI-RADS v2.0 in September 2015, with improved diagnostic expertise and scanning methodology. Previous study has demonstrated that the PI-RADS v2.0 scoring system is useful for diagnosing prostate cancer and increases the positive rate of prostate puncture. [9]. The most current prostate magnetic resonance scoring version PI-RADS v2.1, proposed in 2019 by European Urology, is more granular and selective, decreasing PI-RADS v2.0 The existence of confusing scoring standards, as well as a lack of definition of scoring zones, improves the diagnostic consistency and accuracy of prostate cancer [10]. Nonetheless, owing to the absence of a specific value of objective quantitative parameters, the interobserver agreement might still have some impact due to the expertise level of various readers, often resulting to larger false-positive findings and limiting the detection rate of PCA [11].

(a)

(b)

(c)

(d)

(e)

(f)

(g)
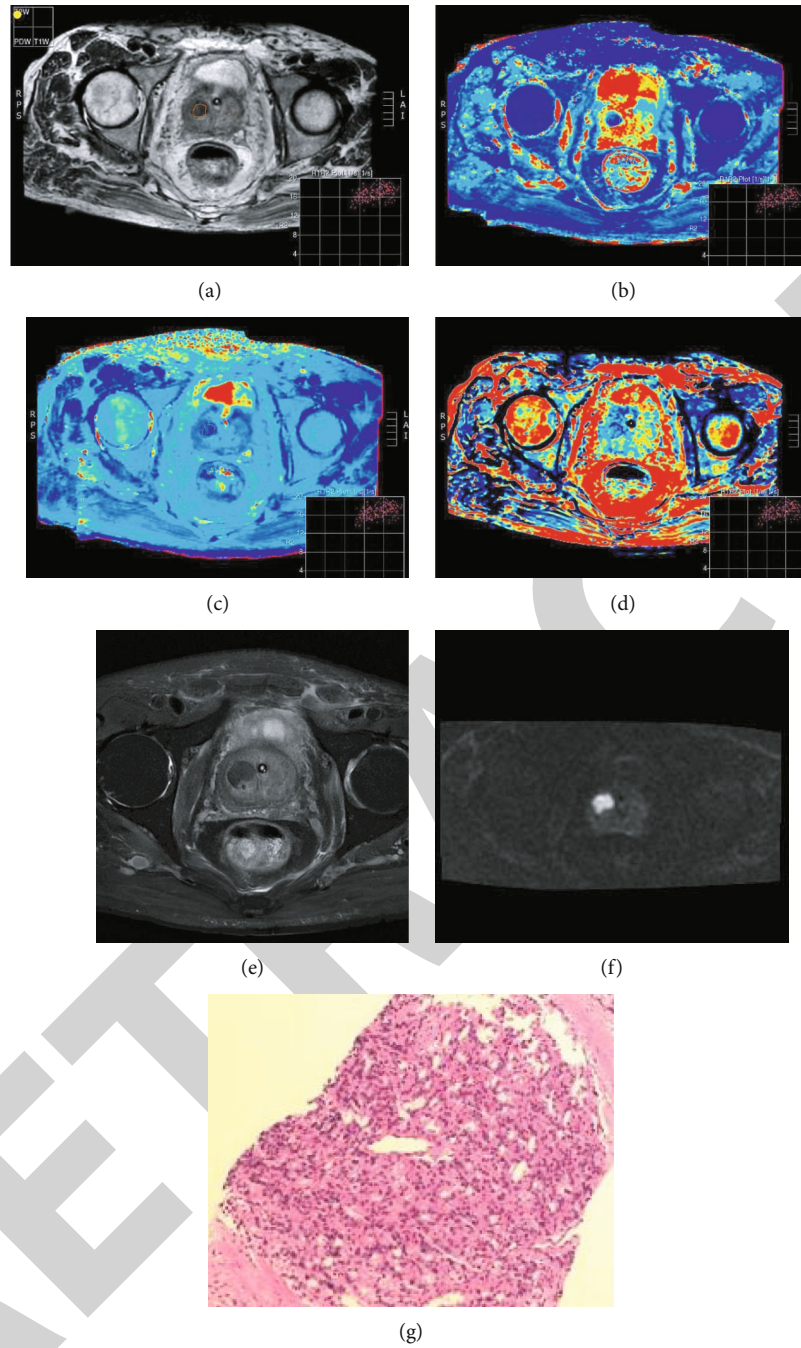
FIGURE 2: Migrated magic images with prostate cancer. (a) is the T2WI, (b) is the T1 value, (c) is the T2 value, (d) is the PD value, (e) is the small field T2W fat pressing axial, (f) is the diffusion-weighted image with b value 2000, and (g) is the pathological result of prostate cancer.

TABLE 1: PI-RADS scores and the ratio of benign to malignant composition of prostate lesions on MP MRI.

PI-RADS score	Transitional zone Benign	Malignant	Total	Malignant rate	Peripheral zone Benign	Malignant	Total	Malignant rate
2	1	0	1	0%	6	0	6	0
3	49	17	66	25.76%	20	9	29	31.03%
4	5	13	18	72.22%	13	38	51	74.51%
5	2	10	12	83.33%	1	18	19	94.74%

TABLE 2: results of different quantitative parameters for benign and malignant lesions of prostate.

TumoR character	Transitional zone			Peripheral zone		
	T1 (ms)	T2 (ms)	PD (pu)	T1 (ms)	T2 (ms)	PD (pu)
Benign proliferation/noncancerous tissue	1561.72 ± 326.08	99.98 ± 13.51	71.80 ± 7.77	2003.27 ± 480.33	132.63 ± 39.50	76.73 ± 8.74
Prostatic	1228.92 ± 302.30	80.04 ± 11.63	67.53 ± 8.33	1310.13 ± 237.64	86.03 ± 14.16	68.87 ± 6.78
t	3.037	5.859	-1.386	2.412	5.787	2.280
p	0.03	<0.001	0.209	0.018	<0.001	0.025

(a) Transitional zone

(b) Peripheral zone
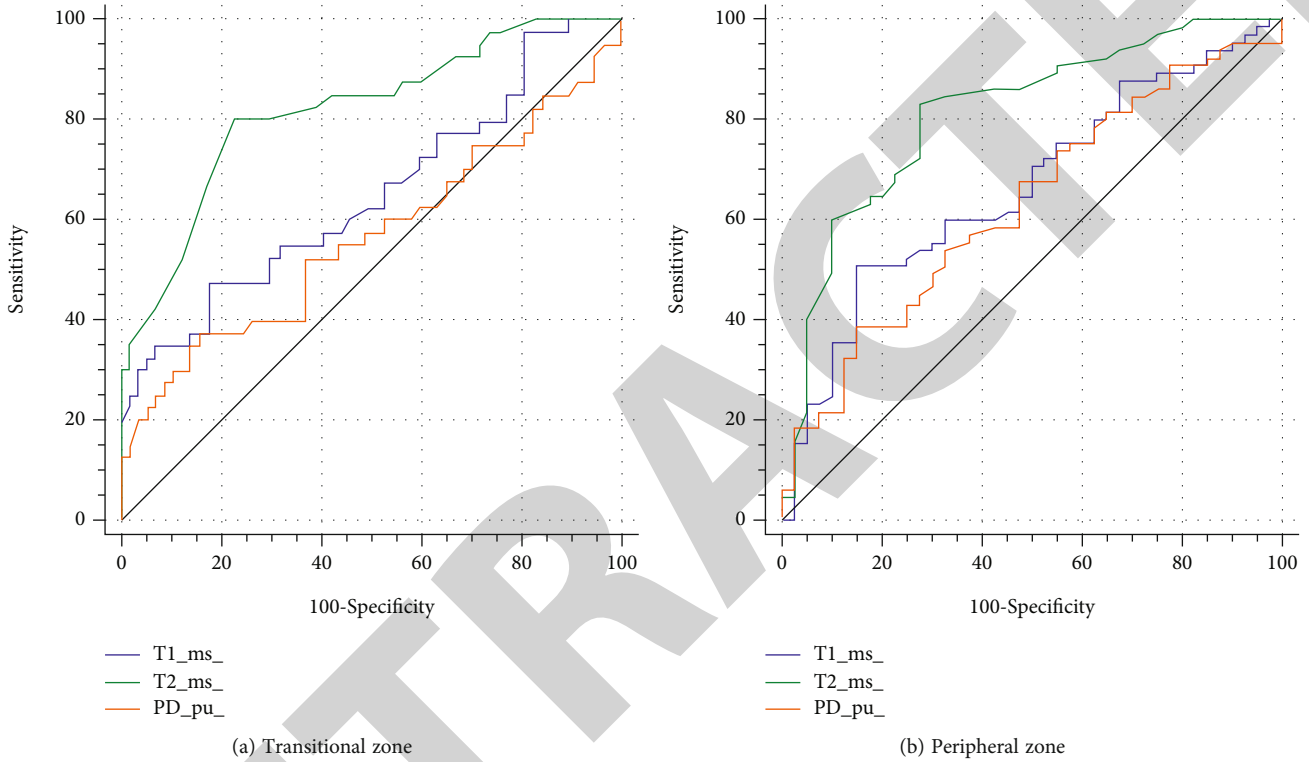
FIGURE 3: ROC curves showing the diagnostic efficacy of T1, T2, and PD values in the migration band and peripheral band areas for differentiating benign and malignant lesions of prostate.

TABLE 3: Comparison of the two scoring methods for the diagnosis of benign and malignant transitional zone lesions.

Scoring method	Susceptibility (%)	Specificity (%)	PPV (%)	NPV (%)	AUC	95% CI
PI-RADS v2.1	57.52	87.70	76.7	74.6	0.735	0.636~ 0.820
PI-RADS v2.1 + T2	82.5	73.68	95.5	74.7	0.846	0.759~ 0.911

TABLE 4: Comparison of the diagnostic values of the two scoring methods for benign and malignant peripheral band lesions peripherin.

Scoring method	Susceptibility (%)	Specificity (%)	PPV (%)	NPV (%)	AUC	95% CI
PI-RADS v2.1	86.15	68.42	82.4	74.3	0.816	0.728~ 0.886
PI-RADS v2.1 + T2	70.8	92.1	93.9	64.8	0.890	0.813~ 0.943

Magic (magnetic resonance image preparation), also known as synthetic MRI, is a ground-breaking one-stop relaxation quantitative MR method capable of detecting T1, T2, and PD values in a single scan. Originally, Magic was intended for use in imaging the central nervous system [12] and then gradually expanded into other systems, pri-

marily on organs with less respiratory activity. It was originally intended for use in imaging the central nervous system and gradually expanded into other systems, primarily in organs with less respiratory activity. There has been little study on its application to prostate illness; however, Cui Yadong et al. investigated the use of quantitative parameters
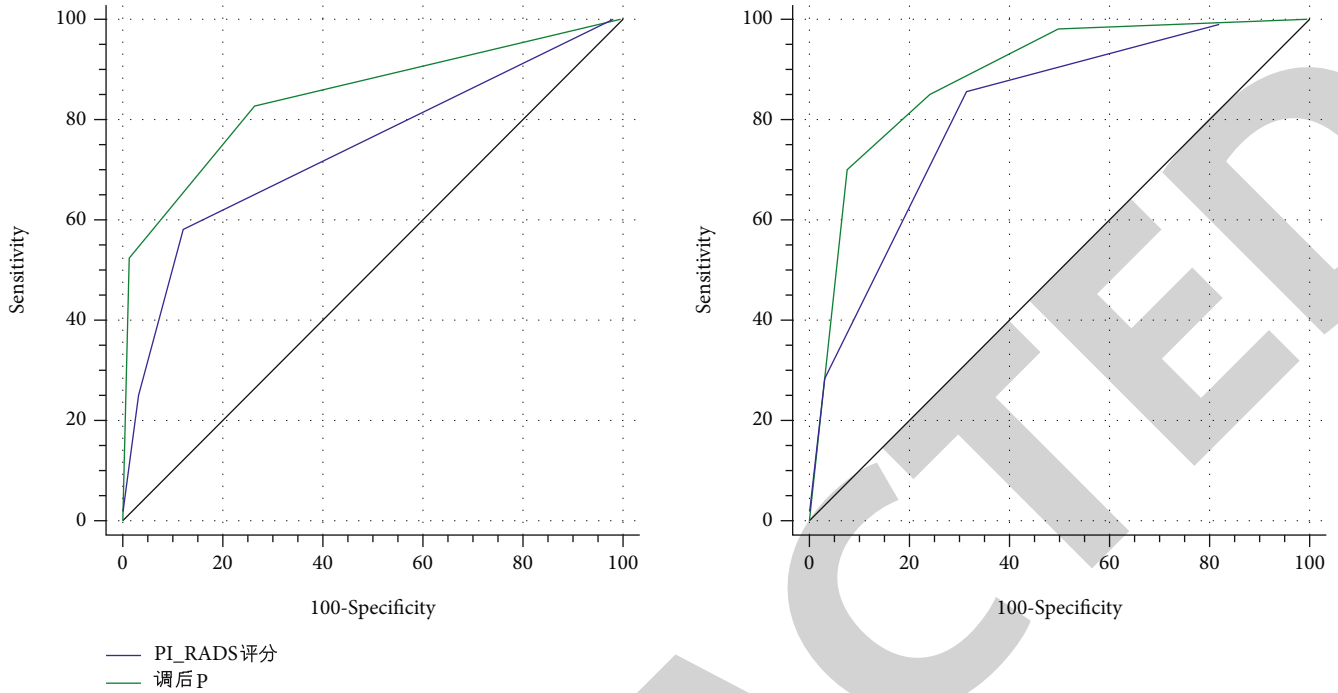
FIGURE 4: ROC curves of the diagnostic values of the two scoring methods for benign and malignant lesions of the prostate.

produced from synthetic MR imaging technology for the detection of prostate cancer [13]. However, since the importance of quantitative parameters T1, T2, and PD values in the diagnosis of prostate disease is not widely accepted, this approach was not included in its scoring system. In this study, we looked for the most meaningful quantitative parameter values for the diagnosis of prostate cancer by interpreting and statistically analyzing different quantitative parameters (T1, T2, and PD values) between prostate cancer and noncancerous areas, and we determined the possible positive and negative indicators for the diagnosis of prostate cancer, counting +1 point for the positive indicator and −1 point for the negative indicator, and we went on to investigate further. Also, talk about if its diagnostic accuracy has increased.

The nodules in this study were all PI-RADS scores 2-5, and the percentage of peripheral band prostate cancer in PI-RADS 2-5 points was 0.31.03, 74.51, and 94.74 percent, and the percentage of transitional band malignant lesions in PI-RADS 2-5 points was 0.25.76, 75.22, and 83.33 percent, which was similar to PI-RADS v2.1 score guideline's accompanying risk of malignancy was fulfilled. The individuals in this investigation with PI-RADS 2-points lesions all exhibited elevated blood prostate-specific antigen levels (> 10 ng/ml) (PSA). We scored 202 lesions by PI-RADS scoreing and generated ROC curves for the quantitative parameters T1, T2, and PD values, respectively, and determined that the quantitative parameter values with the most diagnostic efficacy for prostate cancer were T2 value, shifted band diagnostic value was 77 ms, and peripheral band diagnostic value was 89 ms, which was generally consistent with measurements in previous studies [13, 14].

In this work, we looked at 202 lesions to determine the utility of the magic quantitative parameter maps T1, T2, and PD values in distinguishing PCA lesions from other benign tumors. The T2 values of the lesions were highly significantly different between benign and malignant lesions ($P = 0.001$), the T1 values were statistically different between benign and malignant lesions ($P = 0.03$ for the shifted band and $P = 0.018$ for the peripheral band), and the PD values, although the differences between benign and malignant lesions were not statistically significant for the shifted band ($P = 0.209$), The majority of prior investigations focused on peripheral band prostate cancer and discovered that PCA lesions had considerably lower T2 values than normal PZ [15–17]. The present study's results are consistent with previous studies in that T2 levels are critical in differentiating PCA from non-neoplastic PZ lesions in peripheral bands. Some studies found no statistically significant difference in T2 values between PCA lesions with misplaced bands and hyperplastic prostatic nodules (BPH) [18]. However, one investigation found that transitional PCA lesions had lower T2 values than nontumor TZ lesions [19]. The current research also discovered that T2 values in the transitional band of PCA lesions were considerably lower than those in non-cancerous tissue.

We also discovered that T2 values of transitional band and peripheral band lesions were substantially more efficient than T1 and PD values in distinguishing benign and cancerous prostate. T1 value exhibited slightly greater diagnostic effectiveness than PD value for prostate cancer lesions with a transitional band, but there was no statistical significance between them ($P = 0.3683$); for peripheral band lesions, T1 value had almost the same diagnostic efficiency as PD value.

In this investigation, the AUC of the T2 value in distinguishing peripheral band PCA lesions from non-tumor PZ lesions was 0.813, which was comparable to the findings of a previous study [20]. The AUC of T2 value was 0.819 for the discriminating of PCA lesions and benign hyperplasia in the transitional zone, and the diagnostic effectiveness was greater than that of T1 and PD values, and the findings of earlier investigations (AUC 0.840) were nearly comparable [21]. Because T2 value has been recognized as a quantitative marker reflecting free water in tissues, in prostate cancer patients, the normal free water inside the loose interstitium between the ducts and acini is replaced by densely packed malignant epithelial cells, the free water in the extracellular space is significantly reduced, and thus the T2 value is significantly reduced [22]. Despite being an intrinsic property quantitative parameter of the tissue itself, T1 and PD values were shown to be less effective than T2 value in the research and hence were not deemed positive indications.

In this study, we discovered that T2 value combined with PI-RADS v2.1 score was more valuable than PI-RADS v2.1 alone in the diagnosis of prostate cancer, with AUC values of 0.735 and 0.846 for the shifted band and 0.816 and 0.890 for the peripheral band, which were significantly different ($P = 0.0355$), and the 95 percent confidence intervals of the shifted band versus peripheral band, which were significantly different ($P = 0.0355$), and when compared to the PI-RADS v2.1 score, T2 value coupled with PI-RADS v2.1 score not only showed higher diagnostic efficacy in the diagnosis of benign and malignant prostate, but also had more trustworthy diagnostic results [23]. The current study's findings show that the main improvements in the T2 value combined with the PI-RADS v2.1 score over the PI-RADS v2.1 score in the diagnosis of benign and malignant prostate transitional zone lesions are diagnostic sensitivity and positive predictive value; the main improvements in the diagnosis of benign and malignant prostate peripheral zone lesions were specificity and positive predictive value, demonstrating that the combined score can effectively detect lesions. As a result, the authors propose that lesions with shifting band T2 value >77 ms and peripheral band T2 value >89 ms may be followed up on without needless prostate ultrasound-guided puncture to alleviate patient suffering. Shifting band T2 value 77 ms, peripheral band T2 value 89 ms, or more lesions imply the necessity for prostate ultrasound-guided targeted puncture to increase the diagnostic yield of puncture. The current research contains significant flaws. First and foremost, this is a retrospective research with the potential for bias in patient selection, which requires multicenter or prospective trials to confirm. Second, some of the pathology results in this research were from prostate needle biopsies, which raise the chance of prostate cancer being overlooked. The current research is novel in that it is now vital to combine PI-RADS v2.1 for T2 value in prostate illness, which has received little attention.

5. Conclusion

In conclusion, PI-RADS v2.1 score, when paired with the magic quantitative parameters, demonstrated great diagnostic effectiveness for the detection of prostate cancer using T2 value mixed with PI-RADS v2.1.

Data Availability

All of the data in this article is actually available.

Conflicts of Interest

All the researchers claim no conflicts of interests.

Authors' Contributions

WenJuan Xu and HaiYan Cao contributed equally to this work and should be considered co-first authors.

References

[1] F. Bray, J. Ferlay, I. Soerjomataram, R. L. Siegel, L. A. Torre, and A. Jemal, "Global cancer statistics 2018: GLOBOCAN estimates of incidence and mortality worldwide for 36 cancers in 185 countries," *CA: a Cancer Journal for Clinicians*, vol. 68, pp. 394–424, 2018.

[2] X. Gong, K. Wu, S. Hao et al., "A comparative study on the diagnostic value of MRI dynamic enhancement in prostate cancer reporting and data systems 1.0 and 2.0," *Chinese Journal of Medical Computer Imaging*, vol. 25, no. 2, 2019.

[3] B. Turkbey, A. B. Rosenkrantz, M. A. Haider et al., "Prostate imaging reporting and data system version 2.1: 2019 update of prostate imaging reporting and data system version 2," *European Urology*, vol. 76, no. 3, pp. 340–351, 2019.

[4] S. Y. Park, D. C. Jung, Y. T. Oh et al., "Prostate cancer: PI-RADS version 2 helps preoperatively predict clinically significant cancers," *Radiology*, vol. 280, no. 1, pp. 108–116, 2016.

[5] X. Wang, N. Tu, T. Qin, F. Xing, P. Wang, and G. Wu, "Diffusion kurtosis imaging combined with dwi at 3-t mri for detection and assessment of aggressiveness of prostate cancer," *AJR. American Journal of Roentgenology*, vol. 211, no. 4, pp. 797–804, 2018.

[6] A. Pavilla, G. Gambarota, A. Arrigo, M. Mejdoubi, R. Duvauferrier, and H. Saint-Jalmes, "Diffusional kurtosis imaging (DKI) incorporation into an intravoxel incoherent motion (IVIM) MR model to measure cerebral hypoperfusion induced by hyperventilation challenge in healthy subjects," *Magma*, vol. 30, no. 6, pp. 545–554, 2017.

[7] C. Liu, S. L. Liu, Z. X. Wang et al., "Using the prostate imaging reporting and data system version 2 (PI-RIDS v2) to detect prostate cancer can prevent unnecessary biopsies and invasive treatment," *Asian Journal of Andrology*, vol. 20, no. 5, pp. 459–464, 2018.

[8] J. Byun, K. J. Park, M. H. Kim, and J. K. Kim, "direct comparison of pi-rads version 2 and 2.1 in transition zone lesions for detection of prostate cancer: preliminary experience," *Journal of Magnetic Resonance Imaging*, vol. 52, no. 2, pp. 577–586, 2020.

[9] T. T. Stolk, I. J. de Jong, T. C. Kwee et al., "False positives in PIRADS (V2) 3,4, and 5 lesions: relationship with reader experience and zonal location," *Abdominal Radiology*, vol. 44, no. 3, pp. 1044–1051, 2019.

[10] F. V. Mertan, M. D. Greer, J. H. Shih et al., "Prospective evaluation of the imaging reporting and data version 2 for prostate

Retraction

Retracted: Early Assessment of Cardiac Function by Echocardiography in Patients with Gestational Diabetes Mellitus

Computational and Mathematical Methods in Medicine

This article has been retracted by Hindawi following an investigation undertaken by the publisher [1]. This investigation has uncovered evidence of one or more of the following indicators of systematic manipulation of the publication process:

(1) Discrepancies in scope

(2) Discrepancies in the description of the research reported

(3) Discrepancies between the availability of data and the research described

(4) Inappropriate citations

(5) Incoherent, meaningless and/or irrelevant content included in the article

(6) Peer-review manipulation

The presence of these indicators undermines our confidence in the integrity of the article's content and we cannot, therefore, vouch for its reliability. Please note that this notice is intended solely to alert readers that the content of this article is unreliable. We have not investigated whether authors were aware of or involved in the systematic manipulation of the publication process.

Wiley and Hindawi regrets that the usual quality checks did not identify these issues before publication and have since put additional measures in place to safeguard research integrity.

We wish to credit our own Research Integrity and Research Publishing teams and anonymous and named external researchers and research integrity experts for contributing to this investigation.

The corresponding author, as the representative of all authors, has been given the opportunity to register their agreement or disagreement to this retraction. We have kept a record of any response received.

References

[1] P. Wang, Y. Peng, L. Liu et al., "Early Assessment of Cardiac Function by Echocardiography in Patients with Gestational Diabetes Mellitus," *Computational and Mathematical Methods in Medicine*, vol. 2022, Article ID 6565109, 7 pages, 2022.

Research Article

Early Assessment of Cardiac Function by Echocardiography in Patients with Gestational Diabetes Mellitus

Pin Wang,[1] Yanyan Peng,[1] LiNa Liu,[2] RuiShuang Jiao,[3] YanHong Zhang,[1] Wei Zhao,[1] YingFeng Liu,[1] and CongXin Sun [1]

[1]*Shijiazhuang Obstetrics and Gynecology Hospital Ultrasonography Lab, 050000, China*
[2]*Gucheng County Hospital of Hebei Province Obstetrics and Gynecology Ultrasound Department, 253800, China*
[3]*The Third Hospital of Shijiazhuang Ultrasonography Lab, 050000, China*

Correspondence should be addressed to CongXin Sun; scx19650627@163.com

Objective. To offer a baseline for clinical diagnosis, echocardiography was performed to evaluate the disparities in heart function comparing pregnant women with diabetes mellitus (GDM) and ordinary pregnant women. *Methods*. A prospective case-control study is being conducted on pregnant women with or without gestational diabetes. The sample size for both the intervention and control groups is the same: no diabetes diagnosis or previous forms, a single pregnancy, and no issues (such as preeclampsia or fetal growth restriction). The females were all subjected to routine echocardiograms to examine the morphology and function of their left and right hearts. *Results*. In the research, 51 women with GDM and 50 healthy controls volunteered. Women with GDM had a significantly higher heartrate (82 ± 9 vs. 74 ± 8), left ventricular (LV) relative wall thickness (0.39 ± 0.06 vs. 0.31 ± 0.07; $P < 0.001$), LV early diastolic transmitral valve velocity (E) (0.79 ± 0.14 vs. 0.72 ± 0.13 m/s; $P = 0.031$), and LV late diastolic implementing regulations valve velocity (0.6). Speckle-tracking analysis showed significant decrease in LV right ventricular (RV). A study indicated a reduced pulmonary acceleration time (59 ± 9 vs. 68 ± 12 ms; $P = 0.001$), RV E/A ratio (1.21 ± 0.19 vs. 1.31 ± 0.31; $P = 0.022$), and a greater RV myocardial systolic annular velocity (0.17 ± 0.03 vs. 0.12 ± 0.03; $P = 0.023$). *Conclusions*. Our results revealed that the heart function of diabetic pregnant women differed considerably from that of the control group, such as LV-RWT, LV diastolic transmitral valve speed, and LV late diastolic transmitral valve speed. Given these results, further research into the postpartum cardiovascular healing of pregnant women with gestational diabetes mellitus is required.

1. Introduction

Gestational diabetes (GDM) refers to women who have no symptoms of diabetes before and have symptoms of hyperglycemia during pregnancy [1]. Gestational diabetes may not have obvious symptoms, but it will increase the risk of pregnancy toxemia and depression and the possibility of cesarean section [2]. If a pregnant woman has gestational diabetes and is not properly treated, it may increase the risk of infant overgrowth, postnatal hypoglycemia, or jaundice [3]. In serious cases, it may also cause stillbirth, and the risk of childhood obesity and type 2 diabetes after children grow up is relatively high [4]. Hyperglycemia during pregnancy can lead to abnormal embryonic development and even

death, and the incidence of abortion is 15%-30%. The probability of pregnancy-induced hypertension is 2-4 times higher than that of nondiabetes pregnant women [5]. The incidence of polyhydramnios was 10 times higher than that of nondiabetes pregnant women. The incidence of macrosomia is significantly increased, the probability of dystocia, birth canal injury, and surgical delivery is increased, and the labor process is prolonged, which is prone to postpartum hemorrhage [6]. In addition, it is prone to diabetes ketoacidosis and infection related to gestational diabetes, such as vulvovaginal candidiasis, pyelonephritis, asymptomatic bacteriuria, puerperal infection, and mastitis [7]. If pregnant women with diabetes do not receive timely and effective treatment and management, their future risk of type 2

diabetes will increase. At the same time, pregnant women with diabetes also have a higher risk of preeclampsia and cesarean section [8].

Previous research has shown that gestational diabetes mellitus has an influence on the heart, and in more severe situations, it may even lead to malfunction [9]. This malfunction may express itself in a number of ways, including cardiomyopathy, microvascular protrusions, and subcellular issues [10]. Patients with type 2 diabetes suffer from both structural and functional heart damage as a result of these complications. On either hand, scientists know a little about the implications of hyperglycemia, which for a short period of time, on the hearts of patients who have gestational diabetes [11]. There have been no prospective studies to look at how gestational diabetes impacts the mother's cardiac function. The goal of this study was to compare and contrast the cardiac function of pregnant women who had or did not have diabetes. [12]. Our working hypothesis was gestational diabetes can affect the cardiac function and structure of pregnant women.

2. Material and Methods

2.1. Selection of Subjects. Our hospital will conduct a 12-month prospective study from July 2019 to July 2020. The hospital's Ethics Review Committee (12/L1/2019) approved and carried out the study, and written informed consent was obtained from all pregnant women and their families. An oral glucose tolerance test was used to diagnose GDM in these pregnant women at 20 and 2 weeks. Figure 1 shows ultrasound images of both normal and pregnant women.

2.2. Glucose Tolerance Experiments. Glucose tolerance tests are one method for investigating human blood glucose regulating systems. Subjects were given a single oral dose of 75 g of glucose dissolved in 250 mL of warm boiled water within 5 minutes of drinking completely, venous blood was drawn at each of the three time points (1 hour, 2 hours, and 3 hours), and urine samples were retained after each blood draw for determination of blood glucose and urinary glucose. At the time of fasting, the blood glucose level in normal people is in the range of 3.9-6.1 mmol/L; after 1 hour of oral administration of glucose, the blood glucose concentration reaches a peak, usually in the range of 7.8-9.0 mmol/L; the peak value does not exceed 11.1 mmol/L; the 2-hour blood glucose is less than 7.8 mmol/L; and the blood glucose returns to the fasting level after 3 hours. Urine sugar levels were negative at all testing times. However, diabetic patients' fasting blood glucose levels were often higher than 7.0 mmol/L, their OGTT peak blood glucose level was higher than 11.1 mmol/L, and their 2-hour blood glucose level was similarly higher than 11.1 mmol/L, accompanied by positive urine glucose.

2.3. Inclusion Criteria. There were no prior diabetes or cardiovascular problems (type 1 or 2). Body mass index (BMI) of healthy pregnant women was 30 kg/m^2 with no comorbidities. The pregnant women included in the study had normal blood pressure, single pregnancy, normal fetal development, and no preeclampsia symptoms.

2.4. Echocardiographic Examination. A senior professional examiner evaluated and analyzed the hearts of pregnant women using a Siemens 4v1c color Doppler ultrasonography diagnostic device (ACUSON oxana2). The patient was in the left decubitus position, and the image was detected by sternum and apical angle. Use the hard disk to copy all the data of three heart cycles in the ultrasound instrument and follow-up analysis. The investigation was designed to comply with the most recent standards. Samples were recorded of the left atrial volume (LAVI), the close volume of the left ventricle (LV), the radii of the distal (RD), and proximal RV outflow systems, and other geometric indices(GI) using dorsal long-axis (DLA), quick, and apex five views. The early (E) and late (A) mitral and tricuspid ventricular inflow velocities (IV), acceleration time (T), isovolumetric relaxation (IR), and late mitral leaflet inflow duration may also be determined using dynamic imaging. Tissue with pulsed pulses Doppler imaging is also used to determine the systolic (S), early-diastolic (E), and latdiastolic (A) velocities of heart tissue so at septum, "L", and "RV" walls. "LVM" was determined by applying the following formula, which was derived from the "Essex equation": (LVM) = 0.8 (1.04((LVEDD + IVSd + PWd)3 – LVEDD 3) + 0.6, in which LVEDD is the LV end-diastolic diameter, IVSd is the ventricular septal defect thickness in the diastole, and "PWd" is the posterior wall thickness in the diastole. The LV mass index (LVMI) was calculated by taking the LVM and dividing it by the total surface area of the body. RWT = (2 PWd)/LVEDD was the formula that was used to determine the LV ratio wall thickness (RWT). The recommendations provided by the British Society of Echocardiography were utilized in order to diagnose diastolic dysfunction. These recommendations used values that were adjusted for age and gender and were taken from the 2016 European Society of Cardiology Guidelines for the Diagnosis and Management of Acute and Chronic Heart Failure. Calculations were done based on the apical pictures to determine the LV and RV global longitudinal strain (GLS), as well as the systolic and diastolic (early and late) strain rates. Negative values indicated that the fibers were being shortened. Apical and basal parasternal short-axis photos were utilized to determine LV rotation and derotation, with negative values indicating rotation clockwise. The LV twist distinguishes between the apical and basal rotations of the rotors. To determine LV torsion, divide the LV twist by the diastole length of the LV. There was no statistical analysis for those who refused to participate in more than one section.

2.5. Statistical Analysis. The mean standard deviation of continuous data is shown. The Shapiro–Wilk test is used to test normal distribution. The chi-square test was used to compare categorical data that was given as *n*. (percentages). In order to do group comparisons, we either used the unpaired *t*-test or the Mann–Whitney *U*-test with continuous data. The choice of which test to use was dependent on the distribution of the data. The significance level was set at $P < 0.05$.
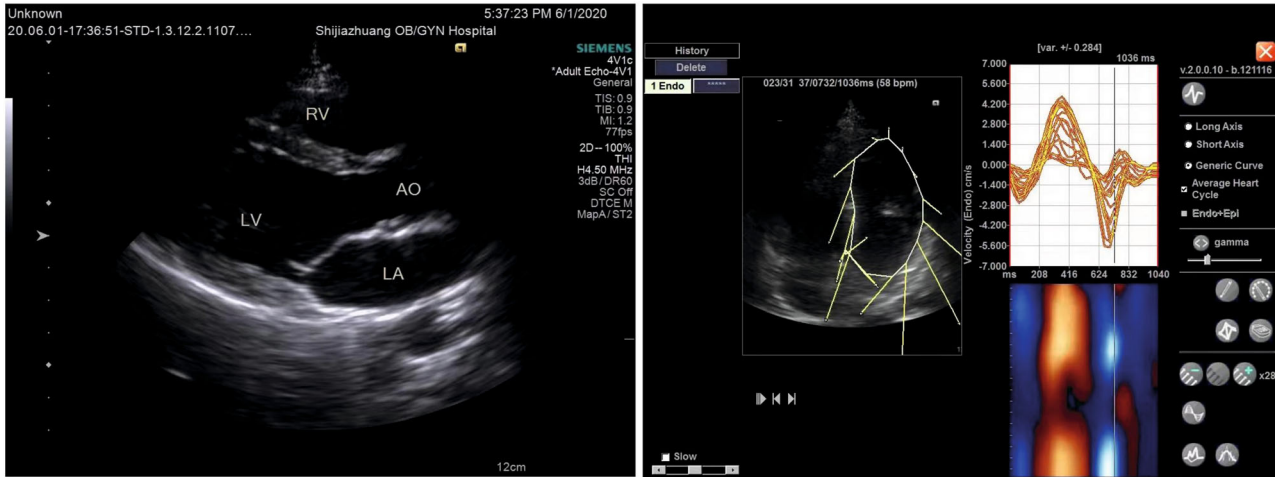
FIGURE 1: Ultrasonogram of normal and pregnant women.
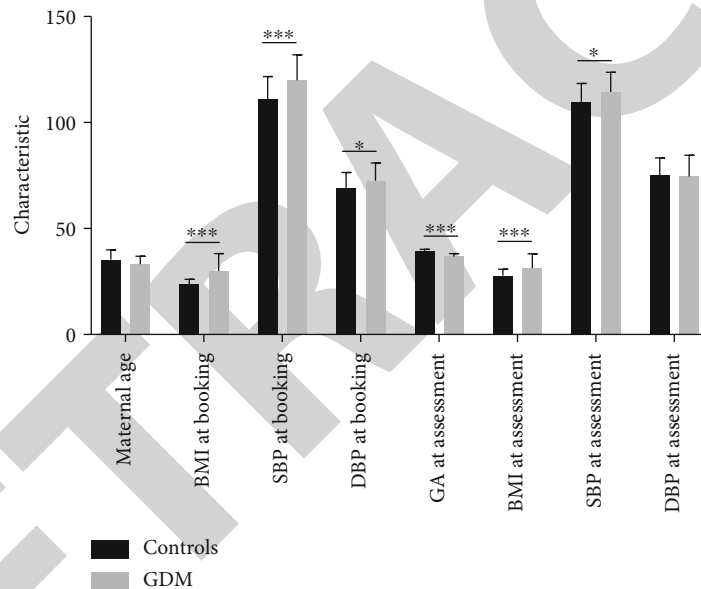
FIGURE 2: Demographic features of all participating pregnant women.

IBM SPSS software version 24 was used for statistical analysis (IBM Corp., Armonk, NY, USA). Previously, our team discovered intra- and interobserver heterogeneity, which was not repeated in our investigation.

3. Results

3.1. Conditions of Participating Study Patients.

This research included 101 pregnant women, 51 of whom had gestational diabetes and 50 who were healthy (control group). All of the ladies underwent routine echocardiogram satisfactorily. Figure 2 depicts the demographic features of the control group and women with gestational diabetes. When compared to controls, women with gestational diabetes had substantially higher BMI and systolic blood pressure.

3.2. Comparison of Ultrasound Parameters.

Figure 3 shows the echocardiographic indices for both groups. There was no statistical significance to the difference. When compared to the controls, the GDM women had significantly greater levels of physical activity, LV-RWT, LV diastolic transmitral valve speed, and LV late diastolic transmitral valve speed. Keeping in mind that the LVM and LVMI did not vary at all between the two groups is critical, since this is a crucial point to remember. When compared to control pregnancies, a chronic strain assessment of the LV showed that global longitudinal strain (GLS), endocardial GLS, and dural GLS all decreased by a lot. This was proven by comparing pregnancies with GDM to those without it. When compared to the control group, women with GDM had a shorter pulmonary acceleration time, a lower RV E/A ratio, and larger RV-S and RV-A values. Also, the RV-S and RV-A values were
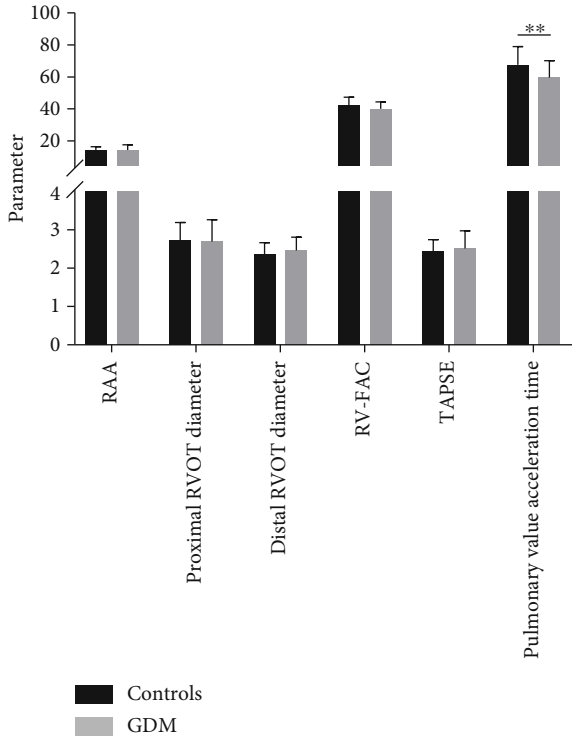
Figure 3: Ultrasonic parameter used in the study.
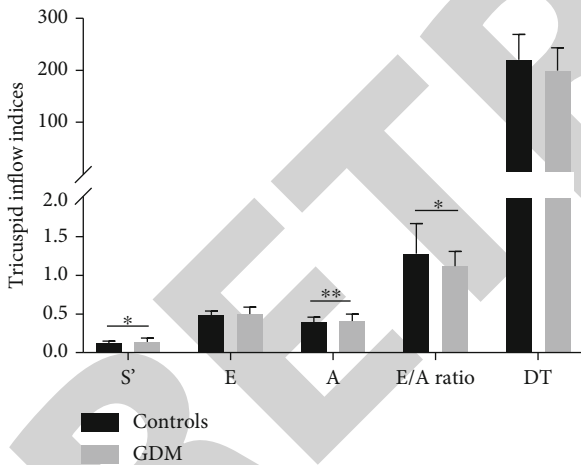
Figure 4: Tricuspid inflow index comparison.

Figure 5: Compare of strain and SR indices.

higher for these women. Speckle-tracking was used to look at the right ventricle, and the results showed that there were no big differences between the women with GDM and the controls (Figures 4–9).

4. Discussion

Patients with gestational diabetes exhibited substantially higher LV-RWT and lower LV-GLS, LV endocardial, and epicardial GLS compared to the control group, according to echocardiographic data [13]. As a result, women with gestational diabetes had significantly worse heart function

throughout pregnancy when compared to the healthy control group [14]. Despite the absence of clinical symptoms in these individuals, this clear cardiovascular adverse response may offer a concern to pregnant women [15]. Previously, researchers employed the speckle tracking technology to examine the systolic function of diabetic patients with normal blood pressure and discovered that GLS and endocardial hypotension of the left ventricle were decreased [16]. However, the cardiovascular effects of diabetes may be mistaken with metabolic syndrome, which includes hypertension and dyslipidemia in addition to high blood glucose levels [17]. The longitudinal and circumferential strains of lv22 and 23 reduced, as did the GLS of rv24, in a study of cardiac alterations in metabolic syndrome [18]. Short-term hyperglycemia during pregnancy has the same effect on heart function as non-pregnant people with a long history of diabetes. Researchers discovered that the GLS of radial strain differed in a retrospective analysis of 18 pregnant women with gestational diabetes in the second trimester of pregnancy [19]. Although the data in this section of the research are comparable to the findings in this study, it cannot be ruled out that these cardiovascular abnormalities are due to the small sample size, early gestational weeks at the time of examination, and brief exposure to hyperglycemia [20].

Recent research has shown that hypertensive disorders of pregnancy and fetal development are linked to major problems with how the heart works in women [21]. GDM is a major risk factor for many diseases [22]. Someone is more likely to get GDM if they have GDM. We may have contributed to exclusion bias by not checking on women who had heart problems because of these pregnancy problems and by leaving out women with GDM who had these worries from a prospective study [23]. According to our data, this means that, unlike when PE or FGR start, when the heart function gets worse, the heart function is normal
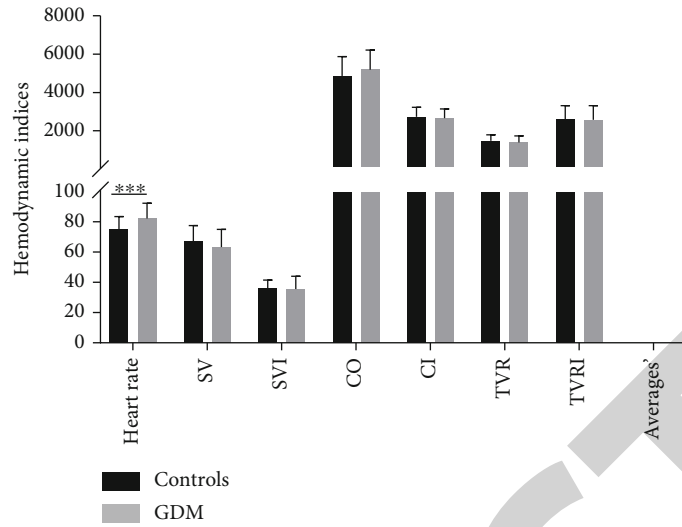
Figure 6: Hemodynamic index comparison.
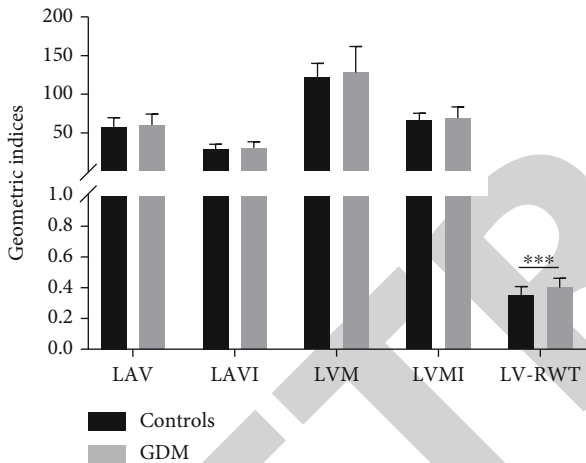
Figure 7: Geometric index comparison.
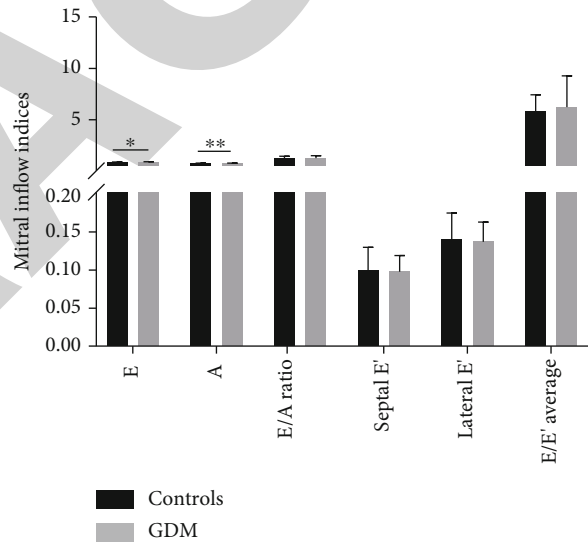
Figure 8: Mitral inflow indices.

during a GDM pregnancy [24]. Despite these problems, women with GDM are about 2.8 times more likely to have diastolic dysfunction than women who have a normal pregnancy to term. Researchers have found that this link makes it more likely for pregnant women to get heart disease [25]. We do not fully understand how diabetes can change the rhythm of the heart in nonpregnant people. Diabetic cardiomyopathy includes a wide range of problems, such as myocardial fibrosis and remodeling, problems with the heart's ability to pump blood, and problems with the heart's ability to pump blood at all. It is usually called diabetic cardiomyopathy. Diabetes has been linked to inflammation, activation of the renin-angiotensin-aldosterone system, microvascular dysfunction, and bad insulin signaling in the heart. Also, people with diabetes are more likely to develop type 2 diabetes [26].

A new meta-analysis shows that women who develop impaired glucose tolerance during pregnancy are 1.5 times more likely to have a heart attack in the first year after giving birth. This higher risk exists whether or not the woman develops type 2 diabetes after giving birth [26]. The authors thought that both GDM and PE might make pregnant women more likely to have heart problems after giving birth. It is interesting to think about how the pathophysiology of GDM fetal circulatory failure could lead to long-term heart damage and fibrosis, like what happens in diabetic cardiomyopathy [27]. Future research should focus on how the heart works after giving birth to a baby with gestational diabetes mellitus. This will help find out if this problem is just caused by the GDM pregnancy or if it is hidden by the effects of other heart risk factors [28]. One of the study's strengths is that it was set up in a prospective way and used both traditional and speckle-tracking sonar to measure how well the left and right hearts worked. A problem with the research is that the women with GDM at the start of the trial had a
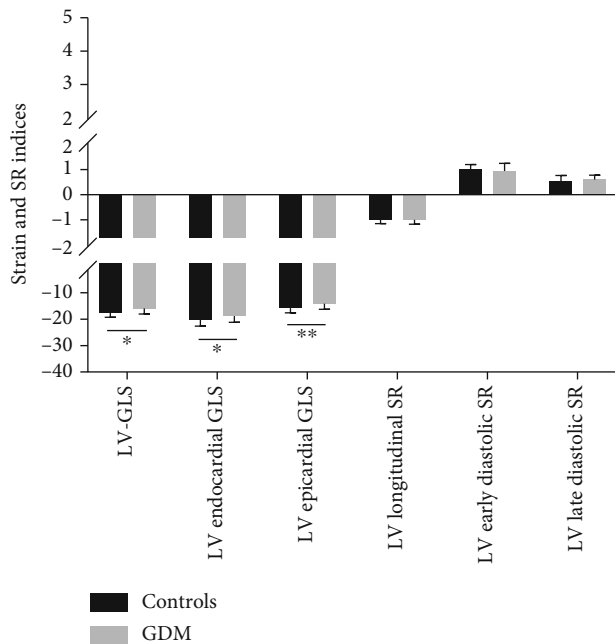
Figure 9: Strain and SR indices part II.

higher BMI and systolic blood pressure. It is impossible to say how much each of the above factors played a role in the development of heart problems during a GDM pregnancy [29]. In our study, heart problems were seen in mothers who did not have diabetes if their BMI was more than $35 \, \text{kg/m}^2$. This was a lot higher than the BMI of our GDM sample. Compared to pregnant women with BMIs less than $35 \, \text{kg/m}^2$, those with BMIs more than $35 \, \text{kg/m}^2$ had much higher SV, CO, and LVM, as well as much lower overall vascular resistance (TVR) [30].

Except for LVMI, all of the differences went away when the weight of the mother was taken into account. In terms of SV, SV index, CO, CI, LVM, LVMI, TVR, and the receipt of the notice index, there was no difference between the GDM group and the controls [31]. So, we know for sure that the difference in speckle tracking and diastolic dysfunction is caused by GDM and not by the higher BMI reported in the GDM group. Surprisingly, it was found that pregnant women with gestational diabetes had more diastolic dysfunction than pregnant women who were obese. Also, women with GDM had their scans done two weeks before women in the control group. Because of the way the mother's heart changes during pregnancy, the second difference would have tended to reduce any differences between GDM and normal pregnancy rather than make them bigger.

5. Conclusions

The occurrence of short-term hyperglycemia in pregnant women with gestational diabetes may have a certain impact on cardiac function. Pregnant women with gestational diabetes have an increased risk of cardiovascular disease after delivery, so it is necessary to take preventive measures for such patients.

Data Availability

All of the data in this article are actually available.

Conflicts of Interest

All the researchers claim no conflicts of interests.

Authors' Contributions

Pin Wang and Yanyan Peng contributed equally to this work and should be considered co-first authors.

Acknowledgments

References

[1] N. Keser, "Echocardiography in pregnant women," *Anadolu Kardiyoloji Dergisi*, vol. 6, no. 2, pp. 169–173, 2006.

[2] E. Mulder, S. Basit, J. Oben, S. van Kuijk, C. Ghossein-Doha, and M. Spaanderman, "Accuracy and precision of USCOM versus transthoracic echocardiography before and during pregnancy," *Pregnancy Hypertens*, vol. 17, pp. 138–143, 2019.

[3] M. U. Barut, F. Güngören, and C. Kaçmaz, "Assessment of clinical and echocardiographic findings of pregnant women with dyspnea," *Medical Science Monitor*, vol. 25, pp. 1032–1037, 2019.

[4] J. Cornette, S. Laker, B. Jeffery et al., "Validation of maternal cardiac output assessed by transthoracic echocardiography against pulmonary artery catheterization in severely ill pregnant women: prospective comparative study and systematic review," *Ultrasound in Obstetrics & Gynecology*, vol. 49, no. 1, pp. 25–31, 2017.

[5] S. Rakha and H. El Marsafawy, "Sensitivity, specificity, and accuracy of fetal echocardiography for high-risk pregnancies in a tertiary center in Egypt," *Archives de Pédiatrie*, vol. 26, no. 6, pp. 337–341, 2019.

[6] W. H. Marshall, S. Gee, W. Lim, and S. Rajpal, "Correlation of echocardiographic probability of pulmonary hypertension with maternal outcomes in pregnant women with elevated right ventricular systolic pressure," *Echocardiography*, vol. 38, no. 5, pp. 760–766, 2021.

[7] L. F. Trasca, E. Poenaru, N. Patrascu, M. Cirstoiu, and D. Vinereanu, "A comprehensive echocardiographic study of the right ventricular systolic function in pregnant women with inherited thrombophilia," *Echocardiography*, vol. 37, no. 7, pp. 1037–1042, 2020.

[8] R. Sarikaya and G. Turkyilmaz, "Is conventional cardiac examination adequate for obese pregnant women? A prospective case-control study," *Taiwanese Journal of Obstetrics & Gynecology*, vol. 61, no. 1, pp. 86–90, 2022.

[9] A. Abdullah, S. Hoq, R. Choudhary, S. Laifer, and S. Zarich, "Cardiac performance is impaired in morbidly obese pregnant females," *The Journal of Obstetrics and Gynaecology Research*, vol. 38, no. 1, pp. 258–265, 2012.

[10] H. Y. Chen, T. Pan, H. Li et al., "Assessment of myocardial injury in neonates born to pregnant women with pregnancy complicated by severe preeclampsia by myocardial work

Retraction

Retracted: Advances in the Application of Liquid Chromatography in the Detection of Pollutants

Computational and Mathematical Methods in Medicine

This article has been retracted by Hindawi following an investigation undertaken by the publisher [1]. This investigation has uncovered evidence of one or more of the following indicators of systematic manipulation of the publication process:

(1) Discrepancies in scope

(2) Discrepancies in the description of the research reported

(3) Discrepancies between the availability of data and the research described

(4) Inappropriate citations

(5) Incoherent, meaningless and/or irrelevant content included in the article

(6) Peer-review manipulation

The presence of these indicators undermines our confidence in the integrity of the article's content and we cannot, therefore, vouch for its reliability. Please note that this notice is intended solely to alert readers that the content of this article is unreliable. We have not investigated whether authors were aware of or involved in the systematic manipulation of the publication process.

Wiley and Hindawi regrets that the usual quality checks did not identify these issues before publication and have since put additional measures in place to safeguard research integrity.

We wish to credit our own Research Integrity and Research Publishing teams and anonymous and named external researchers and research integrity experts for contributing to this investigation.

The corresponding author, as the representative of all authors, has been given the opportunity to register their agreement or disagreement to this retraction. We have kept a record of any response received.

References

[1] X. Hu, "Advances in the Application of Liquid Chromatography in the Detection of Pollutants," *Computational and Mathematical Methods in Medicine*, vol. 2022, Article ID 2152615, 11 pages, 2022.

Hindawi

Research Article

Advances in the Application of Liquid Chromatography in the Detection of Pollutants

XinYu Hu [ORCID]

School of Food Science and Engineering, Shandong Agricultural University, Taian 271000, China

Correspondence should be addressed to XinYu Hu; xinyuhu@sdau.edu.cn

Food is easy to be contaminated because of its complex composition. Therefore, in order to protect people from potential food contaminants, it is very necessary to test for various contaminants in food. Liquid chromatography is widely used in the field of food safety detection. In addition, with the development of liquid chromatography technology, more and more new instruments are combined with liquid chromatography. Compared with traditional liquid chromatography, combined liquid chromatography has great advantages in efficiency and operation. Therefore, it is rapidly promoted in the field of food safety testing. In this paper, the results of the determination of three kinds of food pollutants by different liquid chromatography methods are reviewed, and the indexes are compared and analyzed.

1. Introduction

Food is a variety of finished products and raw materials for human consumption or drinking. It is a very complex compound composed of natural compounds (lipids, carbohydrates, proteins, minerals, vitamins, and trace elements). It is very important to ensure the safety of food. Food should be nontoxic and harmless, meet nutritional requirements, and not cause any acute, subacute, or chronic harm to human health. According to the definition of food safety by Benoy, food safety is "a public health problem of the effects of toxic and harmful substances in food on human health."

Several of these compounds, such as contaminants from food processing, pesticide and veterinary drug residues, and contaminants from natural sources (mycotoxins, etc.), may also be harmful to human health, although they are usually present in small amounts. Countries around the world have formulated corresponding laws, regulations, and standards for various substances that appear in food.

In order to protect people from potential food hazards, detection and risk assessment of toxic and hazardous substances in food are required. It begins by obtaining data from reliable, fit-for-purpose analytical methods to estimate consumer exposure and ingestion levels of contaminants and

residues [1]. Liquid chromatography (LC) is the most commonly used chromatographic method in the analysis of food. In addition, high sensitivity or high resolution can be obtained in combination with other novel detection devices such as mass spectrometry (MS) [2].

The purpose of this review is to describe the differences between different liquid chromatography methods for the determination of contaminants in food samples. It includes references to recently published papers on chromatography in the field of food safety, as well as the application of new technologies. We have listed three common food contaminants. Then, the differences in the determination methods and effects of different liquid chromatography techniques were discussed, and by comparing the chromatographic columns and other related factors, some suggestions were provided for the selection of liquid chromatography for the determination of food contaminants, in order to improve the separation effect of liquid chromatography.

2. Common Liquid Chromatography

Liquid chromatography technology has been widely used in food safety detection. Traditional liquid chromatography mainly includes paper chromatography and thin chromatography. With the development of chromatography technology,

the combination of modern liquid chromatography and mass spectrometry has become the main trend today, with the advantages of high efficiency, rapidity, and convenience. In the field of food safety testing, modern liquid chromatography-mass spectrometry is regarded as a reliable quantitative analysis tool [3].

2.1. Traditional Liquid Chromatography.

Traditional liquid chromatography mainly includes paper chromatography and thin chromatography.

The principle of paper chromatography is the principle of similar compatibility, which is analyzed by the dispersing speed of the split system in the same medium. Paper chromatography is less used in food safety testing because of its slightly inferior efficiency and separation effect. Paper chromatography is less used in food safety testing because of its slightly inferior efficiency and separation effect. Even if it is used, it is improved. For example, Fereshte Mohamadi et al. [4] established a three-dimensional paper chromatography (3D-PC) method for the determination of tartrazine and indigo carmine in food samples (colorimetric method).

Thin-layer chromatography is an analytical method in which an adsorbent and a support agent are uniformly coated on a glass or plastic plate to form a thin layer for chromatographic separation. Compared with paper chromatography, a wider range of corrosive color reagents, mobile phases, and stationary phases can be used than paper chromatography. Therefore, the application in the field of food safety detection is more extensive, and it can also be combined with mass spectrometry and fluorescence detection technology. For example, Claudia et al. [5] established a high performance thin-layer chromatography-fluorescence detection method to determine the emulsifier in food.

2.2. Liquid Chromatography-Mass Spectrometry.

In the field of food safety testing, the most commonly used methods are liquid chromatography-mass spectrometry (LC-MS) and LC-MS/MS, which can realize the analysis of small molecular substances (approx <1200 Da), use traditional mass spectrometers (QqQ and TOF), or use a HRMS hybrid detector (QTOF or Q-Orbitrap, etc.). Sample clean-up techniques also play an important role in LC-MS methods, such as solid phase extraction (SPE) and immunoaffinity columns (IAC) and QuEChERs; in addition to electrospray ionization (ESI), atmospheric pressure chemical ionization (APCI) is also the most commonly used ionization mode for LC-MS methods [6].

In the detection of some types of substances, people often use high performance liquid chromatography-mass spectrometry (HPLC) to determine substances. HPLC is a more efficient separation chromatographic technique than ordinary LC, with high selectivity, sensitivity, and resolution [7]. The working principle of HPLC is shown in Figure 1.

HPLC is a chromatography analytical technique for the separation, quantification, and identification of a variety of compounds. Sample components can be effectively separated by pressurized liquid and sample mixture through a column filled with adsorbent. The principle is that components are separated from the stationary phase at different
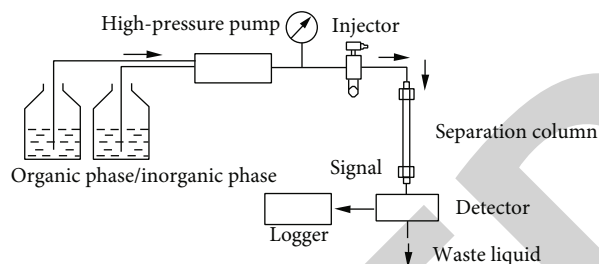
Figure 1: The working principle of HPLC.

times based on hydrophilic or molecular mass, hydrophobic properties, or electric charge through the interaction of the column components with the appropriate type of stationary phase [8]. High performance liquid chromatography has also proved useful in the determination of contaminants in food [9]. Therefore, HPLC is widely used for quantitative analysis of a large number of compounds, including contaminants in food processing, pesticide and veterinary drug residues, and mycotoxins, to evaluate food quality. HPLC can also be used in combination with mass spectrometry (HPLC-MS or HPLC-MS/MS), fluorescence (HPLC-FD), or ultraviolet (HPLC-UV) detection techniques [10]. These methods have been widely used in the field of food safety testing.

3. Application of Liquid Chromatography in Determination of Food Contaminants

There are many kinds of foods, and their characteristics and nutritional components are more complex. Food may be contaminated by various chemical substances during production, transportation, and storage. Excessive amounts of some substances may endanger human health. Therefore, contaminant residues in food are also the focus of people's attention in recent years. With the wider application of HPLC in food safety testing, people can obtain information on various foods through it, which is helpful for people's healthy life.

Acrylamide, veterinary drugs, and mycotoxins are common contaminants in food. Moreover, these three kinds of food pollutants do great harm to the human body. Therefore, this paper analyzes and compares the test accuracy of different liquid chromatography methods based on the detection process and test results of these three common food contaminants. The chromatographic conditions of different chromatographic methods are summarized in Tables 1–3.

3.1. Analysis of Acrylamide.

Acrylamide (AM) is formed during the thermal processing (i.e., frying and baking) of carbohydrate-rich foods and is one of the products of the Maillard reaction in the reaction of asparagine and sugars (glucose and fructose) [11]. The International Agency for Research on Cancer (IARC, 1994) has classified acrylamide (2-acrylamide) as a probable human carcinogen and has called it a neurotoxin for the World Health Organization (WHO, 2002). To this day, the content of acrylamide in

TABLE 1: Liquid chromatography measurement conditions.

Compound	Food product	Chromatographic method	Column	Mobile phase	Flow rate	Ref.
Acrylamide (AM)	Potato chips	LC-MS/MS	Extrasyl ODS1 (200 × 30 mm, 5 μm)	0.5% methanol : water 0.1% 2-propanolacetic acid	0.2 mL/min	[12]
Acrylamide (AM)	Rice, bread and coffee, etc.	Improved LC-MS/MS	C18 (250 × 2 mm, 5 μm)	0.2% acetic acid 1% methanol	0.2 mL/min	[13]
Acrylamide (AM)	Dried fruit and edible seeds	QuEChERS extraction-LS-MS	Gemini RP C18 (250 × 2 mm, 5 μm)	0.1% formic acid 0.1% MeOH : formic acid	0.25 mL/min	[14]
Acrylamide (AM)	Thermally processed seafood	HPLC-MS/MS	C18 (50 × 2 mm, 2.5 μm)	Methanol, 0.1% formic acid Water-methanol	0.2 mL/min	[15]
Acrylamide (AM)	Chinese baked and fried foods	HPLC-UV	ODS-C18 (250 × 4.6 mm, 5 μm)	ACN, water : 0.1% formic acid ACN	0.40 mL/min	[16]

Table 2: Liquid chromatography measurement conditions.

Compound	Food product	Chromatographic method	Column	Mobile phase	Flow rate	Ref.
STZ, SMR, SDZ, SPY, SMZ, SMT, SCP, SMA, SDM, SQX	Honey	LC-MS-MS	Zorbax Eclipse XDB-98 (50 × 4.6 mm, 1.8 μm)	0.5% formic acid in water ACN	0.4 mL/min	[17]
STZ, SMZ, SPY, SGA, SMR, SMA, SDM, SDZ, SIX	Meat and/or egg-based baby foods	LC-QToF-MS	Poroshell 120 HILIC (150 × 3 mm, 2.7 μm) 20 mM ammonium formate aqueous solution at pH	20 mM ammonium formate in water pH 3 : methanol in ACN 1 : 1 v/v	0.2 mL/min	[18]
SDZ, SDM, SMR, SMZ, SMT, SMA, SNM, STZ, SCP, TMP, SDX, SMPZ, SPY, SIX, SBZ, SQX, SCA, SPN	Aquatic products	Online SPE-UHPLC–MS/MS	F5 column (50 × 3.0 mm, 2.6 μm)	0.1% formic acid in water 0.1% formic acid in ACN	0.45 mL/min	[19]
SMR, SMZ, SMA, SMPZ, SDZ, SPY, SDMX, S-STZ, SGA, SCA, SBZ, SNT, SIM, SMTZ, SQX, STZ, SIX, SDX	Animal muscle and liver	HPLC-QqLIT-MS/MS	CHPLC column Purosphers STAR C18 (150 × 4.6 mm, 5 μm)	HPLC-grade water acidified with 10 mM of formic acid ACN with 10 mM of formic acid	0.2 mL/min	[20]
Sulfamethazine (STZ), sulfamonomethoxine (SMM), sulfadiazine (SDZ), SMZ, SMT	Milk	In situ magnetic ionic liquid dispersive liquid-liquid microextraction coupled with HPLC	C18-H column (250 × 4.6 mm, 5 μm)	0.5% MSP-ACN (85 : 15, v/v)	0.2 mL/min	[21]

TABLE 3: Liquid chromatography measurement conditions.

Compound	Food product	Chromatographic method	Column	Mobile phase	Flow rate	Ref.
AFB1, AFB2, AFG1, AFG2	Maize	LC-MS-MS	Purospher Star RP-18 (50 × 2.1 mm, 2 μm)	0.1% acetic acid-methanol (60 : 40)	0.25 mL/min	[23]
AFB1, AFB2, AFG1, AFG2	Wheat, soybeans, peanuts, etc.	LC -ESI-QTOF-MS/MS	ZORBAX Eclipse XBD-C18 (100 × 2.1 mm, 1.8 μm)	1% formic acid and 2 mM ammonium formate in water 1% formic acid in methanol	0.3 mL/min	[24]
AFB1, AFB2, AFG1, AFG2	Glycyrrhiza uralensis	HPLC-MS/MS	C18-H column (250 × 4.6 mm, 5 μm)	0.5% MSP-ACN (85 : 15, v/v)	2 mL/min	[25]
AFM2, AFM1, AFB2, AFB1	Milk	Micro-SPE-HPLC-UV	C18 Hypersil gold (250 × 4.6 mm, 5 μm)	Acetonitrile : methanol 3 : 2 (v/v)	1.2 mL/min	[26]
AFB1, AFB2, AFG1, AFG2	Pistachios and groundnuts	HPLC-FLD	ACE 5 C18, 100 A (250 × 4.6 mm, 5 μm)	Water-acetonitrile-ethanol (6/2/3, $v/v/v$)	2-3 mL/min	[27]

foods has been of concern, especially in fried and baked goods containing carbohydrates and amino acids (asparagine) [12]. Therefore, it is necessary to use new liquid chromatography methods to determine the content of acrylamide in food. For the determination of acrylamide in food, the following section lists some different liquid chromatography methods.

3.1.1. LC-MS/MS. Roach et al. [13] used an Extrasyl ODS1 (200 × 30 mm, 5 μm) chromatographic column for the determination of acrylamide in potato chips by a reversed-phase LC-MS/MS method. It can be known from the original literature that the mobile phase they used is acetic acid-methanol-Milli-Q water (0.1 : 1.0 : 98.9), and the flow rate is 0.2 mL min^{-1}. Cheong Tae et al. [14] improved the LC-MS/MS method and used it to determine the content of acrylamide in processed food. The selected chromatographic column is Aqua C18 HPLC (2 × 250 mm, 5 μm particles). It is 0.2% acetic acid aqueous solution and 1% methanol, and the flow rate is 0.2 mL/min.

Eleonora et al. [15] used RP C18 column (Phenomenex, Torrance, CA, USA) in the QuEChERS extraction and LC-MS combined detection method established in the experiment of detecting the content of acrylamide in dried fruit (250 mm × 2 mm 5 μm particle size) and edible seeds (Phenomenex, Torrance, CA, USA). They chose a pore size of 110 A based on the molecular weight of acrylamide (Mr = 71.078). The mobile phases chosen were 0.1% formic acid in water (99.5%, solvent A) and 0.1% formic acid in methanol (0.5%, solvent B) with a flow rate of 0.25 mL/min at ambient temperature.

3.1.2. HPLC-MS/MS and HPLC-UV. Lubomir et al. [16] used HPLC-MS/MS for the determination of AM in thermally processed seafood using a shorter narrow-bore column (Phenomenex Synergi Fusion-RP C18 column 50 mm × 2 mm, 2.5 μm), replacing traditional columns like those listed above (250 or 150 mm × 2 or 4.6 mm). Its polar endcaps operate in 100% water and provide acceptable retention and peak shape for acrylamide. In addition, the 50 mm column length reduces analysis time (only 8 minutes of run time, including wash and equilibration time per analysis). Mobile phase A consists of 5% methanol, 0.1% formic acid, and 95% water. Mobile phase B is methanol at a flow rate of 0.2 mL/min.

Haiyan et al. [17] used Hypersil ODS-C18 (250 mm × 4.6 mm, 5 μm) (Thermo Scientific, Waltham, MA, USA) solvent A for the determination of acrylamide in Chinese baked or fried foods. With a mixture of 10% acetonitrile and 90% water containing 0.10% formic acid, solvent B was pure acetonitrile, and the flow rate was 0.40 mL/min.

3.2. Analysis of Veterinary Drugs. Veterinary drug residues are the residues formed in animal visceral tissues and their products (egg, milk, etc.) after veterinary drugs act on animals, which usually includes sulfonamides, antibiotics, and pesticides. Veterinary drug residues are one of the research hotspots in recent years, and all countries in the world have

strengthened the detection of veterinary drug residues in international trade animal food. In this paper, representative sulfonamides will be selected as the research objects, and the effects and differences of different chromatographic methods will be discussed. For the determination of sulfonamides in food, the following section lists some of the different liquid chromatography methods.

3.2.1. LC-MS/MS. The column used by Marisol et al. [18] in their LC-MS-MS analysis for the presence of sulfonamides in honey products was a Zorbax Eclipse XDB-98 (50 × 4.6 mm, 1.8 μm), supplied by Agilent. Chromatographic separation was performed with 0.5% aqueous formic acid (mobile phase A) and ACN (mobile phase B) as mobile phases at a flow rate of 0.4 mL/min.

Petrarca et al. [19] used a Poroshell 120 HILIC column (150 × 3 mm, 2.7 μm) in their LC-QTOF-MS analysis of sulfonamide antibiotic residues in meat and/or egg baby food (Agilent Technologies, Santa Clara, CA, USA). The mobile phase was 20 mM ammonium formate in water, pH 3 : methanol, 1 : 1 *v/v* (solvent A) and acetonitrile (solvent B) at a flow rate of 0.2 mL/min.

3.2.2. HPLC and HPLC-MS/MS. Tian and Kaifeng [20] used Amethyst C18-H (250 × 4.6 mm, 5 μm) as a chromatographic column in the simultaneous determination of sulfonamides in milk by in situ magnetic ionic liquid dispersion liquid-liquid microextraction-high performance liquid chromatography. A 0.5% sodium dihydrogen phosphate aqueous solution-acetonitrile (85 : 15, *v/v*) was used as the mobile phase, the flow rate was 2.0 mL/min, and the measurement wavelength of the UV detector was set to 270 nm for simultaneous detection.

Tao et al. [21] used an F5 column (50 × 3.0 mm, 2.6 μm, Phenomenex, Torrance, CA, USA) for the detection of sulfonamide antibiotic residues in aquaculture by online solid-phase extraction-UHPLC-MS/MS. For chromatographic separation, the mobile phases of UHPLC were 0.1% formic acid water (A) and 0.1% formic acid ACN (B), and the total flow rate of the liquid phase was controlled at 0.45 mL/min.

Hoff et al. [22] used a high performance liquid chromatography column purrospher STAR C18 (150 × 4.6 mm, 5 μm) for the determination of sulfonamide antibiotics and metabolites in animal liver, muscle, and kidney samples by HPLC-Qqlitm-MS/MS method. The mobile phase consisted of HPLC-grade water acidified with 10 mM formic acid and ACN acidified with 10 mM formic acid at a flow rate of 0.2 mL/min.

3.3. Analysis of Mycotoxins. Among the mycotoxins, aflatoxins are more typical. Aflatoxins (AFs) grow in food, including AFB1, AFB, AFG, and AFG2. They are toxic chemicals produced by a variety of fungi, which can cause a variety of food contamination and pose a threat to human health [23]. Likewise, the following section lists several different liquid chromatography methods for the detection of aflatoxins in foods.

3.3.1. Analysis of LC-MS/MS.

3.3.1. Analysis of LC-MS/MS. Purospher Star RP-18 column (50 × 2.1 mm, 2 μm) was selected for the study by Abdallah et al. [24] for the detection of aflatoxin B in maize by LC-MS/MS. The mobile phase was 0.1% acetic acid-methanol (60 : 40) at a flow rate of 0.25 mL/min.

Ala' Yahya et al. [25] used a ZORBAX Eclipse XBD-C18 (100 × 2.1 mm, 1.8 μm) for the determination of aflatoxins in food by the LC-ESI-QTOF-MS/MS method (PN. 928700-902) column at a flow rate of 0.3 mL/min. The mobile phase was 1% formic acid and 2 mM ammonium formate in water (A) and 1% formic acid in methanol (B).

3.3.2. Analysis of HPLC-MS/MS and HPLC-FD/FLD. Riwei et al. [26] used Zorbax SB-C18 column (50 × 2.1 mm, 3.5 μm) in the determination of aflatoxin in Ural licorice by HPLC-MS/MS, mobile phase A was water, eluent B is acetonitrile, both contain 0.1% formic acid, and the flow rate is 2 mL/min.

Nor Shifa and Bahruddin [27] used a C18 Hypersil gold (250 × 4.6 mm, 5 μm) column for the determination of aflatoxins in milk by in-syringe dispersive microsolid phase extraction by HPLC-FD with the mobile phase of acetonitrile : methanol 3 : 2 (*v/v*) flow rate of 1.2 mL/min.

Fatma et al. [28] used ACE 5 C18, 100 A (250 × 4.6 mm, 5 μm) in the determination of aflatoxins in pistachios and peanuts by HPLC-FLD, and the mobile phase was water-acetonitrile-ethanol (6/2/3, *v/v/v*); the flow rate is 2-3 mL/min.

4. Discussion

4.1. Analysis of Chromatogram Peaks. The flow rate is the main factor that affects the peak area of the final result chromatogram. Among all liquid chromatography methods for the determination of acrylamide, there are three methods (LC-MS/MS, improved LC-MS/MS, and HPLC-MS/MS) at similar flow rates. Under the condition that this factor remains unchanged, comparative analysis is carried out by comparing the final chromatograms. There are multiple chromatograms according to (and other peak resolution, peak symmetry, and sharpness) filter. The three methods all use the multiple reaction detection mode (MRM). Under different voltages, the transition changes of the ion collision energy are different, and the chromatograms under such conditions are also different. A comparison of the best chromatograms screened for each method is shown in Figure 2. By comparison, we found that the improved LC-MS/MS method has more symmetry in the shape of the chromatographic peaks than the LC-MS/MS method. It is much better and easier to calculate the peak area, and the HPLC-MS/MS method can produce peaks within two minutes and has good symmetry, so the HPLC-MS/MS method is an extremely useful method for the determination of acrylamide in food. The optimal method shortens the analysis time and improves the quality of sample analysis.

The best chromatographic peaks (Figure 3) for the determination of acrylamide content by HPLC-UV were produced when the mobile phase was 10% (*v/v*) acetonitrile at a flow rate of 0.40 mL/min. In both cases, 15% (*v/v*) acetonitrile with a flow rate of 0.40 mL/min and 10% (*v/v*) acetonitrile with a flow rate of 0.50 mL/min were not as effective as the first mobile phase and flow rate The chromatographic peaks produced by the selection are effective, so simply increasing the flow rate and the acetonitrile concentration cannot improve the chromatographic peaks.

In the experiment of determination of sulfonamides by liquid chromatography, the differences of the corresponding methods of different chromatographic peaks were analyzed under the condition that the flow rate was almost constant. In the experiment of the HPLC-QqLIT-MS/MS method for the determination of sulfonamides, there are 16 kinds of tested substances. In this experiment, two extraction methods, PLE and USE, were set up for comparison and verification. By observing the shape of their chromatographic peaks (Figure 4), Figure 4(a) is the chromatogram of the PLE method, and Figure 4(b) is the chromatogram of the USE method. From the symmetry, the degree of separation, and the sharpness of the different substances in the chromatogram, it is inferred that the chromatogram of the USE method is more accurate and precise. By comparing the shape of the chromatogram peaks, it is concluded that the USE method is more accurate than the PLE method, and this conclusion has also been confirmed by Valente et al. in the laboratory for many years.

In the determination of sulfonamides in food by the HPLC-QqLIT-MS/MS method and in situ magnetic ionic liquid dispersive liquid-liquid microextraction-HPLC method, the former can use the USE extraction method to obtain the determination chromatogram of each compound, while the latter is a chromatogram with multiple peaks, including a variety of substances, which is not easy to distinguish. In general, the HPLC-QqLIT-MS/MS method is more suitable for the simultaneous detection of multiple compounds and has higher resolution. In the research on the determination of sulfonamides in food by LC-MS/MS, the overall effect of the chromatographic peaks obtained by the SPE extraction method is good, but the peaks of the three substances are stuck or overlapped together, which is inconvenient to observe and calculate the final result, affecting its accuracy.

In the determination of aflatoxin in food, the HPLC-FLD method and the LC-ESI-QTOF-MS/MS method also have similar flow rates, so they have little effect on the peak area, and the standard solution is also measured first. Therefore, it is easier to compare under this condition. It can be clearly seen in Figure 5 that the LC-ESI-QTOF-MS/MS method has a higher sharpness and a faster peak time, which is also due to the combination with the QTOF analyzer, which is combined use.

4.2. Recovery and Precision Analysis. The precision of LC-QTOF-MS was 1.0-18.1%, which was similar to that of LC-MS/MS with 3.0-19.5%, but the average recovery was 70-120%, which was higher than that of LC-MS/MS with 89-114%. It can be seen that the combination of the QTOF analyzer can also improve the recovery and precision of liquid chromatography.

(1) HPLC-MS/MS
(2) Improved LC-MS/MS
(3) LC-MS/MS
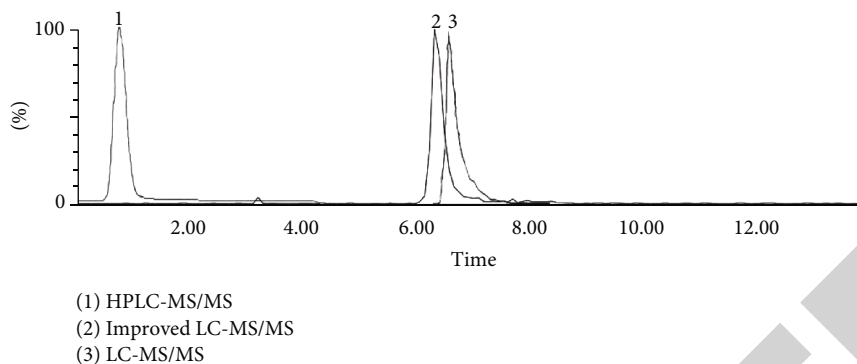
Figure 2: Schematic diagram of chromatographic peak comparison.
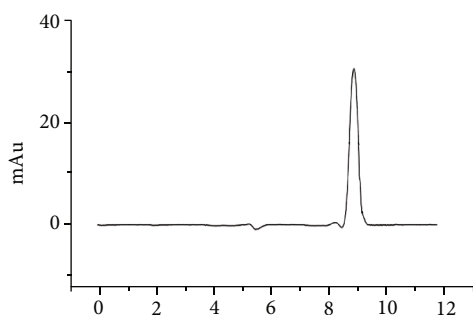
Figure 3: Optimal chromatographic peaks of HPLC-UV.

In experiments for the determination of aflatoxins, the precision of the LC-MS/MS method was less than 11% and the recovery was 50-120%. The precision of the HPLC-FD method was 1.2-14.3%, and the recovery was 73-110%. The precision when analyzed by immunomagnetic solid-phase extraction coupled with UHPLC-MS/MS was less than 15.2%, and the recovery was 84.5–112.7%. By comprehensively comparing the above data, the lower the precision, the higher the average recovery, the better, so it is very desirable to use immunomagnetic solid-phase extraction on the basis of UHPLC-MS/MS.

4.3. Column Size and Particle Size. In terms of column selection, if the inner diameter of the column is halved, the sensitivity increases by a factor of four to five (assuming the same injection volume). For example, injecting the same amount of sample into a 2.1 mm id column produces peaks that are about 5 times higher than injection into a 4.6 mm id column. Parameters such as column efficiency, number of theoretical plates, backpressure, and analysis time are independent of the reduction in column ID as long as the linear flow rate remains constant.

In the separation process, the following sections pursue narrower peak broadening and the best column efficiency under the condition of approximate retention time. For this, we refer to the Van Deemter equation, which is the most famous chromatographic equation to date [29]. This equation expresses the change in column height equivalent to one theoretical plate (HETP) with linear mobile phase velocity:

$$H = A + \frac{B}{u} + C \times u. \tag{1}$$

In the above formula, H is the height of the theoretical plate, which represents the peak broadening in the separation process. u (longitudinal molecular diffusion) is related to the inner diameter of the column and the flow rate of the mobile phase, and $C \times u$ (mass transfer resistance) is related to the particle size of the filler and the flow rate of the mobile phase. According to the calculation, we can obtain an optimal flow rate when A, B, and C are fixed values. For example: the optimal flow rate $u0$ of a column with a diameter of 4.6 mm and a particle size of $5\,\mu$m is 1 mL/min. However, according to the data in Tables 1–3, the 4.6 mm diameter, $5\,\mu$m particle size column has different flow rates. In the determination of acrylamide, the actual flow rate is 0.4 mL/min, which is less than the optimum flow rate. In the determination of sulfonamides, the actual flow rate is 0.2 mL/min, which is also less than the optimum flow rate. In the determination of aflatoxin, the actual flow rate is 1.2 mol/min, 2 mol/min, and 2-3 mol/min; these three data are larger than the optimal flow rate. So, the following sections will discuss the effect of the actual flow rate on the column efficiency (peak broadening) when the actual flow rate is greater than $u0$ and less than $u0$.

According to Figure 6 and formulas, we can conclude that when the actual flow rate is less than $u0$, B/u (longitudinal molecular diffusion) plays a major role on the plate height, $C \times u$ (mass transfer resistance) plays a secondary role on the plate height, and A (vortex diffusion) has a negligible effect on plate height. Therefore, under this condition, the larger the actual flow rate, the lower the theoretical plate height, and the higher the column efficiency. When the flow rate is greater than $u0$ and the actual flow rate is greater than $u0$, $C \times u$ (mass transfer resistance) plays a major role in the height of the tray, and A (vortex diffusion) plays a secondary role in the tray. Under this condition, as the flow rate increases, the height of the theoretical plate also increases, and the column efficiency decreases slowly. In addition, at the same flow rate, the smaller the particle size of the filler, the smaller the height of the theoretical plate, and the better the column efficiency. It
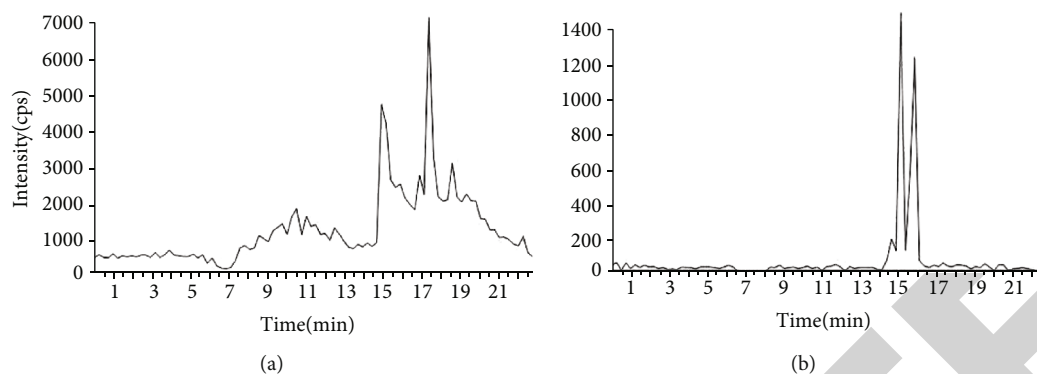
Figure 4: (a) Chromatograms obtained by the PLE method and (b) the USE method.
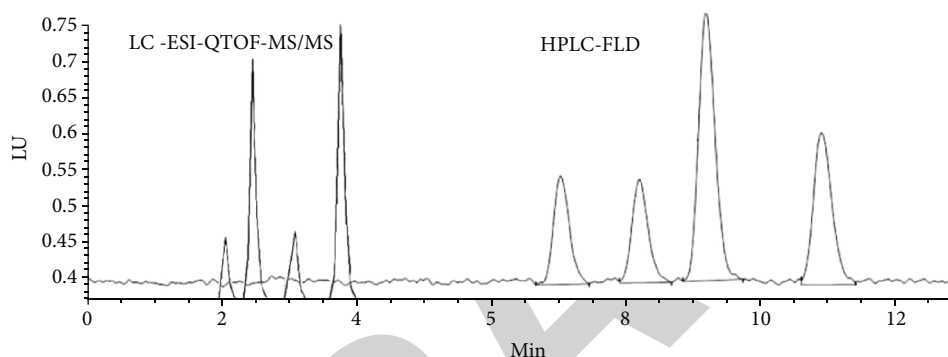
Figure 5: Comparison of chromatographic peaks between HPLC-FLD and LC-ESI-QTOF-MS/MS.
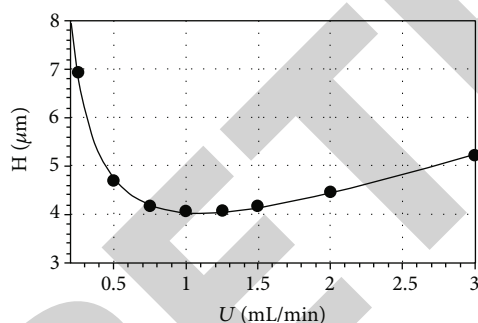
Figure 6: Vandermuth equation image reference optimal flow rate determination [30].

can be inferred that the HPLC-FD method used in the determination of aflatoxin is superior to HPLC-MS/MS and HPLC-FLD. HPLC-MS/MS is superior to improved LC-MS/MS in the determination of acetamide content.

According to the above theory, it can also conclude that the newer methods such as fluorescence detection, UV detection, QTOF, or QuEChERS extraction combined with liquid chromatography are much better than the original liquid chromatography.

As for the selection of stationary phase and mobile phase, in the above liquid chromatography, mostly is reverse phase chromatography. In the process of determination, the nonpolar stationary phase such as C18 is mostly used, while the mobile phase is usually water or buffer. This combination of stationary and mobile phases is suitable for the sepa-

ration of nonpolar and low-polar compounds. In the mobile phase, the commonly used water-soluble organic solvents are methanol, formic acid, ammonium formate, acetonitrile, isopropanol, acetone, tetrahydrofuran, and so on. These substances can regulate the retention time.

5. Conclusion

In this paper, by enumerating three types of food contaminants, referring to and citing different liquid chromatography methods in the literature to determine the indicators and the final results, a comparison was established in terms of chromatographic peaks, recovery, and accuracy, and the immobilization was summarized. For the principles for the selection of phase and mobile phase, with the increase of the molecular weight of the tested substance, the position of the peak in the chromatogram is correspondingly backward, and the analysis time is also correspondingly increased. When there are multiple compounds in the analyte, HRMS hybrid detectors such as QTOF analyzers can be used, which is more efficient and convenient than traditional QqQ and TOF. It should also have good clean-up techniques like PLE, USE, SPE, or QuEChERs [31]. Choosing the appropriate mobile phase ratio and flow rate of the stationary phase will help to enhance the symmetry of the chromatographic peak shape and the degree of separation and also help to improve the precision and recovery rate, so that a more efficient liquid chromatography technology can be established and used. The field of food safety testing has been more widely used.

Data Availability

The datasets used and/or analyzed during the current study are available from the corresponding author on reasonable request.

Conflicts of Interest

The author declared no potential conflicts of interest with respect to the research, authorship, and/or publication of this article.

References

[1] J. H. Simon, P. Y. L. Benjamin, S. Rainer, and K. Rudolf, "Liquid chromatography-mass spectrometry for the determination of chemical contaminants in food," *TrAC Trends in Analytical Chemistry*, vol. 59, pp. 59–72, 2014.

[2] O. Núñez, H. Gallart-Ayala, C. P. Martins, P. Lucci, and R. Busquets, "State-of-the-art in fast liquid chromatography-mass spectrometry for bio- analytical applications," *Journal of Chromatography B*, vol. 927, no. 5, pp. 3–21, 2013.

[3] D. A. Medina, J. V. Borsatto, E. V. Maciel, and F. M. Lancas, "Current role of modern chromatography and mass spectrometry in the analysis of mycotoxins in food," *TrAC Trends in Analytical Chemistry*, vol. 135, article 116156, 2021.

[4] G. Fereshte Mohamadi, A. Morteza, and H. Bahram, "A three-dimensional origami microfluidic device for paper chromatography: application to quantification of tartrazine and indigo carmine in food samples," *Journal of Chromatography A*, vol. 1621, article 461049, 2020.

[5] O. Claudia, L. Katharina, and S. Wolfgang, "Characterization of E 472 food emulsifiers by high-performance thin-layer chromatography with fluorescence detection and mass spectrometry," *Journal of Chromatography A*, vol. 1618, article 460874, 2020.

[6] G. Brett, C. Olivier, Q. Brian, M. B. Luis, and T. E. Christopher, "Redefining dilute and shoot: the evolution of the technique and its application in the analysis of foods and biological matrices by liquid chromatography mass spectrometry," *TrAC Trends in Analytical Chemistry*, vol. 141, article 116284, 2021.

[7] S. Esslinger, J. Riedl, and C. Fauhl-Hassek, "Potential and limitations of non-targeted fingerprinting for authentication of food in official control," *Food Research International*, vol. 60, pp. 189–204, 2014.

[8] M. Esteki, Z. Shahsavari, and J. Simal-Gandara, "Food identification by high performance liquid chromatography fingerprinting and mathematical processing," *Food Research International*, vol. 122, pp. 303–317, 2019.

[9] A. Hercegová, M. Dömötörová, and E. Matisová, "Sample preparation methods in the analysis of pesticide residues in baby food with subsequent chromatographic determination," *Journal of Chromatography A*, vol. 1153, no. 1-2, pp. 54–73, 2007.

[10] M. Kamal and R. Karoui, "Analytical methods coupled with chemometric tools for determining the authenticity and detecting the adulteration of dairy products: a review," *Trends in Food Science & Technology*, vol. 46, no. 1, pp. 27–48, 2015.

[11] T. Labuza, "Dr Ted Labuza Univ. of Minnesota topic 12 acrylamide FScN 1102 case study #1".

[12] J. Keramat, A. Lebail, C. Prost, and N. Soltanizadeh, "Acrylamide in foods: chemistry and analysis. A review," *Food & Bioprocess Technology*, vol. 4, no. 3, pp. 340–363, 2011.

[13] J. A. G. Roach, D. Andrzejewski, M. L. Gay, D. Nortrup, and S. M. Musser, "Rugged LC-MS/MS survey analysis for acrylamide in foods," *Journal of Agricultural and Food Chemistry*, vol. 51, no. 26, pp. 7547–7554, 2003.

[14] K. Cheong Tae, H. Eun-Sun, and L. Hyong Joo, "An improved LC-MS/MS method for the quantitation of acrylamide in processed foods," *Food Chemistry*, vol. 101, no. 1, pp. 401–409, 2007.

[15] L. Eleonora, M. Giuseppe, M. Francesca, G. Davide, B. Martino, and A. Andrea, "Determination of acrylamide in dried fruits and edible seeds using QuEChERS extraction and LC separation with MS detection," *Food Chemistry*, vol. 217, pp. 191–195, 2017.

[16] K. Lubomir, W. Thomas, and A. Elke, "Determination of acrylamide in roasted chestnuts and chestnut-based foods by isotope dilution HPLC-MS/MS," *Food Chemistry*, vol. 114, no. 4, pp. 1555–1558, 2009.

[17] W. Haiyan, F. Feng, G. Yong, S. Shaomin, and M. F. C. Martin, "HPLC-UV quantitative analysis of acrylamide in baked and deep-fried Chinese foods," *Journal of Food Composition and Analysis*, vol. 31, no. 1, pp. 7–11, 2013.

[18] J.-B. Marisol, P. Angela, D. Eva, and E. Isabel, "Routine quality control in honey packaging companies as a key to guarantee consumer safety. The case of the presence of sulfonamides analyzed with LC-MS-MS," *Food Control*, vol. 50, pp. 243–249, 2015.

[19] M. H. Petrarca, P. A. de Campos Braga, F. G. Reyes, and A. P. Bragotto, "Exploring miniaturized sample preparation approaches combined with LC-QToF-MS for the analysis of sulfonamide antibiotic residues in meat- and/or egg-based baby foods," *Food Chemistry*, vol. 366, article 130587, 2022.

[20] Y. Tian and D. Kaifeng, "Simultaneous determination of sulfonamides in milk: in-situ magnetic ionic liquid dispersive liquid-liquid microextraction coupled with HPLC," *Food Chemistry*, vol. 331, article 127342, 2020.

[21] L. Tao, W. Ce, X. Zhaoan, and C. Amit, "A coupled method of on-line solid phase extraction with the UHPLC–MS/MS for detection of sulfonamides antibiotics residues in aquaculture," *Chemosphere*, vol. 254, article 126765, 2020.

[22] R. B. Hoff, T. M. Pizzolato, M. D. Peralba, M. S. Díaz-Cruz, and D. Barceló, "Determination of sulfonamide antibiotics and metabolites in liver, muscle and kidney samples by pressurized liquid extraction or ultrasound-assisted extraction followed by liquid chromatography–quadrupole linear ion trap-tandem mass spectrometry (HPLC–QqLIT-MS/MS)," *Talanta*, vol. 134, pp. 768–778, 2015.

[23] N. A. AlFaris, J. Z. ALTamimi, Z. A. ALOthman et al., "Analysis of aflatoxins in foods retailed in Saudi Arabia using immunoaffinity column cleanup and high-performance liquid chromatography-fluorescence detection," *Journal of King Saud University-Science*, vol. 32, no. 2, pp. 1437–1443, 2020.

[24] O. Abdallah, C. Adil, C. Hanane, A. Abdelmajid, and A. Elhabib Ait, "Optimization and validation of a liquid chromatography/tandem mass spectrometry (LC-MS/MS) method for the determination of aflatoxins in maize," *Heliyon*, vol. 5, no. 5, article e01565, 2019.

[25] S. Ala' Yahya, T. Guan Huat, and C. S. W. Richard, "Determination of aflatoxins in food using liquid chromatography coupled with electrospray ionization quadrupole time of flight

Retraction

Retracted: Clinical and Biological Significances of a Ferroptosis-Related Gene Signature in Lung Cancer Based on Deep Learning

Computational and Mathematical Methods in Medicine

This article has been retracted by Hindawi following an investigation undertaken by the publisher [1]. This investigation has uncovered evidence of one or more of the following indicators of systematic manipulation of the publication process:

(1) Discrepancies in scope

(2) Discrepancies in the description of the research reported

(3) Discrepancies between the availability of data and the research described

(4) Inappropriate citations

(5) Incoherent, meaningless and/or irrelevant content included in the article

(6) Peer-review manipulation

The presence of these indicators undermines our confidence in the integrity of the article's content and we cannot, therefore, vouch for its reliability. Please note that this notice is intended solely to alert readers that the content of this article is unreliable. We have not investigated whether authors were aware of or involved in the systematic manipulation of the publication process.

Wiley and Hindawi regrets that the usual quality checks did not identify these issues before publication and have since put additional measures in place to safeguard research integrity.

We wish to credit our own Research Integrity and Research Publishing teams and anonymous and named external researchers and research integrity experts for contributing to this investigation.

The corresponding author, as the representative of all authors, has been given the opportunity to register their agreement or disagreement to this retraction. We have kept a record of any response received.

References

[1] X. Yang, X. Hu, and N. Guo, "Clinical and Biological Significances of a Ferroptosis-Related Gene Signature in Lung Cancer Based on Deep Learning," *Computational and Mathematical Methods in Medicine*, vol. 2022, Article ID 6495301, 15 pages, 2022.

Research Article

Clinical and Biological Significances of a Ferroptosis-Related Gene Signature in Lung Cancer Based on Deep Learning

Xiaosong Yang [ID],[1] Xuanjian Hu [ID],[1] and Na Guo [ID][1,2]

[1]*Department of Anesthesiology, Sun Yat-sen University Cancer Center, State Key Laboratory of Oncology in South China, Collaborative Innovation Center for Cancer Medicine, 651 Dongfengdong Road, Guangzhou 510060, China*
[2]*Guangdong Esophageal Cancer Institute, Guangzhou 510060, China*

Correspondence should be addressed to Na Guo; guona@sysucc.org.cn

Acyl-CoA synthetase long-chain family member 4 (ACSL4) has been linked to the occurrence of tumors and is implicated in the ferroptosis process. Deep learning has been applied to many areas in health care, including imaging diagnosis, digital pathology, classification of cancer, and prediction of metastasis. Nonetheless, neither the level of ACSL4 expression nor its predictive significance in non-small-cell lung cancer (NSCLC) is well understood at this time. Predictions of the ACSL4 mRNA expressions in NSCLC and its link to NSCLC prognosis were made with the aid of the Oncomine and TCGA databases. By performing real-time PCR, we detected the levels of ACSL4 expression that were present in human NSCLC samples. Analyses of the diagnostic, as well as the prognostic significance of ACSL4 in NSCLC, were performed with the use of Kaplan-Meier curves. To assess the influence of ACSL4 on ferroptosis in NSCLC cell lines, an inducer of ferroptosis, namely, erastin, was utilized in this study. In NSCLC tissues, there was a substantial decrease in the level of ACSL4 expression ($p < 0.001$), and this was in line with the findings of the inquiry into the Oncomine and TCGA databases. After that, the findings of the immunohistochemistry analysis revealed that the ACSL4 staining was weakened in NSCLC samples in contrast with the normal samples. It was shown that the differential expression of ACSL4 was substantially linked to the stages of cancer, smoking behaviors, and the status of nodal metastases (all $p < 0.001$). According to the findings of the survival analysis, both RFS and OS were favorable among NSCLC patients who had elevated expression of ACSL4. The ferroptosis sensitization in cancer cells may be reestablished with upregulation of ACSL4 through gene transfection. Mechanistically, protein ubiquitination could perform a remarkable function in ACSL4-induced ferroptosis. ACSL4, which has a function in ferroptosis as both a contributor and monitor, was shown to be downregulated in NSCLC. This finding suggests that ACSL4 might function as a helpful diagnostic and prognostic biological marker and might also be considered a novel possible treatment target for NSCLC.

1. Introduction

Lung cancer is the most prevalent type of malignancy worldwide and the major contributor to cancer-associated fatalities [1]. Lung cancer is divided into small-cell lung cancer (SCLC) and non-small-cell lung cancer (NSCLC). In the case of NSCLC, it is further classified into squamous cell carcinoma (SCC) and adenocarcinoma (ADC) which is responsible for the highest percentage of all lung cancer cases [2]. The processes that drive the growth of tumors in NSCLC

and the treatment approaches that might be implemented are still important research topics.

Cancer cells often exhibit innate or acquired resistance to the programmed cell death process known as apoptosis. As a result, the identification of nonapoptotic types of regulated cell death has emerged as a promising therapeutic approach for treating cancer [3]. A previously undiscovered type of programmed cell death known as ferroptosis, which is distinctive from autophagy, necrosis, and apoptosis, was initially discovered in cancer cells with oncogenic Ras

mutations [4]. Ferroptosis plays a role in the disorders of the neurological system, kidneys, and cardiovascular system and performs an integral function in cancers, including NSCLC [5–7]. Ferroptosis may be induced by a variety of agents, including drugs, chemical compounds, and small molecule drugs. Erastin, which is a cell-permeable piperazinyl-quinazolinone substance, is one of the compounds that is utilized extensively in the investigation of the molecular processes behind ferroptosis [8]. Erastin can produce iron accumulation and lipid peroxidation by interfering with several sites, such as the glutathione peroxidase 4 (GPX4) and the cystine/glutamate exchange transporter (SLC7A11).

Even though it has only been recently discovered that various regulators are responsible for modulating erastin-mediated ferroptosis in a variety of experimental settings, the key modulator of lipid metabolism in ferroptosis of cancerous cells is still not well comprehended. In 2002, a mutation in a gene called acyl-CoA synthetase long-chain family member 4 (ACSL4) was found to be the cause of the non-specific X-linked mental retardation [9]. ACSL4 had a substrate predilection for arachidonic acid (AA) and eicosapentaenoic acid (EPA). Even more intriguing is the fact that the levels of free AA may, in turn, influence the levels of ACSL4 protein within the cells [10]. To this day, it has been shown that ACSL4 dysregulation is linked to many illnesses, which include diabetes, acute kidney injury, and malignant tumors [7, 11, 12]. Recent research has shown that ferroptosis and the dysregulation of ACSL4 are strongly connected [13]. ACSL4 knockdown was shown to suppress erastin-mediated ferroptosis in HL-60 and HepG2 cells, whereas the upmodulation of ACSL4 was found to reestablish the susceptibility of K562 and LNCaP cells to erastin [9]. As a consequence, the levels of ACSL4 expression could be linked to the progression of NSCLC because of its role in triggering ferroptosis. Nonetheless, neither the expression profiles nor the roles of ACSL4 in NSCLC have been investigated to this point. Hence, the present research sought to examine the ACSL4 expression in NSCLC and its link to the clinical-pathological characteristics and patients' prognoses, as well as the involvement of ACSL4 in ferroptosis through experimental and bioinformatic analyses.

2. Material and Methods

2.1. Bioinformatics Analyses of ACSL4. To begin, the Oncomine database (https://www.oncomine.org/) was retrieved in order to make a prediction about the level of ACSL4 mRNA expression found in lung cancer samples and normal samples. Next, the Cancer Genome Atlas (TCGA) LUAD and LUSC database was retrieved to evaluate the link between ACSL4 mRNA expression and clinical prognostic outcomes of NSCLC patients based on the data from UALCAN (http://ualcan.path.uab.edu/). In The Human Protein Atlas (HPA) (https://www.proteinatlas.org), the immunohistochemical (IHC) image was utilized to perform a comparative evaluation of the levels of ACSL4 protein expression between human NSCLC samples and normal samples. The prognostic utility of ACSL4 mRNA expression was investigated with the use of an electronic database

referred to as Kaplan-Meier (KM) plotter (https://kmplot.com/analysis/). cBioPortal (http://www.cbioportal.org/) was employed to conduct an analysis of ACSL4 coexpression genes based on the TCGA-LUAD and LUSC datasets. To examine the ACSL4 functions, we utilized the GO and KEGG in the Database for Annotation, Visualization, and Integrated Discovery (DAVID) (https://david.ncifcrf.gov/).

2.2. Human Lung Cancer Samples. From 2018 to 2019, we recruited 36 NSCLC patients (18 cases of ADC and 18 cases of SCC) at the Sun Yat-sen University Cancer Center. For the subsequent real-time PCR tests, samples of tumor tissues and surrounding tissues that were five centimeters distant from the margin of the cancerous tissues were collected. Before receiving surgery, these participants did not undergo any adjuvant treatment, like radiotherapy, chemotherapy, or any other kinds of treatment. This research was subjected to approval by the Academic Committee of the Cancer Center at Sun Yat-sen University Cancer Center, and each patient gave their informed consent before taking part in the research.

2.3. Cell Culture and Treatment. The human lung cancer cells A549 and SPC-A-1 cell lines were procured from the American Type Culture Collection (ATCC; Manassas, VA, USA). Next, we cultured the A549 cells in Gibco™ Dulbecco's modified Eagle's medium (DMEM; Thermo Fisher Scientific, Inc., Paisley, UK), whereas the SPC-A-1 cells were grown in Roswell Park Memorial Institute 1640 Media (RPMI 1640; Gibco, USA) comprising 10% fetal bovine serum (FBS), 100 U/ml of penicillin, and 0.1 mg/ml of streptomycin (Thermo Fisher Scientific, Inc.) in a humid incubator with 5% CO_2 and 37°C culture environment. A549 cells were subjected to treatment with 5 μM erastin (Sigma-Aldrich, St. Louis, MO, USA) for 24 hours for the purpose of performing subsequent relevant analyses. Following that, the cells were collected in the manner detailed below in preparation for further examination.

2.4. Cell Proliferation. An evaluation of the capacity for cells to proliferate was carried out with the aid of a Cell Counting Kit-8 assay (CCK-8, Sigma-Aldrich; Merck KGaA, Darmstadt, Germany) in compliance with the specifications stipulated by the manufacturer.

2.5. Quantitative Real-Time PCR Analysis. Synthesis of first-strand cDNA was accomplished following the guidelines provided by the manufacturer of the Reverse Transcription System Kit (OriGene Technologies). cDNA obtained from the cells was amplified utilizing the appropriate primers (ACSL4: 5′-GCTATCTCCTCAGACACACCGA-3′ and 5′-AGGTGC TCCAACTCTGCCAGTA-3′), and the data were normalized to actin RNA (5′-CACCATTGGCAATGAGCGGTTC-3′ and 5′-AGGTCTTTGCGGATGTCCACGT-3′).

2.6. RNA Interference and Gene Transfection. OriGene Technologies supplied the human ACSL4-cDNA used in this study. The Lentivirus Transduction System (Sigma) or the Lipofectamine™ 3000 (Invitrogen) was used to carry out

the transfections following the guidelines provided by the respective manufacturer.

2.7. Iron Assay. In order to conduct the iron assay, we made use of an Iron Assay Kit (Sigma Aldrich, Milwaukee, WI, USA) to assess the level of total iron present per cell line. Subsequently, in a short time, 2×10^6 cells were quickly homogenized in a range of 4 to 10 volumes of iron assay buffer. The insoluble material was separated from the samples by centrifuging them at a rate of $13,000 \times g$ for 10 minutes at a temperature of 4°C. Iron reducer (in a volume of $5 \mu l$) was introduced into each sample well so that Fe^{3+} could be converted to Fe^{2+} to measure total iron. After the samples were well agitated by pipetting or with a horizontal shaker, the solutions were subjected to incubation for 30 minutes in the darkness at ambient temperature. Thereafter, $100 \mu l$ of iron probe were introduced into each well that contained either a standard sample or a test sample. Once the samples were well agitated either by pipetting or with a horizontal shaker, the solutions were allowed to incubate for 60 minutes at ambient temperature in the darkness. At last, the absorbance was evaluated at 593 nm.

2.8. Lipid ROS Assays. In order to analyze lipid ROS, the cells were first trypsinized before resuspension in a medium supplemented with 10% FBS. After that, $10 \mu M$ of C11-BODIPY (Thermo Fisher Scientific, Inc.) was introduced into the samples before incubating them for 30 minutes at 37°C with 5% CO_2, in the darkness. To get rid of any residual C11-BODIPY, the cells were rinsed two times in PBS. By employing a flow cytometer (Beckman Coulter Inc., Brea, CA, USA), the fluorescence of C11-BODIPY 581/591 was quantified by simultaneously recording red signals and green signals.

2.9. Statistical Analysis. GraphPad Prism 6.0 (GraphPad Software, Inc., USA) and SPSS 22.0 (IBM SPSS, Chicago, IL) were utilized to conduct all analyses of statistical data in this study. The results obtained from statistical analyses are presented as means ± SD. We examined whether there were significant differences across the groups with the help of the two-tailed Student's *t*-test or one-way analysis of variance (ANOVA) test. The threshold for significance was set at a *p* value < 0.05.

3. Results

3.1. ACSL4 Expression Is Downmodulated in Lung Cancer. We began by retrieving the Oncomine database, where we discovered that the level of ACSL4 mRNA expression in lung tumor samples was considerably lowered in contrast with that in normal samples (Figure 1). A tissue qPCR was undertaken to determine the expression of ACSL4 in postoperative lung tumor samples relative to normal lung samples. The findings illustrated that the relative ACSL4 expression level was remarkably lowered in tumor samples ($n = 18$) in contrast with the normal samples ($n = 18$) ($p < 0.001$, Figures 2(a) and 2(b)). After that, we scrutinized the HPA dataset to ascertain ACSL4 protein expression. It was discovered that normal lung tissues showed intense staining for ACSL4 (Figure 2(c)).

Conversely, it was demonstrated that all malignant tissues had weak staining for ACSL4 (100%, 12 of 12 cases). In addition, the staining was predominantly present in the cytoplasm and the cell membrane (Figures 2(d) and 2(e)). The findings matched up perfectly with those found in the TCGA database (Figure 3(a)).

3.2. Decreased ACSL4 mRNA Expression Is Associated with Malignant Clinical-Pathological Characteristics in NSCLC Patients. In the current investigation, we examined whether there was a correlation between the expression of ACSL4 mRNA and clinical and pathological characteristics. In both ADC and SCC patients, the findings illustrated that ACSL4 mRNA expression was linked to the cancer stages, smoking behaviors, and the status of nodal metastases ($p < 0.001$, Figure 3). KM curves of overall survival (OS) and relapse-free survival (RFS) were constructed premised on the survival data obtained from the KM plotter to investigate the link between ACSL4 mRNA expression and NSCLC patients' prognoses. According to the findings, patients with ADC who had a high level of ACSL4 expression experienced considerably better OS and RFS ($p = 0.007$, $p = 0.026$, correspondingly, Figures 4(a) and 4(b)). Additionally, patients with SCC who had a high level of ACSL4 expression experienced exhibited an improved OS and RFS, whereas the differences did not meet the significance threshold ($p = 0.16$, $p = 0.13$, correspondingly, Figures 4(c) and 4(d)).

3.3. Overexpression of ACSL4 Promotes Ferroptosis. We transfected ACSL4 cDNA into SPC-A-1 and A549 cells to ascertain the potential of ACSL4 expression to modulate the anticancer function of erastin (inducer of ferroptosis) in lung cancer (Figure 5(a)). Gene transfection was used to overexpress ACSL4, which resulted in a considerable enhancement of the susceptibility of SPC-A-1 and A549 cells to the erastin-mediated cell death (Figures 5(b) and 5(c)), indicating that ACSL4 is a necessary part of the ferroptosis-related regulatory mechanism. Both the peroxidation of lipids and the accumulation of iron are necessary elements in the process of ferroptosis activation. As a result, we examined whether ACSL4 affected these events during ferroptosis. Erastin caused a considerable increase in the generation of lipid ROS when ACSL4 was upregulated (Figure 5(d)). On the other hand, the upmodulation of ACSL4 did not have any effect on the erastin-mediated accumulation of iron (Figure 5(e)). Based on these data, ACSL4 may be a factor contributing to erastin-mediated ferroptosis through modulating lipid peroxidation; however, it does not seem to be a contributor to iron accumulation.

3.4. GO Functional Annotation and Pathway Enrichment of ACSL4. To investigate the fundamental process of ACSL4's participation in the pathologically aggressive biological behavior of lung cancer, we conducted a TCGA-LUAD and LUSC gene coexpression network analysis. We identified the remarkably coexpressed genes with ACSL4 in TCGA-LUAD and LUSC by utilizing the cBioPortal of Cancer Genomics. A criterion of absolute Spearman's *r* of ≥0.5 was utilized to determine whether genes in LUAD and LUSC

Analysis type by cancer	Cancer vs. Normal	
Bladder cancer		1
Brain and CNS cancer		3
Breast cancer		5
Cervical cancer		
Colorectal cancer	4	
Esophageal cancer		
Gastric cancer		
Head and neck cancer	2	
Kidney cancer	2	
Leukemia		3
Liver cancer	6	
Lung cancer		4
Lymphoma	4	
Melanoma		
Myeloma	1	
Other cancer		1
Ovarian Cancer		
Pancreatic cancer	1	1
Prostate cancer		
Sarcoma		
Significant unique analyses	20	18
Total unique analyses	366	

1 5 10   10 5 1   Cell color is determined
by the best gene rank
percentile for the
analyses within the cell.
%

(a)

Figure 1: Continued.

(b)

(c)

Figure 1: Continued.

(d)

(e)

Figure 1: Continued.

(f)

(g)
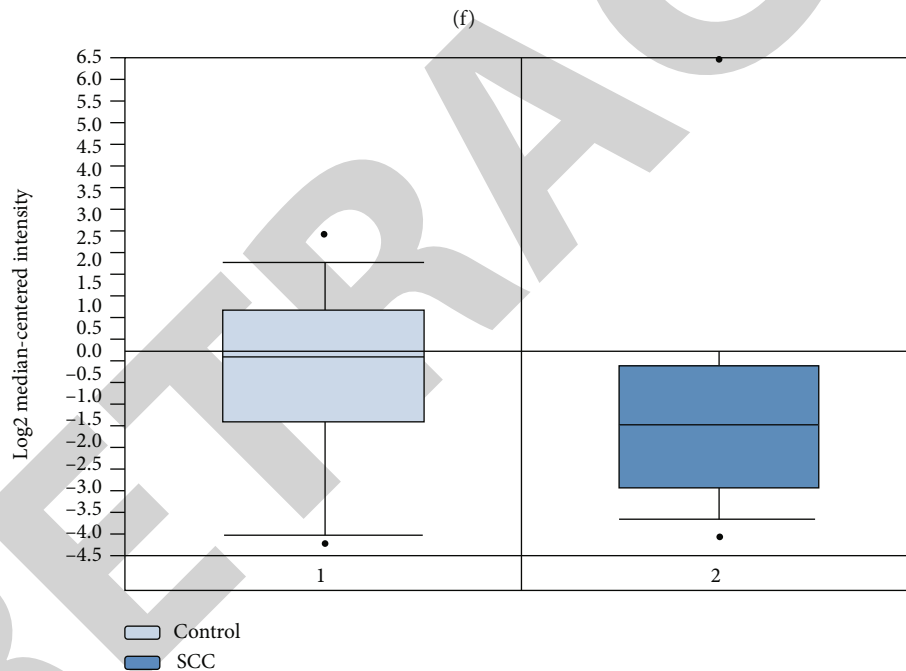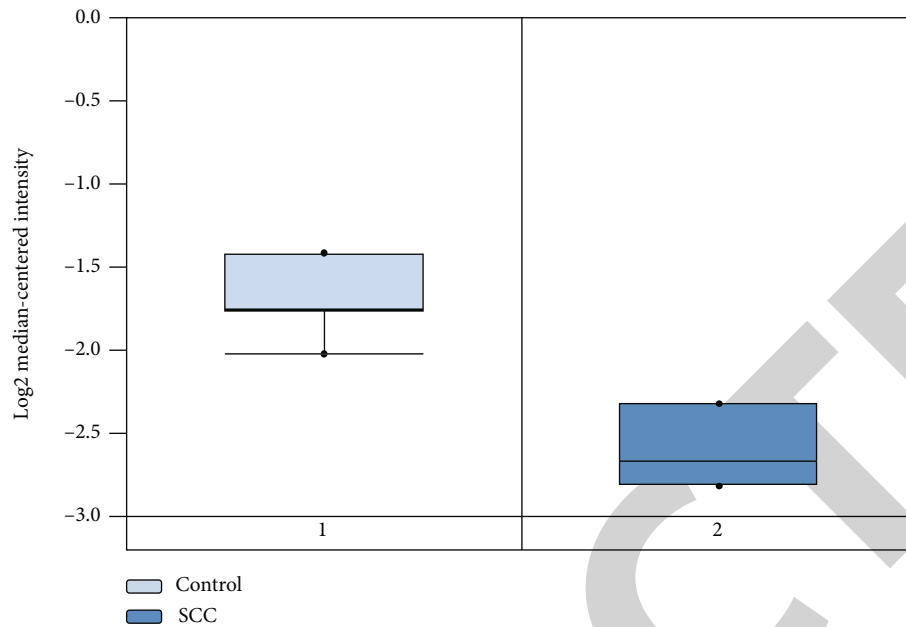
Figure 1: The Oncomine database indicates that NSCLC tissues had low levels of ACSL4 mRNA expression. An investigation of ACSL4 mRNA levels was carried out by retrieving the Oncomine database for (a) overall cancer type, (b–d) ADC, and (e–g) SCC grouped by NSCLC and normal lung tissue. All $p < 0.001$ vs. control.

were coexpressed with ACSL4, and the findings illustrated a coexpression of ACL4 with 56 genes in LUAD and 63 genes in LUSC. After that, these genes were entered into DAVID so that additional GO analysis and KEGG pathway analysis could be undertaken. Table 1 contains a list of the three most significant terms derived from the GO functional annotation and the KEGG pathway enrichment analysis. The ubiquitin-induced proteolysis pathway was the one that was most relevant for the gene enrichment that occurred as a result of ACSL4 coexpression. Protein ubiquitination (GO: 0016567)

and ubiquitin-protein transferase activity (GO: 0004842) accounted for the substantial proportion of enriched GO categories in the biological process and molecular function. In the cellular component ontology, the endocytic vesicle (GO: 0030139) ranked at the top in the pathophysiological process.

4. Discussion

Ferroptosis was not discovered until 2012 when Dixon et al. published their findings on a study they had conducted on a

(a)

(b)

Control

ADC

(c)

(d)
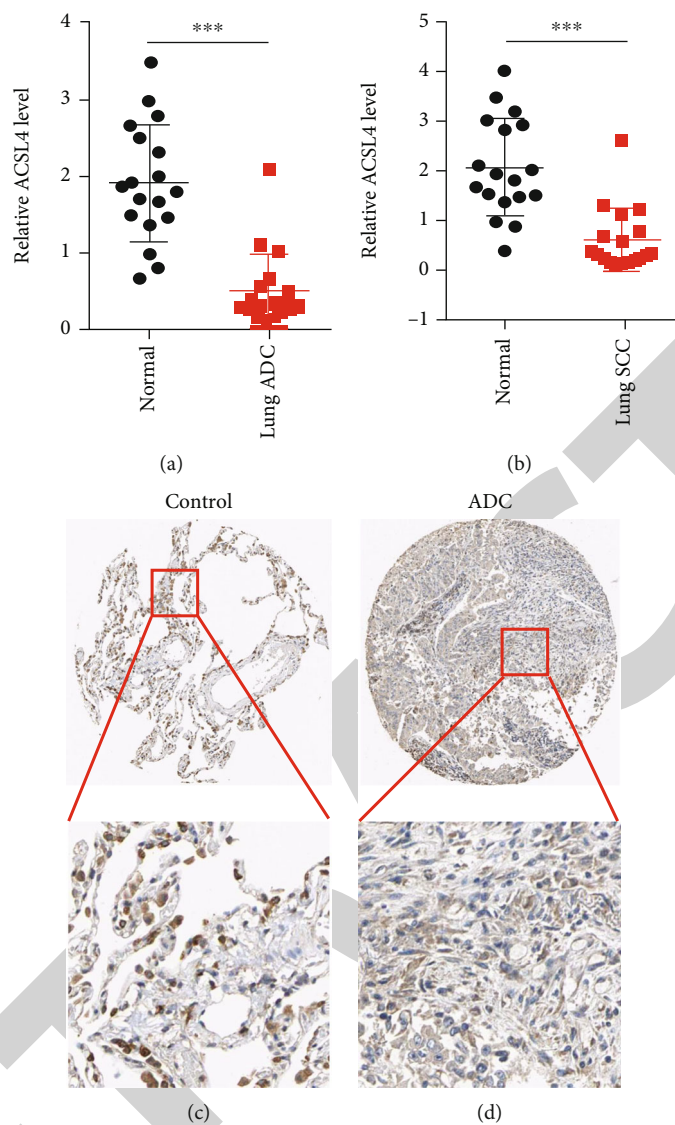
FIGURE 2: Continued.

SCC

(e)
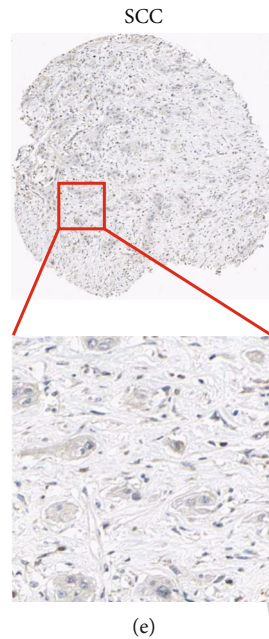
FIGURE 2: Compared with normal lung samples, NSCLC tissue samples showed a considerable reduction in ACSL4 expression. (a, b) A qPCR was utilized to examine ACSL4 mRNA expression in 18 pairs of NSCLC and corresponding neighboring normal lung tissues. ACSL4 IHC demonstrated strong staining in normal lung tissues (c); weak staining in NSCLC tissue (d, e). $^{***}p < 0.001$ vs. control.

small compound known as erastin [4]. The process of ferroptosis is a novel kind of regulated cell death that is reliant on iron and is linked to oxidative stress [14]. The typical characteristics of ferroptosis encompass lipidic and cytoplasmic accumulation of ROS, a decrease in the volume of mitochondria, an enhancement in the density of the mitochondrial membrane, rupture or loss of mitochondrial cristae, and rupture of the mitochondrial outer membrane [4, 15]. Following gene scanning using genome-wide CRISPR and microarray analyses of anti-ferroptosis cell lines, it was recently shown that ACSL4 is a significant factor involved in the ferroptosis process [13]. In the current investigation, the patterns of ACSL4 expression, as well as the clinical and pathological characteristics of NSCLC patients, were analyzed. Furthermore, we present the substantiation that ACSL4 is implicated in the accumulation of lipid intermediates in the process of ferroptosis. The degree of cellular susceptibility to the ferroptosis caused by erastin is correlated with ACSL4 expression. Mechanistically, it is conceivable that the ubiquitin-mediated proteolysis pathway is necessary for the ferroptosis that is triggered by ACSL4.

According to several reports, ferroptosis has a very strong correlation with a variety of human disorders [15, 16]. However, there has not been much research done on ferroptosis in NSCLC. Lai and his colleagues found that ferroptosis as an antitumor factor is inhibited in NSCLC [17]. In Li's study, NSCLC cells possessing chemotherapy based on cisplatin-resistant characteristics (N5CP cells) were acquired from the surgical excision of clinical samples taken from patients suffering from NSCLC [18]. They discovered that stimulation of the Nrf2/SLC7A11 pathway was closely linked to the resistance of cells to the cisplatin-based chemotherapeutic treatment. As a consequence, the modulation of

Nrf2 or SLC7A11 expression by erastin or sorafenib can make tumor cells more or less sensitive to the treatment that is on the basis of cisplatin. Both erastin and sorafenib, which are both small compounds, successfully triggered ferroptosis in N5CP cells. This process was facilitated by the accumulation of lipid ROS within the cells. In addition, to successfully induce N5CP cell ferroptosis, modest dosages of erastin or sorafenib might be employed in conjunction with chemotherapeutic treatment premised on cisplatin. Accordingly, ferroptosis inducers such as sorafenib and erastin might be deemed as a new therapeutic regimen for patients who have NSCLC, especially individuals whose chemotherapeutic regimen was unsuccessful due to the use of cisplatin [18].

Through its role as a central marker and modulator of ferroptosis, ACSL4 also performs an indispensable function as a crucial factor of ferroptosis susceptibility by modifying the lipid content of the cells [7]. ACSL4 deletion cells exhibited resistance to lipid peroxidation as well as ferroptosis [9]. Ferroptosis was partially caused by the formation of 5-hydroxyeicosatetraenoic acid (5-HETE), which was mediated by ACSL4. The generation of 5-HETE was attenuated by zileuton's pharmacological suppression, which inhibited ACSL4 upregulation-mediated ferroptosis [10]. ACSL4 increases the level of long polyunsaturated ω6 fatty acids that are present in cell membranes. In addition, ACSL4 is selectively expressed in a group of breast cancer cell lines that have a basal-like phenotype, which is predictive of the cell lines' susceptibility to ferroptosis [19]. Deletion of ACSL4 in prostate cancer (PCa) cells that express endogenous ACSL4 results in the attenuation of cell capacity to proliferate, migrate, and invade, whereas ectopic production of ACSL4 in ACSL4-negative PCa cells results in an enhancement of the proliferative, migratory, and invasive capacity

(a)

(b)

(c)

(d)
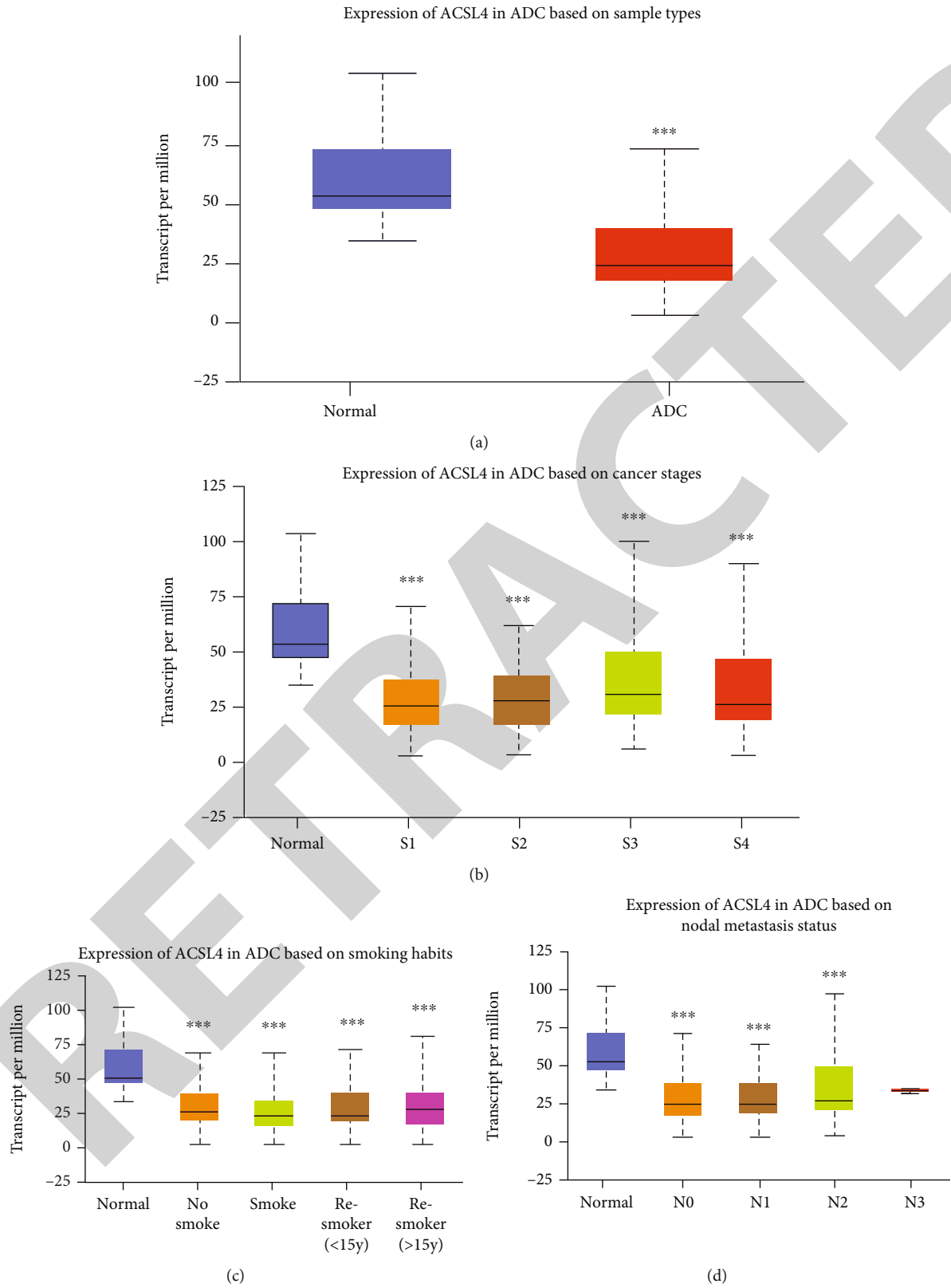
Figure 3: Continued.
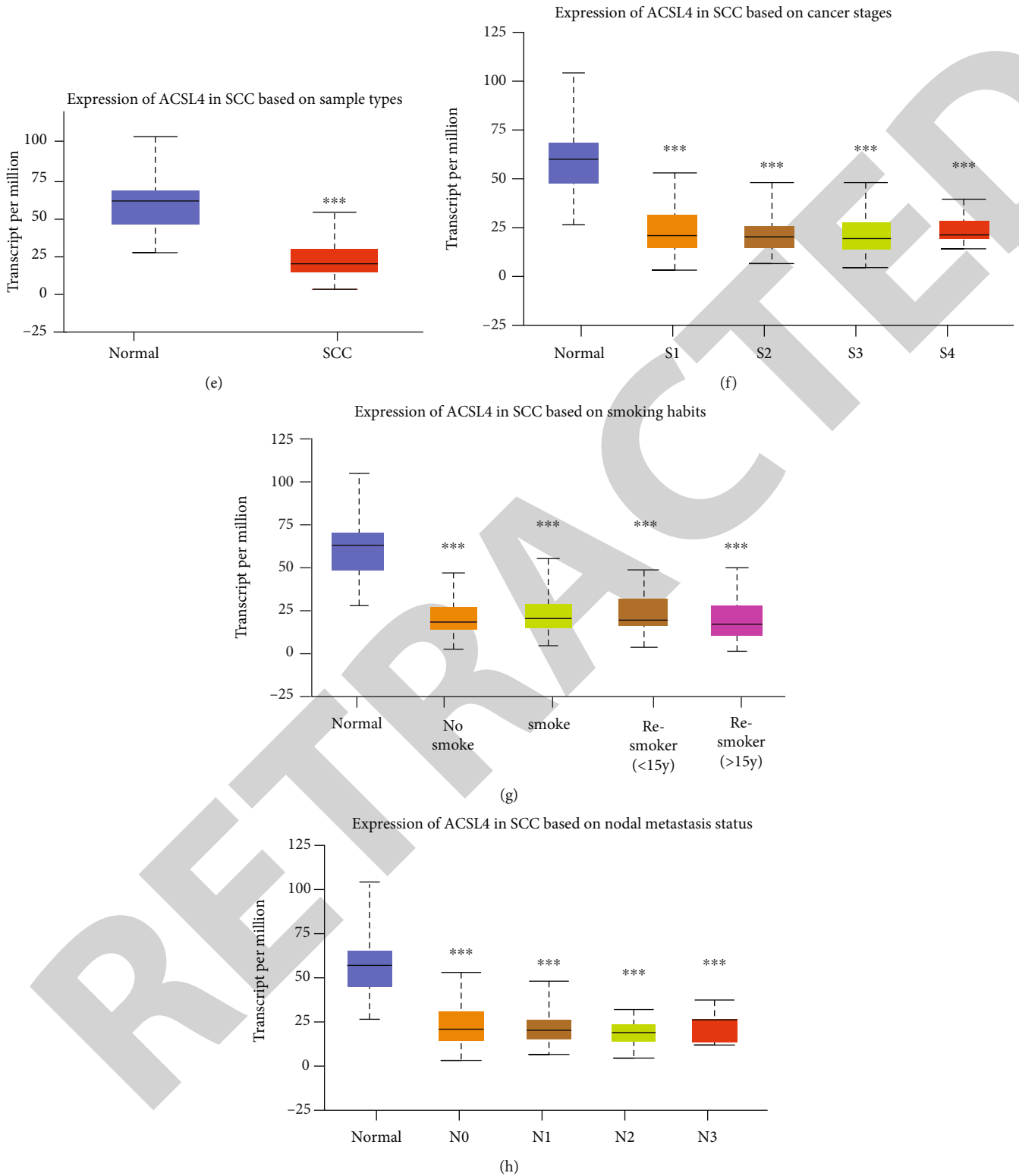
Figure 3: Levels of ACSL4 mRNA expression in patients suffering from NSCLC that were included in the TCGA dataset cohorts. (a, e) A comparison of the ACSL4 expression in ADC and SCC tissues with that of normal controls is depicted in the plot chart. (b–d) Plots chart illustrating the expression of ACSL4 mRNA between cancer stages, smoking habits, and nodal metastasis status in ADC patients. (f–h) Plots chart illustrating the expression of ACSL4 mRNA between cancer stages, smoking habits, and nodal metastasis status in SCC patients. $^{***}p < 0.001$ vs. control.
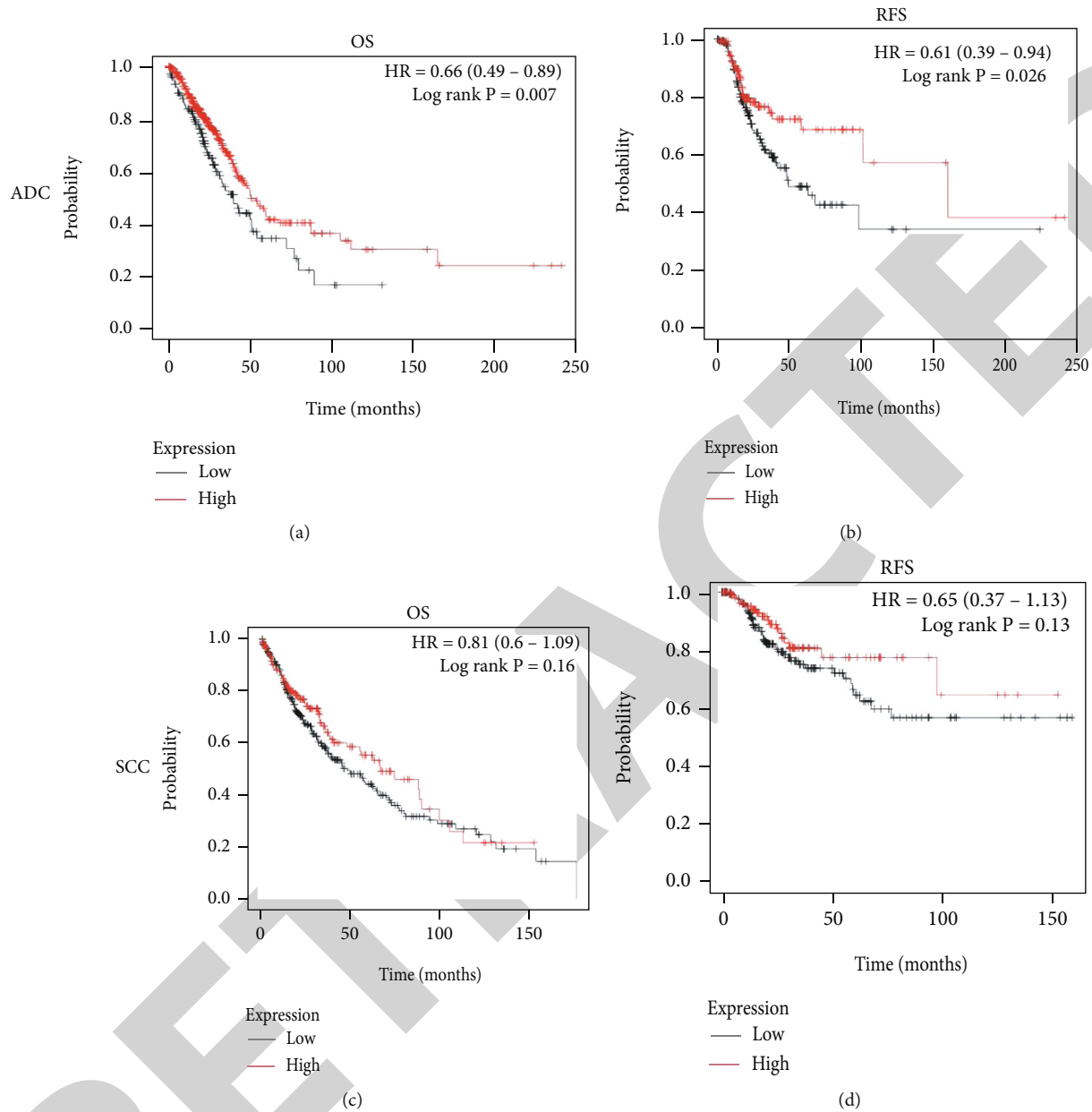
Figure 4: Patients diagnosed with NSCLC who had high levels of ACSL4 expression attained a better chance of survival. (a, b) Overall survival (OS) and recurrence-free survival (RFS) were analyzed utilizing Kaplan–Meier curves for all patients diagnosed with ADC. (c, d) Kaplan–Meier curves of OS and RFS for all cases of SCC.

of cells [20]. According to the findings of the research, ACSL4 is responsible for the upmodulation of many different pathway proteins, including β-catenin, LSD1, and p-AKT [20]. As a consequence of this, ACSL4 is considered to be a sensitive modulator of the ferroptosis process. On the other hand, ACSL4 has not yet been explored in ferroptosis-linked NSCLC. In this research, we discovered that the expression of ACSL4 was reduced in tumors and that this reduction was associated with an unfavorable prognosis. These findings imply that ACSL4 might function as a biological marker and a possible treatment target for NSCLC.

Ferroptosis, like other types of cell death, is intimately linked to particular signaling pathways. The incidence of ferroptosis is tied closely to the accumulation of iron and the oxidation of lipids, which are the two most important components in the process [14]. To determine whether or not ACSL4 has a function in ferroptosis in NSCLC, an ACSL4 upregulation plasmid was introduced into two distinct NSCLC cell lines and subjected to transfection. According to the findings, ACSL4 overexpression may aggravate erastin-mediated cell death and increase the formation of lipid ROS. Conversely, the expression of ACSL4 did not affect the iron accumulation that was caused by erastin. As a fatty acid activating enzyme, the preferred substrates of ACSL4 are long-chain polyunsaturated fatty acids, including EPA and AA. ACSL4 is responsible for the catalysis of these fatty acids and the synthesis of the associated coenzyme A [10], both of which affect the process of lipid peroxidation.
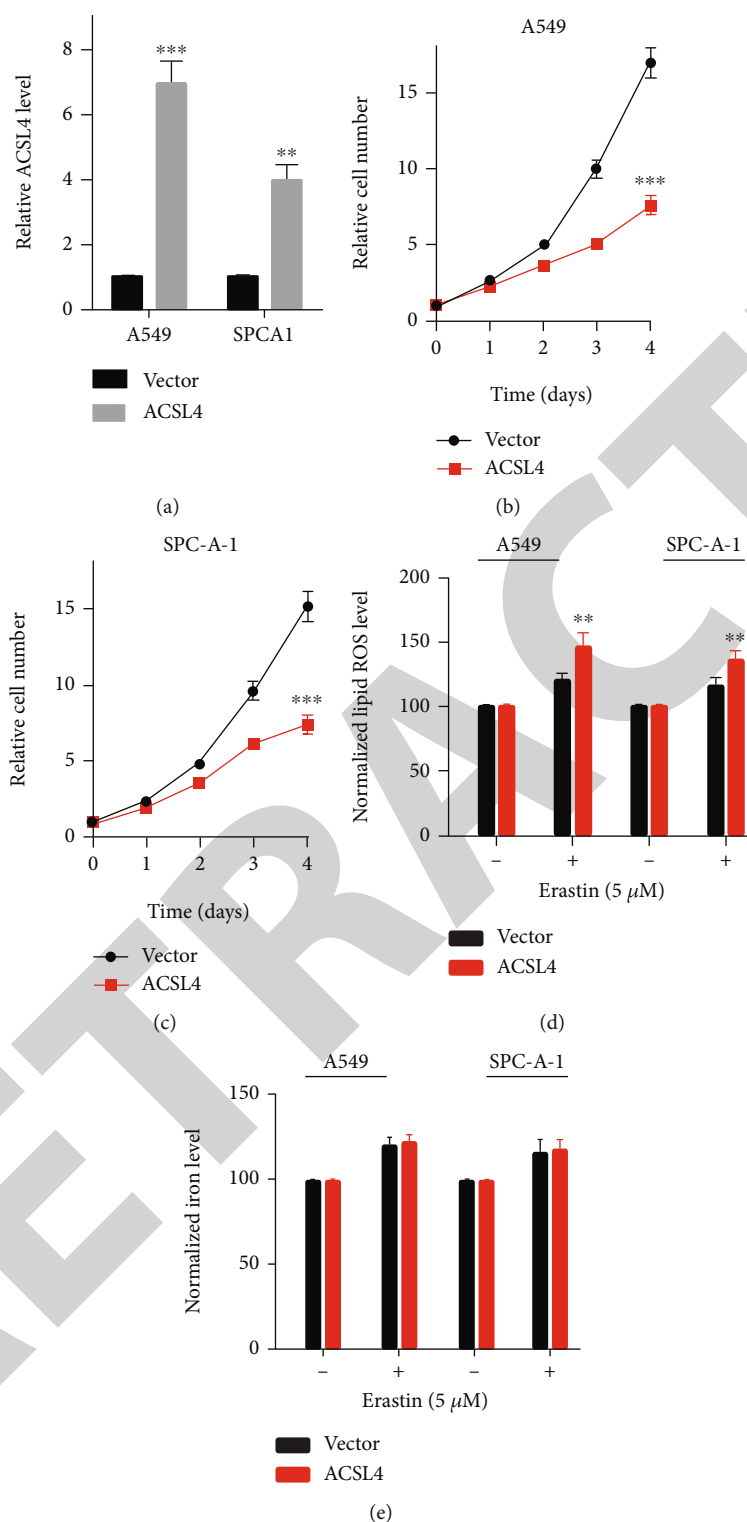
FIGURE 5: Upmodulation of ACSL4 enhances ferroptosis. (a) mRNA expression of ACSL4 after transfection in specified cells. (b, c) In A549 and SPC-A-1 cells, upregulation of ACSL4 enhanced erastin-induced cell death. ($n = 3$, $***p < 0.001$ vs. control cDNA group). (d, e) After 24-hour treatment with erastin, lipid ROS and iron in A549 and SPC-A-1 cells were measured ($n = 3$, $**p < 0.01$ vs. control cDNA subgroup).

Besides exploring the interaction that occurs between ferroptosis and other different kinds of cell death, it is also necessary to research the role and assess the molecular and pathway components that are connected to ferroptosis. Var-ious recently discovered proteins, including metallothio-nein-1G, NCOA4, and PEBP1, have been linked to ferroptosis via the processes of the metabolism of iron and the peroxidation of lipids [21–23]. GO and KEGG analyses

TABLE 1: Gene Ontology and pathway enrichment analysis of the ACSL4 coexpressed genes in TCGA-LUAD and LUSC.

Ontology	ID	Description	p value	p.adjust	Q value
BP	GO:0016567	Protein ubiquitination	1.52e-04	0.040	0.031
BP	GO:0032446	Protein modification by small protein conjugation	1.57e-04	0.040	0.031
BP	GO:0007265	Ras protein signal transduction	1.76e-04	0.040	0.031
CC	GO:0030139	Endocytic vesicle	1.10e-04	0.015	0.012
CC	GO:0044322	Endoplasmic reticulum quality control compartment	1.28e-04	0.025	0.015
CC	Go:0031461	Cullin-RING ubiquitin ligase complex	1.42e-04	0.025	0.015
MF	GO:0004842	Ubiquitin-protein transferase activity	2.30e-05	0.002	0.001
MF	GO:0005095	GTPase inhibitor activity	1.74e-04	0.025	0.015
MF	GO:0019003	GDP binding	2.63e-04	0.032	0.022
KEGG	03050	Ubiquitin-mediated proteolysis	1.13e-05	5.43e-04	2.38e-04
KEGG	04141	Protein processing in endoplasmic reticulum	8.53e-04	0.008	0.003
KEGG	04114	Oocyte meiosis	9.00e-04	0.008	0.003

found that the gene coexpressed with ACSL4 is enriched in the pathway of protein ubiquitination. BAP1 is responsible for encoding a nuclear deubiquitinating enzyme that helps minimize ubiquitination of histone 2A on chromatin. Recent research has shown that the protein BAP1 reduces H2Aub occupancy on the regulator of the ferroptosis inhibitor SLC7A11 and suppresses the expression of SLC7A11 in a deubiquitinating-dependent way and that increased lipid peroxidation and ferroptosis are the direct results of BAP1's suppression of SLC7A11 expression, which impairs cystine absorption [24]. Moreover, BAP1 partially prevents the progression of tumors via SLC7A11 as well as ferroptosis, and cancer-related BAP1 mutants end up losing their capacities to suppress SLC7A11 and to stimulate ferroptosis [25]. The findings of this research indicate that, in addition to SLC7A11 ubiquitination, ACSL4 ubiquitination might well be implicated in the ferroptosis process, which warrants further investigation.

Additional research on ferroptosis is considered necessary not only to shed light on the mechanistic explanation behind the process but also to open the door to the possibility of developing novel therapeutic approaches. Sorafenib resistance, for instance, has been demonstrated to be the outcome of the metallothionein-1G-mediated suppression of ferroptosis during therapy for metastatic hepatocellular carcinoma [21]. In a group of human cell lines derived from a variety of cancerous tissues, Lachaier et al. examined the levels of ferroptosis that were caused by sorafenib and compared them to the levels that were induced by the standard compound, erastin [26]. They discovered that sorafenib promoted ferroptosis in kidney carcinoma cell lines. In addition to this, they discovered that the ferroptotic potency of sorafenib was positively correlated with that of erastin. Sorafenib is the only medication that can achieve ferroptotic efficacy in comparison to other kinase inhibitors, which makes sorafenib the first anticancer treatment to be licensed for use in the clinical setting that can trigger ferroptosis [26]. Doll et al. additionally illustrated that pharmacologically targeting ACSL4 using the antidiabetic compound class, thiazolidinediones, and alleviates tissue death in mice ferroptotic

model, implying that inhibiting ACSL4 might be a useful therapeutic strategy for the prevention of illnesses linked to ferroptosis [13].

5. Conclusion

Our research illustrated that the expression level of ACSL4 is lowered in NSCLC, which was shown to have a correlation with the clinical and pathological characteristics of patients. By stimulating ferroptosis, ACSL4 can partially inhibit the growth of NSCLC cells. These findings suggest that ACSL4 might be considered a viable treatment target for NSCLC, providing a foundation for future research on clinical pathways that involve ACSL4.

Data Availability

The simulation experiment data used to support the findings of this study are available from the corresponding author upon request.

Conflicts of Interest

The authors declare that there are no conflicts of interest regarding the publication of this paper.

Acknowledgments

References

[1] F. R. Hirsch, G. V. Scagliotti, J. L. Mulshine et al., "Lung cancer: current therapies and new targeted treatments," *Lancet*, vol. 389, no. 10066, pp. 299–311, 2017.

[2] B. C. Bade and C. C. Dela, "Lung cancer 2020," *Clinics in Chest Medicine*, vol. 41, no. 1, pp. 1–24, 2020.

Retraction

Retracted: The Efficacy and Safety of Bisoprolol in the Treatment of Myocardial Infarction with Cardiac Insufficiency

Computational and Mathematical Methods in Medicine

This article has been retracted by Hindawi following an investigation undertaken by the publisher [1]. This investigation has uncovered evidence of one or more of the following indicators of systematic manipulation of the publication process:

(1) Discrepancies in scope

(2) Discrepancies in the description of the research reported

(3) Discrepancies between the availability of data and the research described

(4) Inappropriate citations

(5) Incoherent, meaningless and/or irrelevant content included in the article

(6) Peer-review manipulation

The presence of these indicators undermines our confidence in the integrity of the article's content and we cannot, therefore, vouch for its reliability. Please note that this notice is intended solely to alert readers that the content of this article is unreliable. We have not investigated whether authors were aware of or involved in the systematic manipulation of the publication process.

Wiley and Hindawi regrets that the usual quality checks did not identify these issues before publication and have since put additional measures in place to safeguard research integrity.

We wish to credit our own Research Integrity and Research Publishing teams and anonymous and named external researchers and research integrity experts for contributing to this investigation.

The corresponding author, as the representative of all authors, has been given the opportunity to register their agreement or disagreement to this retraction. We have kept a record of any response received.

References

[1] Y. Wang, "The Efficacy and Safety of Bisoprolol in the Treatment of Myocardial Infarction with Cardiac Insufficiency," *Computational and Mathematical Methods in Medicine*, vol. 2022, Article ID 3098726, 5 pages, 2022.

Research Article

The Efficacy and Safety of Bisoprolol in the Treatment of Myocardial Infarction with Cardiac Insufficiency

Yan Wang [ID]

Sixth Department of Cardiology, Cangzhou Central Hospital, Cangzhou, 061000 Hebei Province, China

Correspondence should be addressed to Yan Wang; wangyan@cz96120.org.cn

Background. Bisoprolol is commonly used to treat moderate or severe chronic stable heart failure, coronary heart disease, and hypertension. This study is aimed at analyzing the efficacy of bisoprolol in the treatment of myocardial infarction with cardiac insufficiency and its effect on cardiac function, Hcy, and CRP through meta-analysis. *Methods*. A total of 120 patients with myocardial infarction and cardiac insufficiency from February 2020 to February 2021 were selected and randomly divided into two groups (control and the observation, $n = 60$) according to the random number table method. The control group was given conventional treatment. The observation group was given bisoprolol on the basis of control group. The clinical efficacy, systolic blood pressure, diastolic blood pressure, heart rate, cardiac function indexes, homocysteine (Hcy), and C-reactive protein (CRP) levels were compared between the two groups before and after treatment through data analysis. Adverse reactions were observed during treatment. *Results*. Compared with the control group, the total effective rate of the observation group was significantly increased ($p < 0.05$). After treatment, the levels of heart rate, left ventricular end-diastolic volume (LVEDV), and left ventricular end-systolic volume (LVESV) and serum Hcy and CRP levels in the observation group were significantly lower than those in the control group ($p < 0.05$). Meanwhile, left ventricular ejection fraction (LVEF) level in the observation group after treatment was higher than that of the control group ($p < 0.05$). *Conclusion*. Bisoprolol combined with conventional treatment can reduce serum Hcy and CRP levels in patients with myocardial infarction and cardiac insufficiency and improve cardiac function. Moreover, there are no obvious adverse reactions during the treatment.

1. Introduction

Myocardial infarction refers to acute myocardial ischemia and necrosis. Most myocardial infarctions result from severe and persistent acute ischemia of the corresponding myocardium due to a dramatic reduction or interruption of coronary blood supply. [1]. At present, the incidence of acute myocardial infarction in China is on the rise, and the incidence in rural areas is higher than that in urban areas. The mortality rate of myocardial infarction is on the rise [2, 3]. Cardiac insufficiency is a symptom of a decrease in myocardial contractile function, which reduces the forward blood flow of the heart, resulting in blood stasis in the systemic or pulmonary circulation [4, 5]. Previous studies have shown

that after myocardial infarction, a large number of patients can induce or even aggravate cardiac insufficiency due to the greater impact of myocardial remodeling on cardiac contractility [6]. Myocardial infarction with cardiac insufficiency undoubtedly increases the difficulty of treatment and threatens the prognosis of patients.

Many studies have shown that patients with myocardial infarction and cardiac insufficiency cannot obtain reliable efficacy with conventional medical methods alone [7, 8]. Bisoprolol is a beta1-adrenoceptor blocker, which is commonly used in the treatment of moderate or severe chronic stable heart failure, coronary heart disease, and hypertension [9–11]. Bisoprolol is a widely used beta-blocker, whose primary mechanism is to block the connection between

adrenaline and beta1 receptors [12]. Bisoprolol is more selective for $\beta 1$ receptors than metoprolol and attilol. In addition, reliable efficacy has been achieved in the treatment of congestive heart failure [13, 14]. However, the effect of bisoprolol on myocardial infarction and cardiac insufficiency is unclear.

Therefore, this study tried bisoprolol and conventional treatment to treat patients with myocardial infarction and cardiac insufficiency. The efficacy of bisoprolol for myocardial infarction with cardiac insufficiency and its effects on cardiac function, Hcy, and CRP through meta-analysis were analyzed. This study will provide a reference for clinical treatment of patients with myocardial infarction and cardiac insufficiency.

2. Materials and Methods

2.1. Patients. This is a retrospective study. A total of 120 patients with myocardial infarction and cardiac insufficiency in Cangzhou Central Hospital from February 2020 to February 2021 were randomly divided into two groups according to the random number table method. This study was approved by the Ethics Committee of Cangzhou Central Hospital. The control group included 34 males and 26 females. The age of the patients ranged from 42 to 71 years, with an average of (57.25 ± 4.11) years. NYHA classification of cardiac function showed that the control group included 35 cases at grade II and 25 cases at grade III. The observation group included 36 males and 24 females. The ages of these patients ranged from 44 to 70 years old, with an average of (57.66 ± 4.23) years. NYHA classification of cardiac function showed that the observation group included 38 cases at grade II and 22 cases at grade III. There was no significant difference in general data between the two groups, and they were comparable.

2.2. Inclusion and Exclusion Criteria. Inclusion criteria: all patients signed informed consent. All patients received clinical symptoms, signs, and imaging diagnosis in Cangzhou Central Hospital. The diagnosis was made based on the diagnostic criteria in the "Guidelines for Primary Diagnosis and Treatment of ST-Segment Elevation Myocardial Infarction (2019)". Patients were divided into grades II to III according to the New York Heart Association (NYHA) cardiac function classification. Patients were 60 years of age and older.

Exclusion criteria: patients with other system and organ dysfunction; patients with a history of drug allergy in this study; patients with severe heart failure; and patients with missing clinical data.

2.3. Treatment. The control group was given conventional treatment. After admission, the patients were given basic oxygen inhalation treatment and ECG monitoring. At the same time, cardiac, analgesic, and vasodilator treatments were given according to the patient's condition. The patients were given oral aspirin (Hunan Zhongnan Pharmaceutical Co., Ltd., Chinese medicine H43021055), nitroprom (China Resources Shuanghe Pharmaceutical Co., Ltd., Chinese medicine H11020907), nitroglycerin (Beijing Yimin Pharmaceutical

Co., Ltd., Chinese medicine H11020289), and other drugs. Antiarrhythmic therapy was used in patients with cardiac arrhythmias. For patients with dyspnea, furosemide and diuresis were given. The observation group was given bisoprolol (Beijing Huasu Pharmaceutical Co., Ltd., H10970082) and conventional treatment. The initial dose of bisoprolol was 6.25 mg twice a day. The dosage of bisoprolol is adjusted according to the patient's heart rate and blood pressure. The frequency of drug dose adjustment was 3 to 5 days, and the dose was adjusted to 12.5 mg. Then, the drug dose was gradually increased ($25 \text{ mg/d} \leq \text{drug dose} \leq 50 \text{ mg/d}$). All patients were treated continuously for 6 months.

2.4. Efficacy Evaluation Criteria. Markedly effective: after treatment, the patient's cardiac function improved by more than 2 grades, and the clinical symptoms and signs disappeared.

Effective: after treatment, patient's cardiac function improved to grade 2 or above, and the clinical symptoms and signs improved.

Invalid: the patient's cardiac function, clinical symptoms, and signs did not improve or even worsened after treatment.

$$\text{Total effective} = \text{markedly effect} + \text{effective.} \qquad (1)$$

2.5. Observation Index. The levels of serum Hcy, CRP and clinical efficacy, systolic blood pressure, diastolic blood pressure, heart rate, and cardiac function indexes were compared between the two groups before and after treatment. Meanwhile, adverse reactions were monitored during treatment.

Left ventricular end-diastolic volume (LVEDV), left ventricular end-systolic volume (LVESV), and left ventricular ejection fraction (LVEF) were measured by Mindray DC-N3S color Doppler before and after treatment.

Fasting venous blood (5 ml) before and after treatment was put in a centrifuge and centrifuged at 2500 rpm for 10 min. The extracted serum was placed in the refrigerator for testing. CRP levels were measured using an enzyme-linked immunosorbent assay (ELISA). HCY levels were measured using an automatic immunoassay analyzer.

2.6. Statistical Analysis. All experiments were performed in triplicate. Data were analyzed using SPSS18.0 statistical software. Differences between groups were compared using χ^2 test and t test. Count data were expressed as %, and measurement data were expressed as mean $\pm$ SD. $p < 0.05$ represented statistical significance.

3. Results

3.1. Comparison of Clinical Efficacy between the Two Groups. The observation group found a total of 53 effective people. The data showed that the total effective rate of the observation group was 88.33%. Meanwhile, 44 effective people were found in the control group. The total effective rate in the control group was 73.33%. Compared with the control group, the total effective rate of the observation group was significantly increased ($p < 0.05$, Table 1).

3.2. Comparison of Heart Rate, Systolic Blood Pressure, and Diastolic Blood Pressure between the Two Groups before

Table 1: Comparison of clinical efficacy between the two groups [case (%)].

Group	Case	Markedly effective	Effective	Invalid	Total effective rate
Control	60	23 (38.33)	21 (35.00)	16 (26.67)	44 (73.33)
Observation	60	29 (48.33)	24 (40.00)	7 (11.67)	53 (88.33)
χ^2					4.357
p					0.037*

*$p < 0.05$.

Table 2: Comparison of heart rate, systolic blood pressure, and diastolic blood pressure between the two groups before and after treatment.

Group	Heart rate (times/min)		Systolic blood pressure (mmHg)		Diastolic blood pressure (mmHg)	
	Before	After	Before	After	Before	After
Control	115.22 ± 3.6	98.33 ± 2.2	119.36 ± 21.2	118.60 ± 22.2	74.25 ± 15.4	74.11 ± 14.5
Observation	116.15 ± 4.1	75.65 ± 1.2	120.15 ± 22.1	119.31 ± 23.1	75.10 ± 14.2	72.60 ± 12.7
t	1.312	69.326	0.200	0.172	0.412	0.605
p	0.192	$p \leq 0.001^{**}$	0.842	0.864	0.682	0.546

**$p < 0.01$.

Table 3: Comparison of cardiac function indexes between the two groups before and after treatment.

Group	LVESV (ml)		LVEDV (ml)		LVEF (%)	
	Before	After	Before	After	Before	After
Control	54.21 ± 12.5	50.98 ± 12.7	94.25 ± 16.5	92.68 ± 14.1	38.65 ± 2.55	48.65 ± 5.11
Observation	55.10 ± 11.6	44.83 ± 10.5	94.10 ± 15.8	86.11 ± 5.2	39.11 ± 2.76	54.10 ± 5.41
t	0.403	2.884	0.051	3.380	0.948	7.269
p	0.688	0.005^{**}	0.960	0.001^{**}	0.345	$p \leq 0.001^{**}$

**$p < 0.01$.

Table 4: Comparison of serum Hcy and CRP levels before and after treatment in the two groups.

Group	Hcy (μmol/l)		CRP (mg/l)	
	Before	After	Before	After
Control	19.25 ± 4.02	16.40 ± 2.81	21.45 ± 3.15	12.64 ± 2.47
Observation	19.31 ± 4.11	12.34 ± 3.20	22.50 ± 2.79	8.75 ± 1.24
t	0.081	7.385	1.933	10.902
p	0.936	$p \leq 0.001^{**}$	0.056	$p \leq 0.001^{**}$

**$p < 0.01$.

and after Treatment. After treatment, the heart rate in both groups was significantly decreased. Compared with the control group, the heart rate of the observation group was significantly decreased ($p < 0.01$, Table 2). After treatment, there were no changes in systolic and diastolic blood pressure in the two groups ($p > 0.05$, Table 2). There were no significant changes in systolic and diastolic blood pressure between the two groups ($p > 0.05$, Table 2).

3.3. Comparison of Cardiac Function Indexes between the Two Groups before and after Treatment. After treatment, the levels of LVESV and LVEDV in the two groups were decreased, and the level of LVEF was increased. In addition, compared with the control group, the levels of LVESV and LVEDV in the observation group were significantly decreased, and the level of LVEF was significantly increased ($p < 0.01$, Table 3).

3.4. Comparison of Serum Hcy and CRP Levels between the Two Groups before and after Treatment. After treatment, serum Hcy and CRP levels in both groups were decreased. In addition, the serum Hcy and CRP levels in the

observation group were lower than those in the control group ($p < 0.01$, Table 4). Moreover, there were no obvious adverse reactions during treatment in both groups.

4. Discussion

After myocardial infarction, the myocardium is prone to systolic and diastolic dysfunction, which induces and aggravates the occurrence and development of cardiac insufficiency, and even induces heart failure in severe cases [8, 15]. In the current clinical work, the treatment of myocardial infarction complicated with cardiac insufficiency mainly focuses on cardiotonic, diuretic, and coronary artery expansion [16, 17]. However, these medical treatments are more common. Moreover, long-term use of angiotensin-converting enzyme inhibitors in patients is very likely to induce the phenomenon of "aldosterone escape," causing unnecessary damage to the heart [18–20]. The application of β-blockers can increase the density of β-receptors and have a strong antagonistic effect on catecholamines, thereby reducing cardiotoxicity and enhancing myocardial response [21].

Bisoprolol, as a specific $\beta 1$ adrenergic receptor blocker, is commonly used in clinical practice and has the advantages of low first-pass effect and long half-life [22]. And bisoprolol is also highly absorbed orally and more easily crosses the blood-brain barrier. Bisoprolol not only has a strong blocking effect on part of $\beta 1$ but also significantly reduces the possible adverse reactions to the central nervous system [23]. In addition, it was found that the application of bisoprolol can not only effectively reduce the heart rate but also have a strong inhibitory effect on the release of renin [24]. Bisoprolol can improve the hypoxic state of myocardium and also has a strong recovery effect on myocardial systolic and diastolic function. Therefore, bisoprolol can effectively reduce the scope of myocardial infarction and ultimately achieve the purpose of eliminating and relieving clinical symptoms and signs [25]. It has also been reported that early treatment with bisoprolol can reduce the incidence of arrhythmias to a certain extent [26]. The results showed that bisoprolol and conventional treatment improved cardiac function and reduced heart rate in patients. It indicates that the application of bisoprolol can not only produce a strong vasoconstriction effect but also help to reduce the excitability of sympathetic nerves. Bisoprolol prolongs ventricular diastolic filling time to a certain extent and reduces cardiac load [27]. Ultimately, bisoprolol improves myocardial compliance, increases coronary blood perfusion, and effectively improves clinical symptoms and signs in patients with myocardial infarction and cardiac insufficiency.

At the same time, serum Hcy and CRP levels were also observed in this study. Serum Hcy is considered a commonly used specific indicator for assessing cardiovascular disease outcomes [28]. CRP is a more sensitive indicator of human inflammatory response [29]. The results of this study show that bisoprolol can effectively regulate serum Hcy and CRP levels, further confirming the superiority of bisoprolol in the treatment of myocardial infarction with cardiac insufficiency. In addition, since bisoprolol is metabolized in the

human body through the dual channels of liver and kidney [30], it does not cause serious adverse reactions. However, it should be noted that bisoprolol may cause mild to moderate renal and hepatic insufficiency [31]. In this study, no obvious adverse reactions were found in patients with myocardial infarction and cardiac insufficiency after treatment, indicating that the safety of bisoprolol is still high. In the following research, the sample size and observation indicators will be further increased to better evaluate the application advantages of bisoprolol.

5. Conclusion

Data analysis showed that bisoprolol combined with conventional treatment can effectively improve the heart rate and cardiac function in patients with myocardial infarction and cardiac insufficiency. At the same time, bisoprolol can regulate serum Hcy and CRP levels and do not have adverse reactions. Therefore, bisoprolol is a safe and effective drug for patients with myocardial infarction and cardiac insufficiency.

Data Availability

The datasets used and/or analyzed during the present study are available from the corresponding author on reasonable request.

Conflicts of Interest

The author declares no potential conflicts of interest with the respect to the research, authorship, and publication of this article.

References

[1] H. Hara, K. Takahashi, N. Kogame et al., "Impact of bleeding and myocardial infarction on mortality in all-comer patients undergoing percutaneous coronary intervention," *Circulation. Cardiovascular Interventions*, vol. 13, no. 9, article e009177, 2020.

[2] H. J. Kim, T. Kang, M. J. Kang, H. S. Ahn, and S. Y. Sohn, "Incidence and mortality of myocardial infarction and stroke in patients with hyperthyroidism: a nationwide cohort study in Korea," *Thyroid*, vol. 30, no. 7, pp. 955–965, 2020.

[3] H. S. Kim, D. R. Kang, I. Kim, K. Lee, H. Jo, and S. B. Koh, "Comparison between urban and rural mortality in patients with acute myocardial infarction: a nationwide longitudinal cohort study in South Korea," *BMJ Open*, vol. 10, no. 4, article e035501, 2020.

[4] D. Y. Lee, K. Han, S. Park et al., "Glucose variability and the risks of stroke, myocardial infarction, and all-cause mortality in individuals with diabetes: retrospective cohort study," *Cardiovascular Diabetology*, vol. 19, no. 1, p. 144, 2020.

[5] A. Mikaeilvand, A. Firuozi, H. Basiri et al., "Association of coronary artery dominance and mortality rate and complications in patients with ST-segment elevation myocardial infarction treated with primary percutaneous coronary intervention," *Journal of Research in Medical Sciences*, vol. 25, no. 1, p. 107, 2020.

Retraction

Retracted: Myopia in Chinese Adolescents: Its Influencing Factors and Correlation with Physical Activities

Computational and Mathematical Methods in Medicine

This article has been retracted by Hindawi following an investigation undertaken by the publisher [1]. This investigation has uncovered evidence of one or more of the following indicators of systematic manipulation of the publication process:

(1) Discrepancies in scope

(2) Discrepancies in the description of the research reported

(3) Discrepancies between the availability of data and the research described

(4) Inappropriate citations

(5) Incoherent, meaningless and/or irrelevant content included in the article

(6) Peer-review manipulation

The presence of these indicators undermines our confidence in the integrity of the article's content and we cannot, therefore, vouch for its reliability. Please note that this notice is intended solely to alert readers that the content of this article is unreliable. We have not investigated whether authors were aware of or involved in the systematic manipulation of the publication process.

Wiley and Hindawi regrets that the usual quality checks did not identify these issues before publication and have since put additional measures in place to safeguard research integrity.

We wish to credit our own Research Integrity and Research Publishing teams and anonymous and named external researchers and research integrity experts for contributing to this investigation.

The corresponding author, as the representative of all authors, has been given the opportunity to register their agreement or disagreement to this retraction. We have kept a record of any response received.

References

[1] Y. Yin, C. Qiu, and Y. Qi, "Myopia in Chinese Adolescents: Its Influencing Factors and Correlation with Physical Activities," *Computational and Mathematical Methods in Medicine*, vol. 2022, Article ID 4700325, 10 pages, 2022.

Research Article

Myopia in Chinese Adolescents: Its Influencing Factors and Correlation with Physical Activities

Yao Yin [iD],[1] Cheng Qiu [iD],[2] and Yufei Qi [iD][3]

[1]*Beijing College of Finance and Commerce, No. 15, Shuuizi East Rd., Chaoyang District, Beijing, China*
[2]*People's Public Security University of China, Huangyi Rd., Daxing District, Beijing, China*
[3]*Central South University, 932 Lushan South Rd., Changsha, China*

Correspondence should be addressed to Cheng Qiu; 20052483@ppsuc.edu.cn and Yufei Qi; yufeiqi@csu.edu.cn

Purpose. The study is conducted to analyze the risk factors and the protective factors of myopia in Chinese adolescents and its correlation with physical activities and then to provide 2 formulas to predict the probability of becoming myopic and the probability of preventing myopia. *Methods*. This is a cross-sectional study in which a questionnaire survey was conducted among 650 students aged 14-17 from 5 schools in Beijing in 2021. The students were divided into two groups: nonmyopia group and myopia group. Statistically significant variables were selected after the univariate analysis for a binary logistic regression analysis. *Results*. In the univariate analysis, 18 risk factors of myopia were found and 14 physical-activity-related protective factors were found. In the multivariate analysis, 5 independent factors were found to be positively related to myopia and could be used for calculating the probability of becoming myopic. The 5 factors are gender, staying up late playing smartphones, parental myopia, daily time spent on digital devices, and regular eye examinations. Five physical-activity-related factors were found to be positively related to the prevention of myopia and can be used for the calculation of the probability of preventing myopia. The 5 factors are regular physical activities, attitude towards physical education, daily time spent on in-school physical activities, daily time spent on after-school physical activities, and eye exercises. *Conclusions*. The influencing factors of myopia in adolescents mainly include heredity, habits of using eyes, and environment. Physical activities can effectively reduce the probability of becoming myopic in adolescents and promote eye health. Therefore, taking part in physical activities is an effective way to reduce the prevalence of myopia in adolescents.

1. Introduction

Eye health was defined by the Lancet Global Health Commission as maximized vision, ocular health, and functional ability, thereby contributing to overall health and well-being, social inclusion, and quality of life [1]. The International Agency for the Prevention of Blindness (IAPB) stressed in *2030 IN SIGHT* that the eye health of children and adolescents was the focus of future work and should be integrated into school health policy resulting in schools the world over routinely offering sight tests and eye health promotion and prevention information should be taught within education settings [2].

The incidence of myopia in China has increased significantly in recent years. Some pointed out that 20% to 50% of the students in primary school, 35% to 60% of the students in middle school, and 50% to 75% of the students in college are myopic in China in 2018 [3]. As of October 2021, 52.7% of the children and adolescents in China were myopic, and the rate was 2.5% higher than that in 2019 [4]. Schools, where children and adolescents carry out daily activities, are the main places for the improvement of their physical and mental health. The Ministry of Education attaches great importance to the prevention and control of myopia in young students and has formulated a specific work plan for it in 2018. Multiple measures and much effort have been taken to curb the prevalence of myopia.

Previous studies show that gender, age, region of habitation, family history of myopia, daily reading time, breaks while studying, daily time spent on digital devices, and

learning piano are independent risk factors of myopia in primary school students in China [5]. The pathogenesis of myopia remains unclear so far, which may be related to genetic, environmental, and other factors. Some argued that the influence of environmental factors, such as bad habits of using eyes and visual fatigue, was greater than that of genetic factors [6, 7]. In summary, the eye health of children and adolescents is closely related to the environment, heredity, and intense use of the eyes.

It is regarded as an important part of student management, education, and teaching in China's School Management Standards for Compulsory Education that schools should help students to develop strong constitutions and reduce the prevalence of myopia among students. *Mingmu Gong*, a kind of Chinese eyesight improvement exercise, is said to have a significant effect on the recovery of students' eyesight, which helps to relax the eye muscles and accelerate the eye blood flow and further promote the recovery of eye vision [8]. Smartphone users are more likely to be myopic, showing a moderate positive correlation between playing smartphones and myopia. Outdoor activities reduce the probability of myopia, showing a strongly negative correlation between outdoor activities and myopia [9]. Compared with nonmyopic children, myopic children spend more time watching screens and shorter time on outdoor activities [10]. Outdoor activities help to prevent adolescents from being sedentary and improve their eyesight. Physical education should be integrated with the health service system to promote eye health education.

Based on an in-depth literature review, this study analyzed the influencing factors of myopia in adolescents and predicted the probability of becoming myopic through the analysis of the risk factors of myopia. Physical activities were important factors affecting eye health, and in this study, they were analyzed and used to predict the probability of preventing myopia.

2. Research Objects and Methods

2.1. Participants. A total of 650 questionnaires were distributed to 650 middle school students in Beijing using stratified sampling, and 610 of them were collected. After excluding 31 invalid questionnaires, there were 579 (89%) valid questionnaires left.

2.2. Research Variables. Based on previous studies, this study summarized the influencing factors of myopia in adolescents and the physical-activity-related factors, according to which the questionnaire was designed. 17 binary variables were investigated, such as gender, only child, playing video games, parental myopia, reading posture, writing posture, staying up late playing smartphones, and regular physical exercises. 21 continuous variables were investigated, such as diopter, daily time spent on digital devices, daily sleep duration, distance to the TV screen, illumination while studying, drinking milk, bedtime, get-up time, afternoon nap duration, breaks while studying, reading extracurricular books, daily time spent in reading in extremely weak or strong light, picky about food, eating whole grains and vegetables, frequency of visual acuity tests, regular eye examinations, attitude towards physical education, daily time spent on in-school physical activities, after-school physical activities, and eye exercises.

2.3. Statistical Methods. The data were statistically analyzed by SPSS 26.0. The continuous variables were first tested for normality, and those that do not conform to the normal distribution were analyzed by nonparametric tests. Binary logistic regression was performed for the multivariate analysis, and GraphPad 9.0 was used to draw figures. All participants agreed to participate in the study.

2.4. Ethical Approval. This research was approved by the independent ethics committee of the Institute of Clinical Pharmacology, Central South University (registered number: ctxy-140003). All methods were carried out in accordance with relevant guidelines and regulations. This study was carried out in compliance with the ARRIVE guidelines. Informed consent was obtained from caregivers, and all information was kept strictly confidential.

3. Results and Analysis

3.1. Univariate Analysis. The chi-square test and the nonparametric two-sample test were performed for the univariate analysis of 24 independent variables. The results are as follows (see Table 1).

The results in Table 1 show factors such as gender, playing video games, parental myopia, reading posture, writing posture, staying up late playing smartphones, diopter, daily time spent on digital devices, daily sleep duration, distance to the TV screen, illumination while studying, daily time spent on homework, breaks while studying, reading extracurricular books, daily time spent in reading in extremely weak or strong light, eating whole grains and vegetables, visual acuity tests, and regular eye examinations were found significant ($P < 0.05$). These factors were kept for the multivariate analysis. Factors such as only child, daily sleep duration, drinking milk, get-up time, afternoon nap duration, and picky about food were found not significant, which means they are not the influencing factors of myopia in adolescents. The details are shown in Figure 1.

3.2. Univariate Analysis of Physical-Activity-Related Factors. The chi-square test and the nonparametric two-sample test were performed for the univariate analysis of 13 independent variables. The results are as follows (see Table 2).

The results in Table 2 show that the myopia rate of adolescents who often took part in physical activities is significantly lower than those who occasionally took physical exercise ($P < 0.05$). The myopia rate of adolescents who often participated in football, basketball, table tennis, track and field, swimming, tennis, badminton, volleyball, dance, and other sports is low ($P < 0.05$). Continuous variables such as attitude towards physical education, daily time spent on in-school physical activities, after-school physical activities, and eye exercises were found significant, and they were kept for the multivariate analysis. The details are shown in Figure 2.

TABLE 1: Analysis of influencing factors of myopia.

| Parameter | | Groups | | Myopia rate | X^2/Z | P |
		Nonmyopia group	Myopia group			
Gender	Male	115	190	62.3%	5.543	0.019
	Female	78	196	71.5%		
Only child	No	94	191	67.0%	0.031	0.860
	Yes	99	195	66.3%		
Playing video games	Occasionally	67	97	59.1%	5.823	0.016
	Often	126	289	69.6%		
Parental myopia	No	76	107	58.5%	8.090	0.004
	Yes	117	279	70.5%		
Reading posture	Poor	123	288	70.1%	7.396	0.007
	Good	70	98	58.3%		
Writing posture	Poor	116	272	70.1%	6.250	0.012
	Good	77	114	59.7%		
Staying up late playing smartphones	Occasionally	116	194	62.6%	5.013	0.025
	Often	77	192	71.4%		
Diopter #		2 (1~4)	3 (2~4)		-4.579	<0.001
<2.0		75	40	10.40%		
2.0-4.0		27	105	27.20%		
4.0-6.0		35	105	27.20%		
6.0-8.0		38	94	24.40%		
>8.0		18	42	10.90%		
Daily time spent on digital devices #		2 (1~3.5)	3 (2~4)		-4.369	<0.001
<1 h		73	39	10.10%		
1-2 h		29	113	29.30%		
3-4 h		43	123	31.90%		
>4 h		48	111	28.80%		
Daily sleep duration #		2 (2~3)	2 (2~2.25)		-1.366	0.172
<6 h		29	75	19.40%		
6-8 h		109	215	55.70%		
>8 h		55	96	24.90%		
Distance to TV screen #		3 (2~4)	3 (2~4)		-2.238	0.025
<1 m		28	89	23.10%		
2-3 m		35	72	18.70%		
3-4 m		48	84	21.80%		
4-5 m		40	73	18.90%		
>5 m		42	68	17.60%		
Illumination while studying #		4 (2~5)	3 (2~4)		-2.97	0.003
Reading lamp (white light)		29	92	23.80%		
Reading lamp (yellow light)		36	64	16.60%		
Pendant lamp (white light)		29	83	21.50%		
Pendant lamp (white light)		45	73	18.90%		
Natural light (sunlight)		54	74	19.20%		
Drinking milk #		3 (2~4)	3 (2~4)		-1.188	0.235
Never		5	13	3.40%		
Occasionally		61	118	30.60%		
Often		57	148	38.30%		
Every day		70	107	27.70%		
Bedtime #		2 (1~3)	1 (1~2)		-2.857	0.004
After 24:00		91	222	57.50%		
23:00-24:00		50	105	27.20%		
22:00-23:00		36	33	8.50%		

Parameter	Groups		Myopia rate	X^2/Z	P
	Nonmyopia group	Myopia group			
21:00-22:00	16	26	6.70%		
Get-up time #	2 (1~3)	2 (1~3)		-0.783	0.434
Before 5:00	57	116	30.10%		
5:00-6:00	51	115	29.80%		
6:00-7:00	67	129	33.40%		
After 7:00	18	26	6.70%		
Afternoon nap duration #	2 (1~2)	2 (1~3)		-0.693	0.488
No	84	178	46.10%		
<20 minutes	72	101	26.20%		
20-40 minutes	29	72	18.70%		
>40 minutes	6	28	7.30%		
Daily time spent on homework #	2 (2~3)	3 (2~3)		-4.201	<0.001
<40 minutes	43	39	10.10%		
40-80 minutes	74	135	35.00%		
>80 minutes	76	212	54.90%		
Breaks while studying #	2 (1~2)	2 (2~3)		-3.451	0.001
Often	60	76	19.70%		
Rarely	89	180	46.60%		
Never	44	130	33.70%		
Reading extracurricular books #	2 (1~2)	2 (1.75~3)		-3.547	<0.001
Dislike	67	96	24.90%		
Like	93	173	44.80%		
Very like	33	117	30.30%		
Daily time spent in reading in extremely weak or strong light #	2 (1~3)	2 (2~3)		-2.528	0.011
<20 minutes	49	66	17.10%		
20-40 minutes	81	161	41.70%		
40-80 minutes	63	159	41.20%		
Picky about food #	4 (3~5)	4 (3~5)		-0.585	0.559
Extremely	4	10	2.60%		
Quite	10	24	6.20%		
Moderate	45	84	21.80%		
Slightly	49	111	28.80%		
Not	85	157	40.70%		
Eating whole grains and vegetables #	2 (2~3)	3 (2~3)		-4.243	<0.001
Never	84	230	59.60%		
Rarely	68	120	31.10%		
Often	41	36	9.30%		
Visual acuity tests #	1 (1~2)	1 (1~2)		-2.011	0.044
Rarely	121	212	54.90%		
Once every 6 months	45	95	24.60%		
Once every 3 months	27	79	20.50%		
Regular eye examinations #	2 (1~2)	2 (1~2)		-2.800	0.005
Never	91	132	34.20%		
Rarely	80	199	51.60%		
Annually	22	55	14.20%		

*Factors ending with # are not normally distributed according to the results of the SW normality test.

3.3. Multivariate Analysis of Influencing Factors of Myopia. 18 significant factors were kept for the multivariate analysis using binary logistic regression, and the factors are gender, playing video games, staying up late playing smartphones, parental myopia, reading posture, writing posture, diopter, daily time spent on digital devices, distance to the TV screen,
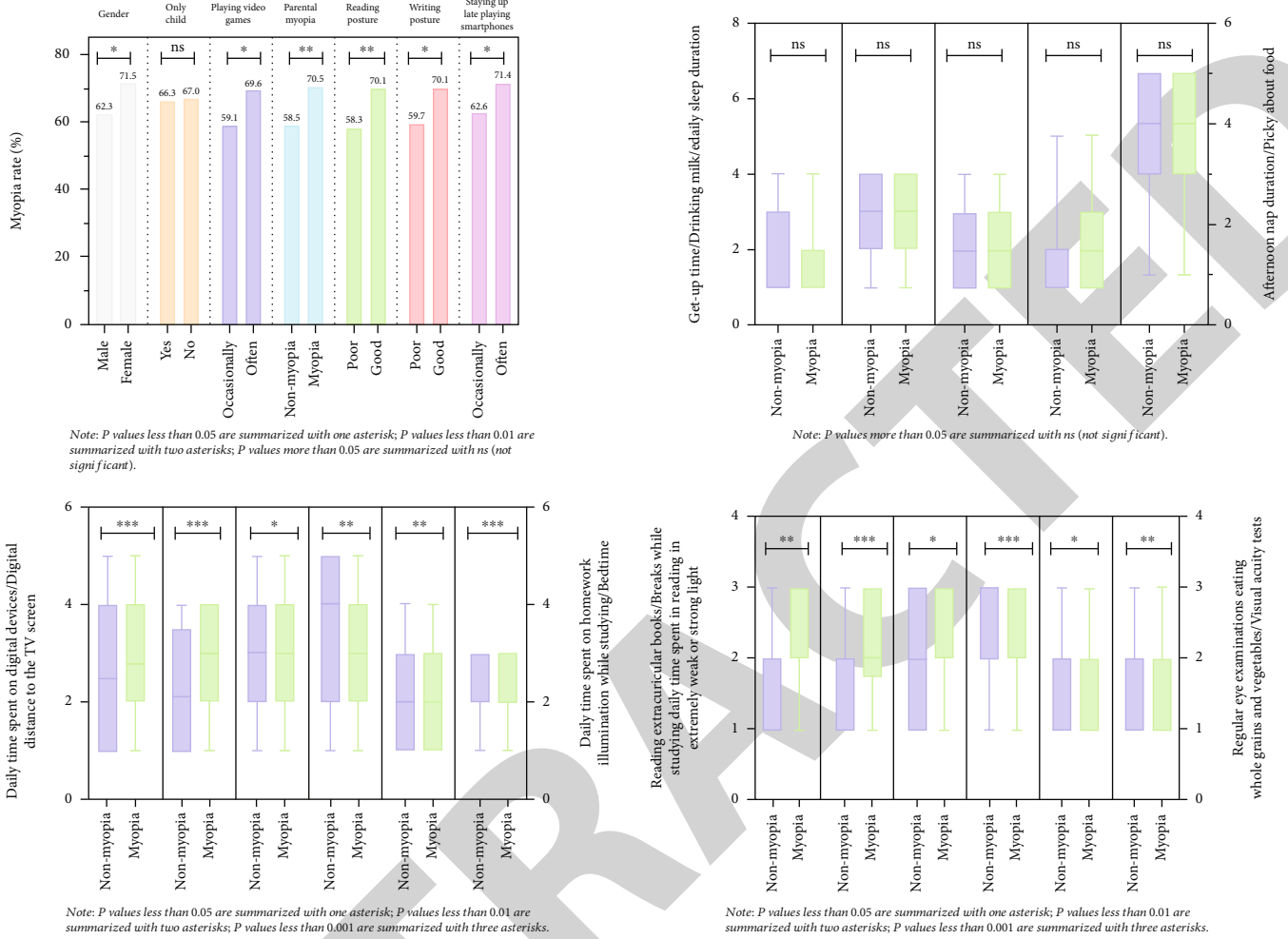
Figure 1: Univariate analysis of the influencing factors of myopia.

illumination while studying, bedtime, daily time spent on homework, breaks while studying, reading extracurricular books, daily time spent in reading in extremely weak or strong light, visual acuity tests, regular eye examinations, and eat whole grains and vegetables. The results are as follows in Table 3.

From the above analysis, it can be clearly concluded that gender is an independent factor affecting the incidence of myopia ($P < 0.05$), and the incidence of myopia in females is 1.679 times higher than that in males. Staying up late playing smartphones is an independent factor of myopia ($P < 0.01$), and the incidence of myopia in those spending a long time playing smartphones is 1.964 times higher than in those spending a short time staying up late playing smartphones. Parental myopia is an independent factor affecting the incidence of myopia ($P < 0.01$), and the incidence of myopia in those who have myopic parents is 1.880 times higher than in those who do not. Daily time spent on digital devices is an independent factor of myopia ($P < 0.01$), and the incidence of myopia in those spending a long time on digital devices is 1.721 times higher than that in those spending a short time on digital devices. Regular eye examinations is an independent factor affecting the incidence of myopia ($P < 0.01$), and the incidence of myopia in those who never (or rarely) have their

eyes examined is 1.614 times higher than that in those who have regular eye examinations annually. The rest factors are not independent influencing factors of myopia ($P > 0.05$). From the above analysis, the forest plot of the five independent influencing factors of myopia was given.

Based on the above five factors in Figure 3 that significantly affect the incidence of myopia, a formula for predicting the probability of becoming myopic is given.

$Z = -3.953 + 0.518 * 1$ (if gender = female) $+ 0 * 1$ (if gender = male) $+ 0.675 * 1$ (if staying up late playing smartphones = true) $+ 0 * 1$ (if staying up late playing smartphones = false) $+ 0.631 * 1$ (if parental myopia = true) $+ 0 * 1$ (if parental myopia = false) $+ 0.543 * 3$ (daily time spent on digital devices > 4 h) $+ 0.478 * 2$ (regular eye examinations = false).

$$P_{\text{myopia}} = \frac{1}{1 + e^{-Z}}. \qquad (1)$$

The following is an example that shows how to predict the probability of becoming myopic of a female student who often stays up late playing smartphones, has myopic parents, spends more than 4 hours on digital devices every

Table 2: Analysis of the correlation between physical activity and myopia.

Parameter		Groups		Myopia rate	X^2/Z	P
		Nonmyopia group	Myopia group			
Regular physical activities	No	109	272	71.40%	11.190	0.001
	Yes	84	114	57.60%		
Football	Rarely	135	299	68.90%	3.869	0.049
	Occasionally	58	87	60.00%		
Basketball	Rarely	79	194	71.10%	4.491	0.034
	Occasionally	114	192	62.70%		
Ping pang	Rarely	112	283	71.60%	13.866	<0.001
	Occasionally	81	103	56.00%		
Track and field	Rarely	75	186	71.30%	4.520	0.033
	Occasionally	118	200	62.90%		
Swimming	Rarely	112	271	70.80%	8.519	0.004
	Occasionally	81	115	58.70%		
Tennis	Rarely	127	285	69.17%	4.044	0.044
	Occasionally	66	101	60.48%		
Badminton	Rarely	82	206	71.50%	6.093	0.014
	Occasionally	111	180	61.90%		
Volleyball	Rarely	68	180	72.58%	6.828	0.009
	Occasionally	125	206	62.24%		
Dance	Rarely	54	143	72.60%	4.713	0.030
	Occasionally	139	243	63.60%		
Attitude to physical education #		4 (3~4)	3 (3~4)		-3.284	0.001
Negative		96	134	34.70%		
Indifferent		27	64	16.60%		
Positive		58	157	40.70%		
Very positive		12	31	8.00%		
Daily time spent on in-school physical activities #		2 (1~3.5)	3 (2~4)		-5.074	<0.001
<20 minutes		48	111	28.80%		
20-40 minutes		29	113	29.30%		
40-60 minutes		43	123	31.90%		
>60 minutes		73	39	10.10%		
After-school physical activities #		3 (2~4)	3 (2~4)		-2.209	0.027
Rarely		72	116	30.10%		
Occasionally		46	92	23.80%		
Sometimes		61	127	32.90%		
Often		14	51	13.20%		
Eye exercises #		2 (1~3)	1 (1~2)		-3.453	0.001
Never		84	217	56.20%		
Rarely		51	107	27.70%		
Occasionally		42	36	9.30%		
Often		16	26	6.70%		

*Factors ending with # are not normally distributed according to the results of the SW normality test.

day, and rarely has her eyes examined.

$$Z = -3.953 + 0.518 * 1 + 0.675 * 1 + 0.631 * 1$$
$$+ 0.543 * 4 + 0.478 * 2 = 0.999,$$

$$P_{\text{myopia}} = \frac{1}{1 + e^{-Z}} = \frac{1}{1 + e^{0.999}} = 73\%. \tag{2}$$

The probability of becoming myopic of the student is 73% (>50%), which means the student will be myopic.

Note: P values less than 0.05 are summarized with one asterisk; P values less than 0.01 are summarized with two asterisks; P values less than 0.001 are summarized with three asterisks.

Note: P values less than 0.05 are summarized with one asterisk; P values less than 0.01 are summarized with two asterisks; P values less than 0.001 are summarized with three asterisks.
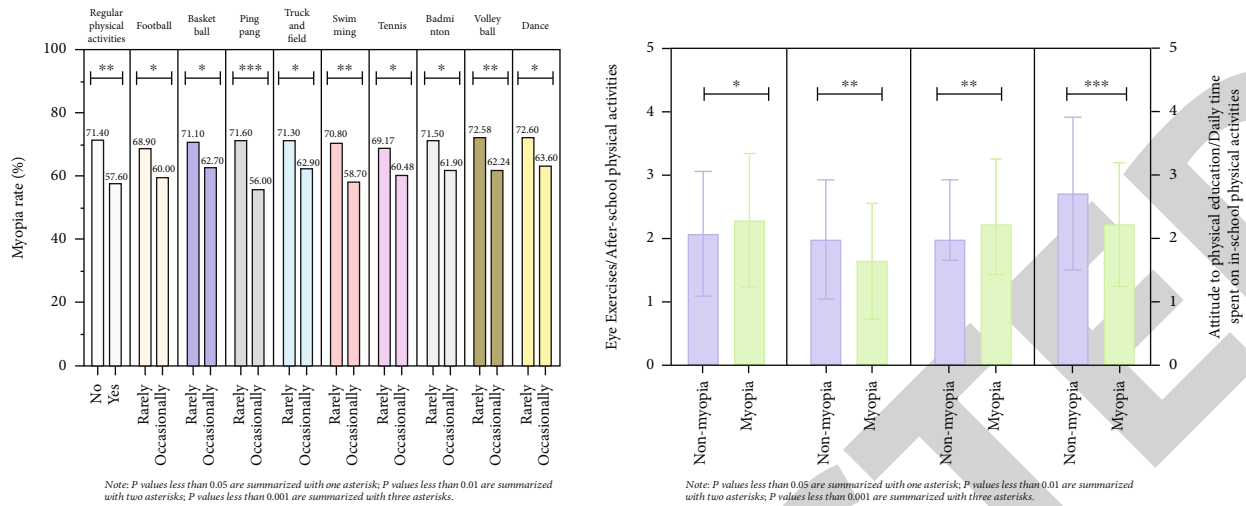
Figure 2: Analysis of the correlation between physical activities and myopia.

Table 3: Binary logistic analysis of influencing factors of myopia.

Parameter	B	S.E.	Wald	DF	P	OR	OR 95% CI Minimum	Maximum
Gender	0.518	0.206	6.302	1	0.012	1.679	1.120	2.516
Playing video games	0.006	0.761	0.000	1	0.993	1.006	0.226	4.474
Staying up late playing smartphones	0.675	0.232	8.488	1	0.004	1.964	1.247	3.093
Parental myopia	0.631	0.216	8.507	1	0.004	1.880	1.230	2.872
Reading posture	-0.590	0.763	0.598	1	0.439	0.555	0.124	2.472
Writing posture	-0.365	0.21	3.034	1	0.082	0.694	0.460	1.047
Diopter	0.136	0.166	0.676	1	0.411	1.146	0.828	1.587
Daily time spent on digital devices	0.543	0.203	7.164	1	0.007	1.721	1.156	2.561
Distance to TV screen	-0.072	0.075	0.905	1	0.341	0.931	0.803	1.079
Illumination while studying	-0.116	0.080	2.100	1	0.147	0.890	0.760	1.042
Bedtime	-0.167	0.115	2.095	1	0.148	0.847	0.676	1.061
Daily time spent on homework	0.130	0.307	0.179	1	0.673	1.139	0.623	2.080
Breaks while studying	0.066	0.212	0.098	1	0.754	1.069	0.706	1.618
Reading extracurricular books	0.081	0.208	0.153	1	0.696	1.085	0.721	1.631
Daily time spent in reading in extremely weak or strong light	0.221	0.147	2.273	1	0.132	1.247	0.936	1.663
Visual acuity tests	0.168	0.134	1.581	1	0.209	1.183	0.910	1.537
Regular eye examinations	0.478	0.153	9.723	1	0.002	1.614	1.194	2.180
Eating whole grains and vegetables	-0.390	0.310	1.581	1	0.209	0.677	0.369	1.243
Constants	-2.393	1.534	2.433	1	0.119	0.091		

3.4. Multivariate Analysis of the Correlation between Physical Activities and Myopia.

In the univariate analysis, 5 significant factors were kept for multivariate analysis using binary logistic regression, and the factors are regular physical activities, daily time spent on in-school physical activities, after-school physical activities, eye exercises, and attitude towards physical education. The results are as follows in Table 4.

From the above analysis, it can be clearly concluded that regular physical activities is an independent factor reducing the incidence of myopia ($P < 0.01$), and the incidence of myopia in those who had regular physical activities was 0.523 times

lower. Daily time spent on in-school physical activities ($P < 0.001$), after-school physical activities ($P < 0.05$), eye exercises ($P < 0.01$), and attitude towards physical education ($P < 0.01$) were all independent factors reducing the occurrence of myopia. According to the above analysis, the forest plot of the five independent influencing factors against myopia was given.

Based on the 5 factors in Figure 4 that significantly prevent myopia, a formula for predicting preventing myopia prevalence is given.

$Z = 1.986 - 0.648 * 1$ (if regular physical activities = true) $- 0.560 * 3$ (if daily time spent on in-school physical
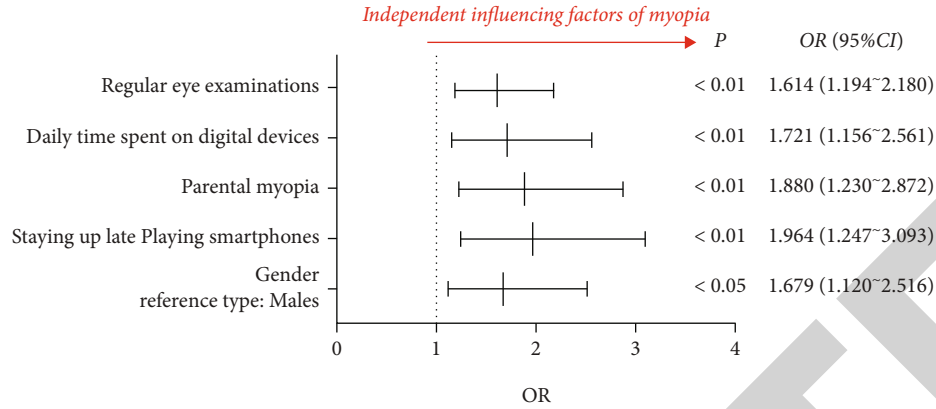
Figure 3: Forest plot of the five independent influencing factors of myopia.

activities = 40-60 minutes) + 0.192 ∗ 2 (if after-school physical activities = occasionally) − 0.366 ∗ 3 (if eye exercises = often) + 0.276 ∗ 4 (if attitude to physical education = very like).

$$P_{\text{nonmyopia}} = \frac{1}{1 + e^{-Z}}. \tag{3}$$

The following is an example that shows how to predict the probability of preventing myopia of a student who takes part in physical activities for 40-60 minutes every day, occasionally takes part in after-school physical activities, often do eye exercises, and like PE lessons very much.

$$Z = 1.986 − 0.648 ∗ 1 − 0.560 ∗ 3$$
$$+ 0.192 ∗ 2 − 0.366 ∗ 3 + 0.276 ∗ 4 = 0.51,$$

$$P_{\text{nonmyopia}} = \frac{1}{1 + e^{-Z}} = \frac{1}{1 + e^{-0.552}} = 51\%.$$
$$\tag{4}$$

The probability of the student not being myopic is 51%, which means the student will not be myopic.

4. Discussion

The univariate analysis showed that factors like playing video games, parental myopia, reading posture, writing posture, distance to the TV screen, daily time spent on homework, breaks while studying, reading extracurricular books, daily time spent in reading in extremely weak or strong light, eating whole grains and vegetables, visual acuity tests, and regular eye examinations are influencing factor for myopia, which is consistent with Luo's study [11]. Students who play digital devices for a long time every day might have eyestrain even keratitis [12]. The incidence of myopia in girls was higher than that in boys, which is consistent with the results of Wen's study [5]. The difference may be due to different environments. Girls like to be quiet and study harder, while boys prefer outdoor activities. Parental myopia, long daily reading time, and less outdoor activity time are the risk factors associated with the increased incidence of myopia [13].

With the popularity of electronic products, most adolescents are equipped with learning and game devices. They often spend 3-4 hours reading, writing, and doing homework without rest, and sometimes they even stay up until the wee hours of the morning, which increases the burden on their eyes. The muscles inside and outside the eyes get tense and cannot get a good rest, which might lead to eye muscle spasms. The multivariate analysis of the significant factors was conducted after the univariate analysis of myopia, and the significant factors obtained by multivariate analysis were regarded as the independent influencing factors of myopia. Through binary logistic regression analysis, it was found that gender, parental myopia, staying up late playing smartphones, daily time spent on digital devices, and regular eye examinations were the independent influencing factors of myopia. According to these independent factors affecting myopia, this study attempted to give a formula for predicting the probability of becoming myopic.

The results of the univariate analysis of the correlation between physical activities and myopia showed that the incidence of myopia was lower in those that took part in regular physical activities and actively participated in sports (basketball, volleyball, and football). Continuous variables such as daily time spent on in-school physical activities, after-school physical activities, eye exercises, and attitude towards physical education are also influencing factors of myopia. Outdoor activities and physical activities are beneficial to reduce the incidence of myopia. For adolescents, sports such as basketball, volleyball, and badminton can effectively reduce the risk of becoming myopic [14]. Factors such as more outdoor activities, exposure to natural light, and outdoor environment are protective for the eyes of adolescents [15–18]. Through binary logistic regression analysis, it is found that regular physical activities, daily time spent on in-school physical activities, after-school physical activities, eye exercises, and attitude towards physical education are the main influencing factors in the prevention of myopia. Based on these independent factors, the prediction formula for preventing myopia is given and the probability of nonmyopia can be calculated according to the specific conditions of the students.

Potential limitations of our study should be mentioned. First of all, it is difficult to investigate the change of myopia

TABLE 4: Binary logistic analysis of the correlation between physical activities and myopia.

Parameter	B	S.E.	Wald	DF	P	OR	OR 95% CI	
							Minimum	Maximum
Regular physical activities	-0.648	0.196	10.965	1	0.001	0.523	0.357	0.768
Daily time spent on in-school physical activities	-0.560	0.092	37.376	1	<0.001	0.571	0.477	0.684
After-school physical activities	0.192	0.094	4.177	1	0.041	1.211	1.008	1.456
Eye exercises	-0.366	0.102	13.002	1	0.000	0.693	0.568	0.846
Attitude towards physical education	0.276	0.094	8.570	1	0.003	1.317	1.095	1.584
Constants	1.986	0.453	19.26	1	<0.001	7.287		
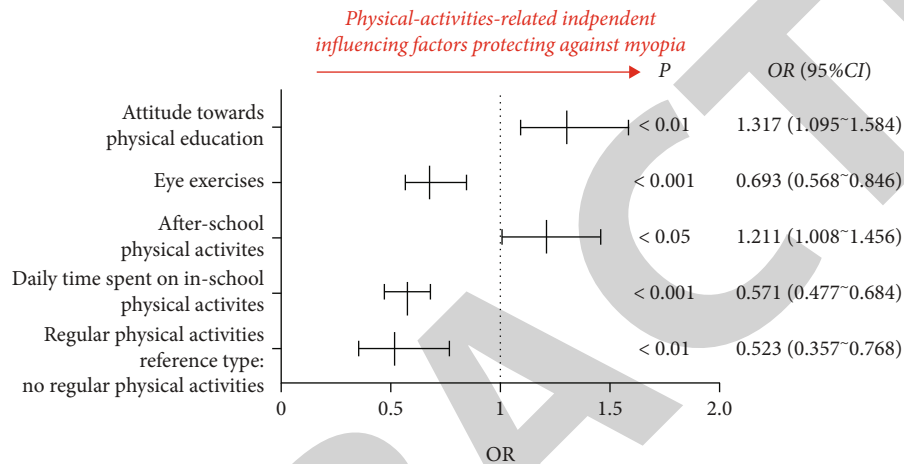
FIGURE 4: Forest plot of the five independent influencing factors protecting against myopia.

with time by a cross-sectional study, and a multilevel linear model should be adopted to obtain a causal explanation in the future. Secondly, compared with previous review studies, this study may only be a potential myopia control strategy, and in future surveys, the time of physical activities and its impact on myopia need to be better defined and quantified.

5. Conclusions

(1) The results of the univariate analysis showed the influencing factors of myopia in adolescents and the factors related to physical activities that affect the prevalence of myopia. (2) The results of the multivariate analysis showed the independent influencing factors of myopia in adolescents and the independent influencing factors related to physical activities that affect the prevalence of myopia. (3) The significant factors in multivariate analysis were used to provide 2 formulas to predict the probability of becoming myopic and the probability of preventing myopia.

Data Availability

The datasets generated during and/or analyzed during the current study are available from the corresponding author on reasonable request.

Conflicts of Interest

No financial or nonfinancial benefits have been received or will be received from any party related directly or indirectly to the subject of this article.

Authors' Contributions

YY was responsible for conceptualization, data curation, formal analysis, investigation, methodology, project administration, supervision, validation, visualization, writing—original draft, and writing—review and editing; CQ was responsible for conceptualization, formal analysis, methodology, project administration, resources, supervision, and writing—review and editing; YFQ was responsible for investigation, methodology, supervision, and writing—review and editing. Cheng Qiu and Yin Yao contributed equally to this work.

Acknowledgments

References

[1] M. J. Burton, J. Ramke, A. P. Marques et al., "The _Lancet Global Health_ Commission on Global Eye Health: vision

Retraction

Retracted: A Meta-Analysis of CT as a Tool for Diagnosing and Treating Shoulder Joint Bankart Injuries

Computational and Mathematical Methods in Medicine

This article has been retracted by Hindawi following an investigation undertaken by the publisher [1]. This investigation has uncovered evidence of one or more of the following indicators of systematic manipulation of the publication process:

(1) Discrepancies in scope

(2) Discrepancies in the description of the research reported

(3) Discrepancies between the availability of data and the research described

(4) Inappropriate citations

(5) Incoherent, meaningless and/or irrelevant content included in the article

(6) Peer-review manipulation

The presence of these indicators undermines our confidence in the integrity of the article's content and we cannot, therefore, vouch for its reliability. Please note that this notice is intended solely to alert readers that the content of this article is unreliable. We have not investigated whether authors were aware of or involved in the systematic manipulation of the publication process.

In addition, our investigation has also shown that one or more of the following human-subject reporting requirements has not been met in this article: ethical approval by an Institutional Review Board (IRB) committee or equivalent, patient/participant consent to participate, and/or agreement to publish patient/participant details (where relevant).

Wiley and Hindawi regrets that the usual quality checks did not identify these issues before publication and have since put additional measures in place to safeguard research integrity.

We wish to credit our own Research Integrity and Research Publishing teams and anonymous and named external researchers and research integrity experts for contributing to this investigation.

The corresponding author, as the representative of all authors, has been given the opportunity to register their agreement or disagreement to this retraction. We have kept a record of any response received.

References

[1] Y. Yang, L. Zou, and Z. Li, "A Meta-Analysis of CT as a Tool for Diagnosing and Treating Shoulder Joint Bankart Injuries," *Computational and Mathematical Methods in Medicine*, vol. 2022, Article ID 9137706, 8 pages, 2022.

Research Article

A Meta-Analysis of CT as a Tool for Diagnosing and Treating Shoulder Joint Bankart Injuries

Yibin Yang, Longqiang Zou, and Zhengnan Li [ID]

Department of Sports Medical, Ganzhou People's Hospital & the Affiliated Ganzhou Hospital of Nanchang University, Ganzhou, 341000 Jiangxi Province, China

Correspondence should be addressed to Zhengnan Li; lizhengnan20210331@163.com

Objective. The shoulder joint is the most flexible joint in the human body. It is a typical multiaxial ball-and-socket joint. The humeral head is approximately spherical, and the glenoid is small and shallow. This article mainly discusses the application value of computerized tomography (CT) in the early diagnosis of skeletal Bankart injury of the shoulder joint. *Methods*. The chemical quality was evaluated according to the physical therapy evidence database PEDro scale. The literature quality evaluation scale and the NO scale are also used to evaluate the quality of each nonrandomized study. The standard quality scores of the literature quality evaluation scale are as follows: (1) the selection of the study group; (2) the comparability of the study group; and (3) (cohort study) clear interest results. Outcome measurement: Postoperative shoulder joint stability and range of motion (ROM) are the main results of Bankart injury patients undergoing open repair surgery and arthroscopic repair surgery. The secondary results of the survey included the Rowe score, the shoulder stability score, the American shoulder and elbow surgery score ASES, the University of California, Los Angeles, shoulder score UCLA, and the operation time. *Results*. Four of the included studies are randomized controlled trials, and the other studies are cohort studies. After meta-analysis, a fixed-effect model ($I^2 = 34\%$) was used to observe the difference in shoulder stability treatment between the two groups and was statistically significant ($P = 0.008$, RR = 0.94, 95% confidence interval: 0.89~0.98). The analysis results showed that compared with patients undergoing open surgery, patients' undergoing arthroscopic repair had better postoperative shoulder motion range ($P < 0.001$, SMD = 0.47, 95% confidence interval: -0.72~0.22), and there is no significant heterogeneity. *Conclusion*. The Bankart injury of the shoulder joint cannot be diagnosed by X-ray examination alone due to its anatomical location and the size of the fracture fragments. CT examination has a better auxiliary diagnostic effect in the early stage of skeletal Bankart injury.

1. Introduction

The shoulder joint is a typical multiaxis ball and socket joint. The glenoid labrum made of fibrocartilage around the glenoid deepens the depth of the joint socket, but still only accommodates 1/4-1/3 of the humeral head. This structure of the shoulder joint determines a greater range of joint motion, but also reduces the stability of the joint. When the shoulder joint is dislocated, the humeral head is often removed from the lower part. Sliding out, dislocation of the front lower part occurred. The incidence of shoulder dislocation injury is relatively high for people who have been doing heavy physical activity and physical exercise for a long

time. Shoulder dislocation brings great pain and inconvenience to patients' life and work. The incidence of skeletal Bankart injury in patients with recurrent shoulder dislocation can reach 41%. Bone Bankart injury is caused by traumatic avulsion of the anterior inferior labrum of the shoulder joint or recurrent unstable shoulder dislocation accompanied by a large bony labrum defect. It is common in anterior shoulder dislocation caused by traumatic factors or anterior inferior dislocation, and the incidence of this injury in clinical work is relatively high, accounting for 5.4%-70% of shoulder instability caused by traumatic factors [1–5]. Due to traumatic factors, the anterior and inferior glenoid bone defects are caused. The glenoid loses its normal

structural characteristics and becomes an "inverted pear-shaped" structure. The humeral head and glenoid lose their normal contact relationship during activities, and joints such as shoulder dislocation occur. Unstable performance. Bankart injury first appeared in 1938 in a report of 27 patients with anterior shoulder instability due to Bankart injury. This injury was caused by the avulsion of the anterior and lower labrum of the shoulder joint, and the general impact did not exceed the 35-year-old crowd. Traditional open Bankart repair surgery is recognized by many surgeons as a recognized standard treatment [6].The traditional open Bankart repair surgery has been proven to significantly improve the stability of the shoulder joint. After this type of surgery, the recurrence rate of patients is less than 10% [7], and the low failure rate of the operation reaches 0-11% [8]. However, limited external rotational activity and secondary osteoarthritis are disadvantages of open surgery. The description of Bankart repair surgery under arthroscopic surgery appeared for the first time in 1993 [9]. In the past two decades, with the development of science and technology, related instruments and surgical implants suitable for arthroscopic surgery have been continuously updated, and with the improvement of surgeons' experience in arthroscopic surgery, arthroscopic Bankart repair surgery has gradually been advocated by some surgeons [10]. Compared with open surgery, arthroscopic surgical treatment has some advantages, such as smaller skin incisions, short operation time, reduced postoperative pain, and reduced complication rate [11]. However, some survey reports show that arthroscopic surgery has a relatively higher recurrence rate compared with standard open surgery [12]. In addition, arthroscopic techniques require experienced surgeons with relatively long learning periods and expensive instruments. So far, some of the newer techniques of arthroscopic repair surgery, such as suture anchor fixation, have the same failure rate as the traditional standard open surgery. However, these available data come from short-term and mid-term follow-up, not long-term follow-up data. Therefore, there is a lack of strong evidence-based medical evidence to determine which surgical method has better clinical effects for patients with skeletal Bankart injury of the shoulder. Some authors have concluded that open repair surgery has a lower recurrence rate, but others believe that there is no significant difference in failure rate between standard open surgery and arthroscopic Bankart repair surgery. In addition, some new high-quality studies have recently been published [13].Therefore, we conducted this meta-analysis to determine which surgical method has a better clinical effect for Bankart injury treatment. In conclusion, Bankart injury cannot be diagnosed by X-ray alone because of its anatomic location and fracture fragment size. CT examination has a better auxiliary diagnostic effect in the early stage of skeletal Bankart injury.

2. Materials and Methods

2.1. Search Strategy.

The correlation in CT as a tool for diagnosing and treating shoulder joint Bankart injuries was searched through the online databases Pub Med (1966 to December 2016) and EMBASE (1966 to December 2016). Only published studies in English are included. The articles in the reference catalogue that may meet the conditions are also checked. The keywords used to search for are as follows: anterior instability of the shoulder joint, Bankart injury, dislocation, and subluxation. To avoid duplication, if multiple research articles include the same number of patients, the results are summarized.

2.2. Inclusion Criteria.

In the literature, DSA and surgery are the gold standards, and double-blind evaluation is used. The patients included in the study are comprehensive, and the included literature has the original number data, can directly or indirectly obtain true and false positive numbers, true and false negative numbers or sensitive data such as degree, specificity, etc. have not been published repeatedly, and the sample size is larger than 10.

2.3. Evaluation of the Literature Quality of the Included Studies.

According to QUADAS2 (Review Manager5.2), independent literature quality evaluation was made for each included literature. When there is a disagreement, negotiate or refer to a third party to resolve.

2.4. Data Extraction.

Two authors independently checked the titles and titles of the retrieved documents according to the inclusion criteria. A preliminary screening of the abstract is carried out. After the preliminary screening, read the full text carefully to eliminate poor quality. For incomplete data and repetitive articles, if there are disagreements, we will agree to quotient solution. Extracted data includes the researcher, the publication year of the paper research, the country where the person is located, the inspection equipment, the number of patients, the reference standard, the inspection department Bits, the number of true and false positives, and the number of true and false negatives.

2.5. Statistical Processing.

Meta-disc 1.4 software was used for statistical analysis. The heterogeneity test level is $a = 0.1$; combined with the magnitude of Iz heterogeneity, Iz G25% is less heterogeneity; 250oGIzG50% is moderate heterogeneity; Iz-50% represents high heterogeneity of research findings. If there is no heterogeneity, combine the effect size, and use Meta-discl. 4 to draw the summary receiver operating characteristic curve (SROC). If the heterogeneity of the included studies is obvious, analyze the reasons for the heterogeneity, and only conduct a descriptive analysis.

2.6. Inspection Method.

Radiology and CT were used to quantify bone loss. Radiographic examination can be used to examine patients with severe pelvic bone loss. CT imaging has good evidence for accurate quantification of pelvic bone loss, shoulder X-ray, and chest fluoroscopy; CT examination of the shoulder joint: The patient lies on his back, with the affected limb straightened down, and scans from the upper edge of the clavicle to 1/2 of the humerus, with a layer thickness of 3 mm. The results of the imaging examination were read independently by an imaging physician and an orthopedic physician.

2.6.1. Result Measurement. The stability and range of motion (ROM) of the shoulder joint after surgery are the main results of Bankart injury patients undergoing open repair surgery and arthroscopic repair surgery. If the patient does not observe dislocation or subluxation of the shoulder joint after surgery, or the fear test is negative, then the shoulder joint is considered stable. The range of motion ROM mainly includes the loss of the range of the external rotation angle when the arm is extended at 90°. The secondary results of the survey included the Rowe score [14], the shoulder stability score [15], the American shoulder and elbow surgery score ASES [16], the University of California, Los Angeles, shoulder score UCLA [17], and the operation time.

2.6.2. Inclusion Criteria

(1) Published English literature

(2) Comparison of open repair surgery and arthroscopic repair surgery for shoulder joint stability in Bankart injured patients

Qualitative

(3) All patients are 18 years old or above

(4) Follow-up for at least 2 years

(5) There are available shoulder joint injury and dislocation recurrence data and shoulder function score

2.6.3. Exclusion Criteria

(1) Nonpublished English documents

(2) The study was followed up for less than 2 years

(3) Insufficient original data for meta-analysis

(4) In vitro studies or noncontrast studies

(5) Research objects include patients younger than 18 years old

(6) The sample size is less than 50

2.6.4. Research Methods. Search the online databases Pub Med (1966 to December 2019) and EMBASE (1966 to December 2019). Only published studies in English are included. The articles in the reference catalogue that may meet the conditions are also checked. The keywords used to search for are as follows: anterior instability of the shoulder joint, Bankart injury, dislocation, and subluxation. To avoid duplication, if multiple research articles include the same number of patients, the results are summarized. Data extraction and methodological quality evaluation. Data extraction and independent evaluation were carried out by two researchers and verified by a third, more senior researcher. The extracted information includes: (1) the characteristics of the included study, including the author, type of study design, and publication date; (2) including the demographic characteristics of the included subjects, including sample size, age, gender, and duration of follow-up

(from injury to surgery time) and details of surgery; and (3) details of the research results. Resolve differences between different authors through discussion. In order to avoid the occurrence of missing necessary data, the authors who are eligible for inclusion in the trial are contacted to obtain relevant data. The methodological quality of each randomized controlled trial (RCT) is evaluated according to the physical therapy evidence database PEDro scale [16]. The literature quality evaluation scale and the NO scale [17] are also used to evaluate the quality of each nonrandomized study. The standard quality scores of the literature quality evaluation scale are as follows: (1) the selection of the study group; (2) the comparability of the study group; and the (3) (cohort study) clear interest results. After a full review, a total of 11 independent studies were included in this meta-analysis, and the cumulative sample size as of the last follow-up was 1, 022. The difference between the two groups was not statistically significant ($P = 0.08$, SMD = −2.01, 95% confidence interval: -4.29 to 0.27), with very significant heterogeneity ($I^2 = 97\%$). Potential publication bias due to study size (tendency for the smaller studies to show larger effects) was explored by plotting the natural logarithm of the estimate of RR (ln RR) versus the inverse of standard error (1/SE). Funnel plot asymmetry was tested using the linear regression method (Figure 1).

After a full review, a total of 11 independent studies were included in this meta-analysis, and the cumulative sample size as of the last follow-up was 1022. Four of the included studies are randomized controlled trials [18], and the other studies are cohort studies [19].

3. Result

All 11 studies evaluated postoperative shoulder stability, including 512 cases in the arthroscopy group and 510 cases in the open group. After meta-analysis, a fixed-effect model ($I^2 = 34\%$) was used to observe the difference in shoulder stability treatment between the two groups was statistically significant ($P = 0.008$, RR = 0.94, 95% confidence interval: 0.89~0.98). Four studies provided ROM data on the range of motion of the shoulder joint.

As a main result of the study, the analysis results showed that patients undergoing arthroscopic repair had better postoperative shoulder motion range, compared with patients undergoing open surgery ($P < 0.001$, SMD = 0.47, 95% confidence interval: -0.72~0.22), with no significant heterogeneity. Meta-analysis showed that there was no significant difference in postoperative functional results for patients with Bankart injury under the two different treatment strategies, and the results were not statistically significant. Rowe score ($P = 0.16$), ASES score ($P = 0.24$), shoulder stability score ($P = 0.32$), and ULCA score ($P = 0.18$).

Data on the number of intraoperative operations were only obtained in 2 trials, including 115 cases in the arthroscopy group and 108 cases in the open group. The difference between the two groups was not statistically significant ($P = 0.08$, SMD = −2.01, 95% confidence interval: -4.29 to 0.27), with very significant heterogeneity ($I^2 = 97\%$). However, patients in the arthroscopic repair group have tendency
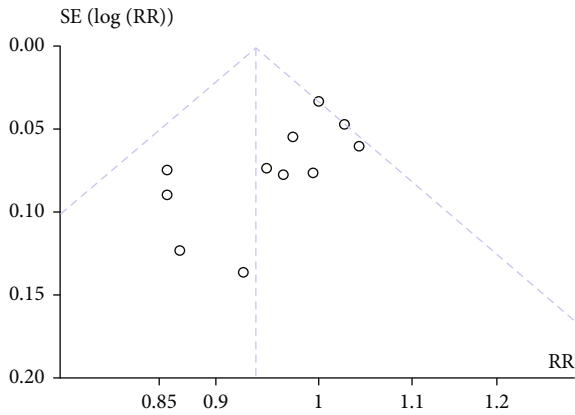
FIGURE 1: Funnel plot to evaluate publication bias.

to reduce the operation time and frequency, compared with patients in the open repair surgery group.

4. Discussion

Skeletal Bankart injury of the shoulder joint is a defect caused by traumatic factors such as bone avulsion in the front of the scapular glenoid of the shoulder joint [20, 21]. This result is caused by repeated dislocations of the shoulder joint and continuous wear and tear of the scapular glenoid edge. Recent studies have shown that in recurrent shoulder joint instability caused by trauma, the incidence of skeletal Bankart injury is as high as 90%. Under the action of a small external force, it is enough to make the humeral head pro-lapse from the glenoid and form a shoulder dislocation. Yang Guohui et al. [22] followed up 88 patients with scapu-lar glenoid Bankart injuries that were clearly diagnosed by imaging. The results of the follow-up study showed that the incidence of poor fracture healing after arthroscopic Bankart repair surgery was 16.6%. The incidence of poor fracture healing was significantly higher in the chronic case group. According to related published literature, there are two main focuses on the repair of bone defects of the shoul-der joint skeletal Bankart injury: ①Reduction and fixation of the scapular glenoid avulsion fracture: the fracture often shifts to the inside of the original physiological position to the shoulder and neck. Therefore, it is necessary to restore the displaced scapular glenoid fracture block to the original physiological position at the level of the scapular glenoid articular surface and fix it firmly during the operation. ②When reducing and fixing the anterior scapular glenoid avulsion fracture, tightening the joint capsule tissue in front of the shoulder joint cannot be ignored either. Xiao Lihua et al. [23] classified the skeletal Bankart injury of the shoul-der joint based on the imaging data of the patient: type I: the fracture piece is separated from the glenoid, and the joint capsule of the shoulder joint is continuous; type II: the severely displaced bone block is deformed. It is connected to the nonanatomical position of the shoulder glenoid mar-gin; type III is divided into two subtypes, namely, type IIIA anterior labrum bony defect area < 25% and type IIIB ante-rior labrum bony defect area > 25%.

Related literature reports that patients with types I and II shoulder joint skeletal Bankart injuries should actively adopt arthroscopic surgery. Type IIIB skeletal Bankart injury with a large and serious bone defect on the scapular glenoid side is mainly used for arthroscopic repair with wire anchors or open surgery with autogenous or allogeneic free bone graft-ing or Brinstow-Latarjet surgery to reconstruct the physio-logical bone retaining structure of the scapular glenoid bone defect and maintain the stability of the shoulder joint [24].

With the development of arthroscopic technology and related equipment, there are different ways of fixing free bones of the skeletal Bankart injury of the shoulder joint under arthroscopy with hollow nails and wire anchors. For imaging diagnosis of patients with small scapular glenoid bone injuries, it is advisable to use single-row single-line anchors for displacement and fixation. For imaging diagno-sis, it is recommended to use a single row of single-line anchors for displacement and fixation; imaging diagnosis shows that the scapular glenoid defect area is larger for bone injury, in order to achieve shoulder joint anatomy. For reduction and firm fixation, most research results show that the use of double-row double-line anchor fixation surgery is recommended. It is reported in the literature that some scholars have experimental studies on the clinical efficacy comparison of arthroscopic single-row single-line anchors and double-row double-line anchors for repairing skeletal Bankart injury of the shoulder joint [25]. In the study, 14 cases of skeletal Bankart injury models of the shoulder joint were made. There is difference in shoulder stability treat-ment between the arthroscopy group, and open group was statistically significant, mainly because the treatment method had effect on the shoulder stability.

The area of the scapular glenoid bone defect reached 25%. The study models were divided into 2 groups. One group was repaired with arthroscopic single-row single-line anchors, and the other group was repaired with arthroscopic double anchors. A row of double-line anchor nails is repaired. After the operation, the shoulder joints of the two groups of subjects were subjected to biomechanical tests such as joint movement. The results of the study show that the arthroscopic double-row double-line anchor repair has a better shoulder joint reduction effect than the single-row single-line anchor repair and the zero position of the shoul-der joint glenoid is more stable. Kim et al. [26] and Bhatia et al. [27] believe that if the area of the scapular glenoid defect is less than 15%, only the soft tissue of the labrum joint capsule can be repaired to restore the stability of the shoulder joint. Jiang et al. [28] studied whether the anatom-ical reduction of the shoulder joint skeletal Bankart injury and the repair of displaced fractures and the healing of the bone defect are necessary under arthroscope. The study selected 50 cases of shoulder joint skeletal Bankart injury and recurrent shoulder with a clear diagnosis of imaging. Patients with anterior joint dislocation of the shoulder joint should be treated with arthroscopic reduction and internal fixation with wire anchors. Before and after the operation, the joint range of motion and Constant-Murley and Rowe scores were used to evaluate the shoulder joint function of

the patients before and after the operation. The results of the study showed that the postoperative imaging data of 3 of the 4 failed patients showed that the repaired area of the glenoid defect was less than 80%. The repaired area of the glenoid defect was greater than 80% in the successful cases. Some researchers at home and abroad have used Latarjet 2 open surgical methods to treat patients with shoulder glenoid defect area > 25% skeletal Bankart injury or engaging Hill-Sachs injury (coracoid parallel transposition and coracoid process, internal rotation 90°index) [29]. After the operation, ASES score, Constant-Murley score, and visual analog scale (VAS) instability score were used to systematically evaluate the patient's shoulder joint function.

The results of the study showed that with the open Latarjet surgical treatment plan, the skeletal Bankart-injured shoulder joint can obtain better static stability and effectively reduce the recurrence rate of shoulder dislocation, Comparison of coracoid transposition and coracoid internal surgery. Compared with the 90° rotation and transposition operation, the imaging data of the postoperative follow-up suggest that the fracture healing rate is relatively higher. At present, the best imaging diagnosis method for skeletal Bankart injury of the shoulder joint is MRI, because MRI has the highest sensitivity and accuracy in diagnosing this injury [30]. However, MRI examinations are expensive, and many primary hospitals are not equipped with MRI equipment. In the early stage of injury, MRI has limited soft tissue resolution. Therefore, how to accurately diagnose shoulder skeletal Bankart injuries in limited conditions is an important issue. CT examination can determine whether the patient has a skeletal Bankart injury of the shoulder joint in a short time. When performing CT examinations on such patients, the accuracy of the examination is determined by the thickness of the slice.

In general, 16-slice or 8-slice CT in county-level hospitals can quickly scan and diagnose fractures, and there will be no low-slice CT, a problem with damage diagnosis. It is worth noting that before the application of CT examination, a strict physical examination of the patient is required. If a patient with skeletal Bankart injury of the shoulder is accompanied by fractures of the acromion and coracoid process, the body surface needs to be projected at the corresponding position under the tenderness and on the CT film. Focus on this position to avoid misdiagnosis or missed diagnosis of the disease. In this study, X-ray and CT examinations were performed on 30 cases of shoulder joint skeletal Bankart injuries diagnosed and treated [31]. The results showed that 18 cases were clearly diagnosed by X-ray, with a diagnosis rate of 60.00%; CT diagnosis accuracy rate was 96.67%, and CT observations found that 30 patients had fractures of different degrees in the front of the glenoid, accompanied by different degrees of displacement. CT examinations can be seen that the information provided is more detailed and the results are more accurate. In addition, MRI is the only effective inspection method for fibrous Bankart injury. If the patient has been excluded from the bone injury by CT, the shoulder joint activities should be followed up during the immobilization treatment. If there is repeated dislocation of the shoulder joint, MRI should

be implemented as soon as possible. Review to fully grasp the condition.

4.1. Research on the Skeletal Bankart Injury of the Shoulder Joint. The shoulder joint is a typical multiaxis ball and socket joint. The head of the humerus is approximately spherical, and the glenoid is small and shallow. The glenoid labrum made of fibrocartilage around the glenoid deepens the depth of the joint socket, but still only accommodates 1/4-1/3 of the humeral head. This structure of the shoulder joint determines a greater range of joint motion, but also reduces the stability of the joint. At the same time, the shoulder joint capsule is thin and loose, and the lower wall is relatively weakest. When the shoulder joint is dislocated, the humeral head is often removed from the lower part. Sliding out, dislocation of the front lower part occurred. The incidence of shoulder dislocation injury is relatively high for people who have been doing heavy physical activity and physical exercise for a long time. Shoulder dislocation brings great pain and inconvenience to patients' life and work. The incidence of skeletal Bankart injury in patients with recurrent shoulder dislocation can reach 41%. Because this type of injury can seriously affect the stability of the shoulder joint and cause repeated dislocations of the shoulder joint, active surgical treatment is required. Bone Bankart injury is caused by traumatic avulsion of the anterior inferior labrum of the shoulder joint or recurrent unstable shoulder dislocation accompanied by a large bony labrum defect. It is common in the anterior dislocation of the shoulder joint caused by traumatic factors or anterior inferior dislocation; the incidence of this injury in clinical work is relatively high, accounting for 5.4%-70% of shoulder instability caused by traumatic factors [32]. Due to traumatic factors, the anterior and inferior glenoid bone defect is caused. The glenoid loses its normal physiological structure and becomes an "inverted pear-shaped" structure. The humeral head and glenoid lose their normal contact relationship during activities, Loss of normal contact between humeral head and pelvis during movement and joint instability in shoulder dislocation. Traditional open Bankart repair surgery is recognized by many surgeons as a recognized standard treatment [33]. The traditional open Bankart repair surgery has been proven to significantly improve the stability of the shoulder joint. After this type of surgery, the recurrence rate of patients is less than 10% [34], and the low failure rate of the operation reaches 0-11%. However, limited external rotational activity and secondary osteoarthritis are disadvantages of open surgery. The description of Bankart's repair surgery under arthroscopy appeared for the first time in 1993. In the past two decades, with the rapid development of arthroscopic instruments and implants and the improvement of surgeons' experience in arthroscopic surgery, arthroscopic surgery Bankart repair surgery is gradually advocated by some surgeons [35]. Compared with open surgery, arthroscopic surgical treatment has some advantages, such as smaller skin incisions, short operation time, reduced postoperative pain, and reduced complication rate. However, some survey reports show that arthroscopic surgery has a relatively higher recurrence rate compared with standard open surgery. In addition,
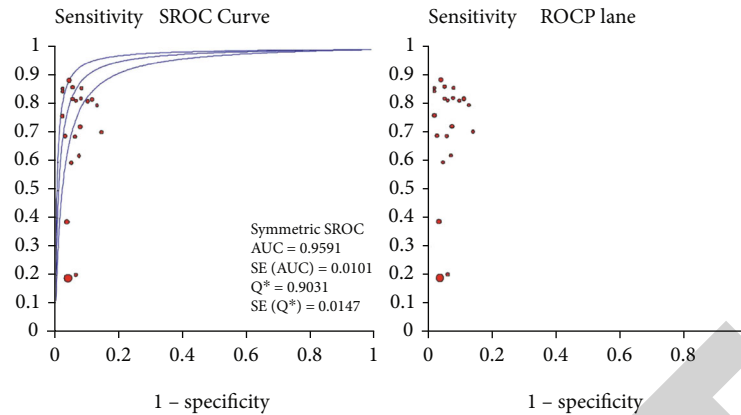
Figure 2: The area under the SROC curve.

arthroscopic techniques require experienced surgeons with relatively long learning periods and expensive instruments. So far, some of the newer techniques of arthroscopic repair surgery, such as suture anchor fixation, have the same failure rate as the traditional standard open surgery. However, these available data come from short-term and mid-term follow-up, not long-term follow-up data. Therefore, there is a lack of sufficient corroborative medical evidence to determine which surgical method should be used for patients with shoulder joint Bankart injury in order to achieve better clinical results. Although some past studies have summarized the results of published studies comparing standard open surgery and arthroscopic Bankart repair surgery, most of these studies are systematic reviews. Some authors have concluded that open repair surgery has a lower recurrence rate, but others believe that there is no significant difference in failure rate between standard open surgery and arthroscopic Bankart repair surgery. In addition, some new high-quality studies have recently been published.

4.2. The Clinical Research Application Value of Meta-Analysis. Although many medical institutions have begun to use CT to diagnose the early diagnosis of skeletal Bankart injury of the shoulder, a large number of research documents at home and abroad are different due to the uneven geographical, ethnic, and equipment conditions, and the research results are also different. The nine documents included in this study are from different countries. Through screening and quality evaluation of the included documents, the quality level of the included documents is guaranteed, thereby ensuring the reliability of the meta-analysis. In this study, the diagnostic effect indicators of nine documents were combined to increase the statistical power. The combined sensitivity of the included literature was 0.98 (95% CI: 0.96-1.00), indicating that CT can better detect early diagnosis of bone and joint and Bankart injury. The combined specificity is 0.99 (95% CI: (0.97-1.00), indicating that CT diagnoses skeletal Bankart injury of the shoulder. The positive likelihood ratio is the ratio of the true positive rate to the false positive rate, and the negative likelihood ratio is false negative. Therefore, the larger the former, the higher the diagnostic value, and the smaller the latter, the higher the

diagnostic value. In this study, the positive likelihood ratio and negative likelihood ratio were 33.14 (95% CI.: 15.74-69.53) and 0.04 (95% CI: 0.02-0.07), both of which indicate that CT has a higher diagnostic value in the early diagnosis of skeletal Bankart injury of the shoulder joint. The diagnostic OR value is that CT has a higher diagnostic value in the early diagnosis of skeletal Bankart injury of the shoulder joint. CT has a higher detection rate of lesions and provides more reliable evidence-based medical evidence. SROC curve is a comprehensive evaluation of the reliability of diagnosis. The SROC curve method performs meta-analysis on multiple diagnostic tests with the same detection target, fits the SROC curve according to the ratio weight, and calculates the area under the SROC curve.

4.3. Mate Analysis Heterogeneity Test. By observing the SROC curve plan, it is found that the result does not show a "shoulder-arm"-like distribution, suggesting that there is no threshold effect. In the test of heterogeneity caused by nonthreshold effects, $P = 0.093$ and $I^2 = 0\%$, which proves that there is no heterogeneity caused by nonthreshold effects. In summary, the heterogeneity between the studies is small. Meta-analysis results: Using random effects model, combined effect size, combined sensitivity, specificity, positive likelihood ratio, negative likelihood ratio, and diagnostic OR value were 0.89 (95% CI: 0.96-10.0), 0.99 (95% CI: 0.97-1.00), 33.09 (95% CI: 15.75-69.53), 0.04 (95% CI: 0.02-0.07), and 1110.47 (95% CI: 37.68-3216.73), respectively. There was no statistically significant difference in the combined effect size of each combination. SROC analysis: The area under the SROC curve (AUC) of CT is 0.99, and the Q index is 0.968 (Figure 2).

Bankart injury of the shoulder joint refers to the avulsion injury of the anterior and inferior shoulder joint glenolabia at the attachment of the anterior inferior glenohumeral ligament complex. It can be accompanied by a fracture of the glenoid edge. After the injury, it is easy to cause instability and habituation in the front of the shoulder joint. Anterior dislocation of the shoulder joint. Burkhart et al. (2000) believe that among patients with a single shoulder dislocation, those without obvious defects in the shoulder glenoid have a 4% risk of redislocation, while those with a glenoid

defect are at risk of redislocation. As high as 67%, therefore, the result of skeletal Bankart injury is more serious than that of fibrous Bankart injury. The treatment methods of fibrous Bankart injury and skeletal Bankart injury are also different: Fibrous Bankart injury can be repaired under arthroscopic surgery to obtain good results, and there are also reports on the treatment of fibrous Bankart by incision and repair of the joint capsule labrum. The damage has been well recovered. For patients with skeletal Bankart injury with or without Hill-Sachs injury, arthroscopic repair is more difficult, and for fracture fragments that cannot provide strong fixation, open reconstructive surgery should be considered. The imaging diagnosis of Bankart damage is currently considered to be the most accurate and sensitive MRI examination, and the accuracy and sensitivity of the water-induced three-dimensional VIBE MR reconstruction in the diagnosis of Bankart damage have been greatly improved. However, most primary hospitals are not equipped with MR equipment, and the resolution of early MRI examination of the injury to the soft tissue is limited. How to make an accurate diagnosis of skeletal Bankart injury under limited conditions is very important. Because the consequences of skeletal Bankart injury are more serious, early diagnosis and treatment are more necessary, and the early diagnosis of skeletal Bankart injury has a positive effect on the recovery of surgical treatment. CT examination can determine whether there is bone in a shorter time. The requirements for CT do not need to be as high as those for cardiac CT examinations. The accuracy of the examination mainly depends on the thickness of the layer. Although there is no clear report on the size of the fracture in the front of the glenoid in the Bankart injury, all patients in this group passed CT examination can clarify the location and displacement of fracture injury. Most county-level hospitals can accurately scan the fracture with 8-row and 16-row CT. There is no concern that low-speed CT cannot diagnose skeletal Bankart injuries. However, the CT examination must be established on the premise of a detailed physical examination. Some Bankart injuries are accompanied by fractures such as the coracoid process and acromion. It needs to be established under the tenderness of the body surface projection of the part. Pay attention to its position on the CT film. Effectively avoid the misdiagnosis and missed diagnosis of Bankart injury. For fibrous Bankart injuries, MRI inspection is the only effective inspection method. For patients whose bone injury is excluded by CT, the shoulder joint movement should be observed at the same time of immobilization treatment. If there is repeated shoulder joint dislocation, MRI review and shoulder arthroscopic surgery should be performed. Most patients can get good recovery.

5. Conclusion

The Bankart injury of the shoulder joint cannot be diagnosed by X-ray examination alone due to its anatomical location and the size of the fracture fragments. CT examination has a better auxiliary diagnostic effect in the early stage of skeletal Bankart injury.

Data Availability

The data used to support this study are available from the corresponding author upon request.

Conflicts of Interest

The authors declare that they have no conflicts of interest.

Authors' Contributions

Yibin Yang, Longqiang Zou, and Zhengnan Li contributed equally to this work.

References

[1] D. Xing, Q. Yanmei, C. Xiaofei, and Z. Sheng, "Technical progress of 3D MRI evaluation of shoulder joint injury," *Journal of Clinical Radiology*, vol. 39, no. 11, pp. 2346–2349, 2020.

[2] W. Zhaoqiang and W. Ping, "Analysis of the application effect of CT in the diagnosis of shoulder joint OA cartilage injury," *China Rural Health*, vol. 13, no. 2, pp. 55-56, 2021.

[3] L. Yujie and Z. Gang, "The progress of arthroscopic techniques in the repair and reconstruction of shoulder joint injuries," *China Orthopedics and Traumatology*, vol. 33, no. 12, pp. 1089–1091, 2020.

[4] B. Chunhui and C. Donghui, "Research on the causes of volleyball players' shoulder joint injury and rehabilitation training," *Contemporary Sports, Science and Technology*, vol. 10, no. 33, pp. 16-17+21, 2020.

[5] J. Zhongjie, "The clinical diagnostic value of MRI scan in shoulder joint injury," *China Medical Device Information*, vol. 26, no. 22, pp. 103-104, 2020.

[6] X. Fei, "The diagnostic effect of MRI scan in shoulder joint injury," *Imaging Research and Medical Application*, vol. 4, no. 22, pp. 184-185, 2020.

[7] Z. Heng, Y. Kun, and L. Li, "The application value of MRI shoulder arthrography in the diagnosis of patients with shoulder joint injury," *Henan Medical Research*, vol. 29, no. 27, pp. 5144–5146, 2020.

[8] C. Chen, "Application of MRI in the diagnosis of shoulder joint injury," *Contemporary Medicine*, vol. 26, no. 28, pp. 47–49, 2020.

[9] W. Yuhao, "Brief analysis of shoulder joint injuries and preventive measures in table tennis sports," *Public Standardization*, vol. 15, pp. 139-140, 2020.

[10] Z. Jixia and Z. Shiqiang, "Seven measures for prevention and treatment of shoulder joint injuries," *Happy Family*, vol. 14, p. 97, 2020.

[11] P. Jiawen, "Investigation and analysis of shoulder joint injuries of Chinese female rugby players," *Chinese Sports Coaches*, vol. 28, no. 2, pp. 66–68+70, 2020.

[12] W. Xing, "The clinical diagnosis analysis of MRI scan in shoulder joint injury," *Imaging Research and Medical Application*, vol. 4, no. 12, pp. 178-179, 2020.

[13] W. Jialian, "The causes and preventive measures of shoulder joint injuries in volleyball sports," *Stationery and Sports Supplies & Technology*, vol. 12, pp. 87-88, 2020.

[14] J. Wenjing and Z. Qiaoling, "Clinical diagnosis analysis of MRI scan in shoulder joint injury," *Electronic Journal of Integrated*

Research Article

Microfeature Segmentation Algorithm for Biological Images Using Improved Density Peak Clustering

Man Li [ID], **Haiyin Sha, and Hongying Liu**

School of Engineering, Guangzhou College of Technology and Business, Guangzhou 510850, China

Correspondence should be addressed to Man Li; xdclm@126.com

To address the problem of low precision in feature segmentation of biological images with large noise, a microfeature segmentation algorithm for biological images using improved density peak clustering was proposed. First, the center pixel and edge information of a biological image were obtained to remove some redundant information. The three-dimensional space of the image is constructed, and the coordinate system is used to describe every superpixel of the biological image. Second, the image symmetry and reversibility are used to obtain the stopping position of pixels, other adjacent points are used to obtain the current color and shape information, and more vectors are used to express the density to complete the image pretreatment. Finally, the improved density peak clustering method is used to cluster the image, and the pixels completed by clustering and the remaining pixels are evenly distributed into the space to segment the image so as to complete the microfeature segmentation of the biological image based on the improved density peak clustering method. The results show that the proposed algorithm improves the segmentation efficiency, segmentation integrity rate, and segmentation accuracy. The time consumed by the proposed biological image microfeature segmentation algorithm is always less than 2 minutes, and the segmentation integrity rate can reach more than 90%. Furthermore, the proposed algorithm can reduce the missing condition and the noise of the segmented image and improve the image feature segmentation effect.

1. Introduction

Image segmentation is an important preprocessing technology that has been widely applied to various fields of computer science, especially in the field of biometric images. However, biometric image segmentation is difficult due to the particularity of such images. The quality of image segmentation results determines the quality of image understanding in the next step, which includes the detection and recognition of targets and the relationship between targets in the scene. According to the development history of biometric recognition, the processing of biometric images has always been the focus of research and computer-aided implementation. In this context, many scholars have carried out research on the microfeature segmentation algorithm of biometric images. For instance, Ji et al. [1] proposed the Synthetic Aperture Radar (SAR) image perceptual hash segmentation algorithm, which reduces speckle noise in the first stage and then uses the principal component analysis

method to reduce redundant information and obtain smooth segmentation results; Tang and Yu [2] proposed an algorithm for retinal vascular segmentation of color fundus images based on the BP model. The algorithm applies the BP neural network to color fundus image segmentation and uses adaptive histogram equalization, morphological processing, and the matched filtering algorithm to segment the image; Zhuang et al. [3] proposed an ultrasonic image segmentation method based on the fractal theory and fuzzy enhancement. With this method, the ultrasonic image is enhanced by fuzzy technology, and then the image is segmented by enhancement technology; Wang et al. [4] proposed an image segmentation algorithm based on the NSST and vector-valued model. The algorithm combines the NSST and vector-valued model and extracts multidimensional data from the image by using the sampling shear wave transform method to realize image segmentation; Reference [5] proposed a cell image segmentation method based on edge intensity cues. In this method, the edge intensity

prompt method is used to recognize the location of leukocytes, and then Grabcut is deployed to segment leukocytes. The above-proposed method can complete the basic segmentation of biometric images. However, it cannot adaptively denoise the noisy biometric images.

To solve this defect, a microfeature segmentation algorithm based on improved density peak clustering is proposed in this paper. The proposed algorithm can reduce the missing condition and the noise of the segmented image and improve the image feature segmentation effect. The contributions of this paper are as follows. (1) The central pixel and edge information of biometric images are obtained, and some redundant information is removed. (2) Image symmetry and reversibility are used to obtain the dwell position of pixels, other adjacent points are used to obtain the current color and shape information, and more vectors are used to express the density with the image preprocessed and the effect of the image feature segmentation optimized. (3) A new clustering algorithm is proposed, which can quickly find the density peak points on the current data and outliers in the dataset and then divide the data points into the nearest classes from the high level to the low level to get the final clustering results.

2. Methodology

2.1. Image Preprocessing. Generally speaking, if the established space is a three-dimensional (3D) space, three kinds of filtering can be used for processing. The dimension of space is closely related to the type of filtering, that is, the larger the dimension of space [6]. The larger the spatial dimension is, the more filtering is involved, and the difficulty of calculation will be exacerbated, resulting in too many variables and difficulty to control, which will cause image damage and improper preprocessing. Suppose there is a sample point x_i, and the edge density before untreated can be expressed as

$$\rho_i = \sum d_{ij} - A_c, \qquad (1)$$

where d_{ij} is the distance between two pixels, A_c refers to the pixel size, and the equation δ_i to calculate the distance between adjacent pixels is

$$\delta_i = \begin{cases} \min\{d_{ij}\} \neq \in I_S^i \neq {}_S^i \neq \varnothing, \\ \max\{d_{ij}\} \neq \in I_S^i \neq {}_S^i = \varnothing, \end{cases} \qquad (2)$$

where I_S^i refers to all the point sets, $\min\{d_{ij}\}$ refers to the minimum distance, and $\max\{d_{ij}\}$ refers to the maximum distance.

Based on the above calculation, further processing is carried out. Based on the different pixel points of each part of the image, the density is also different. The distance between two random pixel points is used as the calculation standard, and the gray value of the image is used as the variable; the

superpixel density equation of the image is obtained [7].

$$\rho_i = \Sigma X(d_{ij} - d_c), \qquad (3)$$

where ρ_i refers to the density of pixels, d_{ij} refers to the distance between two random pixels, d_c refers to the distance between pixels after movement, and X refers to more than one pixel point. It can be transformed into

$$X(x) = \begin{cases} 1, & x \leq 0, \\ 0, & x > 0, \end{cases} \qquad (4)$$

where x refers to the quantity. If the edge in the image is too blurred [8] and the color is not easy to distinguish, the equation can be changed to

$$\rho_i = \sum_j c^{-1 d_j/d_i}. \qquad (5)$$

Equations (4) and (5) are based on the clear core information of the image and cannot represent the segmentation processing of all images [3]. If the part of the image meets the segmentation conditions, the image can be processed as follows:

$$\lambda = \rho \cdot \delta, \qquad (6)$$

where λ refers to the coefficient and δ refers to the distance between two adjacent pixel points.

If there is too much data, multiple decisions will appear during processing, and multiple decisions will be made at the same time, resulting in confusion in image segmentation [9]. Therefore, it is necessary to relatively reduce some unnecessary variables, build a multidimensional space, describe each superpixel using the coordinate system, and then conduct the calculation. Suppose the space is described as (l, a, b), and any random coordinate is expressed as (x, y), and then all recognized pixel points correspond to coordinate points one by one. We can get

$$\begin{cases} (x, y) = (x, y) \cdot /h_s, \\ (l, a, b) = (l, a, b)./h_r, \end{cases} \qquad (7)$$

where h refers to the reduction of times, after which the spacing between pixels in the image will become smaller, resulting in an increase in its density. Therefore, if it is detected that the pixel points in the image gradually increase [10], its density can be expressed as

$$\rho_{SP} = \sum_{p \in SP} p, \qquad (8)$$

where SP refers to the initial density of superpixels and p refers to the quantity.

Then, the stay position of pixel points is obtained by using the symmetry and reversibility of the image [11], and the single feature of each point is found, which is expressed

as (x, y, l, a, b). It can directly describe the main forms of image edge information. Other adjacent points are used to obtain the current color and shape information, and finally, more vectors are used to express the density to complete the image preprocessing.

2.2. Image Center Selection Using Improved Density Peak Clustering. After the above processing, some main information of the image has been mastered. Because the color is easy to distinguish and is not affected by any factors, it can be regarded as a quantitative calculation [12]. There are many remaining density clustering points, so it is necessary to select an optimal clustering center as the variable representative to participate in the density calculation and adopt the improved density peak clustering method in clustering. The process is shown in Figure 1.

The selection of the cluster center should not only consider the quantitative number but also understand the severity of its influencing factors such as noise. The generation of noise will interfere with the image resolution and information transmission. Therefore, the most commonly used denoising method is the two-dimensional entropy denoising method. After the systematic change, the cluster center is finally determined. The expression is shown in

$$\rho_i = \sum_j x(d_{ij} - d_c), \tag{9}$$

where the function range of x is

$$f(x) = \begin{cases} 1, & x < 0, \\ 0, & x \geq 0, \end{cases} \tag{10}$$

where ρ refers to the density, i and j are two adjacent points, and the distance d_c can only be positive and larger than 1. It can be set at will and remain unchanged through the distance equation between two points after clustering [13].

$$\delta_i = \begin{cases} \min_{j, p_i > p_i} (d_{ij}), & i \leq 2, \\ \min_{i \geq 2} (d_{ij}), & i = 1. \end{cases} \tag{11}$$

It can be seen from Equation (11) that the density and clustering reach the peak at the same time. At this time, all pixels within the qualified range can be cluster centers, but there cannot be too many cluster centers [12]. Therefore, it is necessary to continue the operation until the cluster center is obtained.

As long as the density of a point is large, it can be included in the screening range. After various considerations and analyses, the density curve can be drawn and further confirmed by the highest point in the graph. Based on the above density and distance, the information entropy equation is obtained after adding the influence of noise [14].

$$\gamma_i = \rho_i * \delta_i, \tag{12}$$

where γ_i refers to the information entropy. And the three are
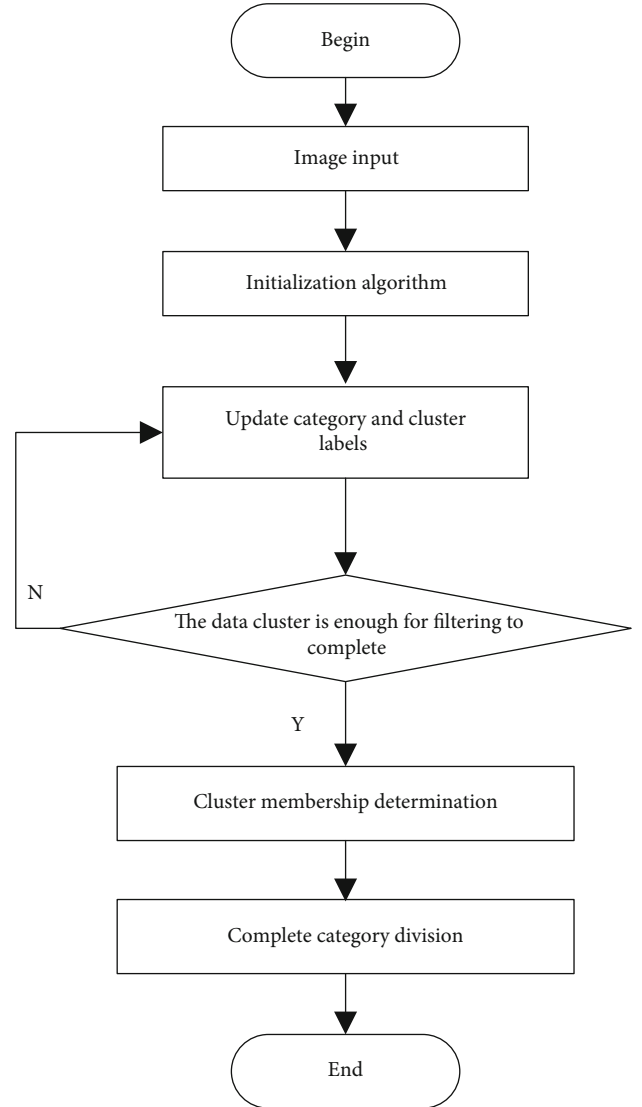
Figure 1: Improved density peak clustering process.

in positive proportion, which will increase with the increase of distance and density. Therefore, the entropy values can be sorted in order, the values in the back row can be removed, and the quantity retained is k. Then, it is determined by other quantitative comparisons [15]. From the previous data, it can be seen that the gray value of the image will fluctuate regularly within a range without interference from any factors. The range is $0 \sim 255$. Therefore, the pixel distance range d_c can be determined as $0 \sim 10$, and the change of k along with the two is $2 \leq k \leq 30$. Then, on the basis of information entropy, the variable gray value is added to obtain the mathematical equation:

$$H = \sum_{255}^{i=0} p_i \log p_i, \tag{13}$$

where H refers to the one-dimensional entropy and p_i refers to the proportion of gray values in the image. The larger the

Input: the clustering center of biological image pixels, and its expression is

$$\rho_i = \sum_j x(d_{ij} - d_c).$$

Output: image microfeature segmentation results
(1) Establish the three-dimensional image space. Assuming that there is a sample point x_i, the edge density before unprocessing is ρ_i
(2) The coordinate system is used to describe each superpixel, and then the residence position of the pixel is obtained by using the symmetry and reversibility of the image
(3) Find the single feature of each point, describe the main form of image edge information, use other adjacent points to obtain the current color and shape information, and use more vectors to express the density ρ_{SP}
(4) The improved density peak clustering method is used to select the optimal clustering center
(5) Calculate the maximum information entropy $\gamma_{\max}$ and evenly distribute the pixels in the three-dimensional space
(6) With the distance between fixed pixels and the position of fixed pixels, the fast segmentation result of biological image is δ_i
(7) End
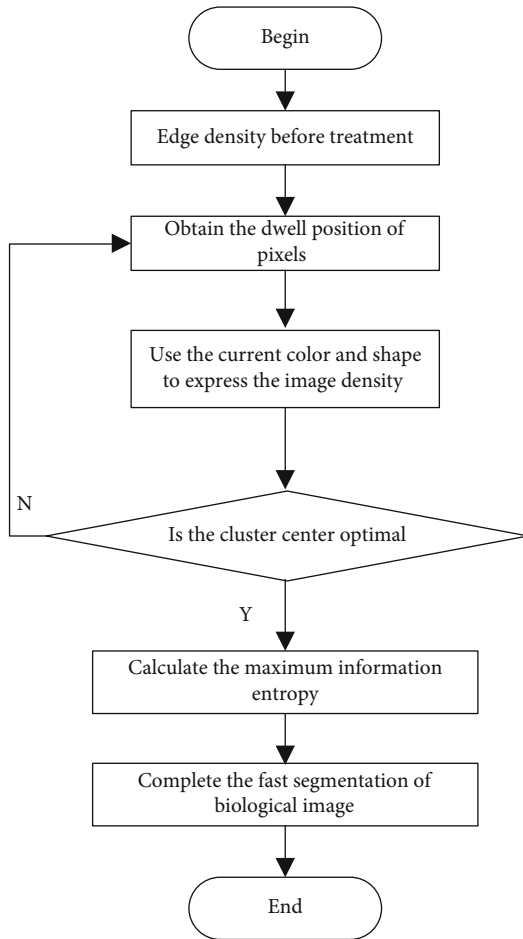
<div align="center">Algorithm 1</div>

Figure 2: Algorithm implementation process.

Therefore, pixels that do not meet the standard can be removed at the same time through multiple calculations [17].

$$D_s = d_{lab} + \frac{m}{S} d_{xy}, \tag{14}$$

where d_{xy} refers to the distance between adjacent pixels when gray values are the same, d_{lab} refers to the distance between adjacent pixels with similar color and different density values, m refers to the index, and S refers to the point area. The equation is as follows [18]:

$$d_{xy} = \sqrt{(x_k - x_i)^2 + (y_k - y_i)^2},$$
$$d_{lab} = \sqrt{(l_k - l_i)^2 + (a_k - a_i)^2 + (b_k - b_i)^2}, \tag{15}$$

where l refers to the color, a refers to the image length, and b refers to the image width. Therefore, the best distance and density can be determined, and the distance between the cluster center and the edge pixel can be obtained by taking the color as the calculation benchmark:

$$s_{ij} = \left\| c_i - c_j \right\|, \tag{16}$$

where $\|\cdot\|$ refers to the actual distance, c_i refers to the spatial characteristic of the pixel point i, and c_j refers to the spatial characteristic of the point j.

In summary, when the density and distance are maximum, the value of information entropy should be maximized, and the number of superpixels should be small. At this time, several adjacent points are recorded to obtain the cluster center.

2.3. Image Feature Segmentation Optimization. After the cluster center is obtained through the constraints of the multidimensional space and vector, the remaining pixels can be evenly distributed into the space [19] so that the distance between each point remains unchanged, and its position remains unchanged, which can be uniformly placed in the

value, the more obvious the color of the representative image, the higher the definition, and the faster the information carried will be extracted [16]. The region of the cluster center is about $2S \times 2S$, in which there is more than one pixel point, and different pixel points correspond to different gray values, which poses certain difficulties to segmentation.
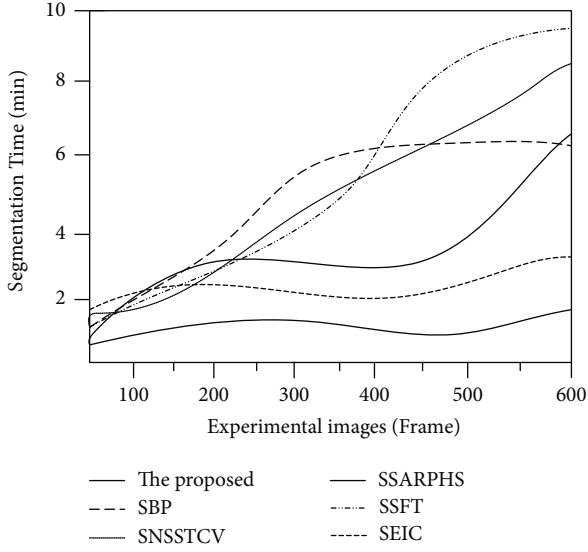
Figure 3: Comparison of segmentation time.

grid. On this basis, iteration and addition are carried out to form a fixed circular pattern to quickly segment biometric images.

If the factors interfering with image segmentation remain unchanged and only noise is left, the spatial isolation method can be used to separate the noise from the data information so that the data can be recorded and reduce the impact of noise [20]. Suppose a point in the space is (x, y), the position of the adjacent pixel point is $(x + \Delta x, y + \Delta y)$, and Δx and Δy are randomly selected in $\{-1, 0, 1\}$. However, the prerequisite is $(\Delta x, \Delta y) \neq (0, 0)$. Different spaces will also lead to changes in the distance between pixels. It can be expressed as

$$d_{ij} = \left\| (\bar{x}_i - \bar{x}_j)^2 \cdot W \right\|_2, \tag{17}$$

where $\bar{x}_i$ refers to the average threshold value of the adjacent space of i, $\bar{x}_j$ refers to the average threshold value of the adjacent space of j, W refers to the variance matrix representing threshold in space, and $\|\cdot\|_2$ refers to the times. In order to make the segmentation more thorough without affecting the data collection in other areas, reduce the noise to the greatest extent. However, some details need to be calculated, and small details often affect the global effect. The distance between superpixels is calculated as [21]

$$\delta_i = \min_{j:\rho_j > \rho_i} (d_{ij}). \tag{18}$$

Redefine the two points as

$$\text{neigh}_i = j. \tag{19}$$

The equation for the pixel with the best performance and

the highest density value is

$$\delta_i = \max_j (d_y), \tag{20}$$

where each pixel exists independently. When the distance is relatively reduced, its density becomes higher, and the maximum density can be obtained in this range [22]. The coordinate points existing in the space are used to accurately segment the region. At this time, the gray value and data information between different regions can be separated:

$$\text{cluster}_i = \exists i : \max (\delta_i + \rho_i), \tag{21}$$

where (x, y) are all independent individuals and n refers to the coefficient of the 3D space. The algorithm based on the above density peak clustering is improved and optimized, assuming that the preconditions remain unchanged. The mathematical equation is

$$\rho_i = \sum_j X(d_{ij} - d_c)P_i,$$

$$X(d) = \begin{cases} 1, & d < 0, \\ 0, & \text{otherwise.} \end{cases} \tag{22}$$

It can be seen from Equation ((22)) that the solution of density is actually related to the distance between neighbors, and the image segmentation is actually related to the proportion of gray values. It can not only calculate the density but also see the sparsity of the segmented region. Therefore, it is particularly important to obtain the main features of each pixel. Therefore, a feature function is established [23].

It is assumed that the collected characteristic samples are $X_1, X_2, \cdots, X_n$, and its function is expressed as $f(x)$, and then the density function is

$$\hat{f}_h(x) = \frac{1}{n}\sum_n^{i=1} K_h(x - X_i) = \frac{1}{nh}\sum_n^{i=1} K\left(\frac{x - X_i}{h}\right), \tag{23}$$

where $K(\cdot)$ refers to the characteristic function, which is usually inversely proportional to the density function, and the constraints are

$$\begin{cases} \int K(u)du = 1, \\ \int uK(u)du = 0, \\ \int u^2 K(u)du = u_2(K) > 0, \end{cases} \tag{24}$$

where u refers to the constraint coefficient, $u = (x - X_i)/h$. When all variables in the equation approach 0, the characteristic function is affected first, and the density function will gradually decrease according to its change. At this time, the microfeatures of all points in the image can be obtained clearly, and the damage to the image is minimal.

FIGURE 4: Experimental image.
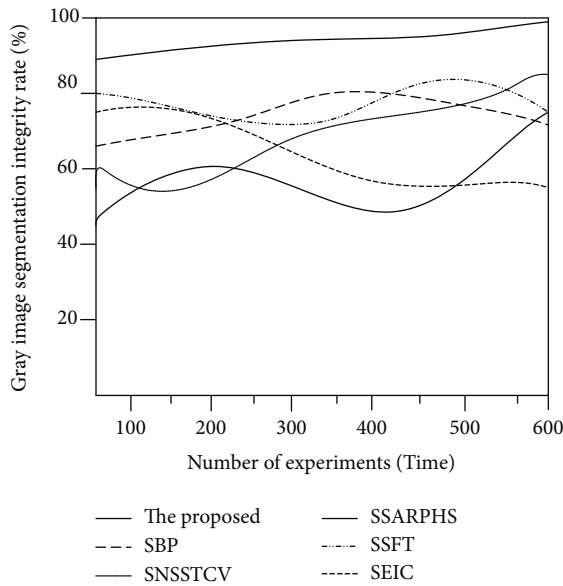
FIGURE 5: Comparison of gray image segmentation integrity.

For the superpixel point i, after its space position and occupation ratio are determined and the best distance is obtained, the image microfeature segmentation result can be obtained. The mathematical equation is expressed as

$$\delta_i = \begin{cases} \min_{j, \rho_j > \rho_i} (s_{ij}), & \text{if} \exists j, \ \rho_j > \rho_i, \\ \max_j (s_{ij}), & \text{otherwise}. \end{cases} \quad (25)$$

After several iterations, it can be cut directly to complete the microfeature segmentation of biometric images.

2.4. The Proposed Algorithm. The improved density peak clustering method is used to cluster the image, and the clus-

tered pixels and the remaining pixels are evenly distributed into the space to realize the microfeature segmentation of the biological image. The microfeature segmentation algorithm of the biological image based on improved density peak clustering is shown in Figure 2.

3. Experimental Analysis and Results

3.1. Dataset. To verify the effectiveness of the biometric image microfeature segmentation algorithm based on improved density peak clustering, experiments are carried out. The SSARPHS algorithm proposed by Reference [1], the SBP algorithm proposed by Reference [2], the SSFT algorithm proposed by Reference [3], the SNSSTCV algorithm proposed by Reference [4], and the SEIC algorithm proposed by Reference [5] are compared with the proposed algorithm, and the segmentation effects of the six methods are compared.

The Python development platform is now finished. The simulation data runs on Windows 10, and the algorithm is written in OpenCV. The ImageNet dataset is a vast visual database used in the development of visual object recognition software. ImageNet manually annotates over 14 million picture URLs. ImageNet has over 20,000 categories, such as "balloon" or "strawberry," each with hundreds of images. The annotation database of the third-party picture URL is available for free from ImageNet. With the Context Dataset Common Objects, all of the image resources in the common objects in the context dataset are linked to the Flickr picture website. The evaluation dataset is partitioned so that 80% of the data is used for training and 20% is used for testing. Initialize the proposed algorithm with the other five segmentation algorithms; store and show the image in BMP format; analyze the image and properly evaluate the experimental findings.

3.2. Experimental Index

3.2.1. Image Microfeature Segmentation Time. Compare the image microfeature segmentation time of the biological image microfeature segmentation algorithm, and record the image feature segmentation time of different algorithms.

3.2.2. Gray Image Segmentation Integrity. The visibility of the segmented image is affected by the image's segmentation integrity while segmenting biological images in a microfeature manner. The gray image segmentation integrity rate calculation equation is as follows:

$$\Re = \frac{\chi'}{\chi} \times 100\%, \quad (27)$$

where χ' is the number of complete segmentation features of the image and χ is the total number of features contained in the image.

3.2.3. Noise after Segmentation. To evaluate the picture's noise, divide it into nonoverlapping image blocks, compute the variance of each image block, rank it from small to large, and select 1% of the total number of blocks to calculate the

(a) The proposed

(b) SSARPHS

(c) SBP

(d) SSFT

(e) SNSSTCV

(f) SEIC
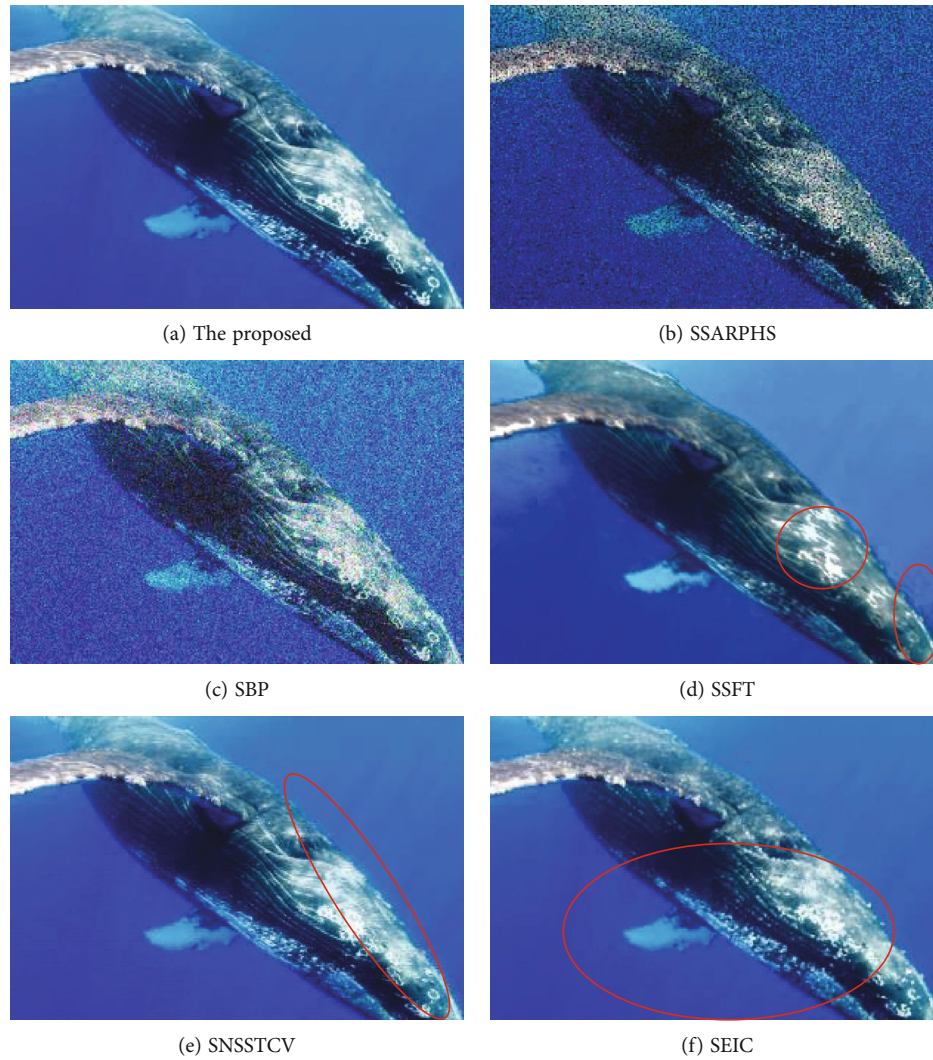
FIGURE 6: Comparison of image noise after segmentation.

mean value of the variance, that is, the image's noise variance. The size of image noise is measured in this experiment by the visual noise results in the image.

3.2.4. Missing Condition after Image Segmentation. After applying various algorithms, the lack of image features is the key metric used to assess the algorithm's application performance. The applicability of this method is low after image feature segmentation, resulting in more missing portions.

3.2.5. Segmentation Accuracy. The segmentation accuracy is mainly reflected by the feature segmentation results of the image. The higher the fitting degree between the segmentation results of the image features and the original features, the higher the application accuracy of this method.

3.3. Results and Discussion. The segmentation time comparison results of the proposed biometric image microfeature segmentation algorithm and the other five segmentation methods are shown in Figure 3.

It is seen from Figure 3 that the feature segmentation time of the SAR image perceptual hash segmentation algorithm proposed by the SSARPHS algorithm is up to 6.5 min, and the faster the segmentation time increases with the increase of the number of experimental images. The segmentation algorithm based on the BP neural network proposed by the SBP algorithm takes up to 8 min, and its time consumed increases linearly. The segmentation algorithm based on the fractal theory proposed by the SSFT algorithm increases rapidly when the number of experimental images is less than 300. When the number of experimental images is more than 300, the feature segmentation time gradually stabilizes and approaches 6 min. Compared with other algorithms, the image segmentation algorithm proposed by the SNSSTCV algorithm takes the most time. When the number of experimental images is 600, the time is 9.5 min. The time consumed by the cell image segmentation algorithm based on edge intensity cues proposed by the SEIC algorithm is closest to that of the proposed method. When the number of experimental images is the highest, the segmentation time is about 2.5 min. The image segmentation algorithm

(a) The proposed

(b) SSARPHS

(c) SBP

(d) SSFT

FIGURE 7: Continued.

(e) SNSSTCV

(f) SEIC
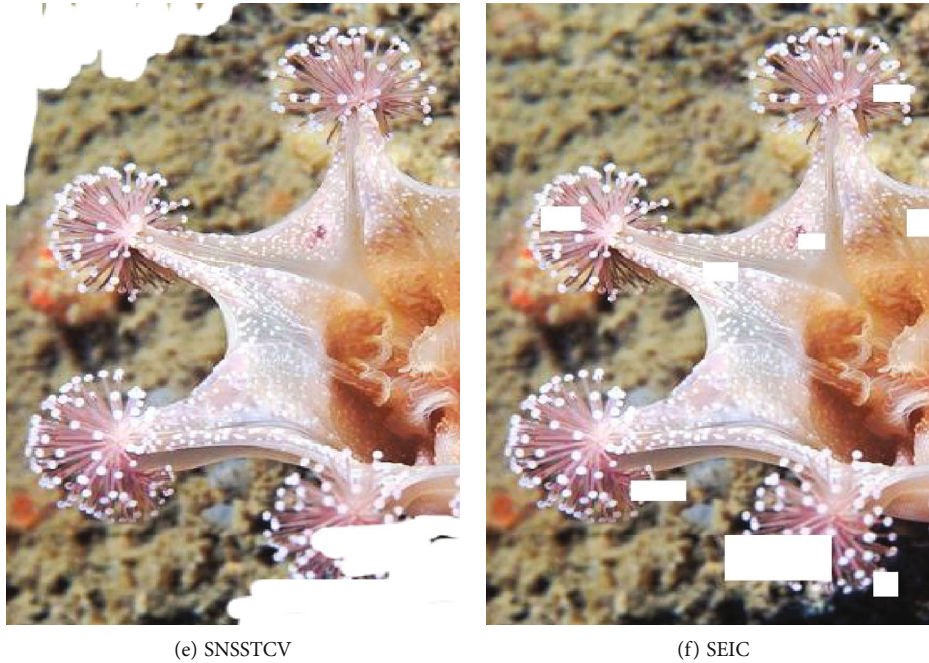
Figure 7: Comparison of missing images after image segmentation.

proposed in this study can complete image segmentation in a short time when the number of images is small or large. The other five methods spend less time when there are 10 images. When there are 60 images, the time increases significantly, and the segmentation algorithm based on the BP neural network takes the most time.

The segmentation integrity rate of the six methods was compared under the gray image, and the experimental image is shown in Figure 4.

The segmentation and comparison results of the six methods are shown in Figure 5.

According to Figure 5, the fluctuation range of the image segmentation integrity rate of the SAR image perceptual hash segmentation algorithm proposed by the SSARPHS algorithm is 40%~70%, and the segmentation integrity test of this algorithm fluctuates greatly with the increase of the number of experimental images. The segmentation integrity rate of the segmentation algorithm based on the BP neural network proposed by the SBP algorithm is up to 75%, and the completion rate of image segmentation decreases with the increase of the number of images. The segmentation algorithm based on the fractal theory proposed by the SSFT algorithm gradually increases the segmentation completion rate to 80% when the number of experimental images is less than 350. When the number of experimental images is more than 350, the image segmentation completion rate gradually decreases to 60%. The image segmentation algorithm based on the NSST and vector-valued C-V model proposed by the SNSSTCV algorithm and the cell image segmentation algorithm based on edge intensity cues proposed by the SEIC algorithm have the greatest fluctuation in segmentation integrity, and the test results are less than 80%. The segmentation algorithm studied has a high segmentation integrity rate, which shows that the proposed method also has a good segmentation effect in the

gray image. The other five methods have low segmentation integrity and are greatly affected by the gray image, which is not as good as the algorithm.

The image noise after segmentation was compared by the six methods, and the results are shown in Figure 6.

It can be seen from Figure 6 that the SAR image perceptual hash segmentation algorithm proposed by the SSARPHS algorithm and the segmentation algorithm based on the BP neural network proposed by the SBP algorithm cannot filter the image noise, and there are obvious noise points, which affect the visual recognition effect of image features. The segmentation algorithm based on the fractal theory proposed by the SSFT algorithm, the image segmentation algorithm based on the NSST and vector-valued C-V model proposed by the SNSSTCV algorithm, and the cell image segmentation algorithm based on edge intensity cues proposed by the SEIC algorithm all have obvious problems of noise points at different positions and cannot clearly show the image. The proposed algorithm has no obvious feature points, and the segmented image quality is high.

The missing situation of the images after the segmentation was compared by the six methods, as shown in Figure 7.

As shown in Figure 7, the SAR image perceptual hash segmentation algorithm proposed by the SSARPHS algorithm has many feature deletion problems after feature segmentation. The image feature segmentation results of the segmentation algorithm based on the BP neural network proposed by the SBP algorithm, the image segmentation algorithm based on the NSST and vector-valued C-V model proposed by the SNSSTCV algorithm, and the cell image segmentation algorithm based on edge intensity cues proposed by the SEIC algorithm are not ideal, and the feature deletion is obvious. Although the missing features of the segmentation algorithm based on the fractal theory proposed by the SSFT algorithm

(a) The proposed

(b) SSARPHS

(c) SBP

(d) SSFT

(e) SNSSTCV

(f) SEIC
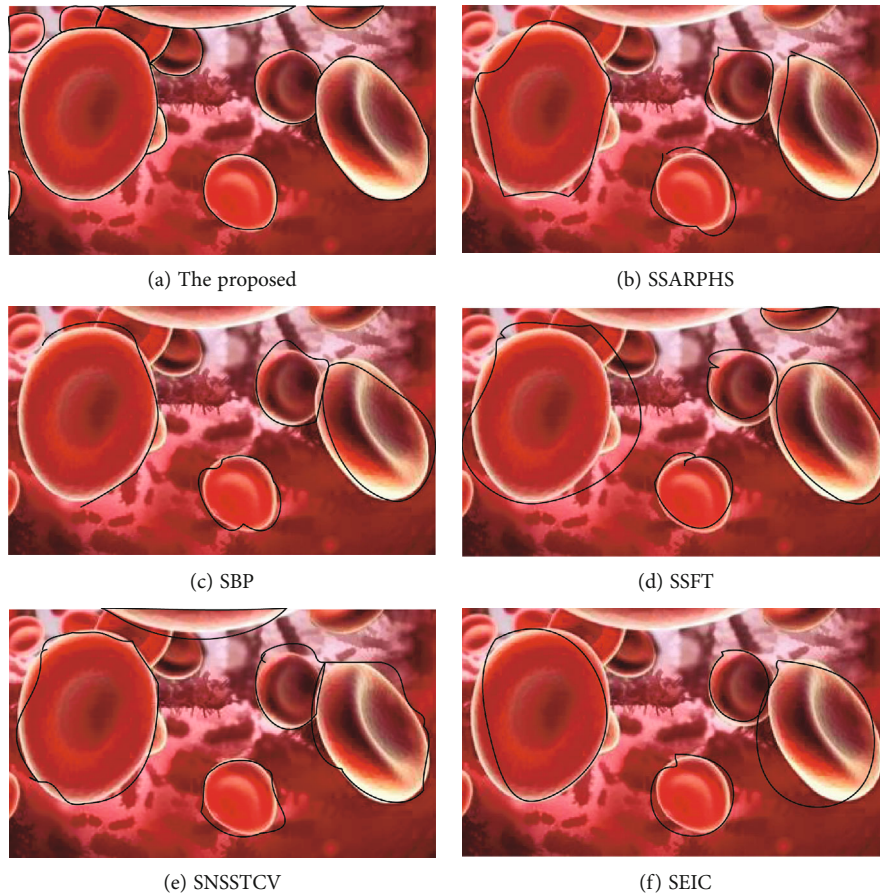
Figure 8: Comparison of segmentation accuracy.

appear in the image edge, it also directly affects the image edge recognition and subsequent processing. The biometric image microfeature segmentation algorithm in this study has no image loss after segmentation, and the other five methods have image loss, which may be caused by oversegmentation.

The segmentation algorithm in this paper is compared with the segmentation accuracy of the other five methods, as shown in Figure 8.

Figure 8 shows the comparison of segmentation accuracy. The SAR image perceptual hash segmentation algorithm proposed by the SSARPHS algorithm, the segmentation algorithm based on the BP neural network proposed by the SBP algorithm, the segmentation algorithm based on the fractal theory proposed by the SSFT algorithm, and the image segmentation algorithm based on the NSST and vector-valued C-V model proposed by the SNSSTCV algorithm all have too large, too small, and too few segmentation ranges, and the segmentation accuracy is not as high as the algorithm. In contrast, the algorithm studied can segment all the targets with high accuracy, and there is basically no oversegmentation and less segmentation.

4. Conclusions and Future Works

Image segmentation technology is one of the key technologies in image analysis and computer vision, and it is the key to subsequent image processing. Due to the interference of many factors in complex images, there is random noise in addition to the target in the image, and the traditional image segmentation algorithm cannot effectively filter this kind of noise. A microfeature segmentation algorithm based on improved density peak clustering is designed. The algorithm of this research not only improves the segmentation efficiency, segmentation integrity, and segmentation accuracy but also reduces the image noise and image loss after segmentation and effectively solves the current problems. However, there are many factors affecting the characteristics of biometric images, and the research methods do not consider too many factors. In order to further enhance the antinoise performance of the segmentation algorithm, targeted optimization should be carried out from a specific link. Therefore, the influencing factors that may affect image segmentation will be fully considered in future works to improve the effect of image segmentation.

Data Availability

The data used to support the findings of this study are included within the article.

Conflicts of Interest

The authors declare that there is no conflict of interest with any financial organizations regarding the material reported in this manuscript.

Acknowledgments

References

[1] J. Ji, Y. Yao, J. Wei, and Y. Quan, "Perceptual hashing for SAR image segmentation," *International journal of remote sensing*, vol. 40, no. 10, pp. 3672–3688, 2019.

[2] S. Tang and F. Yu, "Construction and verification of retinal vessel segmentation algorithm for color fundus image under BP neural network model," *The Journal of Supercomputing*, vol. 77, no. 4, pp. 3870–3884, 2021.

[3] Z. Zhuang, N. Lei, A. J. Raj, and S. Qiu, "Application of fractal theory and fuzzy enhancement in ultrasound image segmentation," *Medical & Biological Engineering & Computing*, vol. 57, no. 3, pp. 623–632, 2019.

[4] X. Wang, X. Zhao, Y. Zhu, and X. Su, "NSST and vector-valued C-V model based image segmentation algorithm," *IET Image Processing*, vol. 14, no. 8, pp. 1614–1620, 2020.

[5] K. Sudha and P. Geetha, "Leukocyte segmentation in peripheral blood images using a novel edge strength cue-based location detection method," *Medical & Biological Engineering & Computing*, vol. 58, no. 9, pp. 1995–2008, 2020.

[6] M. L. Moskopp, A. Deussen, and P. Dieterich, "Bayesian inference for the automated adjustment of an image segmentation pipeline – a modular approach applied to wound healing assays," *Knowledge-Based Systems*, vol. 173, no. 1, pp. 52–61, 2019.

[7] R. Bates, B. Irving, B. Markelc et al., "Segmentation of vasculature from fluorescently labeled endothelial cells in multi-photon microscopy images," *IEEE Transactions on Medical Imaging*, vol. 38, no. 1, pp. 1–10, 2019.

[8] M. Matsuda, Y. Yamanaka, M. Uemura, M. Osawa, and C. Alev, "Recapitulating the human segmentation clock with pluripotent stem cells," *Nature*, vol. 580, no. 7801, pp. 124–129, 2020.

[9] W. Gao, X. Li, Y. Wang, and Y. Cai, "Medical image segmentation algorithm for three-dimensional multimodal using deep reinforcement learning and big data analytics," *Frontiers in Public Health*, vol. 10, article 879639, 2022.

[10] Z. Liu, K. Han, Z. Wang, J. Zhang, and V. S. Sheng, "Automatic liver segmentation from abdominal CT volumes using improved convolution neural networks," *Multimedia Systems*, vol. 27, no. 1, pp. 111–124, 2021.

[11] C. H. Antink, J. Ferreira, M. Paul, S. Lyra, and S. Leonhardt, "Fast body part segmentation and tracking of neonatal video data using deep learning," *Medical & Biological Engineering & Computing*, vol. 58, no. 12, pp. 3049–3061, 2020.

[12] Z. Xiong, Q. Xia, Z. Hu et al., "A global benchmark of algorithms for segmenting the left atrium from late gadolinium-enhanced cardiac magnetic resonance imaging," *Medical Image Analysis*, vol. 67, p. 101832, 2021.

[13] M. Winter, W. Mankowski, E. Wait, D. Cardenas, A. Aguinaldo, and A. R. Cohen, "Separating touching cells using pixel replicated elliptical shape models," *IEEE Transactions on Medical Imaging*, vol. 38, no. 4, pp. 883–893, 2019.

[14] Á. Casado-García, G. Chichón, C. Domínguez et al., "MotilityJ: an open-source tool for the classification and segmentation of bacteria on motility images," *Computers in biology and medicine*, vol. 136, 2021.

[15] H. Hu, A. Liu, Q. Zhou, Q. Guan, X. Li, and Q. Chen, "An adaptive learning method of anchor shape priors for biological cells detection and segmentation," *Computer Methods and Programs In Biomedicine*, vol. 208, article 106260, 2021.

[16] K. W. Chen and C. W. Shih, "Collective oscillations in coupled-cell systems," *Bulletin of Mathematical Biology*, vol. 83, no. 6, pp. 1–60, 2021.

[17] H. O. Ilhan, I. O. Sigirci, G. Serbes, and N. Aydin, "A fully automated hybrid human sperm detection and classification system based on mobile-net and the performance comparison with conventional methods," *Medical & Biological Engineering & Computing*, vol. 58, no. 5, pp. 1047–1068, 2020.

[18] J. He, G. Zhou, S. Zhou, and Y. Chen, "Online hard patch mining using shape models and bandit algorithm for multi-organ segmentation," *Ieee Journal of Biomedical and Health Informatics*, vol. 26, no. 6, pp. 2648–2659, 2022.

[19] S. Sarangi, N. P. Rath, and H. K. Sahoo, "Mammogram mass segmentation and detection using Legendre neural network-based optimal threshold," *Medical & Biological Engineering & Computing*, vol. 59, no. 4, pp. 947–955, 2021.

[20] R. D'Antuono and G. Pisignano, "ZELDA: a 3D image segmentation and parent-child relation plugin for microscopy image analysis in *napari*," *Frontiers in computer science*, vol. 3, article 796117, 2022.

[21] Z. Liu, L. Jin, J. Chen et al., "A survey on applications of deep learning in microscopy image analysis," *Computers In Biology and Medicine*, vol. 134, article 104523, 2021.

[22] J. Grande-Barreto and P. Gómez-Gil, "Segmentation of MRI brain scans using spatial constraints and 3D features," *Medical & Biological Engineering & Computing*, vol. 58, no. 12, pp. 3101–3112, 2020.

[23] C. Stringer, T. Wang, M. Michaelos, and M. Pachitariu, "Cellpose: a generalist algorithm for cellular segmentation," *Nature Methods*, vol. 18, no. 1, pp. 100–106, 2021.

Research Article

Analysis of Rational Drug Use Effect under Hospital Drug Control System

Haoli Huo [ID], Xiaoyan Li, Hui Li, Haiye Wang, Xin Ma, Chen Chen, and Hongfeng Zhang

Department of Pharmacy, Handan Central Hospital, Handan 056008, China

Correspondence should be addressed to Haoli Huo; huohaoli1986@163.com

Objective. To describe and assess the hospital drug control system's measures. *Methods*. From 2017 to 2019, examine the changes in medication percentage, important monitoring drug amount, top 10 medications amount, and usage rate of prophylactic antibiotics for type I incisions. *Results*. The proportion of pharmaceuticals remains below 30%, the number of significant monitoring drugs has decreased, the top ten drugs have shifted from adjuvant to therapeutic drugs, and the use of prophylactic antibiotics for type I incisions has decreased by 10%. *Conclusion*. The percentage of medications that met requirements by using the drug control system has steadily decreased, and the number of pharmaceuticals for important monitoring pharmaceuticals has steadily decreased, in accordance with national medical insurance policy, as well as improved rational drug usage.

1. Introduction

The State Council issued No. 38 in 2015, stating that the public hospital revenue system needed to be changed and that strict control of pharmaceutical costs was unjustified, resulting in a drop in the percentage of public hospital drugs in the pilot city (excluding Chinese medicine drinkers) to around 30% by 2017. Medication ratio management was used as a management measure by a number of medical organizations [1]. The Handan City Health and Family Planning Commission published a notice on boosting the follow-up monitoring of essential pharmaceuticals in public hospitals as the doctor's change advanced, and key medication surveillance was launched at our hospital [2]. Furthermore, the antimicrobial prophylaxis usage rate for class I incisional surgery should be less than or equal to 30%, and such medical records should be carefully verified regularly. Monthly, the quantity and amount of antimicrobial medicine usage were double sorted, and medical record spot checks were undertaken by the top 10 departments and people [3]. Every year, the top 10 medications by medication quantity were statistically analyzed and evaluated [4]. As a public tertiary general hospital at the crossroads of three provinces, our hospital bears the burden of diagnosing and treating critically ill patients in the periphery, the proportion of controlled drugs is somewhat difficult, and it may achieve certain success only by taking multiple measures, combined with clinical, pharmaceutical, and administrative interventions [5]. This study investigates the changes in drug percentage, the amount of attention paid to medication monitoring, the rate of usage of class I incision antibiotic prophylaxis, and other management indicators under various drug administration techniques in relation to the existing policy form [6].

2. Materials and Methods

2.1. Data Collection. The hospital's his system, amygdalin software, the Mecon system, relevant departmental records, and website announcements were used to collect data for this study.

2.2. Research Method. Statistics for 2017-2019, the percentage of total hospital medicines is monthly data, with a focus on monitoring the number of medications in the catalog used annually, the number of the top 10 drugs, and antimicrobial drug consumption in class I incision prevention. EXCAL tables were used for descriptive statistical analysis to compare changes before and after control and indicators.

2.3. Specific Measures

2.3.1. Drug Proportion Control System.

Set up a working leadership committee for the proportion of control drugs, with the dean serving as the leader and the vice dean serving as the vice leader. This will improve medicine, encourage the prudent use of clinical drugs and antibacterial treatments, reduce the drug ratio, and collaborate with our hospital. The group's office is known as the "drug control office." The head of the drug department's clinical department is in charge of management. The leading group established a medical department, a pharmacy department, and an advocacy department to promote drug-related laws and regulations, hospital drug control-related rules and regulations, management methods, and medical modification; to raise awareness of reasonable, legal, and compliant drug use among health care workers, and to promote publicity, inspections, punishments, and rewards. Cardiovascular medications, nervous system drugs, anticancer drugs, adjuvant pharmaceuticals, and certain Chinese medicine injections lose their most critical control, and their most important monitoring is reduced in half. The Drug Control Office gathered clinical pharmacists and other clinical professionals to assess the top 20 most-prescribed medications each month. When there was a trend of super-routine or needless prescriptions, the medicine was halted for three months. For clinical departments to determine the Department drug occupancy goal, the drug control office looks at the actual to target ratio. If the decline is greater than 30%, the department bonus and director are not penalised. If the drop is less than 30%, 50% of the manager's bonus are withdrawn. For nutritional support class auxiliary medication of the hospital's key control and halving shopper medicine newly communicated by the hospital each month, the department level should strengthen the regulation, reduce the medication under the premise of reasonable drug use, and have conversations and penalties with the super routine drug use and personal record inspection departments. You cannot take part in the yearly evaluation if you use four or more drugs. Top 10 physicians with the most monthly prescription expenses were scrutinized for excessive drug usage. The doctor with the highest points for inappropriate drug usage earned an appointment, and the top doctor got a Codonopsis action each month. When the hospital's medication ratio did not achieve the overall aim, the professional or department that did not met the goal was based on their professional characteristics (the same drug ratio target professional, the standard department is not within the sequence). The doctor with the lowest average patient cost had his medical record modified to utilize POA. The doctor and department director who present with inappropriate medication administration make an appointment, minus the doctor's bonus for the month. Half of the department directors complete target management award; medical record points occur within half a year 3 unreasonable doctors to schedule an appointment, suspend prescription rights for 3 months, report to the medical department, and report to the department director by the record review department. The drug control office organizes the clinical pharmacists and other clinical experts in the department of pharmacy every month, and physicians in the top ten of time

average costs, the first two of each specialty, and the first ten of class I incision surgery prevention randomly pick medical records for review. The point review department avoids. Each clinical department head is on the expert panel and must examine reasonable medication usage. Each week, the medical, pharmacy, sensory control, critical care, and laboratory medicine departments ran the rational drug use ward. Walk into a clinical department weekly, evaluate the running medical record for acceptable medication usage, and observe hospital patients. Inquire about the progress of the disease and focus on the use of antibacterial medicines, the rate of perioperative antimicrobial prophylaxis in surgical departments, the rate of antimicrobial drugs before treatment, the intensity of antimicrobial drug consumption, and the incidence of bacterial resistance. The five department union highlights pharmaceutical concerns and reacts in the department face-to-face with the clinical department.

2.3.2. Antimicrobial Drug Management System.

In the implementing regulations of review criteria of Hebei tertiary general hospital (2013 Edition), the operation of class I incision (2 h of surgical time) and the usage of preventive antimicrobials required to be 30 percent. In our facility, the indicator is about 55%, which is substantially more than necessary. Inguinal hernia repair (including patch repair), thyroid disease surgery, breast disease surgery, arthroscopy surgery, carotid endarterectomy, cranial mass resection, and diagnostic surgery via vascular intervention are not prophylactic for antimicrobials, according to 2015 guidelines for the clinical use of implants for the seven diseases. Antimicrobial prophylaxis in the perioperative phase should be 0.5 to 1 hour before surgery, and in class I incision surgery, it should not be more than 24 hours. Antimicrobial agents and postoperative prophylactic medicine should also be regulated. In this management, the medical record of class I incisions was obtained monthly, and the top 10 physicians rated the average prescription cost of antibacterial medicines for class I incision surgery prevention. The medical records of the doctors who ranked first for the subtotal average cost of antimicrobial prophylaxis for class I incision surgery were reviewed using point review and random spot checks. The doctors who showed unreasonable drug use were interviewed by the record review department and had their bonuses taken away for the month. The physicians with three inappropriate drug usage were also interrogated and lost their incentives. Every month, antimicrobial usage was rated. Antimicrobial medications in the top 10 total medication quantity were totalled, and the department of pharmacy created medication points. Using Mecon, medical records were abstracted and named. Medical records were also retrieved at random, with a reference to our hospital's appraisal standards for the sensible use of antimicrobial medications. Based on the grading criteria, persons or departments with fewer than 80 points were interrogated.

2.3.3. Effect of Drug Management System.

Handan City put out a warning to increase important medication tracking and monitoring in public hospitals. Our hospital has created clear guidelines for essential monitored pharmaceuticals and set up a working committee to handle monitoring drugs.
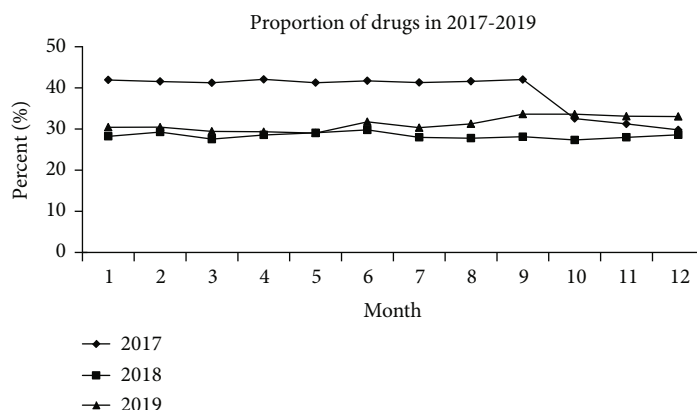
FIGURE 1: The changes in the ratio of drug proportion from 2017 to 2019.

Head of the clinical department oversees medication management. To enhance special point evaluation, monthly sales, and ranking of pharmaceuticals on the list, the doctor who initially monitored drug dose was picked at random. (In the Wellcome system, input the name of the first physician whose dose was recorded, and the medication name, i.e., medical record and prescription, was picked at random.) Before picking a medicine, physicians should weigh its benefits and costs. Also, they should respect the medicine's specifications and Medicare drug list restrictions. Doctors should not allow patients utilize medications unapproved methods. The review study focuses on prescribing medications clinically (drug selection, drug indication, use and dosage, route of administration, drug interactions, compatibility contraindications, etc.). Orders Menu included Review antimicrobial drugs, Assessment criteria for antimicrobial medication usage our hospital created, Monthly drug sequencing and review findings, an unreasonable medication caution by a doctor, and three unnecessary medical visits in half a year.

3. Results

3.1. Changes in Drug Occupancy Indexes. After developing the drug accounting control system in October 2017, clinical departments cooperated to better execute rules and regulations and reduce the drug accounting ratio while enhancing rational drug usage. Figure 1 shows the change in medication percentages from 2017 to 2019. The drug occupancy ratio was around 41% before October 2017 and dropped to less than 30% by December. Each month in 2018 was below 30%, with late 2019 above 30%. The average drug percentage statistics for 2017 (39%), 2018 (29%), and 2019 (30%) meets national criteria.

3.2. Use of Antimicrobial Agents for Class I Incision Prophylaxis. In 2017-2019, the rate of class I incision prevention using antimicrobial medications was derived by our hospital's amygdalin software, as shown in Figure 2. From January to September 2017, the usage rate of antimicrobial agents for class I incision prevention was between 50% and 60%, as shown in the figure, and the use rate reduced dramatically when the medication proportion was restricted in October. Antimicrobial medicine usage declined in 2018 and 2019
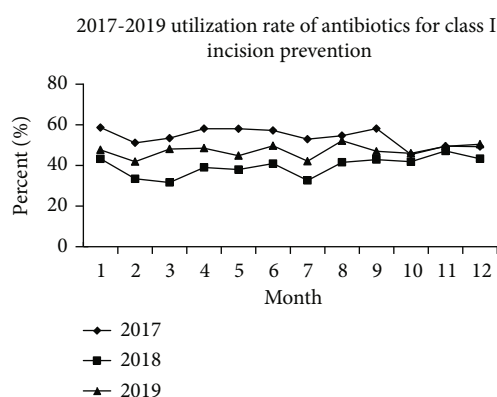
FIGURE 2: Utilization rate of prophylactic antibiotics for type I incisions from 2017 to 2019.

compared to each month of 2017. The average usage rate in 2017 was 53.85 percent, while the use rate of antimicrobial drugs for class I incision prophylaxis was maintained between 35 and 50 percent in 2018 and 2019, reflecting a 10 percentage point decrease in the evaluation. Although current figures do not meet the national minimum of 30%, they have improved dramatically under the drug control system.

3.3. Top Ten Drugs by Amount of Medication. In 2017-2019, the top 10 drug goods by medication quantity were extremely varied (see Table 1). The top 10 in 2017 were all adjuvant medications, the top ten in 2018 contained two, and the rest were primarily therapeutic medications including antineoplastic drugs, anticoagulants, and anti-infective agents. Only one adjunct is in the top 10 in 2019, while the rest are both antineoplastic and antibacterial. Thus, it can be seen that the proportion of drugs took place through the implementation of control and control measures, the special management of adjuvant drugs, key monitoring drugs, and the promotion of physicians' awareness of rational drug use. Adjuvant drug use in hospitals has significantly decreased, with only one fifth of the number in 2018 from ten to one, and therapeutic drugs such as antitumor and antibacterial drugs account for eight, a significant proportion, in 2018.

TABLE 1: The top ten drugs in the amount of medication from 2017 to 2019.

No.	2017	2018	2019
1	Lienal polypeptide injection	Imatinib mesylate	Meropenem
2	Creatine phosphate sodium for injection	Meropenem	Trastuzumab injection
3	Coenzyme complex	Sodium chloride 0.9%	Imatinib mesylate
4	Butylphthalide and sodium chloride injection	Cefoperazone tazobactam	Compound porcine cerebroside and ganglioside injection
5	Edaravone	Lienal polypeptide injection	Cefoperazone tazobactam
6	Calf spleen extract	Cefazolin sodium	Cefamandole
7	Lansoprazole needle	Sodium chloride 0.9% (double valve soft bag)	Paclitaxel liposome for injection
8	Placental polypeptide injection	Ginkgolide injection	Piperacillin sodium and tazobactam sodium
9	Omeprazole	Nadroparin calcium	Cefazolin
10	Brain glycoside carnosine	Piperacillin sodium and tazobactam sodium	Sodium chloride 0.9% (double pipe and double plug)
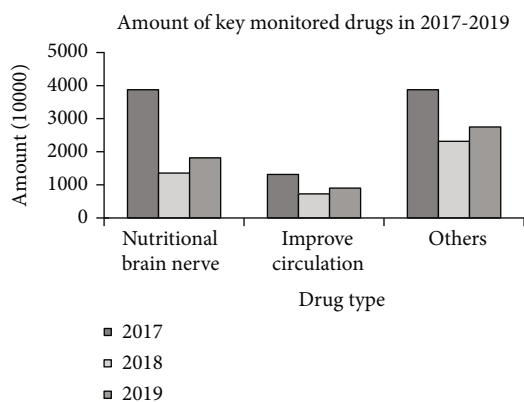
FIGURE 3: The amount of the key monitoring drugs from 2017 to 2019.

3.4. Focus on Monitoring Drug Amounts.
According to the most recent state key monitoring drug catalog for categorization data, see Figure 3 for a comparison of yearly medication usage in our hospital's key monitoring catalog from 2017 to 2019. As seen in the graph, the number of medications in each category declined in 2018 compared to 2017, and the reduction was greater. According to the statistics, the usage of concentrated monitoring declined by about 50% during the course of the year. 2019 is mostly unchanged from 2018.

4. Discussion

4.1. Exploration of the Effect of Drug Control System.
Compared to 2017, the percentage of medications in 2018 and 2019 was all held at 30%, which fulfilled the criteria of national documents, via drug proportion control and control, antimicrobial drug administration, and key monitoring of drug administration [7]. The quantity of antimicrobial usage has fallen dramatically, and the rate of class I incision prophylactic antibiotic treatment has decreased by 10%, although not meeting national guidelines. Concentrated monitoring of the quantity of drug usage in the table of contents decreased by about

50%. The top 10 pharmaceuticals with the highest yearly drug usage quantities also changed structure; in 2017, they were all adjuvant drugs; in 2019, they were mostly antitumor, antibiotic, and other therapeutic drugs [8]. With the adoption of different regulations, numerous medical institutions around the nation began to regulate hospitals and obtained positive outcomes. Our control and control results show that the indicators meet or are close to the national requirements, but we recognize that the proportion of control drugs relates to various aspects of hospital clinical work, social relationship processing, and so on, and reflects the level of management work in the hospital function [9]. The functional department played an important management function in this control and control work, medical and technical departments provided a large amount of technical support, clinical departments with a positive attitude seriously summarized the deficiencies in the medication process and many aspects of the cooperation of multiple departments, so that the control and control work achieved better results [10]. Of course, the decreased drug ratio is undesirable for therapeutic purposes. The fundamental concerns of no indication medication, improper usage, and incorrect selection of antimicrobial kinds for perioperative prophylaxis are already evident in the prescription (medical claims) point review process, but additional minor issues continue to emerge in the point review results [11]. Currently, the drug ratio data has been maintained at about 30%; nevertheless, raising the degree of reasonable drug usage is our ultimate aim of ongoing drug management.

4.2. Focused Surveillance of Drugs and Medicare.
The author compared the basic medical insurance, job injury insurance, and fertility insurance drug catalog of Hebei Province (2017 transition version) and the state-latest Medicare catalog of 2019, and two of the key monitored catalogs (gangliosides and bone peptides) were varieties that did not exist in either [12]. The original 2017 edition had four species (edaravone, alprostadil, murine nerve growth factor, and cinnarizide maleate), however, they were removed from the updated 2019 catalog [13]. The remaining 19 kinds were all novel category B medications introduced in Hebei Province in 2017. According

to a notice issued by the state Medicare administration in 2019, each region must strictly enforce the drug catalog, not self-develop the catalog or increase the list of drugs with the method of transformation, and not self-adjust the set of restricted payment ranges for the drugs in the catalog. Stepwise digesting should take place over a three-year period for category B medications that are increased as specified in the initial provincial prescription list [14]. Provinces should preferentially modify out-of-pocket payments for medications that are included in the area of state focused surveillance during digestion. This means that by 2020, focused monitoring of varieties within the table of contents, six of which are not covered by Medicare and the other 19 newly added varieties, will be prioritized, implying that all varieties within the table of contents may not be in the Hebei Province Medicare table of contents. The continual decline in drug consumption in the table of contents is consistent with national policy, as represented in this drug control and control method. Then, in clinical practice, we provide medical services in accordance with national policy in order to be informed of changes in the Medicare catalog in a timely manner.

4.3. The Role of the Clinical Pharmacist in the Drug Control System. Clinical pharmacy has advanced rapidly in recent years, and clinical pharmacists at our hospital have contributed significantly to the drug control and control process [15]. Docking with clinical departments, each clinical pharmacist docks on professional departments to perform in-hospital medical order review on the responsible department, regularly announced the clinical department's morning meeting, pointed out deficiencies in the medication process, and provided advice to rationalize the medication [16]. Departments such as the combined medical department, laboratory, and hospital feeling carry out the rational drug use ward and walk into different clinical departments once a week. The clinical pharmacist was in charge of evaluating and discussing the department's medical recommendations in person. The requirements for perioperative prophylaxis and antimicrobial use in surgical departments, antimicrobial principles used in treatment, and adjunctive indications were all fully covered. It included in drug proportion control and control, antimicrobial drug double ranking, key monitoring of drug point review work, developing point review criteria, and monthly reporting of point review results to relevant functional departments in accordance with drug instructions and other strict controls. The reports focused on ongoing hospital-wide training, assessment, and timely interpretation of updated Medicare regulations, medication counseling for professionals, and so on.

5. Conclusion

In summary, all indicators such as the proportion of drugs in our hospital and the use rate of antimicrobial drugs for class I incision prevention have clearly improved under the current drug control and control system, the data meet the requirements at the same time, therapeutic drug use dominates, medication problems are improved, and medical staff awareness of rational drug use is increased. This implies that the intervention has a significant influence on the hospital drug control and control system, but it also improves physicians' rational drug use.

Data Availability

All of the data in this article is actually available within the article.

Conflicts of Interest

All the researcher claims no conflicts of interests.

Acknowledgments

References

[1] P. J. Liu and G. A. Hospital, "Quality control system optimization measures of intravenous drug centralized control center," *Journal of Anhui Health Vocational & Technical College*, vol. 17, no. 3, pp. 17-18, 2018.

[2] R. Leon, "ASHP statement on hospital drug control systems," *American Journal of Health-System Pharmacy*, vol. 31, no. 12, pp. 1198–1207, 1974.

[3] R. S. Evans, D. C. Classen, and L. E. Stevens, "Using a hospital information system to assess the effects of adverse drug events," *Proceedings/ the … Annual Symposium on Computer Application [sic] in Medical Care*, pp. , 1993161–165, 1993.

[4] H. Chun-Yip, T. Kay, P. A. Demers, and V. Scott, "Antineoplastic drug contamination on the hands of employees working throughout the hospital medication system," *Annals of Occupational Hygiene*, vol. 58, no. 6, pp. 761–770, 2014.

[5] M. Uhart, L. Bourguignon, P. Maire, and M. Ducher, "Bayesian networks as decision-making tools to help pharmacists evaluate and optimise hospital drug supply chain," *European Journal of Hospital Pharmacy*, vol. 19, no. 6, pp. 519–524, 2012.

[6] E. Fukuoka, S. Kamata, K. Nakajima, T. Orii, and T. Iga, "Development and evaluation of a medication management system for rational inventory control of medicine," *Japanese Journal of Hospital Pharmacy*, vol. 27, pp. 523–530, 2001.

[7] X. Cheng, F. He, M. Si, P. Sun, and Q. Chen, "Effects of antibiotic use on saliva antibody content and oral microbiota in Sprague Dawley rats," *Frontiers in Cellular and Infection Microbiology*, vol. 12, 2022.

[8] O. N. Ang'Wa, "Evaluation of the drug supply system at Kenyatta national hospital," *Bachelor of Pharmacy 2004*.

[9] W. A. Thomas, "Drug distribution in a small hospital," *American Journal of Health-System Pharmacy*, vol. 25, no. 8, pp. 429–433, 1968.

[10] H. D. Administration, "Medical devices; general hospital and personal use devices; classification of implantable radiofrequency transponder system for patient identification and health information," *Final rule. Federal register*, vol. 69, p. 71702, 2004.

[11] B. J. Grilley, L. A. Trissel, and B. M. Bluml, "Design and implementation of an electronic investigational drug accountability system," *American Journal of Hospital Pharmacy*, vol. 48, no. 12, pp. 2616–2618, 1991.

[12] W. L. Gousse, "Computer system for unit dose drug distribution," *American Journal of Hospital Pharmacy*, vol. 35, no. 6, pp. 711–714, 1978.

[13] W. T. Sharp, P. Driver, and P. Bartlome, "Drug-usage evaluation: a system for the prospective evaluation of antibiotic utilization in minimum inhibitory concentration documented infections," *Topics in Hospital Pharmacy Management*, vol. 11, no. 2, pp. 59–69, 1991.

[14] K. Ishimoto, K. Hironaga, A. Koshiro, and S. Nakamura, "Purchasing and inventory control system of drugs utilized ABC analysis theory using personal computer," *Journal of the Nippon Hospital Pharmacists Association*, vol. 12, pp. 415–420, 1986.

[15] E. L. Lynsky, N. D. Richie, and R. L. Taylor, "A hospital narcotic control system for schedule II drugs," *Hospital Formulary*, vol. 12, no. 9, pp. 599-600, 1977.

[16] A. T. Azevedo, P. Edson, R. M. Borges, and C. C. Comini, "Drug-dispensing errors in the hospital pharmacy," *Clinics*, vol. 62, no. 3, pp. 243–250, 2007.

Retraction

Retracted: Analysis of Rotator Cuff Muscle Injury on the Drawing Side of the Recurve Bow: A Finite Element Method

Computational and Mathematical Methods in Medicine

This article has been retracted by Hindawi following an investigation undertaken by the publisher [1]. This investigation has uncovered evidence of one or more of the following indicators of systematic manipulation of the publication process:

(1) Discrepancies in scope

(2) Discrepancies in the description of the research reported

(3) Discrepancies between the availability of data and the research described

(4) Inappropriate citations

(5) Incoherent, meaningless and/or irrelevant content included in the article

(6) Peer-review manipulation

The presence of these indicators undermines our confidence in the integrity of the article's content and we cannot, therefore, vouch for its reliability. Please note that this notice is intended solely to alert readers that the content of this article is unreliable. We have not investigated whether authors were aware of or involved in the systematic manipulation of the publication process.

Wiley and Hindawi regrets that the usual quality checks did not identify these issues before publication and have since put additional measures in place to safeguard research integrity.

We wish to credit our own Research Integrity and Research Publishing teams and anonymous and named external researchers and research integrity experts for contributing to this investigation.

The corresponding author, as the representative of all authors, has been given the opportunity to register their agreement or disagreement to this retraction. We have kept a record of any response received.

References

[1] C. Guo, X. Liu, Y. Yang, D. Zhang, D. Yang, and J. Yin, "Analysis of Rotator Cuff Muscle Injury on the Drawing Side of the Recurve Bow: A Finite Element Method," *Computational and Mathematical Methods in Medicine*, vol. 2022, Article ID 8572311, 10 pages, 2022.

Research Article

Analysis of Rotator Cuff Muscle Injury on the Drawing Side of the Recurve Bow: A Finite Element Method

Cheng Guo [1,2] **Xinlong Liu** [1] **Yi Yang** [3] **Dong Zhang** [4] **Dan Yang** [2] **and Jun Yin** [1]

[1]*Capital University of Physical Education and Sports, 100191 Beijing, China*
[2]*Hebei Institute of Sports Science, 050011 Shijiazhuang Hebei, China*
[3]*Beijing Sport University, 100084 Beijing, China*
[4]*Tsinghua University, 100084 Beijing, China*

Correspondence should be addressed to Jun Yin; yinjun@cupes.edu.cn

Background. This study establishes the shoulder model on the drawing side of recurve archers by the finite element method and finds out the stress changes on the rotator cuff muscles in the position of the humerus and scapula under different stages of special techniques. The aim of this study is to investigate the mechanism of rotator cuff damage on a recurve archer's drawing arm. *Methods.* A 22-year-old healthy male's shoulder CT and MRI data were collected, and the drawing side shoulder joint finite element model was constructed, which contains the structure of the shoulder blades, clavicle, humerus, supraspinatus, infraspinatus, teres minor, and subscapularis. The humerus on the drawing arm was simulated to raising the bow, drawing, holding, and releasing on the scapula plane, and stress changes in rotator cuff muscles are analyzed. *Results.* The peak stress on the infraspinatus increased slowly, and from the start of raising the bow to hold and release, the stress peak increased from 0.007 MPa to 0.009 MPa. The peak stress on teres minor rises slowly from 0.003 MPa at the start of raising the bow to 0.010 MPa at the moment of releasing. The peak stress in the subscapularis increased from 0.096 MPa to 0.163 MPa between the start of raising the bow and releasing. The peak stress on the supraspinatus varied greatly, and from the start of raising the bow to the start of drawing, the stress peak increased markedly from 1.159 MPa to 1.395 MPa. Subsequently, the stress peak immediately decreased to 1.257 MPa at the start of holding and then increased to 1.532 MPa at releasing. *Conclusion.* The position of the humerus and scapula would change with the different stages of special techniques. It causes stress changes in the rotator cuff muscles, and when the stress accumulates over time, the shoulder 5on the drawing side will gradually become injured and dysfunctional. In combination with the depth of the structural site and the surrounding structural features, corrective exercises can be used to prevent injury to the rotator cuff muscles.

1. Introduction

Recurve bow is a static sport that requires strength and endurance in the upper shoulder girdle of the torso. The body is characterized by asymmetries in applying force and the corresponding load. To take the arrow, the athlete must demonstrate a high focus standard while executing a sequence of repetitive, smooth, and consistently accelerated arm motions. One of the most prevalent injuries sustained by archers is a shoulder injury, which may be traced back to overuse, excessive load bearing, and the resulting friction, tugging, and extrusion of tissues between shoulders [1, 2].

Repeating significant movements necessitates the use of the drawing side shoulder.

There have included the supraspinatus, infraspinatus, subscapularis, and teres minor. The rotator cuff muscle is composed of these four muscles. Furthermore, maintain dynamic stability in the shoulder joint while also helping to perform active internal rotation, external rotation, and supination of the shoulder and providing a fulcrum for the other muscles of the shoulder [3, 4].

When abnormalities in the function of the rotator cuff muscles occur, they can lead to shoulder injuries. Most recurve archers suffer from rotator cuff injuries. The rotator

Figure 1: The four distinct movements of a recurve bow: start of raising, drawing, holding, and releasing (reproduced from Cheng et al. [21]).
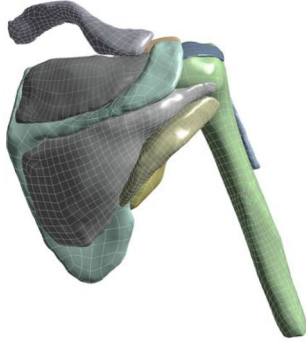
Figure 2: Model establishment of the shoulder muscles and bones.

Table 1: The material parameters of the finite element model for the shoulder.

Materials	Elastic modulus (MPa)	Poisson's ratio
Muscle belly	1.08	0.49
Muscle tendon	1200	0.4
Bone	7300	0.3

Table 2: Stress peak of the rotator cuff muscles at each characteristic action of the recurve bow (MPa).

Muscle name	Raising the bow start	Drawing start	Holding start	Releasing
Infraspinatus	0.007	0.007	0.009	0.009
Teres minor	0.003	0.004	0.005	0.010
Subscapular	0.096	0.150	0.161	0.163
Supraspinous	1.159	1.395	1.257	1.532

cuff injuries are caused by inadequate musculature and muscular strength imbalances. Inadequate muscle strength can lead to compensations in the rotator cuff muscles in a centrifugal state [5]. For example, the supraspinatus is overused when it is used for prolonged periods to simultaneously abduct the shoulder and avoid superior humeral displacement [6, 7]. In addition, when there is an imbalance in the strength of the shoulder's internal and external rotator muscles, this can lead to tendonitis in the muscle [8, 9].

Elite recurve archers spend considerable time practicing real draws to develop their feeling of movement. Up to 1000 repetitions per day are required for training with the bow, including raising, drawing, holding, and releasing the bow. Due to the apparent repetitive nature of the bow arm shoulder's motion, the rotator cuff muscles become overworked, which leads to inflammation and injury [10]. Furthermore, minimal in-depth study shows that recurve archers suffer from rotator cuff muscle damage [11]. Long-term training may cause substantial damage to the rotator cuff muscles, affecting recurve archers' ability to carry out their daily routines [12].

A finite element approach seeks to break down large objects into tiny units with primary forms so that the pattern of parameters may be modeled in a simple manner [13, 14]. The 3D parameters of soft tissue could be acquired by combining CT and MRI scan data and enhancing the geometric similarity, boundary restrictions, and load similarity of the

3D finite element model. [15]. Finite element analysis has been employed by several research organizations [16–20].

Finite element analysis was used in this work after 3D reconstruction of the humerus, scapula, and rotator cuff muscles. Recurve bow contains four specific motions, and researchers wanted to see how the rotator cuff muscle was affected by tension during each action (Figure 1). We explore the origin of rotator cuff damage in recurve archers and offer a strategy for preventing injuries due to the absence, including in research of internal alterations in those other sports biomechanical testing.

2. Materials and Methods

2.1. Subject. The test subject was a healthy male club-level archer. He was 22 years old, 178 centimeters tall, and 90 kg heavy, with no prior injury or shoulder discomfort history, and the right side is the drawing arm, trained for 2 years.

2.2. Methods. CT and MRI scanning methods were used to capture pictures of the subject in a normal anatomical position, with the right arm in a relaxed state, vertical to the shoulder joint. The rotator cuff and bone were modeled 3D using CT and MRI data (Figure 2). CT and MRI pictures were limited to one millimeter in thickness.

The motion biomechanics of recurve archers were studied in the laboratory. For this study, eight infrared high-speed motion capture lenses from Sweden (Qualisys-OQUS700) were used to get the kinematic data that was needed (acquisition frequency: 200 Hz). The individual was instructed to put on a tight shirt and warm up during the test. Reflective markers were positioned at anatomical surface markers after the stretching. Sports biomechanics were able to record it and use it as the boundary condition for a finite element simulation of bow motion.

2.2.1. Reconstruction of a 3D Model of the Drawing Arm's Shoulder Joint. For finite element analysis, Swanson Analysis, Houston, PA, USA, provided the application ANSYS19.1. Simulating a recurve bow's particular
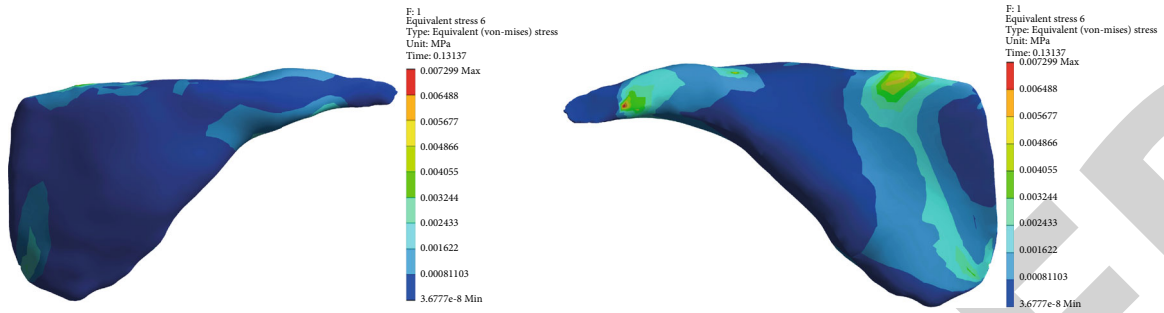
FIGURE 3: Stress changes at the start of the infraspinatus raising stage.
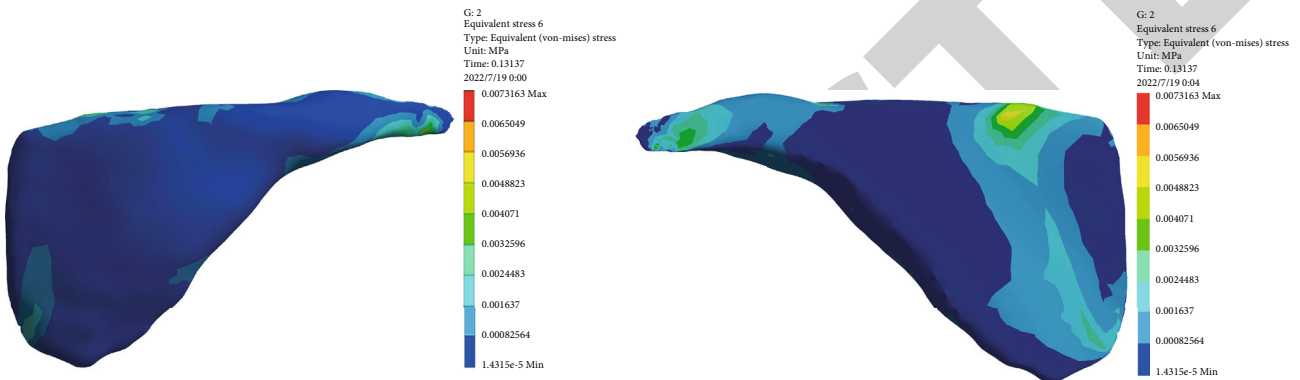
FIGURE 4: Stress changes at the start of the infraspinatus drawing stage.
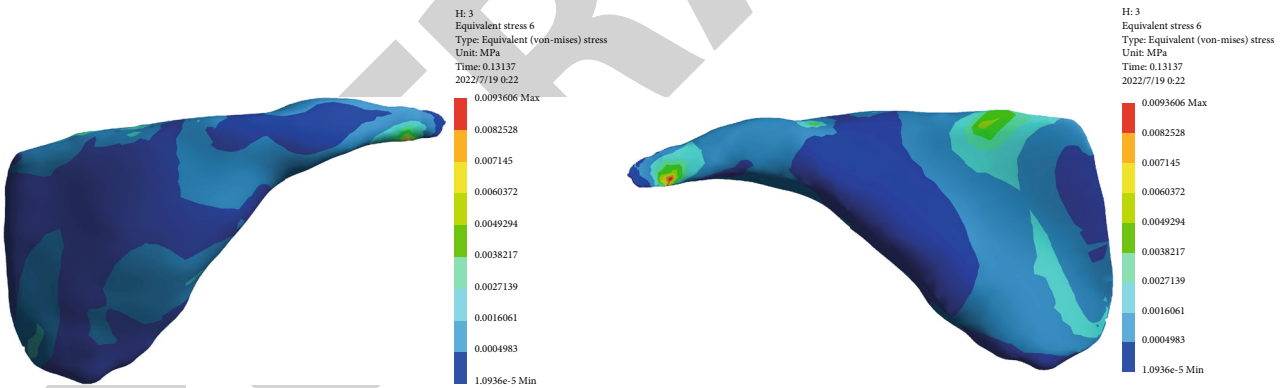
FIGURE 5: Stress changes at the start of the infraspinatus holding stage.
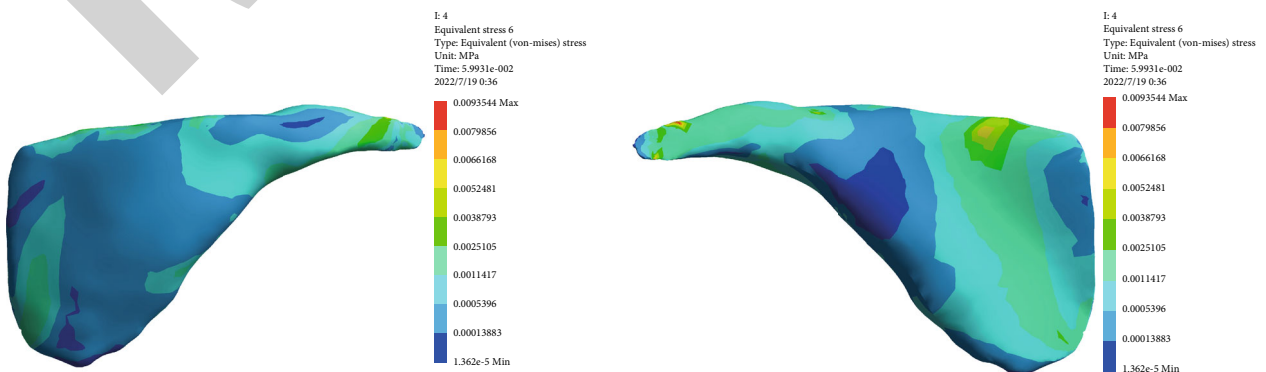
FIGURE 6: Stress changes at the moment of the infraspinatus releasing stage.
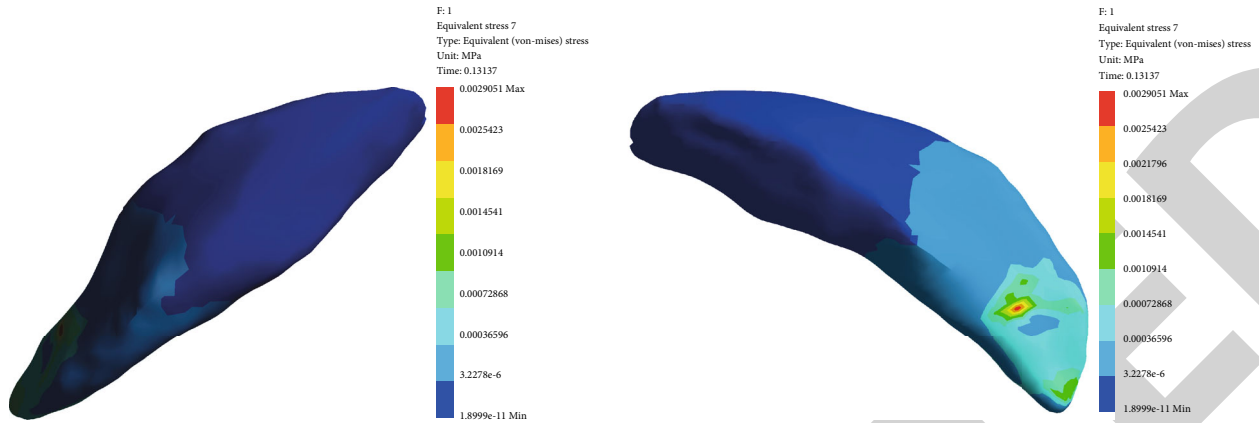
Figure 7: Stress changes at the start of the teres minor raising stage.
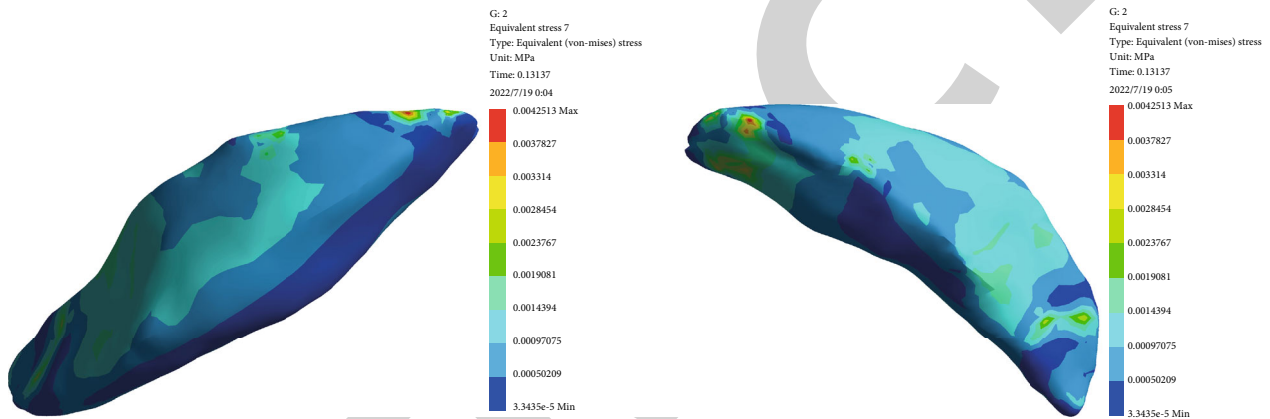
Figure 8: Stress changes at the start of the teres minor drawing stage.
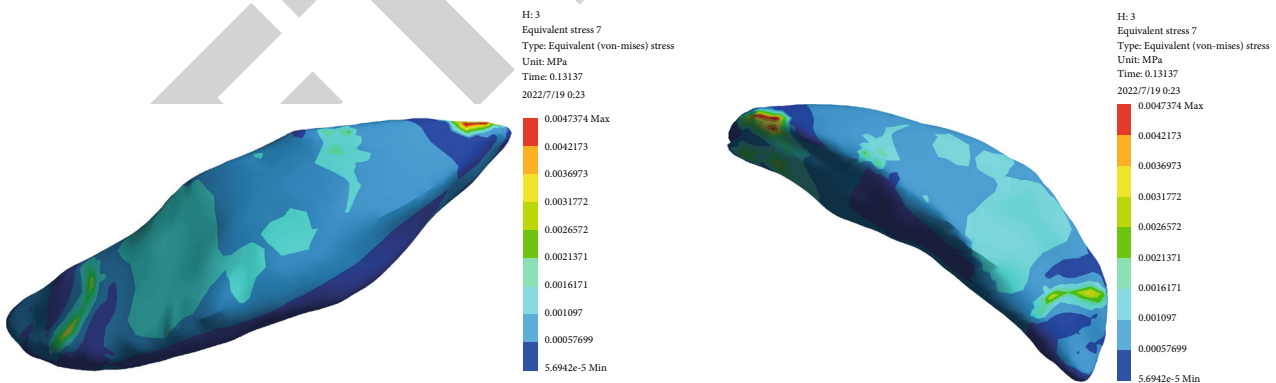
Figure 9: Stress changes at the start of the teres minor holding stage.

movement required the Static Structural module usage. Materialism's Mimics19.0 software (Leuven, Belgium) analyzed CT and MRI medical imaging data, resulting in a 3D reconstruction of the bone and the rotator cuff muscles. Bone and soft tissue were removed from each tomographic picture using software; also, a primary batch of 3D models was created in the opposite order. This was achieved by filling in the blanks on the surface of the 3D model, eliminating unwanted pixels, and smoothing out the edges to produce an

almost-perfect geometric form and structure near the 3D model in terms of genuine human tissue. The scapula, clavicle, humerus, supraspinatus, infraspinatus, teres minor, and subscapular were all included in the final construction. Next, a finite element analysis program simulated the shoulder bone and muscle models in IGES format [22].

2.2.2. Finite Element Model Reconstruction on the Drawing Side Shoulder. The biomechanical properties of the shoulder
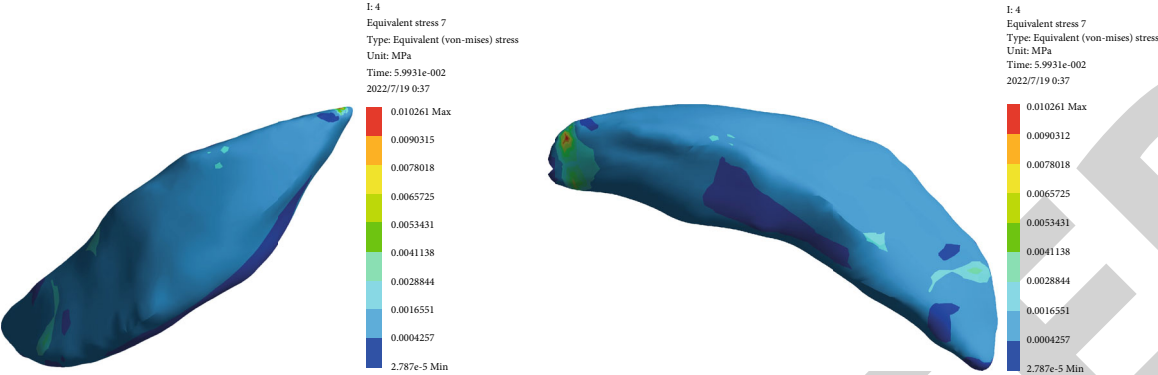
FIGURE 10: Stress changes at the moment of the teres minor releasing stage.
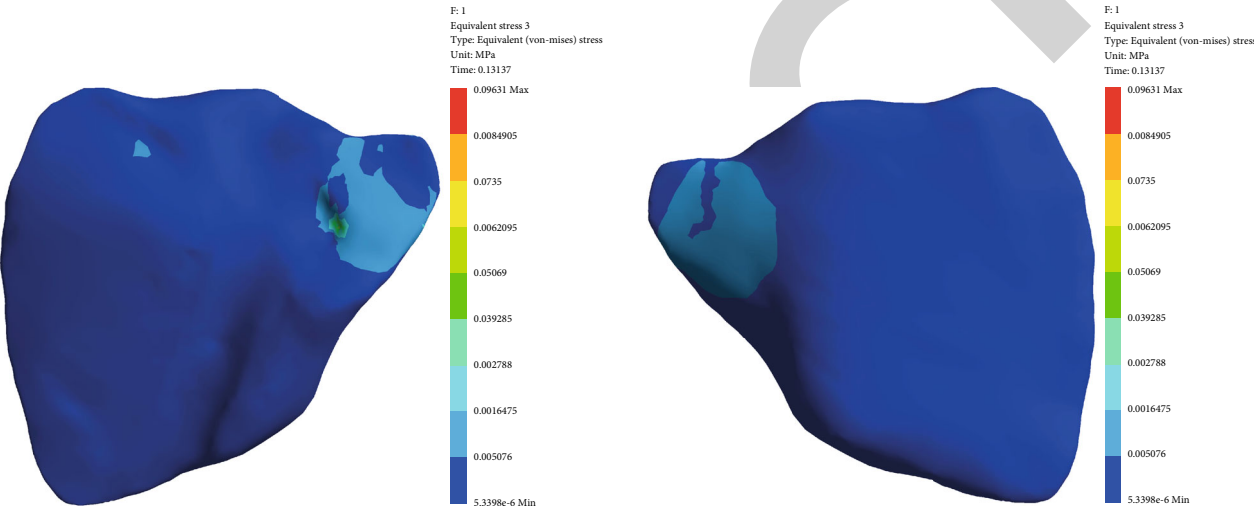
FIGURE 11: Stress changes at the start of the subscapularis raising stage.
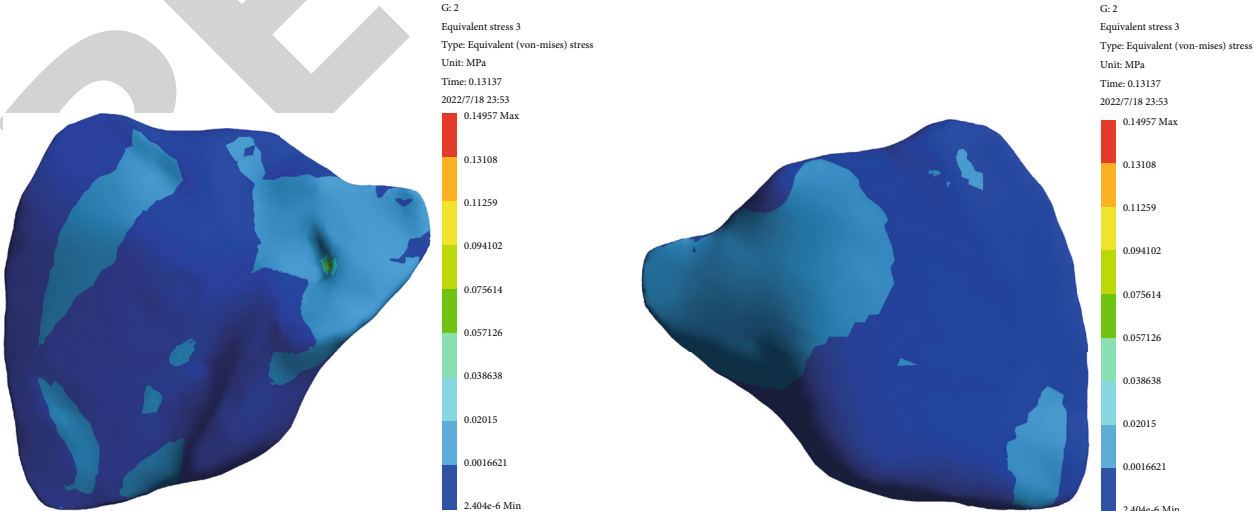
FIGURE 12: Stress changes at the start of the subscapularis drawing stage.
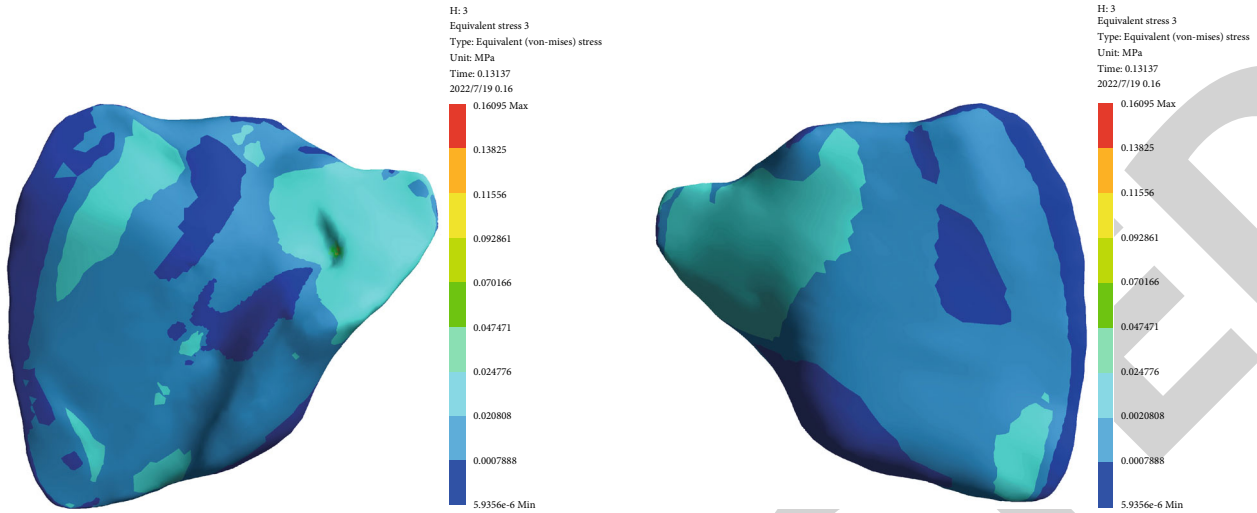
Figure 13: Stress changes at the start of the subscapularis holding stage.
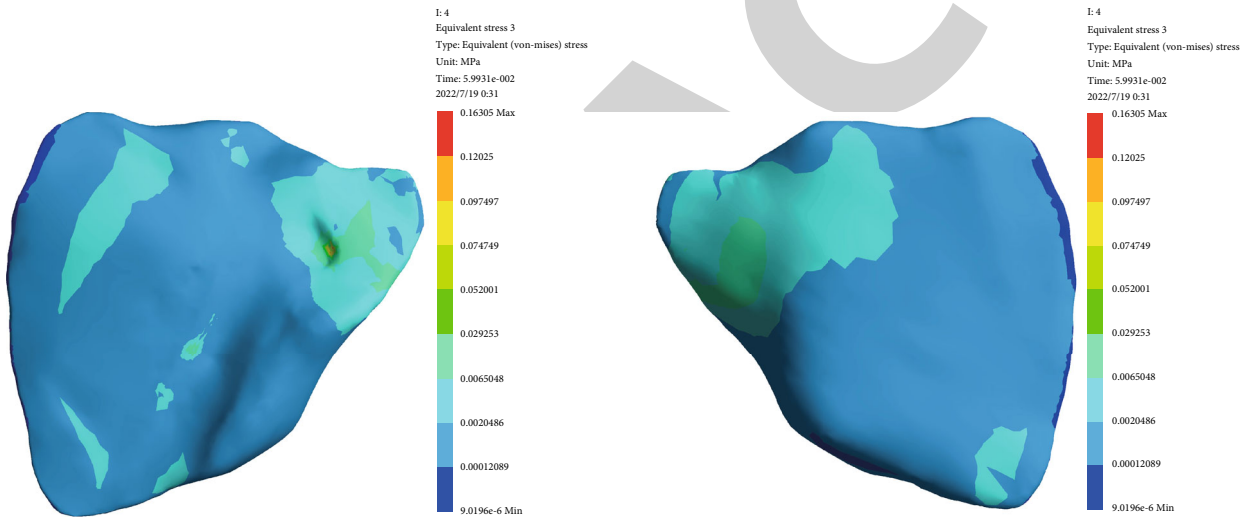
Figure 14: Stress changes at the moment of the subscapularis releasing stage.
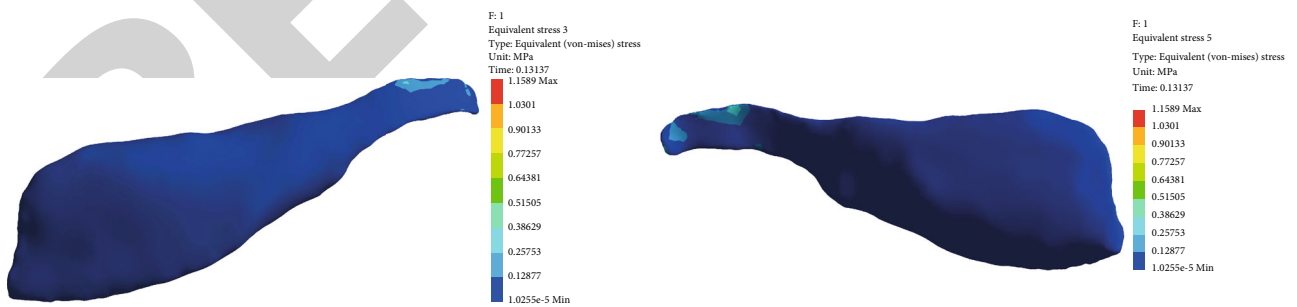
Figure 15: Stress changes at the start of the supraspinatus raising stage.

bone and muscles during the four significant recurve bow motions were examined in earlier investigations [23, 24]. The Static Structural module simulated the structural and mechanical stresses on the shoulder tissue.

The Static Structural module of the AnsysWorkbench19.1 program was used to import the existing 3D model shoulder bone and muscle files. The biomechanical test revealed the rotation angle of the humerus on the drawing arm, which was utilized to establish four separate movements. In the Ansys working interface, four linked simulation projects were formed. By studying the upper arm link's motion characteristics, it was possible to estimate
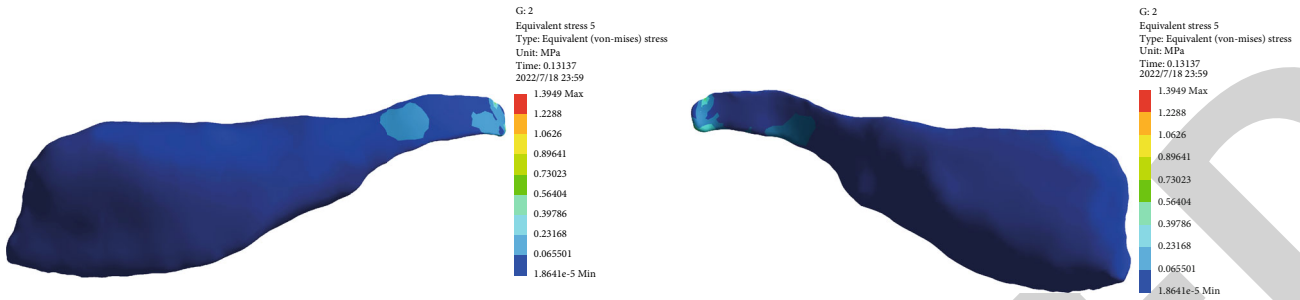
Figure 16: Stress changes at the start of the supraspinatus drawing stage.
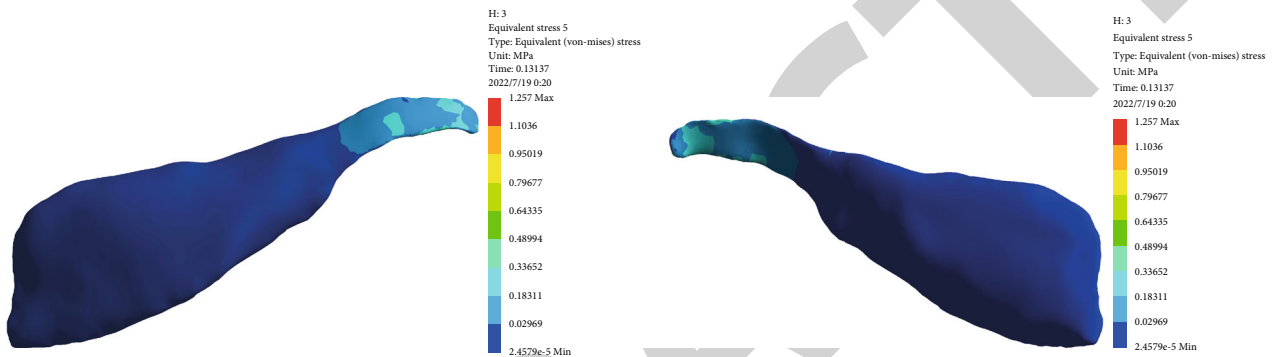
Figure 17: Stress changes at the start of the supraspinatus holding stage.
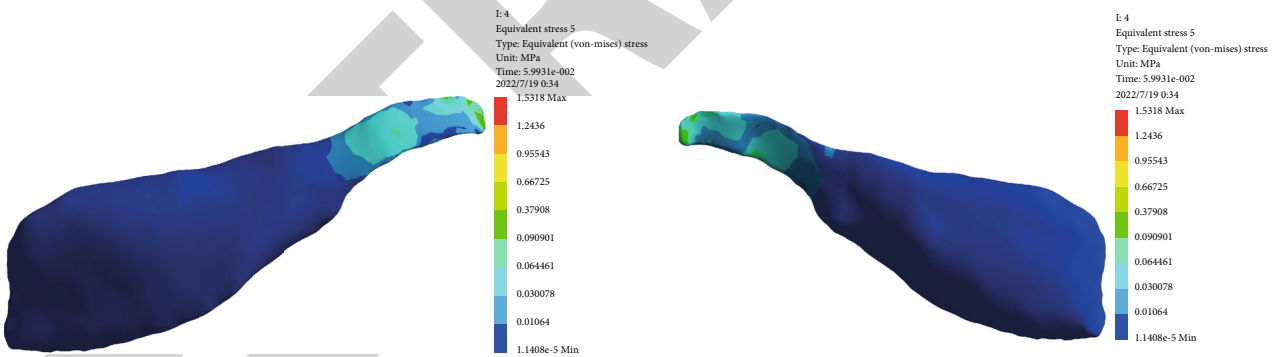
Figure 18: Stress changes at the moment of the supraspinatus releasing stage.

the humeral angle for each of the four key times [25–27]. We utilized the findings of biomechanical 3D photography to establish the joint center positions of the elbow and shoulder when the bow was raising as the humerus assumed a common anatomical condition.

As part of our finite element simulation, we modelled the biomechanical changes in the structure of the shoulder tissue at four different stages of motion: raising, drawing, holding, and releasing. This was done to refer to previous research [28–30]. Meanwhile, for muscle and bone material qualities, isotropic linear elastic materials were used (Table 1).

2.2.3. The Recurve Bow Characteristic Moment Simulation's Loading Mode. There were 1042 scapular and clavicle nodes

secured and restrained in all. Two vectors were used to produce the plane ABC: AB in conventional anatomical position and AC at a regular time.

The shoulder coordinate's origin is the shoulder joint's A-center. The negative direction of the humeral vector AC would be used to create the shoulder x-axis. The shoulder coordinate system for finite element analysis uses a y-axis parallel to plane ABC's average vector. This identifies the humerus' rotation axis and direction.

The 720-node humerus model was selected. Biomechanical testing measured the humerus rotational load around the y-axis rotation angle in the created shoulder joint coordinate system. Two space vectors were constructed based on the four usual raising, drawing, holding, and releasing

moments and the frame's shoulder joint and elbow point coordinates. The angle between the two space vectors was computed using formula (1). The angular stress of humeral rotation was then calculated using this information. The material parameters of the shoulder finite element model were determined according to previous study [21].

$$\text{available } \cos = \frac{\overrightarrow{AB} \cdot \overrightarrow{AC}}{|\overrightarrow{AB}| \cdot |\overrightarrow{AC}|}. \tag{1}$$

3. Results

The infraspinatus' peak stress gradually increased. From drawing and holding the bow until releasing it, the peak stress rose from 0.007 MPa to 0.009 MPa. The peak stress in the teres minor rises slowly from 0.003 MPa at the start of raising the bow to 0.005 MPa at the start of holding. Following this, the peak stress increased to 0.010 MPa at the point of releasing. The peak stress in the subscapularis increased from 0.096 MPa to 0.150 MPa between raising and drawing; the peak stress then continued to grow to 0.161 MPa and 0.163 MPa at the start of holding and releasing. The supraspinatus peak stress rose from 1.159 MPa to 1.395 MPa between raising and drawing; it then fell to 1.257 MPa at the start of holding and climbed to 1.532 MPa at releasing (Table 2). Stress variations at each stage are indicated in Figures 3–18.

4. Discussion

The infraspinatus, teres minor, subscapularis, and supraspinatus muscles form the dynamic stability structure of the shoulder. The rotator cuff muscles encircle the shoulder capsule and the glenoid labrum. By contracting centripetally, the rotator cuff muscles enable the joint capsule to tighten. The supraspinatus and deltoid muscles keep the shoulder joint stable during an abduction. The subscapularis allows for internal rotation of the shoulder joint, while the infraspinatus and teres minor muscles help with the external process of the shoulder joint. They are all essential muscles that stabilize the shoulder joint [31]. Their stress changes directly affect the stability of the shoulder joint.

The peak stress in the infraspinatus muscle tends to rise gently except during the drawing to holding phase when the peak stress increases more rapidly. The stress rises quickly from the drawing stage to the holding stage. This variation reflects that the specific technique requires sustained force from the infraspinatus. When the infraspinatus muscle is weak, a muscle strength imbalance occurs with the internal rotators of the shoulder (pectoralis major, latissimus dorsi, rhomboid, etc.). The state of mechanical instability of the glenohumeral joint would lead to the shoulder injury.

During the first three stages of the particular technique of the recurve, the stress on the teres minor is lower. The stress on the teres minor increases suddenly at the stage of releasing. This indicates that the teres minor needs to be activated while exerting external rotation. This makes the muscle elasticity of the teres minor strongly influence the

special techniques to recurve motion. When muscles are less flexible, this can lead to a higher risk of the teres minor injury [32].

The subscapularis muscle has the lowest stress value when raising the bowing stage. From the drawing stage, the subscapularis stress value increases and then remains at a constant level until the releasing. The specific technique of the recurve motion requires the drawing arm to be in prolonged abduction. The abduction movement causes the space below the rostral process to become narrow. The squeezed subscapularis puts stress on the tendon. This can lead to subscapularis injury [33].

The supraspinatus completes the supination of the humerus in the first three stages of the particular technique and presses down on the head of the humerus during the releasing stage. Frequent involvement of the supraspinatus in shoulder activities can put it under high tension for long periods. The supraspinatus is under increased stress for long periods, leading to muscle degeneration and injury [6]. The supraspinatus tendons can be damaged by impingement of the coracoacromial ligament and the acromion [34].

As a result, specific corrective exercises are required to enhance the force and prevent deformation and other problems. It improves muscle efficiency and prevents injury by reducing stress on the rotator cuff muscles, as well as helping to improve the performance of recurve archers.

5. Conclusions

After obtaining data from CT and MRI scans, a finite element model of the shoulder was developed, representing the in vivo glenohumeral physiological characteristic on the drawing side of the recurve archers [36].

Shoulder instability and injury can occur when the infraspinatus muscle strength decreases due to poor training. The sudden increase in stress of the teres minor at releasing indicates that it needs to be activated quickly. A decrease in muscle elasticity in the teres minor can lead to injury. The subscapularis is susceptible to compression and consequent damage due to the anatomy of the shoulder in which it is located. Supraspinatus is prone to acromioclavicular impingement and tendon degeneration.

The supraspinatus and subscapularis could be released to enhance the posture of the humeral head during abduction and the area beneath the acromion. This may help avoid muscle damage and dysfunction when combined with the depth and surroundings of the structural features. Corrective exercise can also enhance muscular strength, contributing to the recurve archer's improper and twisted shoulder action.

5.1. Limitation of the Study. The simulation results obtained in this research for the rotator cuff muscles are reliable to a certain extent, but further confirmation is needed with scientific cadaver studies.

Data Availability

The data can be obtained through the responsible author.

Ethical Approval

The ethical committee ethically approved the study of the Hebei Shooting and Archery Centre (ethical approval number: 2019A63).

Consent

All the study participants signed an informed consent form.

Conflicts of Interest

The authors declare that they have no conflicts of interest.

References

[1] D. L. Mann and N. Littke, "Shoulder injuries in archery," *Canadian journal of sport sciences = Journal canadien des sciences du sport*, vol. 14, no. 2, pp. 85–92, 1989.

[2] A. Bac, U. Niemiec, and E. Golec, "Long-term evaluation of treatment of traumatic injuries and motor organ overuse syndromes in archers," *Fizjoterapia Polska*, vol. 11, no. 2, pp. 155–168, 2011.

[3] J. I. N. Baoyong, L. I. Yan, M. A. Lin, Z. H. O. U. Binghua, and T. A. N. G. Kanglai, "Clinical application of rebalancing theory of shoulder joint stabilization mechanism in the treatment of shoulder instability and motor dysfunction," *Chinese Journal of Restorative and Reconstructive Surgery*, vol. 36, no. 3, pp. 380–385, 2022.

[4] X. Cai-Kun, Y. Guang-Xiong, and L. Open, "The effect of vibratory bar training on shoulder joint stability in the fixation-spreading phase of recurve bow athletes," *Sports Research*, vol. 4, pp. 77–82, 2018.

[5] D. M. Mulla, J. N. Hodder, M. R. Maly, J. L. Lyons, and P. J. Keir, "Glenohumeral stabilizing roles of the scapulohumeral muscles: implications of muscle geometry," *Journal of Biomechanics*, vol. 100, no. 109589, p. 109589, 2020.

[6] T. Ishigaki, M. Hirokawa, Y. Ezawa, and M. Yamanaka, "Supraspinatus tendon changes and glenohumeral range of motion in college baseball players," *International Journal of Sports Medicine*, vol. 43, no. 2, pp. 145–150, 2022.

[7] Z. H. O. U. Pinghui, Z. H. O. U. Mijuan, and H. U. Pu, "Efficacy of ultrasound-guided injection in the treatment of periarticular bursitis of the shoulder," *Journal of Practical Medical Imaging*, vol. 21, no. 1, pp. 22–24, 2020.

[8] T. Q. Lee, "Editorial commentary: precise repair of partial subscapularis tendon tears is essential," *The Journal of Arthroscopic & Related Surgery*, vol. 35, no. 5, pp. 1314-1315, 2019.

[9] A.-P. Zou, F.-M. An, and Y.-Q. Xin, "Study on the diagnostic value of the supraspinatus tendon tear check test," *China Orthopaedic Injury*, vol. 35, no. 3, pp. 220–224, 2022.

[10] G. Akhoury, "Prevalence of shoulder pain in competitive archery," *Asian Journal of Sports Medicine*, vol. 8, no. 1, 2017.

[11] W. A. N. G. Shi-Kun, Y. A. N. G. Chen, and K. O. N. G. Xi-Liang, "A review of research progress on shoulder joint injuries in recurve archery athletes," *Bulletin of Sports Science and Technology Literature*, vol. 29, no. 6, 2021.

[12] G. Kocaman, E. Atay, M. Alp, and G. Suna, "Site and type assessments of sports injuries in archers," *Spor Hekimligi Dergisi*, vol. 53, no. 1, pp. 1–8, 2018.

[13] F. Yubo and D. E. N. G. Xiaoyan, *Modeling, Simulation and Application of Biomechanical Technology*, vol. 12, Shanghai Jiao Tong University Press, Shanghai, 2017.

[14] Z. Xizheng and H. Kingston, *Biomechanics of Bone and Joint*, vol. 12, Shanghai Jiao Tong University Press, Shanghai, 2017.

[15] B. Chunyu and M. Qinghua, "Establishment and analysis of biomechanical model of human knee joint based on finite element method," *Journal of Wuhan Physical Education University*, vol. 44, no. 5, 2010.

[16] N. Maurel, A. Diop, and J. Grimberg, "A 3D finite element model of an implanted scapula: importance of a multiparametric validation using experimental data," *Journal of Biomechanics*, vol. 38, no. 9, pp. 1865–1872, 2005.

[17] B. J. Ellis, R. E. Debski, and S. M. Moore, "Methodology and sensitivity studies for finite element modeling of the inferior glenohumeral ligament complex," *Journal of Biomechanics*, vol. 40, no. 3, pp. 603–612, 2007.

[18] S. Gupta and F. C. T. van der Helm, "Load transfer across the scapula during humeral abduction," *Journal of Biomechanics*, vol. 37, no. 7, pp. 1001–1009, 2004.

[19] P. Büchler, N. A. Ramaniraka, L. R. Rakotomanana, J. P. Iannotti, and A. Farron, "A finite element model of the shoulder: application to the comparison of normal and osteoarthritic joints," *Clinical Biomechanics*, vol. 17, no. 9-10, pp. 630–639, 2002.

[20] P. Buchler and A. Farron, "Benefits of an anatomical reconstruction of the humeral head during shoulder arthroplasty: a finite element analysis," *Clinical Biomechanics*, vol. 19, no. 1, pp. 16–23, 2004.

[21] C. Guo, K. Liu, Y. Yang, W. Jin, and J. Yin, "Study of damage to the drawing arm subacromial bursa in recurve archers based on a finite element model," *Journal of Men's Health*, vol. 18, no. 5, p. 123, 2022.

[22] Z. Jing, G. Yuan, and Z. Xushu, "Finite element analysis of the shoulder during lateral impact," *Journal of Taiyuan University of Technology*, vol. 49, no. 6, pp. 886–892, 2018.

[23] J. Ma, H. Xinping, and Z. Yan, "Finite element analysis of the shoulder during lateral impact," *Journal of Qingdao Technological University*, vol. 1, pp. 98–102, 2008.

[24] M. M. Islan, U. E. Lechosa, and H. F. Blaya, "Behavior under load of a human shoulder: finite element simulation and analysis," *Journal of Medical Systems*, vol. 43, no. 5, 2019.

[25] M. Zheng, Z. Zou, P. J. Bartolo, C. Peach, and L. Ren, "Finite element models of the human shoulder complex: a review of their clinical implications and modelling techniques," *Biomedical Engineering*, vol. 33, no. 2, 2017.

[26] Y. Yang, "Model simulation of relationship between motion amplitude and motion injury of joint," *Computer simulation*, vol. 31, no. 7, pp. 391–394, 2014.

[27] L. Li, L. Shiwei, and W. Fang, "Finite element analysis of rotator cuff biomechanics in humeral abduction," *Chinese Journal*

Retraction

Retracted: KIF11 Is a Promising Therapeutic Target for Thyroid Cancer Treatment

Computational and Mathematical Methods in Medicine

This article has been retracted by Hindawi following an investigation undertaken by the publisher [1]. This investigation has uncovered evidence of one or more of the following indicators of systematic manipulation of the publication process:

(1) Discrepancies in scope

(2) Discrepancies in the description of the research reported

(3) Discrepancies between the availability of data and the research described

(4) Inappropriate citations

(5) Incoherent, meaningless and/or irrelevant content included in the article

(6) Peer-review manipulation

The presence of these indicators undermines our confidence in the integrity of the article's content and we cannot, therefore, vouch for its reliability. Please note that this notice is intended solely to alert readers that the content of this article is unreliable. We have not investigated whether authors were aware of or involved in the systematic manipulation of the publication process.

In addition, our investigation has also shown that one or more of the following human-subject reporting requirements has not been met in this article: ethical approval by an Institutional Review Board (IRB) committee or equivalent, patient/participant consent to participate, and/or agreement to publish patient/participant details (where relevant).

Wiley and Hindawi regrets that the usual quality checks did not identify these issues before publication and have since put additional measures in place to safeguard research integrity.

We wish to credit our own Research Integrity and Research Publishing teams and anonymous and named external researchers and research integrity experts for contributing to this investigation.

The corresponding author, as the representative of all authors, has been given the opportunity to register their agreement or disagreement to this retraction. We have kept a record of any response received.

References

[1] Y. Han, J. Chen, D. Wei, and B. Wang, "KIF11 Is a Promising Therapeutic Target for Thyroid Cancer Treatment," *Computational and Mathematical Methods in Medicine*, vol. 2022, Article ID 6426800, 8 pages, 2022.

Research Article

KIF11 Is a Promising Therapeutic Target for Thyroid Cancer Treatment

Yue Han,[1] Jing Chen,[2] Dianjun Wei [iD],[3] and Baoxi Wang [iD][3]

[1]*Department of Clinical Laboratory, The Secondary Hospital of Tianjin Medical University, Tianjin, China*
[2]*Department of Pancreatic Cancer, Tianjin Tumor Hospital, Tianjin, China*
[3]*Department of Clinical Laboratory, Hebei Yanda Hospital, Yanda International Health City, Sibilan Road, Yanjiao Economic and Technological Development Zone, Langfang, 065201 Hebei Province, China*

Correspondence should be addressed to Dianjun Wei; weidianjun01@163.com and Baoxi Wang; wangbaoxi2002@163.com

Objective. To assess KIF11 expression in human thyroid tumor tissues and further evaluate its involvement in thyroid cancer. *Methods*. The expression of KIF11 in 71 cases of thyroid carcinoma as well as corresponding tissues was detected by the immunohistochemical (IHC) method. Patients were divided into the high KIF11 expression as well as low expression groups based on the staining levels. In addition, to study the relationship between the expression of KIF11 as well as clinicopathological features, the effects of KIF11 were detected on the proliferation, apoptosis, and cell cycle of two types of thyroid cancer cells, TPC-1 and KTC-1, through colony formation assays, MTT assays, and FCM assays, respectively. We further assessed the potential effects of KIF11 on tumor growth using an animal model. *Results*. The significantly high expression of KIF11 in thyroid tumor tissues was revealed, and the correlations between KIF11 expression levels as well as clinical pathological features (T stage and intraglandular dissemination) of patients were revealed. We further noticed that KIF11 knockdown remarkably suppressed thyroid cancer cell proliferation as well as induced cell apoptosis of thyroid cancer cells. Additionally, KIF11 contributed to tumor growth of thyroid cancer cells in mice. *Conclusions*. We noticed the involvement of KIF11 in the progression of thyroid cancer.

1. Introduction

Thyroid cancer accounts for 1% of all malignant tumors in the body [1], with low malignancy as well as slow progression [2, 3]. However, its growth rate is among the highest among all solid tumors [4–6]. For metastatic thyroid cancer, the existing treatment methods cannot meet the clinical needs, while targeted therapy shows strong advantages [7]. Several targeted therapeutic drugs, such as vandetanib and sorafenib, have been used to treat this type of cancer [8], whereas more effective therapeutic targets are urgently needed.

Kinesin family member 11 (KIF11) is a molecular motor protein involved in many cellular processes [9, 10]. KIF11 could affect the separation of centrosomes as well as the formation of the spindle [11, 12]. In addition, a previous study indicated that the depletion of KIF11 led to cell division defects and cell cycle arrest, so as to induce the apoptosis of cells [13]. As was known, KIF11 affected cell migration through the regulation of axonal branching and growth cone motility in a non-mitosis-dependent manner [14].

KIF11 affected the prognosis of multiple types of cancers [15–18]. The inhibitor of KIF11, K858, could induce apoptosis and also survivin-related chemoresistance in breast cancer cells [19]. In addition, several compounds that inhibit KIF11 have entered Phase I or II clinical trials as monotherapies [19]. Although KIF11 plays a critical role in a variety of tumors, its potential effects on thyroid cancer remain unclear.

This study was aimed at investigating the expression of KIF11 in thyroid cancer tissues and clarifying its effects on the progression of thyroid cancer. We found that KIF11 was highly expressed in human thyroid cancer tissues. KIF11 knockdown remarkably suppressed thyroid cancer

cell proliferation as well as induced cell apoptosis of thyroid cancer cells, suggesting that KIF11 may be a potential therapeutic target for thyroid cancer.

2. Materials and Methods

2.1. Antibodies, Primers, and Plasmids. Antibodies used are anti-KIF11 antibody (for immunohistochemical, 1 : 100 dilution, for immunoblot, 1 : 1000 dilution, ab5694, Abcam, Cambridge, UK) and anti-β-actin (1 : 2000 dilution, ab8226, Abcam, Cambridge, UK).

Ready-to-package AAV shRNA clone for KIF11 was bought from Addgene; the targeted sequences were as follows: 5′-AATAGTAGAATGTGATCCTGTAC-3′.

2.2. Human Tissue Samples and IHC Assays. A total of 71 human thyroid cancer tissues and adjacent nontumor tissues were collected from the patients receiving surgical resection in our hospital from September 2012 to May 2022 (Table 1). Tumor tissues were isolated from mice in the tumor growth assays.

Sample sections were fixed with 4% PFA for 25 min and subsequently blocked with 2% BSA for 20 min. Sections were incubated with KIF11 antibodies for 2 h. Subsequently, the slices were incubated with biotin-labeled secondary antibody for 1.5 h, and diaminobenzidine was used as a chromogen substrate.

2.3. Cell Culture and Transfection. TPC-1 and KTC-1 human thyroid cancer cells were bought from ATCC. TPC-1 cells were maintained in high-glucose DMEM culture medium (Gibco, USA), and KTC-1 cells were maintained in F-12K culture medium (Gibco, USA), respectively, with 10% of fetal bovine serum at 37°C in a 5% CO_2 incubator.

2.4. Quantitative PCR Assay. This experiment was performed according to the previous study [20]. The TRIzol reagent (15596026, Invitrogen, Carlsbad, CA, USA) was used to extract total RNA. Then, the total RNA was reverse-transcribed by M-MLV (M1701, Promega, Wisconsin, USA).

Total RNA was reverse-transcribed to produce cDNA by the cDNA synthesis system. KIF11 expression was normalized to that of GAPDH.

2.5. Immunoblot Assays. This experiment was performed according to the previous study [20]. Cells or tissues were lysed in RIPA Buffer (9800, Cell Signaling, MA). Then, the samples were analyzed with 8% SDS-PAGE. Subsequently, the polyvinylidene fluoride (PVDF) membranes were blocked with 5% milk and then incubated with the primary antibodies as well as HRP-conjugate secondary antibodies for 2 h, respectively. Signals were visualized with an ECL kit.

2.6. Colony Formation Assays. Approximately 500 TPC-1 and KTC-1 cells were seeded per well (6-well plate). The medium was refreshed every 3 days. After 14 days, cells were fixed with methanol as well as stained with 0.1% crystal violet for 30 min and washed.

2.7. MTT Assays. Thyroid cancer cells were plated into 96-well plates with a density of about 1000 cells each well. Cells were then incubated with MTT for 4 h and removed. Then, 150 μL dimethyl sulfoxide (DMSO) was added, and the OD570 value was measured.

2.8. Cell Cycle Assays. Thyroid cancer cells were fixed with 70% ethyl alcohol for 24 h at -20°C and incubated with 50 μg/mL propidium iodide (PI) at 37°C for 30 min; then, the samples were analyzed using FACS (Beckman Coulter, CA).

2.9. Cell Apoptosis Assays. Cells were resuspended in 100 μL binding buffer with 5 μL of annexin V-FITC and incubated for 10 min. Subsequently, 5 μL of PI solution was added, and cells were incubated for another 5 min.

2.10. Tumor Growth Assays. All animal assay processes were approved by the Animal Ethical and Welfare Committee (AEWC) in Tianjin key laboratory of radiation medicine and molecular nuclear medicine (SYXK-2019-0002). TPC-1 cells were stably transfected with control or KIF11 shRNA. Then, approximately $2 * 10^6$ cells were subcutaneously implanted into athymic nude mice. After 2 weeks, tumors began to be formed and then were isolated, and the volume was measured every 3 days.

2.11. Statistics. GraphPad Prism 5.0 software (GraphPad, USA) was used. All data were represented as the mean ± standard deviation (SD). The correlation between clinical data and KIF11 expression was calculated using χ^2 analysis. ∗ indicates $p < 0.05$ and is considered significant.

3. Results

3.1. KIF11 Was Highly Expressed in Human Thyroid Tumor Tissues. To explore the expression and the performance of KIF11 in thyroid cancer patients, we first detect the expression of KIF11 in different types of cancers. We noticed the high expression of KIF11 in several types of cancers (Figure 1). The mRNA levels of KIF11 were also obviously high (Figure 2(a)). We further noticed that the expression of KIF11 was correlated with the disease-free survival rate of patients (Figure 2(b)).

The expression of KIF11 was detected using tumor tissues and corresponding tissues of thyroid cancer patients in our hospital. Compared with the adjacent tissues, the tumor tissues showed an obviously high KIF11 expression (Figures 3(a) and 3(b)).

3.2. The Clinical Significance Analysis between KIF11 Expression and the Clinical-Pathological Features of Patients with Thyroid Cancer. To conduct the analysis, a total number of 71 tumor tissue samples from patients who underwent thyroid cancer were manually classified into the KIF11 low and high expression groups based on the expression levels (Figure 3(a) and Table 1). We noticed that 14 patients exhibited low expression of KIF11, whereas 57 showed high KIF11 expression (Table 1).

TABLE 1: Relationships of KIF11 and clinicopathological characteristics in 71 patients.

Feature	All $n = 71$	KIF11 expression		χ^2	p
		Low $n = 14$	High $n = 57$		
Age (year)				2.045	0.153
<45	24	7	17		
≥45	47	7	40		
Gender				1.701	0.192
Male	14	5	9		
Female	57	9	48		
T stage				6.751	0.009*
T_1-T_2	29	10	19		
T_3-T_4	42	4	38		
Lymph node metastasis				0.031	0.860
Yes	34	7	27		
No	37	7	30		
Intraglandular dissemination				6.675	0.010*
Yes	32	2	30		
No	39	12	27		

PROTEIN EXPRESSION[i]

Colorectal cancer   Breast cancer   Prostate cancer   Lung cancer   Liver cancer

PROTEIN EXPRESSION SUMMARY [i]

Organ   Expression   Alphabetical

HPA006916   HPA010568   CAB017617

Malignant cells showed moderate to strong cytoplasmic immunoreactivity. Malignant lymphomas and renal cancers were in general weakly stained or negative.
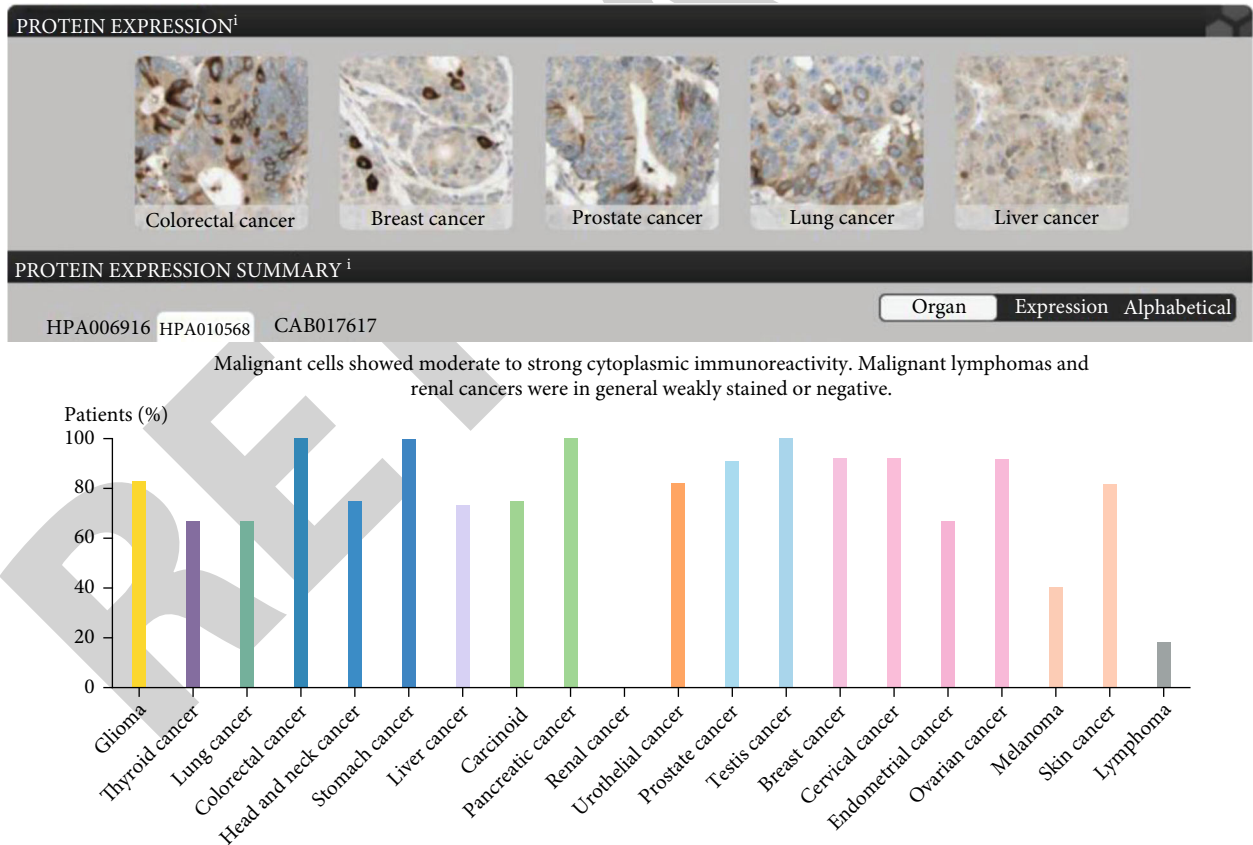
FIGURE 1: KIF11 expression in different types of cancer tissues according to TCGA database.

We then analyzed the clinical-pathological significance between KIF2A expression and clinical features of patients. According to the results, no obvious clinical correlation was found in features including patient age ($p = 0.153$), gender ($p = 0.192$), and lymph node metastasis ($p = 0.860$) between the KIF11 low and high expression groups (Table 1). Notably, our results showed that KIF11 expression was significantly related to T stage ($p = 0.009^*$) and

(a)

(b)
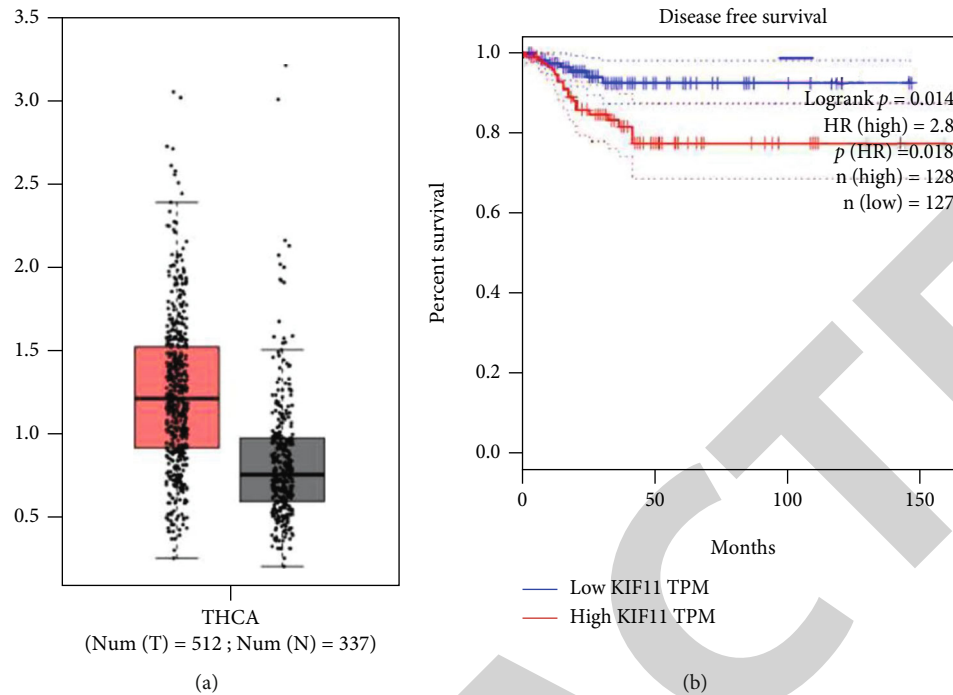
Figure 2: KIF11 expression in tumor tissues and normal tissues according to the GEPIA database.

(a)

(b)
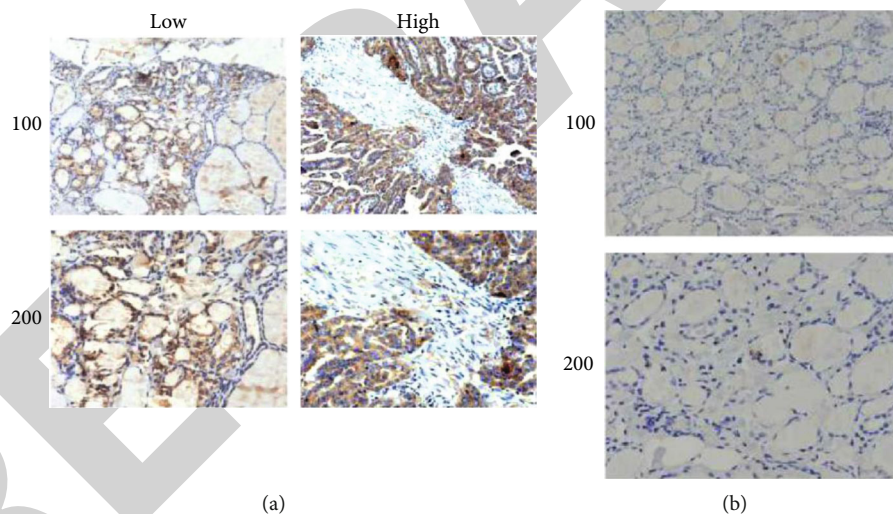
Figure 3: KIF11 was highly expressed in human thyroid tumor tissues. (a) The representative photographs of IHC assays showed the expression of KIF11 in thyroid cancer tissues (100x and 200x magnification, respectively). (b) IHC assays were performed to exhibit KIF11 expression levels in adjacent tissues, and the representative photographs are shown (100x and 200x magnification, respectively). Scale bar, 50 μm.

intraglandular dissemination ($p = 0.010^*$) (Table 1). We therefore indicated that KIF11 expression levels were associated with clinical features including T stage and intraglandular dissemination of thyroid cancer patients.

3.3. KIF11 Fascinates Proliferation and Suppresses Apoptosis of Thyroid Cancer Cells In Vitro. To explore the effects of KIF11 on the progression of thyroid cancer in vitro, shRNA plasmids specifically targeting KIF11 were used to deplete KIF11 in two types of thyroid cancer cell lines, TPC-1 and KTC-1 cell lines. Quantitative PCR (Figure 4(a)) and immu-

noblot (Figure 4(b)) assays were, respectively, performed. The transfection of KIF11 shRNA plasmids effectively decreases its expression in both TPC-1 and KTC-1 cells, respectively.

Subsequently, to explore the possible involvement of KIF11 in the proliferation of thyroid cancer cells, colony formation assays and MTT assays were performed. We found that ablation of KIF11 dramatically decreased the colony numbers of TPC-1 and KTC-1 cells, respectively (Figure 5(a)). Similarly, through MTT assays, we noticed that the OD value (570 nm wavelength) of KIF11-

(a)

(b)
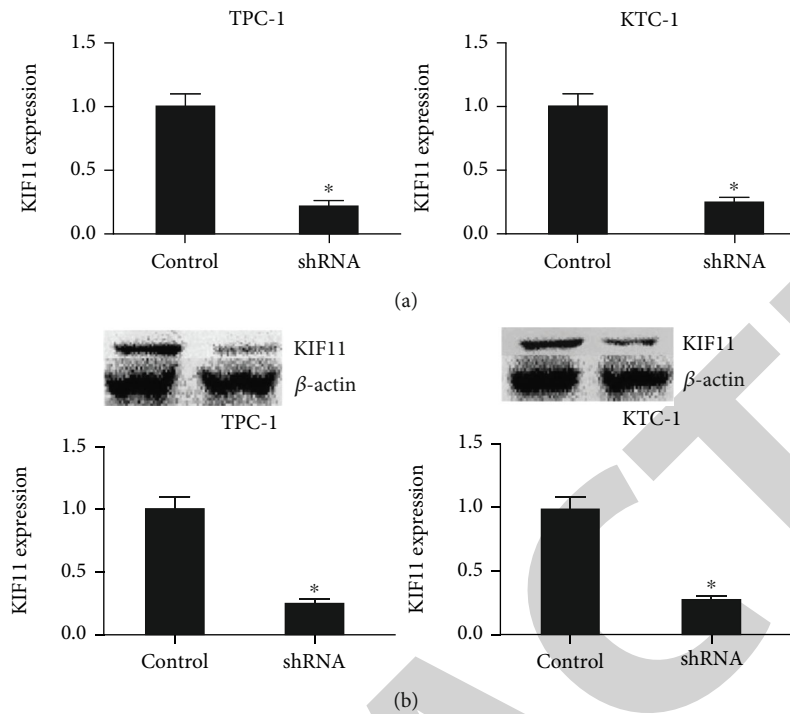
Figure 4: The expression levels of KIF11 were effectively decreased in both TPC-1 and KTC-1 cells caused by the transfection of KIF11 shRNA plasmids. (a) The results of quantitative PCR assays showed the obviously decreased expression levels of KIF11 caused by the transfection of its shRNA plasmids in TPC-1 and KTC-1 cells, respectively. (b) Immunoblot assays showed KIF11 expression levels upon the transfection of control or KIF11 shRNA plasmids in both TPC-1 and KTC-1 cells. Results are presented as the mean ± SD, $^*p < 0.05$.

knockdown groups was obviously decreased after 48 hours in both TPC-1 and KTC-1 cells (Figure 5(b)).

We then performed FCM assays to detect the effects of KIF11 on the apoptosis of TPC-1 and KTC-1 cells. The ablation of KIF11 obviously induced apoptosis in TPC-1 and KTC-1 cells (Figure 5(c)). We also assessed whether KIF11 affected the cell cycle of thyroid cancer cells and revealed that KIF11 depletion obviously induced the arrest of the cell cycle in TPC-1 and KTC-1 cells (Figure 5(d)).

3.4. KIF11 Contributes to Tumor Growth of Thyroid Cancer Cells in Mice. Tumor growth assays were then performed. TPC-1 cells were infected with control or KIF11 shRNA lentivirus and injected into nude mice. After 2 weeks, tumors began to be formed and were isolated every 3 days and photographed, and the volume of tumors was measured. After 29 days, all tumors were isolated. Representative tumors and the growth curve are all exhibited in Figure 6(a). The volume of tumors in the KIF11 knockdown groups was significantly smaller than control (Figure 6(a)). The silencing of KIF11 in tumor tissues from the depletion groups was confirmed (Figure 6(b)).

4. Discussion

Advanced thyroid cancer is still challenging due to the high metastasis and the lack of effective therapy options [21, 22]. The possible role of KIF11 in the progression of cancers has been widely revealed [23]. Firstly, we found the high expression of KIF11 in thyroid cancer tissues through IHC assays.

We also found the correlation between KIF11 and the clinical features of patients. Furthermore, KIF11 depletion led to proliferation inhibition, induced cell apoptosis, and the arrest of cell cycle. Our in vivo results showed that KIF11 ablation suppressed tumor growth in mice.

KIF11 was involved in the progression of multiple types of cancers [17, 23, 24]. This is similar to our results for thyroid cancer [18]. In addition, KIF11 also affected the migration of ovarian cancer cells, which was promoted by death receptor 6 (DR6) [17]. We next should detect whether KIF11 affects the migration of thyroid cancer cells.

Indeed, this therefore resulted in the arrest of cell cycle and the induction of apoptosis, which was also found in this study. Previous studies also revealed the mitosis-independent functions of KIF11, such as neuronal growth cone extension and migration, suggesting that KIF11 might affect the activity of thyroid cancer cells in multiple modes of regulation [25, 26]. However, the precise molecular mechanism underlying KIF11 promoting progression needs further study.

In addition to KIF11, other members of the KIF family could affect the progression and development of cancer; most of them could be potential cancer molecular targets [20]. A previous study indicated that KIF14 could contribute to the growth of hepatocellular carcinoma (HCC) [27]. KIF4A, KIF14, and KIF20A were shown to be highly expressed in many types of cancers [24, 28–30]. Our study investigated another member of the KIF family, KIF11, affecting the proliferation and apoptosis of thyroid cancer cells.

(a)

(b)

(c)

(d)
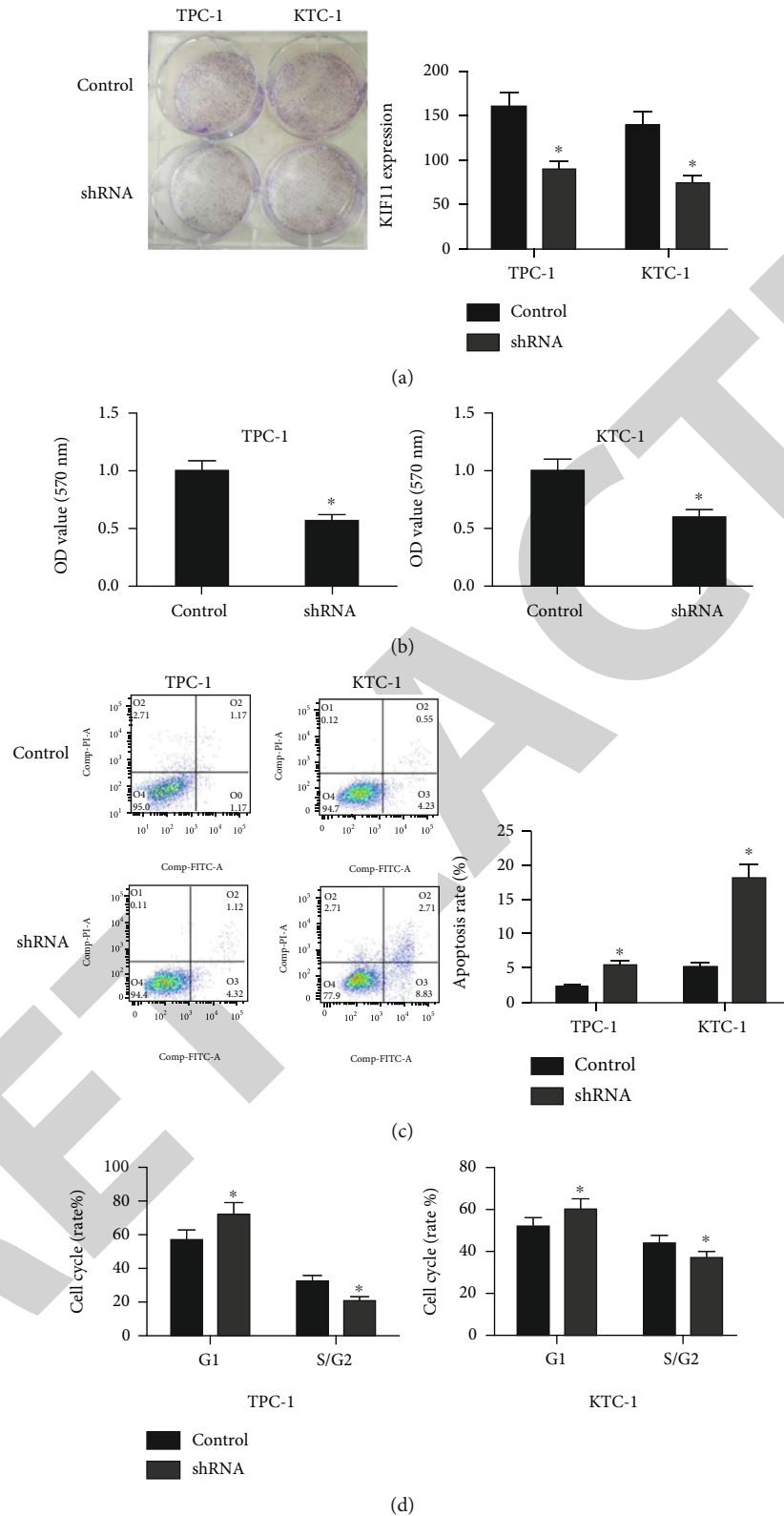
FIGURE 5: KIF11 fascinates thyroid cancer cell proliferation and suppresses cell apoptosis in vitro. (a) Colony formation assays were conducted using TPC-1 and KTC-1 cell transfection, and the number of colonies was counted. Scale bar, 5 mm. (b) MTT assays showed the OD value at 570 nm wavelength of KIF11-depleted cells. (c) FCM assays confirmed the effects of KIF11 depletion on the apoptosis in TPC-1 and KTC-1 cells. (d) FCM assays showed that KIF11 ablation led to the arrest of cell cycle in TPC-1 and KTC-1 cells. Results are presented as the mean ± SD, $^{*}p < 0.05$.
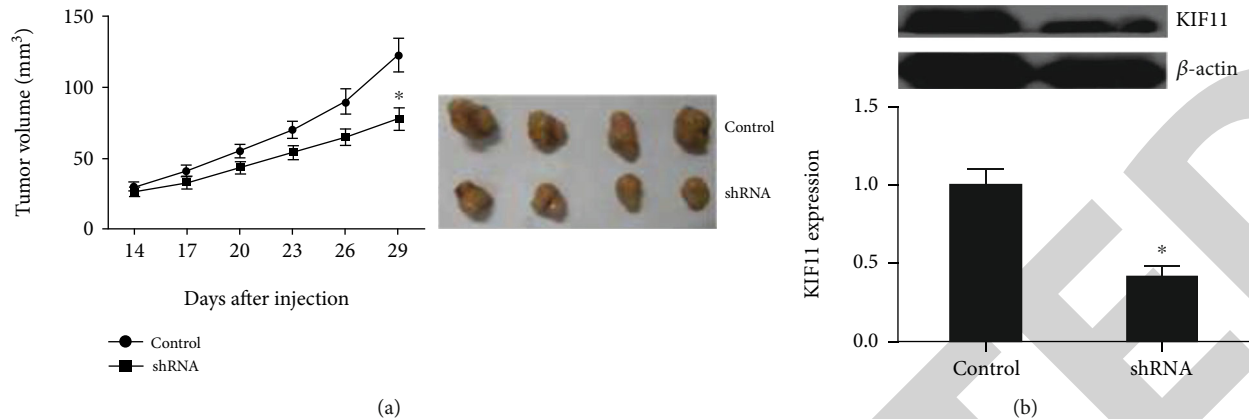
Figure 6: KIF11 promotes tumor growth of thyroid cancer in mice. (a) Tumor growth curves were shown. Scale bar, 5 mm. (b) Immunoblot assays exhibited the expression levels of KIF11 in tumors isolated from mice. Results are presented as the mean ± SD, $^*p < 0.05$.

KIF11, a member of the cell division driver family, is involved in the formation of bipolar mitotic spindles during cell division. Studies have found that these motor proteins are widely expressed and play an important role in cell division and intracellular transport. These microtubule-associated driver proteins, due to their important biological functions in cell division, are closely related to tumor formation and are prognostic factors for a variety of malignant tumors. Therefore, KIF11 has also become a new target for tumor targeted therapy, and our in vitro and in vivo studies further confirm this conclusion.

In summary, we revealed the high expression of KIF11 in human thyroid tumor tissues. We revealed KIF11 in the progression of thyroid cancer and provide a promising therapeutic target for the treatment of thyroid cancer.

Data Availability

The datasets generated during and/or analyzed during the current study are available from the corresponding authors on reasonable request.

Conflicts of Interest

The authors declare that they have no conflicts of interest.

Acknowledgments

References

[1] A. F. Milano, "Thyroid cancer: 20-year comparative mortality and survival analysis of six thyroid cancer histologic subtypes by age, sex, race, stage, cohort entry time-period and disease duration (SEER∗ Stat 8.3. 2) a systematic review of 145,457 cases for diagnosis years 1993–2013," *Journal of Insurance Medicine*, vol. 47, no. 3, pp. 143–158, 2018.

[2] M. Ellis, K. Cohen, E. S. Maman, A. Hercbergs, P. J. Davis, and O. Ashur-Fabian, "The involvement of thyroid hormones in cancer," *Harefuah*, vol. 154, no. 8, pp. 512–515, 2015.

[3] F. Pitoia, F. Bueno, and G. Cross, "Long-term survival and low effective cumulative radioiodine doses to achieve remission in patients with 131iodine-avid lung metastasis from differentiated thyroid cancer," *Clinical Nuclear Medicine*, vol. 39, no. 9, pp. 784–790, 2014.

[4] R. Alvarado, M. S. Sywak, L. Delbridge, and S. B. Sidhu, "Central lymph node dissection as a secondary procedure for papillary thyroid cancer: is there added morbidity?," *Surgery*, vol. 145, no. 5, pp. 514–518, 2009.

[5] S. Faulkner, S. Roselli, Y. Demont et al., "ProNGF is a potential diagnostic biomarker for thyroid cancer," *Oncotarget*, vol. 7, no. 19, pp. 28488–28497, 2016, PMID: 27074571.

[6] G. Accardo, G. Conzo, D. Esposito et al.et al., "Genetics of medullary thyroid cancer: an overview," *International Journal of Surgery*, vol. 41, Suppl 1, pp. S2–S6, 2017.

[7] L. Hou, D. Xu, and W. Dai, "Targeted therapy for thyroid cancer," *Zhonghua Zhong Liu Za Zhi*, vol. 37, no. 11, pp. 801–803, 2015.

[8] V. R. Agrawal, G. Jodon, R. Mushtaq, and D. W. Bowles, "Update on multikinase inhibitor therapy for differentiated thyroid cancer," *Drugs Today (Barc)*, vol. 54, no. 9, pp. 535–545, 2017.

[9] D. A. Nalawansha, I. D. Gomes, M. K. Wambua, and M. K. H. Pflum, "HDAC inhibitor-induced mitotic arrest is mediated by Eg5/KIF11 acetylation," *Chemistry & Biology*, vol. 24, no. 4, pp. 481–492.e5, 2017.

[10] T. Song, Y. Zheng, Y. Wang et al., "Specific interaction of KIF11 with ZBP1 regulates the transport of β-actin mRNA and cell motility," *Journal of Cell Science*, vol. 128, no. 5, pp. 1001–1010, 2015.

[11] X. Wan, Y. Zhang, M. Lan et al., "Meiotic arrest and spindle defects are associated with altered KIF11 expression in porcine oocytes," *Environmental and Molecular Mutagenesis*, vol. 59, no. 9, pp. 805–812, 2018.

[12] M. Venere, C. Horbinski, J. F. Crish et al., "The mitotic kinesin KIF11 is a driver of invasion, proliferation, and self-renewal in glioblastoma," *Science Translational Medicine*, vol. 7, no. 304, p. 304ra143, 2015.

[13] K. Daigo, A. Takano, P. M. Thang et al., "Characterization of KIF11 as a novel prognostic biomarker and therapeutic target for oral cancer," *International Journal of Oncology*, vol. 52, no. 1, pp. 155–165, 2017.

Retraction

Retracted: Clinical Evaluation of the Medium-Term Efficacy of Laparoscopic Sleeve Gastrectomy against Obstructive Sleep Apnea-Hypopnea Syndrome in Obese Patients

Computational and Mathematical Methods in Medicine

This article has been retracted by Hindawi following an investigation undertaken by the publisher [1]. This investigation has uncovered evidence of one or more of the following indicators of systematic manipulation of the publication process:

(1) Discrepancies in scope

(2) Discrepancies in the description of the research reported

(3) Discrepancies between the availability of data and the research described

(4) Inappropriate citations

(5) Incoherent, meaningless and/or irrelevant content included in the article

(6) Peer-review manipulation

The presence of these indicators undermines our confidence in the integrity of the article's content and we cannot, therefore, vouch for its reliability. Please note that this notice is intended solely to alert readers that the content of this article is unreliable. We have not investigated whether authors were aware of or involved in the systematic manipulation of the publication process.

Wiley and Hindawi regrets that the usual quality checks did not identify these issues before publication and have since put additional measures in place to safeguard research integrity.

We wish to credit our own Research Integrity and Research Publishing teams and anonymous and named external researchers and research integrity experts for contributing to this investigation.

The corresponding author, as the representative of all authors, has been given the opportunity to register their agreement or disagreement to this retraction. We have kept a record of any response received.

References

[1] J. Wu, H. Ge, S. Lei et al., "Clinical Evaluation of the Medium-Term Efficacy of Laparoscopic Sleeve Gastrectomy against Obstructive Sleep Apnea-Hypopnea Syndrome in Obese Patients," *Computational and Mathematical Methods in Medicine*, vol. 2022, Article ID 7682706, 9 pages, 2022.

Research Article

Clinical Evaluation of the Medium-Term Efficacy of Laparoscopic Sleeve Gastrectomy against Obstructive Sleep Apnea-Hypopnea Syndrome in Obese Patients

Jianlin Wu [1], **Hong Ge** [1,2] **Sen Lei** [1], **Xiaoping Yang** [1], **Shujuan Zhang** [1], **Yingying Han** [1], **Xiaolong Wang** [1], **Zhimin Liu** [1], **and Qizuo Xu** [1]

[1]*Department of Gastrointestinal Surgery, Zibo Central Hospital Affiliated with Shandong University, Zibo, Shandong 250036, China*
[2]*Department of Respiratory Medicine, Zibo Central Hospital Affiliated with Shandong University, Zibo, Shandong 250036, China*

Correspondence should be addressed to Hong Ge; ludu34849@163.com

Objective. This study was designed to evaluate the efficacy of laparoscopic sleeve gastrectomy (LSG) for obstructive sleep apnea-hypopnea syndrome (OSAHS) in obese individuals and identify the related factors affecting its efficacy. *Methods*. The clinical and follow-up data of 37 obese patients with OSAHS who underwent LSG in the Laparoscopic Surgery Department of Zibo Central Hospital from January 2017 to July 2018 were analyzed retrospectively. The effect of this operation on patients' weight and OSAHS was studied, and the factors affecting weight and OSAHS were examined through univariate and multivariate logistic regression analysis. *Results*. Over 12 months of regular postoperative follow-up with the 37 patients, their body mass index (BMI) decreased, and the percentage of excess weight loss (EWL%) reached 73.2%. Additionally, the rate of successful OSAHS treatment reached 91.89%, and the apnea-hypopnea index (AHI) and lowest arterial oxygen saturation ($LSaO_2$) increased significantly. Univariate logistic regression analysis showed that gender, weight, EWL%, and smoking affected the efficacy of LSG against OSAHS ($P < 0.05$). EWL% and smoking were independent factors that helped determine the efficacy of LSG against morbid obesity ($P < 0.05$). *Conclusion*. LSG can effectively help obese patients lose weight and show medium-term efficacy against OSAHS in obese people. Smoking and EWL% were found to be the factors determining the efficacy of LSG.

1. Introduction

Due to the change of lifestyle and the development of unhealthy eating habits, the number of obese people has increased. It is reported that 27.1% of Chinese adults are overweight, and obesity poses an increasing threat to national public health [1]. Obesity has been recognized as a high-risk factor for many chronic diseases, such as hypertension, hyperlipidemia, coronary heart disease, and type 2 diabetes. In addition, obesity is associated with a high risk of obstructive sleep apnea-hypopnea syndrome (OSAHS) [2]. According to epidemiological studies, the prevalence of OSAHS in obese people was 15-30 times the prevalence in no obese populations [3], and obesity makes OSAHS more difficult to cure. The *Clinical Practice Guideline for Diagnostic Testing for Adult Obstructive Sleep Apnea* (2013 edition), developed in the United States, highly recommends weight-loss therapy for OSAHS patients [4]. Mounting evidences showed that bariatric surgery was the most effective and sustainable treatment approach for obesity and its complications, such as OSAHS and type 2 diabetes [5]. At present, there are three main types of bariatric surgery: laparoscopic Roux-en-Y gastric bypass (LRYGB), laparoscopic sleeve gastrectomy (LSG), and biliopancreatic diversion with duodenal switch (BPDDS). LSG is an operation to reduce the volume of the stomach by removing the fundus and greater curvature of the stomach; this procedure does not otherwise change the anatomical structure of the gastrointestinal tract,

but it alters the levels of gastrointestinal hormones to reduce patients' appetite as a way to help them lose weight [6]. After many years of development, LSG has gradually become the most common method in bariatric surgery. We were the first to introduce LSG to China [7], and a follow-up of patients with OSAHS was carried out in cooperation with our hospital's respiratory medicine department in October 2016. In this study, the clinical and follow-up data of 37 obese OSAHS patients receiving LSG were analyzed.

2. Materials and Methods

2.1. Clinical Data. A retrospective analysis was conducted by selecting 37 patients (9 males and 28 females, aged 19-37, body mass index (BMI): 38.92-58.33 kg/m^2, mean: 42.71 kg/m^2) who were diagnosed with OSAHS and underwent LSG from January 2017 to July 2018 at Zibo Central Hospital. Among the included patients, there were 35 cases of fatty liver, 11 cases of hypertension, and 31 cases of hyperlipidemia. This study obtained the approval of the Ethics Committee of Zibo Central Hospital, following the principle of the Declaration of Helsinki as revised in 2013. The patients and their family members voluntarily signed informed consent.

2.2. Requirements for Participation. To participate in this study, patients needed to meet the following three requirements: (1) their initial BMI was greater than 35.0 kg/m^2; (2) polysomnography (PSG) indicated at least 30 bouts of apnea and hypopnea during 7 hours of sleep every night or an apnea-hypopnea index (AHI) of at least 5 per hour, with the main symptoms of obstructive sleep apnea accompanied by snoring, sleep apnea, and daytime sleepiness; (3) when patients returned for follow-up examinations of 3 months, 6 months, and 12 months after surgery, their BMI, waist circumference, and percentage of excess weight loss (EWL%) were recorded, and PSG was performed.

Exclusion criteria are (1) pregnant or lactating patients; (2) patients with mental disorders or unable to clear expression problems and cooperate with the diagnosis and treatment process; (3) patients who need to take sedative and hypnotic drugs such as diazepam for a long time; (4) patients with congenital upper airway anatomical abnormalities; (5) have severe lung disease or an acute attack of respiratory disease; (6) patients with severe heart disease, severe liver and kidney dysfunction, and acute cerebrovascular disease; (7) patients with tumors; and (8) patients who have received relevant treatment for this disease.

2.3. Surgical Method. Routine tracheal intubation was performed under general anesthesia. The anesthetized patient was positioned in dorsal recumbency with the legs spread, and 5 incisions were made to establish pneumoperitoneum. The observation port was placed above and to the left of the umbilicus, accounting for differences in patient height. A cut was made along the gastrocolic ligament to free the stomach, avoiding areas near blood vessels; the cut began 4 cm from the pylorus, proceeding up along the greater curvature and back to the paries posterior ventriculi and gastric

TABLE 1: AHI and hypoxemia criteria for OSAHS severity in adults.

Degree	AHI (per hour)
Mild	5 ~ 15
Moderate	>15~30
Severe	>30
Degree	LSaO$_2$ (%)
Mild	85~90
Moderate	80 ~ <85
Severe	<80

fundus. The angle of His was fully exposed, and the vasa brevia and spleen were handled carefully. With the assistance of the anesthetist, a 36 F balloon gastric tube was placed through the mouth, and the end was guided through the pylorus into the duodenal bulb. An endovascular gastrointestinal anastomosis (Endo-GIA) stapler was used to cut the stomach wall is cut along the left side of the balloon gastric tube; attention was paid to the gastric angle to prevent stenosis of the remaining stomach. The cut was usually 4-6 staples long, with the final staple typically placed 1 cm from the angle of the His to avoid injuring the cardia. If too little of the gastric fundus is removed, weight loss will be impeded, but if too much is removed, the cardia will be damaged. The cuts were closed with absorbable sutures to reduce the risk of anastomotic leakage and gastric perforation. Finally, the balloon gastric tube was pulled out; no tube was inserted after surgery.

2.4. Polysomnography (PSG). Objects were continuously monitored using the Philips A5 polysomnography system for more than 7 hours overnight. Alcohol, sedatives, hypnotics, and coffee were prohibited on the day leading up to the examination. All sleep stages and respiratory events were identified and marked by the polysomnographic physician, who subsequently made a diagnosis.

2.5. Criteria for OSAHS Severity Classification. According to the *Clinical Practice Guideline for Diagnostic Testing for Obstructive Sleep Apnea and Hypopnea* (2011 edition) by the Respiratory Disturbance Group of the Chinese Thoracic Society [8], the severity of OSAHS is classified as mild, moderate, or severe based on AHI as the primary criterion and LSaO$_2$ as the secondary criterion (Table 1).

2.6. Efficacy Evaluation. Evaluation of postoperative weight loss was conducted according to the international standard [9]. Based on the EWL% after one year of surgery, the results were classified as excellent or good (EWL% ≥ 50%) versus fair or failed (EWL% < 50%) and statistically analyzed. OSAHS was assessed by comparing the AHI and LSaO$_2$ of the sample at different follow-ups. LSG was deemed effective if there were statistically significant improvements in these variables [10]. The effect of LSG on patients with OSAHS was divided into four types defined by AHI [11] to analyze efficacy (cured, excellent, fair, and failed). In addition, patients were divided into two groups-good (cured + excellent) and
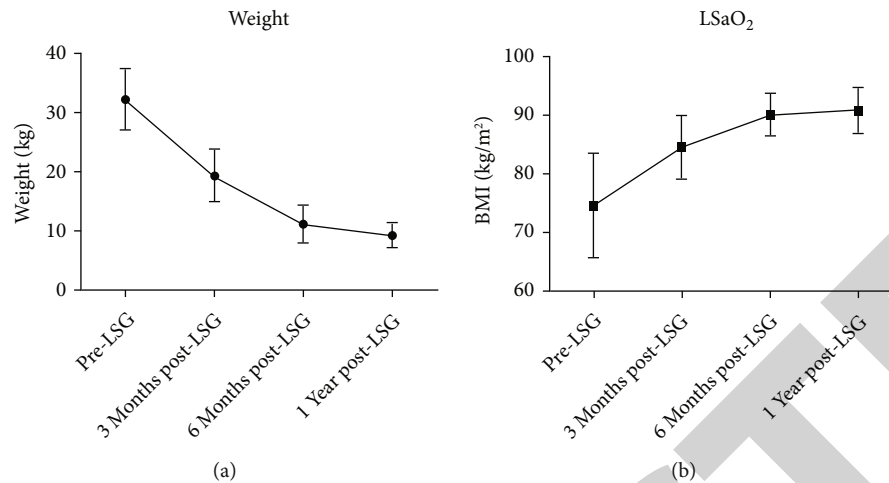
Figure 1: Relationship between OSAHS improvement and BMI. (a) Changes of body weight before and after operation. (b) Changes of LSaO$_2$ before and after operation.

Table 2: Changes in indexes before and after operation.

Indexes	Number of cases	Pre-LSG	Three months	Six months	Twelve months
Weight (kg)	37	121.7 ± 18.3	99.3 ± 11.6[a]	88.1 ± 9.4[b]	80.0 ± 8.2[b]
BMI (kg/m^2)	37	41.5 ± 6.2	35.5 ± 4.4[a]	31.7 ± 2.6[b]	26.4 ± 3.9[b]
EWL%	37		45.1 ± 11.3	65.2 ± 11.4[b]	73.2 ± 16.7[b]
Waistline	37	126.2 ± 15.6	112.3 ± 12.5[a]	104.3 ± 11.7[b]	96.2 ± 10.4[b]
Hipline	37	129.8 ± 17.6	121.1 ± 15.3[a]	115.5 ± 12.7[b]	107.4 ± 9.8[b]
Neck girth	37	51.1 ± 8.2	44.3 ± 6.7[a]	41.8 ± 5.7[b]	38.9 ± 6.7[b]

[a] is compared with the pre-LSG measurement, $P < 0.05$; [b] is compared with the previous time point, $P < 0.05$.

bad (fair + failed)—to analyze the factors affecting efficacy. The four response types were defined by the following postoperative AHI criteria:

(1) *Cured.* <5 per hour

(2) *Excellent.* Decreased by ≥50% compared with preoperative AHI

(3) *Fair.* Decreased by 20-50% compared with preoperative AHI

(4) *Failed.* Not significantly different from preoperative AHI

2.7. *Statistical Treatment.* SPSS 23.0 statistical software was used for data analysis. The patients' age, weight, BMI, EWL%, AHI, and LSaO$_2$ were described as the mean ± standard deviation. Enumeration data were examined by a 2×2 chi-squared test or Fisher's exact test. Student's t-test was used to compare the enumeration data between the two groups, and $P < 0.05$ was taken to indicate a statistically significant test result. Cox regression was used to analyze the factors determining the efficacy of LSG against OSAHS. The variables were examined through univariate logistic regression analysis, and the variables with $P < 0.05$ (implying statistical significance) were included in multivariate logistic regression analysis.

3. Results

3.1. *General Information of Patients.* All patients were operated without conversion to laparotomy. The procedure generally lasted 120-240 minutes and was not accompanied by excessive bleeding. Postoperatively, 1 case of pyloric obstruction and 1 case of marginal leakage were found, but they both recovered after conservative treatment. The length of hospitalization was 3-10 days. All patients were morbidly obese individuals with OSAHS and were followed up for 12 months without malnutrition.

3.2. *Treatment of Morbid Obesity by LSG.* The weight, BMI, and EWL% of patients during the 12-month postoperative follow-up period were analyzed. The data from the preoperative, 3-month, 6-month, and 12-month time points were compared, and the rate of weight loss per month was found to decrease over the follow-up period (Figure 1(a)); nonetheless, patients' weight was significantly reduced at each follow-up time compared with the previous time point. The lowest mean BMI was 26.4 kg/m^2, and the EWL% increased over time, reaching 73.2% at the end of the study
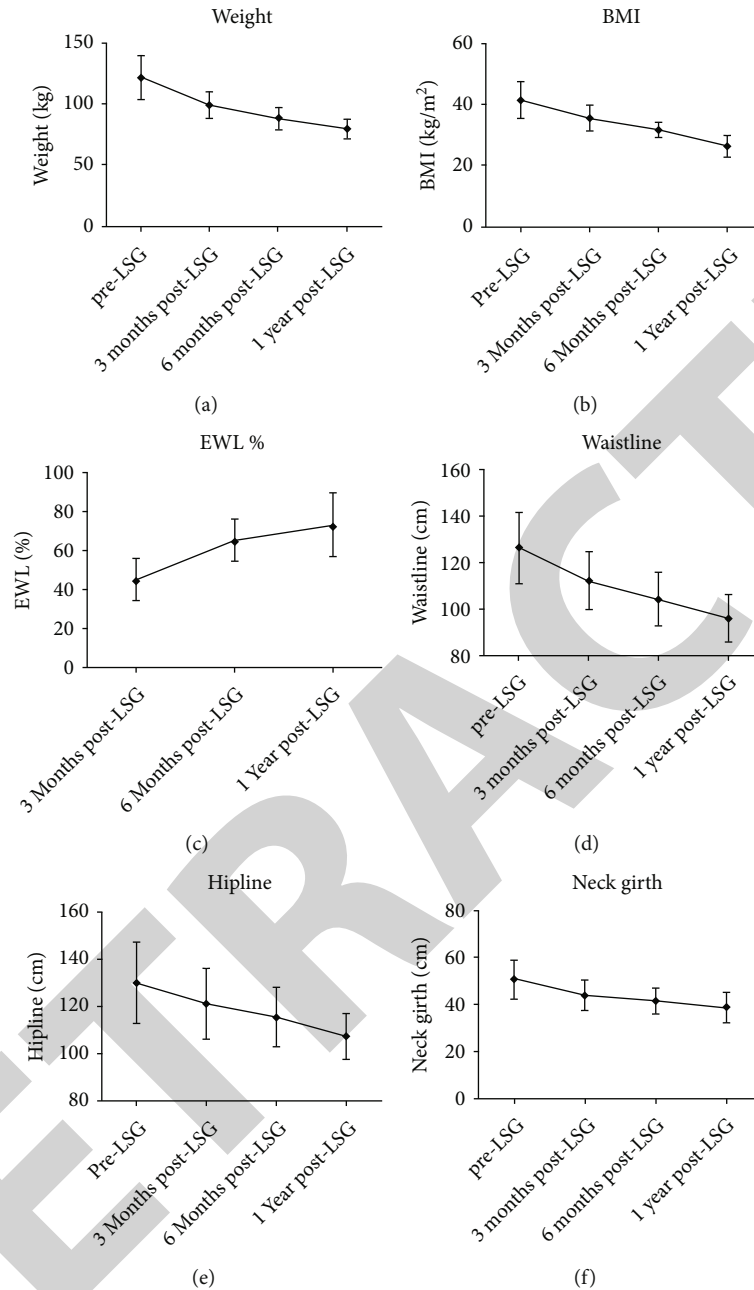
Figure 2: Changes of body weight related indexes before and after operation. (a) Changes of body weight before and after operation. (b) Changes of BMI before and after operation. (c) Changes of EWL% before and after operation.

(12 months after surgery) (Table 2). There were no cases of underweight during the follow-up period. Therefore, we can conclude that LSG has significant efficacy against morbid obesity.

3.3. Treatment of OSAHS by LSG. To evaluate treatment efficacy, we performed follow-up PSG at different time points after surgery and graded the severity of OSAHS according to AHI and $LSaO_2$. By comparing the AHI and $LSaO_2$ before and after surgery, we found that the rate of successful treatment increased over time, measuring 78.38% (29/37), 89.19% (33/37), and 91.89% (34/37) at the 3-, 6-, and 12-

month time points, respectively (Figures 2 and 1(b)). Regarding the degree of OSAHS, PSG showed that all patients initially suffered moderate to severe OSAHS. The severity of OSAHS declined significantly after surgery, especially in the first 6 months, but little difference was found between the 6- and 12-month time points. However, the symptoms of OSAHS continued to decrease for some obese patients (BMI $\geq$ 50 kg/m^2) during this period (Figure 3).

The AHI and $LSaO_2$ values measured by PSG in 37 patients are shown in Table 3. These results showed that AHI and $LSaO_2$ were significantly improved at the 3-, 6-, and 12-month time points (all $P < 0.05$). In addition, both
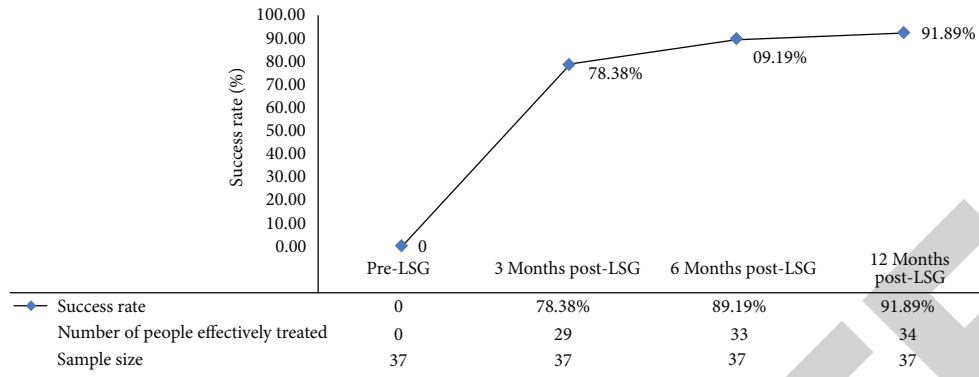
FIGURE 3: Chart of success rate at different follow-up time points.

TABLE 3: Comparison of PSG indexes at different follow-up time points before and after surgery.

Indexes	Number of cases	Pre-LSG	Three months	Six months	Twelve months
AHI (per hour)	37	32.2 ± 5.3	19.3 ± 4.6^a	11.1 ± 3.4^b	9.1 ± 2.2
LSaO$_2$	37	74.6 ± 8.9	84.5 ± 5.4^a	90.1 ± 3.6^b	90.8 ± 3.9

[a] is compared with the pre-LSG measurement, $P < 0.05$; [b] is compared with the previous time point, $P < 0.05$.
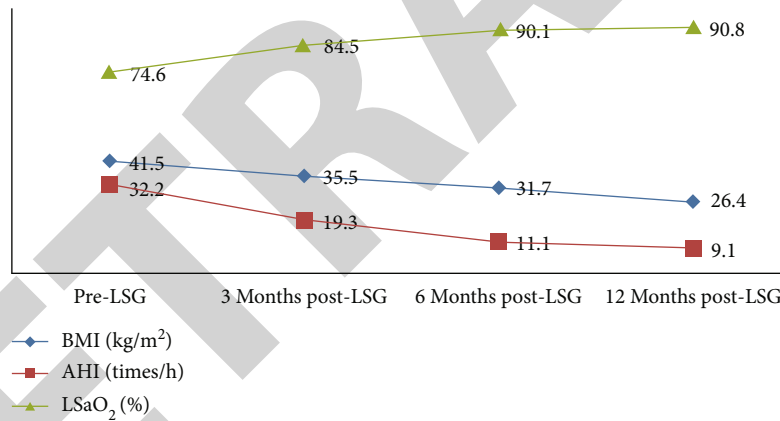
FIGURE 4: Chart of correlation among BMI, PSG, and LSaO$_2$.

indexes were much better at 6 months than at 3 months, although they stabilized beyond 6 months, with no significant difference between the 12-month and 6-month time points (Figure 4).

3.4. Relationship between OSAHS Improvement and BMI. After analyzing the relationship between weight loss and sleep improvement in OSAHS patients after surgery, AHI and LSaO$_2$ improved within 6 months after surgery as BMI decreased. Between 6 months and 12 months after surgery, BMI continued to decline significantly, but AHI and LSaO$_2$ stabilized (Figure 5).

3.5. Factors Affecting the Efficacy of LSG against OSAHS. In order to identify the factors that affect the efficacy of LSG for OSAHS, patients with OSAHS were divided into two groups according to their treatment efficacy: good (cured + excellent) and poor (fair + failed). Sex, age, weight,

BMI, EWL%, hyperlipidemia, hypertension, fatty liver, smoking, fasting blood glucose, and surgical complications were considered as related factors and were analyzed through Cox regression. Through univariate logistic regression analysis, sex, weight, EWL%, and smoking could affect the efficacy of LSG against OSAHS ($P < 0.05$, Table 4). Multivariate logistic regression analysis showed that EWL% and smoking were independent factors determining the efficacy of LSG against morbid obesity ($P < 0.05$, Table 5).

4. Discussion

Overweight and obesity are becoming a major threat to public health as people's lifestyles change and their eating habits become improper. Obesity causes not only an increase in weight but also a sharp rise in the incidence of various
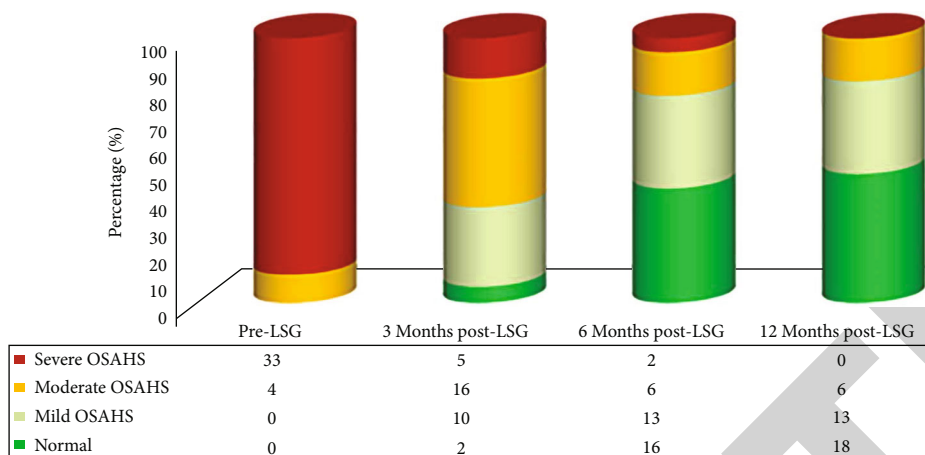
FIGURE 5: Distribution of OSAHS severity at different follow-up time points.

chronic diseases. In addition, the prevalence of obesity in young people is increasing [12]. Obesity is the major contributor to OSAHS [13], and approximately 70% of patients with OSAHS are obese [14–15]. The pathogenesis of obesity-related OSAHS is complicated including factors such as reduction of the cross-sectional area of the upper airway caused by the accumulation of neck fat, stenosis of the pharynx caused by decreased tension in the neck muscles, a decrease in chest volume caused by upward pressure on the diaphragm from the accumulation of visceral fat in the abdomen [16], and changes in hormone and cytokine levels due to lipid metabolism disorders [17–20].

At present, automatic continuous positive airway pressure (auto-CPAP) therapy, the most effective noninvasive treatment for OSAHS, can significantly improve the levels of AHI and $LSaO_2$ and reduce daytime sleepiness. Auto-CPAP is considered the standard treatment method. However, many patients cannot tolerate this therapy in the long term because of respirator-related discomfort, skin irritation, and nighttime noise [4]. Weight loss is another important therapy for OSAHS. The decrease in BMI can improve airway resistance, improve AHI, and shorten the treatment course of Auto-CPAP [21]. The *Clinical Practice Guideline for Diagnostic Testing for Adult Obstructive Sleep Apnea (2013 edition)* in the United States highly recommends weight-loss therapy for OSAHS patients.

Bariatric surgery is the only proven sustainable method to lose weight [22]. LSG has become the most commonly used bariatric surgery worldwide due to its relative simplicity, low rate of postoperative complications, and high efficacy [22]. Over a 12-month follow-up period after surgery, LSG achieved excellent or fair weight-loss results (EWL% ≥ 50%), with a success rate of 75.6%, which was comparable to the rates reported by large weight-loss treatment centers internationally [23–24].

Whether LSG is the best bariatric surgery for OSAHS in obese people has yet to be established. According to a study conducted by Sarkhosh et al. [25], BPDDS is the most effective surgery (99.0%), but few people choose it because of its complexity and relatively high rate of postoperative complications. Regarding the treatment of obese OSAHS patients with LSG

versus LRYGB, the two most widely used bariatric surgeries, there appears to be no significant difference in efficacy between them [3], although some studies suggest that LRYGB is more effective [26]. In this study, all OSAHS patients who underwent LSG surgery were followed up for 12 months, and the rate of successful OSAHS treatment was 91.89%, which was higher than the rate in Sarkhosh's study (85.7%) [25–26] and slightly lower than that in Buchwald's study [27]. In PSG examinations of the entire sample, AHI and $LSaO_2$ significantly improved as BMI decreased within 6 months after the operation, and the correlations between BMI and both PSG indices were significant. The improvement of AHI and $LSaO_2$ from the 6-month time point to the 12-month time point was not statistically significant, but the decrease in BMI in the same period was statistically significant. This degradation of the correlation may result from a short follow-up period; extended follow-up may confirm that PSG improvement is correlated with reduced BMI. However, these results may also indicate that the principle of OSAHS treatment by LSG may not be the decrease in BMI and the change in fat distribution; instead, there could be more complex metabolic and molecular mechanisms. Multivariate logistic regression analysis showed that EWL% and smoking are independent factors that determine the efficacy of LSG against morbid obesity. A large number of oxygen radicals in cigarettes can disrupt the oxidant-antioxidant balance of the respiratory system, causing OSAHS to be worsening [28–29]. Thus, the evidence suggests that the pathogenesis of OSAHS is more complex for obese patients with a history of smoking than for those without; relying solely on surgery to help them lose weight may not achieve significant efficacy [30]. EWL% represents postoperative weight loss; the greater the EWL%, the more efficacious the procedure is for weight loss. The EWL% in our study was consistent with the results of other studies performed in China.

In conclusion, LSG was an effective approach against OSAHS in obese people. It has a high success rate in helping patients lose weight and improving their AHI and $LSaO_2$. LSG has become the most common weight-loss surgery due to its considerable advantages, but its long-term efficacy and molecular metabolic mechanism in the treatment of obesity related OSAHS need to be further evaluated.

Table 4: Univariate logistic regression analysis of factors that affect the efficacy of LSG against OSAHS.

Item	Number of cases	Good efficacy ($n = 23$)	Poor efficacy ($n = 14$)	P value
Sex	37			0.040*
Male	9	3	6	
Female	28	20	8	
Age	37	30.2 ± 9.1	31.5 ± 9.8	0.682
Duration of disease (years)	37			0.575
≥5	30	18	12	
<5	7	5	2	
Weight	37	110.5 ± 15.7	123.8 ± 16.8	0.024*
BMI	37	41.5 ± 6.7	44.5 ± 8.4	0.269
EWL%	37			0.001*
≥50%	21	18	3	
<50%	16	5	11	
Waistline	37	100.5 ± 10.5	93.2 ± 8.9	0.037*
Hipline	37	108.6 ± 11.4	100.4 ± 9.8	0.032*
Neck girth	37	41.5 ± 8.2	37.2 ± 6.8	0.109
Smoking	37			0.001*
Yes	12	2	10	
No	25	21	4	
Hyperlipidemia	37			0.470
Yes	12	6	6	
No	25	17	8	
Hypertension	37			0.173
Yes	17	13	4	
No	20	10	10	
Fatty liver	37			0.582
Yes	18	12	6	
No	19	11	8	
Fasting blood glucose	37	9.3 ± 1.9	10.1 ± 2.5	0.314
Surgical complications	37			0.715*
Yes	2	1	1	
No	35	22	13	

Table 5: Multivariate logistic regression analysis of factors that affect the efficacy of LSG against OSAHS.

Clinical factors	B	SE	P value	OR
Sex	1.382	1.032	0.095	2.896
Weight	1.254	0.874	0.078	3.637
EWL%	0.534	0.788	0.035*	3.758
Waistline	1.364	0.987	0.090	3.657
Hipline	1.297	0.837	0.085	3.897
Smoking	0.686	0.750	0.025*	2.441

Data Availability

The datasets during the current study are available from the corresponding author on reasonable request.

Ethical Approval

This study followed the ethical standards and was approved by the Zibo Central Hospital ethics committee.

Consent

Informed consent was obtained from all individual participants involved in the study.

Conflicts of Interest

The authors declare that they have no conflicts of interest.

Acknowledgments

References

[1] S. Wang, S. Lay, H. Yu, and S. R. Shen, "Dietary guidelines for Chinese residents (2016):comments and comparisons," *Journal of Zhejiang University-SCIENCE B*, vol. 17, no. 9, pp. 649–656, 2016.

[2] K. M. Sharkey, J. T. Machan, C. Tosi, G. D. Roye, D. Harrington, and R. P. Millman, "Predicting obstructive sleep apnea among women candidates for bariatric surgery," *Journal of Women's Health*, vol. 19, no. 10, pp. 1833–1841, 2010.

[3] A. M. Cuccia, G. Campisi, R. Cannavale, and G. Colella, "Obesity and craniofacial variables in subjects with obstructive sleep apnea syndrome: comparisons of cephalometric values," *Head & Face Medicine*, vol. 3, no. 41, pp. 1–9, 2007.

[4] A. Eniwar and E. Erik, "Bariatric surgery for obese patients with OSAS," *Chinese Journal of General Surgery*, vol. 12, no. 6, pp. 538–540, 2018.

[5] Y. Chengcan, W. Wenyue, and W. Bing, "Bariatric surgery for obesity-typed OSAHS," *Journal of Clinical Otorhinolaryngology Head and Neck Surgery*, vol. 30, no. 6, pp. 434–437, 2016.

[6] J. Li, D. Lai, and D. Wu, "Laparoscopic Roux-en-Y gastric bypass versus laparoscopic sleeve gastrectomy to treat morbid obesity-related comorbidities: a systematic review and meta-analysis," *Obesity Surgery*, vol. 26, no. 2, pp. 429–442, 2016.

[7] W. Jianlin, Y. Xiaoping, G. Yingjie, H. Yun, and L. Zhimin, "Opportunities and challenges that basic medical institutions will face in the bariatric surgery," *Journal of Laparoscopic Surgery*, vol. 20, no. 10, pp. 794–796, 2015.

[8] Respiratory Disturbance Group of Chinese Thoracic Society, "Clinical practice guideline for diagnostic testing for obstructive sleep apnea and hypopnea (2011 edition)," *Chinese Journal of Tuberculosis and Aspiration Glaciology*, vol. 35, no. 1, pp. 9–12, 2012.

[9] Classification and Diagnosis of Diabetes, "Standards of medical care in diabetes—2018," *Diabetes Care*, vol. 41, Supplement 1, pp. S13–S27, 2017.

[10] I. C. Aguiar, W. R. Freitas Jr., I. R. Santos et al., "Obstructive sleep apnea and pulmonary function in patients with severe obesity before and after bariatric surgery: a randomized clinical trial," *Multi-disciplinary Respiratory Medicine*, vol. 9, no. 1, pp. 43–43, 2014.

[11] M. Yunli, L. Zhongda, and Z. Zhunjing, "Clinical observation of 60 cases on the treatment for intermingled phlegm and blood stasis typed obstructive sleep apnea syndrome with drug Ninghantang," *Zhejiang Journal of Traditional Chinese Medicine*, vol. 47, no. 10, p. 716, 2012.

[12] Y. Wang, L. Wang, H. Xue, and W. Qu, "A review of the growth of the fast food industry in China and its potential impact on obesity," *International Journal of Environmental Research and Public Health*, vol. 13, no. 11, p. 1112, 2016.

[13] K. M. Sharkey, H. J. Orff, C. Tosi, D. Harrington, G. D. Roye, and R. P. Millman, "Subjective sleepiness and day-time functioning in bariatric patients with obstructive sleep apnea," *Sleep & Breathing*, vol. 17, no. 1, pp. 267–274, 2013.

[14] P. E. Peppard, T. Young, M. Palta, J. Dempsey, and J. Skatrud, "Long-itudinal study of mod-erate weight change and sleep-disordered breathing," *JAMA*, vol. 284, no. 23, pp. 3015–3021, 2000.

[15] J. B. Dixon, L. M. Schachter, and P. E. O'Brien, "Polysomnography before and after weight loss in obese patients with severe sleep apnea," *International Journal of Obesity*, vol. 29, no. 9, pp. 1048–1054, 2005.

[16] Y. Jiasheng and D. Xiufang, "Effect of obesity on obstructive sleep apnea syndrome," *Chinese Prescription Drugs*, vol. 13, no. 1, pp. 1–3, 2017.

[17] H. Ashrafian, C. W. le Roux, S. P. Rowland et al., "Metabolic surgery and obstructive sleep apnoea: the protective effects of bariatric procedures," *Thorax*, vol. 67, no. 5, pp. 442–449, 2012.

[18] K. Spruyt, O. S. Capdevila, L. D. Serpero, L. Kheirandish-Gozal, and D. Gozal, "Dietary and physical activity patterns in children with obstructive sleep apnea," *The Journal of Pediatrics*, vol. 156, no. 5, pp. 724–730.e3, 2010.

[19] K. I. Takahashi, K. Chin, T. Akamizu et al., "Acylated ghrelin level in patients with OSA before and after nasal CPAP treatment," *Respirology*, vol. 13, no. 6, pp. 810–816, 2008.

[20] N. M. Punjabi and B. A. Beamer, "C-reactive protein is associated with sleep disordered breathing independent of adiposity," *Sleep*, vol. 30, no. 1, pp. 29–34, 2007.

[21] C. McDaid, K. H. Durée, S. C. Griffin et al., "A systematic review of continuous positive airway pressure for obstructive sleep apnoea-hypopnoea syndrome," *Sleep Medicine Reviews*, vol. 13, no. 6, pp. 427–436, 2009.

[22] M. Hany and M. Ibrahim, "Comparison between stable line reinforce-merit by barbed suture and non-reinforcement in sleeve gas-trectomy:a randomized prospective controlled study," *ObesSurg*, vol. 8, pp. 2157–2164, 2018.

[23] W. Wang Yuedong, Z. Y. Jia, Z. Yangwen, X. Zhijie, Z. Xiaoli, and Y. Zaiyuan, "Laparoscopic sleeve gastrectomy for obesity," *Chinese Journal of General Surgery*, vol. 26, no. 10, pp. 826–828, 2011.

[24] R. P. Gadiot, L. U. Biter, S. van Mil, H. F. Zengerink, J. Apers, and G. H. Mannaerts, "Long-term results of laparoscopic sleeve gastrectomy for morbid obesity: 5 to 8-year results," *Obesity Surgery*, vol. 27, no. 1, pp. 59–63, 2017.

[25] K. Sarkhosh, N. J. Switzer, M. El-Hadi, D. W. Birch, X. Shi, and S. Karmali, "The impact of bariatric surgery on obstructive

Retraction

Retracted: A Study on the Preventive Effect of Esketamine on Postpartum Depression (PPD) after Cesarean Section

Computational and Mathematical Methods in Medicine

This article has been retracted by Hindawi following an investigation undertaken by the publisher [1]. This investigation has uncovered evidence of one or more of the following indicators of systematic manipulation of the publication process:

(1) Discrepancies in scope

(2) Discrepancies in the description of the research reported

(3) Discrepancies between the availability of data and the research described

(4) Inappropriate citations

(5) Incoherent, meaningless and/or irrelevant content included in the article

(6) Peer-review manipulation

The presence of these indicators undermines our confidence in the integrity of the article's content and we cannot, therefore, vouch for its reliability. Please note that this notice is intended solely to alert readers that the content of this article is unreliable. We have not investigated whether authors were aware of or involved in the systematic manipulation of the publication process.

Wiley and Hindawi regrets that the usual quality checks did not identify these issues before publication and have since put additional measures in place to safeguard research integrity.

We wish to credit our own Research Integrity and Research Publishing teams and anonymous and named external researchers and research integrity experts for contributing to this investigation.

The corresponding author, as the representative of all authors, has been given the opportunity to register their agreement or disagreement to this retraction. We have kept a record of any response received.

References

[1] Q. Wang, M. Xiao, H. Sun, and P. Zhang, "A Study on the Preventive Effect of Esketamine on Postpartum Depression (PPD) after Cesarean Section," *Computational and Mathematical Methods in Medicine*, vol. 2022, Article ID 1524198, 5 pages, 2022.

Research Article

A Study on the Preventive Effect of Esketamine on Postpartum Depression (PPD) after Cesarean Section

Qiwei Wang [ID],[1] **Maoxin Xiao** [ID],[1] **Hao Sun** [ID],[2] **and Pengcheng Zhang** [ID][1]

[1]*Department of Anesthesiology, The Fourth Hospital of Shijiazhuang, Shijiazhuang, 050000 Hebei, China*
[2]*Department of Anesthesiology, The Eighth Hospital of Shijiazhuang, Shijiazhuang, 050000 Hebei, China*

Correspondence should be addressed to Pengcheng Zhang; zhangpengcheng@sjzfcyy.com.cn

Objective. The purpose of this study is to explore and analyze the preventive effect of esketamine on postpartum depression (PPD) after cesarean section. *Methods.* A total of 138 puerperae who underwent cesarean section in our hospital from February 2020 to January 2022 were selected as the research subjects. The control group was given intravenous injection of 2 ml of normal saline after the fetus was delivered. Meanwhile, the observation group was given intravenous injection of a small dose of esketamine (esketamine 0.5 mg/kg+ 2 ml of normal saline) after the delivery of the fetus. The changes of blood pressure and heart rate, the Edinburgh Postnatal Depression Scale (EPDS) questionnaire scores and the incidence of postpartum depression were compared between the two groups. At the same time, the incidence of postoperative adverse events in the two groups was observed. *Results.* There was no significant difference in systolic blood pressure (SBP), diastolic blood pressure (DBP), and heart rate (HR) between the two groups at T1-T3 ($P > 0.05$). Compared with the control group, the SBP, DBP, and HR at T4 and T5 in the observation group were higher ($P < 0.05$). There was no significant difference in SBP, DBP, and HR at T3, T4, and T5 in the observation group ($P > 0.05$). Compared with T3, SBP, DBP, and HR were lower in control group T4 and T5, respectively. There was no significant difference in the EPDS scores between the two groups on the 1st day before delivery ($P > 0.05$). The EPDS scores of the two groups were higher at 3d postpartum and 42d postpartum, respectively, than at 1d before delivery. The EPDS scores of the observation group at 3d and 42d after delivery were lower than those in the control group ($P < 0.05$). Compared with the control group, the incidence of postpartum depression was higher in the observation group at 3 days postpartum and 1 month postpartum, respectively ($P < 0.05$). There was no significant difference in the incidence of postpartum adverse reactions between the two groups ($P > 0.05$). *Conclusion.* The application of esketamine after cesarean section can effectively reduce depression-related scores and the risk of postpartum depression without increasing adverse reactions and has high safety.

1. Introduction

Postpartum depression, also known as postpartum depression, mainly refers to a type of depression that occurs in the puerperium. The main symptoms and manifestations of postpartum depression are different degrees of depression and mental depression. If postpartum depression is not properly dealt with, it will easily lead to the development of the patient's depressive symptoms to a more serious level or even suicide and self-harm, bringing many negative effects and problems to the mother-infant relationship and

the infant's emotional and behavioral growth [1]. Therefore, it is of great clinical significance to take active and effective methods to prevent the occurrence of puerperal depression. The traditional antidepressant drugs used in previous clinical work have slow onset of action, poor cure rate, and preventive effect, and it is impossible to judge whether they can be used for safe breastfeeding [2]. In recent years, studies have shown that small doses of esketamine can play a strong analgesic effect. At the same time, the application of esketamine in the treatment of refractory depression and marital form disorder will also play a good role. This study began

TABLE 1: Comparison of general data between the two groups.

Groups	N	Age (year)	Body mass index kg/m^2	Gestational week (week)	Cesarean section implementation time (min)	Postoperative analgesic drug usage (ml)	Education level (below junior high school/ high school/college and above)
Control group	69	29.21 ± 2.14	24.25 ± 1.21	39.10 ± 1.02	53.35 ± 10.25	110.39 ± 10.77	7/30/32
Research group	69	29.02 ± 2.33	24.30 ± 1.09	39.05 ± 0.99	53.10 ± 11.02	109.24 ± 12.31	10/32/27
t/χ^2		0.490	0.255	0.292	0.138	0.584	1.012
p		0.619	0.799	0.771	0.891	0.560	0.601

to apply esketamine after cesarean section to analyze whether it can prevent the occurrence of postpartum depression. The results are reported below.

2. Materials and Methods

2.1. General Information. A total of 138 puerperae who underwent cesarean section in our hospital from February 2020 to January 2022 were selected as the research subjects. All puerperae were randomly divided into control group and observation group, with 69 cases in each group. The ASA grades of all puerperae were grades I to II, and there was no significant difference in general data between the two groups ($P > 0.05$) (Table 1). Inclusion criteria are as follows: all puerperae who gave birth at term, puerperae who meet the indications for cesarean section, maternal absence of contraindications to spinal canal, and prenatal screening of mothers without severe fetal malformations or defects. Puerperae and their families gave informed consent to this trial. Exclusion criteria are as follows: puerperae with prenatal history of mental illness and brain disease; puerperae who have experienced major life events before birth; maternal coexistence with other types of obstetric diseases, including pregnancy-induced hypertension syndrome, eclampsia, placenta previa, and placental abruption; puerperae with serious comorbidities such as fake Xi'an hyperfunction and high blood pressure were combined; and puerperae with missing clinical data. All the specimens of this study were gotten the informed consent from patients and were approved by the Ethical Committee of Fourth Hospital of Shijiazhuang.

2.2. Methods. All puerperae were given combined spinal-epidural anesthesia treatment, the puerperae were lying on the left side, and puncture treatment was given between the L2-3. After successful epidural puncture, subarachnoid block was administered using the "intra-needle method" with a "pencil tip" spinal needle. After the puncture is successful, turn the bevel of the puncture needle toward the head, and inject 10 mg of bupivacaine (Hunan Kelun Pharmaceutical Co., Ltd., approved by Chinese medicine H43021411) with equal specific gravity at a speed of 10 to 15 s. After injecting the drug, adjust the maternal position to the left lateral decubitus position of 15°, and regulate the anesthesia level at T10. All puerperae selected the same group of obstetricians, made a transverse incision in the pubic bone, and performed cesarean section through the abdominal cavity [3]. The control group was given intravenous injection of 2 ml of normal saline after the fetus was delivered (Beijing Institute of Biological Products Co., Ltd., S10870001). And the observation group was given intravenous injection of a small dose of esketamine after the delivery of the fetus (Esketamine 0.5 mg/kg+ 2 ml of normal saline). No other type of analgesic drugs were used in the two groups of women, and no postoperative analgesia was given.

2.3. Observation Indicators. The changes of blood pressure and heart rate, the Edinburgh Postnatal Depression Scale (EPDS) questionnaire scores and the incidence of postpartum depression were compared between the two groups. At the same time, the incidence of postoperative adverse events in the two groups was observed. The perioperative time points were 15 minutes before administration (T1), 5 minutes before administration (T2), during administration (T3), 5 minutes after administration (T4), and 15 minutes after administration (T5). The evaluation indicators of the EPDS questionnaire included 10 items including mood, fun, self-blame, fear, anxiety, insomnia, coping ability, sadness, crying, and suicide. Each item is scored on a 4-point scale, with a score between 0 and 30. The higher the score, the more severe the depressive symptoms. A score of 10 and above is diagnosed as postpartum depression [4]. Common types of adverse reactions include nausea, vomiting, dizziness, and headache.

2.4. Statistical Processing. SPSS 23.0 statistical software was used to analyze the data. Three replicates were performed for each experiment. Enumeration data were expressed as %, and χ^2 test was used. Measurement data were expressed as mean ± standard deviation (mean ± sd), t-test was used, and F-test was used for comparison of multiple groups. Statistical significance was represented by $P < 0.05$.

3. Results

3.1. Comparison of Changes in Blood Pressure and Heart Rate between the Two Groups. There was no significant difference in SBP, DBP, and HR between the two groups at T1-T3 ($P > 0.05$). Compared with the control group, the SBP, DBP, and HR at T4 and T5 in the observation group were higher ($P < 0.05$). There was no significant difference in SBP, DBP, and HR at T3, T4, and T5 in the observation group ($P > 0.05$). Compared with T3, the SBP, DBP, and HR were lower in the control group T4 and T5, respectively ($P > 0.05$) (Table 2).

3.2. Comparison of EPDS Scores before and after Cesarean Section between the Two Groups. There was no significant

TABLE 2: Comparison of changes in blood pressure and heart rate between the two groups.

Groups	N	Time point	SBP (mmHg)	DBP (mmHg)	HR (every time/min)
		T1	108.44 ± 8.24	68.87 ± 9.23	86.10 ± 16.58
		T2	109.51 ± 9.87	66.20 ± 7.25	87.14 ± 14.20
Control group	69	T3	111.54 ± 8.60	68.14 ± 8.36	87.65 ± 16.87
		T4	103.87 ± 12.54	62.54 ± 11.35	77.29 ± 11.20
		T5	105.54 ± 9.61	65.97 ± 11.66	80.03 ± 10.98
F			2.251	2.336	2.571
P			0.024	0.035	0.040
		T1	112.02 ± 8.31	69.10 ± 10.21	87.56 ± 16.54
		T2	108.36 ± 9.64	67.22 ± 9.54	88.24 ± 15.60
Research group	69	T3	112.02 ± 8.55	69.21 ± 8.30	89.36 ± 18.34
		T4	111.24 ± 12.98	71.39 ± 11.24	92.47 ± 11.87
		T5	108.77 ± 9.54	68.33 ± 10.77	90.54 ± 10.73
F			3.012	3.247	3.559
P			0.034	0.046	0.047

difference in the EPDS scores between the two groups on the 1st day before delivery ($P > 0.05$). The EPDS scores of the two groups were higher at 3d and 42d postpartum than those at 1d before delivery. The EPDS score of the observation group was lower at 3d and 42d after delivery than that of the control group at 3d and 42d after delivery, respectively ($P < 0.05$) (Table 3).

3.3. Comparison of the Incidence of Depression after Cesarean Section between the Two Groups. The incidence of postpartum depression was higher in the observation group than that in the control group at 3 days postpartum and at 1 month postpartum, respectively ($P < 0.05$) (Table 4).

3.4. Comparison of the Incidence of Adverse Reactions between the Two Groups. There were 2 cases of nausea and vomiting and 1 case of dizziness in the control group. In the observation group, there were 3 cases of dizziness and headache. There was no significant difference in the incidence of postpartum adverse reactions between the two groups ($\chi 2 = 0.174$ and $P = 0.676$). There were no serious adverse reactions such as mental symptoms and respiratory depression in the two groups of puerperae.

4. Discussion

Postpartum depression mainly refers to a depression that exists during the puerperium. During the onset of postpartum depression, persistent emotional depression is the main symptom and manifestation, accompanied by changes in thinking and behavior. According to the survey data, in my country, the incidence of postpartum depression is as high as 6.15% to 33.93% [5]. At the same time, clinical data show that the occurrence of postpartum depression on the one hand can have a large and small impact on the physical and mental health of puerperae. On the other hand, postpar-

TABLE 3: Comparison of EPDS scores before and after cesarean section between the two groups (points).

Groups	N	Prenatal 1d	Postpartum 3d	Postpartum 42d
Control group	69	7.21 ± 4.24	8.66 ± 2.07	9.16 ± 2.01
Research group	69	7.18 ± 4.06	7.79 ± 2.14	8.43 ± 2.26
t		0.043	2.427	2.005
P		0.966	0.017	0.047

TABLE 4: Comparison of the incidence of depression after cesarean section between the two groups.

Groups	N	Prenatal 1d	Postpartum 3d	Postpartum 42d
Control group	69	6(9.09)	17(24.64)	15(21.74)
Research group	69	5(7.25)	7(10.14)	6(9.09)
χ^2		0.099	3.957	4.550
P		0.753	0.047	0.033

tum depression can threaten the baby's personality, cognitive ability, and behavioral training [6]. Therefore, it is of great significance to take active and effective preventive measures for the occurrence and development of depression after cesarean section.

In the current clinical work, although the antidepressant drugs taken can achieve a certain antidepressant effect, but antidepressant drugs have general flaws, mainly manifested in a delay of several weeks before it can take effect. In particular, some mothers who need to breastfeed have obvious rejection of most antidepressant drugs [7, 8]. Ketamine hydrochloride was first developed by Parke Davis in 1962 and belongs to a class of derivatives of phencyclidine

(PCP). Ketamine hydrochloride is mainly used for anesthesia and has achieved good effects. Subsequently, after the acquisition of ketamine hydrochloride by Pfizer, a dextrorotatory split of ketamine (esketamine), was developed to exert a stronger and safer analgesic effect [9, 10], clinical data show that esketamine has stronger affinity and potency than ketamine hydrochloride. In addition, the pharmacokinetics of esketamine are controllable, and it can also achieve good results in the treatment of treatment-resistant depression [11, 12]. The mechanism of action of ketamine hydrochloride in the prevention and control of depression and its related symptoms lies in the inactivation of eukaryotic elongation factor-2 kinase through enhanced blocking of NMDA receptors. The inactivation of eukaryotic elongation factor-2 kinase reduces the level of eukaryotic elongation factor-2, avoids the increase of BDNF expression, and finally achieves the purpose of anti-depression. But whether ketamine hydrochloride can play an antidepressant effect after cesarean section is still worthy of research and analysis [13, 14]. Therefore, this study analyzed the preventive effect of esketamine on the occurrence of PPD after cesarean section. The results showed that the SBP, DBP, and HR of the observation group were higher than those of the control group at T4 and T5 time points. There was no significant difference in SBP, DBP, and HR at T3, T4, and T5 time in the observation group. Compared with T3, SBP, DBP, and HR were lower in control group T4 and T5, respectively. It can be seen that the application of esketamine can better ensure the stability of the patient's heart rate and blood pressure. And there is no increase in adverse reactions during the treatment period, ensuring the safety of the drug during the application period. When observing depressive symptoms, it can be seen that the EPDS score of the observation group was lower than that of the control group and the incidence of postpartum depression was higher at 3d and 42d postpartum. The results confirmed that esketamine has a strong antidepressant effect and effect and the depressive symptoms of some puerperae were relatively relieved, which was basically consistent with previous reports [15, 16]. At the same time, esketamine has a faster action speed and a relatively longer action time and has more comprehensive advantages. However, some experts believe that esketamine itself has a strong stimulating effect on the sympathetic nerve, which can easily lead to abnormally high blood pressure in mothers. Therefore, during the use of esketamine, it is necessary to comprehensively evaluate various basic indicators of cesarean section and select an appropriate dose to ensure better tolerance and safety for puerperae [17, 18].

In conclusion, the application of esketamine after cesarean section can effectively reduce depression-related scores and the risk of postpartum depression. And esketamine does not increase adverse reactions and has high safety. In the following clinical work, the sample size can be further expanded, the observation indicators can be increased, and the follow-up time can be extended, so as to better comprehensively evaluate the application effect of esketamine after cesarean section.

Data Availability

Data to support the findings of this study is available on reasonable request from the corresponding author.

Conflicts of Interest

The authors declare that they have no conflicts of interest.

Authors' Contributions

Qiwei Wang and Maoxin Xiao contributed equally to this work.

References

[1] S. Jiaduo, H. Juanming, H. Mengjiao, D. Guonan, X. Shiyuan, and Z. Qingguo, "Effect of pregnancy complicated with diabetes mellitus on maternal ropivacaine subarachnoid block time effect," *Journal of Practical Medicine*, vol. 35, no. 4, pp. 602–605, 2019.

[2] S. Jie, Y. Yingjing, T. Yanmei, and W. Zhangyuan, "Research on the preventive effect of low-dose ketamine on postpartum depression after cesarean section," *Modern Medicine and Health*, vol. 3, no. 18, pp. 2956–2960, 2020.

[3] C. R. Martin and M. Redshaw, "Establishing a coherent and replicable measurement model of the Edinburgh Postnatal Depression Scale," *Psychiatry Research*, vol. 264, pp. 182–191, 2018.

[4] Z. Ling, W. Li, Z. Yan, and C. Xiufang, "Cesarean section rate and composition of cesarean section indications in the past 5 years: analysis of data from a hospital," *Chinese Journal of Family Planning*, vol. 27, no. 11, pp. 92–94, 2019.

[5] W. Zhongmin, L. Lijun, S. Yanan, D. Qi, and W. Zhixian, "Clinical research progress of vaginal delivery in re-pregnancy after cesarean section," *Clinical Misdiagnosis and Mistreatment*, vol. 32, no. 11, pp. 107–111, 2019.

[6] R. Komatsu, K. Ando, and P. D. Flood, "Factors associated with persistent pain after childbirth: a narrative review," *British Journal of Anaesthesia*, vol. 124, no. 3, pp. e117–e130, 2020.

[7] X. Pan Ren, P.,. Y. Jing, M. Zhong, and C. Luying, "Comparison of the effect of quadratus lumborum block for postoperative analgesia after cesarean section and its influence on the consumption of analgesic drugs," *Chinese Maternal and Child Health Care*, vol. 35, no. 10, pp. 1793–1799, 2020.

[8] X. Rui, L. Guangxiang, Z. Wenwen, and W. Luoxuan, "Effects and mechanism of a single injection of ketamine on fear behavior in animal scenarios of post-traumatic stress disorder," *Chinese Journal of Pharmacology and Toxicology*, vol. 34, no. 2, pp. 104–111, 2020.

[9] P. Zanos and T. D. Gould, "Mechanisms of ketamine action as an antidepressant," *Molecular Psychiatry*, vol. 23, no. 4, pp. 801–811, 2018.

[10] J. Kamp, M. Van Velzen, E. Olofsen, M. Boon, A. Dahan, and M. Niesters, "Pharmacokinetic and pharmacodynamic considerations for NMDA-receptor antagonist ketamine in the treatment of chronic neuropathic pain: an update of the most recent literature," *Expert Opinion on Drug Metabolism & Toxicology*, vol. 15, no. 12, pp. 1033–1041, 2019.

[11] V. S. Pereira and V. A. Hiroaki-Sato, "A brief history of antidepressant drug development: from tricyclics to beyond ketamine," *Acta Neuropsychiatr*, vol. 30, no. 6, pp. 307–322, 2018.

[12] Q. Na, J. Li, S. Jiangtao, M. Huimin, L. Guofang, and Z. Hongyang, "Effect of multimodal analgesia on postoperative analgesia and postpartum depression in cesarean section women," *Clinical Misdiagnosis and Mistreatment*, vol. 33, no. 5, pp. 26–32, 2020.

Research Article

The Effect of Exercise Motivation on Eating Disorders in Bodybuilders in Social Networks: The Mediating Role of State Anxiety

Yixin Liu and Yuping Cao [ID]

College of Physical Education, Xinjiang Normal University, Urumqi 830054, China

Correspondence should be addressed to Yuping Cao; xjnucyp@sina.com

The aim of this study is to explore the relationship between exercise motivation and eating disorder and the mediating effect of anxiety in physical exercise. Athletes are in a social network, and the different human-machine relationships and situations generated in this may produce different sports motivations and anxiety states for athletes. The exercise motivation, status-trait anxiety, and eating disorder of 1076 fitness subjects were described and analyzed by questionnaire survey, and the survey data were statistically analyzed by means of correlation, regression, and structural equation model. The results showed that the overall detection rate of eating disorder was 56.3%. The overall detection rate of eating disorder was different between males and females. Exercise motivation has a significant positive correlation with state anxiety and eating disorder. Exercise motivation has a significant positive predictive effect on eating disorder, exercise motivation has a significant positive predictive effect on state anxiety, and state anxiety has a significant positive predictive effect on eating disorder. The mediating effect shows that state anxiety can partially mediate the relationship between exercise motivation and eating disorder, exercise motivation has a direct impact on eating disorder, and state anxiety has an indirect impact on eating disorder. In physical exercise, the exercisers' bad exercise motivation will produce too much anxiety. Poor exercise motivation and anxiety can lead to symptoms of eating disorders. In physical exercise, we should adopt reasonable value orientation and positive psychological suggestion and encourage healthy and reasonable eating behavior, which will help to prevent and treat eating disorders.

1. Introduction

According to the report of the American Psychiatric Association (APA) in 2000, eating disorders have become the third chronic disease among adolescent women, with the incidence rate of about 5%. Including China, Japan, South Korea, and other economically developed eastern countries, the incidence of eating disorders is reported to be increasing year by year [1]. Eating disorder (ED) abnormal eating behavior patterns, such as repeated overeating, or a type of mental disorder with diet as the main clinical characteristics is a kind of psychological disorder, involving persistent disorders in eating habits or other behaviors designed to control weight, body shape, or shape [2]. There are four main categories of eating disorders, including anorexia nervosa

(AN), bulimia nervosa (BN), atypical nervosa, and binge eating disorder (BED), with anorexia and bulimia as the most common disorders. Eating disorders not only impaired physiological function but also highlight the psychological problems of patients. Excessive attention to weight and body shape as well as morbid fear of weight gain is the core features of eating disorders [3]. The origin of eating disorders is widely recognized as a result of multiple factors, with individual risk factors that must be considered in a complex etiological model, including biological factors related to personality traits, heredity and malnutrition, sociocultural factors based on cultural constraints, and family factors based on overprotection and family conflict, and in individuals, only a few studies have reported that eating disorders were associated with adverse life events prior to their occurrence, such as loss

of a close relative or separation from a close friend. Again, this does not seem to be unique to patients with eating disorders, but it also stands out in individuals with other psychological problems. Further risk factors include chronic physical conditions such as diabetes, chronic intestinal disease, and other physical conditions associated with diet and body weight change [4]. Eating disorders often cause harmful manifestations of a series of physical and mental health problems (such as dehydration, arrhythmia, hypotension, decreased self-confidence, anxiety, depression, and even suicide). Therefore, identifying various precipitating factors and the mechanisms that induce eating disorders have become the key issues in the current study of eating disorders.

Studies have shown that participating in sports will bring health, self-esteem, self-confidence, and skill development, and social function brings many benefits [5, 6]. However, some aspects of sports competitions and training may damage the physical and mental health of athletes. The sports environment emphasizes physical development and training as well as nutritional strategies and diet to optimize performance, which may increase the risk of athletes suffering from eating disorders. In addition, the types of exercise motivation are often related to the sport field in which they work, and the need for specific body shape conditions or weight requirements in athletic achievement is related to the increased risk of eating disorders [7, 8]. Thus, there is a correlation between exercise motivation and eating disorders. Many behavioral characteristics describe that the extrinsic motivation and active individuals are related to eating disorders. Individuals with symptoms or diseases of eating disorders often show a high level of ineffectiveness, helplessness, lack of control, and lack of self-esteem [9]. According to the research report by Filaire et al. [10], eating disorders are related to motivation orientation. In gymnasts, an energy gap is usually caused to improve sports goals and performance. In addition, the intervention of extrinsic motivation has a negative relationship with self-esteem and body image. People with high level of extrinsic motivation will show low self-esteem and less satisfactory body image. In this group with higher self-demand, the risk of eating disorders will also increase when the body weight is low [11]. At the same time, according to the results of Homan et al. [12], they found that when teenagers' exercise motivation is to find strong sensory stimulation in sports, they may appear after 20 months having eating disorders; thus, extrinsic motivation and goal motivation are important factors that affect the occurrence of eating disorders in adolescents. However, Calderon et al. [13] learned from the survey of female college athletes that exercise motivation was also highly correlated with eating disorders. Athletes in high-intensity sports (such as basketball and cross-country running) and sports with high requirements for body shape or specific weight (i.e., cheerleading, track and field, and gymnastics) were more likely to have eating disorders in their motivation to participate in sports. That is to say, among the athletes who participated in the above sports, their intrinsic motivation was related to a lower risk of eating disorders, and their extrinsic motivation was related to a higher risk of eating disorders.

In addition, many studies have shown that negative emotions can also have a significant impact on eating disorders. They often confuse emotional state with hunger and satiety, thus relieving anxiety through eating. Environmental factors are one of the important factors affecting ED. For young people (teenagers) with a tendency to overeat, when they live in an obese family environment, they are more likely to relieve anxiety by eating. It has also been verified that physical dissatisfaction and anxiety during adolescence increase the risk of persistent obesity [14]. However, research results by Ackard et al. [15] provide strong and consistent evidence that the dieting frequency of young female college students with normal weight is related to more symptoms and more severe eating disorder behaviors and emotional distress regardless of BMI. The frequency of dieting was also associated with affective disorders such as depression, low self-esteem, difficulty in distinguishing and regulating emotions, mature fear, ineffectiveness, perfectionism, and insecurity. In domestic studies, Chen et al. [16] proposed in a study on negative emotions, overweight or obesity, and abnormal eating behavior that strong negative emotions, such as anxiety, may have a predictive effect on the occurrence of eating disorders. At the same time, exercise motivation also has a significant impact on anxiety. The relationship between exercise motivation and anxiety is mainly reflected in the higher level of motivation which will lead to higher exercise anxiety. Han [17] through the study of women's volleyball athlete exercise motivation understands that the root cause of anxiety lies in the uncertainty of the result of the game. If you have a strong desire to win and do not know what your performance will be in the upcoming competition and whether you can cope with possible difficulties in the competition, you may have high anxiety. Factors such as one's own ability, the evaluation of the importance of the competition, and the level of preparation for the competition may be related to the anxiety experience before the competition. In the research of Ye [18], the exercise motivation of amateur athletes was highly correlated with trait anxiety, and the participation motivation of sports activities significantly predicted the trait anxiety of participants. Amateur sports for sports learned helplessness is a threat to self-esteem anxiety situation.

In summary, according to previous studies, exercise motivation and anxiety can lead to eating disorders, but its internal mechanism is still unclear. At present, there is no conclusion on the relationship between the exercise motivation and eating disorders. In this study, we introduced anxiety into the effect of exercise motivation on eating disorders, aiming to determine how exercise motivation causes eating disorders. In the study, exercisers completed three tests: exercise motivation, eating disorder, and state-trait Anxiety. We assume that exercisers have a high level of exercise motivation, and exercise motivation can also lead to eating disorders, but the introduction of anxiety will reduce the impact of exercise motivation on eating disorders; that is, anxiety plays an intermediary role in the impact of exercise motivation on eating disorders. The determination of the above relationship can clarify how exercise motivation causes eating disorders on the one hand

and strengthen the intervention and regulation of exercisers' anxiety on the other hand, which is of important practical significance for the prevention and treatment of eating disorders.

2. Objects and Methods

2.1. Objects. Using a convenient sampling method, 606 subjects with eating disorders were selected from 1076 subjects in 5 gymnasiums in Urumqi, including 365 males and 242 females, with the average age of 25.7 ± 3.07 years old and the average number of exercises per week of 5.65 ± 0.65. A questionnaire survey was conducted on May 4, 2020. The questionnaire collection followed the voluntary principle, and a total of 1076 questionnaires were collected. No questionnaire was collected, so no tracking was required.

2.2. Questionnaire Survey Method

2.2.1. State Anxiety Scale. S-AI [19] is a subscale of the State-Trait Anxiety Scale (STAI) developed by Spielberger in 1983 and is one of the most widely used scales for studying anxiety and other issues in China and abroad. The questionnaire consisted of 20 items with a 4-point scoring method. Cronbach's reliability coefficient and test-retest reliability of the scale were 0.88 and 0.864, respectively. The results of confirmatory factor analysis showed that $x^2/df = 9.77$, RMSEA = 0.07, GFI = 0.91, NFI = 0.93, CFI = 0.93, and IFI = 0.91, indicating a good structural validity. It has good reliability and validity.

2.2.2. Exercise Motivation Scale. The exercise motivation scale (MPAM-R) [20] adopted the simplified version of the exercise motivation scale revised by Chen in 2013, which was reduced to 15 topics, including five dimensions of fun, ability, appearance, health, and social interaction. The scale was scored using the Likert 5-level scale, and the motivation intensity ranged from "none" to "very strong." Cronbach's reliability coefficient of the five subscales is above 0.7, and the test-retest reliability is 0.91. The results of confirmatory factor analysis showed that $x^2/df = 7.63$, RMSEA = 0.06, GFI = 0.92, NFI = 0.92, CFI = 0.98, and IFI = 0.93. The results of confirmatory factor analysis showed that the scale had good structural validity, indicating that the scale had good reliability and validity [20].

2.2.3. Eating Disorder Scale. The Eating Disorder Attitude Test (EAT-26) [21] consisted of 26 questions with three dimensions: diet, oral control, and gluttony, which was rated on the Richter 6-point scale, ranging from 1 (always) to 6 (never). Eating disorders with a score greater than or equal to 20 were considered "at risk." It is useful and effective in determining the prevalence of eating disorders but does not diagnose specific disorders. The index of Cronbach in this study was α coefficient of 0.91. The results of confirmatory factor analysis showed that $x^2/df = 8.92$, RMSEA = 0.08, GFI = 0.94, NFI = 0.91, CFI = 0.94, and IFI = 0.92, showing good structural validity. EAT-26 has been verified as a reliable and effective tool for screening for eating disorders [22, 23].

2.3. Mathematical Statistics. The SPSS24.0 and AMOS24.0 analysis software packages were used for data management and statistical analysis. The demographic variables of exercisers, exercise motivation, state anxiety, and eating disorders were described in statistical analysis, difference test, correlation analysis, and regression analysis, and the structural equation model was used to test the relationship between exercise motivation, state anxiety, and eating disorders.

3. Results

3.1. Common Method Deviation Inspection. In this study, all the data were collected through a questionnaire using an anonymous questionnaire, balanced project sequence, and different measurement methods.

The test and other program control method [24], so the common method deviation (Harman single factor test) was used to test. The results show that there are seven factors whose eigenvalues are greater than 1, and the variance explained by the first factor is 18.32%, which is less than the critical criterion of 40%, indicating that there is no serious problem of common method deviation.

3.2. Narrative Statistical Results. Table 1 presents the mean (M), standard deviation (SD), and correlation matrices for exercise motivation, state anxiety, and eating disorders. The results showed that exercisers with dysphagia (25.48 ± 1.890) had higher state anxiety (71.53 ± 22.706) and stronger exercise motivation (60.89 ± 9.897) at the same time. Correlation analysis showed a significant positive correlation between state anxiety and eating disorders ($r = 0.503$, $P < 0.01$). There was a significant positive correlation between eating disorders and exercise motivation ($r = 0.137$, $P < 0.01$). There was a positive correlation between exercise motivation and state anxiety ($r = 0.084$, $P < 0.05$). In addition, there were significant differences in state anxiety ($t = 0.460$, $P < 0.05$) and eating disorders ($t = -5.229$, $P < 0.01$) between the sexes, but there was no significant difference in exercise motivation ($t = -0.498$, $P > 0.05$), so gender was not taken as the control variable in the later analysis. The above results indicated that regression analysis could be further conducted.

3.3. Regression Analysis of State Anxiety, Exercise Motivation, and Eating Disorder. The intermediary effect test procedure proposed by Wen et al. [25] was used to test the relationship between eating disorder (EAT) as a dependent variable, exercise motivation (MPAM-R) as an independent variable, and state anxiety (S-AI) as an intermediary variable. In the first step, the independent variable MPAM-R is tested for predicting the dependent variable EAT. The results showed that MPAM-R could explain 1.7% variation of EAT, and exercise motivation of exercisers could significantly positively predict eating disorders ($\beta = 0.313$, $P < 0.01$). In the second step, the prediction effect of independent variable MPAM-R on intermediate variable S-AI is examined. The results showed that MPAM-R could explain 0.5% variation of S-AI, and exercise motivation of exercisers could

TABLE 1: Average score of all variables, the standard deviation, and the correlation coefficient.

Variable	$M \pm SD$	S-AI	EAT	MPAM-R
S-AI	46.77 ± 8.165	1	0.503^{**}	0.084^*
EAT	71.46 ± 22.527	0.503^{**}	1	0.137^{**}
MPAM-R	60.96 ± 9.879	0.084^*	0.137^{**}	1

Note: S-AI: state anxiety; EAT: eating disorders; MPAM-R: training motivation. $N = 606$. $^*P < 0.05$, $^{**}P < 0.01$: the same below.

significantly positively predict state anxiety ($\beta = 0.069$, $P < 0.05$). In the third step, the prediction effects of independent variable MPAM-R and intermediate variable S-AI on dependent variable EAT are tested simultaneously. The results showed that MPAM-R and S-AI could explain 2.6% variation of EAT, exercisers' intermediary variable S-AI could significantly positively predict eating disorder ($\beta = 1.366$, $P < 0.01$), and the standard regression coefficient of exercise motivation on eating disorder changed from 0.313 to 1.366, but it was still at a significant level as shown in Table 2.

3.4. Path Analysis. First, according to the research assumptions and regression analysis, the relationship model of exercise motivation, state anxiety, and eating disorders was constructed. Exercise motivation could significantly positively predict eating disorders, exercise motivation significantly positively predicted state anxiety, and state anxiety significantly positively predicted eating disorders. Then, AMOS24.0 was used to fit the data. The fitting results are shown in Table 3 and Figure 1. In this study, CMIN/DF was 1.919, GFI, TLI, CFI, and IFI were all greater than 0.9, and RMSEA was less than 0.5. The fitting indexes all met the criteria. The above fitting indexes indicated that the model constructed in this study was good, and the relationship between exercise motivation, state anxiety, and eating disorder could be explained based on the model in Table 3 and Figure 1.

From the results of path analysis, exercise motivation had a significant and direct positive prediction effect on state anxiety ($\beta = 0.05$, $P < 0.05$). State anxiety had a significant direct positive prediction of eating disorders ($\beta = 0.05$, $P < 0.05$). Exercise motivation had a significant positive prediction of eating disorders ($\beta = 0.07$, $P < 0.05$). The state anxiety in this model played a part of the intermediary role.

4. Discussion

4.1. The Relationship between Exercise Motivation and Eating Disorders. This study showed that in the regular exercise population, the exercise motivation of exercisers had a significant positive prediction of eating disorders, which was consistent with the hypothesis of this study. The causes of eating disorders are very complex. Studies have shown that neurobiological factors, sociological factors, family factors, and individual psychological factors are all factors contributing to eating disorders. Bad exercise motivation, as a psychological factor, is also an important factor inducing eating disorders. This result is similar to that of Mau-

gendre et al. [11], in that the purpose and mobility of sports affect the severity of eating disorders in exercisers who participate in intensive sports. Exercisers want to achieve the high level stipulated in the sports, which prompted them to put forward very high requirements for themselves, in order to achieve a high level of state and to strengthen the physical fitness. This kind of external motivation intervention makes the psychological and physical image have a negative relationship; with a high level of external motivation, people will show low self-esteem and less satisfactory physical image, which leads to an increase in the risk of eating disorders, but individuals do not think that this behavior is negative. In general, people who exercised regularly had higher characteristics of health motivation, ability motivation, appearance motivation, social motivation, and fun motivation. The effects of different motivation types on eating disorders were different, and the severity of eating disorders was determined with the duration of time.

4.2. The Relationship between Exercise Motivation and State Anxiety. This study showed that in the regular exercise population, the exercise motivation of exercisers had a significant positive predictive effect on state anxiety, which was consistent with the hypothesis of this study. Exercise motivation that is too weak or too strong will not smoothly complete the task and achieve ideal results; the former will reduce the level of individual emotional excitement and be easy to cause concentration to be easily interfered by irrelevant stimuli. On the contrary, the latter excessively focuses consciousness on specific goals and produces anxiety, which will affect individual motor performance. Understand that anxiety may originate from focusing on whether or not a goal is being achieved. If you have a strong purpose and are not sure whether you can deal with the difficulties that may occur in the exercise and whether the effect is significant after the exercise, anxiety may occur. Similar to amateur athletes, exercise motivation is highly correlated with anxiety, especially for learned helplessness athletes who take part in sports; sports is an anxiety situation threatening their self-esteem [18]. Similarly, among exercisers, women with physical anxiety will not participate in physical exercise due to negative evaluation of others, especially among young women; anxiety has become an obstacle to participate in exercise [26]. In addition, some survey results show that people with high BMI and social anxiety are more likely to avoid sports [27], so the relationship between sports motivation and anxiety needs further study.

4.3. The Intermediary Role of State Anxiety. The results of this study showed that among exercisers, state anxiety played a part of the intermediary role in the relationship between exercise motivation and eating disorders. Exercise motivation not only has a direct effect on eating disorders but also has an indirect effect on eating disorders through state anxiety. The results of this study explained that exercisers with higher exercise motivation were often accompanied by anxiety, and at the same time, this group of people had higher appearance, ability, social interaction, fun, and health motivation. These motivations lead to anxiety and

TABLE 2: Regression analysis of the influence of exercise motivation and state anxiety on eating disorder.

	The first step Eating disorders		The second step State anxiety		The third step Eating disorders	
Fitting index	β	t	β	t	β	t
Training motivation	0.313	3.405**				
Training motivation			$\beta = 0.069$	2.067*		
Exercise motivation and state anxiety					$\beta = 0.218$	2.727**
					$\beta = 1.366$	14.110**
F	11.592		4.274		17.249	
R	0.137		0.084		0.512	
R^2	0.017		0.005		0.260	

TABLE 3: Model fitting index.

Model	CMIN	DF	CMIN/DF	GFI	CFI	IFI	RMSEA
Model	47.967	25	1.919	0.981	0.991	0.991	0.039

Note: ellipse represents latent variable, and box represents observed variable. The arrow between the ellipse and the box indicates the factor load, and the arrow between the ellipses indicates the path coefficient.
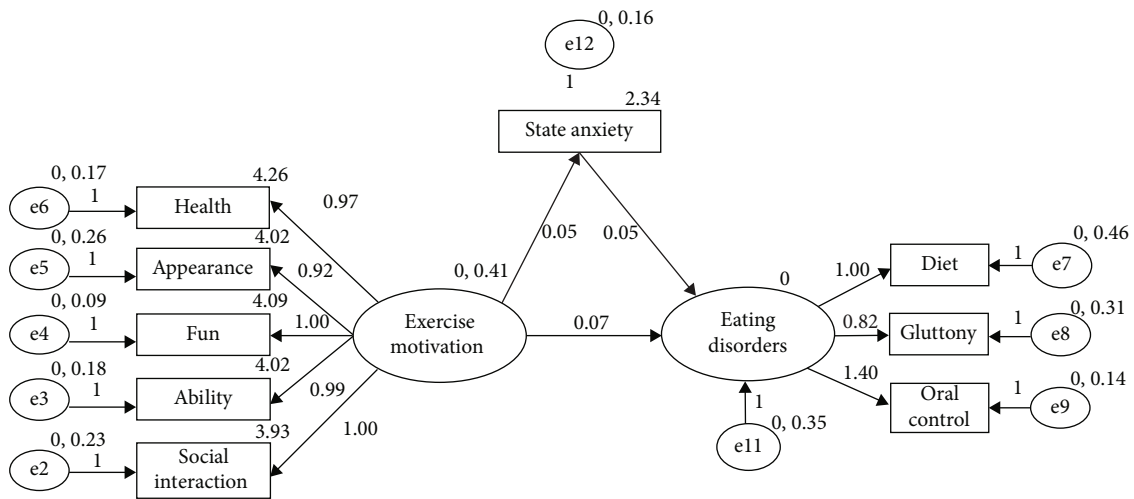
FIGURE 1: Relationship model of exercise addiction, state anxiety, and eating disorder.

demanding eating behaviors. At the same time, this excessive psychological pressure will have an impact on body shape, extreme eating behaviors (anorexia, bulimia, etc.), and exercise behavior itself, resulting in individuals showing a high level of ineffectiveness, helplessness, lack of control, and lack of self-esteem, indicating that negative emotions have a significant impact on eating disorders. They usually connect the emotional state with hunger and satiety, so as to relieve anxiety through eating.

5. Conclusions and Recommendations

5.1. Conclusion. (1) The total detection rate of eating disorders among exercisers is 56.3%, which is more than half,

indicating that the prevalence of eating disorders is higher in the population with regular exercise. (2) Gender has significant difference in eating disorders, and the prevalence of male is higher in women, which is different from the previous research results, indicating that the male population cannot be ignored. (3) Correlation analysis shows that there is a significant positive correlation among exercise motivation, state anxiety, and eating disorder, indicating that exercise motivation of exercisers is often closely related to state anxiety and eating disorder. (4) The intermediary effect results show that state anxiety plays a partial intermediary role between exercise motivation and eating disorders. Exercise motivation indirectly affects eating disorders through state anxiety

5.2. Recommendations. The results of this study indicated that exercisers were among the high risk population of eating disorders, which resulted in this result because of wrong views on exercise and diet. For exercisers with eating disorders, scientific views on exercise, diet, and psychological counseling were urgently needed from professionals. At present, as a result of the popular aesthetic standards in the society, women regard thinness as their beauty and men pursue the acme figure. This requires the family, school, and society to establish a healthy and reasonable value orientation for teenagers, instead of an extreme and unique aesthetic standard. This article provides a preliminary survey of state anxiety, eating disorders, and exercise motivation that, if left untreated, eating may still plague those who want to be happy but miserable. However, the harmfulness of eating disorder goes beyond this. Psychological education on motor dysfunction should be provided for this group of people, and they should be aware that this is not as important as imagined to reduce negative emotions. Future studies should continue to investigate the relationship between the components of dysfunctional locomotion and eating disorders and explore the effects of different forms of exercise on exercise motivation, eating disorders, and anxiety. In addition, studies should include a more diverse sample size to ensure replicable studies. Also, the analysis of typical individual cases should be carried out. It is hoped that future studies will continue to investigate the influencing factors of exercise and diet in order to create more targeted treatments.

Data Availability

The datasets used and analyzed during the current study are available from the corresponding author on reasonable request.

Conflicts of Interest

The authors declared no potential conflicts of interest with respect to the research, authorship, and/or publication of this article.

Acknowledgments

References

[1] S. Lee and A. M. Lee, "Disordered eating in three communities of China: a comparative study of female high school students in Hong Kong, Shenzhen, and rural Hunan," *The International Journal of Eating Disorders*, vol. 27, no. 3, pp. 317–327, 2000.

[2] American Psychiatric Association, "DSM-5 Development [EB]," 2010, http://www.dsm5.org/pages/default.aspx.

[3] H. Simon, "Eating disorders: anorexia and bulimia [EB]," http://adam.about.

[4] R. K. Dodd and R. E. Vetter, "College females' self-perceptions of their overall physical self-worth," *American Journal of Health Studies*, vol. 30, no. 3, pp. 110–118, 2015.

[5] A. Snyder, J. Martinez, R. Bay, J. T. Parsons, E. L. Sauers, and T. C. V. McLeod, "Health-related quality of life differs between adolescent athletes and adolescent nonathletes," *Journal of Sport Rehabilitation*, vol. 19, no. 3, pp. 237–248, 2010.

[6] J. M. Holm-Denoma, V. Scaringi, K. H. Gordon, K. A. Van Orden, and T. E. Joiner Jr., "Eating disorder symptoms among undergraduate varsity athletes, club athletes, independent exercisers, and nonexercisers," *The International Journal of Eating Disorders*, vol. 42, no. 1, pp. 47–53, 2009.

[7] M. K. Torstveit, J. H. Rosenvinge, and J. Sundgot-Borgen, "Prevalence of eating disorders and the predictive power of risk models in female elite athletes: a controlled study," *Scandinavian Journal of Medicine & Science in Sports*, vol. 18, no. 1, pp. 108–118, 2008.

[8] F. V. Froreich, L. R. Vartanian, J. R. Grisham, and S. W. Touyz, "Dimensions of control and their relation to disordered eating behaviours and obsessive-compulsive symptoms," *Journal of Eating Disorders*, vol. 4, pp. 1–9, 2016.

[9] J. Morgan, F. Reid, and J. Lacey, "The SCOFF questionnaire: assessment of a new screening tool for eating disorders," *BMJ*, vol. 319, no. 7223, pp. 1467-1468, 1999.

[10] E. Filaire, M. Rouveix, M. Bouget, and C. Pannafieux, "Prevalence of eating disorders in athletes," *Science Sports*, vol. 22, no. 3-4, pp. 135–142, 2007.

[11] M. Maugendre, E. Spitz, and J. B. Lanfranchi, "Longitudinal study of sport motivation's effects about eating disorders among girls," *Evolution Psychiatrique*, vol. 74, no. 3, pp. 430–444, 2009.

[12] K. J. Homan, S. L. Crowley, and L. A. Sim, "Motivation for sport participation and eating disorder risk among female collegiate athletes," *Eating Disorders*, vol. 27, no. 4, pp. 369–383, 2019.

[13] C. Calderon, M. Fornsy, and V. Varea, "Implication of the anxiety and depression in eating disorders of young obese," *Nutricion Hospitalaria Organo Oficial De La*, vol. 25, pp. 641–647, 2010.

[14] K. Anastasia, D. Tammy, and K. Akihito, "College women with eating disorders: self-regulation, life satisfaction, and positive/negative affect," *The Journal of Psychology*, vol. 137, no. 4, pp. 381–395, 2003.

[15] D. M. Ackard, J. K. Croll, and C. A. Kearney, "Dieting frequency among college females: association with disordered eating, body image, and related psychological problems," *Journal of Psychosomatic Research*, vol. 52, no. 3, pp. 129–136, 2002.

[16] G. U. I. Chen, C. A. I. Taisheng, L. Zhihua, and W. Liu, "Decision-making deficits in overweight and obese individuals: evidence from the open door and delayed discounting task," *Chinese Journal of Clinical Psychology*, vol. 23, no. 1, pp. 38–47, 2015.

[17] H. A. N. Xu, *Study on Training Motivation of Henan Women's Volleyball Team*, Henan University, China, 2007.

[18] Y. E. Ping, "The relationship between motivation to participate in extracurricular sports activities and trait anxiety," *Journal of Chengdu Institute of Physical Education*, vol. 27, no. 3, pp. 85–87, 2001.

[19] L. Zengrang and Z. Xi, *Anxiety theory and diagnosis and treatment strategies*, People's Publishing House, Beijing, 2015.

[20] C. Shanping, Y. Wang, R. Jianzhong, X. Pan, and J. Bao, "Construction and reliability and validity analysis of a simplified version of exercise motivation scale," *Journal of Beijing Sport University*, vol. 2, pp. 66–78, 2013.

[21] D. Garner, M. Olmstead, and J. Polivy, "Development and validation of a multidimensional eating disorder inventory for anorexia nervosa and bulimia," *International Journal of Eating Disorders*, vol. 2, no. 2, pp. 15–34, 1983.

[22] B. Cook, H. Hausenblas, D. Tuccitto, and P. R. Giacobbi Jr., "Eating disorders and exercise: a structural equation modelling analysis of a conceptual model," *European Eating Disorders Review*, vol. 19, no. 3, pp. 216–225, 2011.

[23] D. Garner, M. Olmsted, Y. Bohr, and P. E. Garfinkel, "The eating attitudes test: psychometric features and clinical correlates," *Psychological Medicine*, vol. 12, no. 4, pp. 871–878, 1982.

[24] H. Zhou and L. Long, "Statistical test and control method of common method deviation," *Advances in Psychological Science*, vol. 12, no. 6, pp. 942–950, 2004.

[25] W. Zhonglin, Z. Lei, H. Jietai, and L. Hongyun, "Mediation effect test program and its application," *Journal of Psychology*, vol. 36, no. 5, pp. 614–620, 2004.

[26] R. Ma and H. Chunmei, "A review of social physical anxiety and exercise motivation and behavior," *Martial Arts Scientific*, vol. 10, no. 5, pp. 107–109, 2013.

[27] A. Horenstein, S. C. Kaplan, R. M. Butler, and R. G. Heimberg, "Social anxiety moderates the relationship between body mass index and motivation to avoid exercise," *Body Image*, vol. 36, no. 2, pp. 185–192, 2021.

Retraction

Retracted: 23G Minimally Invasive Vitrectomy Combined with Glaucoma Drainage Valve Implantation and Phacoemulsification Cataract Extraction for Neovascular Glaucoma Secondary to Proliferative Diabetic Retinopathy with Vitreous Hemorrhage

Computational and Mathematical Methods in Medicine

This article has been retracted by Hindawi following an investigation undertaken by the publisher [1]. This investigation has uncovered evidence of one or more of the following indicators of systematic manipulation of the publication process:

(1) Discrepancies in scope

(2) Discrepancies in the description of the research reported

(3) Discrepancies between the availability of data and the research described

(4) Inappropriate citations

(5) Incoherent, meaningless and/or irrelevant content included in the article

(6) Peer-review manipulation

The presence of these indicators undermines our confidence in the integrity of the article's content and we cannot, therefore, vouch for its reliability. Please note that this notice is intended solely to alert readers that the content of this article is unreliable. We have not investigated whether authors were aware of or involved in the systematic manipulation of the publication process.

Wiley and Hindawi regrets that the usual quality checks did not identify these issues before publication and have since put additional measures in place to safeguard research integrity.

We wish to credit our own Research Integrity and Research Publishing teams and anonymous and named external researchers and research integrity experts for contributing to this investigation.

The corresponding author, as the representative of all authors, has been given the opportunity to register their agreement or disagreement to this retraction. We have kept a record of any response received.

References

[1] X. Shi, N. Dong, Y. Liang, L. Zheng, and X. Wang, "23G Minimally Invasive Vitrectomy Combined with Glaucoma Drainage Valve Implantation and Phacoemulsification Cataract Extraction for Neovascular Glaucoma Secondary to Proliferative Diabetic Retinopathy with Vitreous Hemorrhage," *Computational and Mathematical Methods in Medicine*, vol. 2022, Article ID 7393661, 8 pages, 2022.

Research Article

23G Minimally Invasive Vitrectomy Combined with Glaucoma Drainage Valve Implantation and Phacoemulsification Cataract Extraction for Neovascular Glaucoma Secondary to Proliferative Diabetic Retinopathy with Vitreous Hemorrhage

XiaoLing Shi [1,2] **Nuo Dong** [1,2,3] **Yuanyuan Liang** [4] **Lin Zheng** [1,2] **and Xiaobo Wang** [1,2]

[1]*Eye Institute and Affiliated Xiamen Eye Center of Xiamen University, School of Medicine, Xiamen University, Xiamen, 361100 Fujian, China*
[2]*Fujian Provincial Key Laboratory of Corneal & Ocular Surface Diseases, Xiamen, 361002 Fujian, China*
[3]*Department of Ophthalmology, Affiliated People's Hospital & Zhenjiang Kangfu Eye Hospital, Jiangsu University, Zhenjiang, 212003 Jiangsu, China*
[4]*Huaihe Hospital of Henan University, Kaifeng, 475000 Henan, China*

Correspondence should be addressed to Xiaobo Wang; wangxiaobo@xmuedu.org.cn

Objective. To evaluate the clinical efficacy of the combined application of 23G minimally invasive vitrectomy, glaucoma drainage valve implantation, and phacoemulsification cataract extraction in the treatment of neovascular glaucoma (NVG) secondary to proliferative diabetic retinopathy (PDR) combined with vitreous hemorrhage (VH). *Methods.* Eighty-three patients (91 eyes) with PDR diagnosed as NVG phase III complicated with VH from June 2018 to May 2020 were selected as the study subjects. The subjects were randomly divided into 3 groups: group A was treated with 23G minimally invasive vitrectomy combined with glaucoma drainage valve implantation; group B was given 23G minimally invasive vitrectomy combined with phacoemulsification cataract extraction; and group C was treated with 23G minimally invasive vitrectomy combined with glaucoma drainage valve implantation and phacoemulsification cataract extraction. The uncorrected visual acuity (UCVA), intraocular pressure (IOP), and iris neovascularization (INV) scores were recorded and compared among the 3 groups before and after operation, and then the postoperative pain relief and complications were observed. *Results.* Through observation, there was no significant difference in the UCVA, IOP, and INV scores in the 3 groups before operation. After the operation, the UCVA, IOP, and INV scores of the 3 groups were significantly lower than those before operation. After operation, the UCVA of the 3 groups increased first and then decreased, and it improved most significantly in the 3rd month after operation and decreased in the 4th month after operation. There were significant differences in UCVA among the 3 groups at each time point after operation. From the 1st day to the 6th month after operation, the IOP of the 3 groups showed an upward trend, and there was no significant difference among the 3 groups in IOP at each time point after operation. At the 1st, 3rd, and 6th months after operation, the INV score of group A and group B was higher than that of group C. There was no significant difference in the INV score between group A and group B. The incidence of complications was not significantly different among the 3 groups. *Conclusion.* 23G minimally invasive vitrectomy, glaucoma drainage valve implantation, and phacoemulsification cataract extraction can effectively improve the UCVA, IOP, and INV scores of NVG secondary to PDR with VH, and the combined application of the 3 methods has better security.

1. Introduction

Diabetes is a metabolic disease, which is mainly manifested as hyperglycemia [1]. Long-term hyperglycemia can lead to different degrees of tissue damage, resulting in dysfunction of the eye, kidney, heart, blood vessels, nerves, and so on [2]. Diabetic retinopathy is a common blinding disease. In the course of disease development, 62% of patients with diabetes can develop iris neovascularization (INV), and 41.4% eventually develop into neovascular glaucoma (NVG); therefore, proliferative diabetic retinopathy (PDR) is the most important stage of evolution to NVG [3]. In a few patients, since diabetic retinopathy (DR) was not found early or treatment was delayed, NVG was diagnosed at the time of treatment. So the intraocular pressure (IOP) of these patients was still higher than 21 mmHg after symptomatic administration with the largest amount of IOP-lowering drugs. In order to eliminate INV and/or angle neovascularization (ANV), antiglaucoma surgery should be performed in time to reduce IOP and protect the residual visual function of NVG patients. NVG secondary to PDR with vitreous hemorrhage (VH) is a common refractory glaucoma case. Ocular pain, photophobia, corneal edema, conjunctival congestion, and poor vision are the main manifestations of the disease. With the incidence rate of diabetes increasing year by year, the incidence rate of NVG also showed an obvious increasing trend [4]. In recent years, a few attempts have been made to treat the infantile cataract by crystalline resection using the minimally invasive vitrectomy [5]. It has been reported that simultaneous vitrectomy and AGV implantation in patients with posterior segment disease-related glaucoma may be an effective option to manage complex glaucoma cases [6]. At present, surgical treatment is the most commonly used treatment for this disease, and 23G minimally invasive vitrectomy, glaucoma drainage valve implantation, and phacoemulsification cataract extraction are commonly used. However, due to the different complexity of the disease, only one surgical method is often unable to meet the requirements of treatment. It has been reported that the treatment of NVG secondary to PDR with VH by multiple surgical methods can better treat the disease [7]. In order to improve the success rate of surgery and improve the condition of patients more effectively, the above three surgical methods are combined for treatment.

2. Patients and Methods

2.1. Clinical Data. Eighty-three patients (91 eyes) with PDR diagnosed as NVG phase III complicated with VH from June 2018 to May 2020 were selected as the study subjects. The subjects were randomly divided into 3 groups: there were 28 patients (30 eyes) in group A, 27 patients (30 eyes) in group B, and 28 patients (31 eyes) in group C. This study obtained approval from the Ethics Committee of Xiamen University, following the principle of the Declaration of Helsinki (as revised in 2013). The patients have signed the informed consent forms.

The clinical stage of NVG was as follows [8]: phase I (preglaucoma): the iris or anterior chamber angle neovascularization is found; however, as the function of the atrium angle has not been endangered, the IOP is normal, and the patient may have no symptoms; phase II (open-angle glaucoma): the angle of the atrium was not closed, but the neovascular membrane extended into the trabecular meshwork; the function of the trabecular meshwork was damaged, the outflow of aqueous humor was blocked, and the IOP was increased; and phase III (angle-closure glaucoma): the neovascularization membrane contracted, the angle of the atrium adhered and closed, and the IOP increased sharply.

Inclusion criteria were as follows: (1) the age of the patients was more than 18 years old, the patient's disease was nonabsorbable VH caused by PDR, there was obvious INV, and NVG met the criteria of clinical stage III; (2) IOP was still higher than 21 mmHg after topical and systemic administration of the largest dose of IOP-lowering drugs; (3) the results of gonioscopy or ultrasound biomicroscopy showed that the angle was closed in the range of more than 180 degrees; (4) the fasting blood glucose was below 8 mmol/ml, and HbA1c was less than 8.0%; and (5) no treatment was performed 1 month before admission.

Exclusion criteria were as follows: (1) less than 18 years old; (2) history of ocular trauma; (3) history of strabismus surgery, external retinal detachment reattachment, and other conjunctival surgery or PPV surgery; (4) serious corneal edema or bulla formation and unseen fundus; (5) no light perception; (6) obvious lens turbidity and obvious vitreoretinal proliferation or retinal detachment showed by B-ultrasound; (7) patients with coagulation dysfunction and serious organic diseases such as renal insufficiency and cardiac insufficiency who cannot tolerate surgery; and (8) patients with incomplete clinical data or unwilling to participate in this clinical trial.

Experimental grouping was as follows: in group A, there were 15 males (16 eyes) and 13 females (14 eyes), the average age was 56.7 ± 21.1 years (range, 41-77 years), the course of diabetes was 2-6 years, and the average duration was 3.8 ± 2.7 years; in group B, there were 14 males (16 eyes) and 13 females (14 eyes), the average age was 56.9 ± 22.5 years (range, 41-78 years), the course of diabetes was 2-6 years, and the average duration was 3.7 ± 2.6 years; and in group C, there were 14 males (16 eyes) and 14 females (15 eyes), the average age was 58.0 ± 21.7 years (range, 40-79 years), the course of diabetes was 2-6 years, and the average duration was 3.6 ± 2.5 years.

2.2. Therapeutic Methods. Before operation, routine examinations such as blood routine examination, urine routine examination, liver and kidney function examination, and electrocardiogram examination were carried out for the three groups of patients to understand the general situation and reduce the risk of surgical emergencies. At the same time, another auxiliary specialist examination was carried out, where the patients were given ophthalmic examination; the best-corrected visual acuity (BCVA) and uncorrected visual acuity (UCVA) were examined by the international standard visual acuity chart; the noncontact tonometer (NCT) and Goldmann applanation tonometer (GAT) were used to measure IOP [9]; the cornea, INV, anterior chamber depth, and lens were examined by the slit lamp microscope;

the anterior segment was photographed; fundus examination was performed by the direct ophthalmoscope and anterior ophthalmoscope; B-ultrasound was used to examine the vitreous body and retina; gonioscopy was used to examine INV and angle closure. There was no significant difference in gender, age, IOP, and BCVA among the 3 groups ($P > 0.05$, Table 1).

2.3. The Method of Intravitreal Injection [10]. Three groups of patients were given topical anesthesia; the eyes were routinely disinfected and covered with a sterile towel; then, the operation was completed by the same surgeon. A 4.5 needle was inserted into the center of the vitreous cavity at 4 mm behind the subtemporal cornea perpendicular to the eye wall; after a slow injection of 0.05 ml (0.5 mg) of conbercept, the needle was withdrawn slowly and then covered with sterile gauze and dropped with ofloxacin eye drops.

2.4. 23G Minimally Invasive Vitrectomy [11]. Local anesthesia and disinfection were performed on the patients, and 23G minimally invasive vitrectomy was performed in the flat area of the ciliary body. Three standard incisions were used to peel off the fibrous vascular membrane of the fundus, regulate hemostasis by underwater electrocoagulation, preserve the anterior capsule of the lens, and take out the epithelial cells of the anterior capsule and polish it. Then, cut the vitreous body, completely cut the preretinal fibroproliferative membrane with a 23G cutting head, then perform extensive retinal photocoagulation and silicone oil tamponade, and finally pull out the cutting sleeve.

2.5. Glaucoma Drainage Valve Implantation [12]. Cut the bulbar conjunctiva and fascia of the superior temporal quadrant at 0.50 cm from the membranous margin of the cornea, separate the sclera at an angle of about 85 degrees, and infiltrate the local fascia with 5-fluorouracil for 3 min and then wash with normal saline. Perform suture ligation on the root of the adjusted Ahmed glaucoma drainage device, and use the nonabsorbable suture 5-0 to fix the drainage disc 0.80 cm behind the corneal limbus. At the same time, make a scleral tunnel at 0.25 cm behind the limbus, inject the viscoelastic material in the front at 9 o'clock, insert the drainage tube 0.20 cm away from the anterior chamber, and fix the drainage valve with nylon thread at last.

2.6. Phacoemulsification Cataract Extraction [13]. After the scleral tunnel was established, perform continuous curvilinear capsulorhexis according to the procedure of phacoemulsification. For sufficient subcapsular separation, in other words, inject the perfusate under the anterior capsule membrane with a blunt needle to separate the lens capsule from the subcapsular cortex. The lens nucleus was emulsified by capsule plane segmentation to absorb the residual cortex. Appropriately expand and place the incision according to the size of the intraocular lens in the capsule bag. Then, suture the fascia and conjunctiva, which can lead to postoperative routine anti-infection, bandaging, and hemostasis.

Group A was treated with 23G minimally invasive vitrectomy combined with glaucoma drainage valve implantation. Group B was given 23G minimally invasive vitrectomy combined with phacoemulsification cataract extraction. Group C was treated with 23G minimally invasive vitrectomy combined with glaucoma drainage valve implantation and phacoemulsification cataract extraction. The operation methods of the 3 groups were the same as above.

2.7. Observation Index. Record the UCVA (Log MAR) before operation and at the 1st-6th months after operation. In the absence of antiglaucoma drugs, measure the IOP of the 3 groups by the Schiotz indentation tonometer, and take the mean value of 3 measurements during the above periods. INV was scored according to the Teich and Walsh INV scoring standards, also in the same time period above. The relief of eye pain and complications such as inflammatory exudation of the anterior chamber, anterior chamber hemorrhage, corneal edema, and vitreous rebleeding were observed in the three groups.

2.8. INV Grading Standards [14]. No INV was defined as grade 0 (0 points). The presence of INV in 1-2 quadrants was defined as grade 1 (1 point). The presence of INV in 3-4 quadrants was defined as grade 2 (2 points). The presence of INV with the infiltrating matrix in 1-2 quadrants was defined as grade 3 (3 points). The presence of INV with the infiltrating matrix in 3-4 quadrants was defined as grade 4 (4 points). On the basis of grade 4, combined with INV, glaucoma was defined as grade 5 (5 points).

2.9. Statistical Analysis. SPSS 23.0 software (IBM Corp.) was used for the statistical analysis of the data. The measurement data were expressed as $\bar{x} \pm s$. The *F*-test was used for multigroup comparison, and repeated measurement ANOVA was used for comparison at different time points. The count data were expressed as cases (%), and the comparison was made by the chi-squared test. The difference was statistically significant when $P < 0.05$.

3. Results

3.1. Results of UCVA. Before operation, there was no significant difference in the UCVA among the 3 groups ($P > 0.05$). After operation, the UCVA of the 3 groups increased first and then decreased, and it improved most significantly in the 3rd month after operation and decreased in the 4th month after operation. There were significant differences in UCVA among the 3 groups at each time point after operation ($P < 0.05$). In the 1st month after operation, the UCVA scores of the 3 groups were in the order of group A, group C, and group B from small to large. From the 2nd month to the 6th month, the UCVA scores of the 3 groups were in the order of group C, group A, and group B from small to large. The results are shown in Figure 1.

3.2. Results of IOP. Before operation, there was no significant difference in the IOP among the 3 groups ($P > 0.05$). From the 1st day to the 6th month after operation, the IOP of the 3 groups was significantly lower than that before operation ($P < 0.05$). From the 1st day to the 6th month after operation, the IOP of the 3 groups showed an upward trend, and there was no significant difference among the 3 groups

TABLE 1: Comparison of baseline data among the 3 groups.

| Group | Number of eyes | Sex (male/female, number of cases) | Age ($\bar{x} \pm s$, year) | IOP ($\bar{x} \pm s$, mmHg) | BCVA (number of eyes) | | | | | |
					NLP	LP	HM	CF/BE	0.01-0.1	≥0.1
Group A	30	15/13	56.7 ± 21.1	49.25 ± 9.73	4	2	9	2	11	2
Group B	30	14/13	56.9 ± 22.5	52.07 ± 10.33	3	2	11	2	9	3
Group C	31	14/14	58.0 ± 21.7	48.65 ± 11.79	4	3	8	4	8	4
P		0.910	0.639	0.704				0.301		
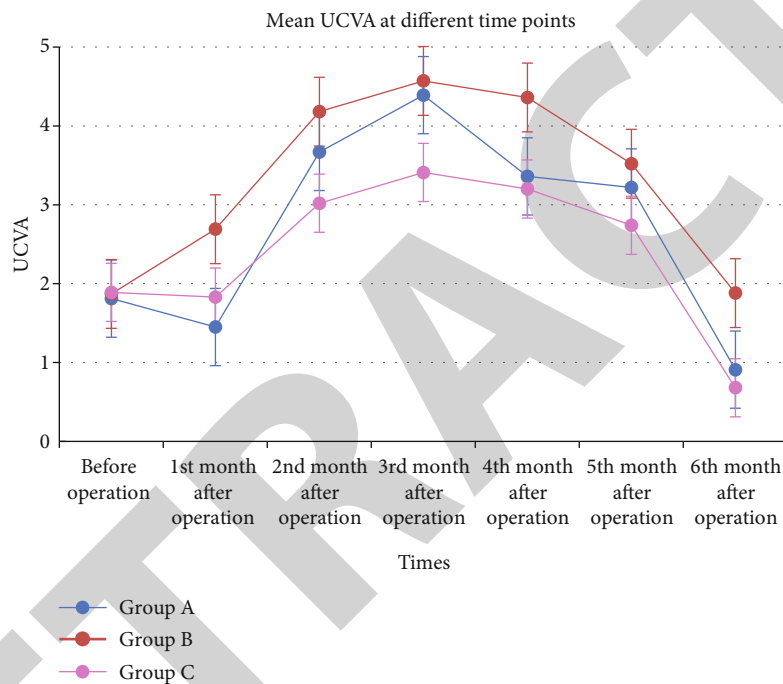
FIGURE 1: Comparison of UCVA among the 3 groups.

in IOP at each time point after operation ($P > 0.05$). The results are shown in Figure 2.

3.3. Results of the INV Score. Before operation, there was no significant difference in the INV score among the 3 groups ($P > 0.05$). At the 1st, 3rd, and 6th months after operation, the INV score of the 3 groups was significantly lower than that before operation ($P < 0.05$). The INV score of group A and group B was higher than that of group C ($P < 0.05$). There was no significant difference in the INV score between group A and group B ($P > 0.05$). The results are shown in Table 2.

3.4. Results of Postoperative Pain Relief and Complications. Three days after operation, no obvious eye pain was found in all 3 groups, and the clinical symptoms were relieved. Postoperative complications such as anterior chamber inflammatory exudation, anterior chamber hemorrhage, corneal edema, and vitreous rebleeding occurred in all 3

groups. The incidence rate of complications in group A, group B, and group C was 23.3%, 20.0%, and 25.8%, and there was no significant difference among the 3 groups ($\chi^2 = 0.315$, $P > 0.05$). The results are shown in Table 3.

3.5. Typical Cases. Figures 3–6 show the comparison of the same patient before and after operation. The patient is a 68-year-old male with a 10-year history of diabetes, and he uses insulin to control his blood sugar, but his blood sugar is not well controlled. The patient's visual acuity decreased for 1 year, with severe pain in the right eye accompanied by headaches for 4 days. The specialist examination results were as follows: the visual acuity of the right eye includes light perception, conjunctival hyperemia, corneal haze edema, mydriasis, and disappearance of light reflection. The depth of the anterior chamber was normal, a large number of new blood vessels were seen in the iris, the lens opacity was (+ +), and the fundus was not clear. The results of ocular ultrasound were as follows: DR and VH in the right
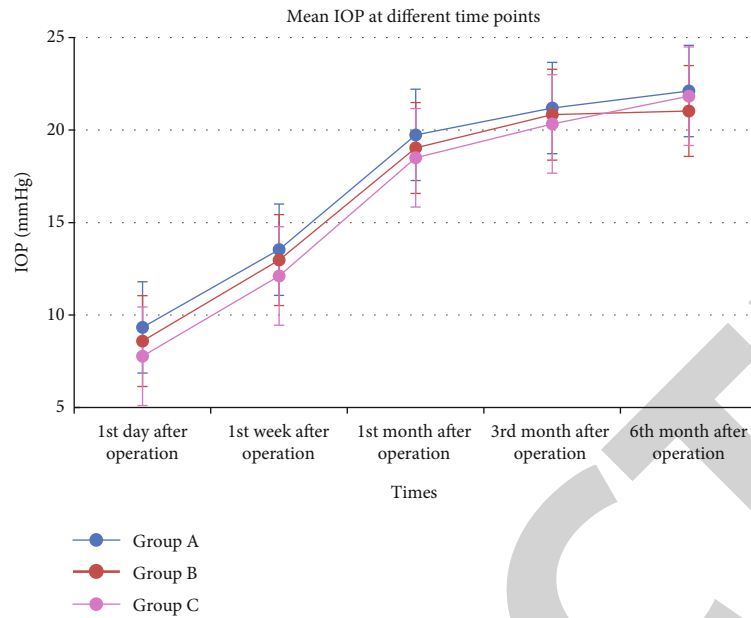
FIGURE 2: Comparison of IOP among the 3 groups.

TABLE 2: Comparison of the INV score among the 3 groups ($\bar{x} \pm s$, point).

Group	Number of eyes	Before operation	1st month after operation	3rd month after operation	6th month after operation
Group A	30	4.47 ± 0.36	$3.07 \pm 0.62^{*\#}$	$2.06 \pm 0.39^{*\#}$	$1.83 \pm 0.41^{*\#}$
Group B	30	4.51 ± 0.31	$2.95 \pm 0.57^{*\#}$	$2.04 \pm 0.28^{*\#}$	$1.77 \pm 0.24^{*\#}$
Group C	31	4.55 ± 0.29	$2.04 \pm 0.33^{*}$	$1.26 \pm 0.22^{*}$	$0.82 \pm 0.30^{*}$

Note: * means compared with the data before operation in the same group, $P < 0.05$; $^{\#}$ means compared with group C, $P < 0.05$.

TABLE 3: Comparison of postoperative complications among the 3 groups (number of eyes/%).

Group	Number of eyes	Anterior chamber inflammatory exudation	Anterior chamber hemorrhage	Corneal edema	Vitreous rebleeding occurred	Incidence rate (%)
Group A	30	2	3	1	2	23.3%
Group B	30	1	2	2	1	20.0%
Group C	31	3	2	1	2	25.8%
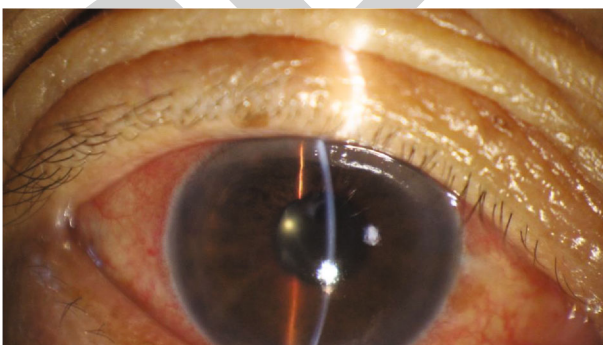
FIGURE 3: Photograph of the right eye of a patient before operation.

eye. Then, he was treated with 23G minimally invasive vitrectomy combined with glaucoma drainage valve implantation and phacoemulsification cataract extraction. One week after operation, the regression of INV could be observed.

4. Discussion

The main cause of PDR complicated with NVG is retinal ischemia or hypoxia caused by central retinal vein occlusion and diabetic retinopathy, which eventually leads to refractory glaucoma. The pathogenesis is the release of the vascular endothelial growth factor (VEGF), platelet-derived growth factor (PDGF), and basic fibroblast growth factor (bFGF) from the ischemic retina and damaged vascular wall to the adjacent retinal tissue, deep choroid tissue, and vitreous cavity; these angiogenesis-promoting factors specifically act on the receptors of vascular endothelial cells and promote the mitosis of vascular endothelial cells; when the adjacent retinal neovascularization proliferates, the remaining proliferative factors diffuse into the vitreous body and enter the posterior chamber, then, with the circulation of aqueous humor through the posterior chamber and anterior chamber, it reaches the angle of the atrium, causing the formation
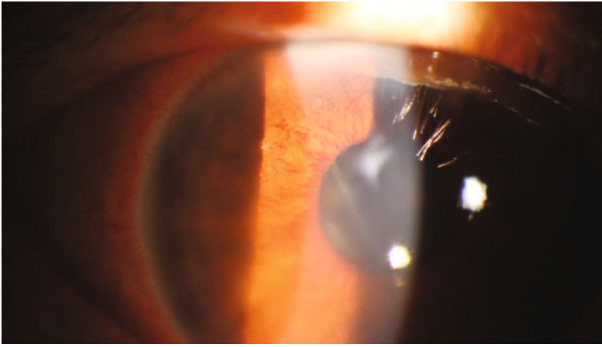
Figure 4: Enlarged photograph of iris neovascularization.
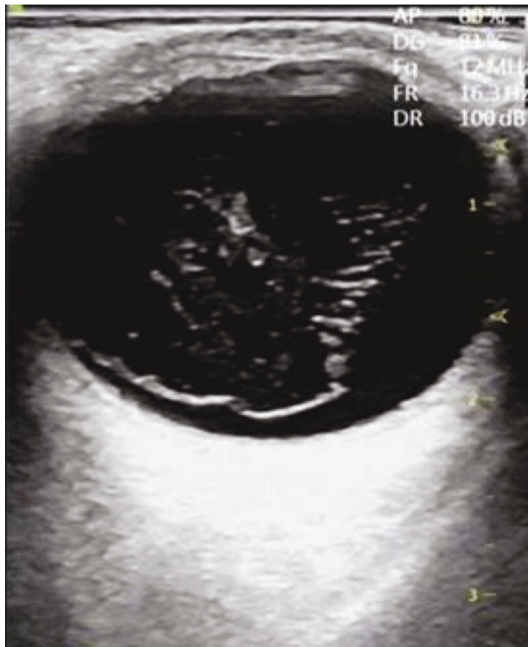
Figure 5: Ultrasound picture of vitreous hemorrhage before operation.
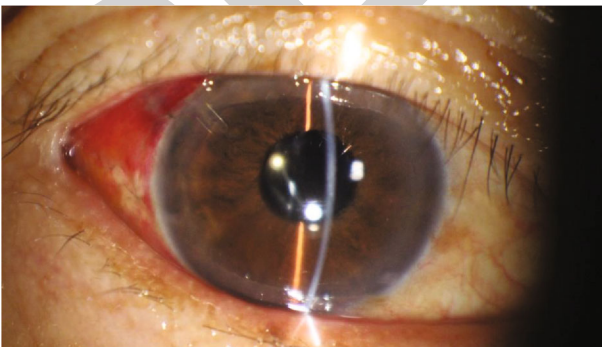
Figure 6: Photograph of the right eye of a patient after operation.

of neovascularization in these parts [15]. Neovascular glaucoma with vitreous hemorrhage is not only complicated in the local eye but also difficult to establish an effective filtering channel through filtering surgery. At present, the treatment of neovascular glaucoma includes the following: the

treatment of primary disease, the elimination of the retinal ischemic state (panretinal photocoagulation), and the drug or surgical control of IOP. The main surgical methods include filtration surgery, aqueous humor drainage implantation, and ciliary body destruction surgery [16]. Because the neovascularized fibrous membrane can cause extensive peripheral anterior synechia and destroy the anatomic structure of the angle of the anterior chamber, it is difficult to cut the iris root, easily injure the ciliary body, and cause serious bleeding, so anterior chamber hemorrhage is a common complication after operation [17]. In addition, because of intraoperative and postoperative bleeding, fibrin exudates and blocks the filtering mouth, resulting in adhesion and atresia; the filtration operation is difficult to work. However, because of the difficult curative effect and serious complications, all kinds of ciliary body destructive surgery are not usually chosen by clinicians. Therefore, we use glaucoma decompression valve drainage implant surgery, greatly improving the success rate of surgery.

The principle of the glaucoma decompression valve is to increase the formation of functional filtering blebs by means of a drainage disc on the surface of the sclera. The decrease of IOP depends on the drainage of aqueous humor around the drainage disc. Aqueous humor passively diffuses or penetrates into the intercellular space of orbital tissue and is absorbed by capillaries or lymphatic vessels, resulting in the decrease of IOP [18]. The thinner the wrapping wall, the lower the IOP, and the larger the surface area of the package, the lower the IOP. The Ahmed glaucoma valve is designed as a drainage disc with a large surface area to enlarge the area of scleral surface wrapping. The second is to provide a one-way pressure-sensitive valve to limit the outflow resistance of aqueous humor, which can prevent excessive drainage of aqueous humor before the surface of the drainage disc is wrapped, which can play a long-term role in controlling IOP [19]. In this study, vitrectomy should be combined with other methods because of vitreous hemorrhage. The purpose of vitrectomy is to remove the turbid vitreous hemorrhage, find out the causes of vitreous hemorrhage, and prevent the occurrence of hemocytosis or hemolytic glaucoma. After vitrectomy, the vitreous cavity becomes a liquid cavity, which provides the conditions for the implantation of the aqueous humor drainage tube through the pars plana of the ciliary body, which is more important for those patients who cannot be implanted with the aqueous humor drainage tube through the anterior chamber. Phacoemulsification is to smash the nucleus of the lens into a chylous shape and then suck it out together with the cortex. It can keep the posterior capsule of the lens, which is conducive to the implantation of the posterior chamber intraocular lens.

All patients were given the conbercept injection before operation. Conbercept is a commonly used antivascular endothelial growth factor drug in the clinic. It has high bioavailability and can penetrate the retina well, inhibit the binding of the vascular endothelial growth factor and receptor and neovascularization, and reduce the permeability of new blood vessels, which is conducive to follow-up surgical treatment [20]. The results of this study show that the

UCVA, IOP, and INV scores of the 3 groups significantly improved after operation; the reason may be that the neovascularization of the iris and retina can be controlled by conbercept before operation. Vitrectomy can relieve vitreoretinal traction, peel off the fibrovascular membrane and proliferative membrane, remove vitreous hemorrhage, and inhibit neovascularization in PDR eyes to a certain extent. In glaucoma drainage valve implantation, the drainage valve was installed in the corresponding position of the anterior chamber or vitreous cavity and conjunctiva to fascia so as to inhibit neovascularization and reduce IOP by establishing an outflow channel of aqueous humor. Phacoemulsification can remove the turbid lens and put in the intraocular lens; the angle of the anterior chamber is wider than that of the anterior chamber, which is beneficial for the posterior aqueous humor to enter the anterior chamber, reduce the IOP, and further inhibit the formation of neovascularization [21]. In this study, all the 3 groups had postoperative complications, but there was no significant difference in the incidence of complications among the 3 groups, suggesting that the combination of multiple methods for the treatment of NVG with PDR and VH is safe; this may be due to the 3 surgical methods causing less eye irritation, hence fewer complications.

5. Conclusion

23G minimally invasive vitrectomy can be combined with glaucoma drainage valve implantation and phacoemulsification cataract extraction. The combination of the 3 methods can effectively improve the UCVA, IOP, and INV scores of PDR patients diagnosed as NVG complicated with VH. In addition, the combined application of the 3 methods is more effective than that of the two methods, and the combined application of the 3 methods has better security. Therefore, the combination of the above 3 methods in the treatment of NVG with PDR and VH is worthy of clinical promotion.

Data Availability

The datasets used and/or analyzed during the current study are available from the corresponding author on reasonable request.

Ethical Approval

The study was approved by the Ethics Committee of our hospital. Patients who participated in the study had complete clinical data.

Consent

Signed written informed consent forms were obtained from the patients and/or guardians.

Conflicts of Interest

The authors declare that they have no competing interests.

Authors' Contributions

XiaoLing Shi and Nuo Dong contributed equally to this work.

Acknowledgments

References

[1] M. George Kristen, "Sex differences in the association of diabetes with cardiovascular disease outcomes among African-American and White participants in the Atherosclerosis Risk in Communities study," *American Journal of Epidemiology*, vol. 187, no. 3, pp. 403–410, 2018.

[2] S. H. Qiu, C. Xue, Z. L. Sun, J. M. Steinacker, M. Zügel, and U. Schumann, "Attenuated heart rate recovery predicts risk of incident diabetes: insights from a meta-analysis," *Diabetic medicine : a journal of the British Diabetic Association*, vol. 34, no. 12, pp. 1676–1683, 2017.

[3] K. Ishikawa, R.-i. Kohno, K. Mori et al., "Increased expression of periostin and tenascin-C in eyes with neovascular glaucoma secondary to PDR," *Graefe's Archive for Clinical and Experimental Ophthalmology: Incorporating German Journal of Ophthalmology*, vol. 258, no. 3, pp. 621–628, 2020.

[4] S. Yoshida, Y. Kobayashi, S. Nakao et al., "Differential association of elevated inflammatory cytokines with postoperative fibrous proliferation and neovascularization after unsuccessful vitrectomy in eyes with proliferative diabetic retinopathy," *Clinical Ophthalmology*, vol. Volume 11, pp. 1697–1705, 2017.

[5] P. Meierl, I. Sterker, H. Tegetmeyer, and P. Wiedemann, "23-Gauge-Lentektomie zur operativen Behandlung einer angeborenen Katarakt," *Der Ophthalmologe*, vol. 107, no. 3, pp. 241–245, 2010.

[6] S. Subasi, N. Yuksel, V. L. Karabas, B. Yilmaz Tugan, and E. Basaran, "Ahmed glaucoma valve implantation for secondary glaucoma post-vitrectomy," *International Ophthalmology*, vol. 42, no. 3, pp. 847–854, 2022.

[7] S. Yaoyao, Y. Liang, Z. Peng et al., "Anti-VEGF treatment is the key strategy for neovascular glaucoma management in the short term," *BMC Ophthalmology*, vol. 16, no. 1, p. 150, 2016.

[8] M. A. Karpilova and M. Durzhinskaya, "Anti-VEGF drugs in the treatment of neovascular glaucoma," *Vestnik Oftalmologii*, vol. 135, no. 5, pp. 299–304, 2019.

[9] A. S. Elwehidy, N. H. L. Bayoumi, A. E. Badawi, S. M. Hagras, and A. Abdelkader, "Intravitreal ranibizumab with panretinal photocoagulation followed by trabeculectomy versus viscotrabeculotomy in management of neovascular glaucoma," *Asia-Pacific Journal of Ophthalmology (Philadelphia, Pa.)*, vol. 8, no. 4, pp. 308–313, 2019.

[10] V. A. D. Vries, F. L. Bassil, and W. D. Ramdas, "The effects of intravitreal injections on intraocular pressure and retinal nerve fiber layer: a systematic review and meta-analysis," *Scientific Reports*, vol. 10, no. 1, p. 13248, 2020.

Hindawi

Retraction

Retracted: MiR-579 Inhibits Lung Adenocarcinoma Cell Proliferation and Metastasis via Binding to CRABP2

Computational and Mathematical Methods in Medicine

This article has been retracted by Hindawi following an investigation undertaken by the publisher [1]. This investigation has uncovered evidence of one or more of the following indicators of systematic manipulation of the publication process:

(1) Discrepancies in scope

(2) Discrepancies in the description of the research reported

(3) Discrepancies between the availability of data and the research described

(4) Inappropriate citations

(5) Incoherent, meaningless and/or irrelevant content included in the article

(6) Peer-review manipulation

The presence of these indicators undermines our confidence in the integrity of the article's content and we cannot, therefore, vouch for its reliability. Please note that this notice is intended solely to alert readers that the content of this article is unreliable. We have not investigated whether authors were aware of or involved in the systematic manipulation of the publication process.

Wiley and Hindawi regrets that the usual quality checks did not identify these issues before publication and have since put additional measures in place to safeguard research integrity.

We wish to credit our own Research Integrity and Research Publishing teams and anonymous and named external researchers and research integrity experts for contributing to this investigation.

The corresponding author, as the representative of all authors, has been given the opportunity to register their agreement or disagreement to this retraction. We have kept a record of any response received.

References

[1] Q. Yi, Y. Miao, Y. Kong et al., "MiR-579 Inhibits Lung Adenocarcinoma Cell Proliferation and Metastasis via Binding to CRABP2," *Computational and Mathematical Methods in Medicine*, vol. 2022, Article ID 9111681, 9 pages, 2022.

Research Article

MiR-579 Inhibits Lung Adenocarcinoma Cell Proliferation and Metastasis via Binding to CRABP2

Qijun Yi ⓘ**, Yu'e Miao** ⓘ**, Ying Kong** ⓘ**, Yan Xu** ⓘ**, Jinghao Zhou** ⓘ**, Qi Dong** ⓘ**, and Haiyan Liu** ⓘ

Department of Chemotherapy, The Second Affiliated Hospital of Shandong First Medical University, Tai'an City, Shandong, China

Correspondence should be addressed to Haiyan Liu; liuhaiyan@sdfmu.net.cn

Background. Lung cancer is the cancer with the highest morbidity and mortality. Lung adenocarcinoma (LUAD) is a subtype of lung cancer. The aim of this study is to explore the functions of miR-579 and CRABP2 in lung adenocarcinoma. *Methods.* Cell counting kit-8 (CCK-8) and colony formation assays were applied to calculate cell proliferative abilities. Transwell assay was utilized to measure cell invasive ability. *Results.* MiR-579 is low expressed in LUAD tissues and cell lines. MiR-579 inhibits cell viability and invasion of lung adenocarcinoma. Knockdown of CRABP2 inhibits cell proliferation and invasion of Calu-3 cells. MiR-579 suppresses cell proliferation and invasion by regulating CRABP2 in Calu-3 cells. *Conclusion.* Our study reveals that miR-579 acts as a tumor suppressor in LUAD and miR-579 can target and regulate the expression of CRABP2 to mediate cell proliferation and invasion. This study indicates that miR-579 has a potential to be a candidate biomarker for the treatment of LUAD.

1. Introduction

Lung cancer is a health killer with high incidence, and its mortality rate ranks first among all cancers for many years [1]. Lung adenocarcinoma (LUAD) is a kind of non-small cell lung cancer, which is a subtype of lung cancer [2]. Despite advances in the diagnosis and treatment of lung cancer, the prognosis of patients remains poor with a 5-year survival rate less than 16% [3]. The lack of understanding of the biological mechanisms associated with LUAD limits the efficacy of treating LUAD. Due to the lack of effective diagnostic biomarkers, patients with LUAD are mainly diagnosed at an advanced stage. Therefore, it is crucial to explore the pathogenesis mechanism of LUAD to improve clinical efficacy.

microRNAs (miRNAs) are a class of conserved, small non-coding RNAs with 19 to 25 nucleotide that regulate developmental and physiological processes [4]. MiRNAs usually negatively regulate gene expression in a post-transcriptional manner by degrading mRNA or inhibiting translation [5, 6]. Accumulating evidences suggest that dysregulation of miRNAs frequently occurs during lung adenocarcinoma initiation [7]. For instance, miRNA-885 inhibits docetaxel chemoresistance in lung adenocarcinoma by downregulating Aurora A [8]. MiR-22 is downregulated in lung adenocarcinoma and may serve as a biomarker for the diagnosis and prognosis of lung adenocarcinoma [9]. MiR-19b promotes lung adenocarcinoma metastasis via Hippo pathway [10]. These works strongly suggest a role of miRNAs in control of LUAD. It has been reported that miR-579 was expressed in non-small lung cancer [11]. However, the functions of miR-579 in lung adenocarcinoma are still unclear.

Cellular retinoic acid binding protein 2 (CRABP2), a cytosol-to-nuclear shuttling protein, encodes a member of the retinoic acid, which binds protein family and lipocalin/cytosolic fatty-acid binding protein family [12]. CRABP2 is a cytosol-to-nuclear shuttling protein, which facilitates RA binding to its cognate receptor complex and transfer to the nucleus. CRABP2 is found to be upregulated in thyroid

carcinoma and promoted the invasion, migration, and EMT of THCA cells [13]. Downregulation of CRABP2 inhibits proliferation and metastasis and promotes cell apoptosis of hepatocellular carcinoma [14]. This work reveals that miR-579 targets CRABP2 to regulate the biological process of lung adenocarcinoma and provides a research direction for the targeted therapy of LUAD.

2. Material and Methods

2.1. Sample Collection. During January 2012 to December 2018, 57 lung adenocarcinoma patients were collected from our hospital, and we obtained 57 pairs of LUAD tissue samples and corresponding paracancerous tissue samples through surgical operation. After surgical resection, all the tissues were rapidly frozen in liquid nitrogen and stored at $-80\,°C$. All the informed consents were obtained before this study, and the scheme was approved by the Ethics Committee of The Second Affiliated Hospital of Shandong First Medical University.

2.2. Cell Culture. Human LUAD cells (H1650, A549, and Calu-3) and a normal cell BEAS-2B were purchased from BeNa Culture Collection (Suzhou, Jiangsu, China). All the cells were cultured in Roswell Park Memorial Institute (RPMI)-1640 (Thermo Fisher Scientific Company, Waltham, Massachusetts, USA) supplemented with 10% fetal bovine serum (FBS; Hyclone, Logan, UT) at $37\,°C$.

2.3. Cell Transfection. MiR-579 mimic, miR-579 inhibitor, pcDNA3.1-CRABP2, si-CRABP2, and control were synthesized and purchased from GenePharma (Shanghai, China). Calu-3 cells were seeded in 6-well plat and cultured to the confluence of 70%. Cells were transfected using the Lipofectamine 2000 kit (Invitrogen, Carlsbad, CA, USA). Lipofectamine 2000 and serum-free medium were mixed and placed in a sterile Eppendorf (EP) tube for 5 minutes. Meanwhile, mix the vector and serum-free medium into another sterile EP tube. The solution in the above two test tubes was mixed and allowed to stand at room temperature for 20 minutes to obtain a complex of RNA and liposomes. This mixture was added to a petri dish containing cells to be transfected and then cultured the cells.

2.4. Real-Time Quantitative Polymerase Chain Reaction (RT-qPCR). The reverse transcription was performed to synthetize the first cDNA chain by using the PrimeScript RT Reagent Kit. Subsequently, RT-qPCR was performed using the SYBR Green qPCR mix kit (Takara, Kyoto, Japan) to quantify the relative levels of mRNAs and miRNAs. Glyceraldehyde 3-phosphate dehydrogenase (GAPDH) and U6 are used as internal references for CRABP2 and miR-579, respectively. The primers were CRABP2 Forward: $5'$-CCCTGTAAGGTGAGTGCCAG-$3'$, Reverse: $5'$- CCTG GGGTCTCCCAGAGAAT-$3'$; GAPDH Forward: $5'$-AAGG TCGGAGTCAACGGATT-$3'$, Reverse: $5'$-CTGGAAGAT GGTGATGGGATTT-$3'$; miR-579 Forward: $5'$-GTGCAG GGTCCGAGGT-$3'$, Reverse: $5'$-TTAACAAAGTG CTCA

TAGTGC-$3'$; U6 Forward: $5'$-CTCGCTTCGGCAGCACA-$3'$, and Reverse: $5'$- AACGCTTCACGAATTTGCGT-$3'$.

2.5. Proliferation Assays. Cell counting kit-8 (CCK-8) assay was used to detect cell proliferation. Calu-3 cells were seeded into 96-well plates at a density of 2×10^3 cells/well. Absorbance was measured at 24, 48, and 72 h after incubation with CCK-8 solutions for 2 h at $37\,°C$. At each time point, cells were added $10\,\mu l$ of 5 mg/ml CCK-8 (Keygen Biotechnology, Nanjing, China) and then incubated for 4 h. The absorbance was measured at 570 nm on the spectrophotometer.

2.6. Colony Formation Assay. For colony formation assays, 300 cells were seeded in 6-well plates and cultured for 12 days. PBS was utilized to wash the colonies and fixed the colonies with 4% paraformaldehyde for 30 min. Crystal violet was applied to stain the colonies with staining solution for 10 minutes, followed by the colonies which were washed with water and air-dried. Finally, the cell colonies are imaged and counted using a microscope.

2.7. Transwell Assay. Transwell inserts covered with Matrigel (Becton Dickinson, NJ, USA) were utilized to measure cell invasive ability. The upper chamber was added $100\,\mu l$ cell suspension with a density of 5×10^4 cells/ml. The lower chamber was filled with $500\,\mu l$ medium containing 10% FBS as a chemoattractant. The cells were incubated at $37\,°C$ for 24 h in a humidified environment with 5% CO2. A cotton swab was employed to remove the cells still on the top surface of the insert. The invade cells were fixed with methanol and stained with crystal violet at room temperature. After washed by PBS, the number of cells in five randomly fields were counted under a light microscope (Olympus Corporation, Japan).

2.8. Western Blotting Assay. RIPA lysis buffer (Beyotime, China) was utilized to lyse cells. The proteins were separated by electrophoresis through 10% sodium dodecyl sulfate-polyacrylamide gel electrophoresis (SDS-PAGE). The gels were followed transferred onto polyvinylidene fluoride (PVDF) membranes (MilliporeCorp, Billerica, MA, USA), and they were incubated by primary antibodies overnight in $4\,°C$. The primary antibodies were Anti-CRABP2 (ab211927, Abcam, Shanghai, China) and Anti-GAPDH (ab8245, Abcam, Shanghai, China). The blots was incubated for 1 h with anti-rabbit horseradish peroxidase conjugated antibody. Proteins were visualized with ECL-chemiluminescent kit (ADANTI, Wuhan, China).

2.9. Dual-Luciferase Reporter Assay. Based on the binding site predicted by Starbase, wild-type and mutant sequences of CRABP2 were inserted into the pcDNA3.1 vector to construct CRABP2 wild-type (CRABP2-WT) and CRABP2 mutant (CRABP2-MT). Cells were co-transfected with wild-type/mutant vector and miR-579 mimic/NC using Lipofectamine 2000. Promega (Madison) dual luciferase reporter detection system was used to determine luciferase activity.
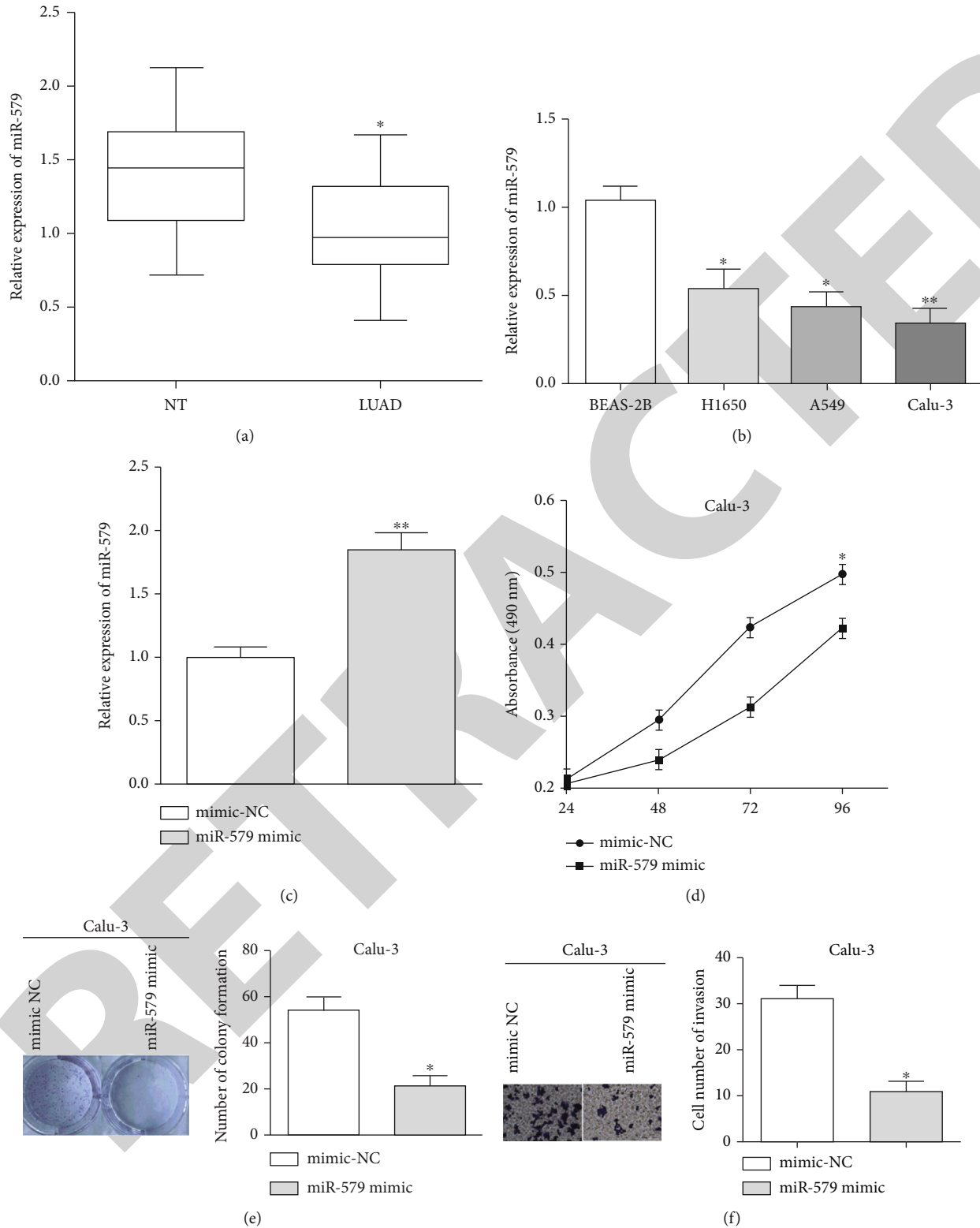
Figure 1: Overexpression of miR-579 inhibits cell viability and invasion of lung adenocarcinoma. (a) MiR-579 expression was downregulated in LUAD tissues compared with corresponding paracancerous tissues. (b) MiR-579 expression was lower in LUAD cell lines H1650, A549, and Calu-3 than BEAS-2B. (c) MiR-579 mimic was overexpressed miR-579 in Calu-3 cells. (d) Overexpression of miR-579 suppressed cell proliferation. (e) Overexpression of miR-579 inhibited colony formation ability. (f) Overexpression of miR-579 inhibited cell invasive ability of Calu-3 cells.

(a)

(b)

(c)

(d)
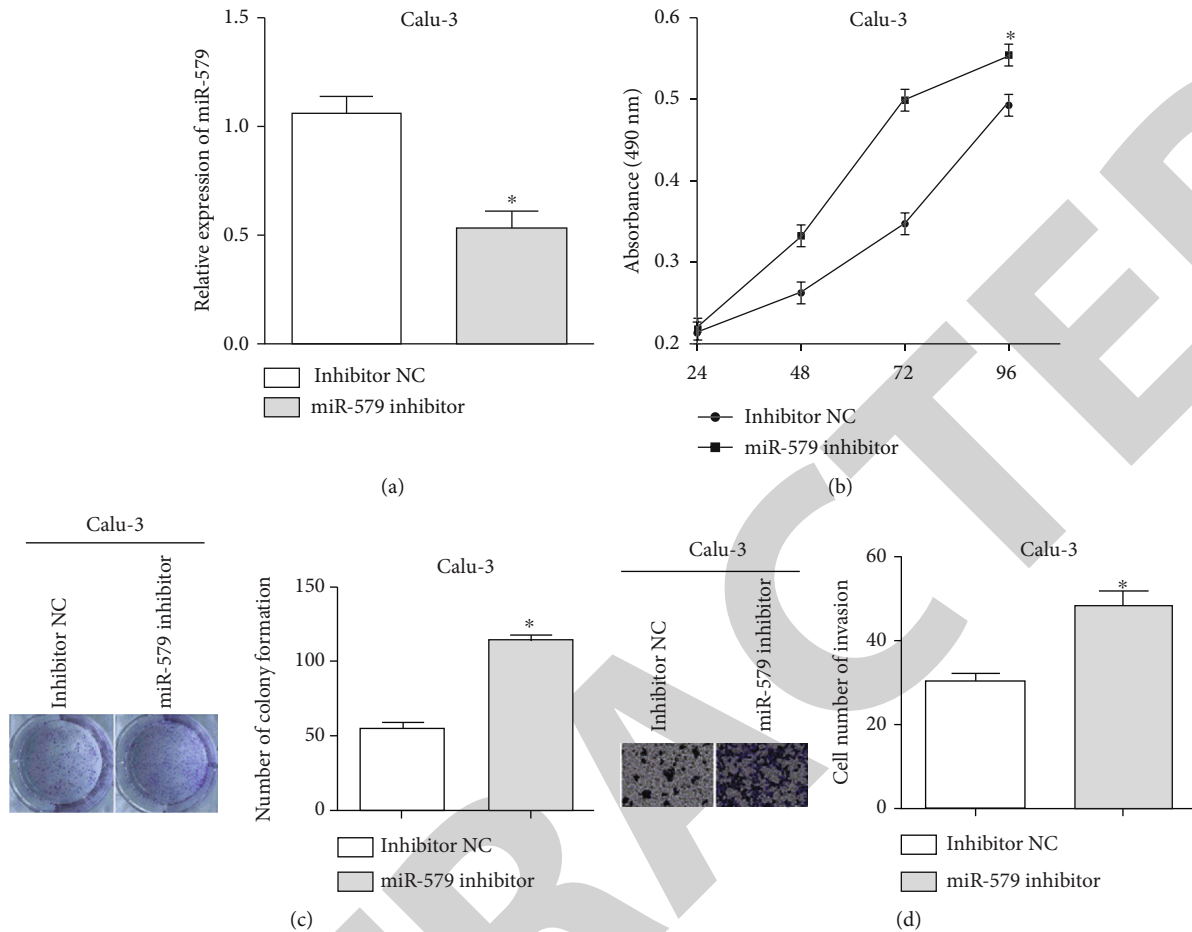
Figure 2: Knockdown of miR-579 promotes the viability and invasion of Calu-3 cells. (a) MiR-579 inhibited the expression level of miR-579 in Calu-3 cells. (b) Knockdown of miR-579 promoted cell proliferation. (c) Knockdown of miR-579 promoted colony formation ability. (d) Knockdown of miR-579 inhibited cell invasion ability of lung adenocarcinoma.

2.10. Statistical Analysis. Data are expressed as mean ± standard deviation (SD) from triplicate recordings. Statistical processing was carried out using SPSS and GraphPad Prism 6 software. The unpaired Student's *t*-test was used to compare date between groups that were normally distributed. *P* values less than 0.05 were considered statistically significant.

3. Results

3.1. Overexpression of miR-579 Inhibits Cell Viability and Invasion of Lung Adenocarcinoma. To detect the expressions of miR-579 in lung adenocarcinoma by using RT-qPCR, we first profiled differentially expressed genes in LUAD and corresponding paracancerous tissue samples. And we discovered that miR-579 expression was downregulated in LUAD tissues compared with corresponding paracancerous tissues ($P < 0.05$) (Figure 1(a)). Also, the expression of miR-579 was lower in LUAD cell lines H1650, A549, and Calu-3 than normal human bronchial epithelial cell line BEAS-2B ($P < 0.05$) (Figure 1(b)).

The biological function of miR-579 is determined through the gains and losses of functional experiments. MiR-579 mimic was used to overexpress miR-579 in Calu-3 cells. The transfection efficiency was measured by RT-

qPCR ($P < 0.05$) (Figure 1(c)). We found that overexpression of miR-579 suppressed cell proliferation ($P < 0.05$) and colony formation ability ($P < 0.05$) (Figures 1(d) and 1(e)). In addition, overexpression of miR-579 inhibited cell invasive ability of Calu-3 cells ($P < 0.05$) (Figure 1(f)). Overall, the findings indicated that miR-579 regulated the viability and invasion of Calu-3 cells in vitro.

3.2. Knockdown of miR-579 Promotes the Viability and Invasion of Calu-3 Cells. To further clarify the potential function of miR-579, miR-579 inhibitor was synthesized and then transfected into Calu-3 cells, and its transfection efficiency was checked. MiR-579 inhibited the expression level of miR-579 in Calu-3 cells ($P < 0.05$) (Figure 2(a)). Knockdown of miR-579 promoted cell proliferation and colony formation abilities ($P < 0.05$) (Figures 2(b) and 2(c)). In transwell experiments, knockdown of miR-579 inhibited cell invasion ability of lung adenocarcinoma ($P < 0.05$) (Figure 2(d)).

3.3. CRABP2 Is Regulated by miR-579. Through TargetScan, we discovered that CRABP2 was a target gene of miR-579, so we wonder whether mIR-579 affected the expression of CRABP2, and then affected the biological function of cells
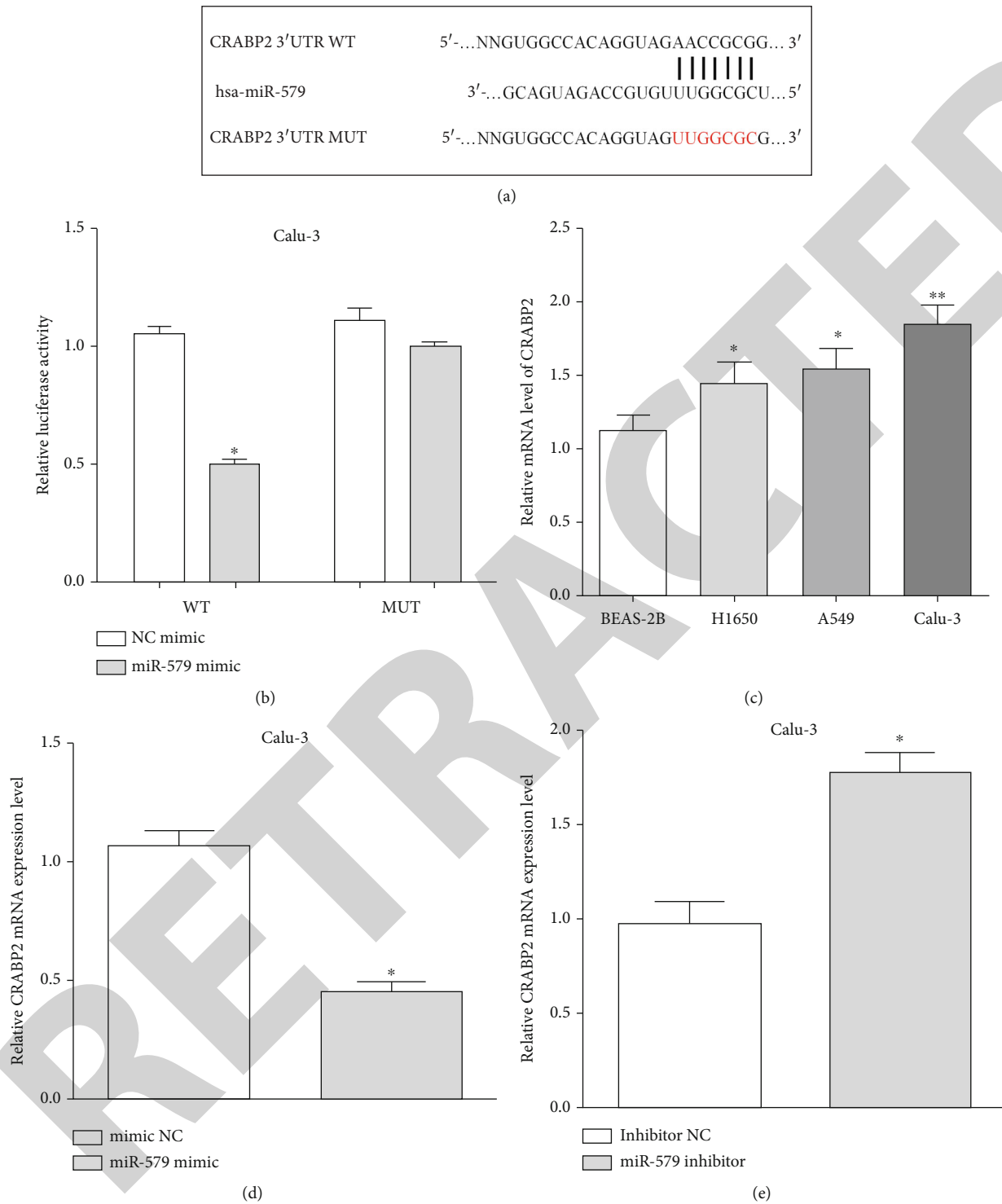
Figure 3: CRABP2 was regulate by miR-579 (a) Through TargetScan, we found that CRABP2 is a direct target gene of miR-579. The miR-579 binding sequences on CRABP2 mRNA were mutated from $5'$-…AACCGCG…-$3'$ to $5'$-…UUGGCGC…-$3'$. (b) Co-expression of miR-579 mimic and wild-type CRABP2 $3'$UTR could reduce luciferase activity, and it had no change in Calu-3 cells that co-transfected miR-579 mimic and CRABP2 MUT $3'$UTR. (c) CRABP2 was overexpressed in H1650, A549, and cells verse BEAS-2B. (d) The expression of CRABP2 was calculated after exogenous change miR-579. (e) CRABP2 expression was increased by inhibiting miR-579 in Calu-3 cells.

through CRABP2. The miR-579 binding sequences on CRABP2 mRNA were mutated from $5'$-…AACCGCG…-$3'$ to $5'$-…UUGGCGC…-$3'$ (Figure 3(a)). To verify that miR-

579 directly target CRABP2 in Calu-3 cells, two plasmid vectors were co-transfected containing WT or MUT CRABP2 $3'$-untranslated regions (3'UTR) and miR-579 mimic in
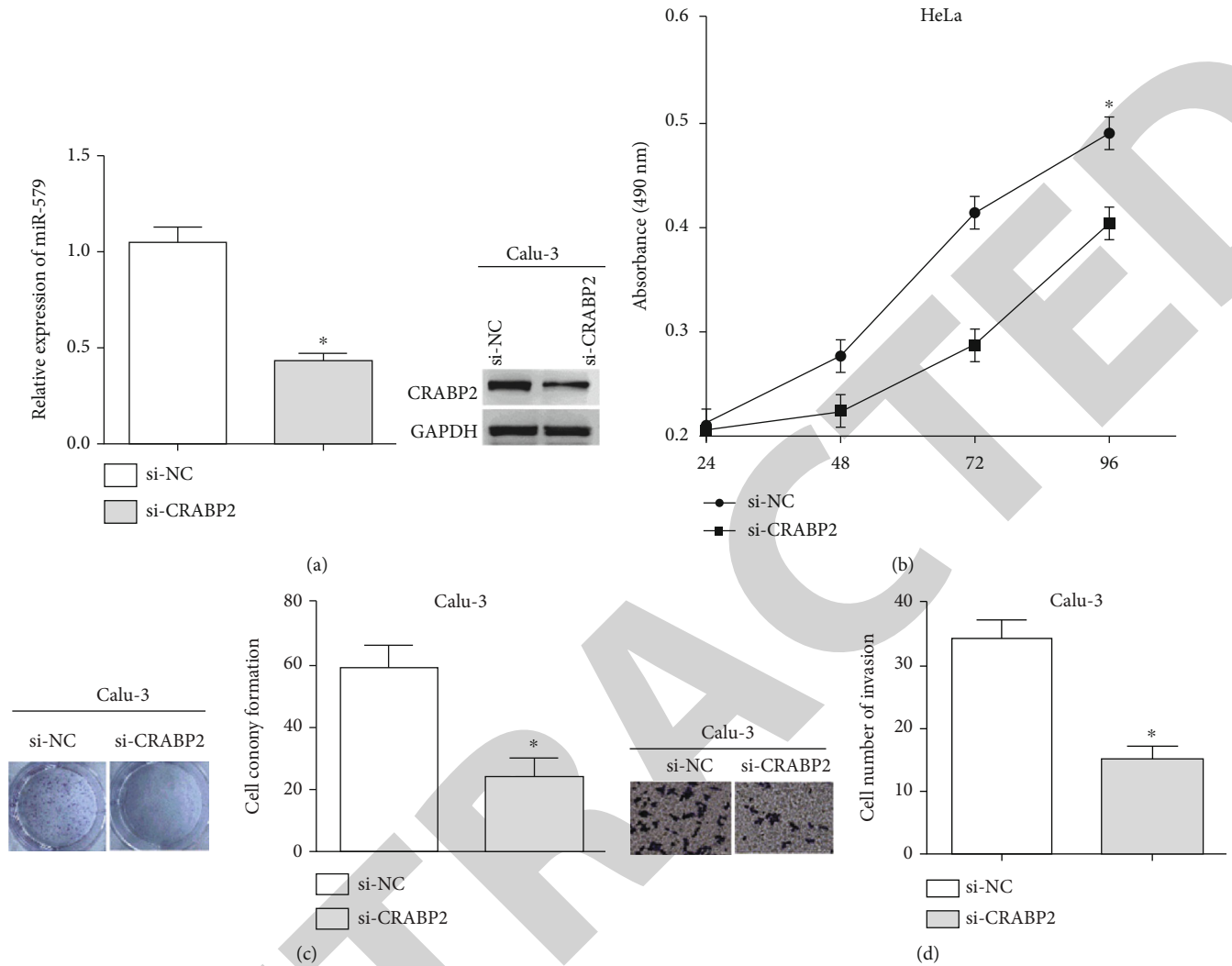
FIGURE 4: Knockdown of CRABP2 inhibits cell proliferation and invasion of Calu-3 cells. (a) Si-CRABP2 was used to silence CRABP2 in Calu-3 cells, and the transfection efficiency was calculated by RT-qPCR and western blot. (b) Cell proliferation was suppressed when knockdown of CRABP2 in Calu-3. (c) Knockdown CRABP2 inhibited cell colony formation ability. (d) Cell invasion ability was reduced by silencing CRABP2 in Calu-3 cells.

Calu-3 cells and then measure the luciferase activity. As we found, co-expression of miR-579 mimic and wild-type CRABP2 3'UTR could reduce luciferase activity ($P < 0.05$). In contrast, the luciferase activity had no change in Calu-3 cells that co-transfected miR-579 mimic and CRABP2 MUT 3'UTR ($P > 0.05$) (Figure 3(b)). The expression of CRABP2 was measured in LUAD cells H1650, A549 and Calu-3 and BEAS-2B. On the contrary with the expression of miR-579, we discovered that CRABP2 was overexpressed in H1650, A549, and Calu-3 cells verse BEAS-2B ($P < 0.05$) (Figure 3(c)). Also, the expression of CRABP2 was calculated after exogenous change miR-579. CRABP2 expression was reduced by overexpressing miR-579 ($P < 0.05$), and it was increased by inhibiting miR-579 in Calu-3 cells ($P < 0.05$) (Figures 3(d) and 3(e)).

3.4. Knockdown of CRABP2 Inhibits Cell Proliferation and Invasion of Calu-3 Cells.

Si-CRABP2 was used to silence CRABP2 in Calu-3 cells, and the transfection efficiency

was calculated by RT-qPCR ($P < 0.05$) and western blot (Figure 4(a)). CCK8 assay indicated that cell proliferation was suppressed when knockdown of CRABP2 in Calu-3 ($P < 0.05$) (Figure 4(b)). Cell colony formation assay displayed that knockdown CRABP2 inhibited the cell number of colony formation ($P < 0.05$) (Figure 4(c)). Transwell assay indicated that cell invasion ability was suppressed by silencing CRABP2 in Calu-3 cells ($P < 0.05$) (Figure 4(d)).

3.5. Overexpression of CRABP2 Reverses the Inhibition of miR-579 on Cell Proliferation and Invasion in Calu-3 Cells.

CRABP2 plasmid and miR-579 mimic were co-transfected in Calu-3 cells. The RNA and protein levels of CRABP2 in Calu-3 was measured by RT-qPCR ($P < 0.05$) and western blotting (Figure 5(a)). We demonstrated that the miR-579 mimic inhibited cell proliferation, while CRABP2 overexpressed reversed the inhibition of miR-579 on cell proliferation ($P < 0.05$) (Figure 5(b)). Similarly, cell number of clone formation was found to be reduced by overexpressing miR-
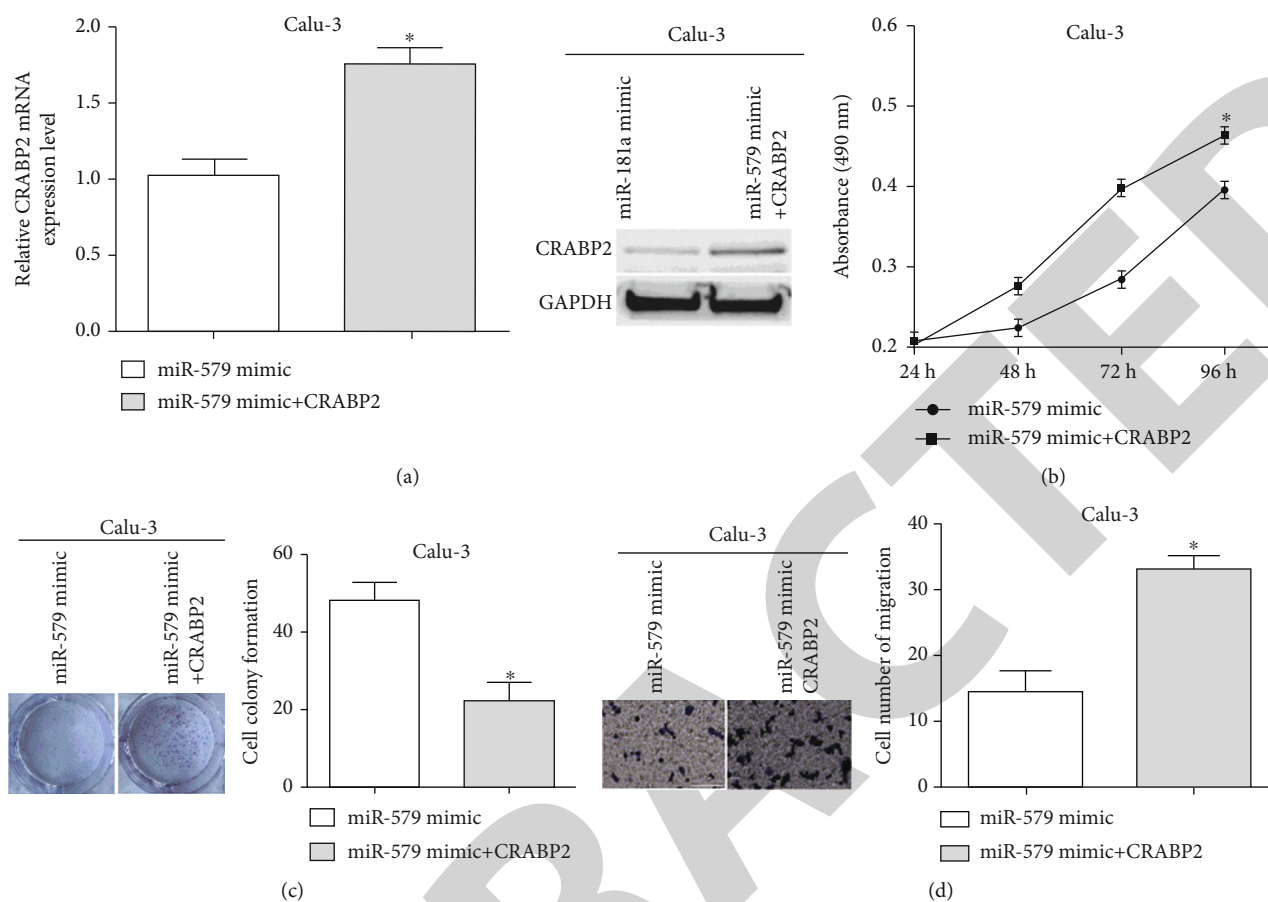
Figure 5: MiR-579 suppresses cell proliferation and invasion by regulating CRABP2 in Calu-3 cells. (a) CRABP2 plasmid and miR-579 mimic were co-transfected in Calu-3 cells. (b) MiR-579 mimic inhibited cell proliferation, while CRABP2 overexpressed reversed the inhabitation of miR-579 on cell proliferation. (c) Clone formation was found to be reduced by overexpressing miR-579, while CRABP2 inversed the reduction of miR-579. (d) MiR-579 mimic inhibited the invasion of Calu-3 cells, while CRABP2 reversed this reduction.

579, while CRABP2 inversed the reduction of miR-579 ($P < 0.05$) (Figure 5(c)). Transwell assay analysis demonstrated that miR-579 mimic suppressed invasion of Calu-3 cells, whereas CRABP2 reversed this reduction ($P < 0.05$) (Figure 5(d)). The addition of CRABP2 into Calu-3 cells could reverse the tumor suppression effects of miR-579 mimic.

4. Discussion

Lung adenocarcinoma has a high mortality rate possibly due to delays in diagnosis due to insignificant symptoms [15]. In early LUAD, most patients are asymptomatic. Approximately 57% of lung cancers metastasize and affect the normal function of other organs and tissues [16]. Thus, the tumor biomarkers are important for early diagnosis and treatment of cancer patients.

MiRNAs are a class of small endogenous noncoding RNAs that modulate multiple human genes by mRNA degradation or repression [17]. MiRNAs can complementarily bind to the $3'$-UTR of the corresponding target gene, ultimately inhibiting gene translation at transcriptional or post-transcriptional level [18]. MiR-579 has been shown to

play crucial roles in biological progresses. MiR-579 is a negative prognostic factor and acts as a suppressor in melanoma [19]. MiR-579 is downregulated in squamous cell lung carcinoma and inhibits the proliferation, invasion, and migration [20]. However, the functional mechanisms of miR-579 have not been elucidated in lung adenocarcinoma. We discovered that miR-579 was low expressed in LUAD tissues and cell lines compared with corresponding paracancerous tissues and bronchial epithelial cell. MiR-579 inhibited the proliferation, colony formation, and invasion of Calu-3 cells. We also found that CRABP2 was a direct target gene of miR-579 and miR-579 regulates cell progression via targeting CRABP2 in Calu-3 cells.

CRABP2, an intracellular lipid binding protein associated with retinoic acid, is considered a key regulator of intracellular retinoic acid signaling [21]. Increasing researches indicate that CRABP2 may act as a transcription coactivator and can involve in biological behavior independent [22]. For example, CRABP2 promotes cell migration and invasion and the EMT in non-small cell lung cancer cells [23]. Consistent with the above findings, silencing of CRABP2 suppressed the proliferation, colony formation, and invasion in Calu-3 cells. On the contrary, CRABP2 acts as a

suppressor factor and is related to ethnicity, nerve invasion, and postoperative treatment [24]. Similarly, CRABP2 suppresses the EMT, invasion, and metastasis of ER breast cancer cells in vitro and in vivo [25]. Therefore, we speculate that CRABP2 has tissue specificity.

5. Conclusion

All the results indicated that the tumor suppressor function of miR-579 is exerted partly by the negative regulation of CRABP2 in LUAD. However, the specific regulatory mechanism of miR-579 remains to be further investigated. Our next work will require further investigation of the roles of miR-579/CRABP2 axis in tumorigenesis using animal model.

Data Availability

Data to support the findings of this study is available on reasonable request from the corresponding author.

Conflicts of Interest

The authors declare that they have no conflicts of interest.

Authors' Contributions

Qijun Yi and Yu'e Miao contributed equally to this work.

References

[1] Z. Chen, C. M. Fillmore, P. S. Hammerman, C. F. Kim, and K. K. Wong, "Non-small-cell lung cancers: a heterogeneous set of diseases," *Nature Reviews. Cancer*, vol. 14, no. 8, pp. 535–546, 2014.

[2] T. Miyazawa, H. Marushima, H. Saji et al., "PD-L1 expression in non-small-cell lung cancer including various adenocarcinoma subtypes," *Annals of Thoracic and Cardiovascular Surgery*, vol. 25, no. 1, pp. 1–9, 2019.

[3] M. Ni, X. L. Shi, Z. G. Qu, H. Jiang, Z. Q. Chen, and J. Hu, "Epithelial mesenchymal transition of non-small-cell lung cancer cells A549 induced by SPHK1," *Asian Pacific Journal of Tropical Medicine*, vol. 8, no. 2, pp. 142–146, 2015.

[4] H. Mollaei and R. Safaralizadeh, *MicroRNA replacement therapy in cancer.*, vol. 234, no. 8, pp. 12369–12384, 2019.

[5] Y. S. Lee and A. Dutta, "MicroRNAs in cancer," *Annual Review of Pathology*, vol. 4, no. 1, pp. 199–227, 2009.

[6] R. Rupaimoole and F. J. Slack, "MicroRNA therapeutics: towards a new era for the management of cancer and other diseases," *Nature Reviews. Drug Discovery*, vol. 16, no. 3, pp. 203–222, 2017.

[7] J. Huang, Q. Weng, Y. Shi et al., "MicroRNA-155-5p suppresses PD-L1 expression in lung adenocarcinoma," *FEBS Open Bio*, vol. 10, no. 6, pp. 1065–1071, 2020.

[8] J. Cao, J. Geng, X. Chu, R. Wang, G. Huang, and L. Chen, "miRNA-885-3p inhibits docetaxel chemoresistance in lung adenocarcinoma by downregulating Aurora A," *Oncology Reports*, vol. 41, no. 2, pp. 1218–1230, 2019.

[9] D. J. Ma, X. Y. Zhou, Y. Z. Qin, Z. H. Tian, H. S. Liu, and S. Q. Li, "MiR-22-3p expression is down-regulated in lung adeno-

[10] J. Chen, K. Zhang, Y. Zhi et al., "Tumor-derived exosomal miR-19b-3p facilitates M2 macrophage polarization and exosomal LINC00273 secretion to promote lung adenocarcinoma metastasis via hippo pathway," *Clinical and Translational Medicine*, vol. 11, no. 9, article e478, 2021.

[11] J. Li, Z. Zhu, S. Li, Z. Han, F. Meng, and L. Wei, "Circ_0089823 reinforces malignant behaviors of non-small cell lung cancer by acting as a sponge for microRNAs targeting SOX4," *Neoplasia*, vol. 23, no. 9, pp. 887–897, 2021.

[12] X. Jiao, R. Liu, J. Huang et al., "Cellular retinoic-acid binding protein 2 in solid tumor," *Current Protein & Peptide Science*, vol. 21, no. 5, pp. 507–516, 2020.

[13] H. Zhao, X. Zhu, Y. Luo et al., "LINC01816 promotes the migration, invasion and epithelial-mesenchymal transition of thyroid carcinoma cells by sponging miR-34c-5p and regulating CRABP2 expression levels," *Oncology Reports*, vol. 45, no. 5, 2021.

[14] Q. Chen, L. Tan, Z. Jin, Y. Liu, and Z. Zhang, "Downregulation of CRABP2 inhibit the tumorigenesis of hepatocellular carcinoma in vivo and in vitro," vol. 2020, Article ID 3098327, 2020.

[15] F. R. Hirsch, G. V. Scagliotti, J. L. Mulshine et al., "Lung cancer: current therapies and new targeted treatments," *Lancet*, vol. 389, no. 10066, pp. 299–311, 2017.

[16] T. H. Huang, A. T. Wu, T. S. Cheng et al., "In silico identification of thiostrepton as an inhibitor of cancer stem cell growth and an enhancer for chemotherapy in non-small-cell lung cancer," *Journal of Cellular and Molecular Medicine*, vol. 23, no. 12, pp. 8184–8195, 2019.

[17] G. Bertoli, C. Cava, and I. Castiglioni, "MicroRNAs: new biomarkers for diagnosis, prognosis, therapy prediction and therapeutic tools for breast cancer," *Theranostics*, vol. 5, no. 10, pp. 1122–1143, 2015.

[18] J. Hayes, P. P. Peruzzi, and S. Lawler, "MicroRNAs in cancer: biomarkers, functions and therapy," *Trends in Molecular Medicine*, vol. 20, no. 8, pp. 460–469, 2014.

[19] L. Fattore, R. Mancini, M. Acunzo et al., "miR-579-3p controls melanoma progression and resistance to target therapy," *Proceedings of the National Academy of Sciences of the United States of America*, vol. 113, no. 34, pp. E5005–E5013, 2016.

[20] R. R. Wu, Q. Zhong, H. F. Liu, and S. B. Liu, "Role of miR-579-3p in the development of squamous cell lung carcinoma and the regulatory mechanisms," *European Review for Medical and Pharmacological Sciences*, vol. 23, no. 21, pp. 9464–9470, 2019.

[21] J. F. Meng and M. J. Luo, "CRABP2 involvement in a mechanism of Golgi stress and tumor dry matter in non-small cell lung cancer cells via ER dependent hippo pathway," *Acta Biochimica Polonica*, vol. 69, no. 1, pp. 31–36, 2021.

[22] L. Wei, Y. Liu, Y. Ma et al., "C-X-C chemokine receptor 2 correlates with unfavorable prognosis and facilitates malignant cell activities via activating JAK2/STAT3 pathway in non-small cell lung cancer," *Cell Cycle*, vol. 18, no. 24, pp. 3456–3471, 2019.

[23] J. F. Meng, M. J. Luo, and H. B. Li, "Correlation between plasma cellular retinoic acid-binding protein 2 and proliferation, migration, and invasion of non-small-cell lung cancer cells," *Critical Reviews in Eukaryotic Gene Expression*, vol. 31, no. 3, pp. 81–89, 2021.

carcinoma," *Acta Biochimica Polonica*, vol. 68, no. 4, pp. 667–672, 2021.

Retraction

Retracted: Effect of Stereotactic Body Radiation Therapy Combined with Thermoplastic Fixation on Set-Up Errors in Breast Cancer Patients Undergoing Radiotherapy

Computational and Mathematical Methods in Medicine

This article has been retracted by Hindawi following an investigation undertaken by the publisher [1]. This investigation has uncovered evidence of one or more of the following indicators of systematic manipulation of the publication process:

(1) Discrepancies in scope

(2) Discrepancies in the description of the research reported

(3) Discrepancies between the availability of data and the research described

(4) Inappropriate citations

(5) Incoherent, meaningless and/or irrelevant content included in the article

(6) Peer-review manipulation

The presence of these indicators undermines our confidence in the integrity of the article's content and we cannot, therefore, vouch for its reliability. Please note that this notice is intended solely to alert readers that the content of this article is unreliable. We have not investigated whether authors were aware of or involved in the systematic manipulation of the publication process.

Wiley and Hindawi regrets that the usual quality checks did not identify these issues before publication and have since put additional measures in place to safeguard research integrity.

We wish to credit our own Research Integrity and Research Publishing teams and anonymous and named external researchers and research integrity experts for contributing to this investigation.

The corresponding author, as the representative of all authors, has been given the opportunity to register their agreement or disagreement to this retraction. We have kept a record of any response received.

References

[1] L. Zhu, J. Liu, Y. Li et al., "Effect of Stereotactic Body Radiation Therapy Combined with Thermoplastic Fixation on Set-Up Errors in Breast Cancer Patients Undergoing Radiotherapy," *Computational and Mathematical Methods in Medicine*, vol. 2022, Article ID 8370842, 7 pages, 2022.

Research Article

Effect of Stereotactic Body Radiation Therapy Combined with Thermoplastic Fixation on Set-Up Errors in Breast Cancer Patients Undergoing Radiotherapy

Luchao Zhu [iD],[1] **Jun Liu** [iD],[2] **Yimin Li** [iD],[1] **Qiaolu Yang** [iD],[3] **Qiong Wu** [iD],[2] **Qing Lin** [iD],[1] **and Sijia Chen** [iD][2]

[1]*Department of Radiation Oncology, Xiamen Radiotherapy Quality Control Center, Xiamen Cancer Center, Xiamen Key Laboratory of Radiation Oncology, The Third Clinical Medical College of Fujian Medical University, The First Affiliated Hospital of Xiamen University, School of Medicine, Xiamen University, Xiamen, Fujian, China*
[2]*Radiation Oncology, The First Affiliated Hospital of Xiamen University, Xiamen, Fujian, China*
[3]*Department of Breast Surgery, The First Affiliated Hospital of Xiamen University, Xiamen, Fujian, China*

Correspondence should be addressed to Sijia Chen; cscscsj@sina.com

Objective. To investigate the effect of stereotactic radiotherapy (SBRT) combined with thermoplastic fixation on set-up error in breast cancer (BC) patients undergoing radiotherapy. *Methods.* Ninety BC patients undergoing radiotherapy who were treated in our hospital (May 2019-May 2020) were selected as the research objects and equally divided into the experimental group and control group according to the order of hospitalization, with 45 patients in each group. The control group received conventional radiotherapy combined with breast bracket, and the experimental group received SBRT combined with thermoplastic fixation. The incidences of adverse reactions, 1-year survival rates, and set-up errors were compared between the two groups. *Results.* Compared with the control group, the experimental group had much lower total incidence of adverse reactions and remarkably higher 1-year survival rate. The translational errors (*X* direction, *Y* direction, and *Z* direction), translational errors after rotation (*X* direction, *Y* direction, and *Z* direction), and rotation errors (*X* direction, *Y* direction, and *Z* direction) in the experimental group were obviously lower compared with those in the control group. *Conclusion.* Implementing SBRT combined with thermoplastic fixation in BC patients undergoing radiotherapy can effectively improve set-up efficiency and treatment accuracy and reduce set-up errors. Compared with the breast bracket, the combination of SBRT and thermoplastic fixation has higher application value, and further studies are conducive to providing patients with a better solution plan.

1. Introduction

Breast cancer (BC), a malignant tumor occurring in the breast epithelium or ductal epithelium, was the most common cause of death in women, and the diagnosed BC patients account for the largest part of cancer patients in the world [1, 2]. The pathogenesis of BC is complex and has not yet been elucidated, but most scholars believe that genetic and endocrine factors are high-risk factors for BC [3]. According to pertinent literature, BC is the most prevalent cancer among women worldwide, and its incidence accounts for 24.1% of the total incidence of all female cancers. Most of the BC patients come from developing countries [4]. Jacobs et al. [5] have noted that more than 290,000 women are diagnosed with BC in China each year, and its incidence is much higher in economically developed and eastern coastal regions. According to statistics, on average, one out of 17 women worldwide develops BC in their whole life, and the majority of the patients with breast malignant tumor are the ones with hormone receptor-positive breast cancer, which account for about 65% [6]. Ho et al. [7] have stated that BC is the most prevalent malignant

tumor among women, and its incidence, which has been increasing in recent years, accounts for 14% of all malignant tumors in the female body. According to pertinent literature, the BC incidence among Asian women increased by approximately 1.7% per year from 2006 and 2015, so it is urgent to provide effective treatment for BC patients [8].

Radiotherapy, as a conventional treatment for BC in the clinic, occupies a key position in preoperative assistance, postoperative assistance, and the treatment of advanced breast cancer, and its efficacy has been widely accepted [9]. Stereotactic body radiation therapy (SBRT) can directly irradiate the tumor areas at a high dose with less irradiation to surrounding normal tissues and significantly improves the treatment effect of the patients who cannot receive surgery or refuse surgery. Meanwhile, the efficacy of SBRT has been confirmed in nonsmall cell lung cancer (NSCLC) [10]. In recent years, with the rapid development of precision radiotherapy, image-guided radiotherapy has also entered a new stage, so higher demands are made on such aspects as position fixation devices, target delineation, computed tomography (CT) localization, and the design and implementation of treatment plans. At the same time, position fixation devices not only affect the patients' set-up errors but also affect the repeatability of later treatment positions. Although the conventional breast bracket has certain treatment effect, its set-up accuracy fails to live up to the expectation, so it cannot meet the clinical demand. Thermoplastic fixation, with the characteristics of low cost, better fixed effect, and high comfort, has been widely applied to clinical practice and has remarkable effect. According to pertinent literature, the position fixation method directly affects the set-up accuracy and plays a pivotal role in the design and implementation of the treatment plan [11]. Therefore, this study has investigated the effect of SBRT combined with thermoplastic fixation on set-up errors in BC patients undergoing radiotherapy and implemented combined clinical intervention in research objects, so as to provide more evidence-based proofs for such patients.

2. Materials and Methods

2.1. General Data.
Ninety BC patients undergoing radiotherapy who were treated in our hospital (May 2019–May 2020) were selected as the research objects and equally divided into the experimental group and the control group, with 45 patients in each group. This study conformed with the *Declaration of Helsinki (2013)* [12]. This study obtained approval from the Ethics Committee of the First Affiliated Hospital of Xiamen University. The patients have signed informed consent.

2.2. Recruitment of Research Objects.
Inclusion criteria: (1) The patients met the diagnostic criteria of breast cancer stipulated in the Guideline and Standard for the Diagnosis and Treatment of Breast Cancer by Chinese Anti-Cancer Association (2021 edition) [13], and their conditions were confirmed via pathological diagnosis. (2) The patients were less than 75 years old. (3) Their breast tumor had measurable lesions. (4) Their treatment site did not receive any

form of radiotherapy before this study. (5) The patients were not the ones with advanced tumor and dyscrasia.

Exclusion criteria: (1) The patients had severe acute or chronic diseases (like acute pancreatitis, acute myocardial infarction, cerebral hemorrhage, and cardiac failure) or had familial dyslipidemia. (2) The patients had mental illness. (3) The patients' important organs had lethal lesion or infection. (4) The patients were the experimenters of clinical drugs, or the interval between this study and the end of the last clinical test in which they were involved was less than one month. ⑤ The patients were complicated with severe skin disease or limb injury, which affected the radiotherapy.

2.3. Methods

2.3.1. Experimental Group

(1) SBRT. The patients in the experimental group received the stereotactic X-ray treatment system (Manufacturer: Varian Medical Systems, Inc.; model: TrueBeam). The patients took the supine position and were guided to lie on the thermoplastic film. The patients maintained the position by manipulating the negative pressure suction and moulding. When adopting the respirator, the patients were told to keep stable respiration. Then, the CT scanning and localization (Manufacturer: General Electric Company; model: LightSpeed RT) were performed on the patients, and CR scanning images were sent to the Eclipse platform. After stipulating the radiotherapy plan, the radiotherapy oncologists precisely map the position and shape of the tumors from the reconstruction of the three-dimensional CT images, so as to determine the target regions: breast tumor target, clinical target volume (5-millimeter outward expansion of the breast target), and planning target volume (5-millimeter outward expansion of the breast target). The radioactive ray might involve the organ region (like the digestive tract, heart, lung, and so on). At the same time, the medical physicists should pay attention to irradiate the organs adjacent to the tumors as less as possible to ensure ray exposure of the adjacent organs ≤ 29%. The margin dose of the planning target volume was 3 Gy/time–3.6 Gy/time, 5 times a week and 10 times in total, and 90% isodose lines covered 100% planning target volume. The margin dose of the tumor target was 5.5 Gy/time–6.2 Gy/time, 5 times a week, and 80% isodose lines covered 95% clinical target volume.

(2) Thermoplastic Fixation. CIVCO Posiret™-2 was adopted to support the patients' arms, and the breast bracket was used to fix the lifting positions of the head and arms. Before positioning, the patients were guided to try lying down and adjust the position of the upper arms. At the same time, the position of the knee pads were adjusted to make the patients feel comfortable. When the patients put down their arms, the radiation therapists started to make thermoplastic mask. When the patients lifted their arms to the original position, the radiation therapists started to draw positioning lines at the breast level and the middle axillar lines. If the patients had large breasts, a positioning line was added along the lower edge of the breast crease to ensure relative fixation

of the patients' and bracket plate's positions. At the same time, the breast, neck, and other areas needing irradiation should not be covered, and the doses on the skin and superficial organs were reduced. When the above process was continuously verified for 3 times and the verification results showed no error, the patients received treatment according to the data results.

2.3.2. Control Group

(1) Conventional Radiotherapy. The patients took the supine position and kept the chest wall stable. Then, they were guided to raise the upper arms. After locating the laser radiation point, the conventional radiotherapy plan was implemented in target areas. A reasonable and systematic irradiation program was made in combination with the radiotherapy plan. The radiation dose was 1.8 Gy/time, 45-50.4 Gy up to 28 fractions with boost 59-66.6 Gy up to 37 fractions.

(2) Breast Bracket. The patients were guided to lie flat in the center of the bracket, and their long body axis coincided with the longitudinal axis of the bracket. The arms' positions were adjusted to fully expose their armpits and chest, and the patients should keep the chest flat as much as possible. The bed was moved to make the breast in the healthy side be fully exposed. The bed was elevated so that the horizontal laser line was at the median level of the body. Then, the index line was drawn on the skin according to the laser line. At the same time, the corresponding bracket scale was recorded. Then, the bed was moved again to make the laser line irradiate the center of the affected breast (chest wall). Later, the index line was drawn on the body surface, and the bracket scale was recorded. If the patients' supraclavicular lymph nodes on the diseased side need to be irradiated, the patient should be instructed to put the head to the healthy side or to put the head straight. When the above process was continuously verified for 3 times and the verification results showed no error, the patients received treatment according to the data results.

2.4. Observational Indexes. The patients received baseline assessment three months after the end of radiotherapy, and the patients' adverse reactions (cardiac injury, acute radiation-induced skin reaction, and lung injury) were observed and recorded.

The two groups' 1-year survival rates were counted and recorded through telephone follow-up or other follow-up methods.

The cone beam CT (CBCT; Manufacturer: Varian Medical Systems, Inc.) was adopted to confirm the displacement data after the radiotherapy placement. Under the pelvis model, the reconstructed image matrix of $510 * 510$ was scanned by half fan, and the gantry angle rotated 180°-175°. Then, the grayscale registration and automatic registration were performed in CBCT images and locating CT images. After determining the error to be less than 5 millimeters, the radiotherapy could be conducted. If the error is more than the allowed value, the error should be corrected

in time. The frequency of the CBCT scan was 1 time a week, and the registration conditions were kept the same as those in the first scan, so as to obtain the set-up errors. The translational errors, translational errors after rotation, and rotation errors in different directions of the two groups were observed and recorded.

2.5. Statistical Treatment. This study adopted SPSS 20.0 as the data processing software and GraphPad Prism 7 (GraphPad Software, San Diego, USA) to draw graphs of the data. Each experiment was repeated at least three times. This study included count data and measurement data and adopted χ^2 test, t test, and normality test. When $P < 0.05$, the difference was taken as remarkably significant.

3. Results

3.1. Comparison of Baseline Data. No notable difference in age, body mass index (BMI), menstrual status, histological grading, pathological type, occupation, education level, religious belief, household income, and place of residence was observed between the two groups ($P > 0.05$), as illustrated in Table 1.

3.2. Comparison of Incidences of Adverse Reactions. Compared with the control group, the experimental group had much lower total incidence of adverse reactions ($P < 0.05$; Table 2).

3.3. Comparison of 1-Year Survival Rates. According to research results, the median survival period in the experimental group was 9 months, and the survival rate was 95.56% (43/45) with 43 surviving patients. In the control group, the median survival period was 8 months, and the survival rate was 80.00% (36/45) with 36 surviving patients. Compared with the control group, the experimental group had remarkably higher 1-year survival rate ($P < 0.05$; Figure 1).

3.4. Comparison of Translational Errors. Compared with the control group, the translational errors (X direction, Y direction, and Z direction) in the experimental group were obviously lower ($P < 0.001$; Table 3).

3.5. Comparison of Translational Errors after Rotation. Compared with the control group, the translational errors after rotation (X direction, Y direction, and Z direction) in the experimental group were obviously lower ($P < 0.001$; Table 4).

3.6. Comparison of Rotation Errors. Compared with the control group, the rotation errors (X direction, Y direction, and Z direction) in the experimental group were obviously lower ($P < 0.001$; Table 5).

4. Discussion

As a common malignant tumor in the department of breast surgery, breast cancer, with a high morbidity and mortality, seriously threatens patients' life safety [14]. Currently, surgery, chemotherapy, and radiotherapy are the main

TABLE 1: Comparison of baseline data.

Items	Experimental group ($n = 45$)	Control group ($n = 45$)	X^2/t	P
Age ($\bar{x} \pm s$, years old)	50.56 ± 8.33	50.93 ± 7.87	0.217	0.829
BMI (kg/m^2)	20.54 ± 0.31	20.48 ± 0.29	0.948	0.346
Menstrual status			0.049	0.824
Nonmenopause	30 (66.67%)	29 (64.44%)		
Menopause	15 (33.33%)	16 (35.56%)		
Histological grading				
I	10 (22.22%)	11 (24.44%)	0.062	0.803
II	21 (46.67%)	22 (48.89%)	0.045	0.833
III	14 (31.11%)	12 (26.67%)	0.216	0.642
Pathological type				
Specific cancer	11 (24.44%)	12 (26.67%)	0.058	0.809
Nonspecific cancer	25 (55.56%)	26 (57.78%)	0.045	0.832
Mixed type	9 (20.00%)	7 (15.56%)	0.304	0.581
Occupation				
Teacher	14 (31.11%)	15 (33.33%)	0.051	0.822
Financial staff	15 (33.33%)	14 (31.11%)	0.051	0.822
Others	16 (35.56%)	16 (35.56%)	0.000	1.000
Education level				
Primary school and junior high school	19 (42.22%)	20 (44.44%)	0.045	0.832
Senior high school and junior college	11 (24.44%)	12 (26.67%)	0.058	0.809
University and higher	15 (33.33%)	13 (28.89%)	0.207	0.649
Religious belief			0.047	0.829
Have	18 (40.00%)	17 (37.78%)		
No	27 (60.00%)	28 (62.22%)		
Household income			0.062	0.803
≥3000 yuan/(month·person)	34 (75.56%)	35 (77.78%)		
<3000 yuan/(month·person)	11 (24.44%)	10 (22.22%)		
Place of residence			0.049	0.824
Urban areas	29 (64.44%)	30 (66.67%)		
Rural areas	16 (35.56%)	15 (33.33%)		

TABLE 2: Comparison of incidences of adverse reactions [n (%)].

Group	n	Cardiac injury	Acute radiation-induced skin reaction	Lung injury	Total incidence of adverse reactions
Experimental group	45	1 (2.22%)	2 (4.44%)	1 (2.22%)	4 (8.89%)
Control group	45	3 (6.67%)	5 (11.11%)	4 (8.89%)	12 (26.67%)
X^2					4.865
P					<0.05*

*$P < 0.05$.

treatments in the clinic. Conventional radiotherapy kills or inhibits cancer cells by irradiating the target area with different energy rays, but this treatment has difficulty in meeting the clinical demand because of the large radiotherapy area, poor shape-adaptability of the target area, and many adverse effects [15, 16]. SBRT gathers the X-ray in the tumor location with accurate location and reasonable dose distribution in the target area, and the adjacent tissues only receive a safe dose. This treatment can effectively control the tumor growth and improve the patients' quality of life [17, 18]. In

this study, there were 4 patients and 12 patients having adverse reactions in the experimental group and control group, respectively, indicating that SBRT had higher safety compared with conventional treatment. Meanwhile, after one-year follow-up, the experimental group had remarkably higher 1-year survival rate compared with the control group ($P < 0.05$), indicating that SBRT combined with thermoplastic fixation could effectively improve the patients' quality of life. The reasons behind this are speculated as follows. SBRT effectively destroys the DNA of tumor cells to make them
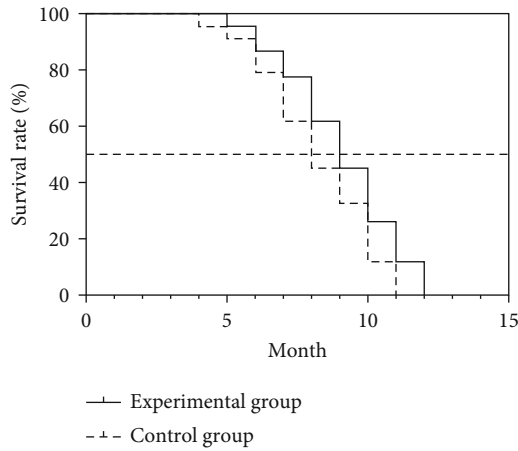
Figure 1: Comparison of 1-year survival rates ($\bar{x} \pm s$).

Table 3: Comparison of translational errors ($\bar{x} \pm s$).

Group	n	X direction (cm)	Y direction (cm)	Z direction (cm)
Experimental group	45	0.14 ± 0.06	0.20 ± 0.09	0.13 ± 0.07
Control group	45	0.29 ± 0.12	0.34 ± 0.11	0.32 ± 0.15
t		7.500	6.608	7.699
P		$<0.001^*$	$<0.001^*$	$<0.001^*$

$^*P < 0.05$.

Table 4: Comparison of translational errors after rotation ($\bar{x} \pm s$).

Group	n	X direction (cm)	Y direction (cm)	Z direction (cm)
Experimental group	45	0.18 ± 0.08	0.20 ± 0.09	0.22 ± 0.09
Control group	45	0.29 ± 0.15	0.32 ± 0.15	0.35 ± 0.12
t		4.341	4.602	5.814
P		$<0.001^*$	$<0.001^*$	$<0.001^*$

Table 5: Comparison of rotation errors ($\bar{x} \pm s$).

Group	n	X direction (°)	Y direction (°)	Z direction (°)
Experimental group	45	0.57 ± 0.21	0.56 ± 0.15	0.41 ± 0.12
Control group	45	0.95 ± 0.08	1.15 ± 0.23	1.10 ± 0.34
t		11.343	14.414	14.325
P		$<0.001^*$	$<0.001^*$	$<0.001^*$

lose the growing ability and resulting in apoptosis, and then, the tumor is naturally absorbed and metabolized by the body. Position fixation is the prerequisite of the whole radiotherapy, and thermoplastic fixation can effectively ensure the set-up accuracy and reduce errors, so as to enhance the treatment effects.

Han et al. [19] have pointed out that the advancement of radiotherapy technology in recent years has led to the diversification of position fixation techniques, and set-up repeatability and accuracy have become the focus of attention. At the same time, different position fixation devices directly affect the treatment effect, and wider physical activities during radiotherapy can lead to unsatisfactory set-up effect, thus damaging the patients' trachea, heart, lungs, and other organs. The conventional breast bracket, with a simple bracket structure, has many disadvantages. Because the bracket lacks a personalized mold, the patients may move or have difficulties in resetting their positions in magnetic resonance imaging (MRI) localization, CT localization, and CBCT scan and treatment, thus affecting the radiotherapy effect [20, 21]. The thermoplastic fixation makes up for the deficiencies of conventional fixation. The head mask and baseplate in the thermoplastic fixation can effectively fix the patients to make them feel comfortable and safe during treatment, and the groove and fixing lugs in the baseplate not only facilitate the fixation of headrest but also increase the comfort level [21–23]. Besides, Tokunaga et al. [24] have pointed out that thermoplastic fixation has remarkably smaller set-up errors compared with the breast bracket and can effectively enhance radiotherapy effect and benefit the patients' prognoses. Tables 3, 4, and 5 in this paper present the analysis results of set-up errors of the breast bracket and thermoplastic fixation. Remarkable differences in the translational errors (X direction, Y direction, and Z direction), translational errors after rotation (X direction, Y direction, and Z direction), and rotation errors (X direction, Y direction, and Z direction) between the two groups were found, fully illustrating that the thermoplastic fixation can reduce the set-up errors in the X direction, Y direction, and Z direction and better protect normal tissues by further increasing the target dose of the patients with breast cancer. Yuen et al. [25] analyzed the set-up errors of 58 patients who underwent modified radical mastectomy (emphasizing radiotherapy) for breast cancer, with 29 patients receiving the breast bracket, and the other 29 patients receiving thermoplastic fixation. Their study showed that the set-up errors in the thermoplastic fixation group were remarkably lower than those in the breast bracket group, and the reasons behind this are speculated as follows. The personalized thermoplastic fixation, fully fitting and wrapping every part of the patients' body, can effectively shape the patients' body according to their curves. Besides, this fixation can appropriately fix the breast position, limit the patients' chest range, and reduce the involuntary movement errors caused by various factors. The deficiencies of this study are as follows. Firstly, the cases in this study are the ones treated in our hospital, and the source region of the cases is single. In addition, limited to the observation time, this clinical study fails to include enough samples, causing bias of the study results. Finally, the death of patients may be influenced by other uncontrollable factors, resulting in biased data results. Therefore, the study design should be improved and the follow-up period should be extended in the future studies to deeply and in more detail explore the effect of SBRT combined with thermoplastic fixation on set-up errors in BC patients undergoing radiotherapy from multiple perspectives. In conclusion, more studies need to be conducted in the future to improve the preliminary conclusions in this study.

Data Availability

The datasets during the current study are available from the corresponding author on reasonable request.

Conflicts of Interest

The authors declare that they do not have any commercial or associative interest that represents a conflict of interest in connection with the work submitted.

Acknowledgments

References

[1] Y.-X. Chen, Y. Zhuang, P. Yang et al., "Helical IMRT-based stereotactic body radiation therapy using an abdominal compression technique and modified fractionation regimen for small hepatocellular carcinoma," *Technology in Cancer Research & Treatment*, vol. 19, article 1533033820937002, 2020.

[2] K. Sasamura, R. Suzuki, T. Kozuka, R. Yoshimura, Y. Yoshioka, and M. Oguchi, "Outcomes after reirradiation of spinal metastasis with stereotactic body radiation therapy (SBRT): a retrospective single institutional study," *Journal of Radiation Research*, vol. 61, pp. 929–934, 2020.

[3] E. Vargas, M. S. Susko, P. V. Mummaneni, S. E. Braunstein, and D. Chou, "Vertebral body fracture rates after stereotactic body radiation therapy compared with external-beam radiation therapy for metastatic spine tumors," *Journal of Neurosurgery: Spine*, vol. 33, no. 6, pp. 870–876, 2020.

[4] B. J. Pielkenrood, J. M. van der Velden, Y. M. van der Linden et al., "Pain response after stereotactic body radiation therapy versus conventional radiation therapy in patients with bone metastases-a phase 2 randomized controlled trial within a prospective cohort," *International Journal of Radiation Oncology • Biology • Physics*, vol. 110, no. 2, pp. 358–367, 2021.

[5] B. L. Jacobs, M. Hamm, F. de Abril Cameron et al., "Radiation oncologists' attitudes and beliefs about intensity-modulated radiation therapy and stereotactic body radiation therapy for prostate cancer," *BMC Health Services Research*, vol. 20, p. 796, 2020.

[6] L. T. Tchelebi, E. J. Lehrer, D. M. Trifiletti et al., "Conventionally fractionated radiation therapy versus stereotactic body radiation therapy for locally advanced pancreatic cancer (CRiSP): an international systematic review and meta-analysis," *Cancer*, vol. 126, no. 10, pp. 2120–2131, 2020.

[7] H.-W. Ho, S. P. Lee, H.-M. Lin et al., "Dosimetric comparison between RapidArc and HyperArc techniques in salvage stereotactic body radiation therapy for recurrent nasopharyngeal carcinoma," *Radiation Oncology*, vol. 15, p. 164, 2020.

[8] B. Frey, J. Mika, K. Jelonek et al., "Systemic modulation of stress and immune parameters in patients treated for prostate adenocarcinoma by intensity-modulated radiation therapy or stereotactic ablative body radiotherapy," *Strahlentherapie und Onkologie*, vol. 196, no. 11, pp. 1018–1033, 2020.

[9] M. J. Sotelo, S. Cabezas-Camarero, A. Riquelme, and C. Bueno, "Long-term survival of a patient with programmed death ligand 1-negative lung adenocarcinoma and oligoprogressive disease treated with nivolumab and stereotactic body radiation therapy," *Journal of Cancer Research and Therapeutics*, vol. 16, no. 4, pp. 941–945, 2020.

[10] Y. Liu, W. Wang, K. Shiue et al., "Risk factors for symptomatic radiation pneumonitis after stereotactic body radiation therapy (SBRT) in patients with non-small cell lung cancer," *Radiotherapy and Oncology*, vol. 156, pp. 231–238, 2021.

[11] J. D. Brooks, J. D. Boice Jr., R. E. Shore et al., "A case-control study of the joint effect of reproductive factors and radiation treatment for first breast cancer and risk of contralateral breast cancer in the WECARE study," *Breast*, vol. 54, pp. 62–69, 2020.

[12] World Medical Association, "World Medical Association Declaration of Helsinki: ethical principles for medical research involving human subjects," *Journal of the American Medical Association*, vol. 310, no. 20, pp. 2191–2194, 2013.

[13] Z. Jiaqiang, C.-Y. Lu, C. Chien-Hsin et al., "Effect of pathologic stages on postmastectomy radiation therapy in breast cancer receiving neoadjuvant chemotherapy and total mastectomy: a cancer database analysis," *Breast*, vol. 54, pp. 70–78, 2020.

[14] A.-S. Boudy, C. Ferrier, L. Selleret et al., "Prognosis of HER2-positive pregnancy-associated breast cancer: analysis from the French CALG (Cancer Associé à La Grossesse) network," *The Breast*, vol. 54, pp. 311–318, 2020.

[15] L. A. Solis-Castillo, G. S. Garcia-Romo, A. Diaz-Rodriguez et al., "Tumor-infiltrating regulatory T cells, CD8/Treg ratio, and cancer stem cells are correlated with lymph node metastasis in patients with early breast cancer," *Breast Cancer*, vol. 27, pp. 837–849, 2020.

[16] N. Tanaka, A. Hirano, A. Hattori et al., "Effect of adjuvant chemotherapy in patients with ER + /HER2- breast cancer, assessed by propensity score matching: significance of nuclear grade and nodal status," *Breast Cancer*, vol. 28, pp. 40–47, 2021.

[17] K. Seiffert, K. Thoene, C. z. Eulenburg et al., "The effect of family history on screening procedures and prognosis in breast cancer patients - results of a large population-based case-control study," *The Breast*, vol. 55, pp. 98–104, 2021.

[18] L. Tang, Z. Ma, Y. Ishikawa, H. Matsushita, T. Ishida, and K. Jingu, "Effect of radiotherapy after breast-conserving surgery in elderly patients with early breast cancer according to the AJCC 8th Edition Breast Cancer Staging System in Japan," *Breast Cancer*, vol. 28, pp. 465–470, 2021.

[19] H. Yiqun, J. Wang, and B. Xu, "Clinicopathological characteristics and prognosis of breast cancer with special histological types: a surveillance, epidemiology, and end results database analysis," *The Breast*, vol. 54, pp. 114–120, 2020.

[20] Y. Yamamoto, H. Yamashiro, U. Toh et al., "Prospective observational study of bevacizumab combined with paclitaxel as first- or second-line chemotherapy for locally advanced or metastatic breast cancer: the JBCRG-C05 (B-SHARE) study," *Breast Cancer*, vol. 28, pp. 145–160, 2021.

[21] J. Dan, J. Tan, J. Huang et al., "The dynamic change of neutrophil to lymphocyte ratio is predictive of pathological complete response after neoadjuvant chemotherapy in breast cancer patients," *Breast Cancer*, vol. 27, no. 5, pp. 982–988, 2020.

Hindawi

Research Article

Exercise-Diet Therapy Combined with Insulin Aspart Injection for the Treatment of Gestational Diabetes Mellitus: A Study on Clinical Effect and Its Impact

Amei Mu [iD],[1] **Yan'e Chen** [iD],[2] **Yongmei Lv** [iD],[3] **and Wenxing Wang** [iD][4]

[1]*Interventional Department of Nephrology, The Affiliated Qingdao Central Hospital of Qingdao University, The Second Affiliated Hospital of Medical College of Qingdao University, Qingdao 266042, China*
[2]*Department of Neurology IV, Jiyang People's Hospital, Jinan 251400, China*
[3]*Department of Pharmacy, Zhangqiu District People's Hospital, Jinan 250200, China*
[4]*Department of Obstetrics I, Yantaishan Hospital, Yantai 264000, China*

Correspondence should be addressed to Wenxing Wang; wangwenxing@ytsyy.com.cn

Objective. To explore the clinical effect and impact of exercise-diet therapy combined with Insulin Aspart Injection on gestational diabetes mellitus (GDM). *Methods*. The objects of study were patients with pregestational diabetes mellitus (PGDM) and 62 patients with GDM who were diagnosed by oral glucose tolerance test (OGTT) and insulin release test from February 2017 to February 2019. According to the severity of the disease, enrolled patients were informed to have appropriate exercise and diet control or Insulin Aspart Injection on this basis until the completion of delivery. By using 50 pregnant women with normal glucose as the control, the fasting plasma glucose (FPG), 1-hour postprandial glucose (1hPG), 2-hour postprandial glucose (2hPG), nocturnal glucose, and glycosylated hemoglobin (HbA1c) levels were compared between the PGDM group and the GDM group before and after treatment; besides, further comparison was made in terms of glucose compliance rate, islet B-cell secretory function, and insulin resistance after treatment. The pregnant women were examined by B-ultrasound at 24 and 26 weeks of gestation to check if the fetus had abnormalities in the central nervous system and the heart. Further B-ultrasound examination was performed at 32 and 37 weeks of gestation to check the problems such as polyhydramnios and stillbirth. In addition, a comparative analysis was carried out in terms of the adverse pregnancy outcomes and complications, associated with the comparison of the results after treatment with control group. *Results*. After treatment, the levels of FPG, 1hPG, 2hPG, nocturnal glucose, and HbA1c were decreased in the PGDM group and GDM group than those before treatment, especially in the GDM group, with significant difference still when compared with the control group ($P < 0.05$). Statistical analysis revealed that the blood glucose compliance rate in the GDM group was higher than that in the PGDM group, showing a better therapeutic effect. Fasting insulin (FINS) and homeostasis model assessment index for insulin resistance (HOMA-IR) in the GDM group were significantly higher than those in control group, but lower than those in the PGDM group ($P < 0.01$), while the level of HOMA-β was lower in the GDM group than that in the control group and higher than that in PGDM ($P < 0.01$). Further ultrasound examination revealed the presence of fetal cardiac abnormality, polyhydramnios, stillbirth, and problems, showing a higher incidence in the PGDM group but almost nonexistence in the control group. In addition, the incidence of hypertension, macrosomia, premature rupture of membranes, postpartum hemorrhage, and infection were obviously higher in the PGDM group than those in the GDM group and control group ($P < 0.05$). *Conclusion*. Exercise-diet therapy combined with Insulin Aspart Injection can effectively control the blood glucose level of pregnant patients with GDM, improve the pregnancy outcome to a certain extent, and ensure the health of pregnant women and fetus, which is worthy of clinical application.

1. Introduction

Diabetes mellitus is a type of metabolic disease characterized by high blood glucose, with insulin secretion defect or biological damage acting as its major reason of pathogenesis. The diagnostic criteria for hyperglycemia during pregnancy was revised by the Chinese Diabetes Society (CDS) in the 2016 Guidelines [1]. Pregnancy associated with diabetes mellitus can be divided into the following two types, diabetes mellitus patients getting pregnant (pregestational diabetes mellitus, PGDM) and pregnant patients with diabetes mellitus (gestational diabetes mellitus, GDM). According to previous research [2–4], about 1%~15% of pregnant women have GDM annually. It can be explained by the impact of pregnancy that may change the immune system and endocrine system of females, resulting in increased demand for glucose, insufficient insulin secretion, or insulin resistance and hence increasing the risk of diabetes mellitus. It is well known that hyperglycemia during pregnancy has an intimate association with maternal, fetal, and neonatal morbidity. Diabetes mellitus is a high-risk factor for adverse pregnancy outcomes and complications. For instance, compared with pregnant women with normal blood glucose, patients with diabetes mellitus have higher risk to develop fetal intrauterine dysplasia, neonatal malformation, macrosomia, and other symptoms, while the mothers are prone to have preeclampsia and develop into type 2 diabetes mellitus after delivery in the case of poor control. Therefore, the risk of adverse pregnancy outcomes of GDM patients is significantly higher than that of pregnant women with normal blood glucose, and that of PGDM patients is higher than that of GDM, which has been concerned greatly in recent decades. In this regard, there is a need to pay much attention to the nursing methods in order to ensure the health and safety of pregnant women and newborns.

It has been reported that the application of medical intervention to patients with diabetes mellitus can greatly reduce the probability of perinatal diseases, ensure women's health, improve their related quality of life, and reduce the risk of birth of unhealthy fetuses and dystocia [5]. It is thus necessary for patients with gestational hyperglycemia to receive appropriate treatment. However, according to different medical conditions of patients and treatment goals, still 10%-30% of patients with gestational hyperglycemia require medical treatment on the basis of lifestyle intervention [6]. Insulin is the preferred choice for treating patients with hyperglycemia [7, 8]. While in view of the advantages of oral hypoglycemic drugs in cost and convenient use, it has aroused great interest in the treatment of gestational hyperglycemia recently. Comparison on the safety and effectiveness of oral hypoglycemic drugs with insulin and insulin analogues has become the major focus of the current concern in the treatment of gestational hyperglycemia. For example, existed systematic analysis on the treatment of GDM with insulin has compared and analyzed the safety and effectiveness between insulin and oral hypoglycemic drugs. Corresponding results revealed that insulin and oral hypoglycemic agents produced similar efficacy in major health outcomes. At present, insulin is the first choice for the treatment of gestational diabetes mellitus, as an effective drug for blood glucose control. Accordingly, the present study was conducted to explore the clinical effect and adverse pregnancy outcomes of Insulin Aspart Injection combined with exercise-diet therapy in the treatment of GDM, and the report is as follows.

2. Materials and Methods

2.1. General Data. The objects of study were 55 patients with PGDM and 62 patients with GDM ($n = 117$ in total) diagnosed in our hospital from February 2017 to February 2019 according to the *Guidelines for the Diagnosis of Gestational Diabetes Mellitus (2016 Edition)* [9]. According to the severity of disease, all patients were treated with appropriate exercise, diet control, and intensive therapy with Insulin Aspart Injection during hospitalization. The control group was pregnant women with normal blood glucose level ($n = 50$). The exclusion criteria were subjects with severe infection; genetic disease; failure of important organs; endocrine disease; refusal of drug therapy; allergy to the medicine used in this study; and acute complications such as diabetic ketoacidosis, damage in the heart, liver and kidney, hyperthyroidism, pancreatitis, anemia, and other diseases affecting blood glucose level [10]. This study obtained approval from the Ethics Committee of our hospital, following the principle of the Declaration of Helsinki (as revised in 2013). The patients have signed informed consent. Table 1 shows the general data of enrolled subjects.

2.2. Therapeutic Methods [11–14]. The therapeutic methods were described in detail as follows: the diet style of patients was having more meals a day but less food at each, with attention paid to avoid foods with high sugar content, reduce the amount of staple food, and increase the proportion of coarse food grains as the best choice. It was recommended to strengthen appropriate exercise after three meals (such as walking for 15-30 minutes) and keep individualized diet and some exercise support. Basic insulin should be injected at bedtime every day, and Insulin Aspart should be injected before three meals (NovoRapid, Novo Nordisk China Pharmaceutical, National medicine approval No. J20100124, 3 ml: 300 IU). The dosage was adjusted to 0.5-1.0 IU/kg/d according to the severity of the patient's condition and the monitoring results of blood glucose. The treatment was continued until delivery. The method of blood glucose level monitoring was as follows: (1) blood glucose monitoring. Patients were instructed to measure the blood glucose individually and use the blood glucose meter regularly. The blood glucose level is directly proportional to the incidence of complications in pregnant women and fetuses. Hence, the fluctuation of blood glucose must be monitored in a strict manner to provide an effective basis for subsequent treatment. (2) Medication instruction. The correct method of Insulin Aspart Injection and the working mechanism of insulin were explained in detail in stages, so as to cultivate the consciousness of patients to measure blood glucose voluntarily and form the habit gradually. It was expected to ensure that patients could understand the adverse reactions

TABLE 1: General data of enrolled subjects ($\bar{x} \pm s$).

Items	PGDM group	GDM group	Control group	χ^2	P
Cases	55	62	50		
Age (year)	29.54 ± 4.31	28.71 ± 4.73	29.37 ± 5.07	0.352	
Weight (kg)	78.8 ± 11.3	76.2 ± 13.2	78.1 ± 12.5	1.247	
Gestational age (week)	25.75 ± 3.50	28.50 ± 5.25	27.25 ± 3.75	4.833	>0.05
Gravidity and parity (times)	1.17 ± 0.33	1.06 ± 0.23	1.12 ± 0.26	0.113	
With family history of disease	26 (47.3)	11 (17.7)	-	0.638	
HbA1c (%)	16.3 ± 2.5	15.6 ± 1.7	4.8 ± 0.34	8.576	

PGDM: pregestational diabetes mellitus; GDM: gestational diabetes mellitus; FINS: fasting insulin.

TABLE 2: Blood glucose index ($\bar{x} \pm s$) and blood glucose compliance rate (%).

Group	Time	Case	FPG (mmol/L)	1hPG (mmol/L)	2hPG (mmol/L)	Nocturnal glucose (mmol/L)	HbAlc (%)
PGDM group	Before treatment	55	6.83 ± 0.46	11.27 ± 1.94	9.84 ± 1.23	5.71 ± 0.22	7.7 ± 0.6
	After treatment		5.61 ± 0.37[a]	8.06 ± 0.47[a]	7.08 ± 0.42[a]	4.65 ± 0.28[a]	6.1 ± 0.7[a]
GDM group	Before treatment	62	6.62 ± 0.33	11.66 ± 1.64	9.76 ± 1.27	5.57 ± 0.24	7.2 ± 0.4
	After treatment		5.15 ± 0.34[a]	7.57 ± 0.32[a]	6.54 ± 0.39[a]	4.04 ± 0.26[a]	5.3 ± 0.4[a]
Control group		50	4.06 ± 0.21	7.13 ± 0.26	5.73 ± 0.34	3.86 ± 0.23	4.7 ± 0.3
P			<0.05*	<0.05*	<0.05*	<0.05*	<0.05*
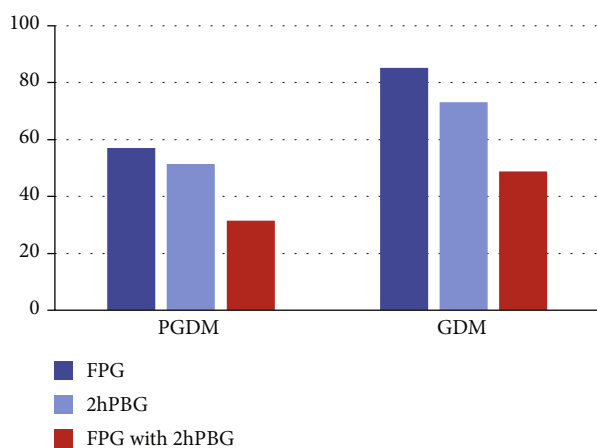
FIGURE 1: The blood glucose compliance rate (%) of the PGDM group and GDM group after treatment.

and possible results of drugs fully and enhance their awareness of the standard medication. (3) Diet care. According to the individual blood glucose level, patients were guided to strictly control the total calorie intake of food daily, so as to better control the blood glucose; besides, based on the dietary habit and preference, patients were informed to choose the type of food for regular and quantitative intake, and spare a certain space; patients could select favorite food in a certain range, improve their compliance behavior as much as possible, but do not increase or reduce the amount of food unadvisedly. Meanwhile, patients should have more food with high cellulose, supplement some fresh fruits and food containing trace elements needed by the human body, and prohibit spicy, raw, and cold food with high sugar and large amount of oil, so as to ensure a light diet in the daily life. (4) Excise care. Patients were instructed to take exercise 1 hour after meal for 30 min/time each time and pay attention to have moderate exercise to experience the feeling of a little weak and slight sweating after exercise and comfortable feel after rest. It was recommended to avoid strenuous exercise, fasting excise, excise when there was physical discomfort, and excise during the waiting time for meals after insulin injection and have exercise safely to prevent falling to induce abortion. Proper exercise may be beneficial to maintain the health of pregnant women and fetus, better control of blood glucose, reduce patients' demand for insulin, and improve glucose tolerance.

2.3. Diagnostic Criteria. According to the recommended criteria mentioned in the Guidelines for the Diagnosis of Gestational Diabetes Mellitus (2016 Edition), 75 g OGTT was used to measure blood glucose at 24-28 weeks and on the first visit after 28 weeks of gestation. Patients were confirmed with GDM when any of the blood glucose values reached or exceeded the above criteria: PG5: 1~6.9 mmol/L, blood glucose ≥ 10.0 mmol/L 1 h after OGTT, and blood glucose ≥ 8.5 and <11 mmol/L 2 h after OGTT. Besides, PGDM was diagnosed in patients with definite history of diabetes mellitus before pregnancy.

2.4. Observational Indexes. Blood glucose indexes, including fasting blood glucose (FPG), 1-hour postprandial glucose (1hPG), 2-hour postprandial glucose (2hPG), and nocturnal glucose and glycosylated hemoglobin (HbA1c) levels, were recorded before and after treatment. In terms of the major observational indexes, the blood glucose control of gestational hyperglycemia was performed in accordance

TABLE 3: Comparison of islet-B-cell secretory function and insulin resistance-related indexes among groups ($\bar{x}\pm s$).

Group	Time	Cases	FINS (mU/L)	HOMA-β (%)	HOMA-IR
PGDM group	Before treatment	55	37.13 ± 5.47	5.18 ± 0.21	3.64 ± 1.13
	After treatment		12.31 ± 2.56^a	7.03 ± 0.41^a	2.93 ± 0.66^a
GDM group	Before treatment	62	36.75 ± 6.38	5.68 ± 0.24	3.58 ± 1.27
	After treatment		6.64 ± 1.75^a	8.36 ± 0.37^a	2.31 ± 0.35^a
Control group		50	2.41 ± 1.03	9.22 ± 0.15	1.72 ± 0.12
χ^2			14.537	6.263	4.712
P			$<0.05^*$	$<0.05^*$	$<0.05^*$

Note: PGDM: pregestational diabetes mellitus; GDM: gestational diabetes mellitus. Compared with pretreatment condition, $P^a < 0.01$. Comparison between the PGDM group and the GDM group, $P < 0.01$. Compared with the control group, $P < 0.01$.

with the standard recommended by the *Guidelines for the Diagnosis of Gestational Diabetes Mellitus (2016 Edition)*. FPG should be controlled between 3.3~5.3 mmol/L, 2hPG ≤ 6.7 mmol/L, 1hPG ≤ 7.8 mmol/L, and nocturnal blood glucose > 3.3 mmol/L, and HbA1c during pregnancy should be $<5.5\%$. Moreover, the secretory function of islet-B-cells and insulin resistance-related indexes were recorded [6, 15], associated with the detection of fasting insulin (FINS). Furthermore, islet B-cell secretion index (HOMA-β) and homeostasis model assessment index for insulin resistance (HOMA-IR) were used to evaluate islet B-cell secretory function and insulin resistance, of which $HOMA-\beta = FINS \times 20/(FPG - 35)$; $HOMA-IR = FPG \times FINS/22.5$. Simultaneously, the adverse pregnancy outcomes were analyzed, including polyhydramnios, macrosomia, postpartum hemorrhage, and postpartum infection. In this study, blood glucose was measured 4-7 times a day, and it was controlled in the above range by combining the intensive therapy of Insulin Aspart Injection. The experiment was repeated three times.

2.5. Use of Instruments. The instrument for measuring peripheral blood glucose used BaiAnJin blood glucose meter (7600P, Bayer HealthCare LLC.). Other instruments included ion-exchange high-performance liquid chromatography (BIO RAD VARIANT II, Bio-Rad Laboratories, Inc., USA) and glycosylated albumin monitoring kit (Abbott I16200, Abbott, USA).

2.6. Statistical Analysis [16]. The SPSS 23.0 statistical software was used to analyze and process the data in this study. The count data (%) were tested by χ^2 test, and the measurement data ($\bar{x}\pm s$) were examined by t-test. $P < 0.05$ meant that the difference was statistically significant.

3. Results

3.1. Comparison of Blood Glucose Index and Blood Glucose Compliance Rate. Measurement results were compared according to the blood glucose control criteria in the *Guidelines for the Diagnosis of Gestational Diabetes Mellitus (2016 Edition)*. As shown in Table 2, after reasonable treatment, levels of FPG, 1hPG, 2hPG, nocturnal glucose, and HbA1c were decreased in the PGDM group and GDM group than

those before treatment, especially in the GDM group when compared with the PGDM group, with significant difference still when compared with the control group, with statistical significance ($P < 0.05$). Further analysis of the blood glucose compliance and calculation of corresponding rate [17] showed that the rate was much higher in GDM (Figure 1), exhibiting better therapeutic effect.

3.2. Comparison of Islet-B-Cell Secretory Function and Insulin Resistance-Related Indexes among Groups. After treatment, FINS and HOMA-IR in the GDM group and PGDM group decreased significantly [18], which were better in the control group when compared with combined diabetes mellitus group, while HOMA-β was increased in the GDM group and PGDM group, which was the highest in the control group (Table 3).

3.3. Monitoring of the Unborn Fetal Health. According to the results of B-ultrasound [19, 20] of pregnant women in the second and third trimester, the fetal health of the GDM group was better than that of the PGDM group after treatment, and there was almost no adverse reaction in the control group (Figure 2).

3.4. Comparison of Adverse Outcomes and Complications of Pregnant Women. As shown in Table 4, after treatment, the adverse pregnancy outcomes and complications of the GDM group were better than those of the PGDM group ($P < 0.05$); comparison among groups showed that the control group had a better adverse pregnancy outcomes and complications.

4. Discussion

The incidence rate of pregnancy combined with diabetes mellitus [21] is as high as 17.5% in China. It includes two types, as described below. In the first type, subjects have got diabetes mellitus before pregnancy in the absence of blood glucose test, which is known as PGDM; as for the second type, there is no abnormality in the level of blood glucose before pregnancy, while the internal hormone changes due to the special physiological reaction of pregnant women during pregnancy, resulting in impaired glucose tolerance and diabetes mellitus, which is called GDM. In general, diabetes mellitus may produce variety of perinatal
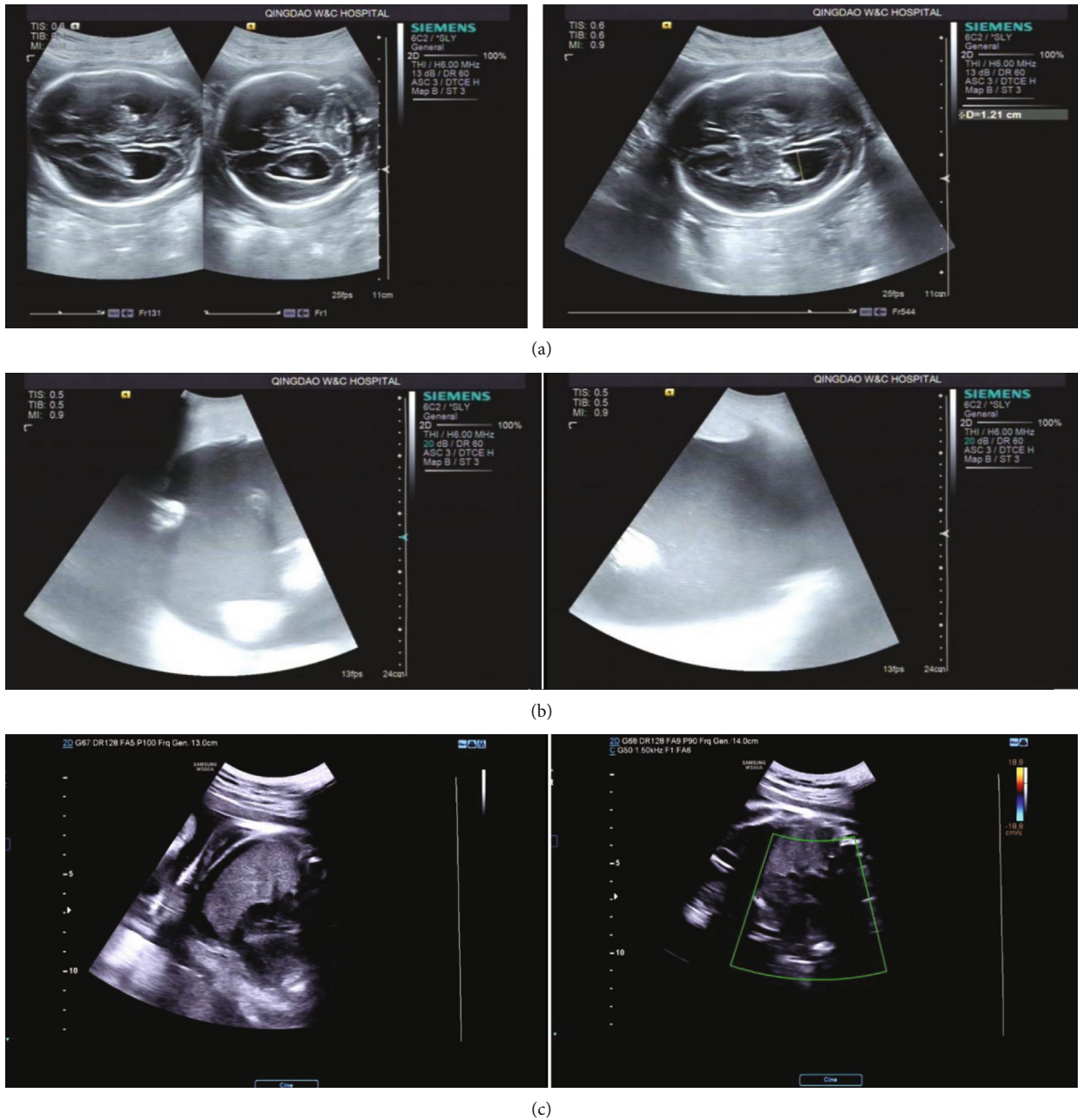
Figure 2: Monitoring of the unborn fetal health. (a) A 30-year-old PGDM patient with intrauterine pregnancy. (b) A 28-year-old GDM patient with intrauterine pregnancy. (c) A 31-year-old PGDM patient with single fetus.

Table 4: Comparison of adverse outcomes and complications of pregnant women ($n(\%)$).

Group	Cases	Hypertension	Premature rupture of membranes	Macrosomia	Postpartum hemorrhage	Postpartum infection
PGDM group	55	10 (18.2)	8 (14.5)	6 (10.9)	5 (9.1)	8 (14.5)
GDM group	62	5 (8.1)	3 (4.8)	1 (1.6)	2 (3.2)	2 (3.2)
Control group	50	2 (4.0)	1 (2.0)	0 (0)	1 (2.0)	0 (0)
χ^2		8.316	4.092	6.500	3.210	8.667
P		<0.05*	<0.05*	<0.05*	<0.05*	<0.05*

PGDM; pregestational diabetes mellitus; GDM: gestational diabetes mellitus.

complications that may have a great impact on the development of pregnant women, fetuses, and newborns [22, 23]. The absence of timely and effective control of blood glucose of pregnant women, the mother, and baby during the prenatal period may develop various serious complications and even death. It has been documented that several important factors can lead to the occurrence of GDM, such as obesity, old age, family history of diabetes mellitus, and poor birth history [24]. In addition, emotional, psychological, and physiological guidance for women with GDM are of great significance in reducing the incidence of complications and improving pregnancy outcomes.

There exists a cause-effect relationship between pregnancy and diabetes mellitus in GDM. Pregnancy may result in the domination of diabetes mellitus and may also lead to the aggravation of hyperglycemia in pregnant women. Diet therapy, exercise therapy, and insulin therapy are all available choice for the treatment of GDM in the clinical setting [25]. In the mild stage, diet therapy combined with moderate exercise therapy may play a therapeutic effect on controlling the blood glucose effectively, while for patients with moderate and severe conditions, there is a need to apply intensive therapy using insulin. During pregnancy, pregnant women may experience extremely obvious increase in estrogen and progesterone secretion. It may further increase insulin secretion, cause antagonistic effect, and finally generate insulin resistance, resulting in abnormal blood glucose level of pregnant women [26]. At present, HOMA-IR has been recognized to be the most commonly used index to evaluate the degree of insulin resistance. In our study, there was a significantly higher level of HOMA-IR in the PGDM group and GDM group than that in the control group, suggesting a more obvious insulin resistance in patients with diabetes mellitus. Furthermore, following the decrease of insulin sensitivity and the increase of insulin resistance, for the purpose of regulating the blood glucose level, the function of islet B-cells may exhibit a compensatory enhancement to maintain the blood glucose within the normal range. It may consequently show an enhanced secretion of islet B-cells. Nevertheless, in the case of excessive enhancement in insulin resistance, the blood glucose may increase when the insulin secreted by islet B-cells is not enough to compensate. As revealed in our study, HOMA-β was evidently lower while FINS was much higher in the PGDM group and GDM group than those in the control group. The insufficient islet secretion in patients combined with diabetes mellitus may be attributed to the deficiency of primary B-cell secretion. In addition, high blood glucose can inhibit the secretion of islet B-cells, which can also suppress the secretion ability of islet B-cells, and even cause permanent damage to islet B-cells. Consequently, the insufficient insulin secretion may further increase blood glucose, which will eventually aggravate insulin resistance repeatedly, forming a vicious circle. Insulin Aspart [27, 28] is a common choice in the medicinal treatment of GDM. Our study carried out a comparative analysis concerning the effect of Insulin Aspart Injection on patients with PGDM and GDM. Corresponding results indicated a certain decrease in the blood glucose index and adverse pregnancy outcome in both groups. It may suggest that Insulin Aspart Injection can achieve an effective control on the blood glucose level, regulate oxidative stress state of patients, and consequently ensure the safety of pregnant women, fetus, and newborn. In accordance with the aforementioned interpretation, it can be found that Insulin Aspart can exert the hypoglycemic effect of insulin, and its activity is close to that of natural insulin. It has rapid work and absorption and can reach the peak of plasma concentration quickly, with relatively short half-life.

To sum up, GDM patients may experience obvious compensatory insufficient insulin secretion and insulin resistance, as well as high risk of adverse pregnancy outcomes compared with pregnant women with normal blood glucose. Therefore, once GDM is diagnosed during pregnancy, it is recommended to actively adopt a series of interventions such as drugs and diet. The exercise-diet therapy combined with Insulin Aspart Injection applied in our study can improve the pregnancy outcome of patients with GDM, effectively control blood glucose, and improve maternal and neonatal complications.

Data Availability

The datasets during the current study are available from the corresponding author on reasonable request.

Conflicts of Interest

The authors declare that they do not have any commercial or associative interest that represents a conflict of interest in connection with the work submitted.

References

[1] R. Martis, C. A. Crowther, E. Shepherd, J. Alsweiler, M. R. Downie, and J. Brown, "Treatments for women with gestational diabetes mellitus: an overview of Cochrane systematic reviews," *Cochrane Database of Systematic Reviews*, vol. 8, no. 8, 2018.

[2] S. Park and S. H. Kim, "Women with rigorously managed overt diabetes during pregnancy do not experience adverse infant outcomes but do remain at serious risk of postpartum diabetes," *Endocrine Journal*, vol. 62, no. 4, pp. 319–327, 2015.

[3] M. Subiabre, L. Silva, F. Toledo et al., "Insulin therapy and its consequences for the mother, foetus, and newborn in gestational diabetes mellitus," *Biochimica et Biophysica Acta (BBA)-Molecular Basis of Disease*, vol. 1864, no. 9, pp. 2949–2956, 2018.

[4] G. Hawthorne, "Maternal complications in diabetic pregnancy," *Best Practice & Research. Clinical Obstetrics & Gynaecology*, vol. 25, no. 1, pp. 77–90, 2011.

[5] M. Balsells, A. García-Patterson, I. Solà, M. Roqué, I. Gich, and R. Corcoy, "Glibenclamide, metformin, and insulin for the treatment of gestational diabetes: a systematic review and meta-analysis," *BMJ*, vol. 350, p. h102, 2015.

[6] J. Brown, L. Grzeskowiak, K. Williamson, M. R. Downie, C. A. Crowther, and Cochrane Pregnancy and Childbirth Group, "Insulin for the treatment of women with gestational diabetes," *Cochrane Database of Systematic Reviews*, vol. 11, no. 11, article CD012037, 2017.

[7] J. Brown, R. Martis, B. Hughes, J. Rowan, C. A. Crowther, and Cochrane Pregnancy and Childbirth Group, "Oral anti-diabetic pharmacological therapies for the treatment of women with gestational diabetes," *Cochrane Database of Systematic Reviews*, vol. 2017, no. 1, article CD011967, 2017.

[8] J. Tieu, S. Coat, W. Hague, P. Middleton, E. Shepherd, and Cochrane Pregnancy and Childbirth Group, "Oral anti-diabetic agents for women with established diabetes/impaired glucose tolerance or previous gestational diabetes planning pregnancy, or pregnant women with pre-existing diabetes," *Cochrane Database of Systematic Reviews*, vol. 2017, no. 10, article CD007724, 2017.

[9] E. Chiefari, B. Arcidiacono, D. Foti, and A. Brunetti, "Gestational diabetes mellitus: an updated overview," *Journal of Endocrinological Investigation*, vol. 40, no. 9, pp. 899–909, 2017.

[10] D. Emily, "Gestational diabetes mellitus," *Endocrinology and Metabolism Clinics of North America*, vol. 48, no. 3, pp. 479–493, 2019.

[11] J. Brown, N. A. Alwan, J. West et al., "Lifestyle interventions for the treatment of women with gestational diabetes," *Cochrane Database of Systematic Reviews*, vol. 2017, no. 5, article CD011970, 2017.

[12] P. Raman, E. Shepherd, T. Dowswell, P. Middleton, C. A. Crowther, and Cochrane Pregnancy and Childbirth Group, "Different methods and settings for glucose monitoring for gestational diabetes during pregnancy," *Cochrane Database of Systematic Reviews*, vol. 2017, no. 10, article CD011069, 2017.

[13] E. Shepherd, J. C. Gomersall, J. Tieu et al., "Combined diet and exercise interventions for preventing gestational diabetes mellitus," *Cochrane Database of Systematic Reviews*, vol. 2017, no. 11, article CD010443, 2017.

[14] L. Suhonen, V. Hiilesmaa, R. Kaaja, and K. Teramo, "Detection of pregnancies with high risk of fetal macrosomia among women with gestational diabetes mellitus," *Acta Obstetricia et Gynecologica Scandinavica*, vol. 87, no. 9, pp. 940–945, 2008.

[15] A. Kautzky-Willer, D. Bancher-Todesca, A. Pollak, A. Repa, M. Lechleitner, and R. Weitgasser, "Gestationsdiabetes (GDM)," *Wiener klinische Wochenschrift*, vol. 124, Supplement 2, pp. 58–65, 2012.

[16] R. Donald, "Gestational diabetes mellitus," *Clinical Chemistry*, vol. 59, no. 9, pp. 1310–1321, 2013.

[17] J. Skupień, K. Cyganek, and M. T. Małecki, "Diabetic pregnancy: an overview of current guidelines and clinical practice," *Current Opinion in Obstetrics & Gynecology*, vol. 26, no. 6, pp. 431–437, 2014.

[18] A. Garrison, "Screening, diagnosis, and management of gestational diabetes mellitus," *American Family Physician*, vol. 91, no. 7, pp. 460–467, 2015.

[19] S. Bano, V. Chaudhary, and S. Kalra, "The diabetic pregnancy: an ultrasonographic perspective," *The Journal of the Pakistan Medical Association*, vol. 66, 9 Supplement 1, pp. S26–S29, 2016.

[20] I. Yehuda, J. Nagtalon-Ramos, and K. Trout, "Fetal growth scans and amniotic fluid assessments in pregestational and gestational diabetes," *Journal of Obstetric, Gynecologic, and Neonatal Nursing*, vol. 40, no. 5, pp. 603–616, 2011.

[21] K. Benhalima, R. Devlieger, and A. Van Assche, "Screening and management of gestational diabetes," *Best Practice & Research. Clinical Obstetrics & Gynaecology*, vol. 29, no. 3, pp. 339–349, 2015.

[22] J. Tieu, A. J. McPhee, C. A. Crowther, P. Middleton, E. Shepherd, and Cochrane Pregnancy and Childbirth Group, "Screening for gestational diabetes mellitus based on different risk profiles and settings for improving maternal and infant health," *Cochrane Database of Systematic Reviews*, vol. 2017, no. 8, article CD007222, 2017.

[23] J. E. Park, S. Park, J. W. Daily, and S. H. Kim, "Low gestational weight gain improves infant and maternal pregnancy outcomes in overweight and obese Korean women with gestational diabetes mellitus," *Gynecological Endocrinology*, vol. 27, no. 10, pp. 775–781, 2011.

[24] A. Nankervis, S. Price, and J. Conn, "Gestational diabetes mellitus: a pragmatic approach to diagnosis and management," *Australian Journal of General Practice*, vol. 47, no. 7, pp. 445–449, 2018.

[25] D. Farrar, M. Simmonds, M. Bryant et al., "Treatments for gestational diabetes: a systematic review and meta-analysis," *BMJ Open*, vol. 7, no. 6, article e015557, 2017.

[26] G. F. Jacobson, G. A. Ramos, J. Y. Ching, R. S. Kirby, A. Ferrara, and D. R. Field, "Comparison of glyburide and insulin for the management of gestational diabetes in a large managed care organization," *American Journal of Obstetrics and Gynecology*, vol. 193, no. 1, pp. 118–124, 2005.

[27] K. Benhalima, K. Robyns, P. Van Crombrugge et al., "Differences in pregnancy outcomes and characteristics between insulin- and diet-treated women with gestational diabetes," *BMC Pregnancy and Childbirth*, vol. 15, no. 1, p. 271, 2015.

[28] L. Hartling, D. M. Dryden, A. Guthrie et al., "Screening and diagnosing gestational diabetes mellitus," *Evidence Report/Technology Assessment*, vol. 210, pp. 1–327, 2012.

Hindawi

Research Article

Application Value of Nutrition Support Team in Chemotherapy Period of Colon Cancer Based on Internet Multidisciplinary Treatment Mode

Jianfeng Chen ⬤, Bo Wang, Xiaobin Yin, Qifei Liang, Yucheng Li, Xingjiang Xie, and Xuehui Zeng

Gastrointestinal Surgery, People's Hospital of Wenjiang District, 611130 Chengdu City, Sichuan Province, China

Correspondence should be addressed to Jianfeng Chen; chenjianfeng@wj120.org.cn

Objective. To explore the application value of the nutrition support team in chemotherapy period of colon cancer based on the internet multidisciplinary treatment mode. *Methods.* For the method of retrospective study, 90 patients with colon cancer admitted to our hospital from August 2018 to August 2020 were selected as the study subjects. They were equally divided into the experimental group ($n = 45$) and the control group ($n = 45$) according to the order of initials and the method of parity group. The control group was given conventional nutrition support, and the experimental group was given the nutrition support under the internet multidisciplinary treatment mode. The serum tumor marker levels (CEA and CA19-9), immune function indexes, nutrition indicators, and the incidence of adverse reactions were compared between the two groups before and after intervention. *Results.* The serum tumor marker levels in the experimental group after intervention were significantly lower than those in the control group ($P < 0.001$). The immune function indexes in the experimental group after intervention were significantly better than those in the control group ($P < 0.001$). The nutrition indicators in the experimental group after intervention were significantly better than those in the control group ($P < 0.001$). The incidence of gastrointestinal adverse reactions above grade 2 in the experimental group was significantly lower than that in the control group ($P < 0.05$). There were 20 patients with myelosuppression, 2 patients with neurotoxicity, and 1 patient with hand and foot syndrome in the experimental group, while 22 patients with myelosuppression, 4 patients with neurotoxicity, and 2 patients with hand and foot syndrome in the control group, with no significant difference in the incidence of adverse reactions between the two groups ($P > 0.05$). *Conclusion.* The nutrition support team under the internet multidisciplinary treatment mode can improve the immune function of chemotherapy patients with colon cancer and enhance their nutritional level, thereby reducing the incidence of adverse reactions and improving the chemotherapy effects.

1. Introduction

Colon cancer is a malignant tumor originating from epithelial cells of colon mucosa, and the incidence rate has shown an upward trend in recent years, with the incidence rate of 0.3‰ [1]. Surgery and chemotherapy are the focus of comprehensive treatment programs. For colon cancer patients with radical resection, the application of adjuvant chemotherapy before or after surgery can improve the 3-year recurrence-free survival of patients and reduce the possibility of metastasis [2, 3]. For colon cancer patients who cannot be treated surgically, chemo-

therapy reduces the lesions, which allows patients to regain the opportunity for surgery. Therefore, chemotherapy is recommended as the core treatment measure for patients with colon cancer in the guidelines of the National Comprehensive Cancer Network (NCCN) [4]. In recent years, the practice has gradually confirmed that adjuvant chemotherapy improves the median survival period of colon cancer patients, and the patients with liver metastasis benefit more especially [5]. However, patients with colon cancer often have multiple diseases before chemotherapy, and the incidence of malnutrition is about 40.0% [6]. Long-term or short-term chemotherapy can

cause adverse reactions such as nausea, vomiting, and myelo-suppression, which further affects the uptake rate of nutrients. If patients with intestinal obstruction have a poor dietetic level before chemotherapy, severe malnutrition will be more likely to occur during chemotherapy, and the immunosuppression will be more obvious [7]. Patients with colon cancer are more prone to anemia due to the malnutrition, thereby reducing the level of plasma protein, which affects the absorption, metabolism, and excretion of chemotherapy drugs. The incremental drug toxicity reduces the number of chemotherapy, and some patients even give up chemotherapy completely [8]. Scholars Kaška et al. have found that the survival period of patients with low body mass treated by comprehensive therapy is significantly shortened, confirming that nutritional status can affect the prognosis of patients with chemotherapy and surgery [9]. Therefore, it is crucial for patients with colon cancer to receive nutrition support during chemotherapy.

NCCN has proposed that patients with colon cancer need multidisciplinary treatment during chemotherapy to closely assess their condition changes [10]. Multidisciplinary treatment (MDT) means that the medical staff coming from different subjects provide patients with independent suggestions about diagnosis and treatment, implement efficient medical services, and formulate the best treatment plans with individual differences according to patients' condition based on the support of data system. In 2016, the National Family Planning Commission in China pointed out that the oncology department should actively implement the treatment mode of single disease and multiple subjects [11]. However, the plan of nutrition support team under the MDT mode has not been implemented due to the practical factors. In recent years, with the continuous development of smart healthcare, the experience accumulated by internet diagnosis and treatment has provided a better reference model for the development of MDT. In particular, big data of medical has become an important data source for MDT. In the internet MDT mode, the working efficiency of the nutrition support team may be significantly improved, which is conducive to improving the effect of nutrition support in patients with colon cancer during chemotherapy. In the internet MDT mode, the work efficiency of the nutrition support team may be significantly improved, which is conducive to improving the nutrition support effect of patients with colon cancer during chemotherapy. Based on this, this study explored the application value of nutrition support team in the chemotherapy period of colon cancer under the internet MDT mode.

2. Materials and Methods

2.1. Research Design.
The retrospective study was conducted in our hospital from August 2018 to August 2020. The study subjects and researchers did not understand the grouping of this experiment, and the research designers were responsible for arranging and controlling the experiment.

2.2. Inclusion and Exclusion Criteria.
Inclusion criteria: (1) The patients were diagnosed with colon cancer by colonoscopy, which met the diagnostic criteria in the Guidelines for the Diagnosis and Treatment of Colon Cancer [12], and they

were diagnosed and treated with interventional therapy for the first time. (2) Patients had definite clinical stages and had indications for chemotherapy. (3) Patients had no abnormal immune function before chemotherapy. (4) Patients were expected to survive more than 3 months. (5) Patients had no history of long-term fasting. (6) Patients could cooperate with the comprehensive therapeutic strategies in the MDT mode. Exclusion criteria are as follows: (1) patients with metastasis in vitals such as abdominal cavity and liver, (2) patients with dysfunction in vitals, (3) patients with the second primary tumor, (4) patients with the contraindication of chemotherapy, (5) patients with the contraindication of nutrition support, (6) patients with language dysfunction and who could not communicate with others, (7) patients with low immune function before chemotherapy and poor tolerance to chemotherapy, and (8) patients with endocrine system diseases

2.3. General Information.
In the study, 90 patients were equally divided into the experimental group ($n = 45$) and the control group ($n = 45$) according to the order of initials and the method of parity group. On the day when the patients agreed to participate in the study, the study group collected the data of sociodemography and clinical manifestation. It was found that there was no statistical difference in the patients' general information between the two groups by comparison ($P > 0.05$), which was comparable. In the experimental group, there were 25 males and 20 females with an average age of 51.27 ± 5.20 years old. Before intervention, the body weight was 55.65 ± 2.65 kg, the BMI was 21.22 ± 1.23 kg/m^2, and the ECOG score was 0.67 ± 0.60 points. In Dukes staging, grade A had 2 cases, grade B had 18 cases, grade C had 18 cases, and grade D had 7 cases. There were 8 cases with hypertension, 6 cases with diabetes mellitus, and 15 cases with intestinal obstruction. In the control group, there were 26 males and 19 females with an average age of 51.22 ± 2.43 years old. Before intervention, the body weight was 55.74 ± 2.40 kg, the BMI was 21.24 ± 1.28 kg/m^2, and the ECOG score was 0.64 ± 0.60 points. In Dukes staging, grade A had 1 case, grade B had 19 cases, grade C had 19 cases, and grade D had 6 cases. There were 8 cases with hypertension, 7 cases with diabetes mellitus, and 17 cases with intestinal obstruction.

2.4. Moral Consideration.
This study was in line with the principles of Declaration of Helsinki (2013) [13], and patients signed the informed consent.

2.5. Methods

2.5.1. Chemotherapy.
Patients in both groups were treated with the FOLFOX4 regimen. On the first day, they received oxaliplatin (Jiangsu Hengrui Pharmaceutical Co., Ltd.; NMPA approval No.: H20050962) by intravenous infusion at a dose of 85 mg/m^2. On the first and second days, they received calcium leucovorin (New Asiatic Pharmaceutical Co., Ltd.; NMPA approval No.: H20113395) by intravenous infusion at a dose of 200 mg/m^2 and received 5-fluorouracil (Beijing Zizhu Pharmaceutical Co., Ltd.; NMPA approval No. H11020069) by intravenous infusion at a dose of 400 mg/m^2. With 14 days as a chemotherapy cycle, two chemotherapy cycles were performed.

The measures of symptomatic treatment such as the prevention of vomiting and the protection of stomach were routinely taken before chemotherapy.

2.5.2. Control Group. The control group was given conventional nutrition support. Firstly, patients were given complete parenteral nutrition, with the heat maintained at 30 kcal/kg/d and the energy ratio of lipid emulsion to glucose as 2 : 3. They were given the enteral nutrition gradually, supplemented by nutritional agents with the daily heat supply of 500 kcal. Patients with severe gastrointestinal reactions also received parenteral nutrition until the surgery was performed.

2.5.3. Experimental Group. The experimental group was given the nutrition support under the internet MDT mode. (1) The MDT team about colon cancer was established. The team members included doctors and nursing staff coming from department of medical oncology in alimentary system, colorectal surgery, anesthesia department, intervention department, nutrition department, imaging department, laboratory department, and pharmacy department, and all participants joined the MDT WeChat group. The doctor and nursing teams were divided into the data, administration, and instruction groups. The managers were clinicians and nursing staff with high qualification and rich experience, whose primary responsibilities were to make an induction and summary of the data and monitor the implementation of the team work. The team members needed to deeply understand the MDT mode through the ways of master lectures and evidence-based medicine and fully learn how to formulate the medical decisions based on the data and apply the decisions to medical process. (2) The internet database was established with the help of the hospital diagnosis and treatment platform, which contained the patient data, medical data, nursing data, and literature data. The patient data were primary data mainly including the basic information of patients (name, gender, the duration of hospitalization, etc.), treatment information (attending physicians, surgeons, surgical methods, etc.), economic information (medical expenses), and MDT information (medical process, neoadjuvant therapy, adjuvant therapy, etc.). The medical data included doctors' orders and all kinds of inspection and examination information and patients' data of clinical symptoms and test indicators. The nursing data included doctors' orders and the implementation of inspection and examination, the common clinical scales such as the scale of Hamilton negative emotion and the scale of NRS nutrition risk assessment, and the questionnaire data collected from patients. The literature data included the data from Chinese and foreign professional literature on colon cancer for doctors and nurses to consult. (3) The instruction group established a diagrammatic figure of MDT nutrition support for colon cancer patients according to the data collected from the internet database and divided the work about nutrition support into three stages during chemotherapy. The first stage was the preparation of nutrition support, which is aimed at comprehensively developing the nutrition support strategies combining the mental status, nutritional status, and various clinical indicators to improve the treatment and nursing compliance and meeting the needs of mental and physical health of patients. The second stage was the implementation of nutrition support, which is aimed at improving the patients' immune function, alleviating the adverse reactions of chemotherapy, and providing good support for subsequent treatment by targeted measures of nutrition support. The third stage was from the end of chemotherapy to discharge, which was dominated by collecting feedback from patients to provide health guidance for them. (4) The administration group formulated the flow chart according to the tasks of each stage and supervised the implementation. The data group dynamically collected the internet data at each stage to facilitate the team to evaluate the implementation effects of the nutrition support under the MDT mode at any time. In the instruction group, the chief experts updated the progress once every 3 days, and the doctors and nursing staff made supplements and discussions in the WeChat group with weekly meetings offline. (5) The measures of nutrition support in the experimental group were formulated by the MDT team according to the above steps on the basis of the control group. The nursing navigators accompanied the patients and answered their questions throughout the intervention and delivered messages dynamically and timely between the MDT nutrition support team and the patients.

2.6. Observation Indexes

2.6.1. The Serum Tumor Marker Levels. The fasting venous blood was taken from the patients in the morning before and after intervention to measure the levels of CEA and CA19-9 by radioimmunoassay using a Roche electrochemiluminescence analyzer with original matching reagents (NMPA (I) 20113402843) and to measure the CA72-4 level by enzyme-linked immunosorbent assay (Beijing Kewei Clinical Diagnostic Reagent Co., Ltd.; NMPA approval No. S20060028).

2.6.2. Immune Function Indexes. The fasting venous blood was taken in the morning before and after intervention to measure the levels of $CD4^+$, $CD8^+$, $CD4^+/CD8^+$, Treg, Th9, and Th17 by a flow cytometry (ACEA BIO (Hangzhou) Co., Ltd.; Zhejiang Medical Products Administration Certified No. 20142400581).

2.6.3. Nutrition Indicators. The body weight of the two groups after intervention was recorded. The fasting venous blood of patients in the morning was taken before and after intervention to measure the levels of total protein (TP), albumin (ALB), and hemoglobin (Hb) by an automatic biochemical analyzer with original matching reagents (Sysmex CHEMIX-800 automatic biochemical analyzer, NMPA approval No. 20112403311).

2.6.4. Incidence of Adverse Reactions. The adverse reactions of patients in the two groups during chemotherapy were recorded according to the World Health Organization (WHO) evaluation criteria for adverse reactions to anticancer drugs [14], and the incidence of adverse reactions was calculated.

(a)

(b)

(c)
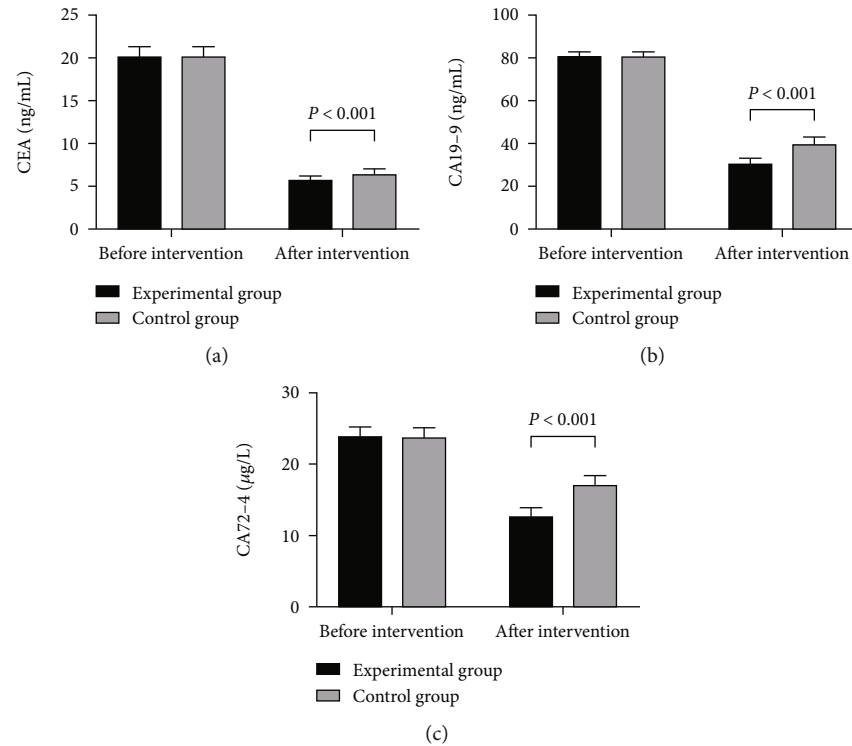
FIGURE 1: Serum tumor marker levels ($\overline{x}\pm s$). (a) CEA level. (b) CA19-9 level. (c) CA72-4 level.

2.7. Statistical Treatment. In this study, the experimental data were processed by SPSS20.0, and GraphPad Prism 7 (GraphPad software, San Diego, USA) was used to draw pictures of the data. The items included in the study were enumeration data and measurement data tested by χ^2 and t-test. When $P < 0.05$, the differences were considered to be statistically significant.

3. Results

3.1. Serum Tumor Marker Levels. The serum tumor marker levels in the experimental group after intervention were significantly lower than those in the control group ($P < 0.001$) (see details in Figure 1).

There was no statistical difference in the levels of CEA, CA19-9, and CA72-4 between the experimental group and the control group before intervention (20.11 ± 1.22 vs. 20.15 ± 1.24, 80.54 ± 2.65 vs. 80.67 ± 2.41, and 23.98 ± 1.25 vs. 23.87 ± 1.20, $P > 0.05$). The levels of CEA, CA19-9, and CA72-4 in the experimental group after intervention were significantly lower than those in the control group (5.67 ± 0.53 vs. 6.44 ± 0.60, 30.55 ± 2.68 vs. 39.68 ± 3.11, and 12.68 ± 1.25 vs. 17.12 ± 1.30, $P < 0.001$).

3.2. Immune Function Indexes. The immune function indexes in the experimental group after intervention were significantly better than those in the control group ($P < 0.001$) (see details in Figure 2).

There was no statistical difference in the levels of $CD4^+$, $CD8^+$, and $CD4^+/CD8^+$ between the experimental group and the control group before intervention (37.52 ± 3.65 vs. 37.60 ± 3.45, 25.98 ± 2.65 vs. 26.05 ± 2.41, and 1.35 ± 0.32 vs. 1.38 ± 0.30, $P > 0.05$). The levels of $CD4^+$, $CD8^+$, and $CD4^+/CD8^+$ in the experimental group after intervention were significantly better than those in the control group (30.98 ± 3.11 vs. 35.11 ± 3.02, 36.98 ± 2.65 vs. 28.98 ± 3.11, and 08.9 ± 0.12 vs. 1.12 ± 0.23, $P < 0.001$).

There was no statistical difference in the levels of Treg, Th9, and Th17 between the experimental group and the control group before intervention (10.11 ± 0.54 vs. 10.15 ± 0.60, 1.40 ± 0.15 vs. 1.42 ± 0.15, and 5.05 ± 0.35 vs. 5.10 ± 0.36, $P > 0.05$). The levels of Treg, Th9, and Th17 in the experimental group after intervention were significantly better than those in the control group (5.11 ± 0.34 vs. 8.96 ± 0.57, 0.67 ± 0.05 vs. 1.32 ± 0.44, and 2.67 ± 0.24 vs. 3.68 ± 0.30, $P < 0.001$).

3.3. Nutrition Indicators. The nutrition indicators in the experimental group after intervention were significantly better than those in the control group ($P < 0.001$) (see details in Figure 3).

There was no statistical difference in body weight and the levels of TP, ALB, and Hb between the experimental group and the control group before intervention (55.65 ± 2.65 vs. 55.74 ± 2.40, 58.62 ± 2.56 vs. 58.67 ± 2.47, 33.65 ± 2.65 vs. 33.24 ± 2.57, and 115.65 ± 2.65 vs. 116.00 ± 2.14, $P > 0.05$). The body weight and the levels of TP, ALB, and Hb in the experimental group after intervention were significantly better than those in the control group (59.55 ± 2.65 vs. 56.65 ± 2.47, 70.12 ± 2.65 vs. 60.55 ± 2.75, 40.65 ± 2.47 vs. 33.84 ± 2.68, and 128.98 ± 5.98 vs. 119.21 ± 4.50, $P < 0.001$).

3.4. Incidence of Adverse Reactions. There were gastrointestinal reactions of different degrees during chemotherapy in
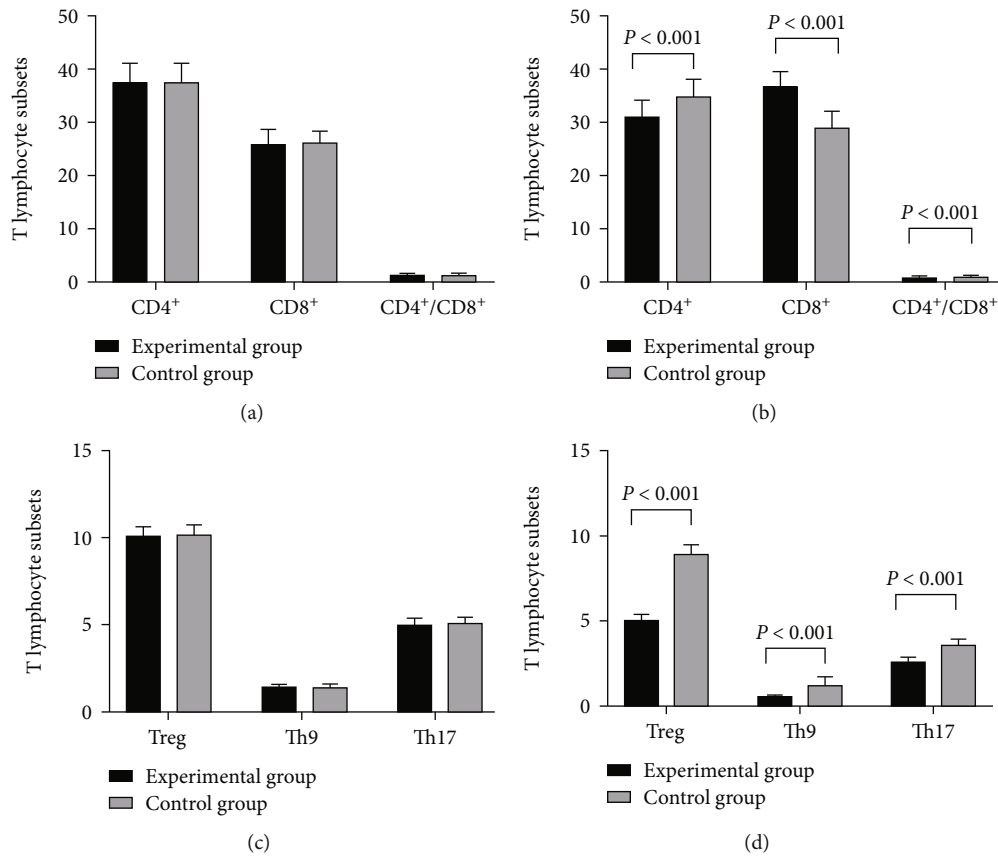
FIGURE 2: Levels of immune function indexes ($\bar{x} \pm s$). (a) Levels of CD4$^+$, CD8$^+$, and CD4$^+$/CD8$^+$ before intervention. (b) Levels of CD4$^+$, CD8$^+$, and CD4$^+$/CD8$^+$ after intervention. (c) Levels of Treg, Th9, and Th17 before intervention. (d) Levels of Treg, Th9, and Th17 after intervention.

the two groups. In the experimental group, there were 18 patients with nausea and vomiting, 10 patients with diarrhea, 6 patients with nausea and vomiting above grade 2, and 5 patients with diarrhea above grade 2. There were 26 patients with nausea and vomiting, 18 patients with diarrhea, 15 patients with nausea and vomiting above grade 2, and 13 patients with diarrhea above grade 2 in the control group. The incidence of gastrointestinal adverse reactions above grade 2 in the experimental group was significantly lower than that in the control group ($P < 0.05$). In addition, there were 20 patients with myelosuppression, 2 patients with neurotoxicity, and 1 patient with hand and foot syndrome in the experimental group and 22 patients with myelosuppression, 4 patients with neurotoxicity, and 2 patients with hand and foot syndrome in the control group. There was no significant difference in the incidence of adverse reactions between the two groups ($P > 0.05$).

4. Discussion

The incidence rate of colon cancer has increased year by year, and the number of patients who need nutrition support during perioperative period has gradually increased. The combination of chemotherapy and surgery is an important comprehensive treatment program approved by many international guidelines for diagnosis and treatment of colon cancer [15].

The clinical value of chemotherapy (or adjuvant chemotherapy) has been confirmed by many studies in recent years, but this program inevitably needs coordination with other treatment measures such as nutrition support. Scholars Plassmeier et al. have claimed that the incidence of malnutrition in patients with malignant tumors is 39.0%, while the incidence of patients with advanced gastrointestinal cancer is higher [16], and the probability of malnutrition in patients with colon cancer is 40.0–50.0% [17]. More and more reports showed that the nutrition support for patients with malignant tumors during chemotherapy can improve the chemotherapy tolerance and enhance the chemotherapy compliance, thereby improving the chemotherapy effect. Therefore, nutrition support is an indispensable part of the comprehensive treatment programs for colon cancer patients, and it is extremely important to deepen the application exploration of nutrition support under the MDT mode.

The MDT mode means that the medical staff coming from different fields provide treatment programs with individual differences for specific patients, so that patients can obtain the best support for treatment. Previous practice has shown that the MDT mode can realize the integration and sharing of medical resources, improve the accuracy of treatment, and shorten the treatment time of patients [18, 19]. With the support of internet big data, smart medical platform provides more possibilities for the application of the MDT mode in
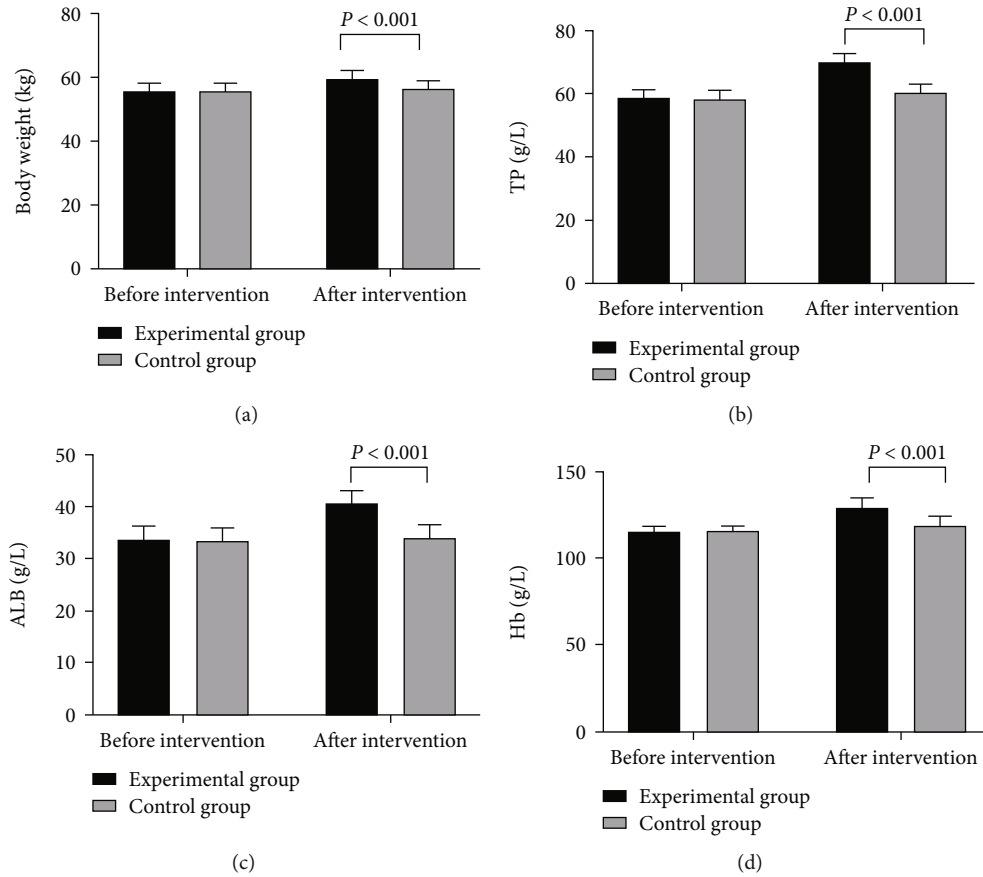
FIGURE 3: Levels of nutrition indicators ($\overline{x}\pm s$). (a) Body weight. (b) TP level. (c) ALB level. (d) Hb level.

nutrition support. In this study, the targeted nutrition support strategies were formulated based on the data obtained from the hospital diagnosis and treatment platform. The study also found that the personalized nutrition support strategies supported by data could better improve the psychological and physical condition of patients and enhance their compliance of nutrition support. The MDT nutrition support team could dynamically adjust the nutrition support plans of patients by online discussion and offline meeting in the experimental group according to the data feedback, so that patients could obtain better nutrition support. Therefore, the nutrition indicators in the experimental group after intervention were significantly better than those in the control group ($P < 0.001$). Since the decline of immune function is an important manifestation of malnutrition in patients with malignant tumors [20], the immune indexes of patients will be improved with the improvement of nutrition status, so that the immune status of patients in both groups after nutrition support is improved. Under the condition of malnutrition, the immune cells of patients such as Treg, Th9, and Th17 show excessive differentiation, which weakens the kill effect of specific and nonspecific immune response on tumor cells, so that patients cannot inhibit cancer through the immune system. The combination of neoadjuvant chemotherapy and nutrition support can ensure that patients obtain sufficient energy sources to enhance self-defense mechanism and improve the metabolic function of organs, thereby enhancing the targeting of chemo-

therapy without excessively damaging the normal cells [21]. Scholars Keskin et al. have shown that neoadjuvant chemotherapy and nutrition support can improve the levels of $CD4^+$, $CD8^+$, and $CD4^+/CD8^+$ in elderly patients with colon cancer [22]. In this study, patients had better improvement in immune function under the internet MDT mode due to the better nutrition indicators in the experimental group.

Nutrition support can maintain the continuity of their gastrointestinal function by improving the immune function and nitrogen balance of colon cancer patients, thereby enhancing the barrier and immune function and accelerating the recovery of intestinal mucosa [23], so that patients in the experimental group were less likely to have gastrointestinal adverse reactions above grade 2. According to Guo, adverse reactions are the important factors affecting patients' willingness and the effect of chemotherapy, and severe toxicity reduces the number of chemotherapy in patients and affects the promotion effect of neoadjuvant chemotherapy for surgery [24]. The reduction of adverse reactions makes patients more willing to accept chemotherapy, and the improvement of immune function also makes them more resistant to the chemotherapy. This study showed that the nutrition support under the internet MDT mode could act on many aspects such as immunity and gastrointestinal function by improving the nutritional indicators to synergistically enhance the chemotherapy effect of patients from different aspects. The performance was that the serum tumor marker levels in the experimental group after

intervention were significantly lower than those in the control group ($P < 0.001$). Another study has shown that the MDT mode is able to improve the 5-year survival rate of patients with advanced colorectal cancer [25]. The survival rate of patients was not counted in this study, and the influence of nutrition support under the internet MDT mode on the survival rate of patients with colon cancer needs to be explored and demonstrated further.

5. Conclusion

The nutrition support team under the internet multidisciplinary treatment mode can improve the immune function of chemotherapy patients with colon cancer and enhance their nutritional level, thereby reducing the probability of adverse reactions and improving the effect of chemotherapy.

Data Availability

Data to support the findings of this study is available on reasonable request from the corresponding author.

Conflicts of Interest

The authors have no conflicts of interest to declare.

References

[1] L. Petrick Jessica and E. Barber Lauren, "Warren Andersen Shaneda et al. Racial disparities and sex differences in early- and late-onset colorectal cancer incidence, 2001-2018. Front," *Oncologia*, vol. 11, p. 734998, 2021.

[2] A. Gupta, E. Gupta, R. Hilsden et al., "Preoperative malnutrition in patients with colorectal cancer," *Canadian Journal of Surgery*, vol. 64, no. 6, pp. E621–E629, 2021.

[3] F. Genua, B. Mirković, A. Mullee et al., "Association of circulating short chain fatty acid levels with colorectal adenomas and colorectal cancer," *Clinical Nutrition ESPEN*, vol. 46, pp. 297–304, 2021.

[4] D. Christine, "Kupfer Sonia S, Colorectal cancer screening recommendations and outcomes in Lynch syndrome," *Gastrointestinal Endoscopy Clinics of North America*, vol. 32, no. 1, pp. 59–74, 2022.

[5] E. R. Tabriz, M. Ramezani, A. Heydari, and S. A. Aledavood, "Health-promoting lifestyle in colorectal cancer survivors: a qualitative study on the experiences and perspectives of colorectal cancer survivors and healthcare providers," *Asia-Pacific Journal of Oncology Nursing*, vol. 8, no. 6, pp. 696–710, 2021.

[6] Y. Wang, L. H. Nguyen, R. S. Mehta, M. Song, C. Huttenhower, and A. T. Chan, "Association between the sulfur microbial diet and risk of colorectal cancer," *JAMA Network Open*, vol. 4, no. 11, article e2134308, 2021.

[7] T. X. Wong, S. T. Chen, S. H. Ong, S. Shyam, P. Kandasami, and W. S. S. Chee, "Study protocol for an open labelled randomised controlled trial of perioperative oral nutrition supplement in breast and colorectal cancer patients undergoing elective surgery," *Trials*, vol. 22, no. 1, p. 767, 2021.

[8] S. K. Murthy, L. Antonova, C. Dube et al., "Multivariable models for advanced colorectal neoplasms in screen-eligible individuals at low-to-moderate risk of colorectal cancer:

towards improving colonoscopy prioritization," *BMC gastroenterology*, vol. 21, p. 383, 2021.

[9] M. Kaška, E. Havel, L. Javorská et al., "Can early postoperative parenteral nutrition have some impact on postoperative inflammatory response intensity?," *Clinical Nutrition ESPEN*, vol. 45, pp. 150–154, 2021.

[10] A. Zöhrer Patrick and A. Hana Claudia, "Gilbert's syndrome and the gut microbiota – insights from the case-control BILI-HEALTH study," *Frontiers in Cellular and Infection Microbiology*, vol. 11, p. 701109, 2021.

[11] A. Bhimla, T. Mann-Barnes, H. Park et al., "Effects of neighborhood ethnic density and psychosocial factors on colorectal cancer screening behavior among Asian American adults, Greater Philadelphia and New Jersey, United States, 2014-2019," *Preventing Chronic Disease*, vol. 18, article E90, 2021.

[12] S. Sato, M. Shiozawa, S. Nukada et al., "Preoperative prealbumin concentration as a predictor of short-term outcomes in elderly patients with colorectal cancer," *Anticancer Research*, vol. 41, no. 10, pp. 5195–5202, 2021.

[13] World Medical Association, "World Medical Association Declaration of Helsinki: ethical principles for medical research involving human subjects," *Journal of the American Medical Association*, vol. 310, no. 20, pp. 2191–2194, 2013.

[14] C. Macaron, G. N. Mankaney, M. Haider, M. Mouchli, K. Hurley, and C. A. Burke, "Chemoprevention considerations in patients with hereditary colorectal cancer syndromes," *Gastrointestinal Endoscopy Clinics of North America*, vol. 32, no. 1, pp. 131–146, 2022.

[15] S. Jafari Nasab, M. Ghanavati, P. Rafiee et al., "A case-control study of Dietary Approaches to Stop Hypertension (DASH) diets, colorectal cancer and adenomas among Iranian population," *BMC Cancer*, vol. 21, no. 1, p. 1050, 2021.

[16] L. Plassmeier, M. K. Hankir, and F. Seyfried, "Impact of excess body weight on postsurgical complications," *Visceral Medicine*, vol. 37, no. 4, pp. 287–297, 2021.

[17] W. Y. Wang, C. W. Chen, T. J. Wang, K. L. Lin, and C. Y. Liu, "Outcomes of early enteral feeding in patients after curative colorectal cancer surgery: a retrospective comparative study," *European Journal of Oncology Nursing*, vol. 54, p. 101970, 2021.

[18] K. R. Koller, A. Wilson, D. P. Normolle et al., "Dietary fibre to reduce colon cancer risk in Alaska Native people: the Alaska FIRST randomised clinical trial protocol," *BMJ open*, vol. 11, no. 8, article e047162, 2021.

[19] N. A. Humphry, T. Wilson, M. C. Cox et al., "Association of postoperative clinical outcomes with sarcopenia, frailty, and nutritional status in older patients with colorectal cancer: protocol for a prospective cohort study," *JMIR research protocols*, vol. 10, no. 8, article e16846, 2021.

[20] L. Huang, J. Liu, X. Huang et al., "Serum C-reactive protein-to-body mass index ratio predicts overall survival in patients with resected colorectal cancer," *Technology in Cancer Research & Treatment*, vol. 20, 2021.

[21] R. Sikavi Daniel and H. Nguyen Long, "The sulfur microbial diet and risk of colorectal cancer by molecular subtypes and intratumoral microbial species in adult men," *Clinical and translational gastroenterology*, vol. 12, no. 8, article e00338, 2021.

[22] H. Keskin, S. M. Wang, A. Etemadi et al., "Colorectal cancer in the Linxian China Nutrition Intervention Trial: risk factors and intervention results," *PLoS One*, vol. 16, no. 9, article e0255322, 2021.

[23] S. P. Yang, T. J. Wang, C. C. Huang, S. C. Chang, S. Y. Liang, and C. H. Yu, "Influence of albumin and physical activity on postoperative recovery in patients with colorectal cancer: an observational study," *European Journal of Oncology Nursing*, vol. 54, p. 102027, 2021.

[24] T. Guo, "Study on the effect of PICC in parenteral nutrition support for colorectal cancer," *American Journal of Translational Research*, vol. 13, no. 8, pp. 9839–9845, 2021.

[25] X.-Y. Li, S. Yao, Y.-T. He et al., "Inflammation-immunity-nutrition score: a novel prognostic score for patients with resectable colorectal cancer," *Journal of Inflammation Research*, vol. 14, pp. 4577–4588, 2021.

Retraction

Retracted: Analysis of Intervention Effect and Satisfaction of Holistic Nursing after Oral Tumor Resection

Computational and Mathematical Methods in Medicine

This article has been retracted by Hindawi following an investigation undertaken by the publisher [1]. This investigation has uncovered evidence of one or more of the following indicators of systematic manipulation of the publication process:

(1) Discrepancies in scope

(2) Discrepancies in the description of the research reported

(3) Discrepancies between the availability of data and the research described

(4) Inappropriate citations

(5) Incoherent, meaningless and/or irrelevant content included in the article

(6) Peer-review manipulation

The presence of these indicators undermines our confidence in the integrity of the article's content and we cannot, therefore, vouch for its reliability. Please note that this notice is intended solely to alert readers that the content of this article is unreliable. We have not investigated whether authors were aware of or involved in the systematic manipulation of the publication process.

Wiley and Hindawi regrets that the usual quality checks did not identify these issues before publication and have since put additional measures in place to safeguard research integrity.

We wish to credit our own Research Integrity and Research Publishing teams and anonymous and named external researchers and research integrity experts for contributing to this investigation.

The corresponding author, as the representative of all authors, has been given the opportunity to register their agreement or disagreement to this retraction. We have kept a record of any response received.

References

[1] L. Qu, Y. Yin, N. Zhao, Y. Lv, and H. Xu, "Analysis of Intervention Effect and Satisfaction of Holistic Nursing after Oral Tumor Resection," *Computational and Mathematical Methods in Medicine*, vol. 2022, Article ID 3788605, 7 pages, 2022.

Research Article

Analysis of Intervention Effect and Satisfaction of Holistic Nursing after Oral Tumor Resection

Lingling Qu [ID],[1] Yan Yin [ID],[2] Na Zhao [ID],[3] Yongmei Lv [ID],[4] and Hangyong Xu [ID][5]

[1]*Rehabilitation Department, Yantaishan Hospital, Yantai 264000, China*
[2]*Department of Infectious Diseases, Qingdao Eighth People's Hospital, Qingdao 266100, China*
[3]*Department of Otorhinolaryngology, Zhangqiu District People's Hospital, Jinan 250200, China*
[4]*Department of Pharmacy, Zhangqiu District People's Hospital, Jinan 250200, China*
[5]*Department of Oral and Maxillofacial Surgery, Zhangqiu District People's Hospital, Jinan 250200, China*

Correspondence should be addressed to Hangyong Xu; xuhangyong@zqrmhospital.cn

Objective. To explore the intervention effect and satisfaction analysis of holistic nursing after oral tumor resection. *Methods.* A total of 70 oral tumor patients who underwent surgical treatment in our hospital from April 2020 to September 2021 were randomly divided into two groups, with 35 patients in each group. The control group was given basic oral care, the observation group was given overall oral care, and the actual effects of the two groups of care were compared, including the emotional status, compliance and nursing satisfaction, hospital stay and nursing quality scores, pain level, quality of life, and complications occurred. *Results.* After nursing, the patients in the observation group had good mood, higher compliance and nursing satisfaction, shorter hospital stay, higher nursing quality and quality of life scores, lower pain level, and lower incidence of complications, when compared with the control group. *Conclusion.* Holistic nursing has obvious effects on patients after oral tumor surgery, which can relieve patients' negative emotions, improve patients' compliance with treatment, improve their quality of life, and effectively reduce the degree of pain and the occurrence of complications, which is worthy of clinical promotion.

1. Introduction

Oral tumors are the most common malignant tumors of the head and neck, with a high incidence rate, accounting for 8.0% of systemic tumors [1–3]. In clinical medicine, surgical treatment is generally used as the way of treatment, but due to the complex surgical method, long operation time, and large postoperative wound, the internal self-cleaning effect of oral cavity is reduced to a certain extent, resulting in a high probability of bacterial infection. Once infection occurs, the patient's quality of life will be reduced, the wound will not heal well, and even the peripheral organs and tissues will be involved, seriously or even directly endangering life [4–6]. In addition, the postoperative facial damage leads to the accumulation of negative emotions such as depression and anxiety, which greatly affects the wound healing and postoperative recovery of patients. Therefore, a set of targeted and time-sensitive care plans is needed to reduce the negative emotions of patients and promote disease outcomes. In this study, 70 patients who underwent radical resection of oral tumors in our hospital were selected for nursing intervention, and the effects were satisfactory.

2. Materials and Methods

2.1. Basic Information. A total of 70 oral tumor patients who underwent surgical treatment in our hospital from April 2020 to September 2021 were selected, and the patients were randomly divided into the observation group ($n = 35$) and the control group ($n = 35$). There were 21 males and 14 females, ranging in age from 31 to 67 years old, with an average age of 44.5 ± 5.5 years, and the course of disease was 2.3 to 10.5 months, with an average of 5.3 ± 2.2 months; the control group consisted of 23 males and 12 females, aged

33 years old to 65 years old, average 45.5 ± 4.7 years old, disease duration $2.2 \sim 10.9$ months, and average 5.4 ± 2.3 months. Inclusion criteria are as follows: patients were diagnosed with oral tumors according to clinical medical tests and meets surgical and oral tumor criteria [7], and the patients and their families gave informed consent to this study. Exclusion criteria are as follows: patients were diagnosed with mental illness or confusion and patients who did not cooperate with the treatment and care. There was no significant difference in the basic data of age, gender, and course of disease between the two groups, which was comparable. This study was approved by the ethics committee of Zhangqiu District People's Hospital (approval no. 2020-0632).

2.2. Nursing Methods. The patients in the control group received routine nursing guidance, including admission introduction, guided patient examination, close monitoring of the condition, basic ward nursing, and symptomatic intervention. The patients in the observation group carried out overall nursing intervention under routine guidance, including the following: ① postural care: for patients who are under general anesthesia and have not woken up after surgery, they are placed in a supine position, and their head is kept on the side; for patients with pedicled skin flaps, the head needs to be placed in the median position after surgery, and the supine immobilization is performed for 5-7 days to promote local blood circulation. ② Nutritional intervention: the next day after the operation, the patients were given nasal feeding, about 200 mL each time. It should be injected at a constant speed and nutritionally balanced. The lumen should be properly rinsed before and after the nasal feeding to reduce the occurrence of intestinal infection, the nasal feeding is changed to liquid food, and it is gradually transitioned to normal food [8]. ③ Negative pressure drainage and wound observation: doctor should closely observe the wound to determine whether there are problems such as oozing and swelling, check whether the dressing is damaged or not and whether the dressing is dry, and change the dressing once a day in the early postoperative period, and pay attention to keeping the wound clean and to observe whether the negative pressure drainage is unobstructed. Generally, the drainage volume in 24 hours should be >250 mL. If the drainage fluid is bright red and the amount is too large, it may be that the bleeding has not been completely stopped, and the doctor should be notified in time. ④ Eliminate the patient's saliva and sputum: after the operation, the patient's oral function is reduced, there is difficulty in swallowing, and the drooling is serious. One week after the operation, the patient's tongue is endangered. For example, the patient's tongue can only be extended halfway, and the contraction is difficult, and the internal oral cleaning cannot be carried out. All that needs to be done well is the propaganda work, informing the patient that saliva is beneficial for cleaning the inside of the mouth, moisturizing the throat and assisting the digestion and absorption of food materials, and swallowing the saliva in the mouth as much as possible. Adjust the pressure value and use a suction tube to suck out the saliva and sputum inside the mouth. ⑤ Clean-

ing: the doctor should clean with cotton wool moistened with silver ion mouthwash, in a gentle posture, wipe off sputum scabs and blood clots, and replace with 0.9% sodium chloride injection or silver ion mouthwash for cleaning. Patients with free tongue movement can instruct the patient to use their tongue. Massage the lingual side of the teeth in a certain direction, so that the lingual side of the teeth can be effectively cleaned, until the clear liquid is sucked out. The initial cleaning solution is generally more than 300 mL, and the other cleaning solution is preferably not more than 250 mL each time. It is cleaned twice a day, and patients with malignant tumors are cleaned three times a day. When cleaning, it should be noted that the cleaning solution directly cleans the mouth flap, and the cleaning tube should not touch the mouth flap, while rinsing and sucking, and the patient's tongue should be stirred at the same time [9]. ⑥ Strengthen the pain assessment of patients and do a good job in pain management. In this group of patients, the postoperative trauma was large, and the nerves in the oral cavity were rich and sensitive, but none of them were equipped with analgesic pumps to relieve pain. In knowledge-behavioral intervention therapy, informing patients that postoperative trauma is the main cause of pain, but negative emotions such as anxiety, depression, and irritability are powerful catalysts to increase pain and timely correct patients' bad cognition of pain, so as to avoid pain. The postoperative pain status of patients without tracheotomy was evaluated by the digital grading method. The resting pain was evaluated every 4 hours. Patients with 4 points received drug analgesia according to the doctor's advice. At the same time, patients were instructed to carry out regular breathing and muscle rhythmic exercise to eliminate patients' emotions and muscle tension, and timely and effective drug and physical analgesia methods were adopted. ⑦ Do a good job of psychological care to reduce negative emotions. Due to the special anatomy, oral tumor patients may have different degrees of facial disfigurement or deformity, functional impairment, and even death risk after surgery, which can easily lead to different degrees of mental and psychological disorders in patients after surgery, especially depression, anxiety, and fear. Other negative emotions are more prevalent and severe, and these negative emotions have a serious impact on postoperative recovery and patients' quality of life. Performing regular relaxation training after surgery, instructing the patient to relax the muscles of the whole body, and cooperating with deep breathing, instructing the patient to perform imagery imagination after completing the relaxation training, image pleasant scenes, and beautiful natural landscapes, and transferring postoperative pain such as dry mouth were done. Due to the temporary difficulty in opening the mouth and language dysfunction after the patient, our department uses a writing board to communicate with the patient in a timely manner. Communicating with patients through some simple gestures, shaking their heads, nodding, and other body language were also done.

2.3. Observation Indicators. The Hamilton Depression Scale (HAMD) and Hamilton Anxiety Scale (HAMA) were referred to evaluate the emotional status of the two groups at different
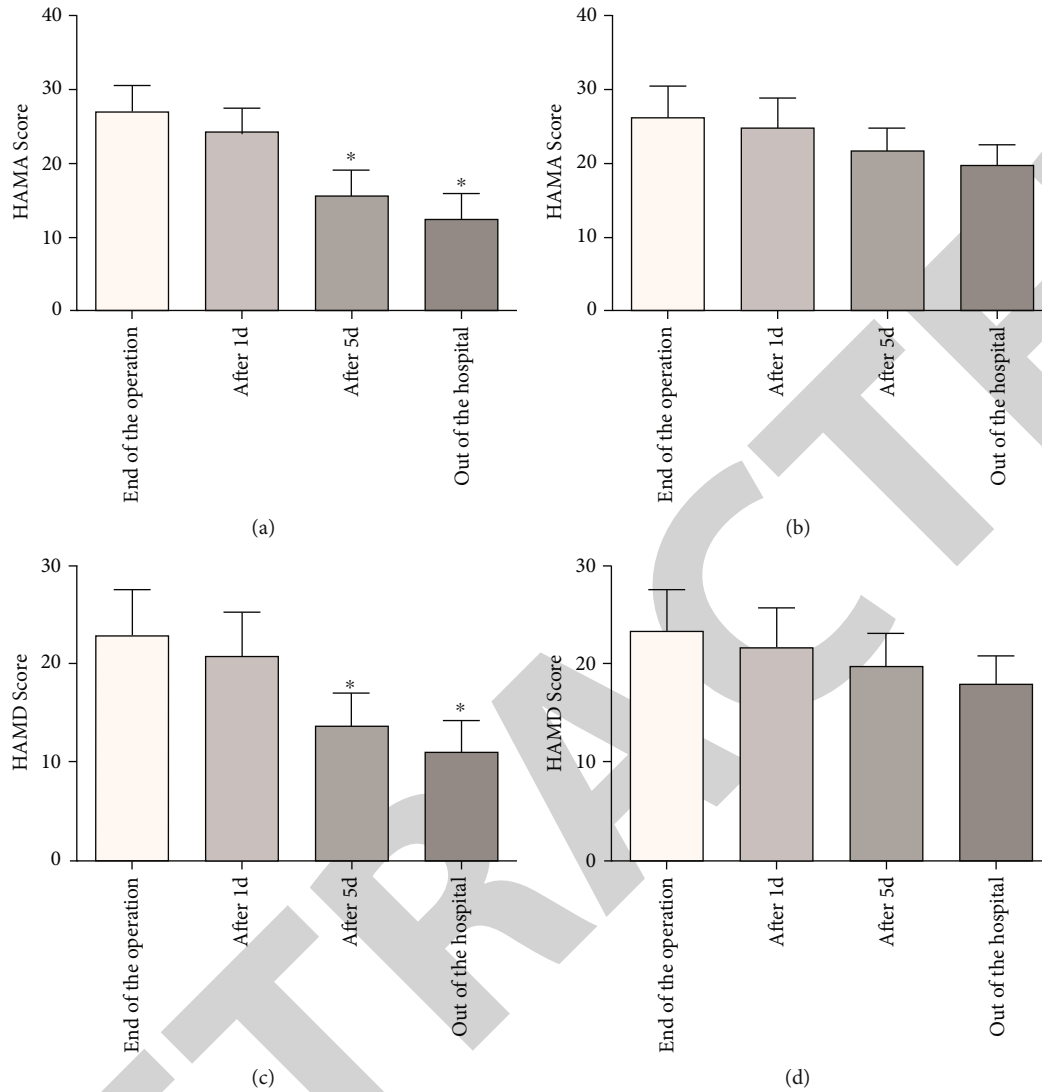
Figure 1: Emotional status of the two groups after surgery in different nursing stages. (a) The HAMA score of the observation group decreased gradually at the end of the surgery, 1 d and 5 d after the surgery, and at discharge. (b) The HAMA score of the control group at the end of the surgery, the surgery after 1 d and 5 d, it gradually decreased at discharge. (c) The HAMD score of the observation group decreased gradually at the end of the operation, 1 d and 5 d after surgery, and gradually decreased at discharge. (d) The HAMD score of the control group was decreased after surgery at the end, 1 d, and 5 d postoperatively and gradually decreased at discharge. $^*p < 0.01$, vs. end of operation.

nursing stages. The lower the score, the more significant the improvement of anxiety and depression were [10].

The self-made nursing questionnaire was used to investigate the compliance, nursing satisfaction, and nursing quality scores of the two groups.

The incidence of complications such as electrocution syndrome, bleeding, infection, and vascular crisis was counted.

The Visual Analogue Scale (VAS) for rating [11] was used to investigate the pain level of patients, with 10 points out of 10, and the lower the score, the less pain and the better the nursing effect.

The quality of life index evaluation scale [12] (Quality of Life Questionnare-Core 30 (QLQ-C30)) was used to evaluate the indicators of quality of life for patients.

2.4. Data Analysis Methods. The counting and measurement data of this study were input into the Statistical Products and Services Solutions 20.0 (Statistical Products and Services Solutions 20.0, SPSS 20.0, IBM, NY, USA) program was used for processing. Specifically, the chi-square and t-tests were completed. The output of the chi-square test results were displayed as (%), t-test results are displayed in the form of $x \pm s$, and $p < 0.05$ indicates that the data difference is statistically significant.

3. Results

3.1. Analysis of Emotional Status in Different Nursing Stages after Surgery. At the end of the operation, there was no significant difference in HAMA and HAMD scores between the

Table 1: Comparison of nursing compliance between the two groups (n (%)).

Group	n	Good	General	Poor	Overall compliance
Observation group	35	26 (74.29)	9 (25.71)	0 (0.00)	35 (100.00)
Control group	35	17 (48.57)	11 (31.43)	7 (2.00)	28 (80.00)
X^2					9.084
p					0.011

Table 2: Comparison of nursing satisfaction between the two groups (n (%)).

Group	n	Very satisfied	General	Dissatisfied	Overall satisfaction
Observation group	35	23 (65.71)	11 (31.43)	1 (2.86)	34 (97.14)
Control group	35	12 (34.29)	13 (37.14)	10 (28.57)	25 (71.43)
X^2					10.987
p					0.004

*$p < 0.01$ vs. the control group.

Table 3: Comparison of hospital stay and nursing quality score ($x \pm s$).

Group	n	Hospital stay (d)	Quality of care			
			Basic care	Safe care	Disinfection care	Ward Care
Observation group	35	8.74 ± 1.44	94.17 ± 2.81	96.09 ± 2.23	97.14 ± 1.61	95.17 ± 2.24
Control group	35	12.00 ± 2.70	79.94 ± 4.08	81.89 ± 3.46	81.09 ± 2.89	83.49 ± 3.02
t		6.294	16.99	20.41	28.68	18.37
p		< 0.001	< 0.001	< 0.001	< 0.001	< 0.001

*$p < 0.01$ vs. the control group.

1–End of the operation
2–After 1 d
3–After 5 d
4–Out of the hospital
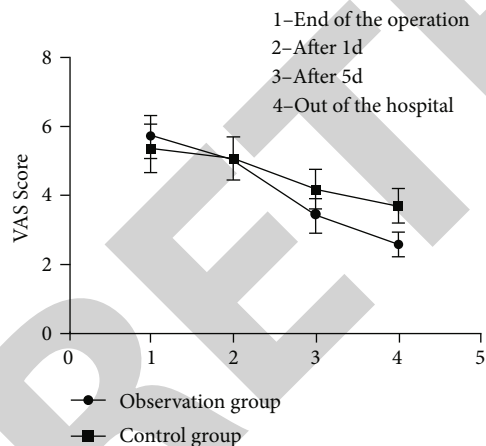
Figure 2: Comparison of pain levels between the two groups. *$p < 0.01$ vs. the control group.

two groups. 1 d, 5 d, and discharge after the operation, the HAMA and HAMD scores of the two groups were lower than those at the end of the operation, and the scores between the two groups were lower than those at the end of the operation (Figure 1).

3.2. Comparison of Patient Compliance and Nursing Satisfaction between the Two Groups. The overall compliance of the observation group was 100%, which was significantly higher than that of the control group (80%). The

nursing satisfaction of the observation group was 97.14%, which was significantly higher than that of the control group (71.43%) (Tables 1 and 2).

3.3. Comparison of Hospital Stay and Nursing Quality Scores between the Two Groups. There were statistically significant differences between the two groups in terms of hospital stay, basic nursing score, safety nursing score, disinfection nursing score, and ward nursing score (Table 3).

3.4. Comparison of Pain Levels between the Two Groups. There was no significant difference in the VAS score between the two groups at the end of the operation, and the VAS score gradually decreased with the increase of the end of the operation time (Figure 2).

3.5. Comparison of Quality of Life before and after Nursing in the Two Groups. Before nursing, there was no significant difference in the indicators of quality of life between the two groups. After nursing, the scores of physical function, role function, emotional function, cognitive function, and social function in the two groups were all increased, and the difference between the observation group and the control group was statistically significant. The scores of insomnia, fatigue, loss of appetite, diarrhea, and nausea and vomiting were obviously decreased (Table 4).

3.6. Comparison of the Incidence of Complications between the Two Groups. There were 1 case, 2 cases, 1 case, and 3 cases of electrical resection syndrome, hemorrhage,

TABLE 4: Comparison of quality of life before and after nursing ($x \pm s$).

Group	n	Nursing time	Physical function	Role function	Emotional function	Cognitive function	Social function
Observation group	35	Before nursing	51.83 ± 8.56	55.54 ± 9.86	49.51 ± 12.07	60.89 ± 6.60	58.71 ± 10.70
		After nursing	78.54 ± 10.71	87.00 ± 5.75	88.00 ± 5.29	81.09 ± 8.55	76.71 ± 10.93
Control group	35	Before nursing	54.20 ± 7.01	54.74 ± 8.59	51.49 ± 13.53	54.00 ± 7.75	59.54 ± 9.86
		After nursing	63.29 ± 11.70	74.29 ± 7.78	70.20 ± 7.01	60.54 ± 9.86	68.09 ± 8.55
$t1$			11.53	16.31	17.27	11.07	6.962
$p1$			< 0.001	< 0.001	< 0.001	< 0.001	< 0.001
$t2$			3.940	9.979	7.264	3.087	3.872
$p2$			< 0.001	< 0.001	< 0.001	0.003	< 0.001
$t3$			5.689	7.779	11.99	9.312	3.679
$p3$			< 0.001	< 0.001	< 0.001	< 0.001	0.001
Group	n	Nursing time	Insomnia	Tired	Anorexia	Diarrhea	Feel sick and vomit
Observation group	35	Before nursing	55.20 ± 12.05	53.31 ± 7.45	47.14 ± 7.75	42.69 ± 5.76	35.09 ± 10.79
		After nursing	20.57 ± 7.82	21.97 ± 6.57	17.14 ± 5.10	24.77 ± 4.70	7.49 ± 2.55
Control group	35	Before nursing	48.49 ± 7.39	52.31 ± 5.76	49.26 ± 6.34	45.00 ± 5.29	32.86 ± 10.67
		After nursing	38.00 ± 6.33	29.40 ± 7.05	31.37 ± 5.82	35.71 ± 7.78	15.43 ± 4.02
$t1$			14.27	18.67	19.12	14.25	14.73
$p1$			< 0.001	< 0.001	< 0.001	< 0.001	< 0.001
$t2$			6.378	14.89	12.29	5.893	9.044
$p2$			< 0.001	< 0.001	< 0.001	< 0.001	< 0.001
$t3$			10.25	4.562	10.88	7.125	9.879
$p3$			< 0.001	< 0.001	< 0.001	< 0.001	< 0.001

Note: $t1, p1$ represent the comparison before and after nursing in the observation group; $t2, p2$ represent the comparison before and after nursing in the control group; $t3, p3$ represent the comparison between the observation group and the control group after nursing. $^{*}p < 0.01$ vs. the control group.
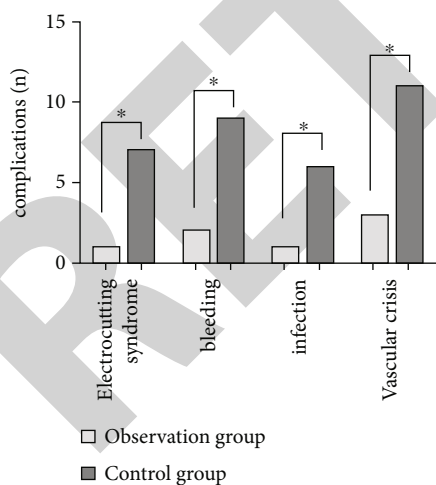
FIGURE 3: Comparison of the incidence of complications. * $p < 0.01$ vs. the control group.

infection, and vascular crisis in the observation group and 7 cases, 9 cases, 6 cases, and 11 cases of electrical resection syndrome, hemorrhage, infection and vascular crisis occurred in the control group, respectively (Figure 3).

4. Discussion

According to statistics, oral tumors account for nearly 8% of human tumors [13, 14]. Due to the poor efficacy of conservative treatment, surgical treatment is currently recommended for diagnosed oral tumors [15]. However, the anatomical structure of the oral cavity is relatively complex, and the lesion site is relatively special. Tissue defects occur under various trauma or surgical treatment conditions. The patient's resistance and oral self-cleaning ability decline. The imbalance of the proportion of the group is very prone to local infection and even the occurrence of complications due to infection, resulting in a worse prognosis [16]. This makes patients generally have a heavy psychological and spiritual burden. Effective nursing interventions are very important. Some data show that [17–19] effective nursing intervention after oral tumor surgery has a significant effect on improving prognosis and improving the quality of life of patients.

Holistic care is one of the important modes of care and an intensification of routine care [20, 21]. It can fully combine the patient's disease characteristics and physical and mental conditions and use psychological education, postural care, nutritional intervention, and other measures to provide systematic services and guidance for patients from various aspects such as psychology, behavioral cognition, diet, and

posture. It can not only ensure the actual effect of oral care but also achieve the comfort of patients, making oral care develop in a safer, more reasonable, more professional, and more personalized direction. At present, the application effect of holistic nursing in international clinical practice has been widely recognized, and its development in oral tumor patients has also been proved to have good effects such as reducing the occurrence of complications and promoting patient recovery [22–25]. This study showed that the HAMA and HAMD evaluation scores of the observation group were significantly lower than those of the control group after this model intervention. The reason is that the overall nursing care used in this study includes psychological nursing. Through the professional relaxation training of medical staff and the timely detection and processing of patients' inappropriate emotions, the patients in the observation group have better emotions than the control group, so the degree of cooperation and nursing satisfaction are higher. Our nursing plan also strengthens pain care and cleaning care for patients, so the results of this study show that the nursing quality score of the observation group is significantly higher than that of the control group, and the incidence of complications is significantly lower than that of the control group, thereby improving the overall quality of life of patients.

5. Conclusion

To sum up, the overall nursing intervention for patients after oral tumor surgery is effective, which can significantly reduce the patient's emotional burden, reduce the patient's pain level, effectively improve the quality of nursing services, reduce the risk of complications, and improve the quality of life. It can improve patients' recognition of nursing work and can be used as an excellent solution for clinical nursing, which is worthy of recommendation.

Data Availability

The datasets used and/or analyzed during the present study are available from the corresponding author on reasonable request.

Disclosure

The funding body had no role in the design of the study; collection, analysis, and interpretation of data; or writing of the manuscript.

Conflicts of Interest

The authors declare that they have no conflicts of interest.

Acknowledgments

The authors deeply appreciate the contributions to this work made in various ways by all of the participants.

References

[1] P. H. Montero and S. G. Patel, "Cancer of the oral cavity," *Surgical Oncology Clinics of North America*, vol. 24, no. 3, pp. 491–508, 2015.

[2] B. W. Neville and T. A. Day, "Oral cancer and precancerous lesions," *CA: a Cancer Journal for Clinicians*, vol. 52, no. 4, pp. 195–215, 2002.

[3] J. A. Valdez and M. T. Brennan, "Impact of oral cancer on quality of life," *Dental Clinics of North America*, vol. 62, no. 1, pp. 143–154, 2018.

[4] T. Shibahara, "Oral cancer -diagnosis and therapy-," *Clinical Calcium*, vol. 27, no. 10, pp. 1427–1433, 2017.

[5] G. Kane, V. Petrosyan, and P. Ameerally, "Oral cancer treatment through the ages: part 1," *Journal of Oral and Maxillofacial Surgery*, vol. 77, no. 7, pp. 1480–1483, 2019.

[6] D. Kim and R. Li, "Contemporary treatment of locally advanced oral cancer," *Current Treatment Options in Oncology*, vol. 20, no. 4, p. 32, 2019.

[7] T. Wong and D. Wiesenfeld, "Oral cancer," *Australian Dental Journal*, vol. 63, Suppl 1, pp. S91–S99, 2018.

[8] C. S. Farah and M. J. McCullough, "Oral cancer awareness for the general practitioner: new approaches to patient care," *Australian Dental Journal*, vol. 53, no. 1, pp. 2–10, 2008.

[9] D. V. Messadi, "Oral cancer: novel concepts for the oral health care practitioner," *Journal of the California Dental Association*, vol. 44, no. 2, pp. 82–84, 2016.

[10] Y. Duan, J. Wei, W. Geng et al., "Research on cognitive function in anxious depression patients in China," *Journal of Affective Disorders*, vol. 280, no. Part A, pp. 121–126, 2021.

[11] Y. T. Sung and J. S. Wu, "The visual analogue scale for rating, ranking and paired-comparison (VAS-RRP): a new technique for psychological measurement," *Behavior Research Methods*, vol. 50, no. 4, pp. 1694–1715, 2018.

[12] O. Husson, B. H. de Rooij, J. Kieffer et al., "The EORTC QLQ-C30 summary score as prognostic factor for survival of patients with cancer in the "real-world": results from the population-based PROFILES registry," *The Oncologist*, vol. 25, no. 4, pp. e722–e732, 2020.

[13] I. Chattopadhyay, M. Verma, and M. Panda, "Role of oral microbiome signatures in diagnosis and prognosis of oral cancer," *Technology in Cancer Research & Treatment*, vol. 18, no. 18, p. 153303381986735, 2019.

[14] A. Paré and A. Joly, "Oral cancer: risk factors and management," *Presse Médicale*, vol. 46, no. 3, pp. 320–330, 2017.

[15] K. Omura, "Current status of oral cancer treatment strategies: surgical treatments for oral squamous cell carcinoma," *International Journal of Clinical Oncology*, vol. 19, no. 3, pp. 423–430, 2014.

[16] A. Pace-Balzan and S. N. Rogers, "Dental rehabilitation after surgery for oral cancer," *Current Opinion in Otolaryngology & Head and Neck Surgery*, vol. 20, no. 2, pp. 109–113, 2012.

[17] M. L. Galante, D. P. D. Silva, M. Gabriel et al., "Brazilian oral health teams in primary care and oral cancer: results of a national evaluation," *Brazilian Oral Research*, vol. 35, no. 35, article e116, 2021.

[18] P. Varela-Centelles, J. Seoane, J. L. Lopez-Cedrun et al., "The length of patient and primary care time interval in the pathways to treatment in symptomatic oral cancer. A quantitative systematic review," *Clinical Otolaryngology*, vol. 43, no. 1, pp. 164–171, 2018.

Research Article

The Clinical Application of Combined Ultrasound, Mammography, and Tumor Markers in Screening Breast Cancer among High-Risk Women

Lin Sun [ID],[1] **Min Qi** [ID],[2] **Xiaomei Cui** [ID],[3] **and Qinghua Song** [ID][4]

[1]*Department of Clinical Laboratory, Yantaishan Hospital, Yantai 264000, China*
[2]*Department of Clinical Laboratory, The Second Affiliated Hospital of Shandong University of Traditional Chinese Medicine, Jinan 250001, China*
[3]*Department of Obstetrics, Affiliated Qingdao Central Hospital, Qingdao University, Qingdao 266042, China*
[4]*Department of Medical Imaging, Qingdao Women and Children's Hospital, Qingdao 266034, China*

Correspondence should be addressed to Qinghua Song; songqinghua@qdfuer.com.cn

In order to explore the clinical application value of color Doppler ultrasound (CDUS), mammography (MAM), and serum tumor marker carbohydrate antigen 153 (CA153) in screening breast cancer (BC) for high-risk women, a total of 38,241 women were surveyed by epidemiological questionnaire on BC high-risk factors. A total of 10,821 cases were screened, accounting for 28.30%. They were randomly divided into US, MAM, and CA153 and combined examination group which has no significant difference in high-risk factors. Breast cancer in high-risk population was screened by CDUS, MAM, and CA153 and combined examination. CA153 was detected by electroluminescence method. The positive detection rate of BC was 360.41/100,000 (39/10,821). The overall difference in the positive detection rate of BC among 10,821 cases in all age groups was statistically significant. The sensitivity and negative predictive value of combined examination were significantly improved compared with each single examination. Combined examination for BC screening can significantly improve the sensitivity of BC early diagnosis and reduce the missed diagnosis rate.

1. Introduction

With the change of people's lifestyle, living environment, and the increase of living pressure, malignant tumor has become one of the most important diseases endangering the health of Chinese residents. Among them, BC is a common malignant tumor in women. In recent years, its incidence rate is increasing, and the age of onset has gradually become younger, which seriously threatens women's health [1]. The onset of BC is insidious without nonspecific symptoms at early stage, and most of them lost the best opportunity for treatment when they were found in the middle and late stage [2, 3]. The prognosis of BC is closely related to its early detection. Early detection, early diagnosis, and early treatment are not only related to the individual survival effect of BC patients but also become a major issue affecting

the national economy and people's livelihood [4]. Therefore, it is particularly important to carry out screening of BC high-risk groups.

At present, the CDUS has become the first choice for the female BC screening which can reveal the internal structure and blood flow of breast masses and observe the morphology, boundary, and internal echo of the lesion and has a strong ability to distinguish solid and cystic masses, but small lesions and calcified lesions easily missed diagnosis and misdiagnose [5, 6]. MAM can image the entire breast with a strong sense of integrity and not easy to miss diagnosis, but with a low resolution for tissue density and inability to clearly show the lesions for dense breast lesions, resulting in low sensitivity and specificity for diagnosis [7, 8]. Thus, there are certain limitations in their application alone. In this study, three methods including CDUS, AMA, and

(a)   (b)
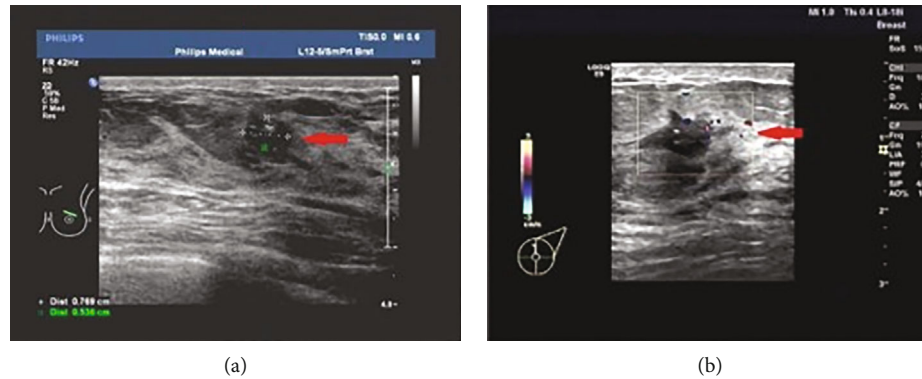
Figure 1: CDUS images of BC. (a) Two-dimensional US images. The arrow showed a two-dimensional US image showing a single nodule in the left breast, about 0.77×0.54 cm in size, with irregular shapes, fuzzy nodule edges, visible burrs, uneven internal echo, low echo, and spotting echo. (b) Color Doppler flow image. Arrows indicated abundant blood flow signals around the nodule. Color Doppler diagnosis was B1-RADS 5.

tumor markers were selected to screen BC in high-risk women. Compare the difference between the value of the combined examination and each single examination to provide a basis for better screening of BC in high-risk groups.

2. Research Objects and Methods

2.1. Research Objects. From January 2016 to December 2018, a total of 38,241 women aged 30-70 from 31 communities in our city were selected for screening BC at high risk. CDUS, MAM, and serum tumor marker CA153 single and combined examination methods were used for BC screening.

2.2. High-Risk Population Screening. Community health service centers publicize the significance and importance of carrying out BC screening to residents through free community diagnosis in communities, distributing of brochures, and household publicity. A questionnaire survey was conducted among female residents aged 30-70 years old who voluntarily participated and sign the informed consent form. Based on the "Harvard Cancer Risk Index" [9], a comprehensive assessment system of individual cancer risk suitable for Chinese population was developed through multidisciplinary expert group discussion and consensus. The respondents completed the "Breast Cancer Risk Assessment Questionnaire" by themselves under the guidance or after being questioned by professionally trained investigators. The basic information of the questionnaire included menarche age, menopause age, delivery history, lactation history, family history of BC, history of benign and malignant breast diseases, dietary habits, changes in postmenopausal weight, and history of long-term use of exogenous estrogen. Each factor has a risk score, and the sum scores of all risk factors constitute the risk score. The risk assessment is performed by collecting the filled data information. Risk scores above 30 were considered high-risk groups and participated in this study.

2.3. CDUS Examination and the Criteria. The diagnostic instrument is PHILIPS iU22, and the frequency of the probe is 5-12 MHz. During the inspection, the examinee was asked to take a supine position, raise arms, and place hands behind the head to fully expose the bilateral breasts, supraclavicular

fossa, and bilateral axillary areas. Each quadrant of the breast, the supraclavicular fossa, and bilateral axillary regions were scanned. Firstly, the lesion location, morphology, mass size, borders, whether the internal echo is uniform, whether there is attenuation of posterior echo, calcification, and association with surrounding tissues, whether lymph nodes metastasize in axillary and clavicle, and other acoustic images were observed, and then, the shape and distribution of blood flow signals inside and around the lesion were observed, and hemodynamic parameters was also measured [10].

Two-dimensional US images revealed obvious masses which were irregular in shape, blurred in boundary, lobulated, burr-shaped, uneven internal echo and attenuation of the rear echo, and calcification (Figure 1(a)). CDUS showed more abundant blood flow in and around the mass (Figure 1(b)).

2.4. Mammography Examination and the Criteria. MAM was performed by a diagnostic instrument GE Senographe 2000D digital MAM machine. In general, internal and external oblique (MLO) and axial (CC) positions were used for photography, and magnification photography or compression photography with small compressors was used for small lesions. The X-ray differential diagnosis of benign and malignant breast diseases is mainly performed from the density, morphology, and indirect signs of the mass. The diagnostic criteria refer to the BI-RADS classification standard (Breast Imaging Reporting and Data System of the American College of Radiology) [11].

MAM examination showed the presence of masses or nodules with irregular, blurred borders, lobular and burr-like changes, micro, granular, or cast calcifications, localized dense infiltration, or skin changes (Figure 2).

2.5. Detection of Serum Tumor Marker CA153. Serum tumor marker CA153 was detected by ELecsys-2010 (Roche, Suisse) using electroluminescence method. All operations were carried out strictly according to the operating instructions, and the quality control met the requirements. The normal reference values of tumor markers is CAl53 ≤ 25.00 U/ml. Serum CA153 > 25.00 U/ml was diagnosed as positive.

(a)

(b)
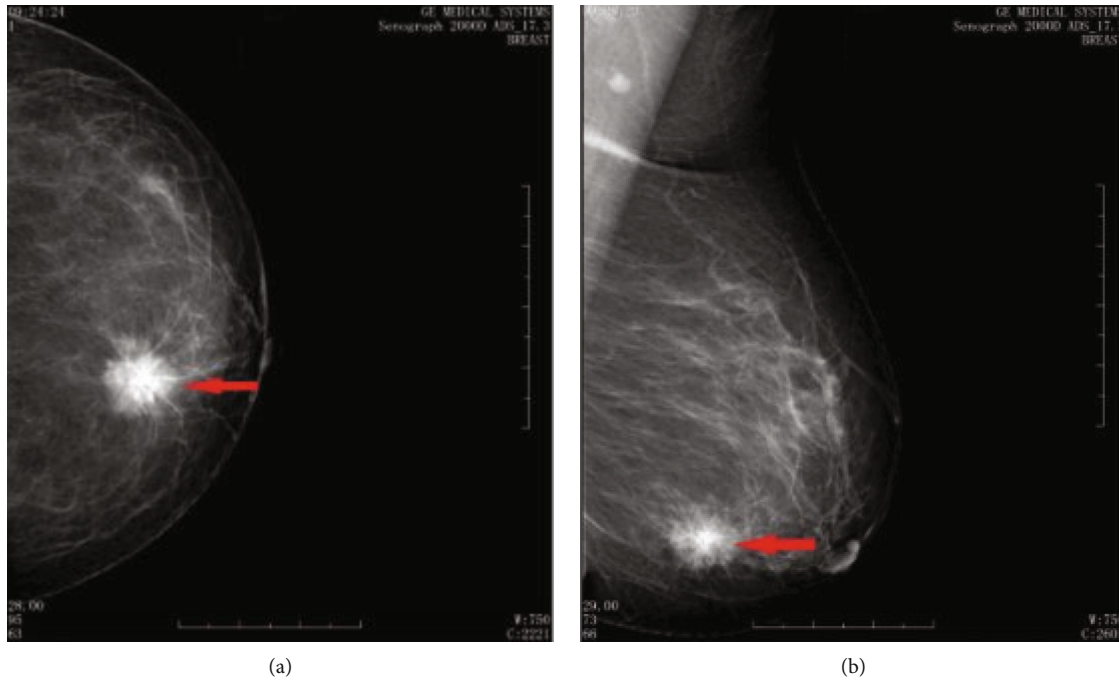
FIGURE 2: MAM image of BC. (a) Axle position (CC). (b) Internal and external oblique position (MLO). The arrow showed a nodule lower-inner of the left breast with a size of about 2.2×2.1 cm, unclear edge, lobular sign, and elongated burr-like changes. MAM diagnosis was B1-RADS 5.

2.6. The Criteria for Combined Examination. In the combined examination, one or more of the positives were judged as positive, and all were negative to judge to be negative.

2.7. Statistical Analysis. The data were processed by SPSS 25.0 statistical software. Data were expressed as mean ± standard deviation($^-x \pm$ sd). The comparison of means between groups was performed by analysis of variance, and the comparison of count data was performed by the χ^2 test. $P < 0.05$ was statistically significant.

3. Results

3.1. Screening Results for High-Risk BC Populations. A questionnaire survey of BC risk factors and assessment of high-risk groups were conducted on 38,241 women. A total of 10,821 eligible people were screened, accounting for 28.30% (10,821/38,241) with an average age of 52.34 ± 10.21 years. They were randomly divided into US group (2705 cases), MAM group (2707 cases), CA153 group (2703 cases), and combined examination group (2706 cases). There was no statistically significant difference in BC risk factors and comprehensive risk scores among the four groups (Table 1), and they were comparable.

3.2. Comparison of Positive Detection Rates of BC in High-Risk Groups of All Age. With pathological examination as the gold standard, 39 cases of BC were confirmed by pathology in 10,821 cases with the high-risk group. The positive detection rates of the groups aged 30-39, 40-49, and 50-70 were 152.13/100,000 (3/1972), 539.08/100,000 (24/4452), and 272.91/100,000 (12/4397), respectively (Table 2). The overall

difference in the positive detection rate of BC among 10,821 cases in the high-risk group in all age was statistically significant ($\chi^2 = 7.277$, $P = 0.026$) (Table 2). There was a significant difference in the positive detection rate of BC between 40-49 and 30-39 years old ($\chi^2 = 4.889$, $P = 0.027$) and between 40-49 and 50-70 years old ($\chi^2 = 3.868$, $P = 0.049$), but there was no significant difference between the ages of 30-39 and 50-70 years ($\chi^2 = 0.845$, $P = 0.358$) (Table 2).

3.3. Comparison of the Value of CDUS, MAM, and CA153 and Combined Examination in Screening BC among High-Risk Population. A total of 426 of the 10,821 cases were confirmed by pathology, including 39 cases of BC and 387 cases of benign lesions. The results of CDUS, MAM, and CA153 and combined examination were determined to be true positive or true negative if they were consistent with pathological diagnosis, otherwise as false positive or false negative. Compared with each single examination, the sensitivity and negative predictive value of the combined examination were significantly improved (Table 3).

4. Discussion

The pathogenesis of BC is not completely clear. It is currently believed that the occurrence of BC is associated with menarche history, menopause history, long-term use of exogenous estrogen history, menstrual marriage history, BC family history, etc. [12, 13]. Aiming at the high-risk factors of BC, screening high-risk BC populations has great significance for the early diagnosis and early clinical intervention of BC. BC screening includes self-examination, clinician physical examination, imaging examination, and

TABLE 1: Comparison of the distribution of high-risk factors among four groups of high-risk BC populations.

Factors	US group ($n = 2705$)	MAM group ($n = 2707$)	CA153 group ($n = 2703$)	Combined detection group ($n = 2706$)	χ^2/F	P
Age (years)						
30-39	485	502	495	490		
40-49	1149	1096	1112	1095	3.285	0.772
50-70	1071	1109	1096	1121		
Menarche age (years)					3.984	0.263
<12	336	295	317	298		
≥12	2369	2412	2386	2408		
Menopausal status					1.691	0.639
Premenopausal	2060	2094	2069	2056		
Postmenopausal	645	613	634	650		
Family history of BC					0.792	0.851
Yes	180	165	175	170		
No	2525	2542	2528	2536		
Breast disease history					1.538	0.674
Yes	157	137	145	150		
No	2548	2570	2558	2556		
Long-term use of exogenous estrogens					2.962	0.397
Yes	39	50	41	35		
No	2666	2657	2662	2671		
Delivery history					2.002	0.572
Yes	2545	2562	2561	2568		
No	160	145	142	138		
Obesity					1.210	0.751
Yes	262	252	240	257		
No	2443	2455	2463	2449		
Risk score ($\bar{x} \pm s$)	39.23 ± 6.59	37.67 ± 7.12	38.56 ± 6.57	39.12 ± 7.01	0.882	0.769

TABLE 2: Comparison of positive detection rates of BC in high-risk groups of all age.

Group	Pathology		χ^2	P
	Positive (n)	Negative (n)		
30-39 years ($n = 1972$)	3	1969	4.889	0.027
40-49 years ($n = 4452$)	24	4428	3.868	0.049
50-70 years ($n = 4397$)	12	4385	0.845	0.358
χ^2	7.277			
P	0.026			

serum tumor marker examination. Imaging examinations mainly include breast CDUS, MAM, and magnetic resonance imaging (MRI). Imaging examination has been proved to be effective in improving the early diagnosis of BC [14]. MRI is not suitable for BC screening because of its complicated operation and high cost; thus, US and MAM are more suitable for BC screening [15]. In addition, serum tumor marker detection which is an in vitro diagnostic test with the advantages of noninvasive, nonrisk, simple operation, and low cost is often used for BC screening.

The advantages of CDUS are noninvasive, nonrisk, convenient, and free of radiation. It can be suitable for any age, whether pregnant, lactating women, or the elderly, and can be repeated. The patient has good compliance. It has been widely used in clinical BC screening. US can scan the lesion from multiple angles and directions to clearly show the characteristics of the lesion, including position, size, shape, boundary, internal echo, and calcification, and clearly display surrounding tissue of the lesion area to judge the invasion of the surrounding tissue [16]. At the same time, according to the characteristics of tumor angiogenesis and blood flow around the lesion, the direction, velocity, and state of blood flow can be analyzed to clearly reflect the information of bleeding flow dynamics and further identify benign or malignant breast mass [17]. US can effectively distinguish cystic lesions from solid lesions [18] and has a strong diagnostic ability for invasive ductal carcinoma, especially for dense breast lesions [19]. The disadvantage of US is that the diagnostic level of the US physician has a large artificial influence on the diagnosis result, it is difficult to find some microcalcification foci and small lesions with unclear echo, and the missed detection rate of ductal carcinoma in situ is high [20, 21].

TABLE 3: Comparison of the value of CDUS, MAM, and CA153 and combined examination in screening BC among high-risk population (%).

Detection indicator	Sensitivity	Specificity	Accuracy	Positive predictive value	Negative predictive value
US	70.00	91.51	88.10	60.86	94.17
MAM	66.67	90.63	86.84	57.14	93.55
CA153	44.44	89.61	81.05	50.00	87.34
Combined examination	90.91[a]	91.67	91.53	68.97	98.02[a]
χ^2	10.106	0.288	5.548	1.710	8.537
P	0.018	0.962	0.136	0.635	0.036

[a]Compared with each single examination, $P < 0.05$.

MAM is also one of the main methods of BC screening. The advantage is that the entire breast can be imaged, the overall sense is strong, and it is not easy to miss the diagnosis. Smaller lesions, calcification of the lesions (especially microcalcifications), and glitches are clearly shown. It has extremely high clinical diagnostic value for ductal carcinoma in situ which is easy to be missed by US, effectively reducing never diagnosis and misdiagnosis. In addition, the MAM examination can transmit the image data in digital form to meet the needs of remote consultation. It is an irreplaceable examination method for BC screening, especially for the diagnosis of tumors with malignant calcification. The disadvantages are that the resolution of tissue density is low and the lesions of dense breast lesions cannot be clearly displayed [7, 8]. Moreover, it is insufficient for the identification of cystic mass and solid mass and the diagnosis of invasive ductal carcinoma. In addition, this test has a large radiation dose and is not suitable for pregnant women, lactating women, and repeated inspections.

Tumor markers are a class of substances secreted by tumor cells or produced by the interaction between tumor and host during the carcinogenesis of tissue cells, including some glycoproteins, hormones, enzymes, and other substances, which can be detected in tissues or peripheral body fluids [22]. Serum tumor markers have gradually become an important means of BC screening, and detecting the level of relevant tumor markers is conducive to the early screening of BC [23]. CA153 is a kind of high molecular weight glycoprotein, which exists in the cell membrane of breast tissue [22]. The cytoskeleton is destroyed when cells become cancerous, resulting in the cell surface antigens falling off and being released into the blood and the increased content of CA153 levels in peripheral blood [24]. CA153, as a classic tumor marker for the diagnosis of BC, has become a routine examination item for women's health examination. However, the sensitivity and specificity of serum CA153 alone as a screening program for BC high-risk population are obviously insufficient.

If BC screening is performed for all females of appropriate age, both the cost and workload are huge and impractical. Therefore, it is necessary to screen out the high-risk population for BC screening on the basis of the high-risk factors of BC. In this study, 38,241 aged 30-70 women were screened for BC risk factors, and a total of 10,821 cases were screened. CDUS, MAM, and serum CA153 were used for single or combined examinations. With pathological diagnosis as the gold standard, a total of 39 cases of BC were screened out, including 15 cases of early stage (stage 0 and stage I), which could be completely cured by early surgery, so the screening effect was significant. Each single examination has its own advantages and disadvantages. The positive detection rate and negative predictive value of the combined examination were significantly higher than those of single examination.

US examination has better resolution of soft tissues, while MAM has a low resolution of tissue density, especially the inability to clearly show dense breast lesions which can easily cause missed diagnosis [25]. Younger women have higher breast tissue density, and US is better than MAM examination, while older people have the opposite [26, 27]. At the same time, the detection of MAM for lesion calcification and carcinoma in situ is better than US, while US has a high detection rate for invasive ductal carcinoma, suggesting that the combined examination of the two is obviously complementary [28]. In addition, the tumor marker CA153 shows an increasing trend in peripheral blood when some BC imaging manifestations are not typical. Therefore, it is a good supplementary experiment for imaging examinations, although this study showed that serum CA153 is not sensitive for screening BC in high-risk populations (44.44%), which is related to early screening. CA153 has not been released into the blood to cause false negatives in early BC. Thus, CA153 is still an essential screening item for BC screening. This study also showed that women aged 40-49 has a high incidence of BC, suggesting that regular medical examinations should be performed to achieve early detection and early treatment.

5. Conclusion

With the increasing incidence of BC, it is necessary to explore its screening model. By screening high-risk groups, early BC can be detected, which can significantly improve the clinical cure rate. US, MAM, and CA153 are commonly used screening methods, but the value of a single examination is limited. The combined test can complement and confirm each other, thereby reducing misdiagnosis and maximizing the positive detection rate of BC screening.

Data Availability

The datasets used and/or analyzed during the present study are available from the corresponding author on reasonable request.

Conflicts of Interest

The authors have no conflicts of interest to declare.

References

[1] K. M. Kelly, J. Dean, W. S. Comulada, and S.-J. Lee, "Breast cancer detection using automated whole breast ultrasound and mammography in radiographically dense breasts," *European Radiology*, vol. 20, no. 3, pp. 734–742, 2010.

[2] Z. Anastasiadi, G. D. Lianos, E. Ignatiadou, H. V. Harissis, and M. Mitsis, "Breast cancer in young women: an overview," *Updates in Surgery*, vol. 69, no. 3, pp. 313–317, 2017.

[3] C. E. DeSantis, J. Ma, A. Goding Sauer, L. A. Newman, and A. Jemal, "Breast cancer statistics, 2017, racial disparity in mortality by state," *CA: a Cancer Journal for Clinicians*, vol. 67, no. 6, pp. 439–448, 2017.

[4] C. Printz, "Breast cancer mortality rates decline internationally, with some major exceptions," *Cancer*, vol. 123, no. 7, p. 1085, 2017.

[5] P. A. Ganz and P. J. Goodwin, "Breast cancer survivorship: where are we today?," in *In Improving Outcomes for Breast Cancer Survivors*, pp. 1–8, Springer, Cham, 2015.

[6] J. H. Yoon, M. J. Kim, H. S. Lee et al., "Validation of the fifth edition BI-RADS ultrasound lexicon with comparison of fourth and fifth edition diagnostic performance using video clips," *Ultrasonography*, vol. 35, no. 4, pp. 318–326, 2016.

[7] C. M. Checka, J. E. Chun, F. R. Schnabel, J. Lee, and H. Toth, "The relationship of mammographic density and age: implications for breast cancer screening," *American Journal of Roentgenology*, vol. 198, no. 3, pp. W292–W295, 2012.

[8] M. Zulfiqar, I. Rohazly, and M. Rahmah, "Do the majority of Malaysian women have dense breasts on mammogram?," *Biomedical Imaging and Intervention Journal*, vol. 7, 2011.

[9] G. A. Colditz, K. Atwood, K. Emmons et al., "Harvard report on cancer prevention volume 4: Harvard Cancer Risk Index," *Cancer Causes & Control*, vol. 11, no. 6, pp. 477–488, 2000.

[10] S. H. Lee, J. Chung, H. Y. Choi et al., "Evaluation of screening US–detected breast masses by combined use of elastography and color Doppler US with B-mode US in women with dense breasts: a multicenter prospective study," *Radiology*, vol. 285, no. 2, pp. 660–669, 2017.

[11] D. Vanel, "The American College of Radiology (ACR) breast imaging and reporting data system (BI-RADS™): a step towards a universal radiological language?," *European Journal of Radiology*, vol. 61, no. 2, p. 183, 2007.

[12] R. Jagsi, S. T. Hawley, P. Abrahamse et al., "Impact of adjuvant chemotherapy on long-term employment of survivors of early-stage breast cancer," *Cancer*, vol. 120, no. 12, pp. 1854–1862, 2014.

[13] L. Chen, Y. Chen, X.-H. Diao et al., "Comparative study of automated breast 3-D ultrasound and handheld B-mode ultrasound for differentiation of benign and malignant breast masses," *Ultrasound in Medicine & Biology*, vol. 39, no. 10, pp. 1735–1742, 2013.

[14] L. L. Humphrey, M. Helfand, B. K. Chan, and S. H. Woolf, "Breast cancer screening: a summary of the evidence for the U.S. preventive services task force," *Annals of Internal Medicine*, vol. 137, no. 5_Part_1, pp. 347–360, 2002.

[15] H.-B. Pan, K.-F. Wong, T.-L. Yang et al., "The outcome of a quality-controlled mammography screening program: experience from a population-based study in Taiwan," *Journal of the Chinese Medical Association*, vol. 77, no. 10, pp. 531–534, 2014.

[16] R. M. Sigrist, J. Liau, A. El Kaffas, M. C. Chammas, and J. K. Willmann, "Ultrasound elastography: review of techniques and clinical applications," *Theranostics*, vol. 7, no. 5, pp. 1303–1329, 2017.

[17] B. L. Sprague, N. K. Stout, C. Schechter et al., "Benefits, harms, and cost-effectiveness of supplemental ultrasonography screening for women with dense breasts," *Annals of Internal Medicine*, vol. 162, no. 3, pp. 157–166, 2015.

[18] E. Y. Chae, W. K. Moon, H. H. Kim et al., "Association between ultrasound features and the 21-gene recurrence score assays in patients with oestrogen receptor-positive, HER2-negative, invasive breast cancer," *PLoS One*, vol. 11, no. 6, p. e0158461, 2016.

[19] M. Štěrba, O. Popelová, J. Lenčo et al., "Proteomic insights into chronic anthracycline cardiotoxicity," *Journal of Molecular and Cellular Cardiology*, vol. 50, no. 5, pp. 849–862, 2011.

[20] M. S. Bae, M. Seo, K. G. Kim, I.-A. Park, and W. K. Moon, "Quantitative MRI morphology of invasive breast cancer: correlation with immunohistochemical biomarkers and subtypes," *Acta Radiologica*, vol. 56, no. 3, pp. 269–275, 2015.

[21] Y. Ma, G. Li, J. Li, and W.-d. Ren, "The diagnostic value of superb microvascular imaging (SMI) in detecting blood flow signals of breast lesions: a preliminary study comparing SMI to color Doppler flow imaging," *Medicine*, vol. 94, no. 36, p. e1502, 2015.

[22] J. W. Choi, B. I. Moon, J. W. Lee, H. J. Kim, Y. Jin, and H. J. Kim, "Use of CA15-3 for screening breast cancer: an antibody-lectin sandwich assay for detecting glycosylation of CA15-3 in sera," *Oncology Reports*, vol. 40, no. 1, pp. 145–154, 2018.

[23] L. Harris, H. Fritsche, R. Mennel et al., "American Society of Clinical Oncology 2007 update of recommendations for the use of tumor markers in breast cancer," *Journal of Clinical Oncology*, vol. 25, no. 33, pp. 5287–5312, 2007.

[24] S. Tang, L. Wei, Y. Sun et al., "CA153 in breast secretions as a potential molecular marker for diagnosing breast cancer: a meta analysis," *PLoS One*, vol. 11, no. 9, p. e0163030, 2016.

[25] M. E. Akbari, H. Haghighatkhah, M. Shafiee, A. Akbari, M. Bahmanpoor, and M. Khayamzadeh, "Mammography and ultrasonography reports compared with tissue diagnosis-an evidence based study in Iran, 2010," *Asian Pacific Journal of Cancer Prevention*, vol. 13, no. 5, pp. 1907–1910, 2012.

[26] F.-L. Wang, F. Chen, H. Yin et al., "Effects of age, breast density and volume on breast cancer diagnosis: a retrospective comparison of sensitivity of mammography and ultrasonography in China's rural areas," *Asian Pacific Journal of Cancer Prevention*, vol. 14, no. 4, pp. 2277–2282, 2013.

[27] S. Shen, Y. Zhou, Y. Xu et al., "A multi-centre randomised trial comparing ultrasound vs mammography for screening breast cancer in high-risk Chinese women," *British Journal of Cancer*, vol. 112, no. 6, pp. 998–1004, 2015.

[28] J. Weigert and S. Steenbergen, "The Connecticut experiments second year: ultrasound in the screening of women with dense breasts," *The Breast Journal*, vol. 21, no. 2, pp. 175–180, 2015.

Retraction

Retracted: Effects of Chinese Herbal Formula on Immune Function and Nutritional Status of Breast Cancer Patients

Computational and Mathematical Methods in Medicine

This article has been retracted by Hindawi following an investigation undertaken by the publisher [1]. This investigation has uncovered evidence of one or more of the following indicators of systematic manipulation of the publication process:

(1) Discrepancies in scope

(2) Discrepancies in the description of the research reported

(3) Discrepancies between the availability of data and the research described

(4) Inappropriate citations

(5) Incoherent, meaningless and/or irrelevant content included in the article

(6) Peer-review manipulation

The presence of these indicators undermines our confidence in the integrity of the article's content and we cannot, therefore, vouch for its reliability. Please note that this notice is intended solely to alert readers that the content of this article is unreliable. We have not investigated whether authors were aware of or involved in the systematic manipulation of the publication process.

Wiley and Hindawi regrets that the usual quality checks did not identify these issues before publication and have since put additional measures in place to safeguard research integrity.

We wish to credit our own Research Integrity and Research Publishing teams and anonymous and named external researchers and research integrity experts for contributing to this investigation.

The corresponding author, as the representative of all authors, has been given the opportunity to register their agreement or disagreement to this retraction. We have kept a record of any response received.

References

[1] M. Liu, "Effects of Chinese Herbal Formula on Immune Function and Nutritional Status of Breast Cancer Patients," *Computational and Mathematical Methods in Medicine*, vol. 2022, Article ID 5900024, 6 pages, 2022.

Research Article
Effects of Chinese Herbal Formula on Immune Function and Nutritional Status of Breast Cancer Patients

Min Liu [ORCID]

Department of Clinical Nutrition, Affiliated Hospital of Shandong University of TCM, Jinan 250011, China

Correspondence should be addressed to Min Liu; liumin@sdzydfy.org.cn

Background. Chinese herbal formulas have certain effects on patients with breast cancer (BC). This article discussed the effect of Buqi Yangxue decoction on the immune function and nutritional status of BC patients and provided an evidence for traditional Chinese medicine (TCM) to improve the quality of life and curative effect of BC patients. *Methods*. 66 cases of BC patients were divided into control group (n=33) and Chinese herbal formula group (n=33). The control group was received with TE chemotherapy, and the Chinese herbal formula group was received with Buqi Yangxue decoction combined with TE chemotherapy. Nutritional status, immune function, TCM symptom quantitative score, and adverse reactions were compared between the two groups. *Results*. There was no difference in all indexes between the two groups before intervention. After 4 weeks, the nutritional indexes ALB, PA, TRF, and TP in Chinese herbal formula group were higher than those in control group, except HGb. CD3+, CD4+, and CD4+/CD8+ in both groups were sharply higher than before treatment, while CD8+ was dramatically lower, and the changes in Chinese herbal formula group were more obvious than those in control group. In Chinese herbal formula group, the levels of IgG, IgA, and IgM were sharply increased compared with control group. The TCM syndrome scores in both groups were decreased significantly after treatment, especially in Chinese herbal formula group. In addition, nausea and vomiting, inappetence, liver function impairment, leukopenia, and thrombocytopenia occurred in both groups. There was no clear difference in the incidence of adverse reactions between Chinese herbal formula group and control group. *Conclusion*. Buqi Yangxue decoction can effectively improve the nutritional status and immune function of BC patients, which has important clinical significance for the later comprehensive treatment.

1. Introduction

Breast cancer (BC) is one of the most common malignant tumors that seriously endangers women's health and life. In recent years, with environmental pollution, the change of people's lifestyle, and the increase of competitive pressure, the incidence of BC is increasing year by year [1, 2]. The incidence of BC in western developed countries accounts for the first place of female malignant tumors [3]. The incidence of BC has increased significantly in China, and the onset age is gradually becoming younger [4]. BC has surpassed cervical cancer and become the most common malignant tumor in urban women. Sadly, BC is becoming younger and younger, which seriously endangers the physical, mental health, and life safety of young women.

The main treatment for BC is surgical resection and postoperative chemotherapy [5, 6]. The depression, damage of qi and blood, hematocele, and fluid accumulation of postoperative BC patients affect the wound healing and body repair [7]. BC patients' weak constitution, combined with the toxic damage of surgical chemoradiotherapy drugs, makes their vital qi more weak. The immune function of patients with BC is generally low [8]. Immune system plays a very important role in reducing postoperative complications and preventing and limiting the occurrence and development of tumors [9]. The postoperative immune function of patients with BC is low, which will increase the risk of infection and tumor recurrence. Therefore, it is very important to restore the patient's immune function as soon as possible. However, due to the damage to the human immune system after treatment, as well as the depression of patients,

it will inevitably lead to insufficient nutritional intake of patients. Persistent nutritional deficiencies can further affect recovery and treatment [10].

In the comprehensive treatment of BC, Chinese herbal formulas play a positive role in increasing curative effect, enhancing physical fitness, improving life quality, and alleviating side effects [11, 12]. Surgery and chemotherapy are the methods of removing evil, which are easy to harm the patient's vital qi, resulting in more deficiency of the patient's vital qi. Malignant tumors belong to qi and blood deficiency syndrome, and massive blood loss caused by surgery will lead to aggravation of qi and blood deficiency [13]. Therefore, BC patients should be treated with Chinese herbal formula during the treatment to achieve the effect of nourishing and eliminating pathogenic factors. In recent years, the basic principle of TCM in treating BC is to replenish T qi and blood. Lee et al. found that Huanglian Wendan Tang improved the prognosis of BC patients [14]. Moreover, Yanghe decoction was found to improve the immune function of BC patients [15]. Buqi Yangxue decoction is a famous prescription for treating deficiency of qi and blood. In recent years, with the application of modern research technology, the pharmacological action of this decoction has been further studied. Studies have shown that Buqi Yangxue decoction can promote the treatment of renal anemia [16]. Furthermore, Buqi Yangxue decoction improved TCM clinical symptoms of patients with advanced colorectal cancer, reduced the side effects of chemotherapy, and provided patients with quality of life [17].

In this study, 66 patients with BC were treated with Buqi Yangxue decoction adjuvant therapy, in order to provide theoretical basis for the study of Chinese herbal formulas to improve the therapeutic effect of BC patients.

2. Materials and Methods

2.1. Clinical Data and Methods. A total of 66 patients with BC from December 2019 to January 2021 were selected as the study subjects. Patients were divided into the control group and Chinese herbal formula group by numerical randomization. There were no significant differences in age, weight, tumor site, TNM stage, and lymph node metastasis between the two groups (Table 1, $P > 0.05$). All patients were clearly diagnosed with BC by preoperative biopsy or intraoperative pathological section. This study was approved by the Hospital's Ethics Committee. All patients were aware of the study and had signed informed consent.

2.2. Inclusion Criteria

(1) Diagnosed with breast cancer by cytology and histopathology

(2) No other malignant tumors

(3) The expected survival was greater than 6 months

(4) Those who agree to participate in the study and sign the informed consent

Table 1: Comparison of general data between the two groups before treatment.

	Chinese herbal formula group	Control group	P
Average age (years)	56.62 ± 8.26	57.23 ± 8.21	>0.05
Weight (kg)	50.37 ± 6.12	49.54 ± 7.15	>0.05
Tumor site			>0.05
Left	12	10	
Right	11	13	
TNM stage			>0.05
I-II	9	8	
III-IV	14	15	
Lymph node metastasis	12	11	>0.05

2.3. Exclusion Criteria

(1) Concurrent use of drugs affecting the results of this study

(2) Failure to follow the prescribed medication

(3) With heart, liver, kidney, and other serious diseases

(4) Mental disorders, unable to cooperate with evaluators

2.4. Interventions. The control group was treated with TE chemotherapy, and received routine nutritional intervention measures. Patients were given targeted dietary guidance according to the actual situation, chose light, digestible, and nutritious food, and avoided spicy stimulation and raw, cold, and greasy food.

The Chinese herbal formula group was treated with Buqi Yangxue decoction on the basis of the control group. The decoction was as follows: 15 g of Astragali Radix, 12 g of Codonopsis Radix, 10 g of Polygonati Rhizoma, 15 g of Rehmanniae Radix Praeparata, 10 g of Poria, 12 g of Radix Paeoniae Alba, 15 g of Angelica sinensis, 15 g of Chinese date, 6 g of liquorice. These herbs were decocted to 300 ml in water and taken twice in the morning and evening once a day, and taken continuously for 4 weeks.

2.5. Nutritive Indexes. In both groups, fasting venous blood was taken in the morning. The levels of hemoglobin (HGb), serum albumin (ALB), prealbumin (PA), transferrin (TRF), and serum total protein (TP) were measured by an automatic biochemistry analyzer (Cobas c702, Roche, Switzerland).

2.6. Cellular Immune Function Detection. Fasting venous blood was collected to detect various immune function indexes. CD3+, CD4+, CD8+, and CD4+/CD8+ were measured by flow cytometry (BeckMan Coulter). Peripheral blood immunoglobulin (IgA, IgG, and IgM) concentration was detected by radioimmunoassay.

2.7. TCM Syndrome Score. TCM syndrome score of patients was evaluated according to the Guidelines for Clinical Research of TCM New Drugs. The main symptoms were

fatigue, self-care ability, nausea and vomiting, dizziness, loss of appetite, and insomnia. Symptoms were rated from 0 to 6 on a scale of severity. The score was 0 for no symptoms, 2 for mild symptoms, 4 for moderate symptoms, and 6 for severe symptoms. The total score was 0-36, with a lower score indicating a milder disease.

2.8. Adverse Reactions. The adverse reactions of BC patients in two groups during treatment were observed and recorded, including nausea and vomiting, loss of appetite, thrombocytopenia, leukopenia, and liver function damage.

2.9. Statistical Analysis. SPSS 24.0 was used to analyze and process the data. t test was used for measurement data analysis, and χ^2 test was used for counting data analysis. $P < 0.05$ indicated that the difference was statistically significant.

3. Results

3.1. Comparison of Nutritional Indexes between the Two Groups. There was no significant difference in nutritional indexes between the two groups before the intervention. After 4 weeks, the nutritional indexes ALB, TP, PA, and TRF in Chinese herbal formula group were superior to the control group, except HGb (Table 2). Our results indicated that Buqi Yangxue decoction can dramatically improve the nutritional status of BC patients.

3.2. Comparative Analysis of Immune Function between the Two Groups. After treatment, CD3+, CD4+, CD4+/CD8+ were significantly increased, and CD8+ was significantly decreased in Chinese herbal formula group and control group (Table 3). And the changes of T lymphocytes in Chinese herbal formula group were clearly higher than that of control group after treatment. There was no obvious difference in the levels of immune indexes (IgG, IgA, and IgM) in both groups before intervention (Table 4). After treatment, the levels of serum IgG, IgA, and IgM in Chinese herbal formula group were notably higher than those in control group. Therefore, the data indicated that Buqi Yangxue decoction might improve the immune function of BC patients.

3.3. Comparison of TCM Symptom Quantitative Score between the Two Groups. Before treatment, there was no difference in observation symptom quantitative score between the two groups. After 4 weeks of treatment, observation symptom quantitative evaluation scale score in Chinese herbal formula group was notably lower than that in control group (Table 5). Our results manifested that Buqi Yangxue decoction might be helpful to improve the clinical symptoms of BC patients.

3.4. Comparison of Adverse Reactions between the Two Groups. Adverse reactions were found to be occurred in both groups during treatment, including nausea and vomiting, inappetence, liver function impairment, leukopenia, and thrombocytopenia. Results of Table 6 showed that there was no clear difference in the incidence of adverse reactions between the Chinese herbal formula group and control group. Therefore, our results indicated that Buqi Yangxue decoction was safe for the treatment of BC.

4. Discussion

BC is a common malignant tumor in women, and its exact pathogenesis has not been clarified yet. TCM believes that deficiency of vital qi and deficiency of blood is the internal cause and root of BC [18]. "Vital qi" in TCM is the immune function of modern medicine. The basis of the occurrence of malignant tumors is the weakness of vital qi, which is manifested in the low immune function. In TCM, the method of "Fuzheng cultivation" is adopted, which is to improve the immune function of the body by tonifying the innate kidney essence and the acquired spleen and stomach [19]. In the process of disease progression, patients often have deficiency syndromes such as spleen and stomach weakness, deficiency of qi and blood, depletion of yang qi, kidney failure, and deficiency of essence. Therefore, the method of replenishing qi and nourishing blood should run through the treatment process of BC [20]. Researches have shown that Chinese medicine has played an important role in the treatment of BC. Chinese herbal formula can be used as a complementary therapy, combined with surgery, chemotherapy, or targeted therapy, to enhance the immune function of patients and reduce adverse reactions [21, 22].

In this study, on the basis of conventional treatment, Buqi Yangxue decoction was used. Astragali Radix [23] and Poria [24] can obviously enhance and regulate the immune function of the body. Codonopsis Radix can tonify and replenish the middle qi, and nourish the heart to tranquilize [25]. Angelica sinensis and Rehmanniae Radix Praeparata have the function of promoting blood circulation and replenishing blood [26]. Polygonati Rhizoma can invigorate qi and nourish Yin [27]. Radix Paeoniae Alba can nourish blood and liver [28]. All the above herbs can nourish and replenish blood, and play the role of replenishing both qi and blood. Combined with licorice and Chinese date can soothe the liver and regulate qi, harmonize the spleen and stomach, and nourish qi and yin [29, 30]. All herbs are used together to play the effect of regulating qi and relieving depression, nourishing blood, and supplementing qi.

Immunosuppressant factors will be secreted or produced during the occurrence and development of tumors, so the immune function of patients with advanced malignant tumors is mostly in a suppressed state, which is the "deficiency of vital qi" in TCM. When the body is lack of vital qi, it will lead to the decline of "zang fu" function over time, and the resistance to disease will also be reduced. The occurrence and development of diseases are closely related to the changes in the number, function, activity, and proportion of CD3+,CD4+ and CD8+ cells [31]. Measuring the changes of CD3+, CD4+, CD4+/ CD8+ can directly reflect the immune function [32, 33]. CD3+ and CD4+ cells were significantly increased in Chinese herbal formula group, while CD8+ cell subsets were decreased, indicating that the cellular immune function of patients was improved. IgG, IgA, and IgM are important indexes of humoral immune response [34]. The

Table 2: Comparison of nutritional indexes between two groups.

	HGb (g/L)	ALB (g/L)	TP (g/L)	PA (mg/L)	TRF (mg/L)
Control group					
Before treatment	110.48±12.62	35.37±6.24	50.16±7.34	254.84±24.17	954.16±154.23
After treatment	120.23±18.50	40.71±4.14	57.31±6.68	270.63±18.55	2001.44±221.68
t	3.517	5.347	11.064	2.368	151.471
P	<0.05	<0.05	<0.05	<0.01	<0.01
Chinese herbal formula group					
Before treatment	110.24±5.47	36.62±4.50	49.67±7.45	262.47±25.39	975.51±183.17
After treatment	122.67±6.59	43.27±6.09	65.25±6.03	293.41±20.65	2517.54±208.61
t	2.647	6.382	10.930	3.417	184.173
P	<0.01	<0.05	<0.01	<0.01	<0.01

Table 3: Comparison of lymphocyte subsets between two groups before and after treatment.

	CD3+ (%)	CD4+ (%)	CD8+ (%)	CD4+/CD8+ (%)
Chinese herbal formula group				
Before treatment	53.34 ± 7.05	31.27 ± 5.40	36.21 ± 4.24	0.86 ± 0.22
After treatment	66.12 ± 5.68	40.22 ± 3.34	31.24 ± 5.37	1.29 ± 0.39
t	13.574	10.367	5.698	1.334
P	<0.01	<0.01	<0.01	<0.01
Control group				
Before treatment	53.15 ± 9.17	31.47 ± 6.25	36.93 ± 5.08	0.85 ± 0.11
After treatment	56.73 ± 6.46	35.04 ± 6.21	35.82 ± 3.63	0.98 ± 0.27
t	14.369	10.084	6.337	2.378
P	<0.05	<0.01	>0.05	<0.05

Table 4: Comparison of immunological indexes between two groups.

	IgG (g/l)	IgA (g/l)	IgM (g/l)
Chinese herbal formula group			
Before treatment	10.26 ± 1.05	2.27 ± 5.40	1.83 ± 4.24
After treatment	13.35 ± 5.68	2.95 ± 3.34	2.16 ± 5.37
t	0.444	0.286	0.559
P	<0.01	<0.01	<0.01
Control group			
Before treatment	10.37 ± 9.17	2.35 ± 6.25	1.79 ± 5.08
After treatment	11.50 ± 6.46	2.33 ± 6.21	2.09 ± 3.63
t	12.241	20.012	13.651
P	>0.05	>0.05	<0.05

results of this study showed that Buqi Yangxue decoction notably increased the levels of IgG, IgA, and IgM, indicating that it can improve the immune function of BC patients.

In addition, the study found that ALB, PA, TRF, and TP in the Chinese herbal formula group were clearly higher than those in the control group, which indicated that Buqi Yangxue decoction could improve the nutritional status of BC patients. Malnutrition in BC patients affects not only the immune system but also the patient's ability to tolerate treatment. Therefore, BC patients should strengthen nutrition during treatment to improve the therapeutic effect. Furthermore, Buqi Yangxue decoction was discovered to improve the TCM symptom. Ultimately, there was no significant difference in the incidence of adverse reactions

TABLE 5: Comparison of TCM symptom score between two groups.

	n	Before treatment	After treatment
Chinese herbal formula group	33	32.52 ± 2.21	17.12 ± 2.58
Control group	33	33.02 ± 2.98	21.61 ± 1.36
t		1.472	3.635
P		>0.05	<0.05

TABLE 6: Comparison of adverse reactions between the two groups.

	n	Nausea and vomiting	Inappetence	Liver function impairment	Leukopenia	Thrombocytopenia	Total incidence (%)
Control group	33	4	3	2	3	4	48.5
Chinese herbal formula group	33	3	3	1	4	3	42.4

between the two groups, suggesting that Buqi Yangxue decoction can be safely used for adjuvant treatment of BC.

To be sure, there are still some shortcomings in our research. For example, the number of experimental patients should be increased to ensure the accuracy of the experiment. The research method was simple and research indicators were few. Furthermore, the observation period was short, and the decoction for Buqi Yangxue decoction should be taken for a long time to verify its effect on BC. In addition, we should study the mechanism of Buqi Yangxue decoction in treating BC patients from the perspective of molecular biology.

5. Conclusion

To sum up, Buqi Yangxue decoction can improve the immune function, nutritional status, and TCM symptoms of BC patients, and with fewer adverse reactions. Our results may provide a new idea for the clinical treatment of BC with combination of Chinese and Western medicine.

Data Availability

The data used to support the findings of this study are available from the corresponding author upon request.

Conflicts of Interest

The author declares no potential conflicts of interest with the respect to the research, authorship, and/or publication of this article.

References

[1] C. Xia, X. Dong, H. Li et al., "Cancer statistics in China and United States, 2022: profiles, trends, and determinants," *Chinese Medical Journal*, vol. 135, no. 5, pp. 584–590, 2022.

[2] H. J. Youn and W. Han, "A review of the epidemiology of breast cancer in Asia: focus on risk factors," *Asian Pacific Journal of Cancer Prevention*, vol. 21, no. 4, pp. 867–880, 2020.

[3] H. Sung, J. Ferlay, R. L. Siegel et al., "Global cancer statistics 2020: GLOBOCAN estimates of incidence and mortality worldwide for 36 cancers in 185 countries," *CA: a Cancer Journal for Clinicians*, vol. 71, no. 3, pp. 209–249, 2021.

[4] K. Wang, Y. Ren, H. Li et al., "Comparison of clinicopathological features and treatments between young (≤40 years) and older (>40 years) female breast cancer patients in West China: a retrospective, epidemiological, multicenter, case only study," *PLoS One*, vol. 11, no. 3, article e0152312, 2016.

[5] T. Fietz, H. Tesch, J. Rauh et al., "Palliative systemic therapy and overall survival of 1,395 patients with advanced breast cancer - results from the prospective German TMK cohort study," *Breast (Edinburgh, Scotland)*, vol. 34, pp. 122–130, 2017.

[6] N. Harbeck, "Neoadjuvant and adjuvant treatment of patients with HER2-positive early breast cancer," *Breast (Edinburgh, Scotland)*, vol. 62, pp. S12–S16, 2022.

[7] T. Shien and H. Iwata, "Adjuvant and neoadjuvant therapy for breast cancer," *Japanese Journal of Clinical Oncology*, vol. 50, no. 3, pp. 225–229, 2020.

[8] J. Cho, M. Lee, S. Kim et al., "The effects of perioperative anesthesia and analgesia on immune function in patients undergoing breast cancer resection: a prospective randomized study," *International Journal of Medical Sciences*, vol. 14, no. 10, pp. 970–976, 2017.

[9] L. Wang, D. Simons, X. Lu et al., "Breast cancer induces systemic immune changes on cytokine signaling in peripheral blood monocytes and lymphocytes," *eBioMedicine*, vol. 52, p. 102631, 2020.

[10] A. Shastri, J. Lombardo, S. C. Okere et al., "Personalized nutrition as a key contributor to improving radiation response in breast cancer," *International Journal of Molecular Sciences*, vol. 23, no. 1, p. 175, 2022.

[11] V. Ho, H. Tan, W. Guo et al., "Efficacy and safety of Chinese herbal medicine on treatment of breast cancer: a meta-analysis of randomized controlled trials," *The American Journal of Chinese Medicine*, vol. 49, no. 7, pp. 1557–1575, 2021.

[12] J. Hong, X. Chen, J. Huang et al., "Danggui Buxue decoction, a classical formula of traditional Chinese medicine, fails to prevent myelosuppression in breast cancer patients treated with adjuvant chemotherapy: a prospective study," *Integrative Cancer Therapies*, vol. 16, no. 3, pp. 406–413, 2017.

[13] Z. Dang, X. Liu, X. Wang et al., "Comparative effectiveness and safety of traditional Chinese medicine supporting Qi and enriching blood for cancer related anemia in patients not receiving chemoradiotherapy: a meta-analysis and systematic

Retraction

Retracted: Effects of Bevacizumab Combined with Chemotherapy on CT, CyFRA21-1, and ProGRP and Prognosis of Lung Cancer Patients under Nursing Intervention

Computational and Mathematical Methods in Medicine

This article has been retracted by Hindawi following an investigation undertaken by the publisher [1]. This investigation has uncovered evidence of one or more of the following indicators of systematic manipulation of the publication process:

(1) Discrepancies in scope

(2) Discrepancies in the description of the research reported

(3) Discrepancies between the availability of data and the research described

(4) Inappropriate citations

(5) Incoherent, meaningless and/or irrelevant content included in the article

(6) Peer-review manipulation

The presence of these indicators undermines our confidence in the integrity of the article's content and we cannot, therefore, vouch for its reliability. Please note that this notice is intended solely to alert readers that the content of this article is unreliable. We have not investigated whether authors were aware of or involved in the systematic manipulation of the publication process.

Wiley and Hindawi regrets that the usual quality checks did not identify these issues before publication and have since put additional measures in place to safeguard research integrity.

We wish to credit our own Research Integrity and Research Publishing teams and anonymous and named external researchers and research integrity experts for contributing to this investigation.

The corresponding author, as the representative of all authors, has been given the opportunity to register their agreement or disagreement to this retraction. We have kept a record of any response received.

References

[1] C. Xi, H. Jiang, Y. Xue, Y. Lv, and C. Wang, "Effects of Bevacizumab Combined with Chemotherapy on CT, CyFRA21-1, and ProGRP and Prognosis of Lung Cancer Patients under Nursing Intervention," *Computational and Mathematical Methods in Medicine*, vol. 2022, Article ID 9422902, 8 pages, 2022.

Research Article

Effects of Bevacizumab Combined with Chemotherapy on CT, CyFRA21-1, and ProGRP and Prognosis of Lung Cancer Patients under Nursing Intervention

Chao Xi [iD],[1] **Hong Jiang** [iD],[2] **Yinling Xue** [iD],[3] **Yongmei Lv** [iD],[4] and **Chao Wang** [iD][5]

[1]*Department of Thoracic Surgery, Zhangqiu District People's Hospital, Jinan 250200, China*
[2]*Department of Imaging, Yantai Yuhuangding Hospital Affiliated to Qingdao University, Yantai 264000, China*
[3]*Department of Urology Surgery, Qingdao Hospital of Traditional Chinese Medicine, Hiser Medical Group of Qingdao, Qingdao 266033, China*
[4]*Department of Pharmacy, Zhangqiu District People's Hospital, Jinan 250200, China*
[5]*Department of Pharmacy, Qingdao Hospital of Traditional Chinese Medicine, Hiser Medical Group of Qingdao, Qingdao 266033, China*

Correspondence should be addressed to Chao Wang; wangchao@qdzyhospital.cn

Objective. Molecular targeted drug therapy and chemotherapy are the main treatments for advanced non-small-cell lung cancer, and the combination of both has advantages in prolonging patients' progression-free survival and overall survival. This study investigated the effects of bevacizumab combined with chemotherapy under nursing intervention on CT, cytokeratin 19 fragment antigen 21-1 (CYFRA21-1), and gastrin-releasing peptide precursor (ProGRP) and prognosis of lung cancer patients. *Methods.* 102 patients with non-small-cell lung cancer admitted to our hospital from January 2018 to May 2019 were divided into observation group and control group, with 51 cases each. The control group was treated with basic chemotherapy, and the observation group was treated with bevacizumab in combination with the control group, and both groups used nursing interventions. The clinical effects, CYFRA21-1 and ProGRP levels, baseline data, CT parameters, 24-month cumulative survival, and the effects of CYFRA21-1 and ProGRP on long-term survival and lung function were compared. *Results.* The disease control rate of the observation group was 94.12%, which was significantly higher than that of the control group (76.47%); after 7 d, 30 d, 60 d, and 90 d of treatment, the levels of CYFRA21-1 and ProGRP were statistically downregulated. The difference in lymph node metastasis, lesion diameter, plain Eff-Z, venous stage, and arterial stage normalized iodine concentrations (NIC) was statistically significant; the survival rate at 24 months in the observation group was 74.51% (38/51); the cumulative survival rate at 24 months in the control group was 52.94% (27/51), and the difference was statistically significant ($X^2 = 4.980$, $P = 0.026$). The cumulative survival rate at 24 months was significantly lower in patients with high expression of CYFRA21-1 and ProGRP compared with those with low expression of CYFRA21-1 and ProGRP. After treatment, in the observation group, the forceful spirometry (FVC), forceful expiratory volume in one second (FEV1), and FEV1/FVC levels were significantly different from those before treatment and were significantly different from those in the control group. *Conclusion.* Bevacizumab in combination with standard chemotherapy regimens with nursing interventions could benefit patients with advanced non-small-cell lung cancer and had a good prospect of application.

1. Introduction

Lung cancer is known as primary bronchial lung cancer, and the incidence rate and death rate of lung cancer in China have been increasing year by year in recent years. Lung can-

cer is divided into small cell lung cancer (SCLC) and non-small-cell lung cancer (NSCLC), of which NSCLC accounts for more than 80% of all lung cancers [1–3]. There are no typical manifestations in the early stage of lung cancer, and its clinical symptoms are easily confused with other benign

lung and respiratory tract lesions, and local spread or distant metastasis has occurred when it progresses to the middle and late stages [4].

Currently, clinical treatment of lung cancer is mainly based on radiotherapy and chemotherapy, which are administered intravenously to induce apoptosis of tumor foci in order to alleviate clinical symptoms. However, long-term clinical studies have found that the use of chemotherapy alone in patients with non-small-cell carcinoma has certain limitations, and the prognosis is not ideal [5–7]. With the continuous development of tumor treatment technology, molecular targeted drug therapy has gradually become the main mode of lung cancer treatment [8, 9]. It has been confirmed by clinical practice that targeted therapy can effectively inhibit tumor cell proliferation, which is of great significance in the treatment of lung cancer [9, 10]. Bevacizumab is the first angiogenesis inhibitor that has been shown to prolong the survival of NSCLC patients in combination with chemotherapy [11]. Akamatsu et al. conducted the first phase III clinical study for Chinese NSCLC patients, and the experimental results showed that the median PFS and OS of paclitaxel + carboplatin combined with bevacizumab were 9.2 and 24.3 months, confirming that bevacizumab combined with chemotherapy could benefit Chinese NSCLC patients [12].

However, while molecularly targeted drugs inhibit tumor cell proliferation and growth in lung cancer patients, they also bring certain risks of adverse effects, causing heavy psychological pressure on patients and leading to negative emotions such as anxiety and depression, which seriously reduce patients' quality of life [13]. This places higher demands on lung cancer nursing, and preventive nursing interventions are a means of emphasizing the safety of the treatment, helping to reduce the burden of multiple symptoms at the physical and psychological levels during treatment, and improving patients' treatment compliance and quality of life [14]. Studies have pointed out that CT is the most commonly used tool for efficacy assessment and is an anatomical imaging technique with good reproducibility, reflecting the patient's condition and predicting the risk of poor prognosis [15]. Cytokeratin 19 fragment antigen 21-1 (CYFRA21-1) levels correlate with tumor load and metastasis in intermediate to advanced NSCLC and can be used as an adjunctive assessment indicator of treatment response and prognosis [16]. Gastrin-releasing peptide precursor (ProGRP) is a new hormonal tumor marker isolated from gastric tissues and widely distributed in gastric nerve fibers and pulmonary neuroendocrine tissues, which is widely used in the diagnosis and monitoring of lung cancer due to its long half-life [17].

In this study, we investigated the clinical efficacy and the effects on CT, CYFRA21-1 level, ProGRP level, and prognosis of 102 lung cancer patients treated with bevacizumab in combination with chemotherapy under preventive care intervention.

2. Materials and Methods

2.1. General Information. The medical records of lung cancer patients admitted to our hospital from January 2018 to May 2019 were collected. Inclusion criteria are as follows: (i) non-small-cell lung cancer diagnosed by surgical pathology or fiberoptic bronchoscopy biopsy, (ii) no history of radiotherapy, (iii) expected survival time of more than half a year, and (iv) complete clinical data. Exclusion criteria are as follows: (1) patients with contraindications to CT examination or contrast allergy; (2) patients within 14 days after major surgery or trauma; (3) patients in the acute phase of infectious diseases, acute exacerbation of various chronic diseases, and acute phase of adverse events in the cardiovascular and cerebrovascular systems; (4) patients with other lung diseases such as pulmonary vasculopathy, pulmonary encapsulation, tuberculosis, or congenital anatomical abnormalities of the lung or respiratory tract; and (5) the presence of severe psychiatric disorders, cognitive impairment, and communication disorders. A total of 102 lung cancer patients were included in this study and divided into an observation group and a control group with 51 cases each. In the control group, there were 29 males and 22 females, aged 51-68 years, with a mean of 57.63 ± 5.39 years. In the observation group, there were 32 males and 19 females, aged 50-70 years, with an average of 57.41 ± 5.98 years. The differences in gender and age between the two groups were not statistically significant ($P > 0.05$) and were comparable. The study was approved by the hospital ethics committee, and all patients gave their informed consent and signed the informed consent form.

2.2. Treatment Method. The control group was treated with a TC chemotherapy regimen: 250 mL of glucose solution mixed with 175 mg/m^2 paclitaxel (Harbin Labotong Pharmaceutical Co., Ltd., National Drug Administration H20067522, specification: 5 mL: 30 mg) was given intravenously on day 1; on the second day, 250 mL of glucose solution was mixed with 300-400 mg/m^2 carboplatin (Zhejiang Haisheng Pharmaceutical Co., Ltd., National Drug Administration H20044177, specification: 100 mg) and then administered intravenously. 21 d was a course of treatment, and there were 3 courses of treatment, with an interval of 1 week between each course.

In the observation group, bevacizumab targeting therapy was given in combination with the TC chemotherapy regimen. The TC chemotherapy regimen was the same as that of the control group. 7.5 mg/m^2 bevacizumab injection was given intravenously on day 1 of chemotherapy. 21 d was a course of treatment, once for each course of treatment, and the efficacy was evaluated after 3 courses of treatment.

2.3. Nursing Method. Nursing interventions were implemented [18].

(1) *Complication Interventions.* Pay attention to the cleanliness and moistening of the patient's radiated skin, avoid direct sunlight stimulation of the irradiated patient's skin, and try to choose clothing made of more comfortable fabrics to avoid damage to the patient's organism skin due to friction. Pay attention to the patient's posture after eating and drinking, and forbid lying down to prevent food reflux,

residue, and other foreign bodies, thus preventing esophagitis. Advise the patient to drink plenty of normal temperature water and to choose the appropriate nebulization input to ensure the smooth flow of the airway

(2) *Lifestyle Interventions.* Observe and count the daily dietary status of the patient and develop a set of targeted individualized diet plans to ensure the daily intake of vitamins, proteins, and other nutrients. Do not consume spicy and stimulating foods, and follow the principle of small and frequent meals. The decline of the patient's physical quality was associated with the level of care, which may lead to negative phenomena such as irritability and anxiety, so the medical staff should communicate with the patient more often to increase the patient's compliance with treatment and to build up their confidence in overcoming the disease. A certain scale of patient conversation could be carried out to further enhance the patient's treatment initiative

(3) *Pain Intervention.* Patients were instructed to carry out healthier physical rehabilitation exercises and targeted interventions such as distraction methods, and watching children's programs and videos were carried out for patients with different pain levels

(4) *Psychological Care.* Strengthen communication with patients and help them to adjust their psychological state, and invite patients with successful treatment cases to "present themselves" to enhance their confidence in the treatment and relieve their negative emotions. Patiently explain the role of radiotherapy and the occurrence of gastrointestinal adverse effects as a normal phenomenon to increase treatment confidence

2.4. CT Scanning Methods. GE gem energy spectrum CT (Discovery CT750 HD) was used for chest plain scan and two-phase enhanced scan. The scan parameters were as follows: tube voltage was switched between high and low energy (80 kVp and 140 kVp) instantaneously (0.5 ms), automatic milliamp, pitch 1.375 : 1, layer spacing 5.0, layer thickness 5.0 mm, matrix 512×512, collimation 64×0.625 mm, and frame rotation time 0. 6 s. The scan area included the lung tip to the rib diaphragm angle. After plain scanning, nonionic contrast agent iohexol was injected through the median cubital vein for 1.6 mL·kg^{-1}, time ≤ 30 s, and the CT value of the thoracic aorta was monitored. After reaching the threshold value of 150 HU, the scanning was delayed for 5.7 s, and the venous phase images were delayed for 30 s after obtaining arterial phase images. The images were uploaded to the workstation and reviewed by 2 attending physicians. The solid component of the lesion was selected as the region of interest (ROI), and the ROI of each phase was measured once at each of the three adjacent levels, with consistent size, morphology, and location, and the average value was obtained. The effective atomic number (Eff-Z) was recorded, and the normalized iodine concentrations (NIC) were calculated as NIC = iodine content in the ROI of the lesion/aortic iodine content.

2.5. Observation Index

(1) Compare the clinical efficacy of the two groups after 3 courses of treatment, in which complete remission (CR): CT scan showed no target tumor, no cavity, pulmonary atelectasis, etc.; partial remission (PR): CT scan showed incomplete cavity of the target tumor, containing liquid or solid components, showing contrast enhancement, part of the target tumor had fibrosis, containing solid components, with enhancement; stable disease (SD): CT scan showed part of the target tumor as a solid nodule with no significant change in volume and reinforcing features; disease progression (PD): CT scan showed newly scattered, nodular, irregular eccentric reinforcement around the treated out tumor again. Total effective rate = number of (CR + PR) cases/total number of cases × 100%

(2) The levels of CYFRA21-1 and ProGRP were compared between the two groups before treatment and after 7, 30, 60, and 90 d of treatment. 5 mL of fasting venous blood was collected from all patients before treatment and left for 20 min in a sterile and light-proof room at 20~26°C, placed in a centrifuge, centrifuged at 3500 r/min for 10 min with a 10 cm radius, and stored the serum in a refrigerator at -20°C for examination. ProGRP level was detected by enzyme-linked immunoadsorbent assay (ELISA), and CYFRA21-1 level was detected by electrochemiluminescence assay

(3) The survival time of patients was recorded by telephone call back every three months after the end of 3 courses of treatment or when the patients were reexamined

(4) Compare the lung function levels of the two groups before and after 3 courses of treatment, and test their forceful spirometry (FVC) and forceful expiratory volume in one second (FEV1) levels

2.6. Statistical Analysis. The SPSS 21.0 statistical software was used to analyze the data, and the measurement data and count data were expressed as $\bar{x} \pm s$ and %, respectively, and t and χ^2 tests were used to compare between two groups. Survival curves were plotted using GraphPad Prism 5 to test the survival of NSCLC patients. The difference was statistically significant at $P < 0.05$.

3. Results

3.1. Comparison of Clinical Efficacy between the Two Groups. The disease control rate of the observation group was 94.12%, which was significantly higher than that of the control group (76.47%), and the difference was statistically significant ($P < 0.05$) (Table 1).

TABLE 1: Comparison of clinical efficacy between the two groups (n (%)).

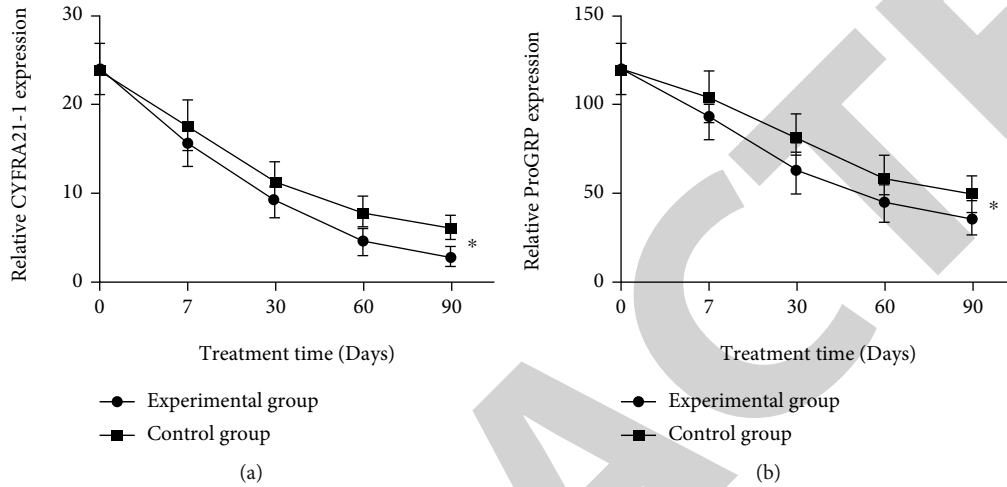| Group	n	CR	PR	SD	PD	Disease control rate
Observation group	51	26 (50.98)	13 (25.49)	9 (17.65)	3 (5.88)	48 (94.12)
Control group	51	18 (35.29)	9 (17.65)	12 (23.53)	12 (23.53)	39 (76.47)
X^2						8.010
P						0.046

FIGURE 1: Comparison of cyFRA21-1 and ProGRP levels between the two groups. (a) After 7 d, 30 d, 60 d, and 90 d of treatment, CyFRA21-1 levels were gradually decreased. (b) After 7 d, 30 d, 60 d, and 90 d, ProGRP levels in both groups were gradually downregulated.

3.2. Comparison of CYFRA21-1 and ProGRP Levels between the Two Groups. After 7 d, 30 d, 60 d, and 90 d of treatment, CYFRA21-1 and ProGRP levels in both groups were gradually adjusted downward, and the differences in CYFRA21-1 and ProGRP levels between the two groups compared with those before treatment were statistically significant ($P < 0.05$), and the levels of CYFRA21-1 and ProGRP in the observation group were significantly lower than those in the control group ($P < 0.05$) (Figure 1).

3.3. The Baseline Data and CT Parameters Were Compared. There was no statistically significant difference in the comparison of gender, age, clinical stage, histological staging, degree of differentiation, smoking history, and drinking history ($P > 0.05$); the difference was statistically significant in the comparison of lymph node metastasis, lesion diameter, plain Eff-Z, venous stage, and arterial stage NIC ($P < 0.05$) (Table 2).

3.4. The Survival Time of the Two Groups Was Compared. The cumulative survival rate at 24 months in the observation group was 74.51% (38/51); the cumulative survival rate at 24 months in the control group was 52.94% (27/51) ($X^2 = 4.980$, $P = 0.026$) (Figure 2).

3.5. Effect of High and Low Expressions of CYFRA21-1 and ProGRP on Long-Term Survival. The 24-month cumulative survival rate of patients with high CYFRA21-1 and ProGRP expression was significantly lower than that of patients with low CYFRA21-1 and ProGRP expressions (Figure 3).

3.6. Comparison of Pulmonary Function. After treatment, the FVC and FEV1 levels in the observation group were 2.55 ± 0.63 L and 2.00 ± 0.46 L, respectively, and the FVC and FEV1 levels in the control group were 2.15 ± 0.61 L and 1.56 ± 0.43 L, respectively. The differences between groups and within groups were statistically significant (both $P < 0.05$). After treatment, the difference in FEV1/FVC between the two groups was statistically significant (both $P < 0.05$) (Figure 4).

4. Discussion

Lung cancer is a common respiratory malignancy in clinical practice and has a high incidence and morbidity and mortality rate in China. Some data show [19] that the incidence of non-small-cell carcinoma accounts for about 80% of lung cancer. In the early stage, there are mostly no typical symptoms, mainly manifesting as chest tightness, chest pain, cough, hoarseness, fever, and shoulder pain, which are easily confused with other benign lung diseases, leading to the progression of the disease to the middle and late stages when most patients are diagnosed, and the best time for surgery is missed. Chemotherapy can improve patients' clinical symptoms to a certain extent, but after clinical practice, it is found that single chemotherapy can cause many adverse reactions, which can seriously affect patients' subsequent treatment and daily life and cannot better control the development of tumor [20]. Molecular targeted drug therapy has a wide range of applications and can provide good antitumor

TABLE 2: Comparison of baseline data and CT parameters between the two groups.

| Baseline data and CT parameters		Observation group ($n = 51$)	Control group ($n = 51$)	X^2/t	P
Gender	Male	32	29	$X^2 = 0.367$	0.545
	Female	19	22		
Age (years)	≥55	28	30	$X^2 = 0.160$	0.689
	<55	23	21		
Clinical stages	III stage	18	21	$X^2 = 0.374$	0.541
	IV stage	33	30		
Histological staging	Adenocarcinoma	26	28	$X^2 = 0.171$	0.918
	Squamous carcinoma	17	16		
	Adenosquamous carcinoma	8	7		
Degree of differentiation	Well differentiated	29	28	$X^2 = 0.318$	0.853
	Moderately differentiated	19	21		
	Poorly differentiated	3	2		
Smoking history	Yes	32	36	$X^2 = 0.706$	0.401
	No	19	15		
Drinking history	Yes	41	42	$X^2 = 0.065$	0.799
	No	10	9		
Lymph node metastasis	Yes	4	14	$X^2 = 6.746$	0.009
	No	47	37		
Lesion diameter/cm	≥3.5	6	15	$X^2 = 4.411$	0.036
	<3.5	45	38		
Plain Eff-Z		7.91 ± 0.46	7.53 ± 0.43	$t = 4.385$	<0.001
Venous stage NIC/mg·cm^{-3}		0.41 ± 0.11	0.300 ± 0.08	$t = 5.696$	<0.001
Arterial stage NIC/mg·cm^{-3}		0.16 ± 0.05	0.09 ± 0.02	$t = 8.609$	<0.001
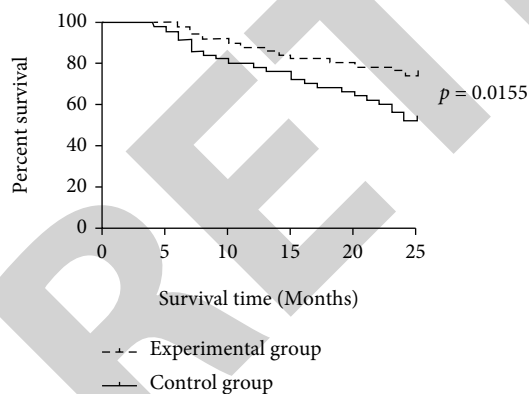
FIGURE 2: Comparison of survival time between the two groups.

support for lung cancer patients in different pathological stages. Moreover, it is easy to operate and highly accepted by patients. However, the long-term use of molecularly targeted drugs during the implementation of targeted therapy for lung cancer patients can easily lead to adverse reactions related to skin reactions mainly [21]. The formation of such problems not only aggravates the painful experience of lung cancer patients but also tends to cause the interruption of targeted therapy. As an important complement to antitumor therapy, the role of nursing care in supporting targeted ther-

apy for lung cancer patients directly affects the recovery status of lung cancer patients. Therefore, it is necessary to select appropriate methods to construct nursing programs for lung cancer targeted therapy patients. In targeted lung cancer therapy, this method uses measures such as missionary intervention, psychological protection intervention, and pain care to improve the risk of adverse reaction formation of targeted therapy, alleviate the severity of adverse reactions of lung cancer patients, and provide the necessary support for targeted antitumor therapy of lung cancer patients.

Bevacizumab, as a targeted drug [22], has the advantages of long half-life, human origin, and high selectivity, which can inhibit the development of tumor cells and play the role of inhibiting tumor cell growth and promoting apoptosis. The results of this study showed that the disease control rates in the observation group were all significantly higher than those in the control group ($P < 0.05$); after treatment, the differences in FVC, FEV1, and FEV1/FVC levels in the observation group were statistically significant compared with those in the control group ($P < 0.05$). It was suggested that bevacizumab combined with chemotherapy regimens and nursing interventions were effective in improving treatment outcomes and lung function in patients with non-small-cell lung cancer. The analysis suggested that bevacizumab initiated complement- and antibody-mediated toxic effects, using the body's immune mechanisms to act as a
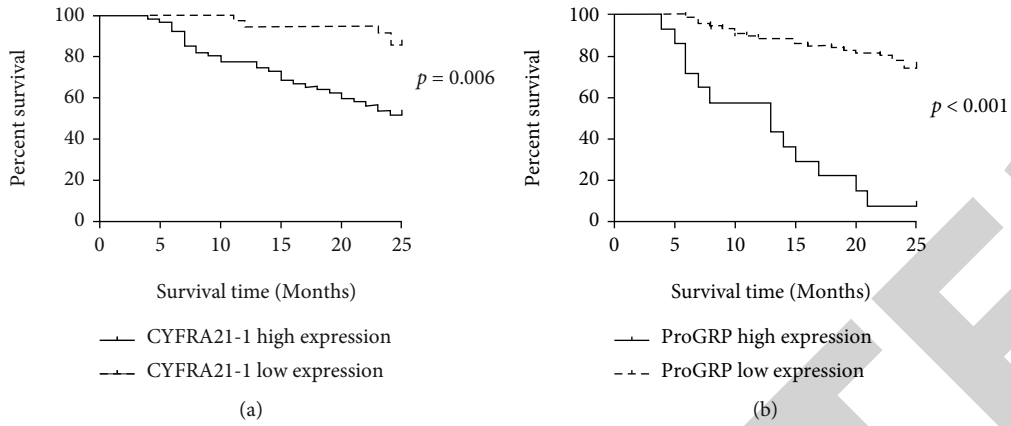
(a)

(b)

Figure 3: Influence of high and low expressions of CyFRA21-1 and ProGRP on long-term survival.
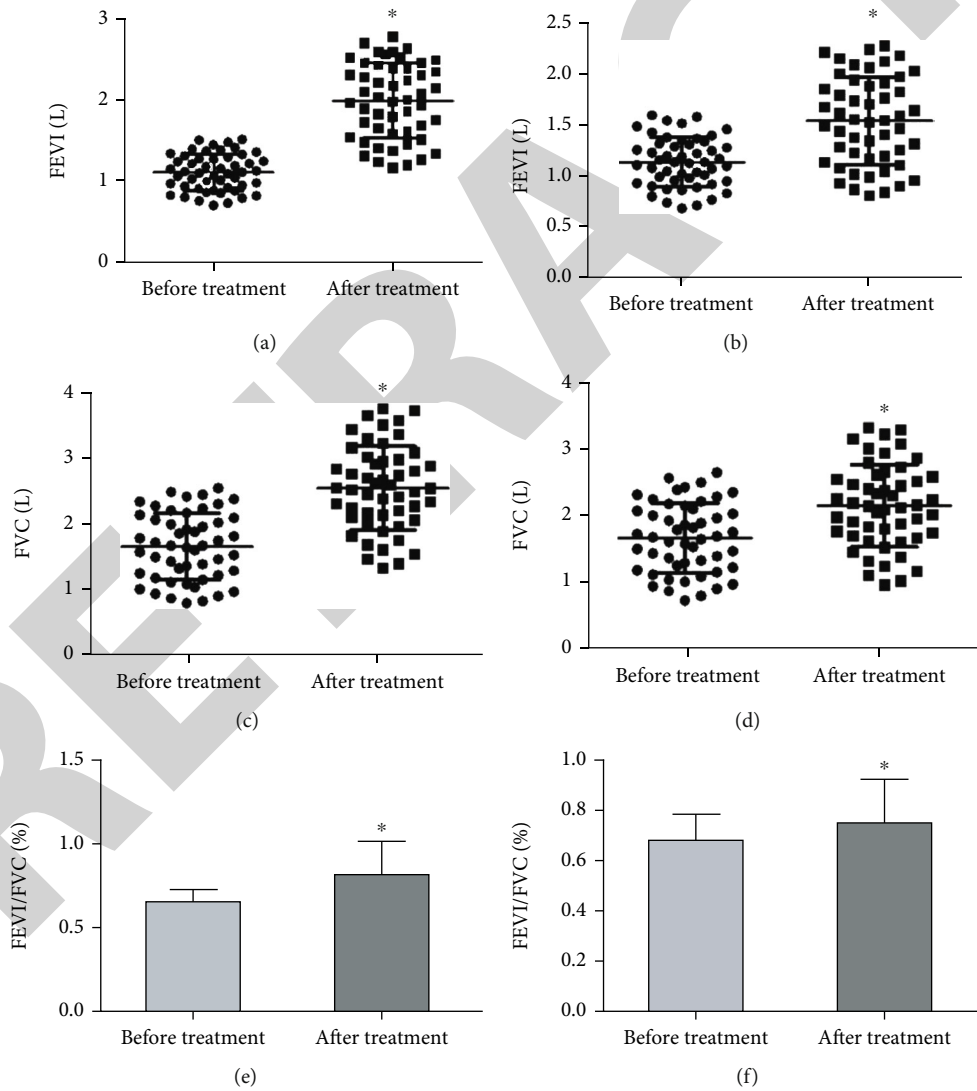

(a)

(b)

(c)

(d)

(e)

(f)

Figure 4: Comparison of lung function between the two groups. (a) Comparison of FEV1 level before and after treatment in the observation group. (b) Comparison of FEV1 levels in the control group before and after treatment. (c) Comparison of FVC levels in the observation group before and after treatment. (d) Comparison of FVC levels in the control group before and after treatment. (e) Comparison of FEV1/FVC levels in the experimental group before and after treatment. (f) Comparison of FEV1/FVC levels in the control group before and after treatment.

lethal agent against tumor cells. Combined with chemotherapy and nursing intervention regimens, treatment not only alleviated toxic effects but also increased drug tolerance, which in turn improved treatment outcomes and lung function in patients with non-small-cell lung cancer. CT is a medical imaging method widely used in recent years for the diagnosis of lung cancer. CT can detect overlapping and micronodules and can determine the specific nature of nodules and has a high sensitivity for the diagnosis of independent nodules in the lung [23]. Plain scan Eff-Z, venous phase, and arterial phase NIC can be used to identify the nature of the lesion. Low of the three can reflect the tumor growth and invasive ability, the neovascularization cannot meet the tumor blood supply-demand, and there are more mucus and necrotic components inside the tumor, and microhemorrhage occurs, and the lesion shows insufficient blood supply, which further reflects the high malignancy of the tumor and the high risk of poor prognosis of the patient. ProGRP is a gastrointestinal hormone [24], mostly found in many neuroendocrine tumors [25], which has high sensitivity and specificity for SCLC and is an important serum marker for the diagnosis of SCLC. CYFRA21-1 is a cytokeratin [26] that shows high expression in patients with non-squamous non-small-cell lung cancer, and the more severe the lesion, the higher the expression level. The results of this study showed that bevacizumab combined with chemotherapy and nursing intervention could effectively reduce the levels of tumor markers CYFRA21-1 and ProGRP in patients with non-small-cell lung cancer. The analysis suggested that bevacizumab inhibited VEGF activity during treatment by binding specifically to VEGF, blocking the nutrient supply to the tumor cell microenvironment, and thus controlling or delaying the formation and proliferation of abnormal neovascularization. In addition, the blocking effect of VEGF to inhibit cell progression also promoted the development of chemotherapeutic drug sensitivity in cancer cells, allowing them to initiate antibody- and complement-mediated toxic effects that used immune mechanisms to destroy cancer cells, thereby reducing or stabilizing serum CYFRA21-1 and ProGRP levels. When bevacizumab was used in combination with a chemotherapy regimen, it could reduce the interstitial pressure in the tumor, enhance the permeability of chemotherapy drugs, improve the effectiveness of treatment, and have a good chemotherapy sensitization effect, which could not only enhance the drug tolerance but also reduce the degree of toxic side effects and symptoms, so that the physical function and health condition of patients could be greatly enhanced, and thus improve the survival time of patients after treatment. Therefore, this study also found that bevacizumab not only improved the treatment effect but also had a good prognosis and a high safety profile.

5. Conclusion

In conclusion, bevacizumab targeted therapy combined with chemotherapy and nursing intervention could improve the clinical outcome and lung function of patients with non-small-cell lung cancer and reduce serum CYFRA21-1 and ProGRP levels while improving the survival time of patients with good prognosis and high safety, which was worthy of clinical reference.

Data Availability

The data used to support the findings of this study are available from the corresponding author upon request.

Conflicts of Interest

The authors declare that they have no conflicts of interest.

Authors' Contributions

Chao Xi and Hong Jiang contributed equally to this work.

References

[1] H. Hoy, T. Lynch, and M. Beck, "Surgical treatment of lung cancer," *Critical Care Nursing Clinics of North America*, vol. 31, no. 3, pp. 303–313, 2019.

[2] F. Wu, L. Wang, and C. Zhou, "Lung cancer in China: current and prospect," *Current Opinion in Oncology*, vol. 33, no. 1, pp. 40–46, 2021.

[3] F. Nasim, B. F. Sabath, and G. A. Eapen, "Lung cancer," *The Medical Clinics of North America*, vol. 103, no. 3, pp. 463–473, 2019.

[4] G. S. Jones and D. R. Baldwin, "Recent advances in the management of lung cancer," *Clinical Medicine (London, England)*, vol. 18, Suppl 2, pp. s41–s46, 2018.

[5] M. Nagasaka and S. M. Gadgeel, "Role of chemotherapy and targeted therapy in early-stage non-small cell lung cancer," *Expert Review of Anticancer Therapy*, vol. 18, no. 1, pp. 63–70, 2018.

[6] A. Rossi and M. Di Maio, "Platinum-based chemotherapy in advanced non-small-cell lung cancer: optimal number of treatment cycles," *Expert Review of Anticancer Therapy*, vol. 16, no. 6, pp. 653–660, 2016.

[7] M. C. Salazar, J. E. Rosen, Z. Wang et al., "Association of delayed adjuvant chemotherapy with survival after lung cancer surgery," *JAMA Oncology*, vol. 3, no. 5, pp. 610–619, 2017.

[8] R. Ruiz-Cordero and W. P. Devine, "Targeted therapy and checkpoint immunotherapy in lung cancer," *Surgical Pathology Clinics*, vol. 13, no. 1, pp. 17–33, 2020.

[9] F. R. Hirsch, G. V. Scagliotti, J. L. Mulshine et al., "Lung cancer: current therapies and new targeted treatments," *Lancet*, vol. 389, no. 10066, pp. 299–311, 2017.

[10] G. S. Shroff, P. M. de Groot, V. A. Papadimitrakopoulou, M. T. Truong, and B. W. Carter, "Targeted therapy and immunotherapy in the treatment of non-small cell lung cancer," *Radiologic Clinics of North America*, vol. 56, no. 3, pp. 485–495, 2018.

[11] M. Reck, G. Shankar, A. Lee et al., "Atezolizumab in combination with bevacizumab, paclitaxel and carboplatin for the first-line treatment of patients with metastatic non-squamous non-small cell lung cancer, including patients with EGFR mutations," *Expert Review of Respiratory Medicine*, vol. 14, no. 2, pp. 125–136, 2020.

[12] H. Akamatsu, Y. Toi, H. Hayashi et al., "Efficacy of osimertinib plus bevacizumab vs osimertinib in patients with EGFR